AD 700896
AGARD CP No. 49

AGARD CONFERENCE PROCEEDINGS No. 49

AGARD

ADVISORY GROUP FOR AEROSPACE RESEARCH & DEVELOPMENT

7 RUE ANCELLE 92 NEUILLY SUR SEINE FRANCE

Ionospheric Forecasting

NORTH ATLANTIC TREATY ORGANIZATION

INITIAL DISTRIBUTION IS LIMITED
FOR ADDITIONAL COPIES SEE BACK COVER

479

Best
Available
Copy

AGARD Conference Proceedings No. 49

NORTH ATLANTIC TREATY ORGANIZATION

ADVISORY GROUP FOR AEROSPACE RESEARCH AND DEVELOPMENT

(ORGANISATION DU TRAITE DE L' ATLANTIQUE NORD)

IONOSPHERIC FORECASTING

Edited by

Vaughn Agy

Institute for Telecommunication Sciences

Environmental Science Services Administration

Boulder, Colorado 80302, U.S.A.

Editorial comment: For the most part, the material in this publication has been produced directly from copy supplied by the authors. Retyping was necessary (and possible) in a few cases. The editor wishes to express his apologies for errors that may thereby have crept in, and his resentment at having found it necessary to arrange for such retyping. Amazement abounds at the number of authors who have not yet learned to read. Apologies are also offered for any changes in meaning or in personal style that his editing may have made in translating oral comments into a printable version. The Discussion section (which includes these comments) should be a useful part of these Proceedings.

Published January 1970

551.510.535.4:
621.391.812.63:
551.509

Printed by Technical Editing and Reproduction Ltd
Harford House, 7-9 Charlotte St. London. W1P 1HD

PROGRAMME CHAIRMAN

Mr. Roger K. Salaman
Institute for Telecommunication Sciences
Environmental Science Services Administration
Boulder, Colorado 80302, U.S.A.

EDITOR-COLLATOR

Mr. Vaughn Agy
Institute for Telecommunication Sciences
Environmental Science Services Administration
Boulder, Colorado 80302, U.S.A.

ELECTROMAGNETIC WAVE PROPAGATION
COMMITTEE CHAIRMAN

Dr. Irvine Paghis
Director, National Radio Propagation Laboratory
Communications Research Center
Ottawa 4, Ontario, Canada

HOST NATION COORDINATOR

Dr. R. E. Barrington
Communications Research Center
Department of Communications, P.O. Box 490
Shirley Bay, Terminal A, Ottawa 2
Ontario, Canada

ELECTROMAGNETIC WAVE PROPAGATION
COMMITTEE EXECUTIVE

Cdr. C. R. Smith, USN
AGARD

THEME

With the continual demand for more communication channels to meet the increasing world traffic requirements, communicators are seeking ways to increase ionospheric communication reliability. Monthly median ionospheric predictions, although not perfect, provide guidelines for circuit planning. To improve system operations, it is necessary to forecast parameters pertinent to system performance on a shorter time period (days and hours). The purpose of this symposium is to stimulate discussion of techniques to improve ionospheric forecasts, and to bring together the scientists and engineers who are developing forecasting techniques, and those who need and use forecasts, so that they might understand each other's problems.

The symposium is primarily concerned with

(1) current forecasting systems and their relation to forecast requirements,

(2) ionospheric forecasting techniques including the use of ionospheric monitors, and

(3) the influence of solar-geophysical events on the ionosphere, and forecasting of these events.

CONTENTS

SESSION I. HISTORY OF IONOSPHERIC FORECASTING

Reference

* * * * * * * * * * * * * * * * *

Errata:

Paper No. 13 (Hughes et al): interchange captions for Figures 2 and 3.

Paper No. 21 (Albrecht): page 21-4, Table I, first column heading should be "Mode Type."

Paper No. 33 (Katz): page 33-3, line 3 of paragraph preceding Summary, change "15 MHz" to "1.5 MHz."

HISTORICAL OUTLINE OF FORECASTING METHODS

by

J.H.Meek

Defence Research Board, Ottawa 4,
Ontario, Canada

ABSTRACT

A historical outline of ionospheric disturbance will be presented. Application to radio communication circuits were started during World War II and have evolved since then towards qualitative and, later, quantitative estimates of ionospheric radio propagation conditions hours and days in advance.

A Historical Outline of Forecasting Methods

by

J.H. Meek
Defence Research Board

1. Introduction

For the purpose of this paper I should like to propose that "Ionospheric Forecasting" signifies the process leading to foretelling the state of the ionosphere for a specified future time at a specified point and estimating its effect on the operability of a given communications circuit.

It is my intention to mention the principal observations and studies which have been done in the past and which have helped bring us to the present "state of the art". I believe that, with the information and knowledge which we have accumulated, a useful quantitative forecasting service could now be devised.

Two other comprehensive reviews of Ionospheric Forecasting exist. These are - Obayashi (1959) and Egeland (1960). The present review and the other two overlap to some extent but each was prepared from its own point of view. In addition Chapman and Bartels (1940), Mitra (1952) and Folkestad (1968) are recommended general references.

2. Early Observations

(a) Magnetic Variations and Aurorae

Hiorter (1747) reported from Upsala, Sweden, a relation between magnetic variations and the aurorae. Balfour Stewart (1861) reporting on the great auroral display August 18 - September 17, 1859, noted the excessive disturbance of the magnetic needle and this led him to postulate the existence of a conducting layer in the upper atmosphere (ionosphere). Carrington (Chapman and Bartels p333, 1940) noted the coincidence of solar outbursts simultaneous with disturbed magnetic elements on September 1, 1859.

Birkeland (1908, 1913) investigated magnetic variations and auroral displays during the International Polar Year 1882-83 and during the Norwegian Expeditions of 1894-1900 and 1900-1903. He pointed out that electrons travelling towards the earth would be deflected by the earth's magnetic field and approach the earth's atmosphere in two zones corresponding to the auroral zones. He demonstrated his theory by experiments using cathode rays, in an evacuated chamber, projected at a model earth (terella) which could be magnetized to various field intensities. Such experiments were extended by Brüche, (1931) and refined by Bennett (1958, 1959) in developing his "Störmertron".

Birkeland discussed his theory with K. Störmer (1906, 1917, 1930), a mathematician, who worked out the theory in detail, based on trajectories of charged particles of various energies approaching the earth and being deviated by its magnetic field. Störmer went on to become renowned (along with his fellow Norwegians Vegard and Krogness) for his meticulous and extensive auroral photography.

In the latter connection Störmer is probably the first to make regular use of a practical ionospheric forecasting or disturbance indication method. He used the reports of perturbations observed on Norwegian telegraph circuits, (Harang, 1951) usually occurring in the afternoon, to indicate the need to prepare his cameras for photography of the aurora that evening.

Vegard (Fleming, 1949) reported in 1916 that the time of strongest aurora, with some notable exceptions, coincided with the interval of highest magnetic activity. Other coincidences were noted by E.O. Hulbert (1929), F.T. Davies (1931), B.W. Currie (1935), while Röstad (1935) correlated the geomagnetic latitude of the auroral display with magnetic variations observed at Potsdam.

The analysis of the 1932-1933 Polar Year data provided a great deal of information on the statistics as well as on associations of individual geophysical phenomena (e.g. Vestine, 1944, 1947; Harang, 1946) with the "visual" ionosphere.

(b) Magnetic Variations and the "Radio" Ionosphere

Magnetic field coincidences with the "radio" ionosphere were reported by Appleton (1937) in 1927 and by Anderson in USA in 1928 as a result of studying the observed signal strengths on radio transmissions.

Detailed investigations of the variations of the ionosphere as observed by radio sounding techniques were carried out by Hafstad and Tuve (1929), Appleton, Naismith and Builder (1933), Wagner, K.W. (1934), Appleton and Ingram, (1935) Shafer and Goodall (1935) and in much detail by Berkner, Wells and Seaton (1939), Berkner and Seaton (1940) and Wells (1947).

(c) Solar Variations

Sabine (1851) studied the relation between sunspots and geomagnetic disturbances from study of magnetic variations at Toronto. The 27 day recurrence of magnetic disturbances (Chapman and Bartels p411 1940) and of long distance radio communications disturbances was well known in the 1930s. Time plots of circuit performance compared closely with those of magnetic variation prepared regularly and distributed by Bartels from Göttingen.

During this period communications engineers were concerned with discovering, empirically, the pattern of the medium and high frequency circuit propagation failures. The 27 day recurrence was found to be quite useful, but qualitative in nature. It was not possible to foretell the amplitude or influence of a disturbance for the next period. On the other hand, circuits normally showed characteristic fadings starting one or two days before a communication "blackout". Thus the maintenance of fixed circuit performance records and accumulated experience allowed the commercial operators to plan with reasonable success.

3. Forecast Methods During the World War II

With the outbreak of World War II came the need for reliable communications over circuits not previously established and to mobile units, ships, aircraft and field forces. Scientists were asked for information and assistance, in order to solve very serious communications problems in temperate and northern latitudes.

The close association of radio disturbances with solar phenomena led to demands on astronomers to provide regular sunspot activity information. It was soon recognized that sunspots themselves were likely not the origin of the earth ionosphere disturbances, but bright active regions such as flares. The fact that some storms occurred where there were no visible active regions on the sun led to the invention of "M regions". Extensive study of all these features was initiated in the United States at the Carnegie Institute of Washington by A.H. Shapley (1946) and others during the period 1942-1945. The results were made available to the communications services and proved to be a useful addition to the 27 day recurrence forecasts.

Operational forecast methods in use during the war were as follows:

(a) In Canada in 1942 F.T. Davies started a daily propagation forecast for the Canadian communicators which was based on:

1) A daily summary of sunspot activity from McMath-Hulbert Observatory followed by weekly photographs of prominences on the series limb,

2) Telegrams reporting reduction to 1/10 sensitivity at the Riverhead N.Y. Magnetic Observatory,

3) Continuous reports on reception and direction of arrival of signals from selected distant short wave transmitters mostly on and across the North Atlantic ocean,

4) A single manually-operated ionospheric sounder at Ottawa.

(b) In Great Britain, in aid of the Royal Navy, Marconi Company made good use of their extensive operational experience.

Sunspots were watched regularly as they appeared around the edge of the sun and, of course, the well recognized 27 day recurrence was used to qualitatively forecast radio communications interruptions. The best indicator was found to be the signs of abnormality of bearings of transatlantic short wave stations such as New York and Yamachiche, Quebec. Vertical incidence ionosonde sweeps which were made every ¼ hour and signs of disturbance were detected very soon after the ionosphere began to be affected. (Tremellen and Cox, 1947). Strip charts of solar surface features received from Russia were of considerable help at times when the sun was not visible in England.

(c) In Germany ionospheric observations were made at a series of stations ranging from Northern Norway to the Mediterranean. Critical frequencies at these stations were transmitted by telex to a central station in Germany and compared. For warning purposes the magnetic variation was the main indication. Long term forecasts based on the 27 day recurrence were also made.

In addition a rough quantitative forecast (quiet, moderate, heavy disturbance) was devised by Kuhn and Rawer for high latitude circuits. It was broadcast every few hours on long waves from a warning centre in northern Norway. Magnetic, visual auroral and ionospheric observations were used as a basis for these forecasts.

(d) In Japan an extensive network of ionospheric stations was operated and predictions were prepared. The Japanese depended upon one or two individuals to do extrapolations. Nearly all circuits were to points south of Japan, or between points in southern or equatorial regions. For these reasons no disturbance warning service, comparable with those mentioned above, was ever set up. (Bailey, 1946).

All the above methods used essentially the same indicators but the importance placed on particular indicators varied with the circumstances. A novel feature was added by RCA, New York, where conjunction and quadrature of the planets were included in the assessment. (Nelson, 1951, 1952).

A meeting in Washington in April 1944 pooled the efforts of British, American and Canadian workers, and led to organized information services for exchange of data on solar activity, magnetic activity, circuit performance and to forecasts which were promulgated regularly from Washington. These forecasts provided rough quantitative estimates for north Atlantic communication circuits which skirt the southern edge of the auroral zone. This service has been continued since without interruption (Moore 1957). A similar forecast service for the North Pacific, from Anchorage, Alaska, was not so useful due to the small number of high priority circuits skirting the sensitive auroral zone in this part of the world.

4. Indicators Used for Forecasting

The forecasting methods have used the following techniques:

1) Daily solar charts of the visual sunspots, flares, prominences and other solar perturbation features to follow their progress across the solar surface.

2) Correlation of the position and time of appearance on the sun of the solar activity, with the commencement of radio communications circuit disturbance and with ionospheric features observed at ionosonde stations in various parts of the world.

3) Estimates of time for passage of disturbance on the sun to the disturbance effect in the earth's atmosphere.

The three main geophysical effects observed were:

(a) Sudden Ionospheric Disturbance - Birkeland's (1908) cyclo-median storm - the Dellinger (1937) - Mögel (1930) effect. This effect is simultaneous with visual solar observations, so that it is an indicator for the subsequent ionospheric disturbance effects. It is most intense in equatorial regions near the subsolar point and not normally seen at high latitudes.

(b) Polar Cap Events - (Reid and Leinbach, 1959; Collins, Jelly and Mathews, 1961; Agy, 1957; Holt, 1968). A radio wave absorption phenomenon occurring in the polar regions several hours after the solar disturbance due to arrival of high energy particles and lasting from several minutes to one or two hours. Solar Radio wave outbursts, as well as visual features, have been associated with these events. (Denisse, 1952) (Simon, 1956) (Hakura and Goh, 1959).

(c) Auroral Zone Disturbance. This is, of course, the main disturbance which arrives one to three days after the solar event and which causes our radio communications problem. Although the disturbance is most frequent and most intense in auroral belt regions, the occurrence of disturbance effects at temperate, equatorial and high polar latitudes, while less frequent, are important and are more sporadic both temporally and spatially. (Vestine et al, 1947; Meek 1952).

(d) Other temperate and equatorial disturbance phenomena are reported from time to time. Explanation of them is often associated with "wishful thinking".

The practical indicators to the communicator remained,

1) The 27 day occurrence effect.

2) Progress of observed sunspots, prominences and other solar features across the sun.

3) Early detection of communication circuit deterioration (amplitude and bearing of the signal).

4) Geomagnetic field variation.

5) Methods of continuous measurement of frequency range availability, by monitoring several frequencies simultaneously over specific radio communications circuits.

5. Discussion of Forecast Methods

The principal defect of methods based on solar observations was that one could not forecast the quantitative effect on any particular communication path but only a rough picture of the probable state of the earth's ionosphere as a whole. The shortcoming of communications circuit monitoring is that one merely sees the disturbance shortly before it seriously effects circuits. One cannot make a quantitative forecast or reliably relate the observations to other circuits. One could not forecast the spatial position and extent, intensity or longevity of a disturbance as it affected a communication circuit. Nor was the communicator provided with information which would allow him to prepare to make the most efficient alternate choice (path or frequency) on which to carry out his communications.

However, the wartime effort did lead to recognition of the main features of the disturbances affecting short wave communications. The ionosphere was described and its variations estimated statistically.

6. Post War Activities

After the war, and with the readjustment to civilian activities the urgency for practical radio forecasts decreased. The main scientific effort was diverted to understanding the phenomenon. However, several groups had by this time set up routine methods for collating ionospheric data and high frequency radio communication circuit performance in order to issue a propagation forecast (e.g. Moore, 1957).

The forecasts have been made available regularly and they have been useful for evaluating circuit performance in retrospect as well as for estimating the future conditions.

The forecasting methods have been "statistics"-oriented and actually semi-empirical. The combination led to information which is not easy to apply practically to individual circuits with more reliability than a good radio communication engineer's accumulated experience can provide.

7. Morphological Studies

A number of workers have looked at the state of the ionosphere morphologically, in spite of the too-large separation of permanent ionospheric stations. The early work of Berkner and Seaton (1940), studying foF2 variations, was noted above as was the observance by Rawer in Germany during the war of the north-south changes in the ionosphere.

During 1948-49 a mobile ionospheric magnetic-auroral observatory was operated in Canada between Portage la Prairie, Manitoba and Churchill. This enabled comparison to be made of the movement and intensity of ionospheric phenomena with movement of the aurorae during disturbances, previously studied by Harang (1951) and others. Meek (1949) gave some data for the frequency of occurrence of Sporadic E ionization at a series of points running south from the centre of the auroral zone and on the speeds of motion of sporadic clouds in the range of altitudes 100-300 km. Lawrence (1953) plotted Continental maps of the history of four ionospheric disturbances. Matsushita (1959) has studied the maximum depression of foF2 with geomagnetic latitude moving south from the auroral zone. Morphological plots of both Δ foF2 (deviation of foF2 from the monthly mean) and absorption (number of hours of vertical ionosonde blackout) have been made for selected disturbances. (Meek, 1952, 1957) (Agy, 1957).

An important step in morphological plotting was made by a series of Japanese workers who prepared hourly hemispherical charts of Δ foF2, followed the history, expansion and movement around the world of the radio ionospheric disturbances and compared them with the geomagnetic variations. A few references are as follows: N. Fukushima (1953) T. Sato (1959) T. Obayashi (1959, 1960) Y. Hakura (1961).

Several workers have followed ionospheric movements through adjacent groups of ionosonde stations. One may mention the F region travelling waves of Munro (1950), the movement of spread F by Agy in Alaska. A study made on movement of Es in the United States using aviation radio operator observations on 10 meters organized by O. Ferrell of CQ magazine is worth noting (Gerson, N. 1951).

A detailed study of selected disturbances was carried out by Meek (1953, 1954) at Saskatoon in order to determine the correlation between magnetic auroral and ionospheric variations throughout the history of each disturbance.

8. Ionospheric Disturbance for Forecasting Purposes

Referring back to the three fundamental ionospheric disturbance phenomena mentioned in section 3 above

(a) The SID is at present unpredictable. One can foresee considerable detailed study of the sun before any progress will be made in forecasting the birth of an individual activity on the sun. However one should be able to relate it to the subsequent polar cap event.

(b) The polar cap event as an absorption phenomenon is treated well in the literature of the past 15 years. One cannot yet forecast the history of a particular event but the general pattern of its growth and expansion in the polar region has been described. It is a useful precursor for the subsequent long duration auroral zone distrubance.

(c) The auroral zone disturbance is the most extensive and most effective phenomenon in the ionosphere. It has been recognized longest but relatively little progress has been made in describing its history. The reason for this is of course due to the fact that most effort has been spent on the statistics of the observations. The statistical picture has proven to have very little relation to an individual event. Work on some aspects of the individual disturbance problem may be summarized as follows:

1) The magnetic disturbance is adequately described by Birkeland's (1908) model. A magnetic field is set up around a line current of limited length flowing in an east-west direction in the ionosphere along the auroral zone. The H component traces out a positive or negative magnetic lay depending upon which side, north or south of the main current line, the observing station is situated and whether it occurs during the evening hours or early morning hours. The intensity of the disturbance decreases as one observed it from farther south or north of the main current. Harang (1951) described the vertical currents associated with the disturbance.

2) Literature on the movement and extent of auroral arcs, curtains and rays are found in several references (Harang, 1951; Meek, 1954; Kim and Currie 1958). The latter two references are results from all-sky camera series of photographs. Until the advent of all-sky cameras and the intensive IGY 1957-1958 observations the auroral disturbance was identified with a fictitious statistical auroral zone belt. The excellent work of T.N. Davis (1962) and others in Alaska, in plotting the geographical details of auroral displays and their dynamics has increased our knowledge markedly. As examples a) the "breakout" probably corresponding to a sudden charge influx and ionization change in the ionosphere b) the curling northward of the auroral curtain near local midnight c) the wave movement of series of parallel curtains, north-south and also east-west. All these give us recorded details of ionospheric fine structure only observed visually and marvelled at before.

3) The ionospheric disturbances have been well "sampled" at hourly intervals and at widely spaced stations. The local studies of movements of ionization waves and Sporadic E spread F will be related to the larger disturbance pattern sooner or later. E region sporadic ionization has been studied intensively but apart from cloud tracing by the radio amateur program mentioned above our detailed knowledge is sparse.

Good work has been done using ground backscatter by way of the ionosphere yielding geographic plots of E and F region disturbance events (Villard Peterson and Manning, 1952) and a number of radio operating groups have used ground backscatter to aid in choosing "on-the-spot" communications frequencies. The method is yet to be properly coordinated with other ionospheric studies.

The Alouette satellites have turned many new features immediately applicable to radio communications problems. One should mention middle and high latitude ionization troughs (Muldrew, 1965) and the slope of the ionization contours (Nelms, 1966) but there are many others.

Unfortunately one must admit that with all the detail available we have not yet put together a reasonable model for the ionospheric disturbance.

The very simple model which I presented about ten years ago (Meek 1958) still appears to be a good starting point for building up a picture of an auroral zone disturbance as it is observed. I repeat the figure from this paper here.

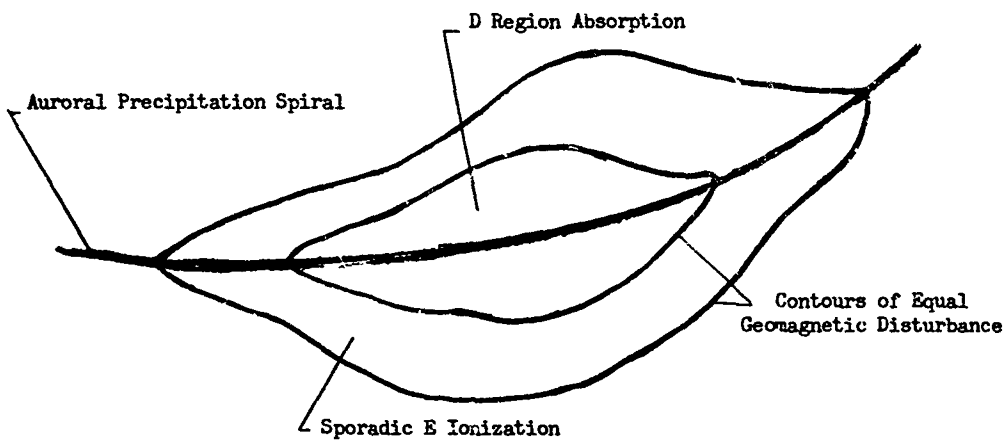

Fig. 1 Model of a single auroral zone upper atmospheric disturbance

One should then consider an auroral zone storm made up of a number of these elements overlapping, their geographical positions being determined by the energy and intensity of the charged particle influx.

9. Summary and Conclusions

Many facts about ionospheric disturbances were known in the 19th century. During the 1920's and 1930's radio disturbances were observed but not understood. During the 1940's empirical disturbance forecasting without understanding was attempted.

In the 1950's, as we have seen, considerable effort was put into studying the detailed history of individual disturbances, the spatial extent and movement of the abnormal effects and the correlation of the radio-ionospheric effects with visual, magnetic and cosmic ray effects. In the 1960's the Alouette satellites have increased enormously the amount of data available and have led to an outstanding improvement in our understanding of the morphology, both vertically and horizontally, of the upper atmosphere. We have acquired a considerable insight into the processes involved. We have not yet been able to track the solar disturbance to its final ionospheric locality. Pertinent work was reported at the URSI XVI General Assembly August, 1969, Ottawa by D.L. Carpenter "Some Recent results of whistler studies of the thermal plasma of the magnetosphere" and D.J. McLean "Solar Mapping".

In this paper I have treated only the "high frequency" ionosphere. This does not mean that there are no problems due to ionospheric disturbances for communications on LF or VHF frequencies. The fact is that very little progress has been made on localizing the effects in these frequency bands. The problem has been overcome largely by brute force methods at great expense in increasing transmitter power. Such methods have of course increased the interference problems at the receiving end and on other circuits. There are still some parts of the world (such as northern Canada) where economy of equipment and power are still important. Much study is required to understand and solve these problems.

What do we really know about the intensity, size and movement of waves, troughs and sporadic ionization clouds at all altitudes? What are their influences on long distance radio communications?

Finally one must not forget the probable relation between ionospheric geomagnetic disturbances and meteorological variations (e.g. Woodbridge et al, 1959). The latter are not, in fact, better understood than ionospheric variations but the forecasting methods are far in advance.

For some time to come we must look to empirical patterns for success in our forecasting methods. However more than enough data exists to enable useable patterns to be outlined, even if our understanding of the processes is still rather vague.

Agy, V. 1954 — J.Geophys Res 59 pp267-272, pp499-512
1957 — Agardograph 29 pt 2 p129 Pergamon Press
Appleton, E.V. and LJ Ingram, 1935 — Nature 135 p548
Appleton, E.V., R Naismith, G. Builder, 1933 Nature 131 p340
Appleton, E.V. 1937 — Proc. Roy Soc A 162 p451
Bailey, D.K. 1946 — Report on Japanese Research on Radio Wave Propagation Vol I p22-27. Gen. H.Q. U.S. Army Force Pacific OCSO Tokyo
Bennett, W.H. 1958 — Astrophys J. 127
1959 — Review Sci.Inst. 30 p63
Berkner, L.V., H.W. Wells, S.L. Seaton, 1939 Terr Mag 44 p441
Berkner, L.V., S.L. Seaton, 1940 — Terr Mag 45 p419
Birkeland Kr, 1908, 1913 — Norwegian Aurora Polaris Expeditions 1902-1903 2 Vol, Christiania
Brüche, E. 1931 — Terr Mag 36 p41
Chapman, S, J. Bartels, 1940 — Geomagnetism, Oxford
Collins, C. D.A. Jelly, A.G. Matthews, 1961 Can. J. Phys 39 p35
Currie, B.W. 1935 — Terr Mag 40 p317
Davies, F.T. 1931 — Terr Mag 36 p199
Davis, T.N. 1962 — J. Geophys Res 67 p75
Dellinger, J.H. 1937 — Proc IRE 25 pp1253-90
1937 — Terr Mag 42 p49
Denisse, J.F. 1952 — Ann Geophys 8 p55
Egeland, A. 1960 — Scientific Report No. 1 Contract No. AF61(052)-237 Kiruno Geophysical Observatory (AFCRL TN-60-611)
Fleming, J. 1949 — Terrestrial Magnetism and Electricity p614,McGraw-Hill
Folkestad, K. 1968 — Ionospheric Radio Communications, Plenum Press
Fukushima, N. 1953 — J.Fac.Sci. Tokyo Univ. Soc II Vol VIII pt V
Gerson, N.C. 1951 — Can J. Phys, 29pp 251-261
Hafstad, L. M. Tuve, 1929 — Terr Mag 34 p39
Hakura, Y and Goh, T. 1959 — J. Radio Res Lab Japan 6 p635
Hakura, Y. 1961 — Rpt Ion and Space Res Japan 15 p1
Harang, L. 1946 — Terr Mag 51 p353
1951 — The Aurorae, Wiley
Heppner, J.P. 1954 — J Geophys Res 59 p329
Hiorter, O.P. 1747 — Svensk.Vet. Acad. Handel. 27
Holt, O, 1968 — p32 Ionospheric Radio Communications Ed.K. Folkestad, Plenum Press
Hulbert, E.O. 1929 — Phys. Rev. 34 p344
Jouaust, R. Bureau, L. Eblé, 1937 — Computer Rondus 205, p1427
Kim, J.S., B.W. Currie, 1958 — Can J. Phys 36 p160
Lawrence, R.S. 1953 — J Geophys Res 58, p219
Matsushita, S. 1959 — J Geophys Res 64, p305
Meek, J.H. 1949 — J Geophys Rec 54, p339
1952 — J Geophys Res 57, p177
1953 — J Geophys Res 58, p445
1954 — J Geophys Res 59, p87
1954 — Astrophys J. 120, p603
1955 — J A.T.P. 6, p313
1957 — Agardograph No. 29, pt 2, p120 Pergamon Press
1958 — Conference on Solar Terrestrial Relationship, Defence Research Telecommunications Establishment, Ottawa
Mitra, S.K. 1952 — The Upper Atmosphere, 2nd Edition. Up.Asiatic Soc Cal
Mögel, H. 1930 — Telefunken Zeitung 11 pp14-31
Moore, R.C. 1957 — Agardograph No. 29 pt 2 p147 Pergamon Press
Muldrew,D.B. 1965 — J.Geophys Res 70 p2635
Munro, G.H. — Proc Roy Soc London A 202 p208 p348,Wiley
Nelms G.L. 1966 — Electron Density Profiles in Ionosphere & Exosphere/
Nelson, J.H. 1951 — RCA Review 12 pp26-34
1952 — Electrical Engineering, AIEE 71 p421
Obayashi, T. 1959 — J. Radio Res Lab Japan 6 pp375-514
Reid, G. H. Leinbach, 1959 — J. Geophys Res 64 p1801
Röstad, A. 1935 — Geophys Pub 10 No. 10
Sabine, E. 1851 — Phil Trans London pp123-139
1852 — Phil Trans London pp103-124
Sato, T. 1959 — Rpt Ion and Space Res Japan 13 p91

Shafer, J.P., W.M. Goodall, 1935 Proc IRE 23 pp670-81
Shapley, A.H. 1946 Terr Mag 51 p247
Simon, P. 1956 Ann Geophys 12 p167
Stewart, B. 1861 Phil Trans London p423
Störmer, K. 1906 Comptes Rendus 142 p1580
1917 Terr Mag 22 pp23-34, pp97-112
1930 Terr Mag 35 p193
Tremellen, KW, J.W. Cox, 1947 J. IEE 94 pt IIA p200
Vestine, E.H. 1944 Terr Mag 49 p77
Vestine, E.H., L. Laporte, I. Lange, W.E. Scott 1947. Carnegie Inst. of Wash. Pub. No. 580
Villard, O.G., A.M. Peterson, L.A. Manning, 1952. Proc IRE 40 p492
Wagner, K.W. 1934 Elect. Nachr. Techn 11
Wells, H.W. 1947 Terr Mag 52 p315
Woodbridge, D.D., N.J. Macdonald, T.W. Roberts, 1959 J Geophys Res 64

IONOSPHERIC FORECASTING IN THE UNITED STATES 1942-1966

by

J. Virginia Lincoln

Aeronomy and Space Data Center

Space Disturbances Laboratory

ESSA, Boulder, Colorado

SUMMARY

Short-term ionospheric forecasting began in 1942 at the Interservice Radio Propagation Laboratory of the National Bureau of Standards. The techniques used and their development in the Western Hemisphere will be discussed up to the beginning of the computer-oriented types of forecasts.

IONOSPHERIC FORECASTING IN THE UNITED STATES 1942 - 1966

J. Virginia Lincoln

The first attempts at systematic forecasts of HF radio disturbance in the U.S. were undertaken in 1941 by the National Bureau of Standards of the U.S. Department of Commerce. In October 1942, with the establishment of the Interservice Radio Propagation Laboratory at the National Bureau of Standards, which was later to become the Central Radio Propagation Laboratory, CRPL, a weekly "Advance Forecast of Radio Propagation Conditions" was issued. These forecasts were done in collaboration with the Department of Terrestrial Magnetism of the Carnegie Institution of Washington where forecasts had begun in March 1942 by Shapley [1946]. The forecasts were in the form of a number for each of five zones which divided the world by latitude from the polar zone to auroral zone to subauroral zone to the equator. A number was given for each of the next seven days. The forecast scale was from 1 representing useless radio propagation conditions to 9 representing excellent conditions. This scale became known in later years as the CRPL radio quality figure scale.

1 = useless	4 = poor-to-fair	7 = good
2 = very poor	5 = fair	8 = very good
3 = poor	6 = fair-to-good	9 = excellent

By 1944 it was determined that instead of five zone subdivisions three latitude zones sufficed. The A-zone was the polar and auroral zone, the B midlatitude and the C equatorial (Figure 1). These daily quality figure forecasts were in a large part based upon reports that were provided by U.S. military units stationed worldwide.

The principle of 27-day recurrence of geomagnetic activity and its association with radio propagation disturbance was relied upon heavily. This was in the descending phase of cycle 17. The accuracy of the forecasts was enhanced since 27-day recurrence is strongest during this part of the solar cycle and there were well established patterns as shown in Figure 2. Fortuitously in those years there was in addition a strong relationship between the appearance of a bright peak in green line coronal intensity at east limb and the occurrence of a geomagnetic disturbance 3-4 days later. Daily reports made at Climax, Colorado, by the High Altitude Observatory of the University of Colorado were telegraphed to the National Bureau of Standards forecast group. These coronal reports were one of the major tools for determining the forecasts for the next few days.

Persistence was, of course, relied upon for the next day's forecast. If a storm were in progress, the probable average duration of storms was used as the basis for the forecast for the next several days. In 1942-1944 the disturbances were lasting five or more days which made the forecasts easier to make and more accurate.

By February 1944 because the losses of planes returning to the United Kingdom from bombing raids over Germany could be traced to the failure of direction finder equipment to guide the planes back to their air bases during geomagnetic storms, it was determined that a daily short-term forecast should be issued. This forecast consisted of the statement "warning" or "no warning". Even if it were not always an advance forecast, it was found valuable to identify the fact that disturbed conditions existed. A formal "W" or "N" was issued once a day for worldwide Naval Communications use, but arrangements were made with two of the communication companies, RCA and AT&T, to telephone the daily forecaster at any hour of the day or night when appreciable disturbance was noted on earth current recordings at their Long Island receiving sites, or if their trans-Atlantic messages had reached less than commercial quality. If a warning were not in effect, then a dozen or more communication headquarters offices in the Washington area were notified of the disturbed conditions. Thus, operators would be notified that deterioration in message transmissions was due to ionospheric propagation conditions rather than equipment failure. Though sent worldwide the warnings were designed primarily for North Atlantic radio paths, or paths crossing near to or through the northern auroral zone.

In the months after sunspot minimum in February 1944, 27-day recurrence became unreliable as a means of forecasting HF radio conditions several days in advance, and in addition the coronal forecasts were proving inaccurate. Larger sunspots were being observed and more solar flares, so the forecasts were based on the work of H. W. Newton [1943] and C. W. Allen [1944]. This meant that disturbance was expected at the central meridian passage of the large sunspots, and about 2 days after major flares if they were in the sun's central zone.

For warnings of deterioration of HF conditions a few hours ahead reliance was particularly placed upon observations at the NBS field station at Sterling, Va., on a visually recording magnetometer which recorded the horizontal component of the earth's magnetic field on photographic printout paper. The latter was unprocessed and faded out as soon as removed from the equipment, but sudden commencements and K-indices could be estimated in real-time. As it happens, the correlation between K-indices from the Washington area and the planetary Kp is very high. Thus, successful HF propagation forecasts for disturbance in the auroral regions were based upon the observations of high K-indices at Sterling. By 1945 it was also noted that the absolute minimum

reached on the H-component trace during a 24-hour period could be used to determine the degree of propagation disturbance to be expected. Of course, this minimum was merely a rough approximation of the Dst of the main phase of the geomagnetic storm. The deeper the main phase, the more severe were the ionospheric effects. Visual magnetometers recording all three components on permanent chart recordings were developed in the early 1950's. Such records continue to be most useful tools in evaluating existing or anticipated ionospheric conditions, particularly in high latitudes.

In the first months of 1944 HF direction finder monitoring of North Atlantic transmissions was continuous during local daylight hours at the NBS field station. It was determined that the onset of significant disturbance over North Atlantic paths -- or paths transiting the auroral zone -- could be anticipated by these observations. Early path failure or complete loss of signals was indicated if the bearings of the signals from Europe shifted southwards with wider and wider bearing swings. Such monitoring was indicative of rapid fading, and there was usually a loss of signal intensity as well. By 1949 when the field station was manned on a 24-hour basis, HF direction finding was used around the clock to assist in forecasting the onset and severity of disturbance.

With the expansion of U.S. operations in the Alaskan area it was felt that better services could be furnished by establishing a North Pacific Radio Warning Service. In February 1951 such a service was initiated at Anchorage, Alaska, becoming officially operational in October 1951. Advance forecasts were made for the North Pacific Area and short-term forecasts were made 3 times a day. The seasonal effects in the high geographic latitudes did not make every six hour decisions critical, and available manpower could more readily prepare the every eight-hour forecasts. Here, too, direction finding was used, and in October 1960 an automatic equipment developed by K. Miya of the Japanese KDD Company was purchased and installed to record the bearings of selected transmissions graphically permitting the bearings to be followed continuously and their deviations from normal to be recognized in real-time.

During the early years another valuable tool was the vertical incidence ionosonde at the NBS Washington field station. Visual readings were made hourly and plotted for comparison with the expected monthly medians. Lower foF2 critical frequencies and increased f-min were disturbance indicators. The onset of severe disturbance over North Atlantic paths was probable when there was a large enhancement of foF2 values in the late local afternoon hours. At Anchorage blanketing sporadic-E out to a high frequency was found to precede the blackout of signals on polar and auroral paths, and was thus used to anticipate by a few hours severe disturbance in those regions. In such periods visual ionosonde readings were made frequently in order to follow the development of the disturbance.

Field-strength recordings were used to identify abnormal daytime ionospheric absorption and sudden ionospheric disturbances. In 1946 an empirical system was put into effect for forecasting the probability of sudden ionospheric disturbances for the next day, since communication units were experiencing prolonged outages because of SID. These SID forecasts continued until 1950 and were begun again in 1955. Field-strength recordings were used for disturbance indicators, too, by monitoring trans-auroral zone paths. Frequencies to be monitored were changed at the time of evening failure, and early failure signified disturbance. In 1959 at Anchorage fading rate meters were also installed. Anchorage monitored transmitters broadcasting continuously from each of three geographic locations. These transmitters were on two frequencies at each location, one basically a day frequency, and the other a night frequency. The transmitters were at Thule, Adak and Seattle, thereby allowing comparison of a mostly polar path to one skirting the auroral zone to one mostly subauroral.

After polar cap absorption events, PCA, were discovered following the great west limb solar flare of February 23, 1956 [Bailey 1964] it was found worthwhile to have the hourly values of f-min reported to Anchorage from the Barrow Ionosphere Field Station. Continuous blackout could be interpreted as the possible onset of a PCA. In addition, loss of the HF signal from Thule helped to confirm PCA, as given in a note by Hakura and Lincoln [1963] (Figure 3). From 1957 onwards the North Pacific Radio Warning Service took advantage of telephone reports from the Geophysical Institute, College, Alaska, of unusual absorption on the riometer operated by Reid and Leinbach [1959]. By the riometer it was possible to discriminate PCA from auroral zone absorption. By such means several hours advance notice was given for the onset of severe geomagnetic disturbance which would then accompany the failure of HF communications on auroral zone paths. Of course, polar paths had become useless with the onset of the PCA.

The Canadians put several oblique incidence ionosondes into operation. The maximum operational frequencies over the selected paths were clearly apparent. Therefore, in 1958 CRPL requested and received the reception reports on the Ottawa to the Hague path for use in forecast decisions. CRPL itself did not institute any oblique incidence soundings purely for the use of the North Atlantic Radio Warning Service.

It was also known that the severer the magnetic disturbance the farther south propagation disturbance would be found. Gartlein illustrated this same relationship by the southern extent reached by auroral displays. He, therefore, sent telegrams to the forecast center, as early as 1944, whenever he observed bright auroral displays at Ithaca, New York, indicating the southern expansion of the auroral zone. Such auroral displays were regularly associated with poor radio propagation conditions on the North Atlantic paths.

The Canadian ionosphere stations made most useful daily reports which provided both evaluation of the forecasts and data for future forecasts. Vertical incidence data were given for every six hours and the hours of reception of each of the WWV standard frequencies during the past 24-hours were reported. In those years there were no other stations on the WWV standard frequencies, and such monitoring provided an excellent indicator of the range of useful frequencies over the auroral paths involved. Other valuable reports were by the U.S. Coast Guard of the success of their hourly contacts in Washington, D. C., with the weather ships located in the North Atlantic, by the U.S. Army, U.S. Navy, F.C.C., Royal Canadian Air Force, Royal Air Force, B.B.C., C.B.C., R.C.A., AT&T, Mackay Radio and Press Wireless. Their reports were translated into CRPL quality figures.

Though the short-term forecasts had developed into successful anticipation of disturbance a few hours ahead, or in quickly identifying the degree of disturbance and its probable duration, as the sunspot cycle rose towards maximum in 1947, the advance forecasts given for several days in advance were relatively inaccurate. To develop new techniques in 1948 Reber's 160 MHz radio noise equipment was installed at the NBS Sterling, Va., Field Station to follow the sun and study the relationship of solar radio noise bursts with other solar-geophysical phenomena. In the early 1950's Denisse and other French colleagues showed solar regions could be divided into "radio noisy" and "radio quiet". Simon [1956] showed magnetic disturbance was associated with the central meridian passage of the radio noisy spots. Therefore, solar noise reports became an important input to the forecast centers.

There were many more important flares than there were disturbances so a way of sorting out the flares that were to be associated with geomagnetic disturbance was needed. In 1956 Helen W. Dodson and E. Ruth Hedeman at the McMath-Hulbert Observatory shared their work [published 1958] that showed that solar noise bursts on the 200 MHz records of Cornell University could be associated with solar flares regardless of their position on the solar disk. In addition, major solar noise bursts were followed by geomagnetic disturbance 3-4 days later. This meant that the number of false alarm forecasts could be reduced. Rather than optical importance of the solar flare alone, one should know the accompanying solar radio noise effects. Cornell had been reporting their observations to the forecast center from 1953. Wild [1950] had begun swept-frequency spectral measurements of solar radio emissions and had established different types of events. The now well-known Type IV continuum bursts were found to be followed by geomagnetic disturbance. After the great February 1958 geomagnetic storm the forecasters became more knowledgeable in how to identify probable Type IV bursts on fixed frequency records. Such identification is necessary since real-time reports are not possible from the typical photographic spectral recording systems. Therefore, the facsimile sweep-frequency equipment developed at the University of Colorado by Warwick greatly helped forecasters to identify Type IV bursts occurring during Western Hemisphere daylight hours. NBS continued fixed frequency observations moving their radiometers on 167 MHz and 470 MHz to Boulder, Colorado in 1952 where they operated until December 1960 and March 1958 respectively, to be followed by 108 MHz through 1965 and currently by 184 MHz observations.

However, since the sun has events on a 24-hour basis, it has always been necessary to collect data on solar events at the forecast centers by telegraphic means. These arrangements were mostly bilateral until the International Geophysical Year 1957-1958 when under the World Days Program universal data interchange codes were adopted [Annals of the IGY, Vol. VII], and special communication networks were established between Regional Warning Centers. This has resulted in greatly improved daily interchange of solar and geophysical data on a worldwide scale. In 1962 the Ursigram Service and World Days Service were reconstituted as the International Ursigram and World Days Service (IUWDS). It is under the aegis of IUWDS that this international cooperation continues to the present. The current system is explained in the Synoptic Codes for Solar and Geophysical Data, Second Revised Edition 1969.

Returning to specific developments in the CRPL Radio Warning Services in the U.S. on January 15, 1946 the category "U" for unstable was added to the daily warnings. The "W" and "N" warnings had been put onto the WWV standard frequency broadcasts in January 1946. The decision to limit the weekly forecasts to the North Atlantic area took place in 1946. In June 1950 radio propagation quality figures were prepared every six hours over the North Atlantic path. This was followed by changing the short-term forecasts to a four-times-a-day decision in February 1951. The forecast at this time became a letter-number combination: the letter to identify conditions at the time of the forecast, and the number for the conditions to be expected during the next six hours using the CRPL quality figure scale. These forecasts were put onto WWV in July 1952, and similar forecasts continue to the present.

In September 1951 the advance forecasts returned to semi-weekly as 27-day recurrence patterns were being reestablished with the approach to sunspot minimum. A new innovation was the addition of a review paragraph discussing the possible causes of observed disturbances. To assist operators in interpretation of the advanced forecasts, glossaries of terms and brief statements on sun-earth relationships and radio disturbance forecasting were issued periodically from 1951 onward.

Beginning in August 1958 a supplementary special disturbance warning was instituted to be sent by telegram or airmail postcard whenever unexpected disturbance occurred, or if an outstanding solar event suggested disturbance would occur, and obviously had not been known of at the time of the regular advance forecast.

At Anchorage the short-term forecasts, letter-number combination, were placed on WWVH standard frequency transmissions in January 1954. These broadcasts continued until November 1964. At that time the mission of the Anchorage field station was changed to the CRPL High Latitude Space Environment Monitoring Station. Though radio propagation advice was given locally in Anchorage, the North Atlantic Radio Warning Service, which had moved to Ft. Belvoir, Va., in 1954, took over responsibility for the full HF radio propagation disturbance forecasting as the CRPL Forecast Center. At Belvoir their advance forecasts were relabelled as suitable for high latitudes, and were evaluated by averaging North Atlantic and North Pacific radio quality figures which continued to be prepared from monitoring in each of those areas. In October 1965 upon the formation of the Environmental Science Services Administration the station at Ft. Belvoir, Va., was named the Telecommunications and Space Disturbance Services Center, and carried on the same basic functions until its transfer to Boulder, Colorado in July 1968.

In February 1956, to relieve the distribution load at Ft. Belvoir and Anchorage, a Geomagnetic Forecast for General Users was prepared at Boulder, Colorado, for dissemination in particular to communication headquarters personnel or to radio amateurs. A simple GEOCAST telegram forecast one of three levels of magnetic activity and was sent daily to Antarctica beginning April 1958 to be used as a forecast of probable disturbance.

For the NASA communications circuits used for Project Mercury -- the first U.S. man-in-space program -- quality figure forecasts together with average usable frequency ranges were predicted for each of the separate HF radio paths during missions beginning in 1959. These were the first steps towards attempting a quantitative frequency forecast on a short-term basis.

It has been difficult to compress the work of more than twenty years in ionospheric forecasting in the United States in this paper. It is to be hoped that the major developments and techniques have been covered by this review.

REFERENCES

ALLEN, C. W. 1944 Relation between magnetic storms and solar activity. Monthly Notices, Royal Astronomical Society, 104, 13-21.

ANNALS OF THE INTERNATIONAL GEOPHYSICAL YEAR 1959 World days and communications, VII, 1-138.

BAILEY, D. K. 1964 Polar-cap absorption. Planet. Space Sci., 12, 495-541.

DODSON, H. W. and E. R. HEDEMAN 1958 Geomagnetic disturbances associated with solar flares with major pre-maximum bursts at radio frequencies 200 MHz. J. Geophys. Res., 72, 2955.

HAKURA, Y. and J. V. LINCOLN 1963 A suggestion for improving forecasts of geomagnetic storms, J. Geophys. Res., 68, 1563-1564.

NEWTON, H. W. 1943 Solar flares and magnetic storms. Monthly Notices, Royal Astronomical Society, 103, 244-257.

REID, G. C. and H. LEINBACH 1959 Low energy cosmic-ray events associated with solar flares. J. Geophys. Res., 64, 1801-1805.

SHAPLEY, A. H. 1946 The application of solar and geomagnetic data to short-term forecasts of ionospheric conditions. Terrestrial Magnetism and Atmospheric Electricity, 51, 247-266.

SIMON, P. 1956 Thesis of Doctorate at the University of Paris.

WILD, J. P. and L. L. MC CREADY 1950 Observations of the spectrum of high-intensity solar radiation at metre wavelengths. Australian J. Sci. Res. A., 3, 387-398.

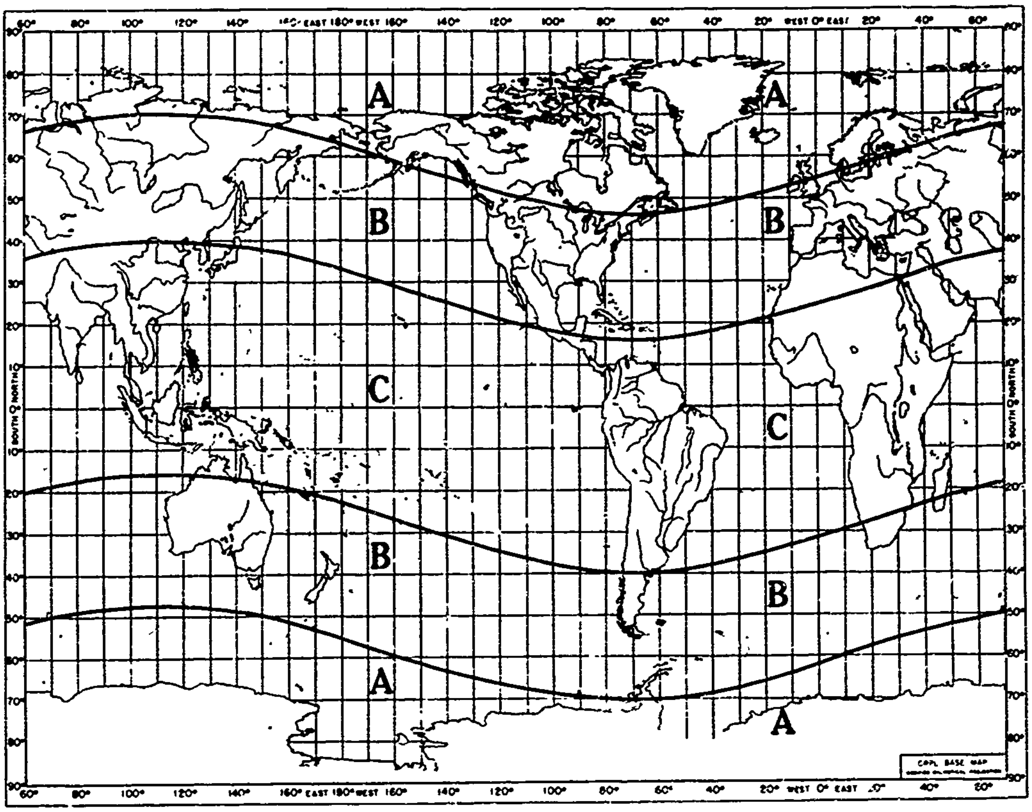

Figure 1 Zones used for CRPL Advance Forecasts

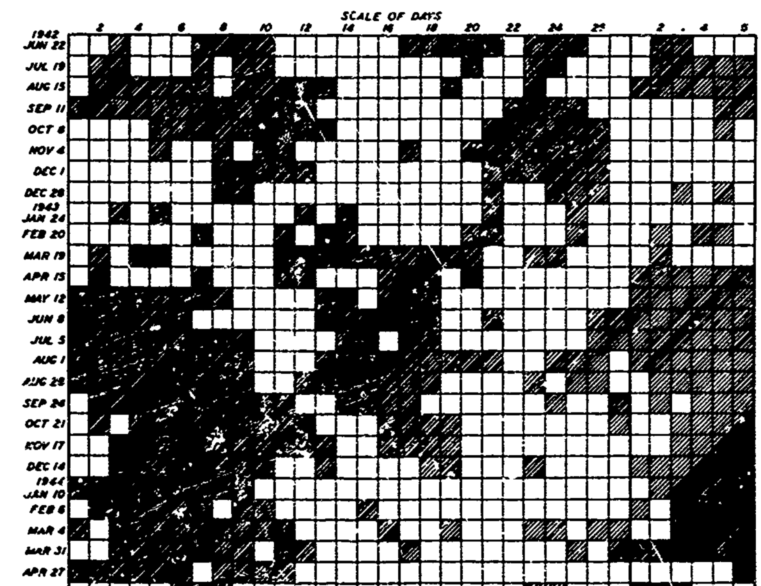

Figure 2 27-day Recurrence of Magnetic Activity June 22, 1942 to January 22, 1945 (after Shapley 1946)

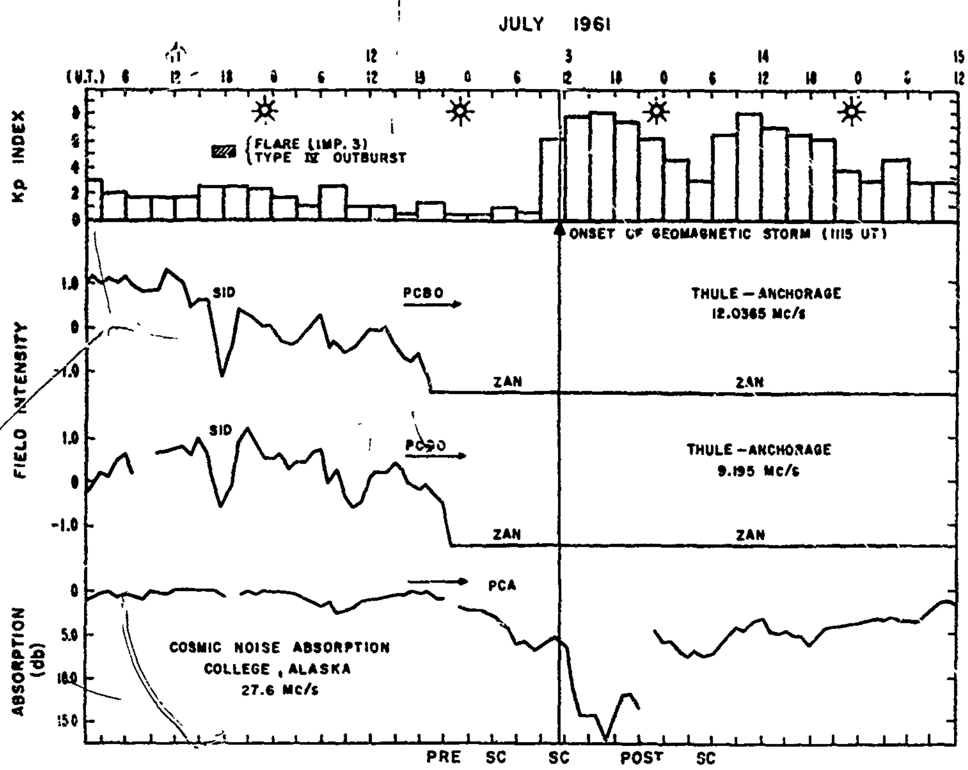

Figure 3 Polar Cap Absorption Detected by Thule-Anchorage Circuits July 11-15, 1961

KEYNOTE COMMENTS

by

T. R. Hartz, P. Simon, R. K. Salaman
J. H. Meek, B. Beckmann, W. L. Hatton

K

KEYNOTE SESSION

VIEWS TOWARD FORECASTING

T. R. Hartz

Communications Research Center
Department of Communications
Shirley Bay, P. O. Box 490, Terminal A
Ottawa 2, Ontario, Canada

The topic of this symposium is Ionospheric Forecasting. When I became involved in plans for the program, I soon found that forecasting meant different things to different people. Those who are using, or attempting to use, forecasts, and those who are engaged in producing them, do not share the same concept. I also found an inherent reluctance on the part of persons in one discipline to speak critically of something from another discipline that they didn't understand too well. Needless to say, I was not alone in my observations, and the program committee felt it most desirable to encourage a frank dialogue and exchange of ideas between the participants at this meeting. In so far as it is possible, we wish to set a discussion atmosphere for the whole symposium, not only in the formal sessions in the conference room, but in the informal intervals as well. We would like to see a continuing discussion throughout the whole week here at Gray Rocks.

This Keynote Session is an attempt to stimulate this type of discussion. In it we present five different points of view toward ionospheric forecasting as an introduction to the more detailed sessions that will follow. The five speakers have been asked to present some rather extreme and contending view points. Each presentation will be limited to ten minutes, so that the speakers will not be able to include all the qualifications and justifications they might otherwise have wished. Furthermore, I have not provided time within this particular session for any discussion; I invite you all to find time in the next four days to discuss these topics thoroughly, along with any others that you might wish. We feel that the symposium cannot be a success without a full dialogue on all aspects of ionospheric forecasting. The points of view to be presented are:

(1) Though there can be no doubt as to the desirability of short-term forecasting of ionospheric conditions for communication purposes, the most serious limitation of any system involves getting reliable forecasts to the operators in a suitable form and within a short enough time scale that they can adapt their operations to the information. (R. K. Salaman)

(2) At present sufficient routine observations of the sun are being made and enough is known about solar-terrestrial relationships that fairly reliable forecasts can be made of gross ionospheric disturbances and storms. (P. A. Simon)

(3) At present enough monitoring of the ionosphere is being done on a global basis, though not necessarily always at the best locations, that short-term forecast of ionospheric propagation conditions depend on pattern recognition of a semi-empirical nature. (J. H. Meek)

(4) The inflexibility of communication circuits and terminal equipment, the difficulties that attend the efficient management of the frequency spectrum, and the limited skill and experience of many operators tend to jeopardize the value of forecasts for all but a rather special class of communication systems. (B. A. Beckmann)

(5) Modern technological developments, such as automatic adaptive communication systems, largely obviate the need for ionospheric forecasts. (W. L. Hatton)

CONTRIBUTION OF THE SOLAR ACTIVITY FORECAST TO THE SHORT TERM FORECAST OF THE IONOSPHERE

P. Simon

Observatoire de Meudon, 92 Meudon, France

During the last decade the reliability of the solar activity forecast has definitely increased. This improvement is related to the contributions of solar radio-astronomy, to the study of the solar magnetic field, to new material obtained by satellites (X-ray, particle flux, etc) and to a good monitoring of the solar activity.

The prediction of solar activity consists mainly of an evaluation of the existing solar activity, a prediction of the evolution of each active center and a forecast of solar events. For a forecast just one day in advance, the success is about 80% i. e. the reported solar activity coincides exactly with the forecast for 80% of the active centers.

The exchange of data between the regional centers in which forecasting is done is carried out for the most part through the International Ursigram and World Day Service (IUWDS). As the secretary of this organization I have visited most of the forecasting centers. In each center they begin with a forecast of solar activity in order to build up their ionospheric forecast. Unfortunately, I must say that the material used for it is very poor: we use mostly the observations made at the Observatory and the reported data are only complementary materials; in these centers, they use mostly reported data and the local data are not sufficient for the issue of a forecast. It is a great pity: they would gain definitely in efficiency using the solar forecast issued by solar astronomers for their ionospheric purpose. It would also lighten the heavy traffic of so much useless data traveling on the IUWDS network.

Another comment is the complementary aspect of the last remark. We issue the solar activity forecast according to the scientific possibilities and in terms of solar activity but we are not certain that this form is the best for the ionosphericists. We would appreciate receiving their comments in order to issue it according to the best criteria for ionospheric prediction.

CAN THE COMMUNICATOR OBTAIN USEFUL IONOSPHERIC FORECASTS?

Roger K. Salaman
Institute for Telecommunication Sciences
Environmental Science Services Administration
Boulder, Colorado 80302 U.S.A.

In the past 4 years, I have had the opportunity to visit a number of communication centers around the world. In most cases, I found that forecasts of radio quality, and even the monthly median MUF-LUF predictions, were seldom used for operations. The quality forecasts were consulted to determine if the actual circuit outages were due to propagation. The monthly median predictions were used only in setting up a new circuit.

These were operational sites, where receivers were tuned, traffic was multiplexed, and HF terminal equipment stood next to troposcatter, microwave, and satellite equipment. The circuit controllers were interested in obtaining HF forecasts that could improve circuit reliability. However, they did not sufficiently understand propagation to know what could be obtained. When they had trouble with a troposcatter or satellite circuit, they consulted the appropriate technical representative. When they unexpectedly lost an HF circuit, they hunted at random for a frequency and often reluctently settled on the frequency that worked yesterday, only to wait until it "came in."

When a controller consults the radio quality forecast, it might say W4 - disturbed conditions, poor to fair. But what he wants to know is what he can do about it. Should he move up or down in frequency? How long will the disturbance last? Shouldn't he be able to consult an HF propagation forecaster - even if that forecaster is located far from the station? Couldn't a disturbance Alert signal be broadcast simultaneously from stations throughout the world (possibly operating at VLF), which would activate a warning light in the operations center?

Do we know enough to facilitate this procedure? Can we really help the communicator during a disturbance? Do we understand the interaction of solar-geophysical events and propagation effects? Is it possible to provide the communicator with the percent change in MUF and LUF - relative to the monthly median predictions, the amount of attenuation for a specific flare, the probability of a magnetic storm and its effect? Shouldn't we be approaching the time when we can predict the flare itself - even if only a few minutes in advance? For the more sophisticated systems of today, we must also be able to forecast the magnitude of unusual phase and frequency perturbations.

In Southeast Asia, we tried for several months to use vertical incidence data in near-real time to forecast specific circuit MUF's. However, it took many hours to communicate these data to a central location, and the forecasts were little better than using persistence alone. It would probably have been more useful for the communicator to record the signal strength over his actual communication circuit, and the noise and interference on an adjacent frequency to determine when he will "lose" his operating frequency.

What we learned from this experiment was that it is not worthwhile trying to forecast conditions that can better be obtained by the communicator. A continual updating forecast of the monthly median MUF-LUF predictions will have little impact if we cannot forecast the onset of significant flare and magnetic storm induced disturbances with reasonable accuracy.

An effort must be made to establish priorities on the parameters to be forecast, based on the telecommunicator's requirements, and not the researcher's interest. A balance must also be maintained between what can be forecast remote from the communication system and what can be better obtained by the communicator himself.

What is needed in communication forecasting? First, it is necessary to distribute forecasts of impending and occurring disturbances immediately and directly to the operators of ionospheric systems. Possibly, this can most economically be done by worldwide broadcasting of a warning signal that can be received by everyone.

Second, it is necessary for the communicator to be able to relate the disturbance to his own communication system characteristics and geographic location. The communicator must then balance the cost of obtaining this information from a regional forecast center against the time he has to perform his own interpolation. For important communication systems, it appears reasonable to establish teletype communications to a central forecast center during critical times, or even to maintain full-time leased lines.

Third, the communicator must be able to relate his outages to actual propagation conditions in a form applicable to communication system analysis.

I hope that during this symposium the papers will be discussed in terms of the communicator's requirements on these three points.

NEW PATTERNS FROM OLD DATA FOR A WORKABLE FORECAST

by

J. H. Meek
Defence Research Board
Ottawa 4, Canada

1. The amount of data is overwhelming

We have been making radio measurements of the ionosphere regularly and on a routine basis since about 1935, and quite intensively since 1945, at over 150 observing stations. This means that there are, according to my rough calculations, more than 2 x 10^8 ionograms in existence from the regular stations and many additional special sets of observations (for example IGY).

These ionograms have been superficially scanned and scaled for a few features, according to rules decided upon 25 years ago. There is a wealth of information yet to be got out of the data, information which cannot be obtained from the tabulated scalings.

Due to the overwhelming mass of observations we seem to have lost the ability to study data thoroughly. There are many scientists who are happy to skim the surface and talk about the interesting new features in a superficial way. It is more difficult to find persons who are happy to work methodically through the data in order to confirm the intuitive discoveries.

There is enough information available today to devise a method of ionospheric forecasting, by study of the data and application of the present knowledge of ionospheric processes and morphological changes.

2. The communicator has lost faith

The communicators have supported our ionospheric research efforts for 25 years. We have not satisfied their requirements - many have given up hope and have turned to expensive alternative systems such as tropospheric scatter, ionospheric scatter and satellite communications. We may be too late to help. Pursuit of some of our basic studies, say for example the cause and distribution of He^+ in the upper atmosphere - while important, cannot be expected to arouse the sympathy of the communicator.

Admittedly we have provided monthly predictions which are useful for general planning purposes. Even there we have failed to provide useful information on the variation about the monthly averages, of the useable frequency range for the communicator.

The communicator needs to know what frequency range will be available to him, say tomorrow at 9.15 a.m., on several specific circuits. He has been waiting 20 years for us to come up with a useable forecast. The best we have provided is a rather qualitative quality figure for the North Atlantic sub-auroral zone circuits. This is based on observations which hopefully detect the radio circuit degradation before it becomes serious to the communicator. He can do about as well himself. He does not gain much by feeding his information to a warning centre to have it returned to him in altered form after a few hours delay.

3. Empirical methods provide the answer

At this stage we still cannot trace the disturbance from its first outburst on the surface of the sun to its final local resting places in the earth's ionosphere. Until we make some progress in following the disturbance through the magnetosphere down into the ionosphere reflecting regions, we shall have to be content with empirical methods.

We must attempt to pick out patterns of change and movement in our data - empirically. The analogy which is quite valid is that of the "breakthrough" in meteorology.

At the beginning of the century meteorological forecasting consisted of detecting low pressure areas and estimating their progress across country according to likely paths based on accumulated statistics. The weather forecast likewise was based on statistical distribution of cloud type and precipitation around the centre of low pressure. This was quite unsatisfactory. V. and J. Bjerknes (1918-21) studied the weather patterns empirically. By sequential comparison of synoptic maps a significant "breakthrough" was achieved and one could make a real forecast of weather for a time and for a locality. We are awaiting the "Bjerknes" of the ionosphere.

4. The Synoptic Ionosphere

A group of Japanese workers - Fuhushua, Obayashi and others, have plotted sequential synoptic maps showing the movements of the ionospheric critical frequency deviations from average. These have been related to other geophysical phenomena. The work has not been carried through to produce a result useful to the communicator.

5. Statement of the project

This type of analysis should be pursued. It should lead to empirical patterns useful for estimating radio communication frequencies over specific paths at specific times. It should propose the setting up of special observing stations for following the ionospheric movements (not necessarily further multifrequency ionosonde stations). It must determine the geographic pattern of these stations which is optimum for the purpose. It must consider the communication of the information from the station to an analysis centre and subsequent dissemination of information to the user. It must be simple - not necessarily scientifically critic-proof. It must be aimed at the communications user rather than the researcher.

6. The challenge

Using presently available ionospheric and radio communications data to determine the patterns and trends, I believe that a small dedicated group of analysts could turn out within a year, a workable system for a useable quantitative high frequency ionospheric forecast.

Who is going to do it?

LIMITATIONS OF FORECASTING APPLICATIONS

B. Beckmann

Fernmeldtechnisches Zentralamt 33
61 Darmstadt, Federal Republic of Germany

A clumsiness with the operation of radio circuits and the use of transmitting and receiving equipment consists in the fact that, once in use, an operating frequency is used as long as possible in order to ensure that but few changes to other frequencies become necessary. This is, however, indispensable if the signal-to-noise ratio drops below the minimum value required for this type of service or if interference is recorded. In both cases an increasing degree of distortion is to be observed which today can be supervised by means of appropriate distortion meters that allow conclusions to be drawn whether or not a change of frequency is necessary.

A number of operation engineers who work at the radio stations of the Deutsche Bundespost are of the opinion that once the introduction of distortion meters into the fixed radio services will have been accomplished, the short-time forecasts can be dispensed with. The switching operations which become necessary whenever a change of frequency is effected can be greatly accelerated today owing to the use of automatic remotely controlled transmitting and receiving equipment.

Now, if for instance due to the out-time attributable to the ionospheric reflection conditions, such a switching operation becomes necessary somewhat earlier than is normally the case, and if the operation engineer has a disturbance forecast at his disposal, he will know that this switching operation occurred in reaction to the influence of this disturbance. However, especially if he is not particularly skilled and experienced, he will then try to be advised which frequency range in this specific case of disturbance is still available for a circuit. The usual formerly provided information contained in a forecast, that is, falling average field strength accompanied by increased or decreased MUF and LUF can, at the utmost, indicate the direction in which the change of frequency would have to be done. The data, taken for themselves, represent already details which do not all follow from the imminent occurrence of a disturbance owing to special solar-terrestrial events. They also require a thorough knowledge of the course of the ionospheric storm which may vary in time and location and of its varying effects on the frequencies of radio circuits of different directions and lengths. The outlook of the course of ionospheric disturbances could be determined from the world-wide notwork of ionospheric stations by means of actual diagram-like presentations of real-time measuring values Δ foF2 and Δf_{min}, provided that a quick transmission of data is possible. Its evaluation concerning the influencing of certain radio circuits will, however, not always be unambiguous since deviations from the great circle due to iono- and ground scatter or side-scatter modes, respectively, may occur. In the case of more pronounced disturbances, these deviations determine to a considerable extent the events in the still possible transmission frequency range and must therefore be taken into account when deciding on radio operation. For this reason it will not be possible to do without systematic field strength recordings. The efficient use of the frequency spectrum will, irrespective of the actually available frequencies, depend on an unambiguous advice concerning the frequency spectrum appropriate in each case.

The aim should be the prediction of such characteristic operational parameter as MUF, LUF, signal-to-noise ratio, fading and distortion. A routine extrapolation in time of these parameters would probably bring us nearer to this aim. To study these problems will be the task of a newly created Working Group of the C.C.I.R.

Since the differentiated effect of the ionospheric disturbance on certain radio circuits, or else the specification of the respective operational parameters required, are subject to another probability than is the occurrence of a ionospheric disturbance due to solar-terrestrial events, only a more coarse approximation will be possible on the basis of such a forecast. Skilled and experienced operation engineers who have received the respective expert training can, however, considerably increase the benefit of such forecasts by means of their logical application. Because of the clumsiness of the operational part of the service and because of the limited availability of alternative frequencies any success will of course always be kept within certain cinfines.

IS THERE A NEED FOR IONOSPHERIC FORECASTING

or

THE IMPACT OF ADAPTIVE SYSTEMS ON FORECASTING

W. L. Hatton

Communications Research Center
Department ot Communications
Shirley Bay, P. O. Box 490, Terminal A
Ottawa 2, Ontario, Canada

When asked to speak in this keynote session on ionospheric forecasting, I expressed the view that the use of adaptive strategies and modern equipment obviated the need for ionospheric forecasting.

(If I wished to be really controversial, at this point, I would suggest that there is no need for thes meeting and move its adjournment). However before I reach this point, I ask myself what I mean by saying that forecasting is not required. From this question I arrive at a remarkably simple answer. If you look upon the complete communication system and the environment as components of a single adaptive feedback system, the interaction of the environment and the system can be related to the time constant of the system and the time constants of the environment.

If the time constant of the system is much smaller than that of the environment the system, by suitable design can follow the variations of the environment.

We can now build systems with time constants smaller than that of the environment. QED forecasting is not required.

If the system time constant is larger than that of the environment, all you can do is make a statistical estimate of the environment. This estimate will have a variance which increases to some maximum value over the correlation interval. The sensitivity of the system performance to this variance will determine the utility of the forecast.

I will now briefly review the typical time constants of the environment and systems to show how their relative position has recently changed.

The time constants of the environment are measured in years for sunspot cycle variations, months for annual variations, hours for diurnal variations, minutes for SID's and seconds for fine grained structural changes of the ionosphere.

In communication systems in the past, we have had time constants of years enforced on us by regulation and of seconds, minutes, hours, days and even months by equipment design. Consequently, systems of the past have been unable to do better than to use statistical estimates of the environment.

A modern adaptive communication systems, such as the MUFFIN system, has a response time of milliseconds, three orders of magnitude improvement over the past systems. Means to overcome the regulation time constant are in the hands of all government users and most commercial users. Therefore there is no reason why complete adaption to the environment is not possible.

In some systems, such as manned spaced systems, the system time constant may be measured in days, in this case adaption to short term variations of the envirohment may be impossible.

Before I leave, I will briefly review how MUFFIN, an adaptive system works. The system automatically measures system performance; if the frequency in use fails an automatic search for a good frequency takes place and communication is continued after only a momentary interruption. For telephone operation only a click may be observed; for teletype, transmission could be held up for one character. The added advantage of simplicity is gained also in as much as the only operator control would be an ON-OFF switch.

It may be said for some complex systems that a more difficult problem exists but since these more complex systems can be considered to consist of a combination of single links, each with a response time of milliseconds, all that is required in a interacting computer control with fast response to optimize the total system.

In the end I conclude that ionospheric forecasting is needed for some systems such as space systems or existing systems but not for modern adaptive communication systems.

U.S. ACTIVITIES IN OPERATIONAL SOLAR-GEOPHYSICAL FORECASTING

by

R.D.Doeker* and D.S.Packnett†

*ESSA, R43, Boulder, Colorado 80302, USA

†Solar Forecast Facility, Department of the
Air Force, Hq. 4th Weather Wing (MAC),
ENT AFB, Colorado, 80912, USA

ABSTRACT

The U.S. Air Force's Solar Forecast Facility

by

Don S. Packnett, Major, USAF

The Solar Forecast Facility's Solar Observing and Forecasting Network (SOFNET) is described. The SOFNET consists of eight worldwide solar/geophysical observatories located at Sacramento Peak Observatory, New Mexico; Sagamore Hill Radio Observatory, Massachusetts; Oahu, Hawaii; National Observatory of Athens, Greece; Manila Observatory, Philippines; Los Angeles, California; Ramey AFB, Puerto Rico; and Tehran, Iran.

The Solar Forecast Facility's Solar Forecast Center at Colorado Springs, Colorado is discussed. The Solar Forecast Center collects and analyses solar and geophysical data received from the SOFNET. From these analyses, routine forecasts are issued for:

(1) Major flare occurrences,

(2) Solar radio flux at 10 cm.

(3) Planetary geomagnetic indices.

Solar Activity Forecast techniques and recent forecast verification data are presented.

Currently planned automation of the Solar Forecast Center is discussed

and

The U.S. National Space Disturbance

by

R.D. Doeker

The U.S. National effort in operational "Space Weather" will be discussed. Emphasis will be placed on the Global Observing System, the real time data gathering, analysis and dissemination system, and the warning/forecast services. The international as well as national role of ESSA forecasting will be defined. Future developments range from automatic data handling to new sources of data, to unique support in future space and telecommunication systems.

Organization

The organization of the Environmental Science Services Administration's (ESSA) and the U.S. Air Force's (USAF) operational solar-geophysical activities are given in Figure 1 and Figure 2 respectively.

Solar Optical and Radio Observing Network

Figure 3 shows the locations of the United States' solar optical and radio observing network sites. ESSA's observing sites are located at:

Boulder, Colorado, USA

Canary Island

Culgoora, Australia

Carnarvon, Australia

The USAF's observing sites are located at:

Sacramento Peak Observatory, New Mexico, USA

Sagamore Hill Radio Observatory, Massachusetts, USA

Palehua Observatory, Cahu, Hawaii, USA

National Observatory of Athens, Greece

Manila Observatory, Republic of the Philippines

Upper Van Norman Observatory, California, USA

Ramey Air Force Base, Puerto Rico, USA

Tehran, Iran

These sites provide real-time (within five minutes) reports of solar optical and radio observations. Figure 4 presents the probability of having daylight at one of the observing sites for June and December. As you can see, the coverage is not complete, varying between 92% and 98% during the year.

A dedicated USAF teletype network (see Figure 5) is used within the U.S. to relay both ESSA and USAF observations. Observations from USAF overseas sites are relayed by the National Aeronautics and Space Administration's (NASA) communications network to Goddard Space Flight Center where they are entered onto the dedicated USAF teletype circuit. Full exchange of observational data is provided among all of the observing sites.

The following solar optical and radio observations are made routinely:

1. Visual and photographic observations of the sun in the light of H-alpha.

2. Photographic observations of the sun in the light of calcium.

3. Visual and photographic observations of the sun in total (white) light.

4. Photographic observations of the solar corona.

5. Observations of the solar flux at discrete frequencies between 200 and 30,000 MHz and swept frequencies between 20 and 40 MHz.

The W-120 (120 mm objective lens) and the W-250 (250 mm) solar optical telescopes, manufactured by Yardney-Razdow Laboratories, Inc., are used for the solar optical patrol. Figure 6 shows the W-120 telescope in use at Boulder, Colorado. These telescopes are equipped with an Halle H-alpha filter, automatic photographic camera, white light telescope, and closed circuit TV of the H-alpha image.

Magnetometer Network

The U.S. Air Force operates a magnetometer network, reporting in real-time, consisting of the following observational sites:

Loring AFB, Maine

Goose AB, Labrador

Thule AB, Greenland

Eielson AFB, Alaska

Fort Belvoir, Virginia (in cooperation with ESSA)

In addition, worldwide geomagnetic indices are received routinely through international exchange provided by SOLTERWARN.

Solar Proton Monitoring Network

ESSA operates a Solar Proton Monitoring Network in Alaska and Greenland equipped with magnetometers, neutron monitors, riometers, and forward scatter circuits (see Figure 7). Real-time reports of Polar Cap Events are relayed by dedicated communications to Boulder, Colorado, and then entered onto the dedicated USAF teletype circuit.

Neutron Monitor Network

The USAF maintains automatically reporting neutron monitors at Durham, New Hampshire and Swarthmore, Pennsylvania. Through cooperation with the Canadian Government, who developed the equipment, the neutron monitor at Deep River, Ontario, Canada, is also hooked up to this same network.

Satellite Observations

Real-time solar-geophysical observations are provided by the USAF's VELA satellite series (earth orbit) and the geostationary ATS-1 satellite. Additional near real-time satellite observations are provided by the Pioneer series (solar orbit), and SOLRAD, OGO, OSO, and ITOS satellites (earth orbit).

Ionospheric Observations

Ionospheric observations will be included in paper 26 and 27 to be presented by Mssrs. Damon and Stonebocker.

Solar-Geophysical Forecast Centers

ESSA's Space Disturbance Forecast Center (SDFC) at Boulder, Colorado, provides solar-geophysical forecasts for civil agencies while the USAF's Solar Forecast Center (SFC) at Colorado Springs, Colorado, provides a similar service for military agencies. Figure 8 indicates, as an example, the services currently being provided by the SFC for military agencies. The two forecast centers use the same observational data base, but tailor their forecast products for their specific users. Continuous coordination is maintained between the two forecast centers.

Everyone is interested in how well we can forecast solar events. Figure 9 shows verification of forecasts of the occurrence of solar flares ≥ Importance Two at the USAF's Solar Forecast Center for the period September 1965 through September 1968. The small white squares represent a major flare occurrence while the gray bars show those times when a "solar flare alert" (probability forecast for a flare ≥ Importance Two is ≥ 50%) was in effect.

Future Plans

Within the year, a large portion of the handling and analysis of solar-geophysical data will be completely automated through use of a UNIVAC 1108 computer at Offutt AFB, Nebraska and terminal equipment at the two forecast centers. At first, forecasts will be partially manual and partially automated. Hopefully, as more techniques are developed and tested, the entire process of observations, analyses, and forecasts can be fully automated.

We are currently testing a new solar H-alpha optical telescope capable of automatically scanning the sun and giving an alarm whenever a solar flare occurs. This should offer a much faster response as well as free observers from having to continuously watch the sun.

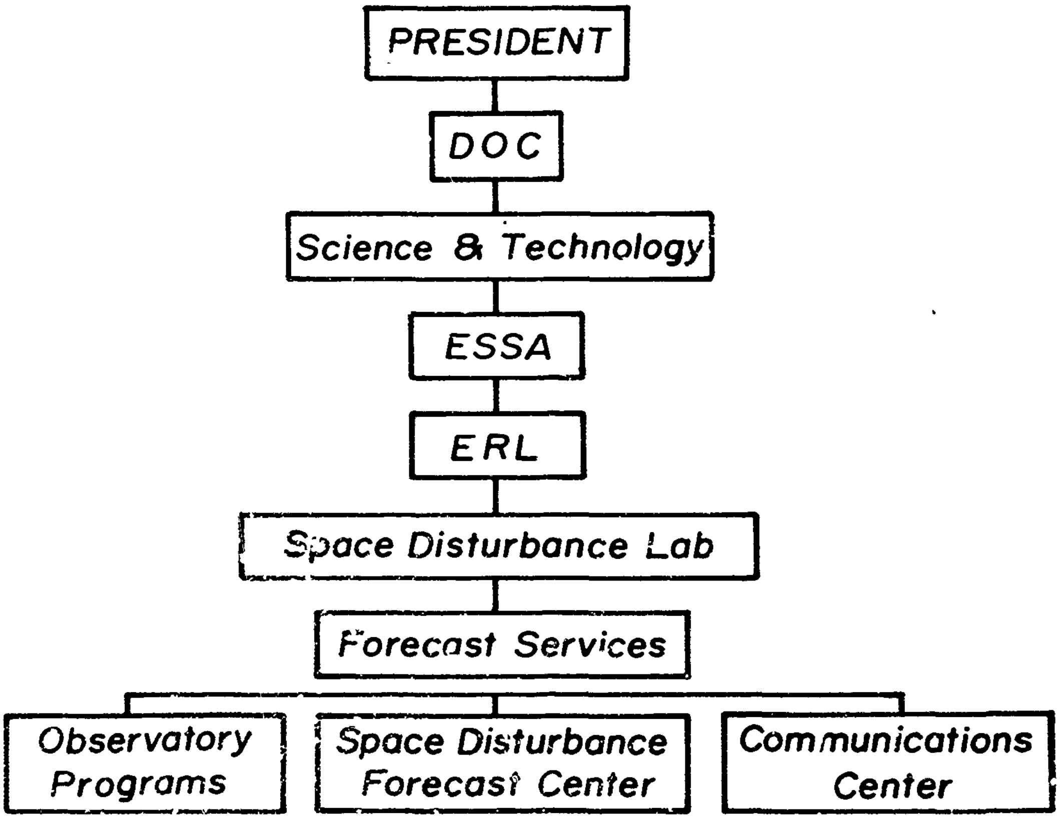

Fig. 1 Organization

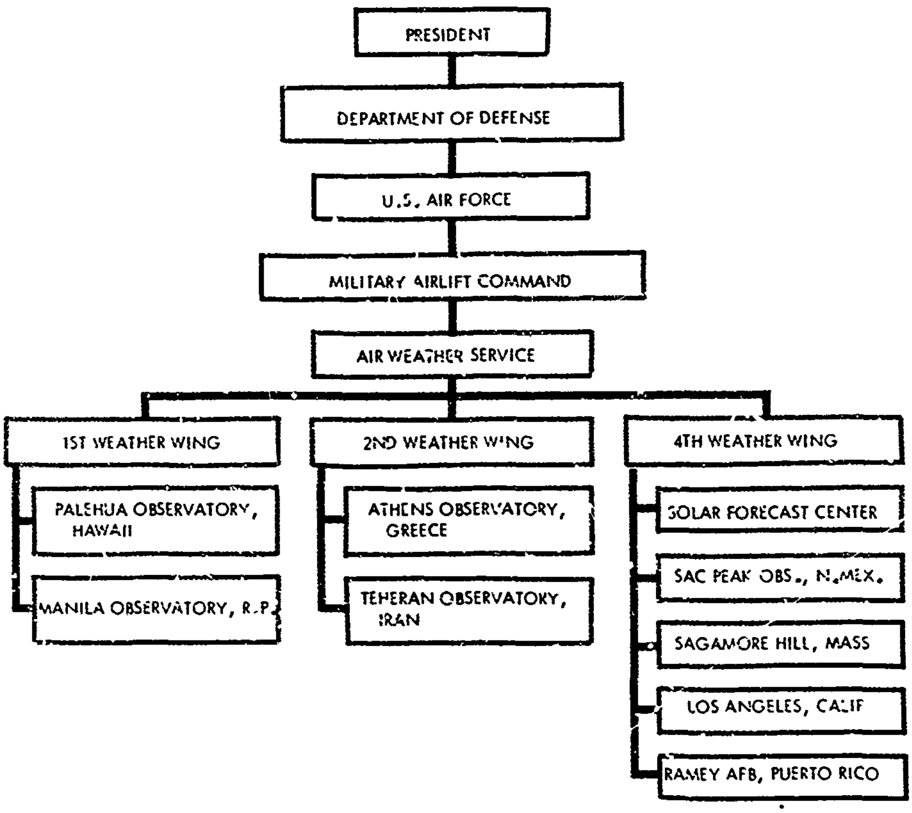

Fig. 2 Organization

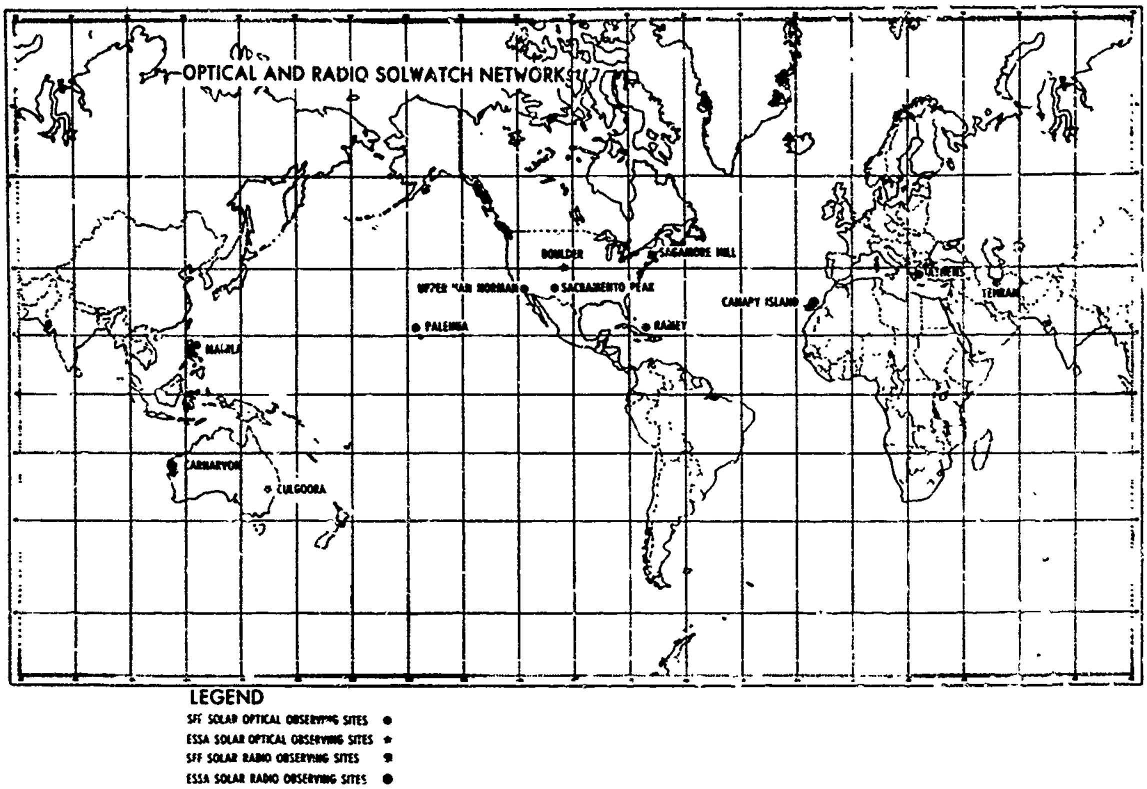

Fig.3 Optical and radio solwatch network

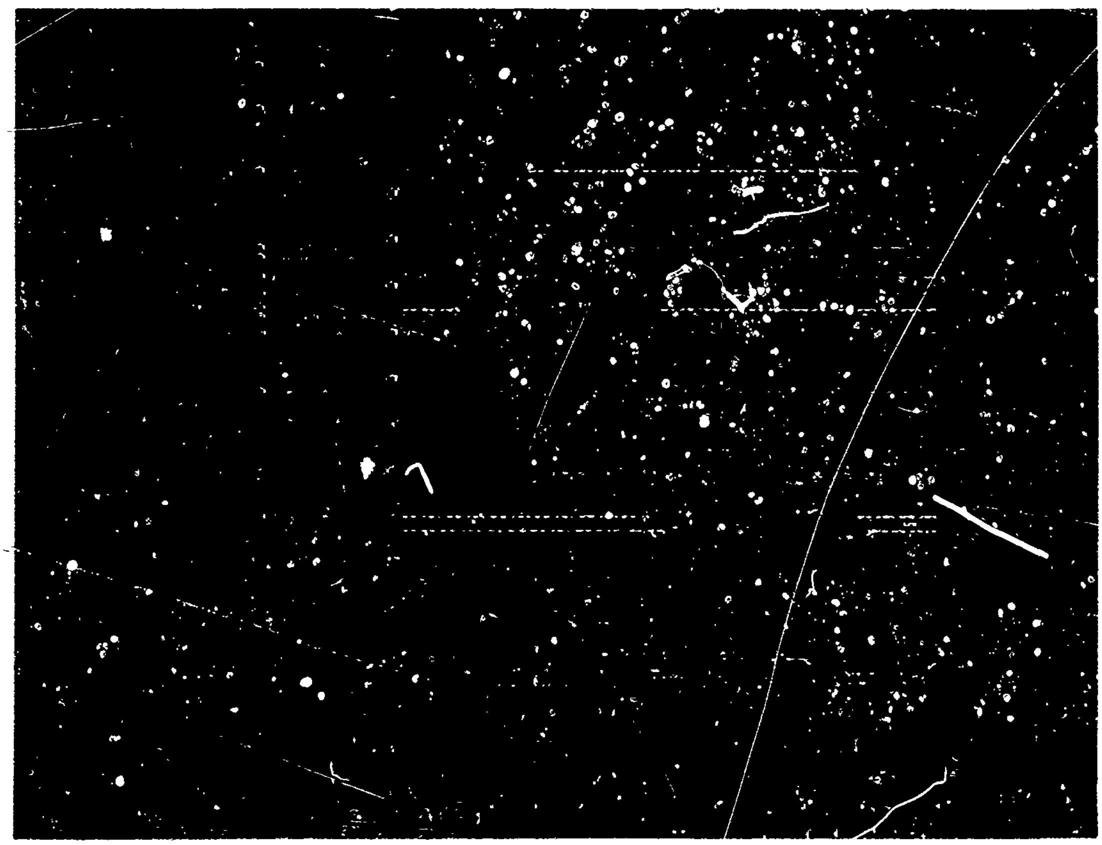

Fig.4 Real-time global solar flare patrol

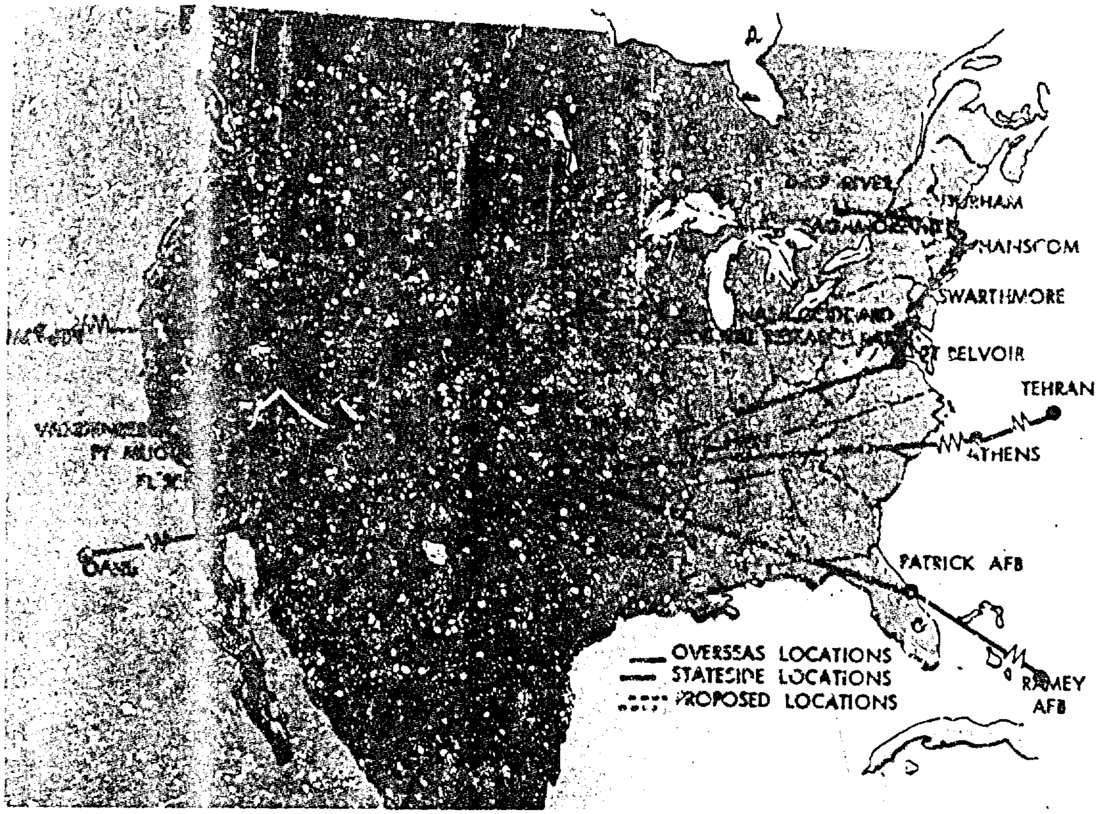

Fig. 5 Solar-geophysical teletype network

Figure 6

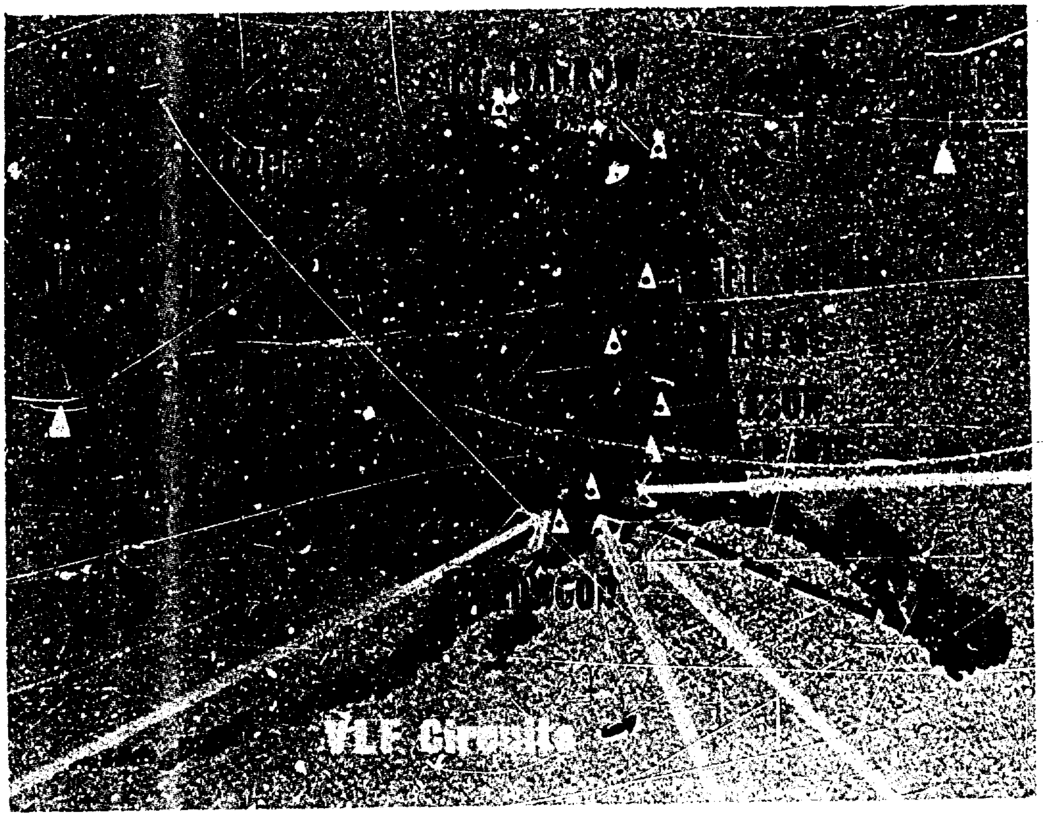

Fig.7 Solar proton monitoring network

SOLAR FORECAST CENTER PRODUCTS

PRIMARY FORECASTS

Issued daily at 2100Z.
Description of the Sun and major solar-geophysical activity.
Probability of an Importance 2 (or greater) flare during the next 3 days.
Probability of a proton event.
Latest observed values and predicted values of the 2800 Mhz solar radio flux and geomagnetic index (A_p).

SECONDARY FORECASTS

Issued daily at 0300Z, 0900Z, 1500Z.
Description of the Sun and major solar-geophysical activity.
24-hour probability of Importance 2 (or greater) flares.
Probability of a proton event.

EXTENDED PERIOD FORECASTS

Issued each Sunday at 1800Z.
Long-range forecast covering general level of solar activity for the next 27 days (one solar rotation).
Forecast of significant 2800 Mhz solar radio flux deviations during the next 27 days.

IONOSPHERIC FORECASTS

Issued to meet specific requests.
Forecasts of general radio propagation conditions, included on primary and secondary forecasts.
Maximum Useable Frequency (MUF) and Lowest Useable Frequency (LUF) forecasts for specific HF communication paths.
Advisories of ionospheric disturbances.

SPECIAL ACTIVITY ALERTS, ALARMS, OR WARNINGS ARE ISSUED IN RESPONSE TO SPECIAL MILITARY REQUIREMENTS.

Figure 8

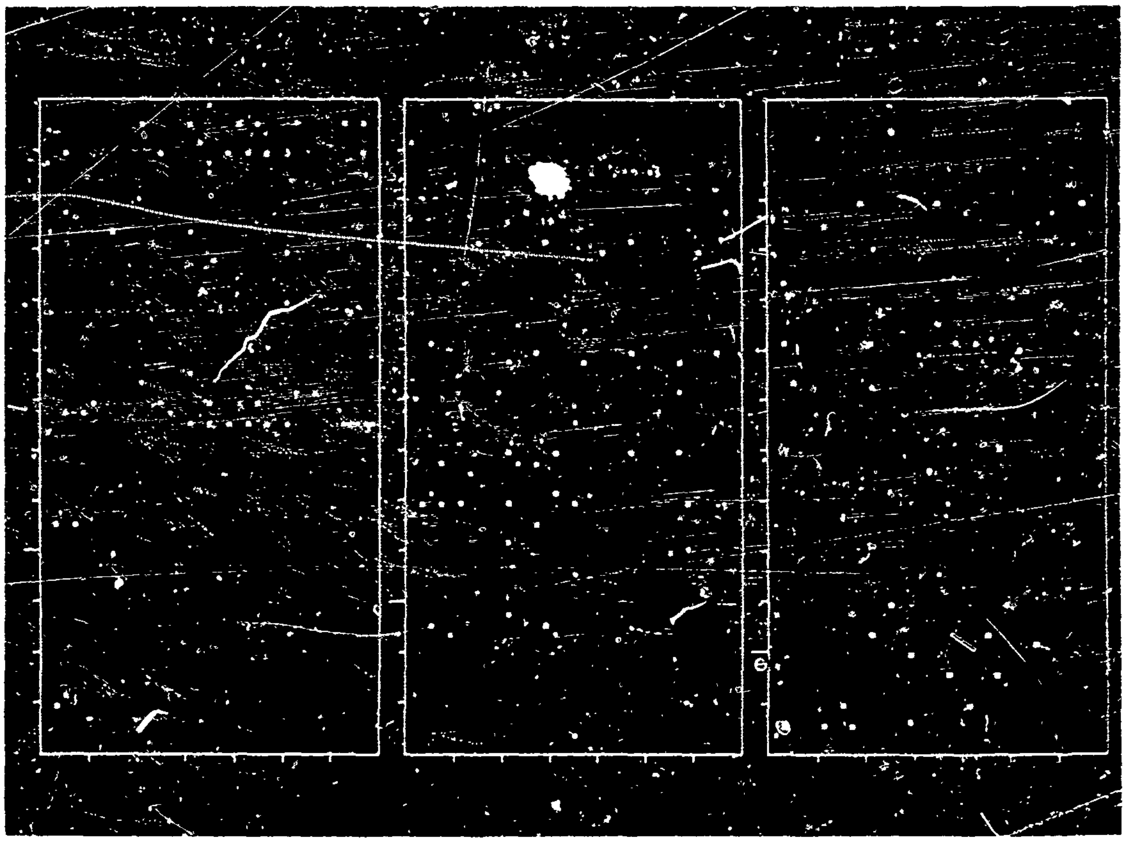

Fig.9 SFC solar flare alerts vs major flare occurrence. September 1965 - September 1968

OPERATIONALLY ORIENTED TELECOMMUNICATION FORECAST SERVICE

by

Roger K. Salaman

Institute for Telecommunication Sciences
Environmental Science Services Administration
Boulder, Colorado 80302 U.S.A.

SUMMARY

Systems to forecast solar-geophysical events and the resultant propagation interactions have been in operation for many years. The purpose of this paper is to stimulate development of forecasting systems which are oriented more to the needs of the telecommunication system operators. Although the specific application referenced here is HF communications, the concepts are applicable to systems working in other areas of the radio spectrum.

OPERATIONALLY ORIENTED TELECOMMUNICATION FORECAST SERVICE

Roger K. Salaman[†]
Institute for Telecommunication Sciences
Environmental Science Services Administration
Boulder, Colorado 80302 U.S.A.

1. BACKGROUND

Ionospheric and solar-geophysical forecasting services have been available for 25 years (see Beckmann, 1969; Lincoln, 1969; and Meek, 1969). During this period of time, HF telecommunication systems have become more sophisticated, and have encountered mounting competition from other systems that provide higher data rates and reliabilities (such as troposcatter and satellite).

In 1965, an effort was made to determine whether new short-term forecasts could better assist HF circuit operation (Slutz et al., 1969; Salaman, 1969). Although this investigation was limited to a few equatorial circuits, the experience gained in working at receiver sites and technical control centers stimulated a study that began in January 1967, to update the HF forecasting technique employed by the United States Department of Commerce at their Fort Belvoir, Va. Telecommunications and Space Disturbance Services Center. The primary objectives of this study were to (1) provide forecasts in terms of parameters directly applicable to telecommunication system operation, (2) expand the service to worldwide coverage, and (3) automate the system to the greatest practical extent. As a result of this study, on July 1, 1968, the existing forecast system was modified, and the operation was moved from the Fort Belvoir field site to the headquarters of the parent organization, the Institute for Telecommunication Sciences, of the ESSA Environmental Research Laboratories, Boulder, Colorado.[††]

This is the first paper describing the philosophies that underlie development of new operationally oriented propagation forecasts, although the concepts are described, all the services mentioned have not yet been implemented.

2. FORECAST NEEDS

The primary objective in short-term telecommunication forecasting is to provide the telecommunication community (principally the system operators) with information necessary to maintain and improve the efficiency of system operations. At the present time, this is accomplished by forecasting detrimental effects that have a solar-geophysical origin.

Currently, the forecasts are limited to propagation induced HF ionospheric communication disturbances and solar noise storms, which have a pronounced effect on VHF communications. Eventually, it may be possible to forecast system degradation brought about by enhanced atmospheric noise (e.g. using satellite weather data), increased interference from man-made radiation sources, and even tropospheric ducting attenuation and abnormal refraction due to atmospheric weather conditions.

The communicator needs a reliable forecast of when his communication system will be degraded to an unsatisfactory level, how long this condition will last, and what he can do to circumvent this problem. For normal HF circuit operation, he needs to know what sequential group of frequencies he must operate on to minimize the number of frequency changes to maximize the probability of successful communications. This choice of frequency is determined, in general, by the prevailing noise or interference level, the signal strength, and the short-term perturbations (amplitude, frequency, and phase) introduced by the propagation medium. Of these factors, emphasis has been placed on forecasting the MUF, signal strength, which affects the LUF, and the large solar noise bursts that raise the receiver noise level at VHF. With advanced HF communication techniques which continue to increase the communication rate, short-term perturbations in the signal stability become an increasingly important problem.

[†] Electronic Engineer

[††] The solar-geophysical forecasting was separated from the telecommunication forecasting in 1966 and commenced from the Space Disturbance Forecast Center, Boulder, Colo., at that time. SDFC and the Solar Forecast Facility in Colorado Springs, Colo., work closely in the solar geophysical forecasting (Packnett and Doeker, 1969).

Remote[†], short-term forecasting alone does not provide the total solution. The state of knowledge upon which these forecasts are based is not sufficiently advanced to provide all the information the communicator needs. The question remains how much information can be provided by the remote forecaster, and what information can be better obtained by the communicator. Indeed, under normal conditions, the operator of existing fixed communication circuits has a good idea of when he will lose communications. A comprehensive system such as CURTS (Dayharsh, 1968) can provide valuable information on the status of communications over a given circuit, when communications will be lost, and the best frequency to maintain communications. Even a simplified version of CURTS, where only the signal-to-noise level and signal characteristics on the actual communication frequency and the noise interference level on potential communication frequencies are monitored, may provide valuable information for frequency selection.

The cause of communication disturbances is a function of the general latitude of the communication circuit. In the arctic latitudes, disturbances due to ionospheric storms are most prevalent. These generally can be traced to solar origin and are associated with disturbances that usually result in a general decrease in the F layer electron density, and an increase in the F layer height (and an associated decrease in the MUF), and an increase in the signal attenuation (i. e. an increase in the LUF). In severe cases, the lowest usable frequency exceeds the maximum usable frequency, and successful communication cannot exist using the conventional HF propagation modes (Hunsucker and Bates, 1969). It is possible (within some error) to forecast these geomagnetic disturbances and their ionospheric effects. The high incidence of Sporadic-E at these latitudes is somewhat more difficult to forecast.

In the equatorial latitudes, disturbances in communication circuits primarily result from large deviations of the MUF (lasting for several hours) from smooth diurnal trends (Salaman, 1969), and from significant increases in the LUF caused by solar flare induced ionospheric absorption. The large MUF deviations are not sufficiently understood yet to allow remote forecasting, and, therefore, a form of on-line monitoring (such as by CURTS or backscatter) may prove more fruitful.

At temperate latitudes, similar effects are found, as in the artic (and equatorial) latitudes, but generally with much less severity.

In the Polar Cap region, Polar Cap absorption events occasionally occur, which cause drastic effects on ionospheric communications. An attempt is made to forecast this phenomena. also.

In addition to forecasts of impending disturbances, the communicator should know what disturbances are in process even though they may not have been forecasted; therefore, it is necessary to have an adequate system for detecting disturbed conditions.

Finally, the communicator must account for communication outages. It is useful to have access to propagation information that might explain operational difficulties afterwards.

3. AN ADVANCED FORECASTING SYSTEM

The purpose of the forecast system is to provide in a timely manner the general and specific disturbance information, described in the previous section to the telecommunication community. To accomplish this, a system must (1) acquire and sort large amounts of solar-geophysical and radio propagation data obtained on a worldwide basis. (2) process the data, as required for generating forecasts and determining the status of disturbed conditions, based on correlations of the interaction of observed events, and the resultant communication effects, and (3) distribute the forecasts, disturbance status information, and historical disturbance information quickly to diverse users.

A system to accomplish these objectives is shown pictorially in figure 1 and schematically in figure 2. The information necessary to prepare the forecasts is received by the communication center and entered into a computer for processing storage and subsequent dissemination. The information in the computer is automatically updated by the input data, and the output provides information concerning disturbances both automatically and upon demand. The duty forecaster, who mans the forecast console, monitors the operation of the forecast system, verifies the validity of the computer generated forecasts and assists the user through either teletype or telephone communications.

[†]The word remote indicates that the forecasting is done some distance from the communication circuit or area.

Data Acquisition

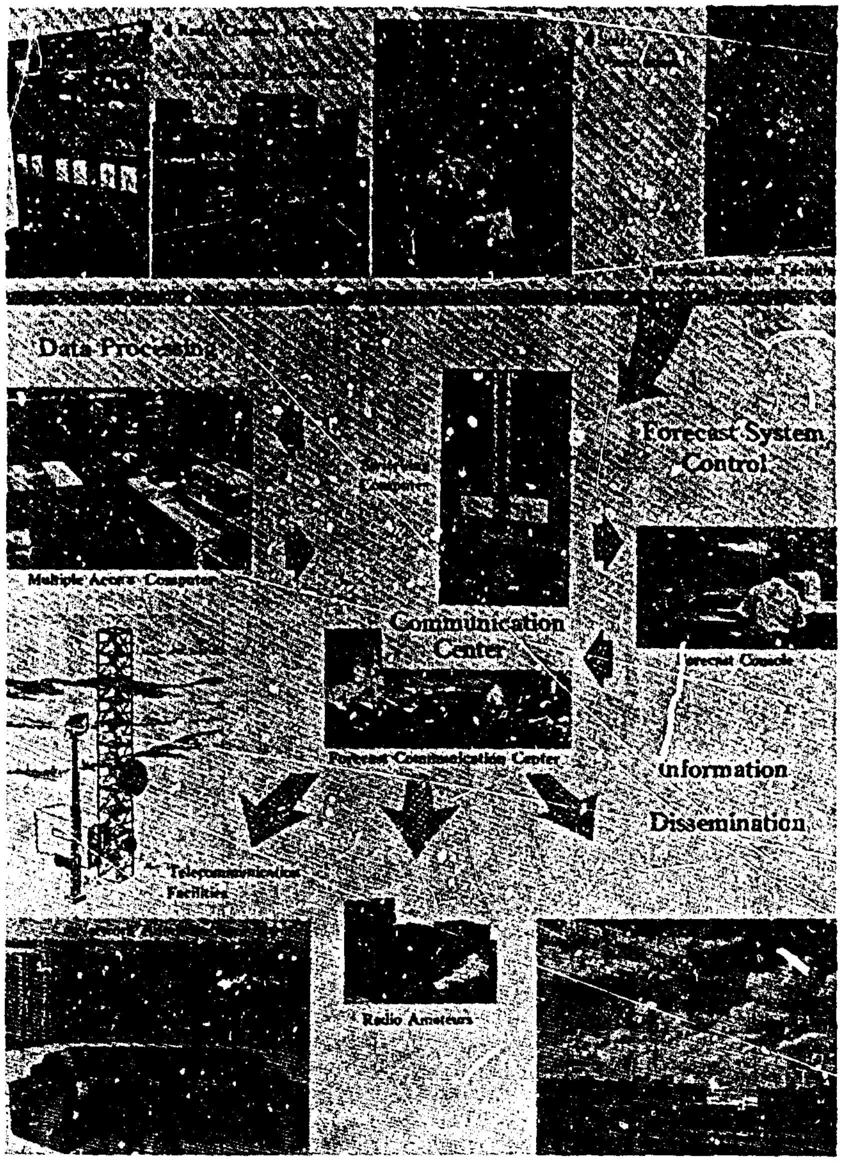

Figure 1. Pictorial representation of forecast disturbance system

3.1 Data Acquisition

Ionospheric telecommunication forecasting requires a large amount of solar-geophysical information on a worldwide basis. In addition to data, forecasts of solar-geophysical activity are also required. Such data and forecasts can be obtained from a system such as described by Packnett and Doeker (1969). It is also necessary to monitor ionospheric radio channel conditions, to verify the forecasts, and to detect unforecasted events. Large areas can be surveyed by backscatter sounding techniques (Bartholomew, 1969). Specific areas and paths can be monitored by remotely tuned receivers that can be located away from the Forecast Center. It is necessary to know as much as possible about the telecommunication system performance characteristics, system parameters, and operational doctrine to provide information in terms that are understood by and meaningful to the user.

3.2 Data Processing

The data discussed above must be processed to (1) provide alerts of disturbances as soon as they can be forecasted or are observed, (2) allow the user to obtain disturbance status messages when he desires as necessary, either for general areas or for his specific paths (these may also

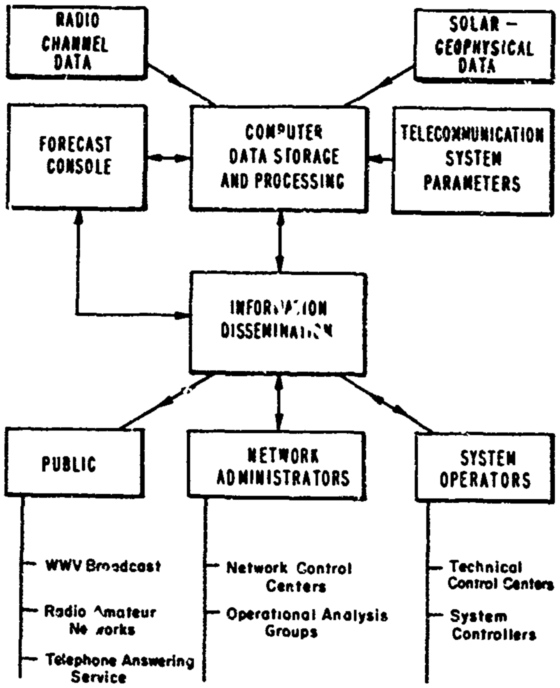

Figure 2. Forecast system

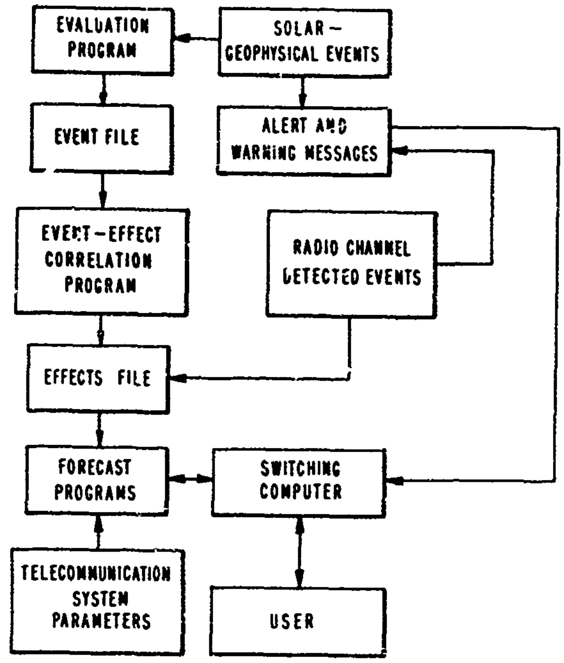

Figure 3. Computer data processing

be made available periodically if he so desires), and (3) allow the user to have access to historical information concerning any specific event or any events which occured in specific time interval. The computer data processing system to accomplish this is shown in figure 3. The computer is employed in a time-sharing mode of operation so that many users can obtain information essentially simultaneously.

The solar-geophysical propagation data which are received over the worldwide networks by teletype codes or available from local observations in digital form are entered directly into the time-sharing computer. Telephone messages and other local observations are entered from the forecast console. The input data are edited to eliminate redundant information and are stored in an event file (an example of which is shown in fig. 4). The events are then evaluated in terms of their potential effect on HF communications with results stored in an EFFECTS file, such as shown in figure 5. A detailed account of the interrelationships between the solar-geophysical events and the communication effects is given by Stonehocker (1969). When the disturbances are observed, it is also noted in the EFFECTS file, the user can, therefore, request information on how a specific disturbance will affect his particular communication system. For large communication systems, information concerning characteristics of the users system is also stored in the computer and applied to the EFFECTS file when a disturbance occurs or when particular information is requested.

·4869						
4867	7280415	2	7280415	18	1.0	-12 55
4868	7280717	2	7280000	28	.2	-10 52
4869	7280826	2	7280829	26	.2	-19 3
4866	7280100	2	7280105	40	.2	-16 27
4865	7271427	2	7270000	23	.2	-14 35
4863	7271310	2	7271313	35	.3	-6 66
4864	7271404	2	7271405	51	.2	-6 55
4862	7271124	2	7271125	56	.3	-6 66
4861	7261607	2	7261610	22	.2	-17 49
4859	7251645	2	7251648	25	.2	-15 30
4860	7251744	2	7251746	33	.2	13-28
4858	7251120	2	7551124	38	1.0	-15 32
4857	7240237	2	7240000	21	.7	-17 85
4856	7231732	2	7231747	27	.2	-12 87
9999	99999999	9	99999999	9999	99999.9	999999
Reference number	Beginning date-time group	Event type	Maximum data-time group	Duration	Magnitude	Flare position

Figure 4. EVENT file

```
4869
1 Ø 4867  11. Ø7280415 Ø7280433   15.5
3 Ø 4867  16. Ø7291712 Ø8011712   5Ø.Ø
1 Ø 4868   1. Ø7280717 Ø7280739    4.5
3 Ø 4868   7. Ø7291950 Ø8011950   5Ø.Ø
1 Ø 4869   1. Ø7280826 Ø7280846    4.5
3 Ø 4869  30. Ø7291711 Ø8011711   5Ø.Ø
1 Ø 4866   1.  7280100  7280122    4.5
3 Ø 4866  21.  7291135  8 11135   5Ø.Ø
1 Ø 4865   1.  7271427  7271449    4.5
3 Ø 4865  19.  7290206  8 10206   5Ø.Ø
1 Ø 4863   2.  7271310  7271334    7.Ø
3 Ø 4863   5.  7290254  8 10254   5Ø.Ø
1 Ø 4864   1.  7271404  7271426    4.5
3 Ø 4864   6.  7290301  8 10301   5Ø.Ø
1 Ø 4862   2.  7271124  7271148    7.Ø
3 Ø 4862   5.  7290108  8 10108   5Ø.Ø
1 Ø 4861   1.  7261607  7261629    4.5
3 Ø 4861   9.  7280416  7310416   5Ø.Ø
1 Ø 4859   1.  7251645  7251707    4.5
3 Ø 4859  21.  7270344  7300344   5Ø.Ø
1 Ø 4860   1.  7251744  7251806    4.5
3 3 4860 100.  7261154  7272359   5Ø.Ø
1 Ø 4858  11.  7251120  7251150   15.5
3 Ø 4858  30.  7262235  7292235   5Ø.Ø
3 Ø 4852   7.  7230929  7260929   5Ø.Ø
3 Ø 4853   5.  7231618  7261618   5Ø.Ø
3 Ø 4851  13.  7230709  7260709   5Ø.Ø
3 Ø 4849  23.  7220636  7250636   5Ø.Ø
3 Ø 4850  14.  7221056  7251056   5Ø.Ø
3 Ø 4846  32.  7211815  7241815   5Ø.Ø
9 9 9999 999. 99999999 99999999 9999.9
```

Magnitude
Ending date-time group
Beginning date-time group
Probability
Reference number
Status
Effect type

Figure 5. EFFECTS file

3.3 Forecast Dissemination

The forecasting system is designed to take action automatically on forecast dissemination and on requests for disturbance information. A switching computer is employed between the user and the forecasting computer. Alerts of impending disturbances are issued immediately and automatically to the user. Requests for routine forecasts (discussed in section 4) are routed to the computer for action, and the reply is automatically sent back to the user. Requests for any unprogrammed information is routed to the forecast console for action by the forecaster on duty.

A telephone is also available at the forecast console for voice communication with the user, including the public, who in general do not have access to teletype equipment.

4. FORECAST SERVICES

Examples of the disturbance forecast services are shown in figure 6. Examples of different types of forecasts are shown in figures 7 through 16. The first four forecasts (Weekly, Advanced, Medium-term, and Short-term) are similar to those that have been available for many years. They are distributed periodically by mail and/or commercial and government teletype to customers who have requested this service. The PROPALERT, PROPWARN, and GENERAL messages are issued automatically by teletype immediately upon sufficient event information; the other forecasts are issued by teletype upon request of the user. The services PROPALERT through GENSUM are directed toward the system operator, network administrator, and operational analysis. The last forecast, GENERAL is directed toward the needs of short-wave listeners, radio amateurs, etc., and should be distributed by voice or teletype as appropriate. In addition, special forecasts are developed and issued as required by the user.

The Weekly forecast, shown in figure 7, is a modification of the Jc series forecast that has been issued for many years. It was modified to eliminate the solar-geophysical information now available in the ESSA Space Disturbance Forecast Center Bulletin. It also includes a forecast of

Radio Conditions based on the computer analysis of current solar-geophysical data discussed above. It is currently distributed to about 500 recipients, on an international basis.

Title	Distributed	Period Covered	Description
Weekly	Mail	Next 7 days	Forecast of HF Radio Conditions for following week, and review of conditions for previous week.
Advanced	Teletype	Next 7 days	Forecast of North Atlantic Radio Quality Figure for following week, in coded format.
Medium-term	Teletype	Next 24 hours	General Quality and frequency usage statements for the North Atlantic for the following day.
Short-term	Teletype WWV	Next 6 hours	Forecast of North Atlantic Radio Quality Figure for the following 6 hours, in coded format.
PROP ALERT	Teletype	Immediate	Forecast notice of impending disturbance.
PROP WARN	Teletype	Immediate future	Forecast of time, location, and magnitude of disturbance.
DETAIL	Teletype	That of disturbance	Forecast of attenuation or MUF for specified circuit or area due to specific disturbance.
ADMIN	Teletype	Previous to next 24 hr	Summary for previous day and forecast for following day, giving time, location, probability, and magnitude or excess attenuation and unstable MUF.
CURRENT	Teletype	Previous to next 24 hr	Brief summary of ADMIN Forecast.
GENSUM	Teletype	Specified period	Summary of radio disturbances for specified previous period.
GENERAL	Voice/ Teletype	As necessary	Forecast of disturbances of interest to the public.

Figure 6. Forecast Services

U. S. Department of Commerce
Environmental Science Services Administration
Research Laboratories

WF-248 TELECOMMUNICATION SERVICES CENTER 23 July 69
ESSA/ITS, R614
Boulder, Colorado 80302

Weekly Radio Telecommunication Forecast

A. Forecast of HF Radio Conditions - 24-30 July 1969

1. Radio conditions should be generally good. Increased geomagnetic activity particularly during local night hours, is expected through 26 July with MUFs somewhat below normal.
The daily high latitude radio quality is expected to be:

• 6-6 7-7 7-7-7

2. Sporadic Excess Attenuation (Solar Flare-Induced SWF):

DAYLIGHT PATHS ONLY

Relative Attenuation	Probability of Occurrence (each day)
Moderate	20%
Large	5%

3. Ionospheric Storms:

Relative Importance	Period Affected	Prob. of Occurrence
Small	AM 24 July - PM 26 July	25%

4. Polar Cap Absorption:

Probability of Occurrence - Slight

B. Review of HF Telecommunications for the past week: Telecommunications were generally good during the review week. No significant S-SWFs were observed.

High Latitude Observed Radio Quality

July	16	17	18	19	20	21	22
Whole day index	7	7	7	7	7	7	7
6-hour indices	7677	6677	7777	7677	7777	6677	7777
Geomagnetic Activity AFR	11	4	2	3	4	5	9

Figure 7. WEEKLY Forecast

The Advanced, Medium-term, and Short-term forecasts shown in figure 8 continue to be issued to keep continuity with the service that has existed for the past 10 years. Those will be available as needed until the new services have had an adequate review.

The seven new forecast services were designed for a specific purpose. In the classical disturbance sequence a flare might occur, such as listed reference number 4860 in the Effect and Event files. A PROPALERT (fig. 9) would be issued immediately. Although the magnitude of the absorption event may not be known, the communicator would be alerted that a sudden outage which he may just have encountered may be due to a propagation disturbance, rather than, for example, problems with his equipment. The PROPALERT forecast is also used to give an alert of any other disturbance immediately upon detection.

```
231550Z JUL 69

ADFL 23214
ADVANCE FORECAST HIGH LATITUDE RADIO PROPAGATION
CONDITIONS FOR 24-30 JUL 69.
RADIO CONDITIONS SHOULD BE GENERALLY GOOD. INCREASED
GEOMAGNETIC ACTIVITY, PARTICULARLY DURING LOCAL NIGHT
HOURS, IS EXPECTED THROUGH 26 JULY WITH MUFS SOMEWHAT
BELOW NORMAL.
EXPECT DAILY QUALITY TO BE: 6-6-7-7-7-7-7
```

ADVANCED Forecast

```
271900Z JUL 69

DAILY HIGH LATITUDE RADIO PROPAGATION FORECAST FOR 28 JUL 69.
UNSETTLED GEOMAGNETIC CONDITIONS AND FAIR RADIO CONDITIONS NEXT
24 HOURS. LOWER THAN NORMAL FOT - NORMAL LUHF FOR NEXT 24 HOURS.
THERE IS A SLIGHT CHANCE OF S-SWF.
```

MEDIUM-TERM Forecast

```
STAFO 28002
THE 28/0500Z SHORT TERM RADIO FORECAST FOR 0600-1200 IS U5.
*
```

SHORT-TERM Forecast

Figure 8. ADVANCED, DAILY, and SHORT-TERM forecast

```
U.S. DEPT. OF COMMERCE
ESSA/ITS, BOULDER, COLORADO

"PROPALERT" FORECAST    7251744Z

A SOLAR FLARE IS OCCURRING OR IMMINENT. PROPAGATION PATHS IN DAYLIGHT
MAY HAVE EXCESS SIGNAL ATTENUATION. PROPWARN FORECAST TO FOLLOW
IF SIGNIFICANT.
```

Figure 9. ALERT forecast

As soon as sufficient information is available to provide a forecast of the magnitude, geographic extent, start time, and duration of the disturbance, a PROPWARN is issued (see fig. 10). The operator should then have sufficient information to take action which would minimize the disturbance effects.

```
U.S. DEPT. OF COMMERCE
ESSA/ITS, BOULDER, COLORADO

"PROPWARN" FORECAST  7251747Z

SMALL EXCESS SIGNAL ATTENUATION MAY BE EXPECTED ON DAYLIGHT PATHS
FROM ABOUT 7251744Z TO 7251806Z
ALSO
SMALL MUF CHANGES WITH INCREASED SIGNAL ATTENUATION AND VARIABILITY
MAY BE EXPECTED ON HIGH LATITUDE PATHS FROM ABOUT 7261200Z TO
7290000Z.

FOR SPECIFIC CIRCUIT REQUEST "DETAIL" REF. NR. 44860.
```

Figure 10. WARNing forecast

If the communicator wants further information on the effect of the disturbance on his particular system or circuit, he can request the DETAIL forecast, as shown in figure 11, referenced in the PROPWARN forecast. In this way, by answering certain questions (as underlined in fig. 11), the

```
U.S. DEPT. OF COMMERCE
ESSA/ITS, BOULDER, COLORADO

"DETAIL" FORECAST

DO YOU WISH A PROGRAM DESCRIPTION?          TYPE 0 FOR NO, 1 FOR YES:1
THIS PROGRAM ENABLES THE OPERATOR TO OBTAIN TWO TYPES OF FORECASTS:
1-A FORECAST OF ABSORPTION FOR A PARTICULAR SHORTWAVE FADEOUT (SWF)
  FOR AN INDIVIDUAL CIRCUIT. THE TFC  REFERENCE NUMBER OF THE SWF
  (OBTAINED FROM "GENSUM" OR OTHER FORECAST) AND CIRCUIT NUMBER MUST BE
  SUPPLIED. THE OPERATOR ALSO HAS THE OPTION OF ENTERING THE GEOGRAPHIC
  COORDINATES OF  THE END POINTS OF THE CIRCUIT INSTEAD OF THE CIRCUIT
  NUMBER FOR SWF FORECASTS.
2-A FORECAST OF EXPECTED MUF VARIATIONS FOR A PARTICULAR MAGNETIC
  (IONOSPHERIC) STORM FOR A PARTICULAR CIRCUIT (USED IN PLACE OF MUF
  CIRCUIT DESIGNATOR 99).  THE MEDIAN MUF MUST BE AVAILABLE IN
  A DATA FILE.  IF THIS FILE IS NOT AVAILABLE IT CAN BE PREPARED BY
  TELECOMMUNICATION SERVICES CENTER UPON REQUEST.

TYPE FORECAST WANTED (1 FOR SWF, 2 FOR MUF):1
TYPE REFERENCE NUMBER OF EFFECT(I4):4860
TYPE CIRCUIT DESIGNATOR (01-39) OR 99 TO ENTER
PATH TERMINAL POINTS:01
NEW YORK TO QUITO EQUATOR

  ------------SWF FORECAST-----------
TYPE IN OPERATING FREQUENCY IN MEGAHERTZ WITH DECIMAL POINT
     IF UNKNOWN TYPE 0.0:09.0
TYPE AVAILABLE SIGNAL TO NOISE RATIO IN DB, 2 INTEGERS,00 IF UNKNOWN:00

THE MAXIMUM ATTENUATION AT  9.000 MHZ ON THE PATH GIVEN
     IS EXPECTED TO BE =  5.5 DB
     IN THE INTERVAL FROM JUL 251744Z TO JUL 251806Z
```

Figure 11. DETAIL SWF forecast

user can obtain a forecast of absorption effects (due to a flare, for example), or MUF effects (due to a magnetic storm) for his communication system.

If the communicator wishes to obtain a short summary of the conditions over the past 24 hours, he may request a CURRENT forecast, an example of which is given in figure 12, which could be useful to a controller at the beginning of his duty.

Large network administrators and planners also need as much information as possible concerning radio conditions for the past and the following 24 hours. This information is contained in a forecast called ADMIN (see fig. 13), which forecasts the MUF effects of a magnetic storm re-

```
U.S. DEPT. OF COMMERCE
ESSA/ITS, BOULDER, COLORADO

"CURRENT" FORECAST

            CONDENSED SUMMARY AND FORECAST OF DISTURBED
            HIGH FREQUENCY TELECOMMUNICATION CONDITIONS
                            JUL 280000Z

SUMMARY FOR PREVIOUS 24 HOURS
----------------------------

UNUSUAL ATTENUATION ON DAYLIGHT CIRCUITS COULD HAVE OCCURRED
DURING AT LEAST ONE PERIOD BUT IT IS UNCONFIRMED.

A PERIOD OF UNSTABLE MAXIMUM USABLE FREQUENCIES AT MIDDLE AND HIGH
LATITUDES, ACCOMPANIED BY ERRATIC ABSORPTION IN AURORAL ZONE REGIONS
BEGAN AT JUL 261154Z, AND CONTINUED DURING THIS PERIOD.

FORECAST FOR NEXT 24 HOURS
--------------------------

THERE IS A FAIR CHANCE OF RELATIVELY SHORT PERIODS (5 MIN TO 2 HOURS)
OF UNUSUAL ATTENUATION ON DAYLIGHT CIRCUITS.

A PERIOD OF UNSTABLE MAXIMUM USABLE FREQUENCIES AT MIDDLE AND HIGH
LATITUDES, ACCOMPANIED BY ERRATIC ABSORPTION IN AURORAL ZONE REGIONS
IS EXPECTED TO END AT JUL 290000Z.

FOR A MORE DETAILED SUMMARY AND FORECAST, SEE "ADMIN" FORECAST.
```

Figure 12. CURRENT forecast

```
U.S. DEPT. OF COMMERCE
ESSA/ITS, BOULDER, COLORADO

"ADMIN" FORECAST

              SUMMARY AND FORECAST OF DISTURBED HIGH FREQUENCY
                        TELECOMMUNICATION CONDITIONS
TELECOMMUNICATION SERVICE CENTER                         28 JUL 0000Z

SUMMARY FOR PREVIOUS 24 HOURS
----------------------------

EXCESS ATTENUATION ON DAYLIGHT PATHS MAY HAVE BEEN EXPERIENCED DURING
 THE FOLLOWING INTERVALS:
   TFC REF. NO.          TIME               REL. INTENSITY  PROBABILITY(PCT)
       4563      JUL 271318Z-JUL 271334Z        LOW              2
       4862      JUL 271124Z-JUL 271148Z        LOW              2

      A PERIOD OF UNSTABLE MUF'S AT TEMPERATE AND HIGH LATITUDES AS
WELL AS ERRATIC ATTENUATION ON AURORAL ZONE CIRCUITS WAS REPORTED
TO HAVE STARTED AT JUL 261154Z.
IT IS ASSOCIATED WITH A SMALL MAGNETIC DISTURBANCE.

FORECAST FOR NEXT 24 HOURS
--------------------------

PERIODS OF EXCESS ATTENUATION ON DAYLIGHT PATHS WITH THE INDICATED
CHARACTERISTICS CAN BE EXPECTED WITH THE LISTED PROBABILITY:

      CHARACTERISTIC                                PROBABILITY(PCT)

ATTENUATION WITH PEAK OF UP TO 20 DB                    25
RETURNING TO NORMAL WITHIN 30 MIN.

ATTENUATION WITH PEAK OF UP TO 40 DB                    36
RETURNING TO NORMAL WITHIN 60 MIN.

ATTENUATION WITH PEAK OF UP TO 80 DB                    5
RETURNING TO NORMAL WITHIN 2 HOURS

THE PERIOD OF UNSTABLE MUF'S AT TEMPERATE AND HIGH LATITUDES AND ERRATIC
 ATTENUATION ON AURORAL ZONE CIRCUITS (TFC REF. NO. 4868) WHICH IS
 CURRENTLY IN PROGRESS SHOULD END AT JUL 290000Z.
DURING THE NEXT 24 HOURS THIS STORM SHOULD PRODUCE MUF VARIATIONS
 OF THE FOLLOWING ORDER:

                      PERCENT CHANGE IN MUF
                   LOCAL TIME (PATH MID-POINT)
LATITUDE:         00-06       06-12       12-18       18-99

HIGH NORTHERN   -7TO   1   -8TO   1  -19TO  -4  -15TO  -4
MID-NORTHERN    -7TO   0  -10TO  -5   -7TO  -3   -6TO  -2
LOW              0TO   8   -1TO   8   -3TO   6   -2TO   6
MID-SOUTHERN    -4TO   0   -7TO  -4   -4TO  -2   -3TO   0
HIGH SOUTHERN   -7TO   0   -9TO  -4  -22TO  -8  -14TO  -8
```

Figure 13. ADMIN forecast

sulting from the previously referenced solar flare, a DETAIL forecast for a specific circuit could then be obtained for this event as shown in figure 14.

Should the communicator need to determine the cause of an outage within the past several days, this information, which is stored in the computer, can be obtained directly for any desired time period and area through the forecast GENSUM, illustrated in figure 15. A collection of GENSUM's for the past month can be printed and issued as a Propagation Summary on a monthly basis.

```
U.S. DEPT. OF COMMERCE
ESSA/ITS, BOULDER, COLORADO

"DETAIL" FORECAST

DO YOU WISH A PROGRAM DESCRIPTION?          TYPE 0 FOR NO, 1 FOR YES: 0
TYPE FORECAST WANTED (1 FOR SWF, 2 FOR MUF):2
ENTER MONTH-DAY-TIME GROUPS OF START + END TIMES OF INTERVAL FOR
WHICH FORECAST IS DESIRED-TWO GROUPS OF 8 INTEGERS SEPARATED
BY A COMMA:07261200,07280000
TYPE REFERENCE NUMBER OF EFFECT(I4):4860
TYPE CIRCUIT DESIGNATOR - 99 INVALID(I2):01
NEW YORK TO QUITO EQUATOR

   ------------MUF FORECAST FOR CIRCUIT  1 ---------
                    (MULTI-HOP)
```

MONTH	DAY	HOUR(Z)	MEDIAN MUF	REVISED MUF	% CHANGE
JUL	26	12	22.2	22.9	3
JUL	26	13	23.9	24.6	3
JUL	26	14	23.7	24.4	3
JUL	26	15	23.7	24.4	3
JUL	26	16	24.5	25.2	3
JUL	26	17	25.3	24.5	-3
JUL	26	18	25.4	24.6	-3
JUL	26	19	25.2	24.4	-3
JUL	26	20	25.3	24.5	-3
JUL	26	21	25.9	25.1	-3
JUL	26	22	26.4	25.6	-3
JUL	26	23	26.7	26.4	-1
JUL	27	0	26.4	26.1	-1
JUL	27	1	25.3	25.0	-1
JUL	27	2	23.8	23.6	-1
JUL	27	3	22.5	22.3	-1
JUL	27	4	21.4	21.2	-1
JUL	27	5	20.5	20.1	-2
JUL	27	6	19.3	18.9	-2
JUL	27	7	17.9	17.5	-2
JUL	27	8	16.4	16.1	-2
JUL	27	9	15.6	15.3	-2
JUL	27	10	16.6	16.3	-2
JUL	27	11	15.3	14.1	-8
JUL	27	12	22.2	20.4	-8
JUL	27	13	23.9	22.0	-8
JUL	27	14	23.7	21.8	-8
JUL	27	15	23.7	21.8	-8
JUL	27	16	24.5	22.5	-8
JUL	27	17	25.3	21.3	-16
JUL	27	18	25.4	21.3	-16
JUL	27	19	25.2	21.2	-16
JUL	27	20	25.3	21.3	-16
JUL	27	21	25.9	21.8	-16
JUL	27	22	26.4	22.2	-16
JUL	27	23	26.7	24.6	-8
JUL	28	0	26.4	24.3	-8

Figure 14. DETAIL MUF forecast

```
U.S. DEPT. OF COMMERCE
ESSA/ITS, BOOULDER, COLORADO

"GENSUM" FORECAST

DO YOU WANT INSTRUCTIONS? TYPE 0 FOR NO, 1 FOR YES: 1
THE FOLLOWING TABLE SPECIFIES THE AREAS AVAILABLE -
0-WORLDWIDE
1-E. ATLANTIC
2-W. ATLANTIC, S. AMERICA
3-N. AMERICA, E. PACIFIC
4-MID-PACIFIC
5-W. PACIFIC
6-ASIA
7-NEAR EAST, INDIAN OCEAN
8-EUROPE, AFRICA
9-SPECIFIC CIRCUIT

TYPE AREA NUMBER,0 FOR WORLDWIDE:0

        SUMMARY OF HIGH FREQUENCY TELECOMMUNICATION DISTURBANCES
                                WORLDWIDE

JUL 250000Z-JUL 280000Z

DURING THIS PERIOD,SHORT INTERVALS OF EXCESS ATTENUATION ON CIRCUITS IN
LATITUDES FROM 55S TO 90N MAY HAVE BEEN EXPERIENCED DUE TO SOLAR FLARES.
LIKELY INTERVALS ARE LISTED IN THE FOLLOWING TABLE. "C" AND "U" FOLLOW-
ING THE REFERENCE NUMBER INDICATE CONFIRMED OR UNCONFIRMED RESPECTIVELY.
```

TSC REF. NO.	INTERVAL	IMPORTANCE	LONG.EXTENT
4865-U	JUL 271427Z-JUL 271449Z	LOW	105E, 45W
4863-U	JUL 271310Z-JUL 271334Z	LOW	90E, 60W
4864-U	JUL 271404Z-JUL 271426Z	LOW	105E, 45W
4862-U	JUL 271124Z-JUL 271148Z	LOW	60E, 90W
4861-U	JUL 261607Z-JUL 261629Z	LOW	135E, 15W
4859-U	JUL 251645Z-JUL 251707Z	LOW	150W, 0W
4860-U	JUL 251744Z-JUL 251806Z	LOW	165W, 15W
4858-U	JUL 251120Z-JUL 251150Z	MODERATE	60E, 90W

```
AN IONOSPHERIC STORM WHICH PRODUCED ABNORMAL MAXIMUM USABLE FREQUENCIES
AS WELL AS ERRATIC ABSORPTION ON AURORAL ZONE PATHS DURING THE PERIOD
BEGAN AT JUL 261154Z.IT ENDED AT APPROXIMATELY JUL 272359Z. TO OBTAIN AN
ESTIMATE OF THE MUF VARIATIONS FOR A GIVEN AREA, REQUEST AN AREA SUMMARY

DO YOU WISH A SUMMARY FOR ANOTHER AREA OR TIME PERIOD? TYPE 0 FOR NO,
1 FOR YES:0
```

Figure 15. GENSUM service

The PROPALERT, PROPWARN, DETAIL, CURRENT, ADMIN, and GENSUM messages, including the necessary correlations, computations, and text, are generated automatically by the computer, based on available solar-geophysical data, adapted to the user's specific requirements.

The GENERAL forecast is designed for public use, and can be distributed by HF and VLF broadcasting (for example through standard frequency radio stations), as well as through Radio Amateur networks. Besides providing a general statement concerning radio conditions, it could give forecasts of the best frequency range for reception between specific areas, such as the East and West Coasts of North America and the Orient, Hawaii, Australia, South America, Europe, and North and South Africa. This might be in two-hour time blocks, with disturbance updating as necessary. Preferably, it should be transmitted by voice. This service can also be made available through automatic telephone answering in selected cities.

In addition, it is possible to provide forecasts designed to meet special user needs, such as those illustrated in figure 16.

5. CONCLUSIONS

Ionospheric forecasting techniques have improved over the past 25 years. Even in recent years, they have consisted of subjective analysis of solar-geophysical events and their effects weighted heavily by the forecaster's experience. With the greater sophistication in communication technology, demands on ionospheric system capacity and reliability have grown. It is now desirable to replace the subjective analysis with more rigorous correlations and allow the communicator access to the information he needs to maintain his required system efficiency. The complexity of both these problems suggests the application of current computer technology, although the forecaster remains a vital element in the system.

The technique for short-term forecasting and forecast dissemination described here attempts to meet these requirements and is presently undergoing operational evaluation. The use of on-line monitoring in conjunction with remote short-term forecasting should not be overlooked.

TO GSFC
FROM
U.S. DEPT. OF COMMERCE
ESSA/ITS, BOULDER, COLORADO
16/0640Z

NASCOM SHORT TERM LUF/FOT/MUF FORECAST FOR MISSION NCG-725/785
FORECAST FOR 16 JUL 08-13Z
LUF-LOWEST USABLE FREQUENCY, FOT-REVISED MEDIAN OPTIMUM TRAFFIC
FREQUENCY (99 INDICATES LUF EQUAL TO OR GREATER THAN FOT), MUF-REVISED
MAXIMUM USABLE FREQUENCY. WHEN FOT EQUALS MUF, PROPAGATION IS VIA E
LAYER. ALL FREQUENCIES IN MHZ. QUALITY CODE, P-POOR, F-FAIR, G-GOOD.

CIRCUIT	TIME(Z)	LUF/FOT/MUF	QUALITY
TANANARIVE -PARIS	8	17/19/23	F/G
	9	17/20/23	G
	10	17/20/23	G
	11	17/20/24	G
	12	17/21/24	G
	13	17/20/24	G
TANANARIVE -PERTH	8	9/26/29	G
	9	8/25/29	G
	10	7/24/27	G
	11	6/21/24	G
	12	5/15/17	F/G
	13	4/12/14	F/G
TANANARIVE -JOHANNESBURG	8	7/20/23	G
	9	8/19/21	G
	10	8/19/21	G
	11	7/19/21	G
	12	7/19/21	G
	13	6/19/21	G
VANGUARD -BERMUDA	8	2/ 9/12	G
	9	3/10/13 T	G
	10	4/12/15 T	G
	11	5/15/16	G
	12	6/17/17X	F/G
	13	7/18/18X	F/G

X INDICATES POSSIBLE CIRCUIT DIFFICULTIES THIS HOUR.
T INDICATES POSSIBLE(NIGHT TO DAY) TRANSITIONAL CONDITIONS THIS HOUR.

GEOMAGNETIC ACTIVITY HAS INCREASED SLIGHTLY THE PAST
FOUR HOURS. HOWEVER, IONOSPHERIC CONDITIONS ARE EXPECTED
TO CONTINUE TO BE NORMAL. ONE OR TWO MINOR S-SWF
MAY BE EXPECTED ON DAYLIGHT CIRCUITS.

Figure 16. Special forecasts

6. REFERENCES

Bartholomew, R. R. (1969). "Use of Backscatter Measurements to Improve HF Communications Predictions," Proceedings of the AGARD Symposium on Ionospheric Forecasting, 1969.

Beckman, B. (1969), "Ionospheric Forecasting in Germany," Proceedings AGARD EPC Symposium on Ionospheric Forecasting, 1969.

Dayharsh, T. I., J. L. Gnagy, and S. D. Probst (1968), "Automated CURTS HF; Real Time Management and Administration of HF Systems and Frequency Resources," February 1968, SRI Project 6787, DCA Contract 100-67-C-0068.

Hunsucker, R. D. and H. F. Bates (1969), "Survey of polar and auroral region effects on HF propagation," Radio Science, vol. 4, No. 4, April 1969.

Lincoln, J. V. (1969), "Ionospheric Forecasting in the United States 1942-1966," Proceedings of the AGARD Symposium on Ionospheric Forecasting, 1969.

Meek, J. H. (1969), "Historical Outline of Forecasting Methods," Proceedings of the AGARD Symposium on Ionospheric Forecasting, 1969.

Packnett, D. S. and R. B. Doeker (1969), "U.S. Activities in Operational Solar-Geophysical Forecasting," Proceedings of the AGARD Symposium on Ionospheric Forecasting, 1969.

Salaman, R. K. (1969), "An evaluation of short-term radio propagation forecasts for selected Southeast Asia DCA trunk," ESSA Tech. Report, ERL-96-ITS-71.

Slutz, R. J., T. N. Gautier, and M. Leftin (1969), "Short-term radio propagation forecasts in Southeast Asia," ESSA Technical Report, ERL-97-ITS-72.

Stonehocker, G. H. (1969), "Advanced Telecommunication Forecasting Technique," Proceedings of the AGARD Symposium on Ionospheric Forecasting, 1969.

THE SHORT TERM FORECAST OF SOLAR ACTIVITY

AND GEOPHYSICAL EVENTS

by

P. Simon

IUWDS Secretary
Observatoire de Meudon (France)

SUMMARY

We review the information obtained during the last ten years in the field of the solar activity.

The Radioastronomy has given the first possibility of an easy identification of the solar events linked with the most outstanding geophysical events. Then the originating active centers have been carefully studied and now they are identified on the solar disk before the event occurence.

A new improvement is due to the solar magnetographs: the place and the birth of a flare are strongly linked to the structure and to the evolution of these solar magnetic fields.

The detection in the space of a flux of low energy solar particles opens the opportunity to specify the propagation situacion into the deep interplanetary space.

Using all this complementary material, a forecasting center working on a routine basis has predicted the solar activity with a surprising accuracy (between 80 and 90 %) and has announced in advance a considerable number of the most oustanding events (between 50 and 70 %).

SOMMAIRE

Nous passons en revue les acquisitions des dix dernières années dans le domaine de l'activité solaire.

La radioastronomie a permis pour la première fois d'identifier parmi des éruptions à peuprès comparables celles qui sont réellement la cause des effets geophysiques les plus importants. Il a été possible d'étudier les centres actifs correspondants et de les identifier avant l'évènement.

Une nouvelle étape a été parcourue grâce à l'étude des champs magnétiques solaires: la place puis la formation des éruptions sont apparues étrcitement liées à la structure et à l'évolution de ces champs magnétiques.

La mesure des flux de particules solaires de basse énergie permet sans doute de préciser les conditions de propagation dans l'espace interplanétaire.

L'utilisation de toutes ces données complémentaires a permis en fait de prévoir l'activité solaire avec une précision surprenante (de 80 à 90 %) et les évènements les plus importants dans une proportion non négligeable (de 50 à 70 %).

The Short Term Forecast of Solar Activity and Geophysical Events.

by P. SIMON.

I U W D S Secretary

Observatoire de Meudon (France).

A description of the forecasting methods related to the solar activity or to the geophysical events is a hard task: the layers of the sun are studied through several techniques as various as radio astronomy and X ray astronomy. One object like sunspots can be studied in white light in order to study its area; on several lines in order to study their magnetic field (by their Zeeman effect) and the Evershed effect (by the Doppler shift). The chromosphere could be studied in many lines like the H alpha line, a Calcium line, some part of the X ray spectrum and the centimetric radio waves but not two of these techniques gives exactly the same information. The corona can be observed on the limb by the scatterred light and mainly on the disk at different radio wave lengths. The more techniques which exist, the more information we are supposed to obtain but in fact the physical meaning of many of them are not yet very definite and we cannot resume the forecasting methods to the acquisition of few accessible sizes. By the way we must use simultaneously several kinds of data with their own classification and it does not simplify the presentation.

However some scientific basis exists which allows some valuable methods of prediction. Since 1957 with the International Geophysical Year, the development of the Solar Radio Astronomy, the birth of the Space Research, the improvement of the Solar Magnetographs, the organization by the commission X of the I A U of several projects like the Cooperative Study of Solar Active Regions and the 1966 Proton Flare Project, our knowledge of the Solar Activity has been definitely improving during these last years. Now the experience of the solar observers is not the only background for such a prediction. The forecasters must get many data obtained through these various techniques and they can issue their forecast mostly according to a scientific process. The first evidence of this possibility came out during the 1966 Proton Flare Project when the solar astronomers had received on time the prediction of three expected Proton Events that later they had observed. Of course they had been lucky but it is a sign of the future possibility in this field.

Let us point out that this improvement of the forecast concerns mostly the Solar Activity (i. e. the espected growth and complexity of the active centers) and only as a consequence, the prediction of the solar events and of their terrestrial effects. By the way, there is some possibility to improve the daily estimate of the future variation of the ionising radiations: the practical problem is mainly related to a closer cooperation between solar and ionospheric forecasters in order to issue the solar forecast in terms easy to use for the ionospheric forecast.

Let us start with a brief review of the solar events linked to some ionospheric effect. Then we will see what have been in this field the original contributions of radio astronomy, of solar magnetic field observations and of space research. We will conclude with a few comments on the practical limits of the forecast and on an estimate of its success.

We name " geophysical events " the solar flares which go with or are followed by ionospheric disturbances or any other effect perceived near the earth (particles arrival, geomagnetic disturbance, a. s. o. ..) As a matter of fact, any flare activity has a consequence upon the earth, but for now we only take into account their classical and definite effects.As far as the forecasting problem are concerned, we insist upon the fact that there is a wide difference between the duration and geographic extent of the various kinds of events.

The differents kinds of Sudden Ionospheric Disturbance are the consequence of E U V and X Ray bursts occuring during the flash phase of a flare: they are concerned with the enlightened part of the earth and they last about a few tens minutes. They ought to be forecast before the event, but unfortunately we do not have the least indication which allows us to predict the very moment of issue of the flare.

The particle events have a specific geographic field for their arrival. Between 20 and 80 Mev the protons are first concerned with the Polar Cap (P C E) and later on with the auroral zone. The onset of the absorption may be observed from 20 minutes to several hours after the flare and its duration can be several days with a diurnal effect. The highest energy events (Gev or more) are very few but they are concerned with the Ground Level of the Earth (G L E) : the increase of the counting rate of neutron monitors starts 20 minutes after the event and last several hours. According to the earth magnetic field, the way they go into the terrestrial atmosphere is monitored by their energy and their first direction: they can arrive at any place on the surface of the earth. Between these two ranges of energy the particles are detected by balloons flying at their ceiling (or by earth satellites) and the terrestrial magnetic field leads them in direction of the auroral zone on the earth. Forecastsand alerts are possible as far as such events are concerned : the forecast is issued a few days before the event and an alert can be issued several minutes after the beginning of the flare if it has been possible to identify the event before the particles arrival.

Some magnetic storms are related to a flare: they usually start about one or several days after the solar event and the disturbance goes on during one or several days. The solar event to which it had been related can be forecast in a more definite way after the flare appearance, and the geomagnetic storm can be announced in advance.

The main interest of solar radioastronomy consists in observing the high chomosphere and the corona on the disk: the biggest and most sophysticated instruments could locate the sources and follow their evolution and movements. Briefly speaking, the longer the wavelength is, the higher the source, the centimetric wave being generated mostly at a chomospheric level and the meter wavelength around half a solar radius or further in the corona.

The first contribution of the radioastronomy has been to establish a link between the radio burst and the particle emission: amongst the many flares which come out on the solar disk, the only flares which are related to the most energetic particle emission are those which have strong long centimetric bursts (M. PICK, 1961). Most of these events also give birth to a kind of metric or decametric bursts with a very large banwidth which has been classified as a type IV burst (A. BOISCHOT 1958), but taking into account an effect of directivity this component is not easy to observe as far as the events are related to the sides of the solar disk.

The shape of these centimetric burts (mostly those around three centimeters) closely follows that of the X ray burst with an energy situated about 10 - 20 Kev (R. L. ARNOLDY et al. 1968) it seems quite reasonable to admit that they are produced by the same set of electrons. By the way, these kind of flares produce strong sudden ionospheric disturbances (P. SIMON 1960).

The large outbursts are linked with flares on spotted active centers (H. DODSON W. HEIDMAN, 1960). More precisely, the centimetric burst comes out when the brightest part of the flare arrives at a spotted area (J. M. MALVILLE, S. F. SMITH, 1963).

Another family of flares is related though not so strongly to the birth or evolution of metric noise storms (or type I burts) (A. M. LE SQUEREN, 1964).

All of these remarks have their importance: they allow a determination of the first efficient process for an easy identification of most of the flares which are related to an earth particles arrival and to build up a study of the linked active center features.

When studying the centimetric sources on the solar disk, and using a large interferometer, KUNDU has been the first to establish a link between the large centimetric outbursts and the very narrow and bright centimetric solar sources (M. KUNDU, 1959). Later on, TANAKA found a new criterium concerning most of the sources of high energy protons: their spectrum around this wavelength (from 3 to 8 centimeters) is very flat (H. TANAKA, T. KAKINUMA, 1964). Such a difference between the spectra is related to the optical features of the active centers (Y. AVIGNON, M. J. MARTRES, M. PICK, 1966).

More generally, the flare followed by radio outburst usually appears related to two kinds of active configurations: the A configuration with two spotted areas of about the same size and opposite polarities close to each other, or the B configuration with a big unipolar spot surrounded by a dark filament like an eyebrow (Y. AVIGNON et al 1964. C. CAROUBALOS, 1964). Anyway we must point out that as a matter of fact several flares could be reported in that area without any centimetric component: only those which cover spotted areas coincide with X ray burst and centimetric outburst and up to now we ignore when a flare will extend in the direction of spotted area.

The identification of the flares which are reponsible for the geomagnetic disturbances is not easy to be related due to the large delay between the flare and the disturbance. The particle effects (G L E, P C E) made larger the number of easy identifications and made safer the value of the relation between flares and geomagnetic disturbances. According to OBAYASI (T. OBAYASHI, 1962) the delay of the storm related to the flare definitely increases when the geomagnetic disturbance is the first of a succession of disturbances. The flux and the duration of the centimetric burst give a possibility of predicting the delay (C. CAROUBALOS, 1964).

Following such an improvement of our knowledge of the solar activity, many other facts have been pointed out and open a new philosophy concerning the flares process and flare activity.

First of all, the flares are not distributed at random amongst the active centers. With I G Y the survey of the flare activity was improved definitely, thanks to the start of the cinematographic flares patrols and a better coverage all around the world. The flares reports are not homogeneous (H. DODSON et al1964) but, in any case some active centers are good producers of flares when other are very quiet. A prompt identification of 20 % of the most active spots gives a possibility of forecasting 80 % of the flares.

On the other hand, the importance of a flare related to its area and brightness in the H alpha line is not sufficient to allow us to give any estimate of its geophysical effects. The obervers reports may happen to be a source of such a discrepancy; the commission X of U A I has recently improved the publication of the flares reports in the Quarterly Bulletin of the Solar Activity with new rules for the selection with a view to establish a list of confirmed flares. Anyway the conclusion still is that many flares (importane 2 or more), most of them originated in unspotted areas, do not have any important geophysical effect.

Third, the frequency rate of the flare appearence followed by the most spectacular geophysical effects is not proportional to the evolution of the solar cycle as it is computed according to the Wolf number or the 10cm flux. It is obvious in the case of the type IV bursts (L. KRIVSKY, A. KRUGER, 1966) and quite definite in the case of P C A events (Z. SVESTKA, 1966) which occur mostly during the increasing and the decreasing phase of the solar cycle. The philosophy of such a remark comes to the conclusion that the most spectacular geophysical events (and as a matter of fact the flare activity) are by no means linked with the global number of active centers (Wolf number) nor with the 10 cm total flux, but to the time of formation of some specific arrangement of spotted area on the solar disk: for some reason this arrangement is not only the fact of the large number of active centers on the surface of the solar disk.

In view of the forecast of the events, the policy of a forecasting method would consist in predicting the formation of the flaring centers or at least in identifying them as soon as possible as well as following their evolution very closely as to be allowed to forecast the same events. For such a purpose a detailed study of the magnetic structures of the active centers has given us the most exact approach up to now.

Roughly it is possible to classify the solar magnetic field into three classes : a strong magnetic field of several hundred or thousand gauss related to the spotted area, the medium magnetic field between a few tens to a hundred gauss (which is mostly connected with calcium plage) and the weak magnetic fields not so strongly related to the optical features of the disk of the sun.

The weak magnetic field areas have been studied at Mt. Wilson Observatory where experiments on the solar magnetic field are quite a tradition. They seem to be very likely connected with the interplanetary magnetic structures which come to sweep the earth according to the rotation of the sun (N. F. NESS, J. M. WILCOX, 1966). This is of importance as far as the forecast of the recurrent geomagnetic storms is concerned during the decreasing phase of the solar cycle (J. M. WILCOX, N. F. NESS, 1965 ; V. BUMBA,R. HOWARD, 1965).Another interesting element consists of the tendency of the solar activity to follow the stable streams and rows of that kind of weak magnetic field areas (V. BUMBA, R. HOWARD 1969) which is confirmed by previous studies about priviledged longitudes on the sun (M. W. HAURWITZ, 1968; Z. SVESTKA, 1968)but does not keep one from studying the sun with the purpose of determining the date of the events.

The medium magnetic field coincides closely with the calcium plages approaching the isogauss of a few tens gauss (M. J. MARTRES et al 1966) and the inversion line of the longitudinal component is most of the time indicated by a dark filament. The first knots of the flare start along the inversion line (see also G. E. MORETON, A. SEVERNY, 1968). The more complicated the inversion line features are, the larger probability to observe a flare (see also S. SMITH, R. HOWARD , 1968). Sometimes this line is very simple, flare is reported

with the now well described double ribbon shape evolving rapidly into an Y shape (Z. SVESTKA, 1962). These shape and movement have been connected with the process of acceleration of the high energy protons (L. KRIVSKY, 1965) but it is definite that the proton arrivals are reported only for flares on spotted areas and that two ribbons shape is a common feature also of flare occuring on unspotted plages. By the way the flare forecast must be connected with the neutral line feature and also with the sunspot evolution.

The strongest magnetic fields exist in the spotted areas : they give the few precursors of a geophysical event : a gradient (more than0,1Gauss/kilometer) is a good indicator of the coming occurence of a major flare followed by a P C E or by the arrival of 100 Mev protons recorded by balloons or satellites near the earth's atmosphere (S. I. GOPASIUK et al. 1963).

The cooperative study of the solar active regions sponsored by the commission X of IAU gave us the required material for a more precise study of the flare process connected with this spot feature. For a long time it has been evident that there exists a strong relation between the flares and the evolution of the spotted regions as well as their configuration (R. G. GIOVANELLI, 1939). A very carefull study of the hourly evolution of the individual spots in connection with their magnetic polarity (M. J. MARTRES et al. 1968 a, b) and with their magnetic flux (E. RIBES, 1969) allows to establish that the flares occur when two magnetic structures of opposite polarity are close to each other and each of them evolves the opposite way: that is one increasing, the other decreasing in term of total flux or field evolution.

Combining all these results it is definite that the forecast of the flares with their importance and their geophysical effect comes mostly from the precise study of the medium and strong magnetic field data.

The general philosophy of these various results could be specified. The identification of the magnetic areas which are the basic structures of the active centers is the first approach in view of any forecast of the solar activity. Magnetic observations easy to be reduced as well as correlated optical features are the complementary material to use.

The second step consists in the prediction of their future evolution. It involves the forecast of the building of any new " active structure " i. e. a group formed by two spots of opposite polarity very close to each other and the prediction of the way each of its magnetic areas evolves, in view of the flare process.

The last point is that this forecast must involve the evolution of the unspotted plages and of the smallest units of the spotted active areas: these last ones can, as a matter of fact, be very good producers of flares (M. J. MARTRES et al. 1966).

Practically we cannot forecast the place nor the date of birth of any new active center : <u>we must start from its very first appearance and only forecast its evolution.</u>

The complexity of an active center is strongly related to the remnant magnetic field and to the place of the two basic new polarities amongst the existing magnetic areas (M. J. MARTRES, 1968). It makes the regular evolution of a bipolar group change and can promote the anomalous growth of its following part.

The most interesting situation is the almost simultaneous birth of several groups at about an equal longitude and with a slight difference of latitude : they grow very fast, and because of the differential rotation they can give birth to a very wide active configuration. The birth of a new group at the right place near a decreasing active center can produce many flares. Some spots can also move inside a group of spots (Mc INTOSH, 1968) and we cannot avoid the possible influence of other groups at distance from the former (L. KRIVSKY, V. OBRIDKO, 1969) .

The experiments carried out aboard satellites or space probes can give interesting material.

The X ray experiments give new interesting data : our knowledge concerning the detailed solar spectrum is at its beginning concerning its link with the active centers, but for several years we have been collecting the SOLRAD observations for each ten minutes Pass, which give the flux through several windows well distributed among the X ray spectrum. The variation of a colour index between the 1 - 8 Å and 8 - 20 Å flux is a good indicator of the increasing activity (R. MICHARD, E. RIBES, 1968) and the report of a flux on the band 0,5 - 3 Å seems to be the index of the formation of an active configuration (A. CHAMBE, 1969).

A difficult problem comes from the understanding of the observed increase of the flux of the low energy protons (around a few Mev). They are connected with the report of flare producer centers (C. Y. FAN et al. 1968) and the fastimpulses of the fluxe are mostly connected with the flare occurence.

One can also admitt that the report of this flux is more strongly linked with the structure of the interplanetary magnetic field than with an unusual activity of the sunspots group (K. A. ANDERSON, 1969). By the way the prompt report of such increase of the flux is an indication of an easy way for the particles to travel from this place to the earth: in fact during such a permanent flux, sometimes the flares are linked with an increase of the energy of the particles and the low energy flux move suddenly in a P C E and in an high energy event.

According to this scientific basis the forecaster works exactly as the intelligence of a man, using his memory of the past events and his knowledge of the actual status in view of the forecast of the future evolution.

For most of the scientists interested in cosmic ray physics or in space science research, the surprising aspect of a solar forecasting center is the large amount of data flowing day and night for the forecast. In fact this large number of contributing institutions is a problem that we cannot avoid. Until now we cannot forecast the solar activity just with few censors operating day and night: it is the fact of the complexity of the solar activity, of our ignorance of many involved process and also of the effect of the weather on the optical data. We must have an active cooperation between the technicians of the contributinginstitutes and their regional forecasting centers and between the regional warning centers themselves. The data must be sent from the observing stations to the forecasting centers as soon as possible after the observation or sometimes they must be reported on real time. The forecasting centers must exchange their data and supply the centers situated in the dark terrestrial hemisphere. All this coopera-

tion has been arranged by the International Ursigram and World Day Service since 1962 and by its parent services since 1938 under the leadership of U R S I . The last code booklet describing the service and its possibility has been issued this year thanks to U N E S C O assistance.

The obtained data are combined and could be used according to several methods in accordance with the process adopted at each forecasting center.One report can be used for several purposes but most of the time several reports must be used in order to interpret correctly just one event or the evolution of one active center. This point is certainly the most difficult task of the forecasters and several techniques are used in order to help them.

Another difficulty comes from the lack of information on the back side of the solar disk. First of all, some events can have an effect at the earth: the 28 January 1966 event is supposed to be of this kind Second, an active center passing the East limb must be evaluated as soon as possible in terms of its past activity and it is not easy: the perspective effect prevail a good study of the center and the magnetic field cannot be measured before about the 60 ° heliographic longitude. It gives a bad value at the forecast of the east limb activity. Fortunately most of the important events like P C E and high energy proton arrival have an east-west asymmetry and very few solar events at the east limb could disturb the earth's atmosphere apart the S I D effect.

Another limit of the forecast is the importance of the birth of an active center near a decreasing one or of any simultaneous births of several active centers very close together. These two kinds of circumstances could produce a fast evolving center and in fact prevail of any valuable forecast several days in advance. Surely when the solar disk is free of any active region or has just a few scattered decreasing centers the probability of an increase of the solar activity is very low but a complex of regions could turn at the east limb and give X ray bursts and S I D and new births on the disk could produce also many events of this kind after one or two days. The general increase of the activity on all the solar disk is a well known aspect of the solar activity and we ignore why and when it would happen. The passage of a privileged active longitude can increase this possibility but as long as we will ignore when and where an active center will appear, it is only this first appearance which will give a possibility of estimating the importance of this birth.

What is the practical efficiency of a forecast based on this scientific background with the actual circulation of solar data? Due to the delay of the final publication of the solar data and to the amount of the involved work we have just checked up the last three months period of the available Quartely Bulletin of the Solar Activity (July / September 1968) at the Meudon forecasting center. We issue the forecast according to four class of activity (see I U W D S Code Booklet):

A CALM CENTER had less than one flare or confirmed subflare a day.
Several flares or subflares occured daily on the ERUPTIVE CENTERS.
The Geophysical Events are reported on the ACTIVE CENTERS.
The PROTON CENTERS could accelerate a flux of high energy protons (20 Mev or more) .

During this period the rate of the right forecast of the solar activity has been of 82 % and if we consider as a wrong forecast the report of a kind of activity more important than the forecasted activity, the rate of the wrong forecast has been of 7,3 %. One can

see in table I that the solar activity has not been so low during this period.

Another check up has been related to the events: during the last year (June 1968 / April 1969) about a third of the Outstanding Events have been forecast on time, but when we have in mind the difficulty of a prediction of the limb events (especially the East limb) and with the overestimated forecasts, 70 % of the outstanding geophysical events and 50 % of the high energy proton events have been predicted.

It is obvious that the forecast of the solar activity works now with a strong scientific basis and it will improve surely in the future. My own feeling is that at this time the ionospheric forecasters do not know really the actual value of the forecast of the solar activity issued by the solar forecasters. May be, the point is only that the solar forecastersdon't issue their forecast in a useful form for them : anyway a closer cooperation would contribue to a better solution of these problems and the purpose of this paper is of contributing to usefull discussions on these problems.

References.

ANDERSON K. A. , 1969, Solar Physics 6, 111.
ARNOLDY R. L., KANE S. R., WINCKLER J. R. 1968, Proc IAU Symposium Nr 35, p. 490
AVIGNON Y. MARTRES M. J. PICK M. 1964, Ann. Astrophys. 27, 23.
AVIGNON Y. MARTRES M. J. PICK M. 1966, Ann. Astrophys. 29, 33.
BOISCHOT A. 1958, Ann. Astrophys. 21, 273.
BUMBA V. HOWARD R. 1965, Ap. J. 141, 1502.
BUMBA V, HOWARD R. 1969, Solar Phys. 7, 28.
CAROUBALOS C. 1964, Ann. Astrophys. 27, 333.
CHAMBE A. 1969, Solar Phys. in press.
DODSON H. HEIDMAN W. 1960, Astron. J. 65, 51.
DODSON H. HEIDMAN W. 1964, Science, 143, 237.
FAN C. Y. PICK M. PYLE R. SIMPSON J. A. SMITH D. R. 1968, J. G. R. 73, 1555.
HAURWITZ M. W. 1968, Ap. J. 151, 351.
I U W D S Code Booklet, Boulder.
KRIVSKY L. 1965, BAC 16, 27.
KRIVSKY L. KRUGER A. , 1966, B A C,17, 243.
KRIVSKY L. OBRIDKO V. 1969, Solar Phys. 6, 418.
KUNDU M. R. 1959, Ann. Astrophys. 22, 1.
LE SQUEREN A. M. 1964, Ann. Astrophys. 27, 183.
MALVILLE J. M. SMITH S. F. 1963, J G R,68, 3181.
MARTRES M. J. MICHARD R. SORU-ISCOVICI I. TSAP A. 1968 a Proc. UAI Symposium Nr 35 p. 318.
MARTRES M. J. MICHARD R. SORU-ISCOVICI I. TSAP A. 1968 b Solar Phys. 5, 187.
Mc INTOSH P. S. Proton Flare Project, 1968, IQSY Annals 3, in press.
MICHARD R. RIBES E. 1968, Proc. UAI Symposium Nr 35 p. 420.
MORETON G. E. SEVERNY A. 1968, Solar Phys. 3, 282.
NESS N. F. WILCOX J. M. 1966, Ap. J. 143, 23.
OBAYASHI T. 1962, J G R,67, 1717.
PICK - GUTMANN M. 1961, Ann. Astrophys. 24, 183.
SIMON P. 1960, Ann. Astrophys. 23, 102.
SVESTKA Z. 1962, B A C,13, 190.
SVESTKA Z. 1966, B A C,17, 262.
SVESTKA Z. 1968, Solar Phys. 4, 18.
TANAKA H. KAKINUMA T. 1964, Rep. Ion. Res. Japan 18, 32.
WILCOX J. M. NESS N. F. 1965, J G R , 70, 5793.

TABLE I

		REPORTED ACTIVITY				Sum of the Forecasted Activity
		Calm	Eruptive	Active	Proton	
FORECASTED ACTIVITY	Calm	435	41	4	0	480
	Eruptive	35	25	4	1	65
	Active	9	5	1	0	15
	Proton	0	0	1	0	1
Sum of reported Activity		479 85,4%	71 12,6%	10 1,7%	1 (0,17%)	561

Table 1.
The daily forecast activity of any spotted active center (lines) at the time of the reported activity (column) from July 1st to September 29th 1968. During this period 287 subflares, 118 flares importance 1, 34 importance 2 and one importance 3 occured and 13 of them have been accompanied by noticeable centimetric bursts.

TABLE II

		REPORTED ACTIVITY	
		Active	Proton
FORECASTED ACTIVITY	Calm	3	0
	Eruptive	1	2
	Active	5	0
	Proton	5	2
	At The Limb	3	2
Sum of reported activity		17	6

Table 2.
The forecast activity (lines) at the time of the reported events (column) from June 1968 to April 1969. The events are only those looking as outstanding events according to the available data at the end of May 1969.

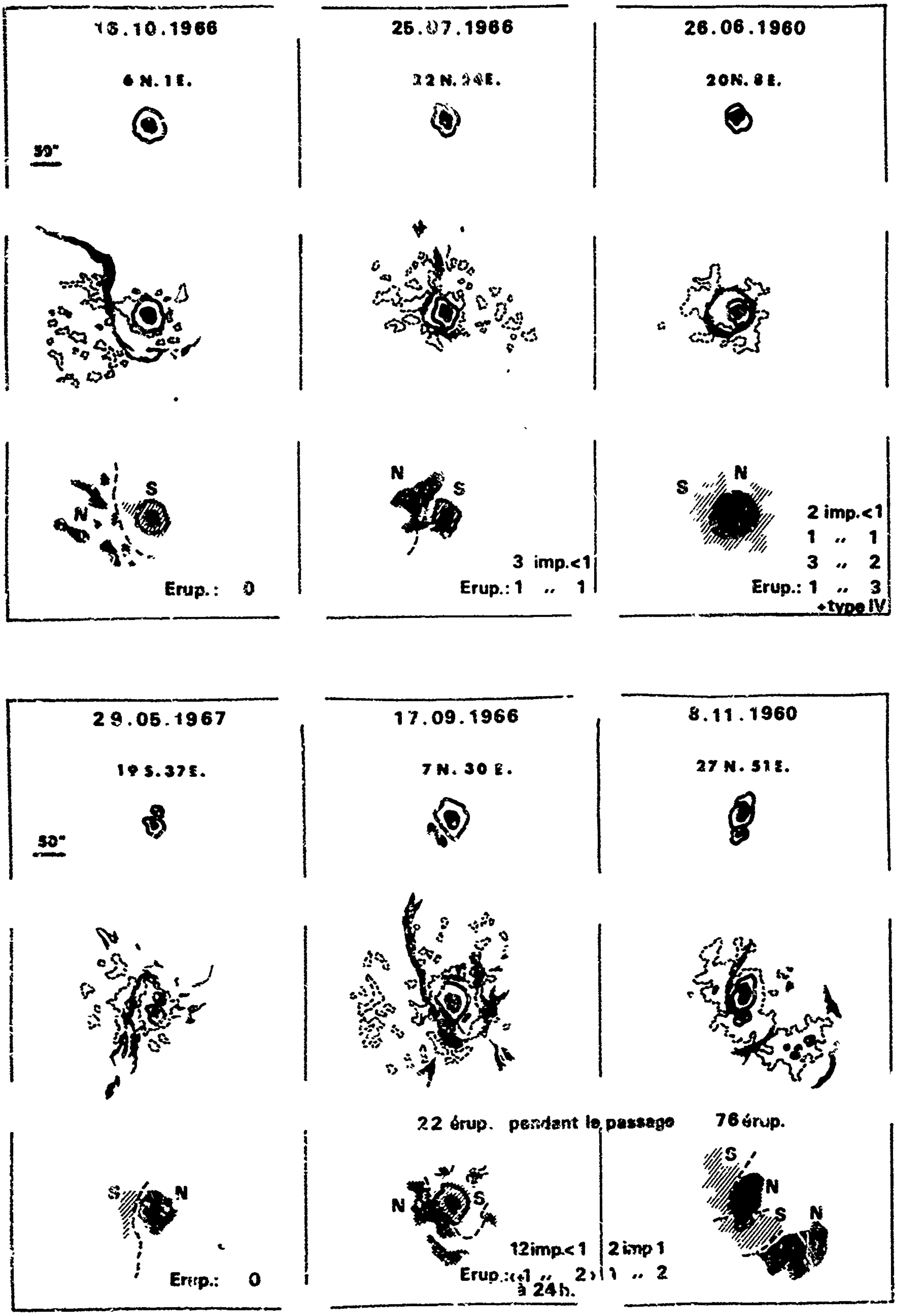

Figure 1 and 2.
Two sets of data in order to demonstrate the importance of the magnetic field data for the forecast. The sunspots (top of the figures) are very similar but the features of the calcium plages and filaments have many differences (medium) that the magnetic field data specify (at the bottom) . The flare activity during the disk crossing is reported.

PREDICTIONS OF SOLAR FLARE ACTIVITY BASED

ON SOLAR X-RAY ENERGY FLUX MEASUREMENTS

by

D.M. Horan and R.W. Kreplin

E.O. Hulburt Center for Space Research
Naval Research Laboratory
Washington, D.C. 20390

SUMMARY

X-ray and particle emission during solar flares can sufficiently increase the electron density in the lower ionosphere to cause disruption of high frequency radio communications. For several years the Naval Research Laboratory has been using satellite-borne detectors to measure solar x-ray energy flux in the 0.5-3A, 1-8A, 8-20A, 1-20A, and 44-60A bands. The daily data sample covers from thirty to ninety minutes over a twenty-four hour span. Based on these measurements, statistical criteria have been established to predict periods of high solar activity during which solar flares capable of disrupting communications might occur. A study of the occurrence of Class 2 or greater flares over a twenty-three month period shows that these large flares are four times more likely to occur when the criteria are met than when they are not met. This result is quite promising considering the sparse x-ray data with which the criteria were formulated.

Predictions of Solar Flare Activity Based on Solar X-Ray Energy Flux Measurements

D. M. Horan and R. W. Kreplin
E. O. Hulburt Center for Space Research
Naval Research Laboratory
Washington, D. C. 20390

I. SOLAR EVENTS AND IONOSPHERIC DISTURBANCES

It is generally agreed that ionospheric disturbances which disrupt radio communications can be caused by x-ray and particle emission from solar flares. Figure 1 demonstrates the close relationship between the x-ray emission from a Class 2B solar flare and a short wave fadeout (SWF) which occurred on October 31, 1968 The x-ray data presented in the figure were obtained from the Naval Research Laboratory's SOLRAD 9 Satellite. The short wave data were obtained from a HF sounder link between California and Hawaii and were made available by the Naval Weapons Center Corona Laboratories. Between 2200 and 2237 UT, the radio data show the normal lowest useable frequency to be between 11 and 12 MHz. At 2237 UT the short wave fadeout begins and becomes complete across the HF band by 2303 UT. By 2332 UT the short wave fadeout has ended and the normal lowest useable frequency is again available for communication. Note that the commencement of the SWF coincides with an x-ray energy flux of approximately 8×10^{-3} ergs/cm^2/sec for the 1-8A band and the peak x-ray flux levels coincide with the totality of the SWF.

There are two important mechanisms by which solar flares can affect the ionosphere. Solar x-rays having wavelengths less than 8A are able to penetrate to the D region. Since these harder x-rays dissipate their energy by ionizing atoms and molecules, the increased emission of these relatively short wavelength x-rays during solar flares results in increased electron concentration in the D region and an effective decrease in altitude for the lower edge of the ionosphere. The higher electron concentrations cause increased absorption of HF signals passing through the D region and the change in altitude of the lower edge of the ionosphere affects VLF signal propagation. X-ray induced ionospheric changes are greatest at the subsolar point and decrease with distance from this point. The time lag between the detection of a solar flare by optical or x-ray sensors and commencement of x-ray induced ionospheric changes is a matter of seconds and the effects generally last less than one hour with occasional disturbances lasting two or three hours.

Changes in the D region are also caused by the increased emission of charged particles during solar flares. As the charged particles approach the earth, they are guided toward the polar regions by the earth's magnetic field. This results in an increased electron density in the lower altitudes of the polar regions and absorption of HF radio signals passing through the polar regions. This phenomenon is called a polar blackout or a polar cap absorption (PCA). Although PCA's are generally confined to the auroral zones, unusually intense solar particle bombardment can cause them to spread to lower latitudes. In 1956 a PCA spread to within 30 degrees of the equator, although its effects were still most pronounced and long lasting at higher latitudes.[1] The time lag between the detection of a solar flare and the onset of a PCA varies from several hours to a day or two, if the PCA occurs at all. Although PCA's are due to solar flares, only a few flares, and not necessarily the largest, produce them. However, when a PCA does occur, it lasts for several days.

II. HISTORY OF NRL SOLAR X-RAY PROGRAM

The existence of solar x-rays and their interaction with the ionosphere had been independently suggested in 1938 by Hulburt[2] and Vegard[3]. In 1949, NRL began a systematic study of solar x-ray emission by means of rocket-borne detectors. Burnight[4], using photographic film packets, first presented evidence for the existence of solar x-rays, although the intensities claimed are incompatible with the fluxes known today. Definitive detection was first obtained by Friedman et al.[5] using x-ray sensitive Geiger counters in September 1949. Experiments by Chubb et al.[6] disclosed that x-ray emission during solar flares was capable of penetrating to the lower ionosphere and was a more reasonable cause of sudden ionospheric disturbances (SID) than was solar Lyman Alpha emission.

Because of the impossibility of observing the initial phases of solar flares by rocket-borne instruments and because of the short duration of the individual rocket flights, earth satellites were used to carry the NRL x-ray detectors beginning with SOLRAD 1 in June 1960. The data from SOLRAD 1 demonstrated that,

if the solar x-ray flux in the band of wavelengths shorter than 8A is less than approximately 2 x 10^{-3} ergs/cm^2/sec, no short wave fadeout would occur. Data from SOLRAD 7B, which was launched in March 1965, showed gradual rises in the energy flux levels of several wavelength bands prior to the sudden large increase which characterizes the flare itself. This was one of the first indications of the possibility of using gradual x-ray changes as a precursor to solar flare activity.

The first five successful SOLRAD Satellites, SOLRADS 1, 3, 6, 7A, and 7B, depended entirely on real-time telemetry, and solar x-ray monitoring could be conducted only when the continuous satellite transmissions could be received and recorded by some ground station. Since there are insufficient ground stations to provide telemetry reception over complete satellite orbits, a serious loss of solar data resulted. To decrease this data loss, SOLRAD 8 (1965-93A) was equipped with a core memory to record samples of solar x-ray data at five minute intervals. Unfortunately the data storage system failed within a month after launch and thereafter only real-time data acquisition was possible as in the cases of the previous satellites. SOLRAD 9 (1968-17A), which was launched on March 5, 1968 is equipped with a core memory to record samples of solar x-ray data at one minute intervals. The SOLRAD 9 memory has worked faultlessly for over fifteen months and continues to provide a wealth of excellent data. A complete description of the spacecraft and its experiments can be found in NRL Report #6800 titled "The NRL SOLRAD 9 Satellite, Solar Explorer B, 1968-17A."

III. SOLRAD 9 DATA DISPLAY FORMAT

Figures 2 and 3 are examples of the manner in which the SOLRAD 9 data are displayed. Figure 2 shows a plot of the real-time solar x-ray data obtained from SOLRAD 9 during the month of July 1968. The x-ray emission is plotted in units of ergs/cm^2/sec on a logarithmic scale with the scales appropriate to each band indicated along the margin. Starting at the top of the plot, the four horizontal lines present the x-ray energy flux in the 44-60A, 8-20A, 1-8A, and 0.5-3A bands. The conversion from the output current of the x-ray detectors to energy flux units for the 44-60A band assumes a 0.5 x 10^6 K color temperature; the 8-20A and 1-8A conversions assume a 2 x 10^6 K color temperature; and the 0.5-3A conversion assumes a 10 x 10^6 K color temperature for the emitting solar region. The abscissa is linear with the integers denoting days of the month. The times at which data are plotted correspond to the times of satellite passes over the NRL ground station.

Figure 3 shows the solar x-ray data for July 5, 1968 which were stored in the satellite's memory. The regularly spaced data gaps of about thirty minutes duration indicate periods of satellite night. The top data curve represents the solar emission in the 8-20A band and the next lower curve represents the solar emission in the 1-8A band. The third curve from the top represents emission in the 0.5-3A band but this curve is quite intermittent because the 0.5-3A solar emission is generally below the threshold level of the detector. The x-ray emission is plotted in units of ergs/cm^2/sec on a logarithmic scale with the scales appropriate to each band indicated along the margin. The abscissa is linear with the integers denoting hours of Universal Time (UT). Charged particle interference with the x-ray detectors, which can cause the plotted flux levels to be higher or lower than the actual flux, is indicated by the lowest data line which is labeled "Background Counts". The number of "counts" is obtained by digitizing the current generated in the 0.5-3A detector by penetrating charged particles when the detector is facing away from the sun. Counts of 10 to 15 indicate no particle interference with the detectors. Counts of 20 to the maximum value of 127 indicate increasing amounts of particle interference. However, the data processing computer program rejects data obviously contaminated by particle interference and this feature causes randomly spaced data gaps of less than 30 minutes duration.

IV. SOLAR X-RAY EMISSION

X-rays, especially in the shorter wavelengths, are not uniformly emitted from the solar disc. Data from five rocket flights during a total solar eclipse on October 12, 1958 and an x-ray photograph obtained with a pinhole camera on April 19, 1960 clearly showed that most of the solar x-ray emission comes from discrete active regions.[7] The locations of these active regions generally coincide with areas of enhanced H alpha and Calcium K line emission, sunspots, and high magnetic fields. More recent x-ray data taken during the eclipse of May 20, 1966 show that the shorter the wavelength of the x-ray band observed, the more localized are the sources of the x-ray emission within the active regions.[8] It has also become clear that solar flares generally occur within these active regions.

The change in solar x-ray emission accompanying the birth of such an active region or the rotation of an existing active region onto the visible portion of the solar disc is shown in Figures 2 and 3. In Figure 2, the apparent discontinuity in the x-ray data lines between the 0430 and 2035 UT satellite passes over the NRL ground station on July 5 was caused by the east limb transit of an active region while the satellite was out of range of our ground station. On July 6 a Class 2B flare and on July 8 a Class 3B flare originated in this region and these events were among the largest x-ray flares recorded. The data obtained during the transit of this active region were stored in the satellite's memory and are presented in Figure 3. The data of Figure 3 show that the flux levels were essentially constant until about 0300 when the rise in energy flux indicated the beginning of the active region's rotation onto the visible portion of the sun. Between 0200 and 0300, the average value of the 1-8A and 8-20A flux was 3.8×10^{-4} and 7×10^{-3} ergs/cm^2/sec respectively. The active region continues its transit without flare activity until approximately 1800 UT when a series of subflares occurs. Between 1700 and 1800 the average values of the 1-8A and 8-20A flux have risen to 9.9×10^{-4} and 1.2×10^{-2} ergs/cm^2/sec respectively. Therefore, the east limb transit of this active region, without flare activity, doubled the 8-20A flux and tripled the 1-8A flux. These increases in x-ray energy flux levels are the basis of our predictions of solar flare activity.

V. CRITERIA FOR SOLAR-FLARE-ACTIVITY PREDICTIONS

The problem of using only data obtained in real-time during a satellite pass over a ground station to establish basic criteria for solar-flare-activity predictions and then comparing the daily data with these predictions is similar to the problem of guessing the information contained in a paragraph when only a few nonsequential words are known. The pattern of data available was such that 10 minutes of continuous data would be followed by 90 minutes of no data. This pattern would be repeated from three to eight times each day; then there would be a data gap of 12 to 20 hours until the daily cycle started repeating again. Frequently, there is no way to tell with certainty whether a 10 minute data sample represented the x-ray output of the active nonflaring sun or the x-ray output during the slow decay of a solar flare. In both cases the data show relatively constant flux values of moderate magnitude for the 10-minute pass. If the flux values change greatly over 10 minutes or if they are relatively constant but very large in magnitude for several minutes, it is safe to consider them as the output from a solar flare. If they are constant and of very small magnitude, it is safe to consider them as the background output from the nonflaring sun.

The interpretation of a sample of data as originating from a flaring or nonflaring sun is extremely important, because the prediction criteria are tied to slow variations in the background x-ray flux values. Study of solar x-ray data acquired over several months showed that there generally is a slow rise in the background x-ray flux values prior to the onset of a period in which numerous solar flares will occur. Therefore, interpreting high background data as of flare origin would fail to generate an appropriate alert, and interpreting isolated flare data as of background origin would generate an unnecessary alert.

The first set of criteria, which was used from August 1966 to early 1967, is as follows:

1. Generally rising but variable flux levels in the 8-20A and 1-8A bands.
2. 1-8A flux levels exceeding 1×10^{-3} ergs/cm^2/sec.
3. Observation of 0.5-3A flux above the 2.0×10^{-6} ergs/cm^2/sec lower limit of the detector.

When all of these criteria were met, it was possible to state with some certainty that a period of solar activity was to be expected during which solar flares capable of producing significant ionospheric disturbances might occur. The fact that these criteria were not met did not preclude the occurrence of a few isolated flares, but, in general, they were good indicators of expected solar-flare-activity. Evidently the gradual rise in the background x-ray flux levels to fulfill the criteria is due to an increase in x-ray emission from an active region as it becomes capable of spawning flares. Although the mere presence of an active region on the visible portion of the sun does cause enhanced background x-ray emission, enhancement sufficient to fulfill the criteria seems to signify something more. Indeed, if it did not signify more, the criteria would not be of much value since the presence of active regions can be more easily verified by optical observations. But since many active regions cross the visible disc without producing major flares, the mere presence of an active region does not mean that flares are imminent. The fulfillment of the x-ray criteria seems to be a way to differentiate between an active region in a relatively dormant, nonflaring state and an active region in a more violet, potentially flaring state.

The first revision of the criteria was not a real change but merely a further quantization of the original criteria. These criteria were first used in early 1967 and are as follows:

1. An increase in the background level of the 1-3A flux by a factor of 10 to 20.
2. An increase in the background level of the 8-20A flux by a factor of 5 to 10.
3. Consistent observation of the 0.5-3A flux above the 2.0×10^{-6} ergs/cm^2/sec level.

As the more active phases of the solar cycle were entered, the minimum background levels encountered began creeping upward. This is due to the sun being rarely devoid of active regions in the phases of the solar cycle approaching solar maximum. Since the difference between low and high background flux levels was smaller, the large increases in background level required to meet the criteria were no longer encountered, and a new set of criteria was needed. The criteria established in early 1968 are as follows:

1. The background levels of the 44-60A flux rises to 2.3×10^{-1} ergs/cm^2/sec or greater.
2. The background level of the 8-20A flux rises to 1.3×10^{-2} ergs/cm^2/sec or greater.
3. The average background level of the 1-8A flux rises to 1.0×10^{-3} ergs/cm^2/sec, and the flux levels fluctuate greatly from pass to pass.
4. Flux levels for the 0.5-3A band fluctuate greatly from pass to pass and are generally greater than 1.0×10^{-5} ergs/cm^2/sec.

Generally criteria 1 and 2 were met a day or two ahead of criteria 3 and 4. However, since the difference between normal background levels and the criteria levels was small in these bands, it often happened that criteria 1 and 2 were met not because of a change in a single active region but because there were a number of discrete, relatively dormant, active regions whose x-ray emissions in these two bands were additively fulfilling the criteria. Therefore, more weight was given to criteria 3 and 4. With the exception of criteria 1, these criteria are still in use. Criteria 1 is not used because of the failure of the 44-60A experiment on SOLRAD 9 in February 1969. Also, there are now times when there are so many active regions on the visible disc that even criteria 3 can be met by adding their x-ray emission contributions. Therefore, greatest weight is now given to criteria 4. The increased significance which must be given to the higher energy bands seems to indicate that a hardening of the emission spectrum may be an essential characteristic as an active region changes from a relatively dormant to a more violent state. This may be an important clue in further improving the prediction criteria.

VI. ACCURACY OF SOLAR-FLARE-ACTIVITY CRITERIA

We wish to examine the usefulness of the solar-flare-activity prediction criteria as employed during 1967 and 1968. The only predictions of solar-flare-activity that NRL actually makes are quite informal and primarily for internal use. Only one person is generally available to make the predictions, and since he is available only 40 hours a week, the nature of the operation is limited. Because of the limited nature of the operation and the discontinuous nature of the x-ray data available, there are many instances where alerts, i.e. positive predictions of solar-flare-activity should have been called but were not. Therefore, actual alerts called are not the best means of testing the accuracy of the criteria. As an alternative, it seems reasonable to compare the number of a selected type of event which occurred on days on which the flare-activity-criteria were met with the number which occurred on days when the criteria were not met. This approach assumes that if a round-the-clock operation had been in effect with continuous real-time data immediately available, an alert would have been called as soon as the background flux levels fulfilled the criteria. This is reasonable, because with the continuous data the background levels would be readily identifiable, and there would be no need for a day or two delay to be certain that observed high flux levels were really background and not isolated flare activity. This alternative approach would examine the validity of the premises on which the prediction operation is based without being tied to the actual predictions which were made and without becoming hopelessly involved in the handicaps under which the rudimentary system was operating.

The next step is to determine what type of event is to be selected as a measure of the accuracy of the criteria. There are three choices: ionospheric disturbances, x-ray events, and solar flares of Class 2 or greater. Although it

would be of great operational significance if the fulfillment of the solar x-ray flux criteria were found to be an accurate predictor of SWF and PCA activity, our lack of complete and reliably interpretable ionospheric disturbance data for the period of test makes the choice of ionospheric disturbances a poor one. Although solar x-ray events are really what NRL is trying to predict and although they have a direct connection to SWF's, the choice of x-ray events is also a poor one because of the incompleteness of available data. The main source of data on x-ray events is the very same data which were used as the bases of NRL's flare activity predictions. These data are extremely discontinuous so that confusion between isolated x-ray flare events and high background levels could easily bias the study. When processing of the stored data from SOLRAD 9 is completed, the choice of x-ray events as a measure of the accuracy of the criteria will be a good one.

This leaves us with the choice of Class 2 or greater solar flares. Good data on solar flares are obtainable for the 1967-1968 period. Although there is no necessary connection between solar flare class and the x-ray emission from the flare, it is usually true that higher flare classifications yield higher x-ray fluxes. Therefore, there is a connection between flare class and ionospheric disturbances, although it is more remote than in the case of x-ray events.

In summary, the accuracy of the criteria will be measured by comparing the number of flares of Class 2 or greater which occurred on days when the solar-flare-activity criteria were met with the number of such flares which occurred on days when the solar-flare-activity criteria were not met.

The Environmental Science Services Administration's series of bulletins IER-FB, titled "Solar-Geophysical Data" was used as a source of information on the date of occurrence and classification of solar flares. The date of occurrence of all Class 2 or greater solar flares occurring between January 1, 1967 and November 30, 1968, was listed. The data for January through December 1967 were obtained from the Revised Solar Flare lists appearing in the volumes IER-FB-275 through 286. In examining these data it was noted that certain stations frequently observed Class 2, 3, and even Class 4 flares at times and places where no other station observed even a subflare. In such cases the flare was counted but was labeled "Questionable." A flare was counted without question if some event was detected by two or more stations and the general consensus of the several observing stations was that a Class 2 or greater flare. This consensus was determined by the group classification given in the tables. The data for January through November 1968 were taken from the Confirmed Solar Flare lists in the volumes IER-FB-287 through 297. The confirmed list differs from the revised list in that questionable flares have been removed from the confirmed list. Therefore, all flares of Class 2 or greater listed in the confirmed lists were counted without question. Table 1 gives a summary of the dates of occurrence of Class 2 or greater solar flares as obtained from the ESSA publication. The portion labeled "All Listed Flares" includes questionable flares and those accepted without question. The numbers appearing in parentheses after a date denote the number of flares when more than one occurred on the same day.

Table 2 identifies the dates on which our solar x-ray data indicate that the criteria clearly are and are not met, the dates on which it is questionable whether the criteria are met, and the dates for which there are no data. The criteria presently being use, i.e. those established in early 1968, were used in compiling Table 2. Questions as to whether the criteria are met arise not only in cases where the flux levels are extremely close to the levels noted in the criteria but also in cases where problems with the SOLRAD 8 spacecraft caused the flux values to be somewhat unreliable. Dates for which there are no data include some dates on which there were data, but the data were too sparse to render a decision.

Table 3 follows directly from the data shown in Tables 1 and 2. It shows the number of Class 2 or greater flares occurring on days when the solar-flare-activity criteria clearly are, possibly are, and clearly are not met, and the number of flares occurring on days when there are no x-ray flux data available. The data presented in Table 3 indicate that, whether you consider all listed flares or just those this study has accepted without question, a Class 2 or greater flare is approximately four times more likely to occur on a day when the solar-flare-activity criteria are met than on a day when the criteria are not met. At the present state of development of this prediction system, this result is considered to be quite promising.

VII. POTENTIAL FOR IMPROVEMENT

The information contained in Table 3 indicates that the solar-flare-activity prediction system, as it is presently used, identifies periods of increased solar-flare activity with sufficient accuracy to warrant continued study of solar x-ray

Table 1

Dates of Occurrence of Class 2 or Greater Solar Flares

Month	Day	Total
	ALL LISTED FLARES	
January 1967	10, 11, 14, 29, 31	5
February	3, 4, 6, 7(2), 13, 18, 22(6), 23(2), 24(2), 27(2)	19
March	6, 20, 22, 26, 30, 31(2)	7
April	1(4), 3, 9(2), 11(2), 20, 28, 30	12
May	2, 3(4), 4, 5, 6(2), 8(2), 10, 13, 19(2), 21, 23(5), 25, 26, 27, 28(3)	27
June	4, 5	2
July	2, 11(2), 22, 24, 25(2), 26, 28(2), 29(4), 30, 31(2)	17
August	1, 4, 6, 9, 12(2), 19(3), 20, 21, 23, 24, 25, 29(2)	16
September	1, 17(2), 18, 19, 20, 28	7
October	8, 13, 19, 20(2), 30(2), 31(2)	9
November	11(3), 13, 16(3), 20(2)	9
December	1, 2(2), 11, 13(2), 15(2), 16(2), 27(2)	12
January 1968	4, 5, 9, 14, 15, 20, 31	7
February	1, 2(2), 10, 15(2)	6
March	25, 27	2
April	--	0
May	--	0
June	9(2), 13, 26	4
July	6, 8, 9, 12, 20	5
August	3, 8(2), 21, 23	5
September	26, 28(2), 29(2)	5
October	3, 4, 21(2), 23, 27, 29, 30(2), 31	10
November	1, 2(2)	3
		189
	QUESTIONABLE FLARES	
January 1967	10, 11, 31	3
February	7, 22(2)	3
March	--	0
April	3, 9, 30	3
May	3(2), 5, 6, 19(2), 23	7
June	--	0
July	2, 11(2), 22, 25(2), 28(2), 29, 30, 31	11
August	12, 20, 25	3
September	20	1
October	13, 19, 20(2), 30(2), 31(2)	8
November	11(3), 13, 20	5
December	1, 2(2), 13, 15(2), 16	7
		51

Table 2
Dates on Which Solar-Flare-Activity Criteria Are, and Are Not, Met

Month	Dates on Which Criteria Are Clearly Met	Dates on Which Criteria Are Possibly Met	Dates on Which Criteria Are Clearly Not Met	Dates on Which No Data Were Obtained
January 1967	30-31	--	15-29	1-14
February	23-28	22	--	1-21
March	1, 30-31	2, 29	--	3-28
April	1-3	--	4-19	20-30
May	19-29	--	15-18, 30-31	1-14
June	1-4	--	18-30	5-17
July	29-31	--	1-5	6-28
August	1-2, 5, 14, 17-21	3-4, 6	7-13, 15-16 22-24	25-31
September	25-26	--	15-24, 27-30	1-14
October	27-30	26, 31	20-25	1-19
November	10, 26, 29-30	4-5, 11-12, 20, 27-28	1-3, 6-9, 13-19, 21-25	--
December	1-2, 15-30	3, 14, 31	4-13	--
January 1968	1-17, 28-31	26-27	18-25	--
February	1-4, 8-11, 19-22 25-26	5-7, 23-24, 27-29	12-18	--
March	1-2, 28	27	3-26, 29-31	--
April	28	--	1-27, 29-30	--
May	18-19, 25, 30	15-17, 20, 22, 24	1-14, 21, 23, 26-29, 31	--
June	25	8-9, 20	1-7, 10-19, 21-24, 26-30	--
July	5-10, 29	--	1-4, 11-28, 30-31	--
August	11-17, 20-22	--	1-10, 18-19, 23-31	--
September	3-4, 8-9, 25-26, 28-29	21	1-2, 5-7, 10-20, 22-24, 27, 30	--
October	15-23, 26-31	--	1-14, 24-25	--
November	1-4, 18-19	17, 25	5-16, 20-24, 26-30	--
Total Days	159	41	338	162

Table 3

Comparison of Flare Occurrence for Days on Which Criteria Are, and Are Not, Met

	Flares Occurring	Number of Days	Flares Per Day
		ALL LISTED FLARES	
Days on Which Criteria Are Met	83	159	0.52
Days on Which Criteria Are Possibly Met	20	41	0.49
Days on Which Criteria Are Not Met	40	338	0.12
Days on Which No Data Were Obtained	46	162	--
		UNQUESTIONED FLARES ONLY	
Days on Which Criteria Are Met	66	159	0.42
Days on Which Criteria Are Possibly Met	11	41	0.27
Days on Which Criteria Are Not Met	33	338	0.10
Days on Which no Data Were Obtained	28	162	--

flux levels as indicators of flare activity. Fortunately, one of the most significant factors to be considered now in evaluating this system, is its tremendous potential for improvement. Suitably complete and continuous records of solar x-ray emission are available only since the launch of NASA's Orbiting Geophysical Observatory 4 (OGO 4) in July 1967, which carried NRL's Solar X-Ray Monitoring Experiment and produced useful data until January 1969. Continuous x-ray data were also obtained between October 1967 and May 1968 from the NRL Wheel X-Ray Experiment on NASA's Orbiting Solar Observatory 4 (OSO 4), and between March 1968 and the present from NRL's SOLRAD 9 Satellite. Processing and preparation of these data is now in the final stages and detailed analysis is expected to begin shortly. The analysis of these data will have several goals. First, it is clear that the direct application of the presently used criteria to the continuous data obtained from a satellite memory does not use these data in the most advantageous manner. Therefore, the data will be studied to identify solar-flare-activity criteria appropriate for use with continuous data. Second, the data will be studied to identify precursors to individual, specific flares rather than general periods of increased flare activity. Third, the data will be studied to more quantitatively establish the relationship between solar x-ray flux levels and various x-ray induced ionospheric events. Fourth, the possibility of identifying a relationship between solar x-ray flare signatures and increased near-earth proton fluxes and their ionospheric effects will be kept in mind while studying the data. This goal will be given less emphasis than those previously mentioned because it is less likely to be successfully achieved using experiments which are not capable of some degree of spatial resolution on the solar disc. The continuous x-ray data will also be available to other investigators who are interested in using them for similar or other studies.

The possibility that experiments with better spectral or spatial resolution would provide more useful information should also be investigated. NRL's X-Ray Spectrometer Experiment aboard the OSO-4 Satellite has provided a considerable number of spectrometer scans within the 1-8A band during both quiet and flaring periods.[9] NRL x-ray spectrometer experiments on the OSO-G Satellite, which is scheduled for launching in July 1969, will be able to scan the solar emission over the 1-25A band. Data from these experiments will be studied to identify discrete spectral lines having characteristic changes which can be used as precursors to solar flares. Experiments which provide spatial resolution by forming an image of the sun in some x-ray line or band would enable an investigator to study the birth, growth, changes, and death of individual active regions on the sun. Such data would be studied to identify characteristic changes in the x-ray emission from a specific region as it transforms from a relatively dormant to a more violent state and finally spawns solar flares.

If, at each stage of improvement described, a suitable precursor to solar flares or ionospheric disturbances is successfully identified, it would ultimately be possible to use a set of satellite-borne detectors having high spatial, spectral, and temporal resolution, which would be aimed at active solar regions of interest and whose data would be continuously transmitted to a central forecasting laboratory, as the basic sensors of a flare or ionospheric disturbance forecasting system. It is readily admitted that several investigations will have to be successfully concluded before such an ultimate system is possible. However, it is important to emphasize that the accuracy of the system, as it is now used, clearly indicates that present investigations to improve the system should be continued and paths along which these investigations should be directed are clearly recognizable.

REFERENCES

1. H. J. Smith and E. Smith. "Solar Flares", New York: MacMillan, p. 242, 1963.
2. E. O. Hulburt, Phys. Rev. 53, 344 (1938).
3. L. Vegard, Geophys. Pub. 12, 5 (1938).
4. Friedman, Lichtman, and Byram, Phys. Rev. 83, 1025 (1951).
5. T. R. Burnight, Phys. Rev. 76, 165 (1949).
6. T. A. Chubb, H. Friedman, R. W. Kreplin and J. E. Kupperian, Jr., Nature, 179, 86 (1957).
7. R. W. Kreplin, Annales De Geophysique. 17, 151 (1961).
8. H. Friedman, Astronautics and Aeronautics, January 1968, p. 16.
9. J. F. Meekins R. W. Kreplin, T. A. Chubb, and H. Friedman, Science, 162, 891 (1968).

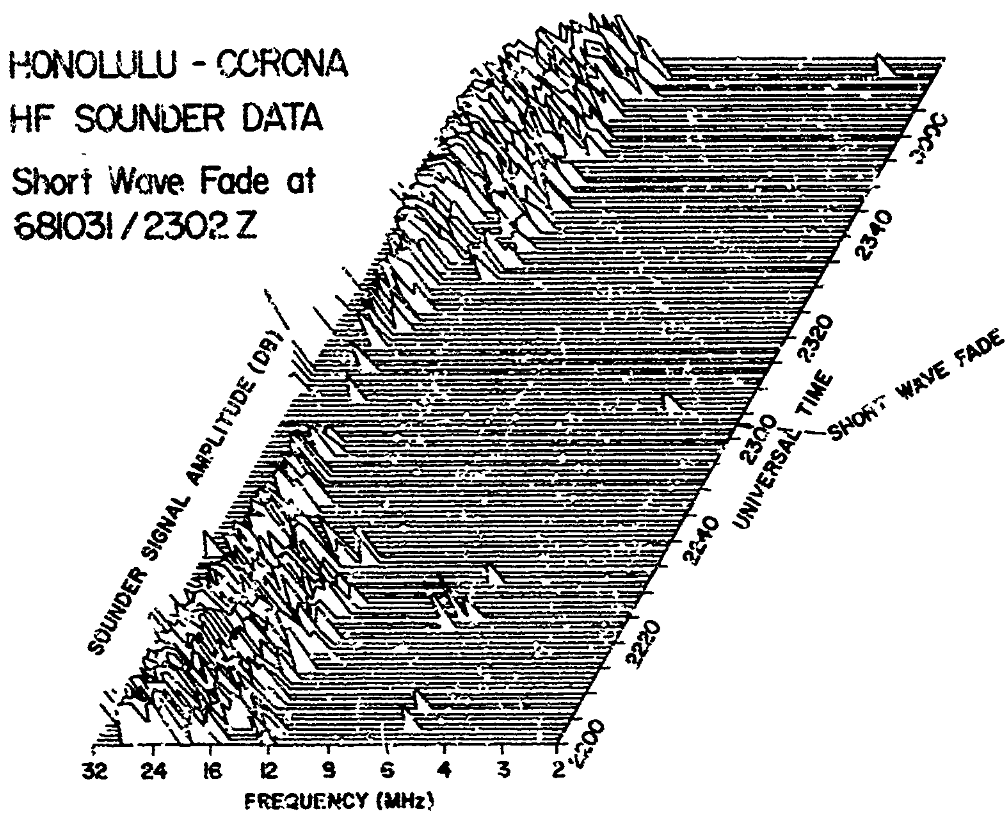

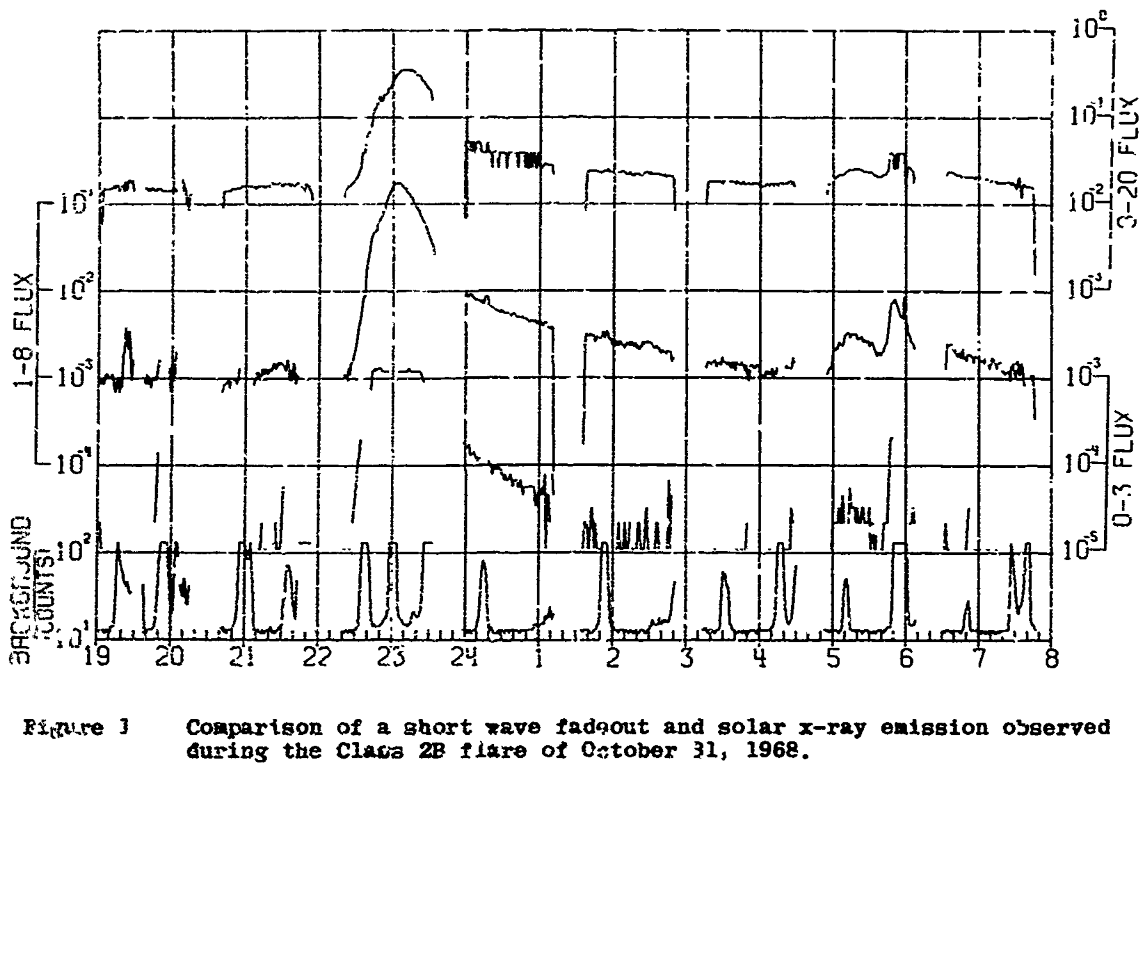

Figure 3 Comparison of a short wave fadeout and solar x-ray emission observed during the Class 2B flare of October 31, 1968.

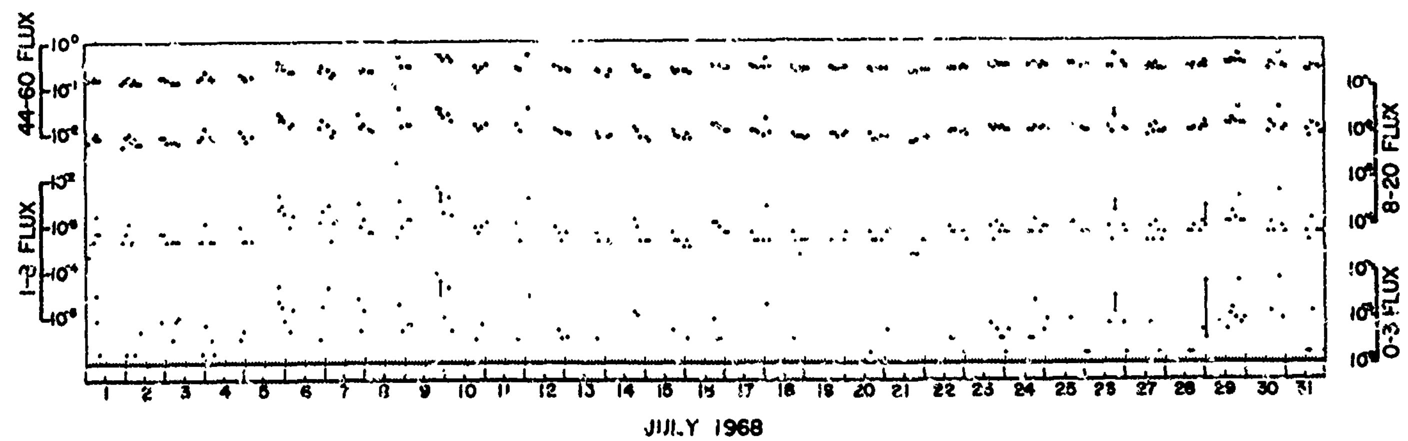

Figure 2 Solar x-ray data received in real-time from the SOLRAD 9 satellite during July 1968.

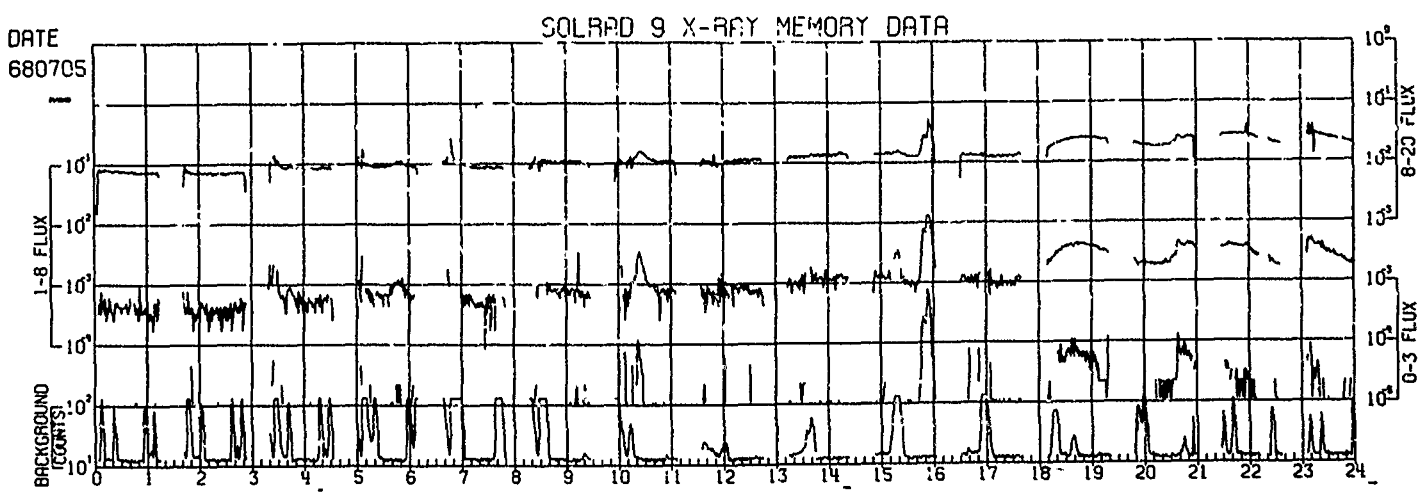

Figure 3 Solar x-ray data for July 5, 1968.

LONG RANGE SOLAR FLARE PREDICTION

by

J.B.Blizard

The University of Denver

SUMMARY

Prediction of solar proton events is essential for the space program. Traditional methods have not solved the problem. Therefore an unconventional approach was taken. A high correlation was found between planetary conjunctions and proton events during 1956-1961. Although a correlation can be demonstrated with individual conjunctions, proton events usually occur after sequences of conjunctions of the planets Mercury, Venus, Earth and Jupiter. A trial prediction method has been attempted since 1965 indicating the dates of the 14-day passage of proton active centers. During the last 3 years the Sensitivity was 63% and the Reliability was 70%, despite the fact that proton events were predicted during only 22% of the total time, using only 5 parameters. Although the theoretical interpretation is not clear at this time, it does not detract from the predictive value of such a method. Proton events have been shown to be related to the positions of four planets which possibly affect the tidal force on the sun or other solar system dynamic variables.

LONG RANGE SOLAR FLARE PREDICTION

J. B. Blizard, Ph.D.*

The University of Denver

Prediction of solar flare proton events is of utmost importance for the space program. The space crew could receive a lethal radiation dose from a single event. Communications are disrupted by polar cap blackouts and by ionospheric disturbances caused by the accompanying solar X-rays. Although many statistical studies dealing with solar events have been made, there is little hope for improvement in prediction capability when these studies are based only on traditional interpretations. The understanding of basic solar physics must be improved, not necessarily our statistical methods. Therefore an unconventional approach was taken in the study of major events of solar cycle 19.

A very high correlation was found between planetary conjunctions and proton events during 1956-61. The probability of such correlation occurring by chance alone is less than 5 in 10,000 using a standard contingency test. Proton events take place on the second or later 27-day passage of an active sunspot group, so positions of the tidal planets - Mercury, Venus, Earth and Jupiter - are observed for a two-month period. Although a correlation can be demonstrated with individual conjunctions, proton events usually occur after sequences of conjunctions of the planets Mercury, Venus, Earth and Jupiter. Occasionally other planets are involved if conjunctions of three or more planets occur. During the two month period preceding major solar events, the number of conjunctions of the four tidal planets is 2 or 3 times the average for a two month period. The concentration of conjunctions is definitely non-random before the solar events. Active longitudes on the sun must also be considered. The northern hemisphere of the sun has three active longitudes, appearing at different times during the 11-year cycle. (Trotter and Billings, 1962)(Warwick, 1965).

The outstanding members of any phenomenon are always worth special study for clues that may throw light on the general behavior of the whole class. Therefore outstanding proton event centers on the sun have been studied in detail. Four active sunspot centers produced 90% of the proton flux during the years of peak solar activity 1956-1961. Each of these active centers caused one or more ground level event (GLE), high energy proton events detected at sea level by neutron monitors. The four centers were responsible for the following major polar cap events (PCE):

23 February 1956; 10, 14, 16 July 1959; 12, 15, 20 November 1960; and 11, 12, 18, 20 July 1961.

In each case the major PCE's followed a sequence of tidal planet conjunctions. Each active center consisted of a giant magnetically complex sunspot group (area >1000 millionths) with a large penumbra enclosing umbrae of opposite polarity, located at an active longitude.

We shall discuss below each of these active centers in turn, utilizing 10 cm. radio flux as an activity indicator. X-rays are a more sensitive indicator and are the direct cause of ionospheric disturbances, but have been monitored only recently. Therefore we will also discuss two active centers of 1966 in cycle 20 in terms of both radio and X-ray flux.

ACTIVE CENTER OF FEBRUARY 1956. The ground level event (GLE) of 23 February 1956 was the highest energy proton event during cycle 19. A giant sunspot stream was first observed on the sun in January. On its second rotation the area had grown to 2410 millionths of the solar hemisphere, with a large bright plage (measured in the light of ionized calcium). The active sunspot group was centered at the Carrington Longitude $L_o = 190°$. The delta configuration (umbrae of opposite polarity in the same penumbra) was present in several parts of the stream. Ninety-eight flares were observed from the active group during its three most active 14-day passages. (The sun's rotation period as viewed from the earth is about 27.3 days; any given sunspot group would be visible from the earth for half of the rotation period, usually reckoned as 14 days.) The sunspot group had a complex magnetic field with maximum field strengths of up to 4000 gauss. On 23 February 1956 the proton flare caused a short wave fadeout (SWF) lasting seven hours. A radio burst lasting 50 minutes was recorded on 10 cm. wavelength. The recorder went off scale, indicating a peak flux in excess of 4700×10^{-22} watts/m^2 (c/s). Bursts were also recorded at 200 Mc/sec, 85 Mc/sec and 20 Mc/sec. The polar cap absorption (PCA) which followed was the first ever observed on the dark hemisphere of the earth.

The longitudinal zone 180°-210° on the northern hemisphere of the sun has been the location of nearly all significant active centers early in the 11-year cycles 18, 19 and 20. Usually only one longitude is active above 20° latitude, and most proton events and active centers early in the cycle form at high latitude. Thus the same Carrington longitude was the location of active centers which produced GLE's on 25 July 1946, 23 February 1956 and 7 July 1966.

On 6 January 1966 a Mercury-Venus conjunction took place in alignment with the active longitude on the sun (Fig. 1). The 10 cm. radio flux was elevated at that time (Table 1) although no important active centers were on the visible hemisphere. The active center which later produced the GLE appeared for its first passage on 13 January and was visible until 26 January. On 31 January a Mercury-Jupiter conjunction occurred opposite (180° away) the active longitude, and the 10 cm. flux was elevated for 5 days (Table 1) although other sunspot groups were now present. Ten cm. radio emission increased 20% upon the appearance of the giant active center in February. However, a major increase of 40% in 10 cm flux took place at the time of the triple conjunction of Earth, Jupiter and Pluto on 16 February in alignment with the active center. While the increase in solar activity was

*Research Physicist

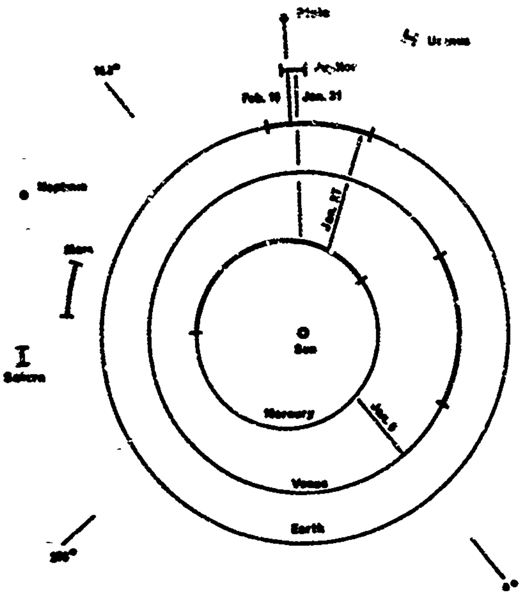

Fig. 1. Planetary Configuration One Month Prior to Proton Event of 23 February 1956.

Conj. Date	Planets	$L_o = 190^o$
Jan 6	Mercury Venus	x
Jan 27	Mercury Earth	
Jan 31	Mercury Jupiter Pluto	x
Feb 16	Earth Jupiter Pluto	x

Table 1. Ten-cm. Daily Radio Flux for January February 1956. Units, 10^{-22} Watts m^2 (c/s). Passages of the Active Center are shown, and the dates of significant conjunctions.

Date		January		February
1		-		114
2		128		116
3		125		116
4		123		116
5		116		106
6		120		103
7	Me-V conj	$\boxed{124}$		107
8		122		109
9		116		116
10		112	E Limb	121
11		116		133
12		124		154
13	E Limb	135		163
14		136		185
15		156		219
16		161	E-J-P conj	$\boxed{240}$
17		170		248
18		177		251
19		174		248
20	CMP	173		244
21		174		236
22		181		229
23		177		204
24		174	W Limb	178
25		153		-
26		137		154
27	W Limb	124		142
28		121		143
29		109		157
30		107		-
31	Me-J conj	$\boxed{110}$		-

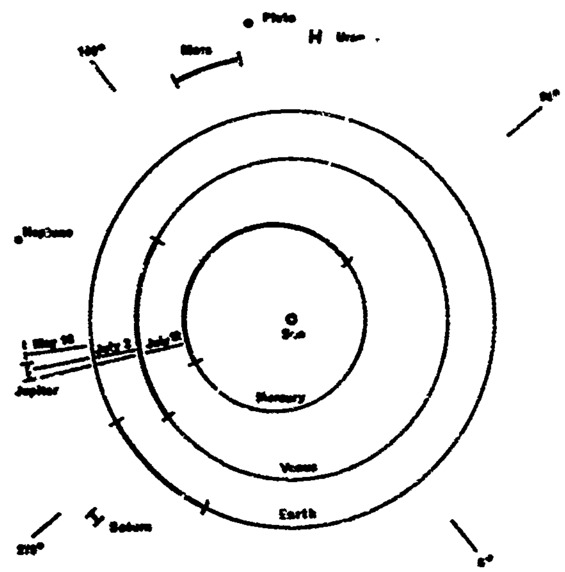

Fig. 2. Planetary Configuration One Month Prior to Proton Events of 10,14,16 July 1959

Conj. Date	Planets	$L_o = 330^o$
May 18	Earth Jupiter	x
Jul 2	Venus Jupiter	
Jul 12	Mercury Jupiter	x

Table 2. Ten-cm. Daily Radio Flux for June, July 1959. Units, 10^{-22} Watts/m^2 (c/s). Passages of the Active Center are shown and the dates of the significant conjunctions.

Date		June		July
1		193	V-J conj	$\boxed{188}$
2	Me-E-J conj	$\boxed{198}$		$\boxed{174}$
3		$\boxed{198}$		171
4		190		177
5		197		176
6		210		188
7		198		192
8		213	E Limb	185
9		223		185
10	E Limb	228		-
11		226		194
12		220	Me-J conj	$\boxed{234}$
13		212		243
14		208		264
15		225	CMP	245
16		220		261
17	CMP	225		240
18		228		231
19		237		222
20		226		208
21		228		189
22		219	W Limb	178
23		220		178
24	W Limb	232		181
25		233		182
26		238		182
27		240		200
28		224		205
29		219		207
30		196		204
31		-		208

clearly noticeable on centimeter wavelengths, the rise was much more striking on the more collimated meter waves. On 16 February, increases took place in mean daily flux of up to an order of magnitude on all frequencies from 81 Mc/s to 200 Mc/sec (Quarterly Bulletin, IAU). An increase of up to 100% took place on meter wavelengths also at the time of the Mercury-Earth conjunction on 27 January, but the change in 10 cm. flux cannot be isolated from the passage of the active center at west limb.

ACTIVE CENTER OF JULY 1959. Late in May 1959, a region developed behind the active center that produced a PCA flare on 10 May. On the second passage in June the complex spot group of area 1110 millionths produced a few large flares but then activity declined. Just before the third passage there were loop prominences, surges and short wave fades indicating reviving activity (Bruzek,1964). On the July passage the area had grown to 2100 millionths with a bright plage of area 12,000 millionths at N16 and Carrington Longitude $L_o = 330^o$. Major proton events occurred on 10, 14 and 16 July, with the 14 July event producing the highest particle flux during a three year period. The 14 and 16 July flares covered all but one of the prinicpal umbrae. Umbral coverage has been noted as a condition for proton events and major radio bursts (Dodson and Hedeman, 1964). Umbrae of both polarity were contained in the same penumbra, and had magnetic fields of up to 3200 gauss. Severe SWF's accompanied all three events. The 16 July event was also associated with sudden enhancement of atmospheric (SEA) and sudden cosmic noise absorption (SCNA) (Ellison et al., 1961). Ten cm. radio bursts occurred on 9 July (peak flux 490 times mean daily flux), 14 July (120 times mean) and 16 July (6500 times mean) (Solar Geophysical Data).

The 1959 July events came midway in the 19th solar cycle and was of lower energy than the February 1956 event, although a high flux of particles resulted. On 18 May 1959 there was a conjunction of Earth and Jupiter and the sunspot group formed about this time. The Carrington longitude $L_o = 330^o$ where the proton events later originated was in line with the Earth-Jupiter conjunction (Figure 2). Activity appeared to be dying out on the June passage but probably revived following the Venus-Jupiter conjunction on 2 July. The revived spot group appeared at east limb on 8 July and grew rapidly to an area of 2100 millionths, one of the largest spot groups in cycle 19. A proton event took place on 10 July. On 12 July the solar longitude $L_o = 330^o$ was in alignment with the conjunction of Mercury and Jupiter, and two GLE's followed on 14 and 16 July. The 10 cm. radio flux was elevated on the days of the Mercury Earth Jupiter conjunction on 2 June and at the time of the Venus-Jupiter conjunction on 2 July (Table 2). The Mercury Jupiter conjunction occurred during continuous major activity and therefore the increase in radio flux is ambiguous. Again, the increases on meter wavelengths were more impressive, but the generally high fluctuating radio emission during the peak of the 11-year cycle makes interpretation difficult.

ACTIVE CENTER OF NOVEMBER 1960. The active region was observed first in October with moderate activity, loop prominences, and yellow coronal line emission. When the region reappeared on 4 November the spot group was very large and complex with a very bright plage.

The Large Sunspot Group - at N 26^o reached a maximum area of 2330 millionths on 13 November, although the maximum plage area of 9200 millionths was observed on 10 November. (HAO Summary.) The Carrington longitude of the F type group was $L_o = 30^o$, one of the three northern active longitudes. The 15 November flare was observed in white light. The two principal umbra were completely covered by both the 12 and 15 November flares (Dodson and Hedeman, 1964). On 12 November the peak fields were north - 2800 gauss, and south - 2700 gauss, but by the time of the flare of 15 November the maximum fields had declined to north - 2500 gauss and south - 1500 gauss, and were unobservable on 20 November. The sunspot type was complex (γ), and the large penumbra enclosed umbra of opposite polarity (the delta configuration). Short wave fadeouts of great severity accompanied all three proton events. Radio Noise - on 10 cm. was outstanding on 12 November with a rare great burst of 5500 flux units, possibly related to the umbral coverage. Type IV emission accompanied all three events.

The active region appeared in early October, following the conjunction of Mercury and Venus on 25 September (Figure 3). The Mercury Jupiter conjunction on 7 October was in alignment with the active center of the sun, and radio emission of up to 100 times average was observed over frequencies from 67 Mc/s to 234 Mc/s for four days following the conjunction. The emission was also elevated on 2800 Mc/s on 7 October (Table 3). Further enhanced radio emission was noted on 17 October, the date of the Venus-Jupiter conjunction (Table 3) and within two days on all frequencies between 67 Mc/s and 234 Mc/s (Quarterly Bull. IAU). On 7 November an inferior conjunction and transit of Mercury took place, and a small radio burst occurred over the active center on that day, according to the radio interferometer observations at 169 Mc/s (Solar Geophysical Data). The correlation between significant conjunctions and elevated solar radio emission is particularly striking for the November 1960 events because of the bursts accompanying the 7 and 17 October conjunctions.

ACTIVE CENTER OF JULY 1961. The active center produced proton events on 11, 12, 20 and 21 July on the second rotation. The maximum area of the giant sunspot group was 1570 millionths on 12 July with a bright plage of area 5100 millionths. The longitude was 70^o, a southern active longitude. The sunspot magnetic field was the complex (γ) type with field strengths of 2100 and 1500 gauss, with three north and 1 south umbrae in a large single penumbra on 12 July (the delta configuration). Short wave fadeouts were observed on many frequencies, persisting for 2 hours on the 18th and 7 hours on the 20th, an abnormally long period for a short wave fade (SWF). On 20 July, other unusually strong ionospheric effects were noted, including SEA and SCNA (Bruzek, 1963). Strong radio bursts on 2800 Mc/s occurred on 12, 18 and 20 July. The peak fluxes were 6000, 2400 and 1800 flux units (10^{-22} watts/m^2 (c/s). The meter bursts on 200 Mc/s were 22,000, 1000, and 4000 flux units on the same three days (Bruzek, 1963). Intense X-ray emission was detected directly by the Injun I Satellite (Van Allen et al., 1965). The counting rate increased to 3 times normal on 18 July and

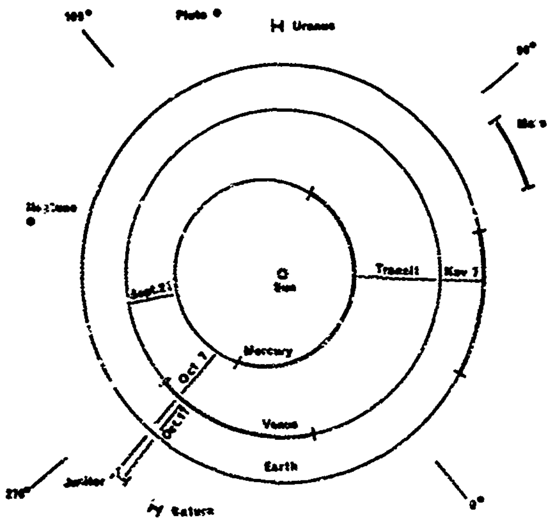

Fig. 3. Planetary Configuration One Month Prior to Proton Events of 12, 15, 20 November 1960.

Conj. Date	Planets	
Sep 24	Mercury	Venus
Oct 7	Mercury	Jupiter
Oct 17	Venus	Jupiter
Nov 7	Mercury	Earth

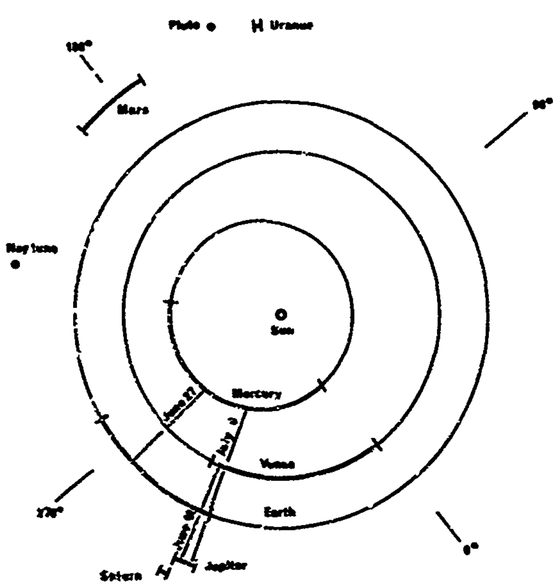

Fig. 4. Planetary configuration One Month Prior to Proton Events of 11-21 July 1961.

Conj. Date	Planets		
Jun 12	Venus	Jupiter	Saturn
Jun 27	Mercury	Earth	
Jul 6	Mercury	Jupiter	Saturn

Table 3. Ten-cm. Daily Radio Flux for October November, 1960. Units, 10^{-22} watts m^2 (c/s). Passages of the Active Center are shown, and the dates of significant conjunctions.

Date		October		November
1		115		124
2		112		129
3		120		130
4		132		131
5		132	E Limb	144
6		132		148
7	Me-J conj	144		157
8		143		168
9	E Limb	151		175
10		159		200
11		152		188
12		159		168
13		162		180
14		166		192
15	CMP	165		183
16		165		174
17	V-J conj	167		164
18		154	W Limb	153
19		153		150
20		149		147
21		144		139
22	W Limb	141		127
23		134		116
24		129		113
25		130		111
26		132		117
27		132		119
28		122		117
29		131		119
30		128		131
31		127		-

Table 4. Ten-cm. Daily Radio Flux for June, July 1961. Units, 10^{-22} watts/m^2 (c/s). Passages of the Active Center are shown, and the dates of conjunctions.

Date		June		July
1		86		104
2		88		99
3		92		104
4		89		103
5		86	Me-J conj	106
6		88		102
7		89	E Limb	105
8		91		107
9	E Limb	100		112
10		102		124
11	V-J conj	110		138
12		108		137
13		114		141
14		123	CMP	136
15		129		136
16		132		132
17	CMP	137		137
18		136		131
19		131		126
20		131		123
21		132		118
22		134		119
23		135		118
24	W Limb	117		118
25		111		117
26		108		115
27		99		111
28		95		105
29		102		103
30		103		92
31		-		91

50 times normal on 20 July in the wavelength band 0-14Å (hard X-rays) in synchronization with the two flares described.

The planetary configuration for the month preceding 11 July is shown in Fig. 4, and significant conjunctions are listed below. The time of Jupiter-Saturn conjunction is felt by many authors to be significant for solar activity. Ten cm. radio emission was elevated on 11 June, the day of the Venus-Jupiter conjunction (Table 4). 25 days later (one solar revolution) the Mercury-Earth conjunction took place. During the first week of July 1961, the five major tidal planets - Mercury, Venus, Earth, Jupiter and Saturn - were within 40° longitude of each other. On 6 July a significant conjunction took place between Mercury and Jupiter and radio emission was elevated (Table 4). The sunspot group grew rapidly following that date.

ACTIVE CENTER OF MARCH 1966. The first important active center of the 20th cycle appeared in late February 1966 at N 18° and longitude 146°. Previous to the appearance of Plage 8207, the sunspot number and 10 cm. radio flux had been at a consistently low level. The Zurich sunspot number had been below 50 except for a few days, and many days had been spotless. Following the February passage, the yellow coronal line (indicating $T = 4x10^6$ degrees K in the corona) was observed at west limb, indicating presence of an active center which could produce protons. The longitude was unusual for an active center early in the cycle, but the latitude was low enough to fit the isolines of a longitude group which appeared for 6 earlier cycles. The March 1966 active center produced 146 optical flares and 155 radio bursts on 10 cm (Solar Geophysical Data), and on 24 March produced a proton event. Although activity declined after the March passage, another center approximately 180° away produced frequent 10 cm. radio bursts and flares, resulting in the March-April period being one of the most active radio periods during the entire year. During the March passage the sunspot group had a maximum area 900 millionths on its second passage. The Carrington longitude was 146°, conforming to one of the northern active longitudes. The plage area was 9500 millionths on 22 May. The magnetic field was beta gamma and the spot group was Zurich class G on 24 March. X-ray bursts over 10 times ambient flux in the 0-8Å band were recorded on 15, 17, 20, 23, 26 and 29 March (see Table 5). Radio type IV continuum emission was recorded daily for nine days from the appearance of the active center on 15 March, and a 10 cm. burst of 1550 flux units occurred on 30 March.

On 3 January there was a conjunction of Venus and Jupiter, and on 26 January of Venus and Earth. No opposition of Jupiter and the earth took place, although the two planets were close in longitude in early January. On 13 February a five planet conjunction took place between Uranus and Pluto in opposition to Mercury, Mars and Saturn. The active center developed soon after and was a radio and X-ray source beginning on 21 or 22 February. Yellow coronal line emission from the region was noted on the same date. On 8 March, another 5 planet conjunction took place between Earth, Uranus and Pluto in opposition to Mars and Saturn. On 19 March, four planets were in alignment, Mercury, Uranus, Pluto in opposition to Saturn. Finally on 21 March there was a conjunction between Mercury and the Earth. The 10 cm. radio flux was elevated at the time of the five planet conjunctions on 13 February and 8 March, and again on 19 March and 21 March, two other conjunction dates. The SOLRAD Satellite had been monitoring solar X-rays in 4 wavelength bands. The flux level in the 0-8Å band is shown for February and March 1966 in Table 5. The increase in X-ray flux is much greater on conjunction dates than for 10 cm. radio flux.

ACTIVE CENTER OF JULY 1966. So much has been written about this active center (Svetska, 1968) that only a few highlights will be repeated here. Although the spot group seemed to appear from nowhere on 28 or 29 June, sequential photos show that remnants of plage No. 8331 probably were incorporated in the new plage. The area grew rapidly from less than 100 on 3 July to 1300 millionths on 7 July The bright plage crossed CMP at 3.4 July at N 35° and Carrington longitude $L_0 = 190°$. The 7 July flare covered all but one of the principal umbrae. Umbral coverage has been noted as a condition for proton events and radio bursts (Dodson and Hedeman, 1964). Magnetic fields of up to 3300 gauss north and 3000 south were recorded in the βγ spot group. Umbrae of both polarity were contained in the same large penumbra (the delta configuration). A rapid increase of magnetic flux was noted on 6 July (Svetska, 1968). Significant X-ray emission was detected by satellite. Radio bursts occurred on 10 cm. on 7 July (peak flux 2650 times mean daily flux), (Solar Geophysical Data), accompanied by Type IV synchrotron radiation. The 7 July event was first recorded case of electron emission from the sun.

The 1966 July event occurred early in the 20th cycle, at the one northern active longitude (L_0=190°) of importance at high latitude. As in February 1956 event, the Earth-Jupiter conjunction seemed to be the triggering factor. (Fig. 6). (Table 6). Earlier on 2 June there was a conjunction of Mercury and Jupiter, on 15 June a quadruple conjunction of Mercury-Uranus-Pluto and Venus and finally on 5 July a conjunction of Earth and Jupiter. The Carrington active longitude 190° which produced the proton event was approximately in line with the 15 June quadruple conjunction. On 5 July the date of the Earth-Jupiter conjunction, the active solar longitude $L_0 = 190°$ was again approximately in line with the conjunction. Although the spot group was born on the disk on 29 June, it grew in size rapidly afterwards to a maximum area of 1300 millionths, one of the larger spot groups thus far in cycle 20.

The 10.7 cm. radio flux was elevated on the day of the Mercury-Jupiter conjunction, and increased very significantly at the time of the Earth-Jupiter conjunction on 5 July (Table 6). Again, the increases on meter wavelengths were more impressive, but the generally high fluctuating radio emission during the peak of the 11-year cycle makes interpretation difficult.

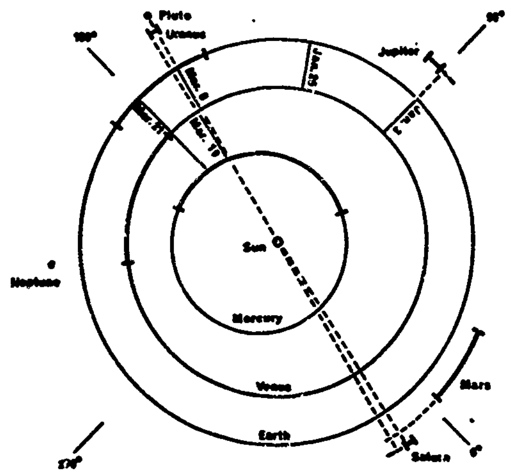

Fig. 5. Planetary Configuration One Month Prior to Proton Event of 24 March, 1966.

Conj. Date	Planets
Jan 3	Venus Jupiter
Jan 26	Venus Earth
Feb 13	Merc. Mars Saturn Uranus Pluto
Mar 8	Earth Mars Saturn Uranus Pluto
Mar 19	Merc. Saturn Uranus Pluto
Mar 21	Mercury Earth

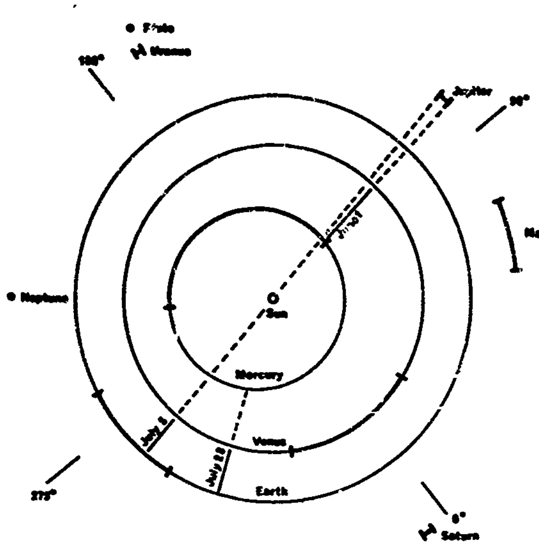

Fig. 6. Planetary Configuration One Month Prior to Proton Event of 7 July 1966.

Conj. Date	Planets
May 27	Mercury Earth
Jun 1	Mercury Jupiter
Jun 14	Merc. Venus Saturn Uranus Pluto
Jul 5	Earth Jupiter

Table 5. Daily X-Ray and Radio Flux for Feb., Mar., 1966. Units: 0-8Å; 10^{-4} ergs/cm^2-sec; 10-cm: 10^{-22} watts/m^2(c/s). The passage of the active center is shown, and the dates of significant conjunctions.

Date		February X-Ray	February Radio		March X-Ray	March Radio
1		0.14	79	W.Limb	11.0	81
2		1.6	79		0.65	78
3		2.0	80		--	77
4		0.65	82		-	77
5		0.35	83		-	76
6		0.30	84		-	76
7		0.60	85		-	76
8		0.33	85		-	77
9		1.30	85	E-Ma-S	3.4	79
10		0.65	85	U-P conj	-	80
11		0.98	86		-	79
12		-	85		-	79
13		-	86		1.9	80
14	M -Ma-U	0.82	86		3.34	82
15	S-P conj	0.65	85		11.7	88
16		0.33	84		5.0	94
17		0.33	84	Me-S-U-	35.0	105
18		0.65	84	P conj	5.4	110
19		-	84		7.1	113
20		-	85	CMP	61.0	114
21		0.98	88	#8207	9.8	120
22		1.6	88		5.1	104
23	CMP #8174	1.6	84		13.0	97
24		0.64	83		8.1	93
25		1.5	81		3.4	90
26		1.1	85		14.0	84
27		4.9	85		6.3	84
28		9.4	85		20.0	87
29		-	-		19.0	95
30	W Limb	-	-	PLAGE	19.0	99
31		-	-	#8223	12.0	110

Table 6. Daily X-Ray and Radio Flux for June, July 1966. Units: 0-8Å:10^{-4} ergs/cm^2 (c/s). The passage of the active center is shown, and the dates of significant conjunctions.

Date		June X-Ray	June Radio		July X-Ray	July Radio
1	Me-J conj	1.6	102		2 4	92
2		1.15	101	CMP	1.4	92
3		1.15	100	#8362	1.3	92
4		1.13	99		1.2	101
5		0.94	99	E J conj	2.0	102
6		1.2	98		1.3	106
7		0.92	94		1.5	110
8		0.96	96		7.3	111
9		1.00	96		14.0	104
10		0.90	93		14.0	105
11		0.85	94		5.1	106
12		1.08	93		4.2	100
13	Me-V-S-U	1.14	93		1.6	97
14	P conj	1.4	93		1.7	97
15		0.79	92		1.7	98
16		0.68	94		1.6	99
17		0.67	96		1.6	98
18		0.65	96		1.1	98
19		0.58	94		1.1	98
20		0.92	92		1.3	98
21		0.84	91		1.9	100
22		0.82	93		1.7	102
23		1.2	96		3.6	111
24		1.3	100		6.5	116
25		2.4	102		5.5	123
26	E Limb	1.04	102		6.0	123
27		1.17	98		3.1	120
28		1.4	98	Me-E	3.9	121
29		1.4	96	conj	3.7	128
30		1.9	97		2.7	123
31		-	-		2.8	121

Table I Proton Events from June 1966 through May 1969 Compared to 120-Day Prediction Ground Level Events are underlined. Parentheses show timing error of less than 4 days.

Year	Predicted 14 d. Periods Starting	Successes	Observed Events (ESSA)
1966	9 Jul	X	<u>9 Jul</u>
	27 Jul	X	28 Jul
	26 Aug	X X	27 Aug, 2 Sep
		X	5 Oct
	12 Nov		
1967	23 Jan	X	<u>28 Jan</u>
	24 Feb	X	11 Mar*
			25, 28 May
	10 Jun	(X)	6 Jun
	7 Aug		
	19 Aug		
	5 Nov	(X)	2 Nov
	13 Dec	X	3, 16 Dec
1968	15 Feb		
	14 Apr		
	24 May	(X)	9 Jun
			3 Jul
	23 Aug		
	22 Oct	X	31 Oct
1969			28 Feb
			30 Mar
	4 Apr	X	<u>10 Apr</u>
TOTAL	17	12	19

*Event on Far Side of Sun

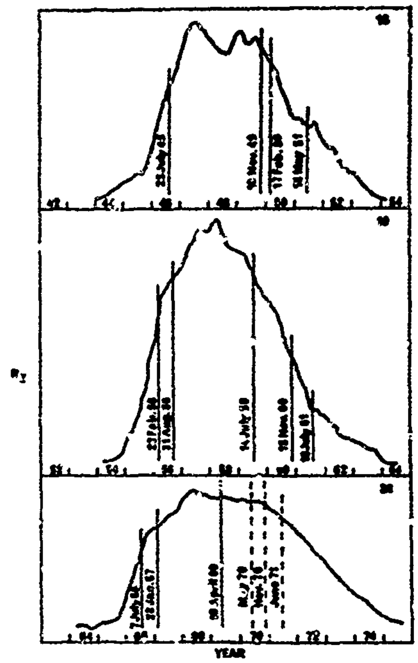

Fig. 7. Major Proton Events of Cycles 18-20, by phase of 11-year cycle. (Fichtel and McDonald, 1967) (Solar Geophysical Data) (Euler 1969) (Blizard 1969).

LONG RANGE PREDICTION, CYCLE 20

A trial prediction method has been attempted over a period of four years, indicating the dates of the 14-day passage of solar active centers which could produce proton events. The forecasts were begun in June 1965, predicting solar activity 120 days in advance. During the first year of forecasting, the active longitudes had not been included, and the method underwent several other improvements. During the latest three years, twelve proton events (PE) have been successfully predicted by the method outlined (Table I). To check the validity of the prediction method we define three ratios. The first, sensitivity (S), is the ratio of the number of correctly predicted PE/total number of PE The second, termed reliability (R), is the ratio of correctly predicted PE/total number of prediction periods. The S and R ratios are commonly used for evaluating predictions, by ESSA personnel among others. The third, alert time (T), is the ratio of the time during which proton events were forecasted/total time. From the totals in Table 1, one can obtain the three ratios for the period from June 1, 1966, through May 31, 1969:

$$S = \frac{12}{19} = 63\% \qquad R = \frac{12}{17} = 70\% \qquad T = \frac{17 \times 14 \text{ days}}{1096 \text{ days}} = 22\%$$

Both the sensitivity (S) and Reliability (R) ratios are high, despite the fact that proton events were predicted only 22% of the total time. Many failures that did occur were due to: (1) the slowly changing active longitudes on the sun, or (2) events taking place on a different passage of the same active center or (3) from events on the far side of the sun, and (4) other planets. Therefore improved Sensitivity and Reliability would result from further study of the longitudes on the sun and the time development of active centers.

Ground level events (GLE) during cycles 18 through 20 are shown in Fig. 7, compared to Zurich smoothed sunspot numbers. Typically one or two GLE's occur early in the cycle 1.5 to 2 years before sunspot maximum, R_m. Two or three active centers produce GLE's late in the cycle, starting at least one year after R_m, and the majority of polar cap absorptions (PCA) occur at this time.

Predictions for the remainder of the 20th cycle are shown with dotted lines in Fig. 7. The predicted smoothed sunspot number is found from a regression formula (Euler 1969) and the GLE dates are estimated from sequences of planetary conjunctions (Blizard, 1969). In the latter case, the total no. of GLE's is also estimated from the overall activity of cycle 20 compared to earlier cycles. The R_m of cycle 20 is about equal to the R_m of cycle 17. On the other hand, the shape of cycle 20 more resembles cycle 18 because both have the same sunspot polarity.

CONCLUSION. Long range prediction of solar activity has now become possible. Proton events have been shown to be related to the positions of Mercury, Venus, Earth and Jupiter, which possibly affect the tidal force on the sun, or the rate of change of solar acceleration in an inertial frame of reference. The lack of a clear explanation at this time of how the planet positions affect solar activity does not detract from the predictive value of such a method. The dates of over 60% of the proton events during the last three years have been predicted in advance, using only 5 parameters.

ACKNOWLEDGMENT. The author acknowledges contract NAS8-21436. Any views expressed are those of the writer and are not necessarily those of NASA Marshall Space Flight Center.

REFERENCES

American Ephemeris and Nautical Almanac, U.S. Naval Observatory, (yearly).

Bigg, E. K., "Effect of Mercury on Sunspot Formation," Astron. J. 72, p. 463 (May 1967).

Blizard, J. B., "Prediction of Solar Flares Months in Advance," Astron. J. 70, p.667 (Nov.1965).

Blizard, J. B., "Long Range Solar Flare Prediction," Astron. J. 73, No. 5 (June 1968).

Bruzek, A., "The Large Flares of July 11, 12, 18 and 20, 1961," in "Physics of Solar Flares," NASA SP 50 (1963).

Castelli, J. P., and Michael, G. A., "Flux Density Measurements of Radio Bursts of Proton-Producing Flares and Non-Proton Flares," J. Geophys. Res. 72, No. 21, pp. 5491-5498 (Nov. 1967).

Dodson, H. W. and Hedeman, E. R., "Problems of Differentiation of Flares with Respect to Geophysical Effects," Planet. Spa. Sci. 12, pp. 393-418 (1964).

Ellison, M., McKenna, S., and Reid, J., "Cosmic Ray Flares," Dunsink Obs. Publ. 1, #5 (1961).

Euler, H. C., "Solar Activity Indices," pp. 188-196, NASA TMX 53782 (Oct. 1968) and "Solar Activity Prediction," (in phase).

Fitchel, C. E., and McDonald, F. B., "Energetic Particles from the Sun," Ann. Rev. Astron. Astrophys. 5, p. 351 (1967).

Head, R. M., "A Triggering Mechanism for Solar Flares," unpublished.

High Altitude Observatory, "Solar Activity Summaries," 1956-61 by D. Trotter and W. O. Roberts.

Jonah, F. C., Dodson-Prince, H., and Hedeman, E. R., "Solar Activity Catalogs, 1954-1963," NASA, Houston.

Jonah, F. C. "Analysis of Polar Cap Absorption Events IV - Almost Necessary and/or Sufficient Condition for Solar Proton Warning," LTV Astro., Div., Report 00.882 (Feb. 1967).

Jose, P. D., "Sun's Motion and Sunspots," Astron. J. 70, No. 3, p. 193 (April 1965).

Malville, J. M., and Smith, S. F., "Type IV Radiation from Flares Covering Sunspots," J. Geophys. Res. 68, pp. 3181-3185 (May 15, 1963).

McDonald, F. B., "Solar Proton Manual," NASA TR R 169, Dec. 1963.

Nelson, J. H., "Planet Position Effect on Short-Wave Signal Quality," Elec. Eng. 421-424(May 1952).

Pimm, R. S., and Bjorn, T., "Prediction of Smoothed Sunspot Number Using Dynamic Relations between the Sun and Planets," Lockheed Report No. HREC-1445-1 (April 1969).

"Quarterly Bulletin of Solar Activity," International Astronomical Union, Zurich, Switzerland.

Sawyer, C., "Statistics of Solar Active Regions," Ann. Rev. Astron. Astrophys. 6, pp.115-34(1968).

Sherry, D. T., editor, "Forecasting Solar Activity and Geophysical Responses," 4WWM 105 1 revised, Ent Air Force Base, Colorado Springs (June, 1968).

Solar-Geophysical Data, ESSA, Dept. of Commerce, Washington, D. C. (monthly).

Svetska, Z., "Proton Flare Project," pp. 513-535 IAU Symp. #35, D. Reidel Publ. Co., Dordrecht, Holland, 1968.

Takahashi, K., "On the Relation between the Solar Activity Cycle and the Solar Tidal Force Induced by the Planets," Sol. Phys. 3, pp. 598 602 (1968).

Trotter, D., and D. Billings, "Longitudinal Variation of a Zone of Solar Activity," Astrophys. J., vol. 136, p. 1140 (Nov. 1962).

Warwick, C., "Longitude Distribution of Proton Flares," Ap. J. 141, pp. 500 504 (1965).

Warwick, C. S., and Haurwitz, M. W., "A Study of Solar Activity Associated with Solar Cap Absorption," J. Geophys. Res. 67, pp. 1317-1332 (1962).

Wood, R. M. and Wood, K. D., "Solar Motion and Sunspot Comparison," Nature 208, pp.129-31 Oct. 9, 1965).

TECHNIQUES OF SOLAR FLARE FORECASTING

by

Patrick S. McIntosh

Environmental Research Laboratories
Environmental Science Services Administration
Boulder, Colorado, USA

ABSTRACT

The Environmental Science Services Administration approach to solar flare forecasting is reviewed and the present forecasting "state of the art" is discussed. The most recent forecasts have shown marked improvement in accuracy and effectiveness in giving warning at least one day in advance of increasing solar activity. Further improvement in forecast performance will depend on: (1) changes in the kind of data reported by the routine solar patrol observatories, (2) an increase in the number of professionally trained forecasters and, (3) the utilization of recent advances in data processing instrumentation.

TECHNIQUES OF SOLAR FLARE FORECASTING

Patrick S. McIntosh

Some solar flares produce enough X-rays to cause ionospheric disturbances. In order to predict these disturbances we must first learn to predict the solar flare. The solar flare is presently defined as a sudden brightening in the solar atmosphere as viewed in hydrogen light. Not all such brightenings produce significant amounts of X-rays or accelerated particles. We must learn to predict which of these brightenings will result in SIDs and ionospheric storms.

This paper is a brief review of flare forecasting techniques that ESSA has examined. Some of the data available to forecasters can be shown to be of no help at all. We will show that the most useful information must presently be evaluated in a subjective manner. There is a need for much more effort on the difficult problem of classifying and quantizing this forecast information.

The relationship between planetary positions and solar activity has been carefully examined at ESSA and we do not find any significant relationship for forecasting (Gray and Sawyer, 1968). Solar activity is not random. The interaction of old active centers and new regions creates persistence and periodicity. Any two periodic phenomena can be compared in a way that appears to show a causal relationship.

Figure 1 presents three commonly-used solar indices for the last quarter of 1968 and shows how they occur relative to the time of major flares. The flare index is derived by adding the number of flares during the day and weighting each flare by its size. The 10.7 centimeter-wavelength radio flux is measured daily at Ottawa. The sunspot number is computed by counting all the spots visible on the sun and adding to it a number ten times the number of sunspot groups. Major flares are those of importance two or greater on a scale of zero to four, based on area of the hydrogen flare.

It appears from this graph that the sunspot number might be a flare predictor since it increases before most of the major flares. We will demonstrate the unreliability of that conclusion below. The history of flare activity show that there is no reliable increase in flare frequency before the major flares. The radio flux averaged over the solar hemisphere, which is a more objective index of general solar activity than the sunspot number, shows the least tendency to correlate with the major flares. Any objective formula which attempts to use these variables for solar forecasting is bound to give poor performance.

The problems with the sunspot number as a predictor can be illustrated by studying Figure 2 and Table 1. The different sunspot R-numbers on the drawings for 30 May and 9 June 1968 are mostly a function of the observer differences. The official Zurich sunspot number was very similar on the two days. This similarity was also reflected in the radio flux, the total area of calcium plage, and the size and type of sunspot groups present. The level of flare activity, however, was very different. On the 30th of May the largest flare was an importance one-normal. On 9 June there were two importance two-bright flares with notable increases in X-ray, radio, and proton radiation. None of the indices in Table 1 predict this difference in activity.

Table 1

	29 May	30 May	8 June	9 June	1968
Boulder R	157	256	178	117	
Zurich R	135	126	119	103	
Ottawa 10.7 cm	151	151	155	149	
Calcium Plage Area	31500	29300	30600	26000	
Flare Index	120	140	210	840	
Largest Flare		1N		2B	

In order to make progress in flare prediction we must understand the physical reasons for flare occurrence. Active centers on the sun are the result of strong, local magnetic fields emerging through the solar surface. Flares occur when these magnetic fields are strong, complex, and changing. With this in mind let us examine the differing structures in the sunspot groups in Figure 2.

Sunspot area has a positive correlation with solar flares and with strong magnetic fields. We might expect that the largest flares on each day occurred in the largest sunspot groups. This was not the case on both of these dates. The one-normal flare on the 30th occurred near a small group in the north-central part of the sun. On the 9th one 2B flare occurred near the large, but simple, spot in the north-east; and the 2B proton flare occurred in the small, decaying group in the south.

Strong magnetic fields are not a sufficient condition for flares. It is also important that the fields be complex with high magnetic field gradients. The largest sunspot groups on these dates were very simple in structure and they apparently were not changing in a way that stores and releases flare energy.

The reasons for the major flares in the two regions on the 9th become apparent when we look at the development of the sunspots leading up to the time of the flares. Figure 3 shows that the region in the north added new spots shortly after appearing at east limb. These spots were opposite in polarity to the large spot. During the days leading up to the flare these spots grew and the distance between them and the main spot diminished. This indicates a steady increase in a high magnetic field gradient across a line of polarity change between an old leader sunspot and the following portion of a new active center. The interaction of new active centers with old centers is the common way of creating complex magnetic field conditions (Martres, 1968).

The region in the south creates the same kind of magnetic field conditions. Although the spots are all small, the close separations of spots of opposite polarity make high gradients across the line of polarity change. The spots within the small penumbra on 6 June form a high gradient which quickly decreases during 8 June as the north-polarity spot undergoes proper motion toward a new spot of south polarity. This movement rapidly builds a new region of high magnetic field gradient in which the major flare occurs.

With just these two examples we see that it is very important to have information on magnetic fields, configurations of spots, and accurate measurements of sunspot growth and sunspot motion. We see in the case of the southern hemisphere region that the region as a whole was decreasing in area and spot count, but one important area was building a high magnetic field gradient. This illustrates the need to look at

portions of regions when we watch for flare conditions. The data being collected today measures either averages over the entire sun or averages over an entire region. It is not surprising that they have poor forecasting value.

Sunspots do not always reveal the reason for a flare. We saw that we had to add magnetic polarity data for the spot evolution to have meaning. Perhaps we could forecast flares with magnetic field data alone. Very likely we could; but magnetic field data is not available often enough nor with enough spatial resolution. There are some expensive magnetographs under development that promise to solve the resolution and availability problems; but, they are already behind schedule, and one or two of these have rescinded their promise to provide data rapidly. Our forecast center must have an alternate source of real-time, solar magnetic data.

We find it is possible with careful interpretation of hydrogen-alpha pictures to infer magnetic data from the pictures that have been a part of the solar patrol programs for decades. Figure 4 shows a picture of some solar active regions enlarged from the solar patrol films at Boulder. This wealth of fine structure forms systems that reveal the orientation and, to some degree, the strength of the magnetic fields. The inferred lines of polarity change are shown below.

In general, active regions in both white light and hydrogen light have a natural tendency to divide their structure according to polarities. Sunspots normally cluster into groups with concentrations at east and west ends and a gap between indicating when the polarities change. The same is true for the bright plage in hydrogen light. Most have a conspicuous corridor at the position of polarity change. In areas without bright plage, the long, dark filaments are the markers of polarity change.

Polarities can be assigned by a simple law that says that the spots on the western side of regions in the northern hemisphere almost always have the same polarity during a solar cycle. Western spots of opposite solar hemispheres have opposite polarities.

This technique for inferring polarities from flare patrol images has been remarkably successful and affords an easy means of patrolling for high magnetic field gradients and watching the evolution of magnetic field configurations. What is lacking now is a procedure for readily placing numerical values on these gradients and configurations. This calls for effort on classification of configurations and ways to quantize inferred magnetic field gradients. We would hope to elicit interest in this area among other forecasters and solar astronomers.

Because the data most useful for forecasting flares is not yet quantitative we must assemble our forecasts in a subjective manner. Although this approach introduces some unwanted human "noise" in our forecasts, we feel it is now the most efficient and most accurate approach to forecasting. Figure 5 shows the forecasts issued during the last quarter of 1968 and the major flares that occurred. This performance is far from perfect, but it is effective for most users of solar forecasts. Most important, the accuracy is better than that obtained by either a persistence forecast or a forecast based on climatology.

We could improve this performance markedly without any further progress in research. We are not yet making full use of the available technology for solar forecasting. In order to increase the effectiveness of our forecasts we need:

(1) Increased automation of data handling and processing so that more of our manpower is available for data analysis.

(2) More applied research on putting sound, subjective forecast techniques on numerical, objective bases.

(3) Continued basic research relating X-ray and particle production to flare structure and active region structure.

(4) An education program in solar activity to enable us to make full use of our limited human resources.

References

Gray, T. and C. Sawyer: 1968, private communication.

Martres, M. J.: 1968, Symposium No. 35 of the I.A.U., 25

Suggested Reading

Kiepenheuer, K. O. ed., "Structure and Development of Solar Active Regions" I.A.U. Symposium No. 35, D. Reidel Publishing Company, Dordrecht, Holland, 1968.

Ohman, Y. ed., "Mass Motions in Solar Flares and Related Phenomena" Nobel Symposium 9, Almqvist and Wiksell, Stockholm, Sweden, 1968.

Xanthakis, J., "Solar Physics", (Proceedings of a NATO Advanced Study Institute Conference, Athens, 1965), Interscience Publishers, London, 1967.

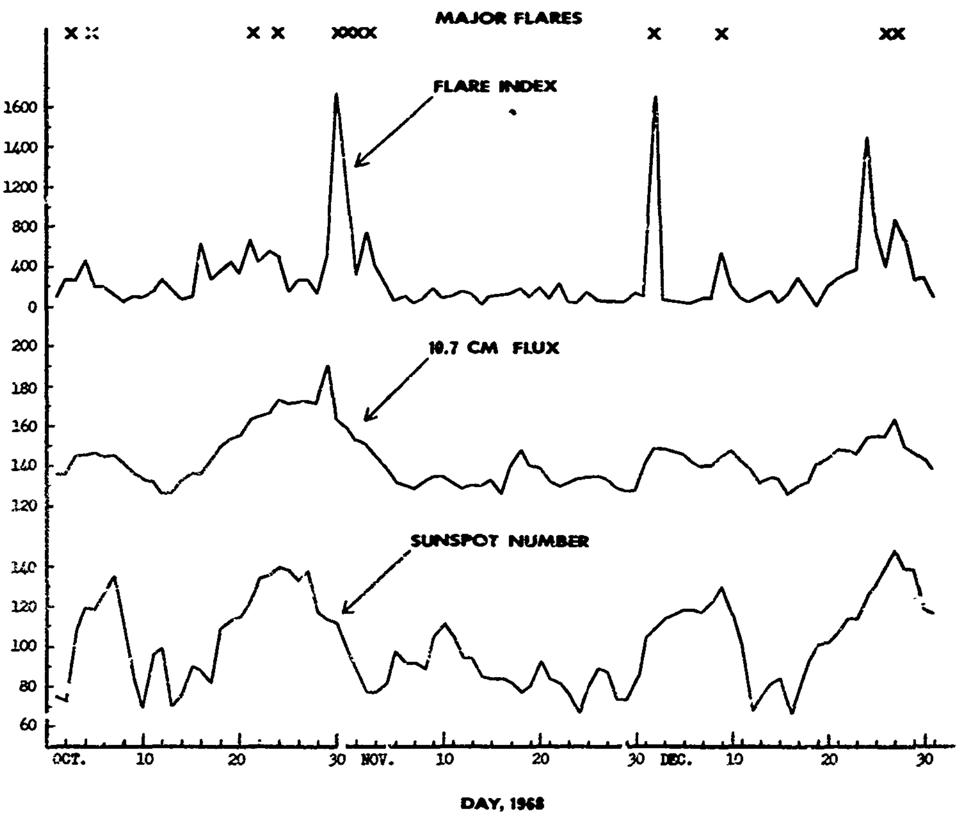

Figure 1. Comparison of three commonly-used solar indices with the occurrence of major solar flares for the last quarter of 1968.

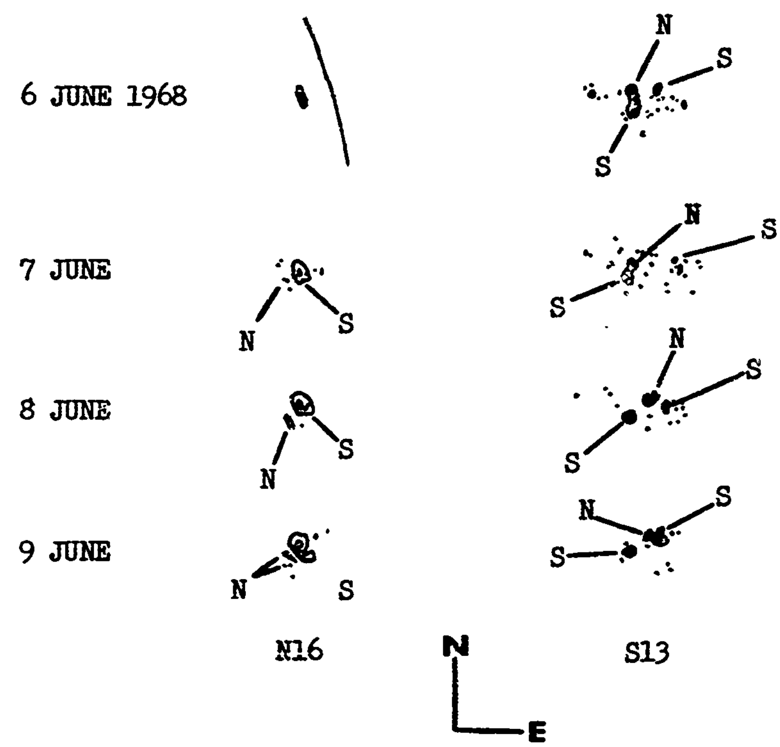

Figure 3. Evolution and magnetic polarities of sunspot groups associated with importance 2B flares on 9 June 1968.

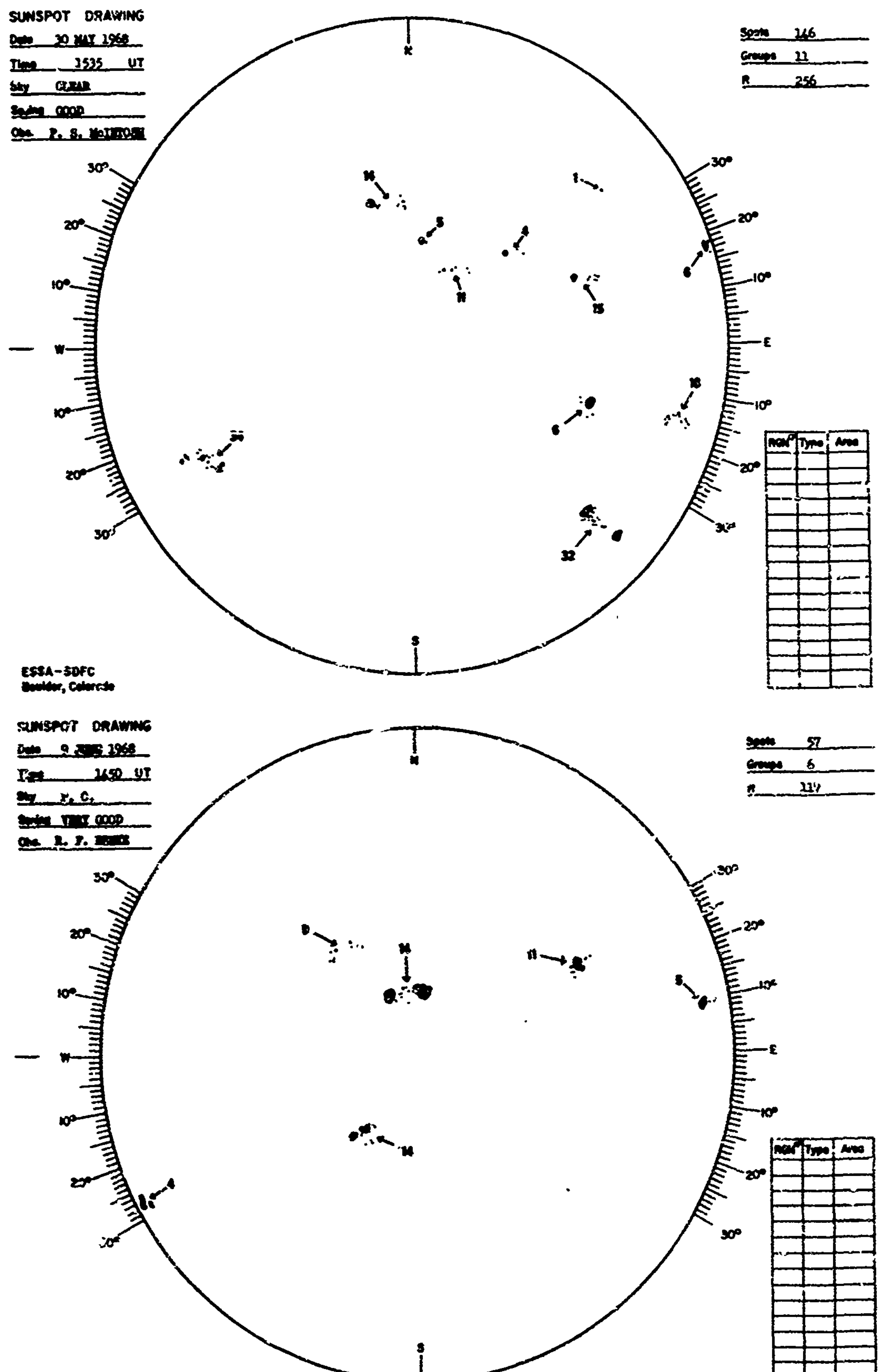

Fig. 2

Figure 2. Comparison of sunspot drawings for dates with similar hemispheric solar indices. No major flares occurred on 30 May, but importance 2B flares occurred on 9 June at N16E40 and S13W85. The drawings were made at the ESSA solar observatory in Boulder, Colorado.

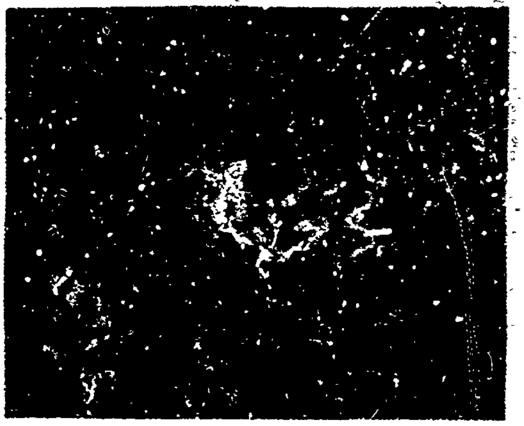

Figure 4. Above: A high-resolution H-alpha filtergram from the ESSA/NASA flare patrol telescope in Boulder, Colorado on 7 August 1968; below: Magnetic polarities and the position of the longitudinal magnetic neutral line as inferred from the H-alpha fine structure.

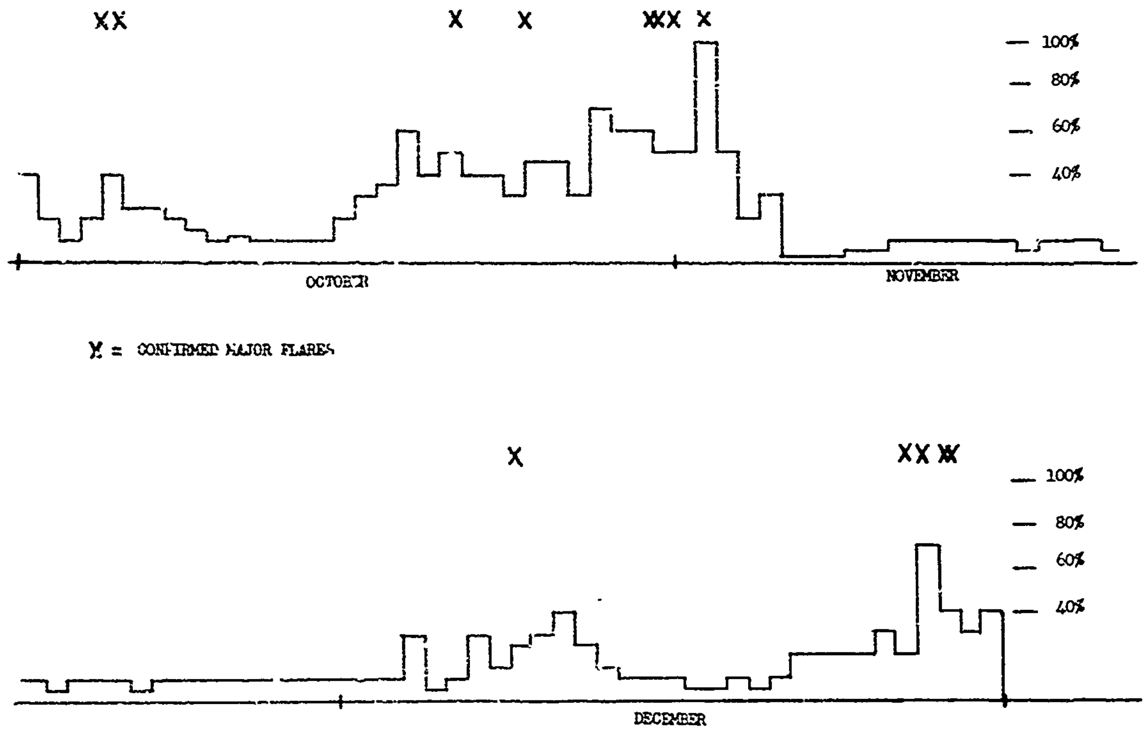

Figure 5. The probability of major flares as forecast one day ahead by the ESSA Space Disturbance Forecast Center compared with the actual occurrence of major flares during the last quarter of 1968.

PROTON EVENTS IN 1967-1968

by

George A. Kuck, Capt, USAF
Air Force Weapons Laboratory
Theoretical Branch, High Altitude Group
Kirtland AFB, New Mexico 87117

SUMMARY

One problem facing the Air Force Solar Forecast Center is the prediction of ionospheric effects related to energetic proton emissions from the sun. The occurrence, intensity, and duration of these charged particle emissions are related to the optical, radio, and x-ray emissions from the solar flares. Data summaries appearing in pre-published form such as the Explorer 34 proton results in the Solar-Geophysical Data bulletins published by ESSA, the Geophysics and Space Data Bulletin by AFCRL, and real time proton and X-ray data from Vela have allowed the evaluation of many important parameters.

Radio and X-ray data give an important indication of proton production. Cm radio bursts with a high flux density and a slope reflecting greater flux values at higher frequencies are often proton productive. Examination of the data summaries have shown that the meter classification of flares as type II or type IV, even though qualitative, should be used in conjunction with the cm radio criteria. The peak intensity of the proton flux $E \geq 25$ meV correlates better with the integrated .5-5 Å X-ray bursts than with the integrated cm radio bursts, peak cm radio flux, or peak X-ray flux.

The proton events were examined in terms of both isotropic and anistropic diffusion theories. The anistropic diffusion theory, which predicts that the plot of $\ln (It^{5/2})$ vs $1/t$ is a straight line during the rising portion of the proton event, can be used to extrapolate proton fluxes for $E \geq 10$ meV during 50% of the events. The isotropic diffusion theory, which predicts that during the entire event the plot of $\ln [It^{(3/2-\beta)}]$ vs $1/t$ is a straight line, can also be used. The isotropic diffusion theory uses a diffusion coefficient.

$$D = Mr^{\beta}.$$

It was found that M and β tended to be functions of flare position on the solar disc.

If there is a direct connection between the polar geomagnetic field and the interplanetary magnetic field, and if there are no accelerating electric fields, the unidirectional interplanetary proton flux is directly related to the proton flux over the polar caps. A measurement of the interplanetary flux in near earth space gives a good indication of the polar cap fluxes. It was found that the 30 MHz absorption over the poles during a PCA is proportional to the square root of the integral proton flux $E > 11$ meV in interplanetary space.

IX. 1. Introduction

One problem facing the Air Weather Solar Forecast Center is the prediction of ionospheric effects related to energetic proton emissions from the sun. The occurrence, intensity, and duration of these charged particle emissions are related to the optical, radio and X-ray emissions from the solar flares. Data summaries appearing in pre-published form, such as the Explorer 34 proton results in the Solar-Geophysical Data bulletins published by ESSA and the Geophysics and Space Data Bulletin by AFCRL, have allowed the evaluation of many important parameters.

An interdisciplinary approach to PCA prediction and ionospheric forecasting allows some effects to be calculated from first principles shortly after the optical flare occurs. Solar radio and X-ray burst observations are useful in determining if protons were actually produced during the flare. These bursts also give an indication of the number of protons produced. The position of the flare on the solar disk and the solar wind velocity can be used to indicate the rise time and the peak intensity of the event in the near earth space. Using the first few proton data points, the proton intensities can be extrapolated into the future. Ground based magnetic measurements can then be used to indicate the spacial extent of the precipitation and its uniformity. Satellite data and real time magnetic measurements can/be used to update the forecasts during the event. On the basis of the extrapolated fluxes, the next step is to calculate the ionization caused by the protons using an atmospheric model and a two-ion D region model for PCA events to calculate the electron profiles. Finally, the absorption on vertical and oblique paths can be calculated for high frequency communication systems across polar regions. Real time riometer measurements can be used to verify the prediction.

This paper covers many of the different phases of PCA prediction. First, the radio and X-ray characteristics of proton producing flares are examined. Then the two theories relating to particle propagation in the interplanetary medium are investigated for their applicability. Auroral measurements and low altitude satellite measurements are then discussed to show the relationship of the spacial extent of the PCA to magnetic activity. Finally, the relationships between 30 MHz riometer aborption and the exospheric proton flux are discussed. The problem of electron profiles and oblique absorption will not be covered in this report.

IX. 2. Prediction of Proton Production

Many different authors have noted the relationship between PCA, discrete frequency cm radio bursts, and Type IV meter radio bursts (Bell, 1963; Kundu, 1965; Yoshida et.al., 1963; DeJager, 1967). Some studies have been based upon sweep-frequency observations (Bell, 1963) while others have been based upon observations at discrete frequencies (Castelli et. al., 1967; Harvey, 1965). This section describes some of the problems involved in trying to use these research results operationally.

The discrete frequency data in the cm wavelength region are more helpful in predicting the large proton events which cause a PCA than the sweep-frequency results. There is quite a large variation in the reported sweep-frequency events. Different observatories tend to record each event differently. Table 1 shows the comparison of the Harvard Observatory, Sagamore Hill, and Boulder sweep-frequency results using the information given in the AFCRL Geophysics and Space Data Bulletin and the ESSA Solar-Geophysical Data bulletins. As one notes from the table, there are large variations in the identification of these bursts from observatory to observatory. Thus the sweep-frequency results tend to be qualitative.

Proton producing flares tend to have distinctive characteristics at cm wavelengths (Castelli et. al., 1967). When examined at each discrete frequency at the flux peaks, many events have a pronounced U-shaped dip in the intensity vs wavelength curves in the 10-100 cm range. The proton producing flares examined by Castelli had a high flux density (10^{-19} watts per m/-Hz in the microwave region up to 10,000 MHz with a slope reflecting greater flux values at higher frequencies. Table 2 shows the result of using these criteria to predict proton fluxes on the basis of the discrete frequency events reported by Sagamore Hill from January 1967 to February 1969. Using the discrete wavelength radio criteria alone gives approximately a reliability of 50%. However, using the Sagamore Hill sweep-frequency data in conjunction with the discrete frequency data tends to increase the forecast reliability even though the sweep-frequency data is a qualitative measurement.

IX. 3. Peak Proton Intensity

If the number of protons accelerated in a solar flare is proportional to the number of electrons accelerated, and if the intensity of X-rays in some wavelength band is proportional to the number of electrons produced, then the integrated intensity of x-radiation in that band should be proportional to the number of protons produced. The Vela .5-5 A X-ray data was integrated by assuming an exponential rise and decay of the intensity.

$$I_{int} = \int_{\infty}^{o} I_{max} \exp(-t/t_r)\, dt \quad + \int_{o}^{\infty} I_{max} \exp(-t/t_d)\, dt$$

$$I_{int} = I_{max}(t_r + t_d) \qquad (1)$$

where t_r and t_d are the exponential rise and decay times, I_{max} is the maximum X-ray intensity, and I_{int} is the integrated X-ray intensity.

The result of plotting the integrated X-ray intensity vs the peak Vela neutron monitor count rate (protons $E \geq 25$ meV) (Singer, 1965) is plotted in Figure 1. The triangle point was omitted in calculating the curvilinear index of correlation. This result indicates that a flare has to have an integrated intensity X-ray burst above a particular value before the protons accelerated are of sufficient intensity to be measurable at the Earth.

IX. 4. Arrival of Protons

There are two theoretical frameworks within which the proton observations could be analyzed. The first is the anisotropic diffusion with boundary theoretical framework (ADB) of Burlaga (1967) while the second is the isotropic diffusion theoretical framework (Parker, 1965; Krimigis, 1965). Both theories have features applicable to predicting the behavior of proton events. However, both theories have definite shortcomings.

The anisotropic diffusion with boundary (ADB) theory assumes that the interplanetary magnetic field lines between the sun and the Earth are spirals with irregularities which can effectively scatter the solar protons. The solar proton flux in this theory will be anisotropic and the flux will be greatest in the direction of the field. Beyond 1 A U., the scattering centers change so that protons cannot be scattered back into the diffusing region once they have reached the transition region. Thus in this model, it is assumed that there is an absorbing boundary at some heliocentric distance greater than 1 A.U.

The ADB model is not particularly useful in predicting the entire behavior of a particular event. The theory uses two different constants to describe the intensity behavior as a function of time. The relationship between the two constants depends upon the position of the absorbing boundary which varies from event to event. If r_1 is the position of the Earth in A.U., the theory may be used to calculate r_1/r for many low energy events. Figure 2 gives this ratio for thirteen events. The theory is obviously not applicable for two cases out of the thirteen because the absorbing boundary is less than 1 A.U. However, this theory could have been used for 60% of the cases examined to extrapolate the proton intensity-time. Figure 3 shows one of the events which had considerable structure. Even though the $\ln(It^{5/2})$ vs 1/t relationship predicted by the theory did not hold for the entire event, the relationship held during the rise of the event and would have allowed a good determination of the peak proton intensity.

The numerous proton events since May 1967 were anlayzed within the ADB theoretical framework. By examining the various particle parameters, one can determine the gross characteristics of the proton events. One of the predictions of the ADB theory is that there should be a linear relationship between the time that the protons reach maximum intensity and θ^2, i.e., the square of the position of the flare with respect to the sun - Earth-Archimedes spiral angle. Figure 4 shows such a plot. The abscissa is determined by the recipe given in the article (Burlaga, 1967), while the ordinate is the time in hours that it took the protons to reach maximum intensity after the start of the flare. The grouping of points above the line for $0 \leq \theta \leq 1$ can be due either to the misidentification of the parent flare or the inapplicability of the theory to these lower energy solar cosmic rays.

TABLE I

EVENT	SAGAMORE HILL (BOULDER)	HARVARD OBSERVATORY (SAGAMORE HILL)	BOULDER (SAGAMORE HILL)
TYPE IV	35	13	66
NOT ON AIR	3 9%	2 15%	10 15%
NO BURST	2 6%	1 8%	13 19%
CONTINUUM	10 27%	3 23%	15 23%
TYPE I	0 0%	0 0%	0 0%
TYPE II	1 3%	0 0%	3 5%
TYPE III	0 0%	1 8%	6 9%
TYPE IV	19 55%	6 46%	19 29%

From 1 Oct 1966 to 30 Jan 1969

TABLE II

Date	Dekameter or Metric Burst	Protons
27 Feb 67	IV	Yes
4 Mar 67	III	No
21 May 67	IV	No
23 May 67	II & IV	Yes
25 Jul 67	Cont I	No
3 May 68	III	No
8 Jul 68	IV	Yes
8 Aug 68	No assoc burst	No
29 Sep 68	III G, II	Yes
27 Oct 68	III, Cont	No
1 Nov 68	IV	Yes
17 Jan 69	IV	No

Castelli Criteria only: 42% proton productive

Castelli Criteria plus Type
II or IV: 71% proton productive

Castelli Criteria plus Type
IV: (one event not called) 66% proton productive

If the ADB theory is valid in this energy region, the line drawn in Figure 4 can be used to determine the normalization factor for the peak proton intensity. This normalization factor is given in Figure 5. The two lines specify the probable limits on the normalization. Within this theoretical framework, there is an effect caused by flare position on both the intensity and the time behavior of the proton event.

One can also anlayze each proton event in terms of the isotropic diffusion theory (Parker; 1963; Krimigis, 1965). In this theory, the diffusion coefficient, D, is given by

$$D = Mr^{\beta} \tag{2}$$

where r is the heliocentric radial distance in A.U., and M and β are parameters which may and often do depend upon the particle energy E. The units of $Mr^{\beta-2}$ are $(\text{hours})^{-1}$. Krimigis showed that for E < 50 meV, the parameter M does depend upon the proton energy. Thus, if one wants the time behavior for 10 meV protons, one must use a data base of 10 meV.

It can be shown that

$$t_{max} = \frac{1}{3M} \frac{r^{2-\beta}}{(2-\beta)} \tag{3}$$

where M and β are the coefficients given in Equ. (2) and t_{max} is the time it takes for the protons to reach maximum intensity. Since t_{max} does depend upon the solar flare heliographic longitude, it is possible to empirically determine M and β as a function of solar flare position even though such an assumption violates the basic theoretical considerations.

Sixteen out of twenty events could be analyzed within the isotropic diffusion framework. Figure 3 shows one of these events. This figure also shows that there is an area of agreement between the ADB theory and the isotropic diffusion theory. A certain amount of judgment was necessary in determining β from the graphs of 1/t vs ln $[It^{(3/2-\beta)}]$ because of poor time resolution and uncertainties in count rates and particle backgrounds. This event also illustrates what happens when a proton event has considerable structure. Many events showed the characteristic hook at small values of 1/t. The value of β used was that value which best fit the first several values of 1/t and which also adequately fit the long time behavior at small values of 1/t.

Figure 6 gives scatter plots of β and M as a function of θ for 10 and 30 meV protons as a function of flare position. The θ was determined in the ADB theoretical framework. Several features do stand out. The low values of β and M for θ less than .25 radians are probably due to the diffusion being one or two dimensional instead of three dimensional as assumed in this analysis. There does seem to be a trend as a function of θ for θ > .5 radians. Although there is a large amount of scatter, the higher energy particles tend to have larger values of M and β than the lower energy particles.

An important conclusion to be drawn from this study is that these results can be refined. Better time resolution will lead to less scatter in the data. The better the time resolution, the easier it was to determine M and β. Data for larger values of θ have not yet become available with the necessary count rate accuracy or time resolution.

IX. 5. Riometer Absorption

Several characteristics of the PCA are related to the magnetic indices. If one examines the data obtained during different PCA's, one does not have enough data to make good statistical predictions on the spacial extent of the proton precipitation. However, by using the mass of observations of the aurorae, one can draw conclusions on the spacial extent.

It has been found that the equatorial edge of the auroral oval is the high latitude edge of those magnetic field lines which connect each hemisphere without being drawn into the earth's magnetic tail. There have been many observations of auroral movement toward the equator as a function of K_p and local time (Feldstein, 1966). As K_p increases, the auroral oval moves toward the equator. Figure 7 shows the latitude distribution of the aurora as a function of K_p for a longitude zone close to geomagnetic midnight. The points represent the peak of the peak hourly occurrence, while the error bars represent the width of 60% of the peak (Gartlein et. al., 1965). Thus the spacial extent of the PCA can be predicted as a function of K_p.

Many theoretical calculations have been done on the energy loss of protons in the atmosphere and the related riometer absorption (Adams and Masley, 1966, Fichtel et. al., 1963). One can now verify, on the basis of satellite data, many of the assumptions made and relate the exospheric proton flux to the riometer absorption.

Several assumptions can be easily verified. Explorer 34 proton measurements have shown that the expontential rigidity spectrum better fits the integral spectral measurements between 10 and 60 meV than exponential energy, power law energy or power law rigidity.

Low altitude satellites have shown that even if the precipitation over the polar caps is not uniform in spacial extent, the unidirectional flux of particles at a point is still isotropic away from the earth. (Stone and Evans, 1969; Blake et.al, 1968)

The Explorer 34 and the Vela satellites make the majority of their measurements in the interplanetary space. These measurements are directly applicable to the polar cap ionospheric measurements. If there are only small electric fields, and if the magnetic field lines connect directly from the polar caps to the interplanetary space, and if the interplanetary proton flux is nearly isotropic, then the proton flux over the polar caps will also be isotropic and of the same intensity as the interplanetary proton flux. If there is no direct connection, the proton precipitation will not be uniform over the polar caps. However, the flux cannot be greater at any point over the polar cap than the flux in interplanetary space.

On the basis of theoretical calculations (Adams and Masley, 1966), it can be concluded that the 30 MHz riometer absorption is proportional to the square root of the incident integral particle flux for $E \geq 11$ meV. (Juday and Adams, 1969). An analysis of the Explorer 34 and Thule riometer data have helped confirm this result.

The Explorer 34 data and Thule riometer data have been examined. Figure 8 is a plot of the results for 10 meV particles. One notes that these 10 meV particles scatter about the line of slope 0.5. The points tend to fall below the line at high absorption values and above the line at low absorption values. When the $E \geq 20$ meV flux is plotted as the abscissa, the points at low absorption tend to fall below the line while those at high values tend to fall above the line. Thus, the absorption is directly proportional to the integral flux somewhere between 10 and 20 meV. Within the limitations of this analysis, therefore, the integral flux for $E \geq 11$ meV is an experimentally verified conclusion.

IX. 6. Summary

An interdisciplinary approach to PCA prediction and ionospheric forecasting allows some effects to be calculated from first principles shortly after the optical flare occurs. Solar radio and X-ray burst characteristics are useful in determining if protons were produced in sufficient quantity to give riometer absorption. The position of the flare on the solar disk and the solar wind velocity can be used to indicate the rise time and peak intensity of the event in near earth space. Using the first few proton data points, the proton intensities can be extrapolated into the future. Ground based magnetic measurements can then be used to indicate the spacial extent of the proton precipitation. Satellite data and real time magnetic measurements can be used to up-date the predictions during the event. Experimental measurements have verified some of the assumptions and theoretical predictions for 30 MHz riometer absorption. Thus the satellite proton measurements can be employed to specify and predict absorption. The approach taken in this report can be continued to give better predictions once more data become available.

ACKNOWLEDGEMENTS

Without the moral support of the personnel assigned to the Solar Forecast Center and the Solar Forecast Facility, this report could not have been written. This work parallels the work being done by the Space Forecasting Plan Working Group at Air Force Cambridge Research Laboratories (AFCRL). Without their technical advice, much of this work could not have been done. My special thanks go to Mr. Ray Conmier of AFCRL for allowing me to use his riometer data. The Vela neutron monitor data and X-ray data were kindly supplied by Dr. Conner and Dr. Bame of Los Alamos Scientific Laboratory. The author is solely responsible for the opinions and material presented in this report. The consent of the above mentioned scientists to use their data does not necessarily imply their agreement with the results.

REFERENCES

1. Adams, G. W. and A. J. Masley (1966) "Theoretical Study of Cosmic Noise Absorption Due to Solar Cosmic Radiation," Planet, Space Sci., 14, 277.

2. Adams, G. W. and L. R. Megill (1957) "A Two-Ion D-Region Model for Polar Cap Absorption Events," Planet. Space Sci., 15, 1111.

3. Bell, B. (1963) "Solar Radio Bursts of Spectral Types II and IV: Their Relations to Optical Phenomena and Geomagnetic Activity," Smithsonian Contr. Astrophys., 5, 239.

4. Bell, B. (1963) "Type IV Solar Radio Bursts, Geomagnetic Storms, and Polar Cap Absorption (PCA) Events," Smithsonian Contr. Astrophys., 8, 119.

5. Blake, J. B., G.A. Paulikas, and S.C. Freden (1968) "Latitude-Intensity Structure and Pitch-Angle Distributions of Low Energy Solar Cosmic Rays at Low Altitude," J. Geophys. Res., 73, 4927.

6. Burlaga, L. F. (1967) "Anisotropic Diffusion of Solar Cosmic Rays," J. Geophys. Res., 72, 4449.

7. Carrigan, A. L., and N. J. Oliver (1967-1968) "Geophysics and Space Data Bulletin," IV-VI Air Force Cambridge Research Laboratories.

8. Castelli, J. P., J. Aarons and G.A. Michael (1967) "Flux Density Measurements of Radio Bursts of Proton-Producing Flares and Nonproton Flares," J. Geophys. Res., 72, 5491.

9. DeJager, C. (1967) "Solar Disturbances Associated with PCA Events," Space Research VII, edited by Smith-Rose and King, North Holland Publishing Co., Amsterdam, 785.

10. ESSA Research Laboratories (1967-1968) "Solar Geophysical Data," IER-FB-281 to IER-FB-295.

11. Feldsten, Y. I. (1966) "Peculiarities in the Auroral Distribution and Magnetic Disturbance Distribution in High Latitudes Caused by the Asymetrical Form of the Magnetosphere," Planet. Space Sci., 14, 121.

12. Fichtell, C. E., D.E. Guss and K. W. Ogilvie (1963) "Details of Individual Solar Particle Events," Solar Proton Manual, NASA Tech. Rept. R-169, edited by F. B. McDonald, 19.

13. Gartlein, C.W., P. M. Millman and G. C. Sprague (Oct 1965) "North American Aurora Visaplots," WDC-A Auroral Data Center, Cornell University, Ithaca, N.Y.

14. Harvey, G.A. (1965) "2800 Megacycle per Second Radiation Associated with Type II and Type IV Solar Radio Bursts and the Relation with Other Phenomena, J. Geophys. Res., 70, 2961.

15. Juday, R.W., and G. W. Adams (1969) "Riometer Measurements, Solar Proton Intensities, and Radiation Dose Rates," Planet. Space. Sci. to be published.

16. Kfimigis, S.M. (1965) "Interplanetary Diffusion Model for the Time Behavior of Intensity in a Solar Cosmic Ray Event," J. Geophys., Res., 70, 2943.

17. Kundu, M. R. (1965) Solar Radio Astronomy, Interscience Publishers, N.Y.

18. Parker, E. N. (1963) Interplanetary Dynamical Processes, Interscience Publishers, N.Y.

19. Singer, S. (1965) "The Vela Satellite Program for Detection of High Altitude Nuclear Detonations," Proc. IEEE, 53, 1935.

20. Stone, E. C., and L. Evans (1969) "A Persistent North-South Asymmetry during a Polar Cap Proton Event," Trans. Am. Geophys. Union, 50, 306.

21. Webber, W. R. (1964) "A Review of Solar Cosmic Ray Events," AAS-NASA Symp. Physics of Solar Flares, NASA SP-50, edited by W. N. Hess, U. S. Government Printing Office, Washington, D.C. 215.

22. Yoshida, S., K. Nagashima, K. Kawabata and M. Morimoto (1963) "Propagation of Solar Particles Deduced from Measurements with Explorer VII," Space Research III, edited by W. Priester, Interscience Publishers, N. Y, 608.

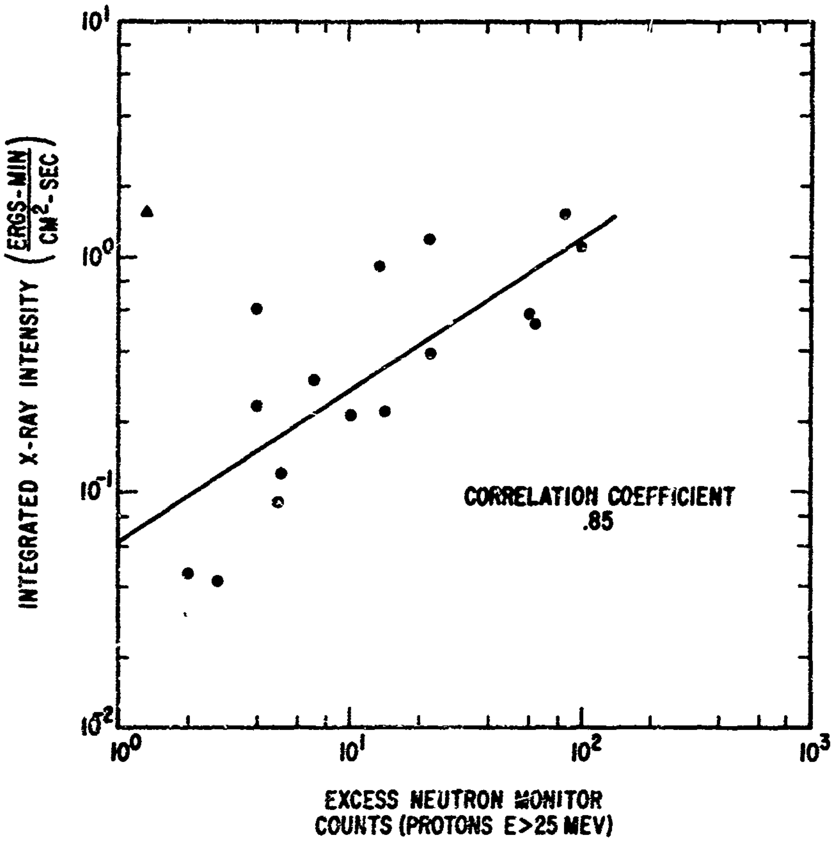

Figure 1: Peak neutron monitor counting rate due to protons E ≥ 25 meV vs the integrated X-ray flux. No correction has been made for the interplanetary propogation factors.

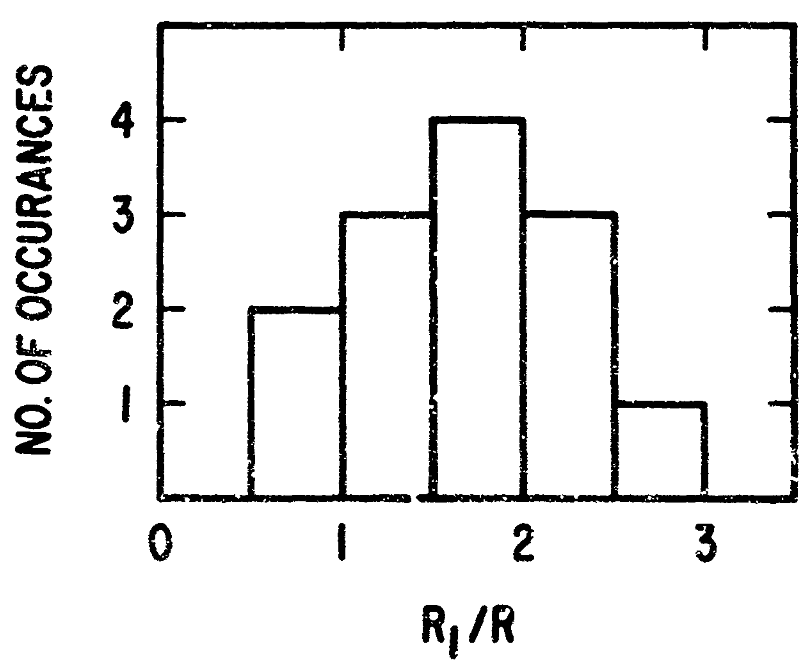

Figure 2: Position of the absorbing boundary for the anisotropic diffusion with boundary (ADB) theory for 13 proton events.

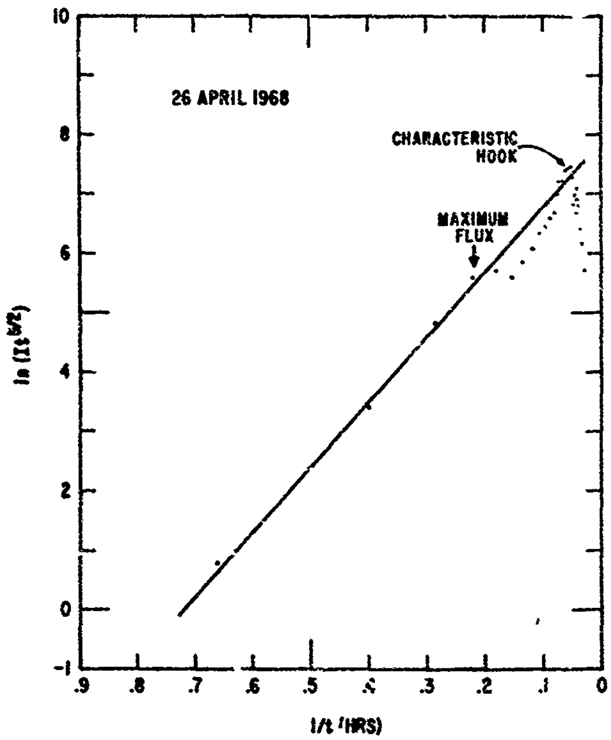

Figure 3: Time-intensity profile for the 26 April 1968 event for E ≥ 10 meV protons measured by Explorer 34. This event had considerable structure.

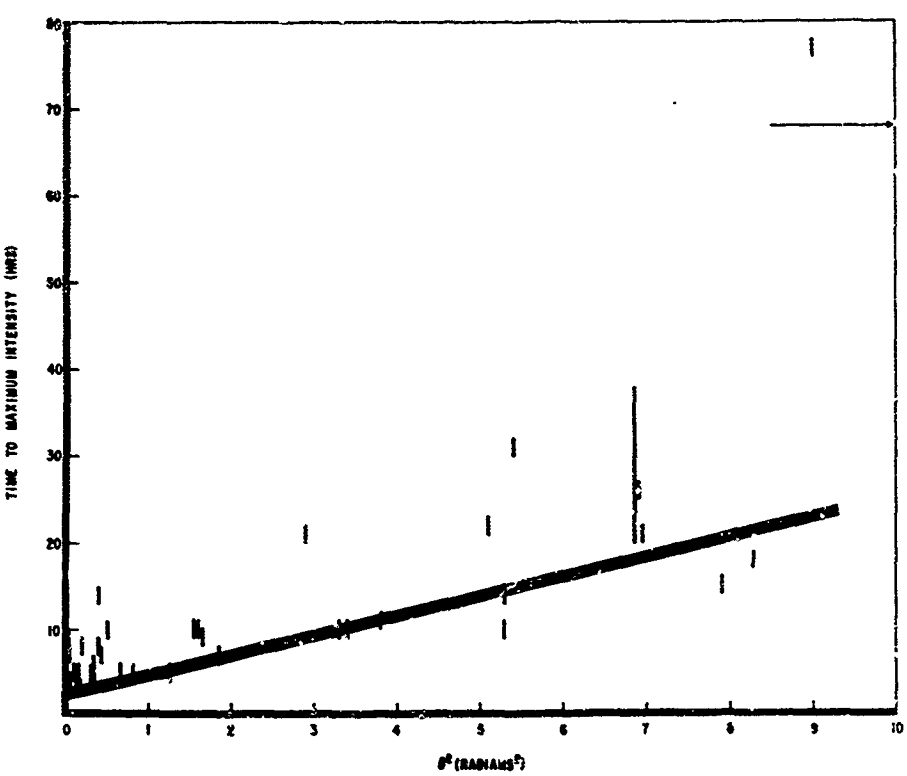

Figure 4: Intensity maximum as a function of the square of the angle of the flare longitude with respect to sun-Earth-Archimedes spiral angle.

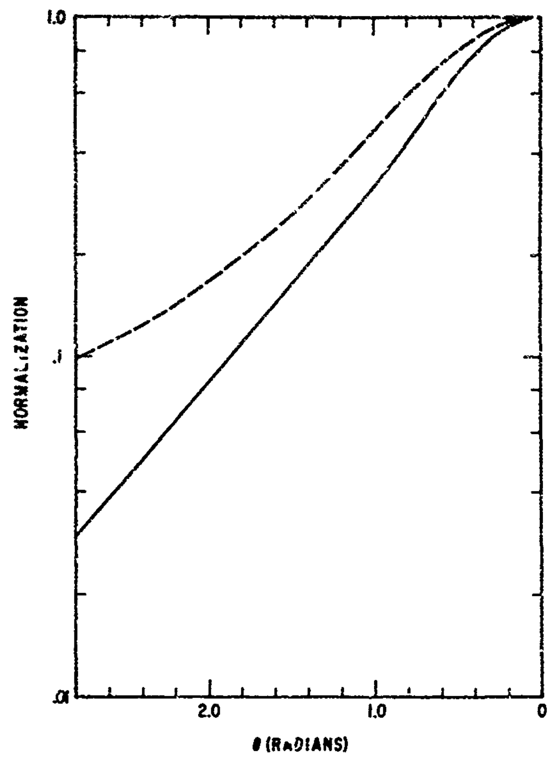

Figure 5: Interplanetary propogation scaling factor as a function of flare position and the sun-Earth Archimedes spiral angle. The two lines show the limits of this normalization factor.

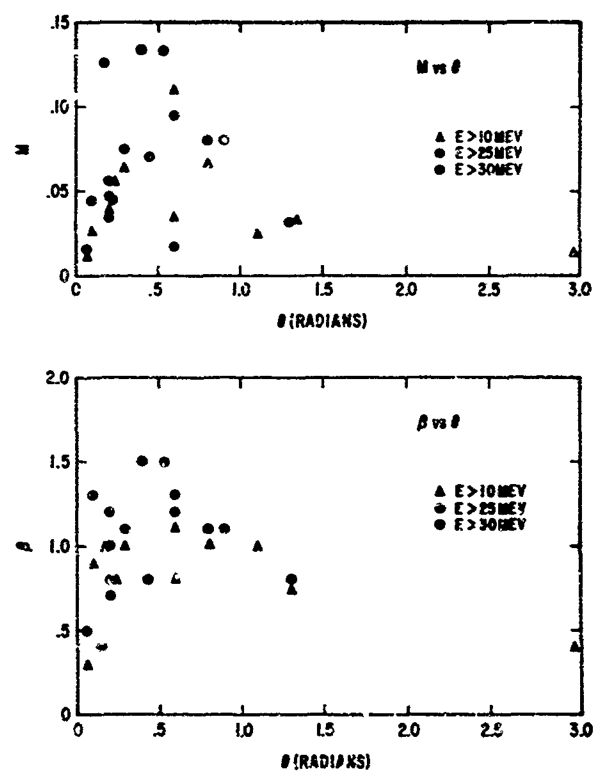

Figure 6: The diffusion coefficients, M and β, as a function of the flare position and the sun-Earth Archimedes spiral angle. The higher energy particles tend to have higher values of M and β than the lower energy particles.

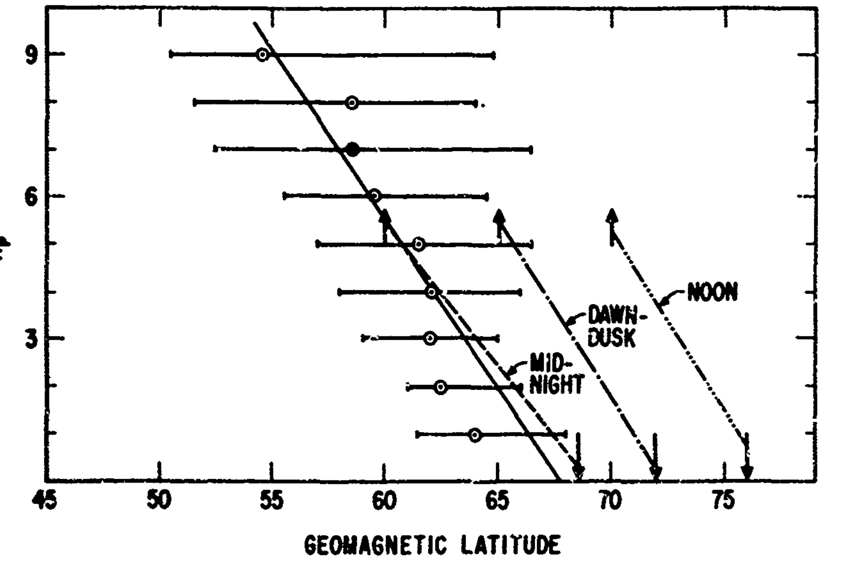

Figure 7: The geomagnetic latitude of the aurora as a function of K_p. The points are the position of the peak hourly occurrence while the lines signify the position of the 60% point.

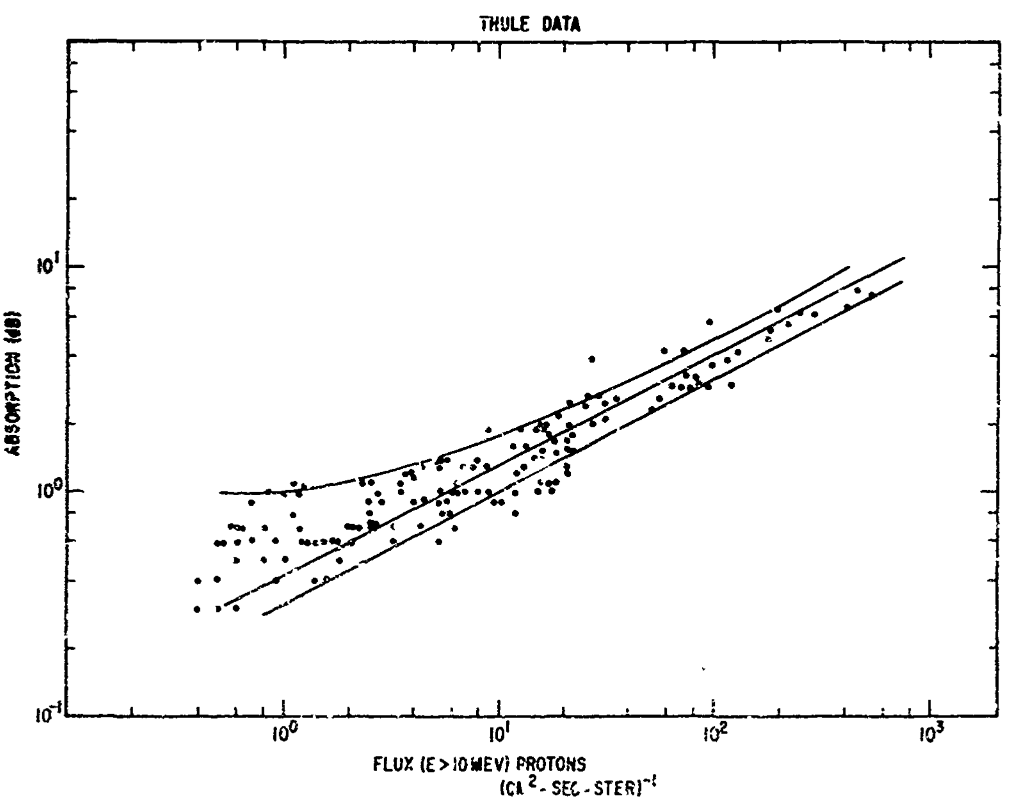

Figure 8: Riometer absorption at Thule as a function of the interplanetary proton flux ($E \geq 10$ meV protons/cm^2/sec/ster). If the square of the riometer absorption were proportional to the flux, the points would fall on the straight line.

MULTIFREQUENCY SOLAR RADIO BURSTS AS PREDICTORS FOR PROTON EVENTS

by

R. M. Straka and W. R. Barron

Air Force Cambridge Research Laboratories
Bedford, Massachusetts

SUMMARY

Success in the use of radio spectral signatures for predicting a PCA event after the occurrence of a solar flare is evaluated. Selected 1966-1968 radio bursts, both proton and nonproton associated, were integrated in flux to obtain the spectral <u>energy</u> characteristics of each event. Large energies in the meter wavelength range were particularly noted with large PCA events. Burst <u>mean</u> flux times duration as a substitute for actual energy values obtained by integration are examined. Energy spectral characteristics are shown as a function of flare longitudinal position. <u>Total</u> radio energies obtained by integration of the energy spectrum in the 500 - 8500 MHz range are obtained and compared in terms of the East-West longitudinal flare position to magnitudes of the associated PCA events.

MULTIFREQUENCY SOLAR RADIO BURSTS AS PREDICTORS FOR PROTON EVENTS

R. M. Straka and W. R. Barron*
Air Force Cambridge Research Laboratories
Bedford, Massachusetts

INTRODUCTION

The ability to forecast a Polar Cap Absorption Event following an intense solar flare can be of vital importance to the communicator who uses the polar region ionosphere in his communications network. Some degree of success in predicting, days in advance, that this proton producing flare will occur is offered through the solar optical measurements of active region spot configurations and sizes, plage areas, magnetic field configurations, and gradients of the field in the active region. However, it is not until the flare actually occurs and a unique radio signature accompanies it, can there be a high degree of certainty that a PCA event will ensue. This allows tens of minutes to tens of hours warning before the maximum absorption of the PCA is attained. These short term forecast capabilities are pointed out by Castelli and Aarons in paper #11 presented at this conference.

The intensity and spectrum of the radio bursts reflect the numbers and energies as well as the magnetic field influences on the accelerated electrons that accompany the flare. If one accepts a similar and simultaneous acceleration of protons, then the radio burst characteristics may well be indicative of what to expect from the protons. Studies, for example, by Webber (1963) and Fletcher (1964) have shown a relationship between the size of the radio event and the intensity of the proton event. To gain further insight to this relationship, this paper investigates multi-frequency integrated flux characteristics of radio bursts (energy spectrum) and their total integrated radio energy over several octaves of spectra. How these values lend themselves to quantitative measures of the magnitude of the accompanying PCA events are investigated.

EFFECTIVENESS OF THE RADIO SIGNATURE AS A PCA PREDICTOR

As part of the incorporation of the AFCRL devised radio signature criteria (Castelli et al., 1967; and Castelli, 1968) into the joint AFCRL-AWS Space Forecasting Program, an independent computer check was made of the successfulness of this yes-no predictor of PCA events. This was accomplished by using Nagoya radio data for the period 1960 through 1963, as well as Hiraiso, Tokyo, and Hollandia meter wavelength burst data. The signature criteria, similar to those cited above, employed in this test were the following:

1) The peak burst flux increased with frequency to a value exceeding 1000 flux units (1 f.u. = 1 x 10^{-22}W/M^2/Hz) in the 9000 MHz range.

2) A peak flux minimum was observed in the 500 - 2000 MHz range.

3) And, a peak flux rise occurred in the low frequency direction.

All radio data tested were from the I.A.U. Quarterly Bulletin of Solar Activity and covered the following frequencies (in MHz). 9500 TOK, 9400 NAG, 3750 NAG, 3000 TOK, 2000 NAG, 1000 NAG, 200 TOK, 200 HIR, and 200 HOL. PCA events were selected from the listings of Obayashi (1962), Bailey (1964), Jonah (1966), and Sakura (1968). Only those PCA events that had identified parent flares occurring within the Nagoya station operating hours were used. Table 1 lists those events that would have been called, confirmed (indicated by a star *) and missed. Underlined dates are those which gave proper radio signatures but were not confirmed as PCA events; for example, the 14 Aug 60 event with peak fluxes of 1540 f.u. at 9400 MHz, 1430 f.u. at 3750 MHz, 775 f.u. at 2000 MHz, 630 f.u. at 1000 MHz, and greater than 2000 f.u. at 200 MHz. Aside from a real False Alarm, it may well be that instrumentation and/or coverage for the PCA detection were insufficient at the time. Radio burst universal times for these "should be" events are included and underlined. Half of the missed events were so small that no absorption values were reported for these events. The Castelli criteria, however, was designed and is most successful for principal PCA events where the absorption >2 dB. Thus, four and possibly five (9 May 60 had dB listed as >1) of the eight misses would not have been considered misses of principal PCA events. Figure 1 summarizes the results of the test. Effectively, it can be said from the 1960-1963 data that 16 of the 20 PCA events were called and confirmed with only four misses and five false alarms. Considering that the instrumentation for radio and PCA detection have increased in number and effectiveness since that time period, it is apparent that the radio burst detection of PCA events currently offers one of the most successful predictive methods indeed. It should, therefore, play a major role in any worldwide PCA forecast scheme.

INTEGRATED RADIO FLUXES

In addition to the yes-no PCA prediction from the radio spectra of bursts, an attempt is made to use the accurate quantitative aspects of these bursts to give an indication of the possible PCA event magnitude. This again assumes the parallel accelerations of electrons which emit the

*Research Physicists in the Radio Astronomy Branch, Ionospheric Physics Laboratory

radio energy by synchrotron emission, and of the protons responsible for the polar cap absorption. One would expect the integrated flux, or energy, in the radio burst to correlate with the energy of the proton event. Webber (1963) shows this correlation between the integrated single frequency 10 cm wavelength flux and the integrated proton fluxes. The 10 cm burst energy study has been greatly expanded by Lopez, Bragg, and Modisette in their NASA Program Apollo Working Papers. With the availability of accurate multi-frequency radio burst recordings from the AFCRL Sagamore Hill Radio Observatory, it was decided by AFCRL to examine integrated fluxes, but on a multi-frequency basis. The question "How did the burst energy spectra relate to the magnitude of the PCA" was pursued. Minute by minute integrations were performed on a number of events. Six of these events are plotted in Figure 2. Note for the two proton flare events (23 May 67 -- 11 dB abs. and 28 Aug 66 -- 4 dB abs.) the distinct increase in energy at the low frequency end of the spectrum. That this increase is important is clearly seen when one looks at the 30 March 66 event for comparison. Although the March event is the second most energetic event plotted, no low frequency energy was observed. It was not a polar cap absorption event. Table II, Special Events, shows this 30 March event to have had over 2000 flux units at 8800 MHz, decreasing to 612 f.u. at 606 MHz, with a continual drop off in flux at the low frequency end.

One event, however, that had a drop in energy at the low frequency end and yet had protons associated with it, was the 27 February 67 event. The presence of protons was not detected by earth based instruments (PCA), but rather by satellite sensors. Paulikas and Blake (1968) report that the ATS-1 satellite (6.6 earth radii out) measured a peak flux in the 21 - 70 MEV range of 13.3 protons/cm^2/sec for this event. This would give somewhat less than 1 dB absorption if it were a PCA event. It, therefore, appears that high energy content at low frequencies is an important prerequisite for any principal PCA event with large absorption.

Another burst of interest is the 4 March 67 event in Figure 2 and Table II. This radio event had very high peak flux values with the proper radio signature. At 606 MHz the peak flux was 9638 f.u. It was not a PCA event. From the energy standpoint it was the weakest event plotted. The reason being that the bursts were of short time duration. For particle events, then, not only must the fluxes be high, but the duration should be long enough to allow a build up of sufficient energy. As a point of interest note that for the PCA events a minimum energy is often observed in the 10 cm range. More cases will be required to draw firm conclusions.

To expand the number of radio events for examination without actually having to integrate minute by minute the multi-frequency events, the approach of obtaining integrated flux by multiplying the burst mean flux times its duration times 2 was used. Exactly the same answer should result if the mean flux values are accurate. Figure 3 plots the actual integrated burst flux versus the value obtained by the Mean Flux Method. The frequency 2695 MHz was chosen for this plot as it could be compared with results from the accurate OTTAWA mean values. Exact correlations would fall on the dashed line. Except for the low frequency data where complicated burst structure makes accurate mean flux values difficult to obtain, one sees the mean flux values can be used rather well in place of the integrated flux.

Using the Mean Flux Method, the energy of other events are obtained and listed in Table III. These are plotted in Figure 4 in a manner such that any relationship of energy spectrum as a function of solar flare East-West position should become apparent. Unfortunately, no particular characteristic of the energy spectra labels it as either an East or West longitude event. The events from W87 through E61 are principal PCA events with greater than 2 dB absorption. All events after the 2 Feb 67 (reading left to right and downward) are nonproton events. Interestingly, principal PCA events have their burst energies in the 10^{-17} to 10^{-15} Joules/m^2/Hz range, except for the weak 2 Feb 67 event, and the strong 23 May 67 and 28 Aug 66 events. Dashed spectra indicate coordinate changes of the energy values. The unusually high energy of the 23 May 67 may well be attributed to the fact that three major solar flares, Imp 2B, 3B, and 2B, occurred during this event. Each flare could have pumped additional particles into the event. On the other hand, the weak 2 Feb 67 PCA event which was assigned the parent flare position of E61 (Masley, 1967) may in fact not have been associated with this flare and its radio burst. There now seems to be reasonable question of this association. The proton event may well have originated from a behind-the-limb active flare region. No radio event would, therefore, have been detected. The integrated burst spectra illustrated for this event may thus have been from an insignificant flare not associated with the 2 Feb 67 PCA event.

SOLAR LONGITUDINAL POSITION OF PCA EVENTS

The solar heliographic longitude of the PCA flare producing centers for 1966 through 1968 were examined after the methods of Warwick (1965), Wilcox and Schatten (1967), Haurwitz (1968) and Dodson and Hedeman (1968). Haurwitz suggests the rotation period of 27^d.213 as being the significant period for longitudinal grouping of events. However, it was possible to use the more convenient Carrington System because of our short data period without introducing significant errors. The results are shown in Figure 5. We see indeed a grouping of PCA events with greater than 2 dB absorption in the heliographic longitude range 160° - 260°. This is in agreement with what Dodson and Hedeman proposed as an apparent concentration for 1962-1966 data. They give the primary zone of concentration with the Carrington longitudes of ~160° - 230°, and a secondary zone from 320° - 50°. The 11.5 dB PCA event of 18 Nov 1968 falls in this seconary zone at 346° in Figure 5. However, the 2 Dec 68 event with 4.7 dB at longitude 348° is presently under investigation as another possible behind-the-limb event. Study of possible behind-the-limb originated events is of vital importance for PCA forecasting. It is suggested that past PCA events be reevaluated in this light.

TOTAL RADIO ENERGY OF SPECTRAL BURST EVENT

To further investigate the energy characteristics of solar radio bursts the energy spectra of these bursts were integrated over a broad frequency range (500 - 8500 MHz) to obtain the total radio energy in the burst event. These results are given in Table III. Of the events, only three that had PCA association were obtained by true flux integration, the others being obtained by the Mean Flux Method. These three events with their total energies are compared with the peak particle fluxes of their PCA's:

Radio Event	Total Energy	Peak Particle Flux
23 May 1967	1430 x 10^{-7} joules/m^2	1936 p/cm^2/sec
28 May 1966	41 x 10^{-7} joules/m^2	256
27 Feb 1967	7 x 10^{-7} joules/m^2	13

Increased particle flux for increased radio energy can be seen in our results.

Throughout our correlative studies use has been made of the peak particle fluxes, rather than the integrated particle fluxes used for example by Webber (1963). This was done at the suggestion of Smart (1969) who states "that the amplitude of the particle flux is best indicated by the peak flux at the earth; whereas, the integrated particle flux is a product of the diffusion rate in interplanetary space, with the latter being quite variable from one event to the other."

The total energies of sixteen burst events in the 500-8500 MHz range are listed in Table III. These values are plotted as a function of the magnitude of the associated PCA in dB Absorption (30 MHz), see Figure 6. The radio events were also subgrouped in the figure according to the longitude intervals of the parent flare positions; i.e., WEST longitudes (30W - 90W ◐), CENTRAL longitudes (30E - 30W ⊙), and EAST longitudes (30E - 90E ◑). East longitude events tend to have small absorptions over a wide range of total energies of the radio bursts. Central longitude events show little association. West longitude events, however, show a distinct alignment. Events occurring in the 30W - 90W longitude zone can have a large variation in magnitude of the PCA even though their total radio energy varies only within a factor of two. While only a few samples are used, there appears to be a radio energy limiting effect for West longitude (30W - 90W) events. The word limiting is used in the sense that East longitude (90E - 30E) events had large variations in total radio energy whereas the West events had near constant energy, almost as though the energy in increasing had reached a maximum value which it did not exceed. Asymmetry in the intense magnetic fields of the leading and trailing sunspots associated with the proton flare could cause East sector radiation to propagate through one magnetic configuration and through a different magnetic configuration for West sector radiation. This latter configuration may impede the radio energy expenditure to a limiting value. The PCA magnitude could also be effected by the magnetic field control of the protons, however, it is more likely that this variation is the result of interplanetary propagation and magnetospheric coupling factors. For a true quantitative prediction of PCA events the sum total of all these factors must be taken into account.

CONCLUSIONS

1) The Castelli and Aarons multi-frequency radio signature criterion for predicting PCA events has a high degree of success (16 of 20 PCA events called and confirmed in the test sample of 1960-1963 Nagoya radio data).

2) Large PCA events tend to have high radio burst energies present in the low frequency end (200 - 600 MHz) of the burst event.

3) Twice the Mean Flux x the Duration of the radio burst gives a practical approximation to the integrated flux (energy) of the event.

4) For most principal PCA events, the energy spectra of radio bursts in the 1000 - 10,000 MHz range falls in the energy range of 10^{-15} to 10^{-17} Joules/m^2/Hz.

5) In addition to high peak flux values of the radio bursts, sufficiently long durations are necessary to give the necessary energies usually found for the association with an important PCA.

6) There is a grouping of the 1966-1968 PCA events with dB > 2 in the solar heliographic longitude range from 160° - 230°.

7) No unique spectral energy characteristic was found as a function of East-West solar longitude of the burst event.

8) The total radio energy of burst events from 500-8500 MHz can be high or low for East longitude (30E - 90E) events, however, the magnitude of the PCA will still be small.

9) West longitude (30W - 90W) originated PCA events have absorption values that appear to be independent of the total radio energy of the event.

10) Every West longit ' ' .rst associated with a principal PCA event had a total radio energy of near 20×10^{-7} Joules/m^2.

REFERENCES

Bailey, D.K. (1964), Planet. Spa. Sci., 12, 495.

Castelli, J.P. (1968), Air Force Surveys in Geophysics, AFCRL-68-0104, No. 203.

Castelli, J.P. and Aarons, J. (1969), AGARD paper presented at XVth Electromagnetic Propagation Committee Symposium on Ionospheric Forecasting, Quebec, Canada.

Castelli, J.P., Aarons, J. and Michael, G.A. (1967), J. Geophys. Res., 72, 5491.

Dodson, W.H. and Hedeman, E.R. (1967), Structure and Devebpment of Solar Active Regions, I.A.U. Symposium No. 35, edited by K.O. Kiepenheuer, D. Reidel Pub. Co.

Hakura, Y. (1968), Table of Outstanding Solar-Terrestrial Events in 1954-1967, NASA TMX-63120.

Haurwitz, M.W. (1968), Ap. J., 151, 351.

Jonah, F. (1966), Analysis of Polar Cap Absorption Events, LTV Aerospace Corp., Rpt No. 00-802.

Masley, A.J. and Goedeke, A.D. (1967), Douglas Missile and Space Systems Division Paper No. 4662, presented at the 10th International Conference on Cosmic Rays, Calgary, Canada, June 1967.

Masley, A.J. (1969), private communication.

Obayashi, T. (1962), Table of Solar Geophysical Events July 1957 - December 1960, Kyoto Univ., Kyoto, Japan.

Paulikas, G.A. and Blake, J.B. (1968), Aerospace Report No. TR-0200 (4260-20)-2.

Quarterly Bulletin on Solar Activity, I.A.U., Zurich, Switzerland.

Solar-Geophysical Data Bulletin, Space Disturbances Laboratory, ESSA, Boulder, Colo.

Smart, D.F. (1969), private communication.

Warwick, C.S. (1965), Ap. J., 141, 500.

Webber, W.R. (1963), AAS-NASA Symposium on the Physics of Solar Flares, NASA-SP-50, edited by W.N. Hess, pp 215-255.

Wilcox, J.M. and Schatten, K.H. (1967), Ap. J., 147, 364.

TABLE I

PCA PREDICTIONS USING NAGOYA BURST DATA (1960-63)

CALLED	MISSED	FLARE	dB	RADIO
18 Feb 60			-	0053 U.T.
29 Mar 60*			3	
3 Apr 60			-	0306
5 Apr 60*			3 - 10	
	28 Apr 60	~0133	3 - 5	
	29 Apr 60	~0209	11	
	9 May 60	0704	> 1 dB	
13 May 60*			4 - 10	
20 Jun 60			-	0128
27 Jun 60*			small	
29 Jun 60*			small	
14 Aug 60			-	0515
3 Sep 60*			5 - 10	
	4 Sep 60	0003	3 - 5	
26 Sep 60*			> 1 dB	
11 Oct 60*			> 1 dB	
11 Nov 60*			small	
14 Nov 60*			>10 db	
15 Nov 60*			20 dB	
	24 Jul 61	~0450	small	
28 Sep 61*			3.3	
28 Feb 62			-	0647
1 May 63*			small	
	9 Aug 63	(sunrise) 2234	small	
15 May 63*			small	
	18 Sep 63	(sunrise) 2230	small	
20 Sep 63*			3.1 dB	
26 Sep 63*			4.6 dB	
	28 Oct 63	0230	small	

*Called and Confirmed as PCA Events

TABLE II

SPECIAL EVENTS

PEAK FLUX VALUES (1 f.u. = 1 x 10^{-22} w/m^2/cps)		$\int$ FLUX (Joules/m^2/Hz)	TOTAL ENERGY (500 - 8500 MHz) (Joules/m^2)	FLARE POS.	dB ABS.
30 March 69					
8800 MHz	2130.0 f.u.	2.1×10^{-15}	92.0×10^{-7}	E47	-
2695 MHz	1550.0 f.u.	2.7×10^{-15}			
1415 MHz	1550.8 f.u.	2.3×10^{-15}			
606 MHz	61[illegible]0 f.u.	0.8×10^{-15}			
4 March 67					
8800 MHz	1330 f.u.	0.8×10^{-17}	0.8×10^{-7}	W69	-
4995 MHz	975 f.u.	1.2×10^{-17}			
2695 MHz	530 f.u.	1.0×10^{-17}			
1415 MHz	90 f.u.	4.6×10^{-17}			
606 MHz	9638 f.u.	7.3×10^{-17}			

TABLE III

TOTAL RADIO ENERGY
(500 - 8500 MHz Range)

DATE	TOTAL ENERGY (1×10^{-7} Joules/m^2)	TIME OF[1] FLARE	POSITION[1] FLARE	dB ABS.[1]
18 Nov 68	12.3	1030E	W87	11.5
2 Sep 66	17.5	0538	W55	13.0
1 Nov 68	13.8	2229 (31 Oct)	W50	4.0
7 Jul 66	27.3	0020	W48	2.1
28 May 67	15.7	0525	W45	3.0
31 Oct 66	16.5	2339 (30 Oct)	W37	5.5
12 Jul 68	3.3	1341	W21	2.4
9 Jun 68	3.2	0835	W08	5.7
28 Aug 66	40.7[2]	1522	E04	4.0
23 May 67	1430.0[2]	1835	E24	11.0
2 Feb 67	0.2	0152	E61	2.6
4 Mar 67	0.8[2]	1715[3]	W69[3]	-
27 Feb 67	7.4[2]	1644[3]	E02[3]	- [4]
21 May 67	3.7[2]	1919[3]	E39[3]	-
30 Mar 66	92.0[2]	1244E[3]	E47[3]	-
6 Jul 68	5.2	0945[3]	E90[3]	-

Notes: 1 PCA flare and abs. data (Masley and Goedeke, 1967; Masley, 1969)
2 Energy values obtained from min/min integration of flux
3 Flare data from Solar-Geophysical Data Bulletin, ESSA
4 13.3 protons/cm^2/sec observed at ATS-1 (Paulikas and Blake, 1968)

	ALERT	CONFIRM	MISS	TOTAL PCA
1960	15	11	4	15
1961	1	1	1*	2
1962	1	0	0	0
1963	4	4	3*	7
TOTAL (1960-63)	21	16	8 (4)*	24 (4)*

* small events - no abs. values reported

Figure 1 RADIO ALERTS OF PCA EVENTS - Using the radio signature criteria for prediction of PCA events, radio events recorded by Nagoya (1960-63) were tested. 'ALERT' are those PCA events that would have met the criteria and have been called. 'MISS' are PCA events without radio events or radio events without the proper signature. 'ALERT' minus the number of 'CONFIRM' equals 'FALSE ALARMS'.

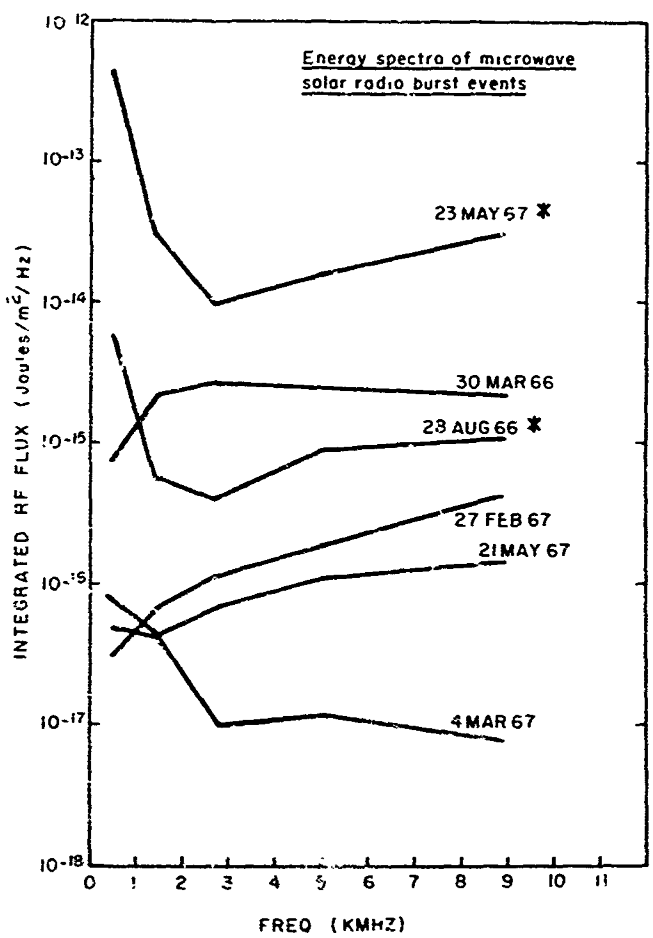

Figure 2 ENERGY SPECTRA OF MICROWAVE SOLAR RADIO BURST EVENTS - Each multi-frequency burst event was minute-by-minute integrated in flux to obtain the energy in Joules/m^2/Hz. The starred events are associated with Polar Cap Absorption Events. Note the increased low frequency energy for these events.

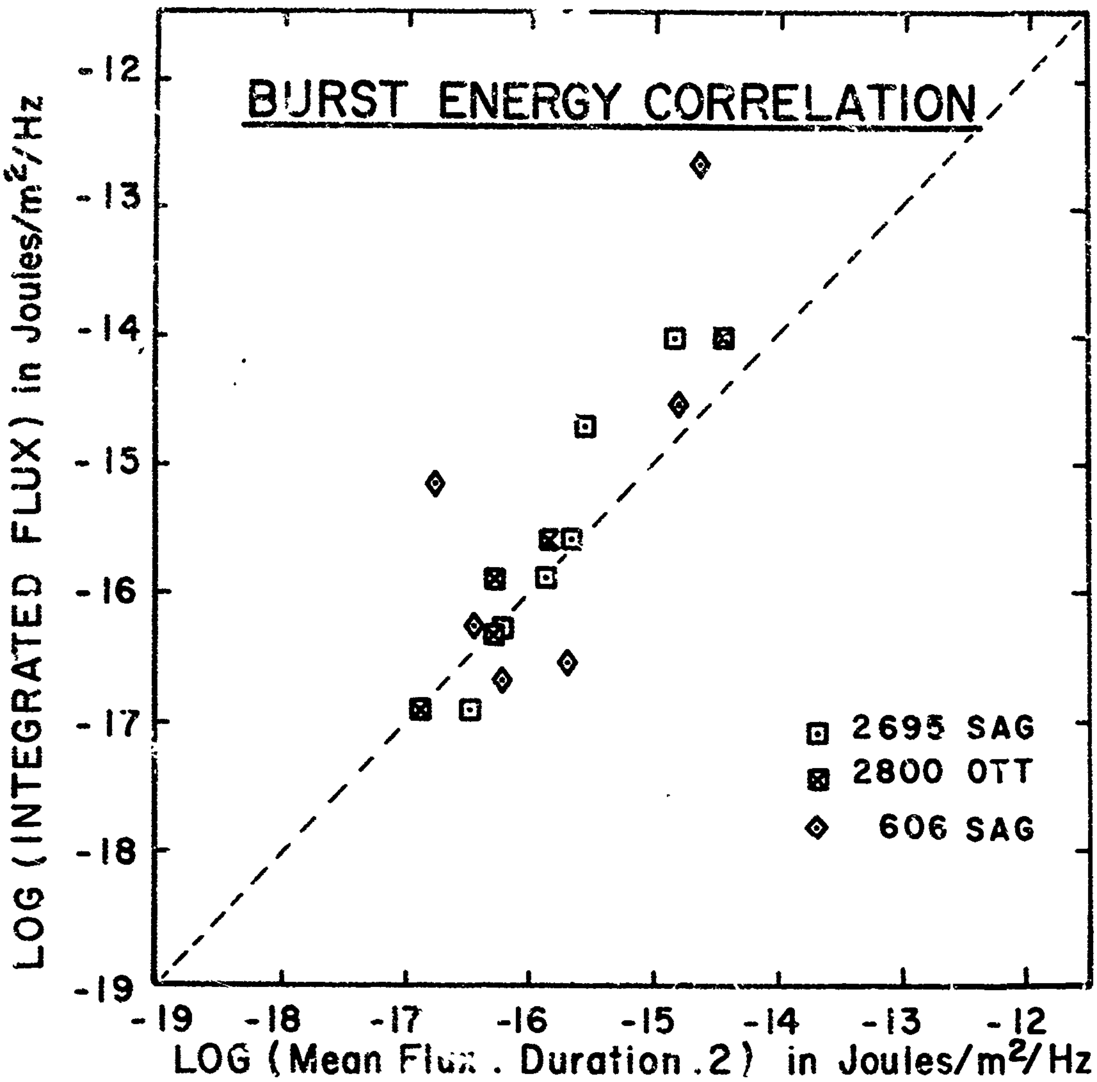

Figure 3 BURST ENERGY CORRELATION - A comparison is made of the energy values obtained when the radio bursts are integrated minute by minute in flux to that energy value obtained by multiplying twice the burst Mean Flux times the duration. Both the ordinate and abscissa are plotted in logarithmic values (e.g. the value -16 = 1 x 10^{-16}). These are in units of Joules/meter^2/Hertz.

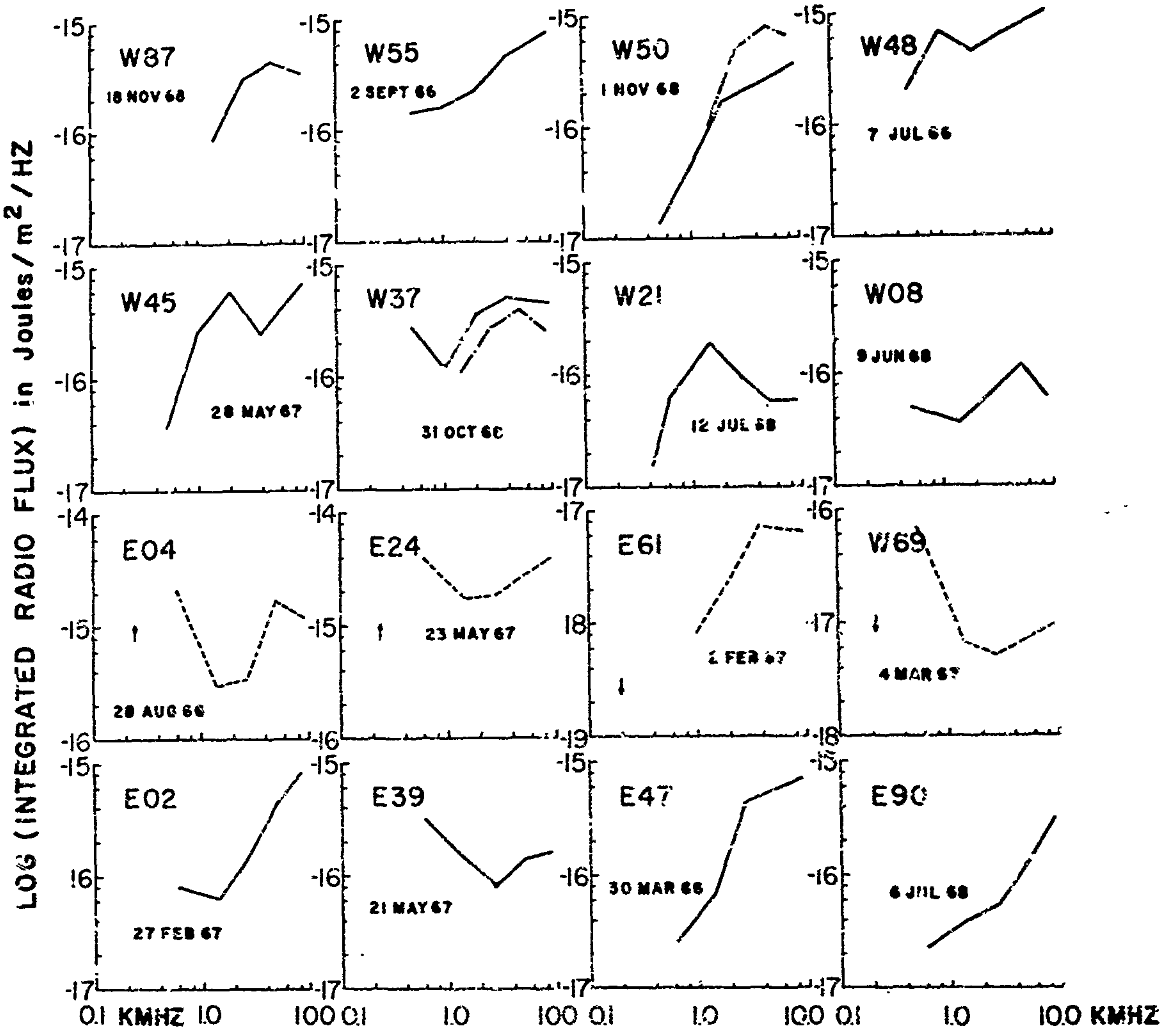

Figure 4 <u>RADIO BURST ENERGY SPECTRA</u> - The spectral energy values obtained by the Mean Flux Method are plotted for a number of 1956-68 radio events. These events are aligned from left to right and top to bottom in declining West solar longitudes (of their associated flares). The first eleven events from W87 to E61 are associated with principal PCA events. The remaining five events from W69 to E90 are non PCA events. In the figures for 1 Nov 68 and 31 Oct 58 the two curves show the difference between Manila values (dashed) and Nagoya values (solid). Dashed curves for the 28 Aug 66, 23 May 67, 2 Feb 67 and 4 Mar 67 represent a change in values of the ordinate. Arrows point the direction of change. Ordinate values are logarithmic as in Figure 3.

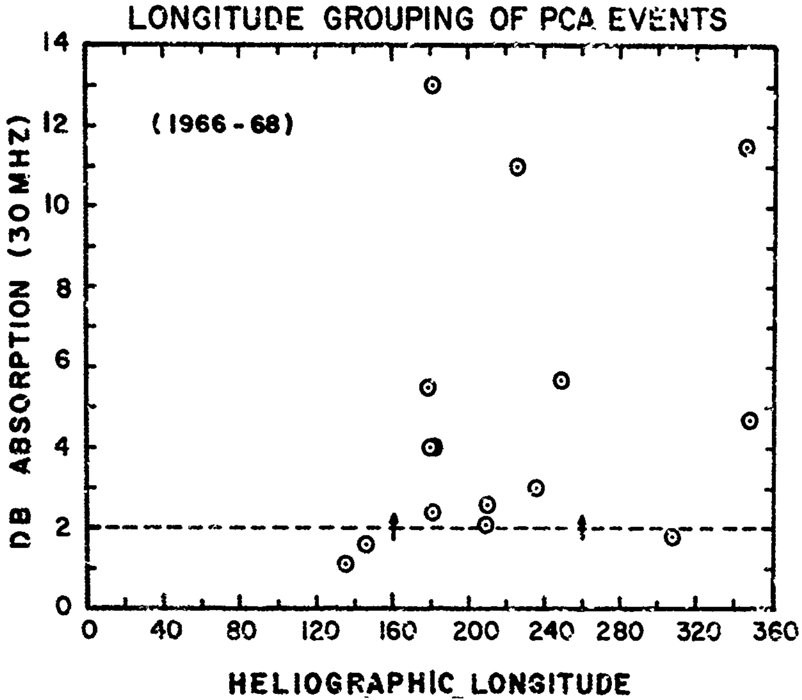

Figure 5 LONGITUDE GROUPING OF PCA EVENTS - The PCA Events for 1966-68 are plotted as a function of Carrington Solar Heliographic Longitude. This fixed longitude system grouping shows a tendency for these PCA events with dB > 2 to eminate from the solar longitude range near 160° - 260°. A second grouping is noted near 360°.

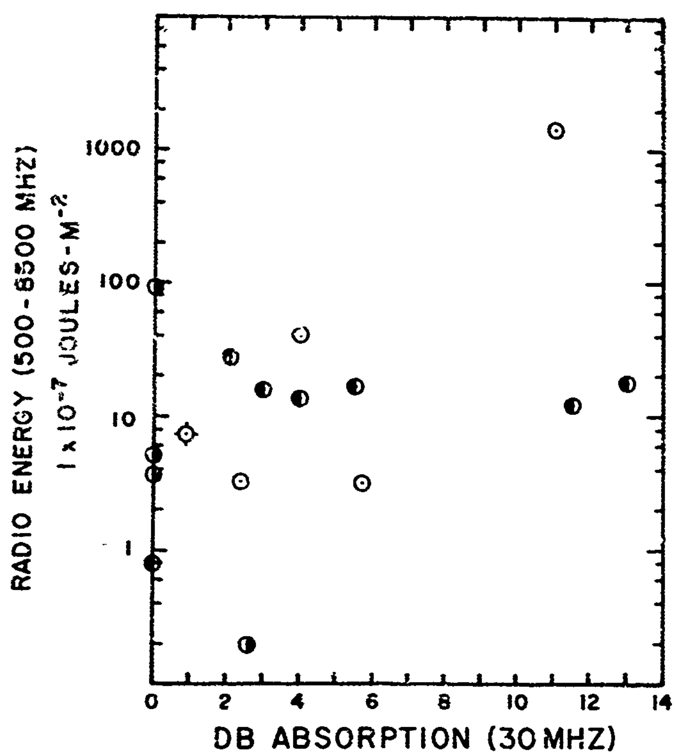

Figure 6 TOTAL RADIO ENERGY FOR 1966-68 PCA EVENTS - The energy spectra of each burst event was integrated over the 500-8500 MHz to obtain the total radio energy in this frequency interval. These total energy values are plotted against the 30 MHz db absorption of their associated PCA events. Longitude sectors of the parent flare positions are given as: (30E - 90E ◑), (30E - 30W ⊙), and (30W - 90W ◐). The event shown as ⊙ is the small non-PCA satellite observed proton event of 27 Feb 67. Note how the West longitude events ◐ vary in PCA magnitude while having near constant total radio energy of about 20 x 10^{-7} Joules/m^2.

RADIO BURST SPECTRA AND THE SHORT TERM PREDICTION OF SOLAR PROTON EVENTS

by

John P. Castelli and Jules Aarons

Air Force Cambridge Research Laboratories
Bedford, Massachusetts

SUMMARY

A short range prediction scheme designed to forecast solar proton events has been described in earlier papers. It depends on highly accurate measurements of solar burst flux densities at a wide range of frequencies. The success of the technique, now used by the Air Weather Service in the Solar Forecasting Network, is examined with data from 1966, 1967 and 1968. The "miss" rate for principal PCA's based on the criteria is close to zero if we discount events apparently associated with far side of the sun flare-bursts. While some radio bursts meeting these criteria are "false alarms", the rate is considerably lower than with any other short term prediction method.

RADIO BURST SPECTRA AND THE SHORT TERM PREDICTION OF SOLAR PROTON EVENTS

John P. Castelli and Jules Aarons*
Air Force Cambridge Research Laboratories
Bedford, Massachusetts

INTRODUCTION

Prediction schemes fall into long and short term categories. Predictions greater than a week in advance of actual events might be called long range. The probability of success is very poor since proton regions seem to evolve rapidly in less than six or seven days. Shorter range predictions make use of the observed development of optical and magnetic features of very large complex sunspot groups (Strickland, 1969). Sometimes the appearance of an active dark filament dividing the spot group provides the clue that a proton flare is likely to occur in this region in the next few hours.

Another approach suggested is to utilize the apparent temperature of solar centers of activity as measured by pencil beam millimeter wavelength systems where the gradients of the temperature of these regions are used to predict whether flare activity will or will not take place in this center.

The short range approach might best be termed an after-the-fact method. One technique currently used is to consider the combination of flare importance and the covering of the spot's inner darker area (umbra) by the H_α flare emission as a forerunner of proton emission likely to be observed within a few minutes to a few hours. Other forecasting schemes employ a combination of several before and after-the-fact criteria including the TYPE IV burst. The Type IV is basically a meter and dekameter featureless type of emission lasting between 10 minutes and several hours.

A traditional identifier of proton emission is the polar cap absorption event (PCA). It is necessary to make a distinction between strong and weak events. Strong or principal events are defined as those having polar region absorption of 37% (2 dB) or more of the normal cosmic background energy at 30 MHz. Weak events are all those with less than 2 dB absorption. Their lower limits can hardly be defined since the use of frequencies below 30 MHz and other propagation methods of measuring the effect of proton flux on the ionosphere would question limits of solar proton detectability.

To satisfy requirements in communications and space programs, the ideal after-the-fact prediction of strong PCA's must accomplish two things. First, there must be 100% success in warning of important proton events and secondly, warning of proton events which apparently do not materialize, "false alarms", must be kept to a minimum.

The prediction technique now in use by the Solar Forecasting Network of the Air Weather Service of the USAF utilizes flux density values of discrete frequency solar radio burst observations in the meter to centimeter wavelength range. The use of certain radio criteria and high accuracy peak flux measurements affords almost total success in predicting PCA's $\geq$ 2 dB from associated flares on the visible hemisphere, and only a small number of "false alarms".

THE RADIO CRITERIA

In predicting principal PCA's, the approach utilizes high accuracy peak flux data at discrete frequencies between 100 and 10,000 MHz. Within the Solar Forecasting Network, both the Sagamore Hill Radio Observatory and the Manila Observatory have been instrumental in developing equipment systems and methodology over a period of years to achieve high accuracies better than $\pm$ 10% at all frequencies. Calibrations involving the Cassiopeia A known flux density and the apparent lunar brightness temperatures provide standard signals for complete system calibration. A small group of observatories throughout the world make a concerted effort to maintain high absolute accuracy in their measurements, others strive for good internal consistency of measurements (relative accuracy).

The radio criteria for the prediction of a principal PCA are the following:

a. Burst flux increase has a value exceeding 1000 flux units (10^{-22} $WM^{-2}Hz^{-1}$) in the 9000 MHz range.

b. Flux minimum is observed in the 600-2000 MHz range.

c. Flux density rises in the low frequency direction.

When these criteria are satisfied, i.e., when the spectrum of the burst has a U-shape, a proton event is most probable.

*J. Castelli is a Research Electronic Engineer in the Radio Astronomy Branch, Ionospheric Physics Laboratory, of which J. Aarons is the Chief of the Radio Astronomy Branch.

In Figure 1, the spectra of principal PCA's for 1966, 1967, and 1968 are shown; although incidental details in form and flux density levels differ, the U-shape is readily apparent and the criteria have been met.

The "miss" rate for principal PCA's based on the criteria is close to zero if we discount events apparently associated with far side of the sun flare-bursts with which neither centimeter radio nor optical disciplines can cope. However, some radio bursts meeting these criteria are "false alarms".

VALIDITY OF APPROACH

The validity of after-the-fact predictions follows from the variable delay time between flare-burst occurrences and the beginning of the absorption. The average delay is about five hours but delays may be as short as 20 minutes. There is generally a considerable delay between first onset and time of maximum absorption or maximum particle flux (Figure 2).

FLARE BURST ASSOCIATION WITH PCA's: The Data:

Principal PCA's for the years 1966-1968 are shown in Table 1. In all but three cases, the PCA would have been predicted by a U-shaped spectrum from discrete frequency peak flux measurements. In two of the three cases there are no apparent radio correlations; there is strong evidence that the parent flares and proton regions were on the invisible hemisphere of the sun. This is almost certain in the case of the January 28, 1967, event which would have been about 64° beyond the west limb at the time of the proton shower (Dodson-Prince, 1969). Since proton regions characteristically produce multiple proton flares one would also expect that the event of February 2, 1967, came from the same region five days later but now 68° further west. A similar line of reasoning might be applied to the December 3, 1968, event. However, a 3N flare located at N18, E80 was observed at 2117 on that date. The time of day was such that no stations operating at wavelengths shorter than 10 cm were in a position to observe it. Though the peak flux was only 270 units at 2700 MHz, it is possible that the flux near 9000 MHz could easily have reached 1000 units if the spectrum of the disturbance were similar to those of other proton events as in Figure 1. A spectral index greater than about 1.07 would have been necessary. The requirement for high meter wavelength flux was met with 6460 flux units at 184 MHz.

The events of the period following the burst at 0948 on July 6, 1968, also require some clarification. It is apparent that the ATS-1 satellite on July 7 measured a proton flux increase which could only have been related to the above activity of July 6. The event at 1712 on July 8 with a spectrum similar to that of the 6th in the range up to about 9000 MHz had probably more effect on the ultimate 2.4 dB absorption recorded several days later.

During the period between October 30 and November 4, 1968, proton activity was extremely high with events occurring in almost daily succession. For that reason, it becomes difficult to isolate the contribution of discrete events. However, it appears that there were at least two principal events and as many as five flare-burst events contributing to particle enhancement. A more detailed study of this period is being prepared.

In the case of flare-burst association with PCA's occurring between 1952 and 1963, it is difficult to thoroughly test the prediction criteria because of incompleteness of radio data in some instances and lack of accuracy in others. However, 73% of the 48 principal PCA's had burst fluxes ≥ 1000 units somewhere in the centimeter range and another 10% most probably had flux exceeding 1000 units based on available information (Castelli, 1968). The small percentage completely lacking centimeter burst correlation may well have been associated with invisible hemisphere flares.

The criteria may also be applied to small proton events. Table II lists a consensus of probable events with absorption less than 2.0 dB. Where an associated flare-burst seems likely, the prediction criteria hold up well. (There is no evidence that the success rate with smaller events would be improved by reducing the peak flux criterion to less than 1000 flux units at 3 cm wavelength.) About half of the events would have been predicted using the criteria. Half would not have been predicted as there exists only nebulous correlation or none at all. Some of these might be associated with small flares and radio events (Sakurai, 1967) probably of fairly long duration while perhaps 3 or 4 might again be from far side flares. Still others have no apparent flare-burst association and may appear as low energy proton events only from directivity considerations from the steady streaming of regions which earlier were the sources of proton events (Fan et al., 1968). These "events" like far-side-of-the-sun proton events are not predictable by present criteria. In only one case would the criteria have led to an erroneous prediction and then the absorption was small and actually ignored by a number of researchers.

FALSE ALARMS

There is strong evidence based on current satellite particle monitors that some of the false alarms are de facto proton events in space without polar cap absorption, an earth oriented effect. The absence of terrestrial effects may be due to the interplanetary field directivity between the sun and earth. It is not entirely clear, however, to what extent the location of a proton flare on the sun influences the magnitude of particle influx at the earth. It is clear that radio events meeting the U-shaped spectral criteria may be associated with PCA's of less than 2.0 dB as well as with proton "events" based on satellite observations for which there are no apparent PCA's.

Figure 3 compares the number of meter wavelength Type IV events with centimeter burst occurrence for the years 1966-1968 at a given location (Sagamore Hill Radio Observatory, Hamilton, Massachusetts). It is apparent that the use of the Type IV criterion as generally understood would lead to an intolerable number of false alarms. Even rejecting those Type IV's with no centimeter burst association does not improve the outlook greatly. It can be shown that spectra rising to large values below 1000 MHz with low flux in the 9000 MHz region are not preferred for proton events. Even though the flux values may be large the spectra essentially run counter to the U-shape shown in Figure 1. The final box in Figure 3 indicates only four false alarms for three years. There were no failures to "call" PCA's $\geq$2.0 dB. Similar statistics could be worked out on a world wide basis if complete frequency and time coverage were assured.

In simple form the physics of the event is as follows:

Both the acceleration of protons to velocities adequate to escape the sun and centimeter radiation take place in the lower atmosphere of the sun. Associated meter wavelength radiation is probably due to relativisitc electrons accompanying the flare spiralling in the coronal magnetic field (synchrotron radiation). This type of radiation may occur apparently without proton emission if energies in the lower atmosphere are inadequate to accelerate protons to escape velocity.

CONCLUSIONS

1. After-the-fact prediction of proton events is valid.

2. The PCA absorption is a useful yes-no indicator.

3. The dm-cm peak flux U-shape spectral criterion appears to be close to perfect for important PCA's with visible hemisphere association.

4. Misses from far-side events will occur; these cannot be predicted with present criteria.

5. A large percentage of smaller PCA's will be predicted using present criteria; an equal number of weak proton events may be missed.

6. The false alarm rate will not be improved by reduction of the peak flux intensity criterion. The inability to associate small PCA's with flare-bursts is the real problem.

7. The number of false alarms from present criteria are so small as to be tolerable.

REFERENCES

Bailey, D.K., Polar Cap absorption, Planetary Space Science, 12, 495-541, 1964.

Castelli, J.P., Observation and Forecasting of Solar Proton Events, Air Force Surveys in Geophysics No. 203, AFCRL-68-0104, 1968.

Dodson-Prince, H.W. and E.R. Hedeman, Solar Physics, 1969 (in press).

Fan, C.Y., M. Pick, R. Pyle, J.A. Simpson and D.R. Smith, J. Geophysical Research, 73, 5, 1968.

Sakurai, K., Report of Ionosphere and Space Research in Japan, 24, 4, 213, 1967.

Strickland, A.C., Editor, Annals of the IQSY, Vol 3, The Proton Flare Project, The M.I.T. Press, 1969.

TABLE 1

PCA's 1966-1968 WITH ABSORPTIONS GREATER THAN 2.0 dB

DATE	APPROX. MAX. TIME FLARE-BURST	FLARE IMPORTANCE	POSITION	ABSORPTION
7 Jul 66	0037 U.T.	3B	N24, W45	2.1 dB
28 Aug 66	1529	4B	N22, E04	4.0
2 Sep 66	0555	3B	N21, W55	13.0
28 Jan 67	*			7.0
2-3Feb 67	*			2.6
23 May 67	1839	3B	N28, E24	11.0
28 May 67	0525	3B	N28, W32	3.0
9 Jun 68	0850	3B	S14, W08	5.[illegible]
9-12Jul 68	[illegible]12 (8 Jul)	3B	N13, E56	2.4
31 Oct 68	0011	3B	S14, W37	5.5
2 Nov 68	0912 (1 Nov)	2B	S18, W47	4.0
13 Nov 68	1028	1B	N23, W85	8.5
3 Dec 68	2117 †	3N	N18, E80	4.7

*Probably on Invisible Hemisphere of Sun

†Radio spectrum incomplete, see text

TABLE 2

PCA's 1966-1968 WITH 30 MHz ABSORPTIONS LESS THAN 2.0 dB

DATE	FLARE-BURST MAX. TIME	FLARE IMPORTANCE	POSITION	ABSORPTION	WOULD PREDICT	NO PREDICTION
24 Mar 66	0238 U.T.	3B	N18, W37	1.6	X	
5-7Feb 67	Unknown			1.6		X
13 Feb 67	1746 U.T.	4B	N22, W10	0.5	PREDICTED NO PCA	
27 Feb 67	1649 U.T.	2B	N27, E02	0.5	X	
11 Mar 67	Unknown*			1.3		X
23 Mar 67	0023 U.T.(22Mar)	3B	N25, E70	0.9		X
5-6Jun 67	Unknown*			1.1		X
2 Nov 67	0858 U.T.	1-2B	S18, E00	0.5	X	
12 Nov 67	Unknown					X
3 Dec 67	Unknown*			1.8		X
16 Dec 67	Unknown			0.8		X
11 Jan 68	1700 U.T.	2B	S25, W38		X	
8 Feb 68	Unknown					X
26 Apr 68	Unknown*					X
8 Jul 68	0946 U.T.(6 Jul)	2B	N14, E89		X	
26 Sep 68	0026 U.T.	1B	N12, E32	1.7	X	
29 Sep 68	1623 U.T.	2B	N16, W52	1.7	X	
4 Oct 68	Unknown			1.6		X
31 Oct 68	2257 U.T.	2B	S15, W49		X	
2 Nov 68	2004 U.T.(1 Nov)			1.3	X	
4 Nov 68	0520 U.T.			1.6	X	

*Possibly on Invisible Hemisphere of Sun

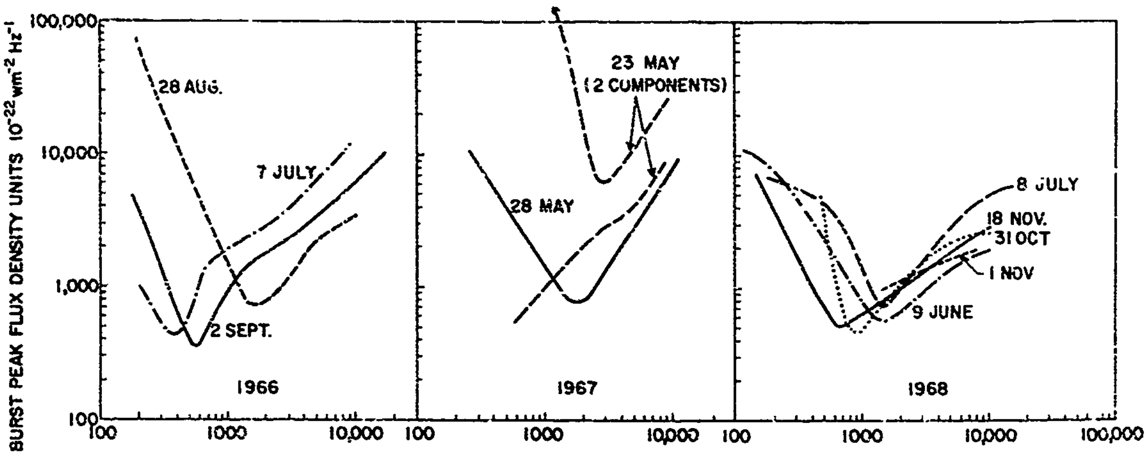

Figure 1 Peak flux spectra of solar radio bursts associated with PCA's ≥2.0 dB at 30 MHz - 1966-1968. Radio maxima are generally observed within a few minutes of each other and associated flare maxima. Flux values are based on published data from many sources.

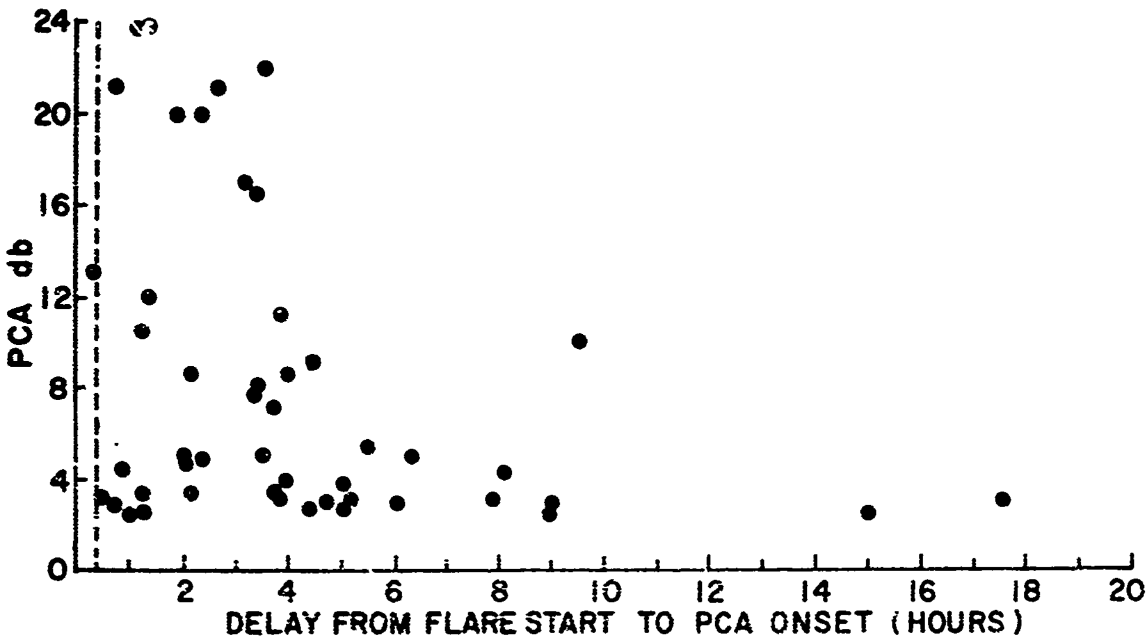

Figure 2 Distribution of principal PCA's (>2 dB) 1952-1963 (Bailey 1964). Mean delay flare start to flare max. (24 minutes) shown by broken line. Mean delay flare start to PCA onset 4 hours. Mean delay PCA onset to max. 18 hours.

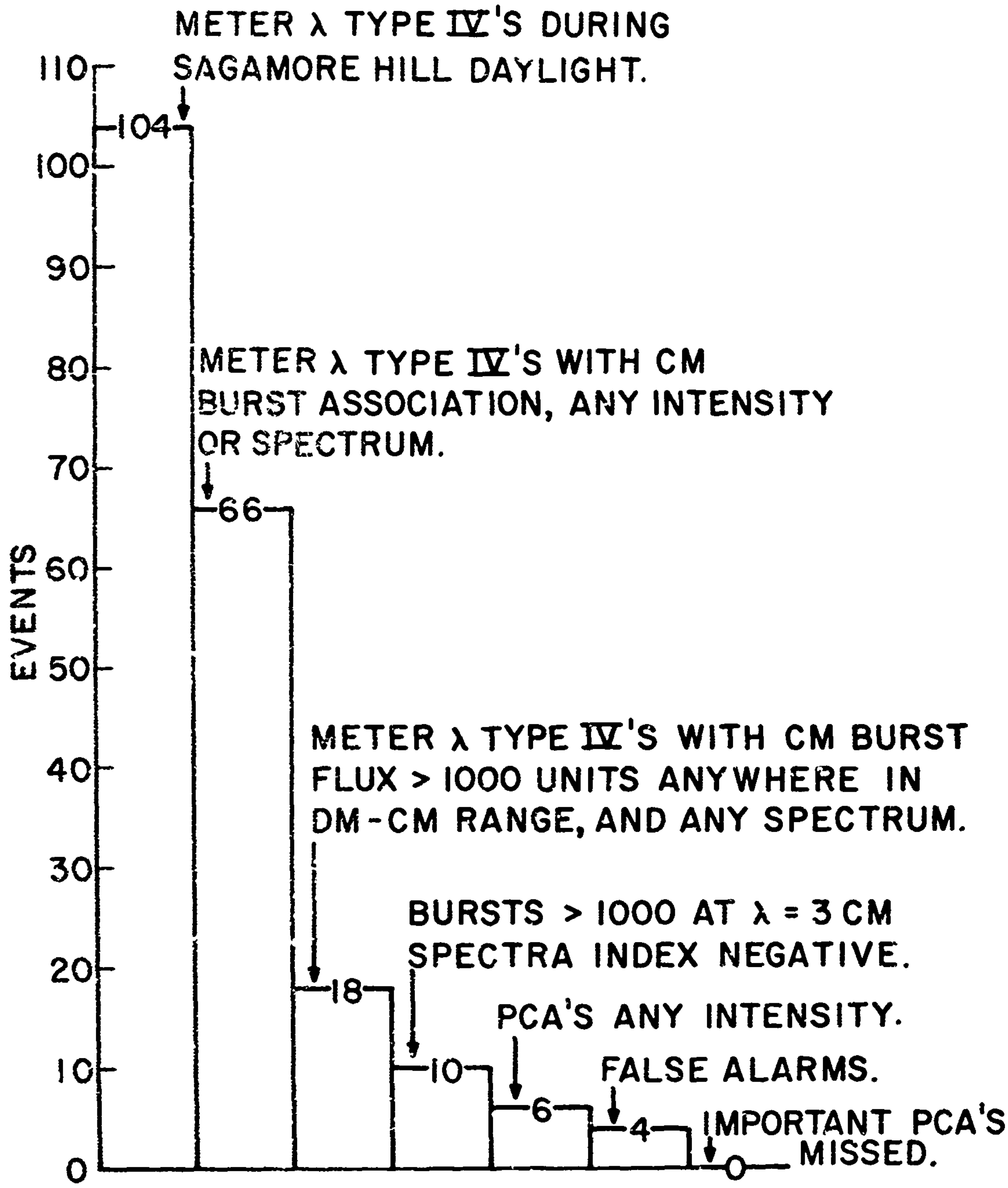

Figure 3 Meter wavelength Type IV events occurring during Sagamore Hill Observatory patrol hours 1966-1968 and distribution of those associated with cm. bursts of different spectra and with PCA's.

AN EVALUATION OF SOME OF THE NEW METHODS OF PREDICTING GEOMAGNETIC DISTURBANCE

by

Kenneth Moe

Space Sciences Department
McDonnell Douglas Astronautics Company/Western Division
Santa Monica, California 90406, USA

ABSTRACT

Although several theories have been proposed, we still do not understand solar flares, nor do we understand how the solar energy propagates into the Earth's magnetosphere. Because of ignorance of the physical mechanisms, attempts to develop methods of predicting geomagnetic disturbance have usually involved correlation studies employing some of the phenomena which are associated with solar flares and geomagnetic storms. It has been known for decades that some geomagnetic storms occur several days after large solar flares, but that in other cases storms will recur for several solar rotations without the recurrence of major flares. The unequivocal separation of flare-associated storms from recurring storms first became possible with the launching of the Mariner Space Probes. The first space probe which has been in a convenient position for predicting recurring storms is Pioneer 7. Even with Pioneer 7 available, serious predictive problems remain, because the energy spectra of solar emissions can vary greatly from storm to storm and not all precursors are invariably present. In this paper, the predictive value of several newly available tools is evaluated: Neugebauer and Snyder's study of the solar wind speed, Castelli et al.'s study of rCA spectra, Anderson and Lin's study of energetic electrons, Fairfield's study of the interplanetary field direction, and Balliff et al.'s study of the perpendicular fluctuations of the interplanetary field. The measurements described in the above studies are introduced in the present investigation into a mathematical formulation to predict the contributions to geomagnetic disturbance of persistent streams and flare-associated streams of solar plasma. Simulated numerical predictions of A_p using various combinations of the precursors are compared with the measured values of A_p .

1. INTRODUCTION

During geomagnetic storms, the air drag on artificial satellites increases, and radio and radar transmissions at high latitudes are impaired. There have been many attempts to develop reliable techniques of predicting magnetic storms in order to improve satellite orbital predictions and arctic radio propagation; but none of these attempts has been completely successful, for several reasons:

1. None of the precursors is wholly reliable.
2. Some of the precursors are monitored for only a fraction of the day.
3. Until the launching of Pioneer VII, there was no practical way of monitoring the long-lived tongues of enhanced plasma which apparently cause the recurring type of geomagnetic storm.

The study described in the present paper utilized Pioneer VII data and several other precursors in an attempt to overcome the limitations enumerated above in predicting the magnetic activity index ΣK_p. The paper begins with a discussion of the kinds of data considered for use. The prediction equations are next explained, and a graphical presentation of the predictions is given. The uncertainties in these simulated predictions are discussed, and suggestions are made for future research.

2. DATA

The following data were considered for use in the prediction formula for ΣK_p:

1. Solar wind speed
2. 10 cm solar radio noise bursts
3. Sudden ionospheric disturbances
4. Outstanding x-ray events
5. PCA events
6. Solar flares
7. Interplanetary field variations
8. Electron events
9. Sunspot areas in equatorial zone of sun
10. Neutron-monitor measurements
11. Magnetic crochets

Data items 1, 5, 7 and 9 were chosen because they had previously been individually correlated with K_p or A_p by Snyder et al. (1), Moe (2), Ballif et al. (3), and Gnevyshev (4), respectively. The remaining items are all associated with geomagnetic activity and were thought to be readily available. The first five data items are used in the final prediction formula and will be discussed in the following section. The last six were rejected for a variety of reasons: The solar flare data, published in Solar-Geophysical Data (5) were found to be too qualitative, incomplete, and unwieldy for the present purposes. Ballif et al. (6) found that the correlation between K_p and interplanetary field variations is greatly reduced when the satellite taking the measurements is more than a few degrees of heliocentric angle from the earth. Thus, such data would probably not be useful for two-day predictions. The prompt fluxes of electrons with energies greater than 40 Kev from solar flare electron events, obtained from Anderson (7), were compared with K_p. There was a good correlation with K_p two or three days later. Prompt electron data were not used in the simulated predictions because they are not yet available for 1968; however, if they were available in real time, they would be useful for predictions. Gnevyshev (4) shows a long-term correlation between A_p and sunspot areas in the equatorial region of the sun. However, analysis of 300 sunspot photographs supplied by Lt. Isbelle of the USAF Solar Observatory at Van Norman Reservoir (near Los Angeles) did not reveal any significant day-to-day or month-to-month correlation. Data items 10 and 11 were not used because of incompleteness.

3. REDUCTION OF DATA

The prediction formula,

$$K(t) = K_M(t) + K_F(t) \quad , \tag{1}$$

where K is the predicted value of ΣK_p, reflects two apparent contributions to the geomagnetic index; K_M is the contribution due to long-lived, active regions on the sun, and K_F is that due to flare-associated burst phenomena.

The basic data to be used in the prediction formula are the solar wind speed measurements made by the Pioneer VII satellite. This data has been published in Solar-Geophysical Data (5) since December, 1967. Pioneer VII orbits the sun in a position such that it sees a particular meridian of the sun τ days sooner than the solar rotation causes the earth to see this same meridian (see Figure 1). Hence, first-order predictions, using only solar wind speed data, can be made τ days in advance. Snyder et al. (1) showed a good correlation between ΣK_p and the solar wind speed U from Mariner IV data according to the formula

$$U = 8.41\Sigma K_p + 330 \text{ km/sec} \quad .$$

In the present study the preliminary formula, patterned after that of Snyder et al., is

$$U = 10\ K' + 300\ \text{km/sec} \quad , \tag{2}$$

where K' is the preliminary prediction of ΣK_p and U is the solar wind speed as measured by Pioneer VII. In applying the Equation 2, the U data must be co-rotated such that U on a certain day predicts ΣK_p at the earth τ days later.

If τ were equal to zero, there would be no need to separate the active region and flare-associated contributions to ΣK_p, since U is assumed to reflect all magnetic activity. Of course, in this case, Equation 2 would no longer be a prediction. Because τ is on the order of days, however, the prediction formula may be improved by considering the two contributions separately; the flare-associated contributions to ΣK_p from a particular event are added to K' at the time of the event, since the data were taken τ days before the event, and are subtracted from it τ days later.

Thus, the final prediction formula in terms of K' is

$$K(t) = [K'(t - \tau) - K_{FS}(t - \tau)] + K_F(t) \quad , \tag{3}$$

where the bracketed term represents $K_M(t)$, and K_{FS} represents flare-associated contributions at the satellite. Implicit in Equation 3 is the assumption that the flare-associated events recorded at the earth affect both the satellite and the earth simultaneously and in the same manner.

The flare-associated events used as precursors of geomagnetic activity in the present prediction scheme are items 2-5 listed in Section 2. The 10 cm solar radio flux measurements are obtained from the Sagamore Hill Observatory of the Air Force Cambridge Research Laboratories. These data are taken continuously during daylight hours. The sum of the mean flux densities of each day's bursts is the parameter used in the predictions. Of the sudden ionospheric disturbances, the sudden phase anomalies are the chosen parameter because of the worldwide distribution of SPA observations. These data are published in Solar-Geophysical Data (5). The reported degrees of phase shift are all assigned a positive sign and then summed for each day. The outstanding x-ray events, published in the same bulletin, are measured by satellite. The 1A to 20A fluxes are summed for each day. The polar cap absorption (PCA) events are recorded at the McDonnell Douglas Astronautics Company's geophysical observatories in the Arctic and Antarctic.

To obtain $K_{FS}(t - \tau)$ and $K_F(t)$ from the precursor data, the raw data are reduced by appropriate scaling factors which take into consideration the solar longitude of the flare associated with a particular precursor and the time delay between precursors and geomagnetic storms. The reduced data are then non-linearly converted to ΣK_p units. (See Reference 8 for details.)

4. DISCUSSION OF RESULTS

Simulated predictions of ΣK_p for 1968 made by the above method are compared with the actual values of ΣK_p in Figure 2. The solid line represents ΣK_p. The dashed line represents K', the predictions based on the co-rotated solar wind measurements alone. The dotted line represents K, the predictions based on both solar wind measurements and flare-associated events, using Equation 3. A solid triangle is placed on the time scale every 27 days, but there is not much evidence of 27-day recurrence in these data, indicating the probability of rapidly evolving tongues of plasma.

There is little difference between the dashed and dotted lines in Figure 2, except during the active period near the beginning of November. This means that flare-associated events made a negligible contribution to the computed K during quiet times, as expected.

Some of the smaller geomagnetic storms which appear not to be flare-associated may actually be associated with flares which did not produce enough penetrating solar radiation to affect riometers (~0.5 db), yet might have been observable with ionosondes at polar stations (9), or by forward scatter (10). A search for small PCA's, using ionosonde and forward scatter data for 1968, would be desirable when such data become available. In an earlier study (2), it was shown that some of the smaller storms during the first six months of the IGY were preceded by PCA's which were detected by ionosondes, but not by riometers.

To compare the predicted K to the preliminary prediction K', which used only solar wind data, the mean of the differences between the prediction and the actual ΣK_p for five ranges of ΣK_p were calculated for each case. The results are listed below.

RANGE	# SAMPLES	$\overline{\lvert K' - \Sigma K_p \rvert}$	$\overline{\lvert K - \Sigma K_p \rvert}$
$0 \le \Sigma K_p < 10$	30	7.2	7.4
$10 \le \Sigma K_p < 20$	148	5.9	6.5
$20 \le \Sigma K_p < 30$	107	9.3	9.4
$30 \le \Sigma K_p < 40$	27	16.9	16.5
$40 \le \Sigma K_p$	5	23.0	9.8

Although the statistical samples are not large, the figures above indicate that K is an improvement over K' for large values of ΣK_p but not for small values of ΣK_p. Referring to Figure 2c, it is obvious that large differences between K and ΣK_p occur after the activity in November when ΣK_p is

small and K becomes negative due to large values of K_{ps} in Equation 3. If, instead of assuming that flare-associated events recorded at the earth affect both the satellite and the earth simultaneously as a sort of expanding plasma shell, it is assumed that geomagnetic activity is caused only by tongues of plasma evolving from flare-producing regions on the sun, as suggested by Balif and Jones (11), then the failure of K as a prediction after the activity in November is explained. That is, K_{ps} cannot be calculated from precursor events observed at the earth; such events must be observed at the satellite. An alternative explanation is that the flare-associated events observed at the earth can be used, but that their effects decrease rapidly with angular distance from the sun's central meridian. This assumption was made in calculating the modified curve for November in Figure 2c. Unfortunately, there were no other large events in 1968 to use for testing the original and modified methods, but many suitable events will occur in the next few years as geomagnetic disturbance reaches its cyclical peak.

To check the present prediction scheme, the standard deviation between ΣK_p and the annual average of the same (used as a prediction for 1968) was compared with the standard deviations between ΣK_p and K, and ΣK_p and K'. The numbers were, respectively, 8.6, 10.8, and 10.5. Surprisingly, the annual average is the best prediction. (Undoubtedly this would not be the case had more activity occurred.)

The conclusions to be deduced from this statistical analysis are that the annual average is, at the present time, better than any of the more sophisticated methods of predicting K_p employed in this paper. More research on the physical nature of flare-associated events is obviously needed.

5. SUGGESTIONS FOR FUTURE RESEARCH

There are two lines along which future research could profitably be conducted: One is to study the usefulness of additional precursors in the prediction of flare-associated magnetic storms. Some of the best precursors are not yet available for the year 1968, but will later become available. These will be discussed in Section 5.1. The second future research area is the instrumentation and evaluation of a space probe which is specifically designed to aid in the prediction of geomagnetic storms. The orbit and instruments which would be desirable for such a research project will be briefly discussed in Section 5.2.

5.1 FURTHER STUDIES INVOLVING PRECURSORS

Although many precursors have been utilized in the present study, some of the precursors used had gaps in geographical or temporal coverage. For example, we only have data on solar radio noise bursts from North America, and the solar x-rays could not be seen by the satellite when the earth was between it and the sun. Other promising precursors are not yet available for the year 1968. Among the unavailable data are polar ionosonde, HF oblique-incidence, polar airglow, and prompt energetic electron measurements. A search for small PCA's would be desirable, using polar ionosonde (12) and HF oblique-incidence measurements (9, 10) for 1968.

To facilitate future research, and for the improvement of the storm-predicting networks, it would be desirable that each high-latitude riometer have an ionosonde near it, and that the ionosonde measurements be reduced immediately. (There is an ionosonde four miles from the riometer at McMurdo Sound, Antartica, but the ionosonde measurements do not become available for several years after they are recorded.) The differences in absorption between day and night, which were studied by Adams and Masley (13), should be studied for diagnostic value, because the energy spectrum of energetic solar particles might be related to radio propagation and magnetic storms in different ways. The sector structure and the southward pointing field component may affect the interaction between solar plasma and the magnetosphere, so this effect should be looked for when these data become available for 1968. Correlated studies for 1968, using long distance HF radio propagation (9, 10) and VLF phase anomalies (14), could be quite informative, especially if the energy spectrum revealed by diurnal variations observed with polar riometers were taken into account.

Some additional precursors have been reported in recent years; Castelli and Arons have reported that the spectrum of solar radio noise bursts can be used to predict geomagnetic storms (15). Adkinson and Hoffman have reported that half of the magnetic storms which occurred between April, 1965, and May, 1966, were preceded by a peculiar transient seen in the geomagnetic records at middle latitudes (16).

Mathews et al. (17) have used super neutron monitor data at many low-latitude stations around the world to study the anisotropy of Forbush decreases and "pre-decreases." The "pre-decrease" may be the result of the turbulent plasma cloud or shock front scattering cosmic rays away from the earth. These "pre-decreases" are sometimes seen at certain low-latitude stations before a storm's sudden commencement. Their possible predictive value should be investigated when the measurements for 1968 become available.

Solar wind data from the Pioneer and Vela satellites should be made available at more frequent intervals than the three or four samples per day which are being published in 1969. (In 1968, only one measurement per day from Pioneer 6 and 7 was published.) Finer time resolution, particularly on Vela data, would also be helpful, especially in evaluating the correlation between geomagnetic storms and changes in the solar wind speed which has been reported by Venkatesan and Sreenivasan (18).

5.2 A SPACE PROBE FOR USE IN PREDICTING ΣK_p

The orbit occupied by the Pioneer VII Space Probe, which is illustrated in Figure 1, is ideal for sampling the long-lived solar streams which will be passing over the earth several days later. Such a space probe, however, should be equipped with instruments for sensing storm precursors in order that the flare-associated contributions to ΣK_p at the satellite might be more accurately predicted, since the data observed at the earth are incomplete, and from the present study it appears that calculating these contributions from earth observations is inaccurate.

For detecting the solar x-rays, UV radiation, and energetic particles that are produced by the major solar flares which often precede geomagnetic storms, it would be desirable for the space probe to be able to scan the sun at one or several UV or x-ray wavelengths. Such a scanning system has been flown on OSO-4, but a less elaborate system would be satisfactory for predicting magnetic storms. The reason that it is important to scan the sun, rather than merely measuring the total solar emission, is that the response at the earth depends strongly on the location of the solar flare-producing regions. In data presently available, it is sometimes impossible to determine the location of flares associated with UV and particulate emissions.

ACKNOWLEDGEMENT

This study was supported by the NASA-Marshall Space Flight Center under Contract NAS 9-30156. We wish to thank the following scientists for unpublished data which were used in this study: Mr. A. J. Masley; Professors P. J. Coleman, Jr., K. A. Anderson, D. E. Jones, and D. Venkatesan; Col. E. J. Zavalick and Lt. T. R. Labolle.

REFERENCES

1. Snyder, C. W., M. Neugebauer and U. R. Rao, "The Solar Wind and its Correlation with Cosmic-Ray Variations and with Solar and Geomagnetic Activity," J. Geophys. Res., 68, 6361-6370, (1963).

2. Moe, K., "A Study of the Reliability of PCA as a Predictor of Geomagnetic Storms," J. Geomag. Geoelectr., 18, 159-66, (1966).

3. Balliff, J. R., D. E. Jones, P. J. Coleman, Jr., L. Davis, Jr., and E. J. Smith, J. Geophys. Res., 72, 4357-64, (1967).

4. Gnevyshev, M. N., "On the 11-Years Cycle of Solar Activity", Solar Physics, 1, 107-120, (1967).

5. Solar-Geophysical Data, ESSA, Government Printing Office, Washington, D. C. (monthly).

6. Balliff, J. R., D. E. Jones, P. J. Coleman, Jr., L. Davis, Jr., and E. J. Smith, "Further Evidence on Correlation," J. Geophys. Res., (in press).

7. Anderson, K., Unpublished data.

8. Moe, K. and N. U. Crooker, "Prediction of Aperiodic Events (Geomagnetic Activity)", Report MDC G1142, McDonnell Douglas Astronautics Company, 1969.

9. Jelly, D. H., "Effects of PCA on HF Oblique-Incidence Circuits", J. Geophys. Res., 68, 1705, (1963).

10. Hakura, Y., and J. V. Lincoln, "A Suggestion for Improving Forecasts", J. Geophys. Res., 68, 1563, (1963).

11. Balliff, J. R. and D. E. Jones, "Flares, Forbush Decreases, and Geomagnetic Storms," J. Geophys. Res., 74, 3499, (1969).

12. Jelly, D. H., and C. Collins, "Some Observations of PCA", Canadian J. Phys., 40, 706, (1962).

13. Adams, G. W., and A. J. Masley, "Theoretical Study of Cosmic Noise Absorption", Planet. Space Sci., 14, 277-290, (1966), (Douglas Paper No. 3112).

14. Chilton, C. J., F. K. Steele and R. B. Norton, "VLF Phase Observations," J. Geophys. Res., 68, 5421-35, (1963).

15. Castelli, J. P., J. Aarons and G. A. Michael, "Flux Density Measurements of Radio Bursts," J. Geophys. Res., 62, 5491-8, (1967).

16. Adkinson, V., and A. J. Hoffman, "Studies of Coincident Phenomena (abstract)", Trans. AGU, 49, 728, (1968).

17. Mathews, T., J. B. Mercer and D. Venkatesan, Anistrophy in Cosmic Ray Intensity, The University of Calgary, (1967).

18. D. Venkatesan and S. R. Sreenivasan, The Solar Wind and the Significance of ΣK_p, University of Calgary, (1967).

LIST OF FIGURES

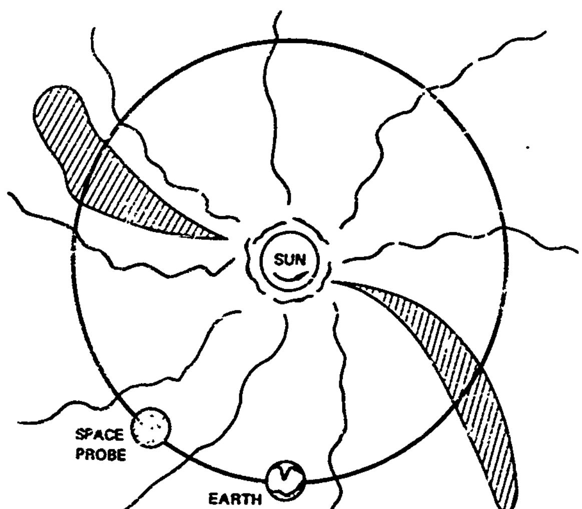

Figure 1. Pioneer 7 Space Probe following Earth in Orbit about the Sun. Because of the Solar Rotation, the long-lived tongues of enhanced solar plasma sweep over the Space Probe 2-days before they sweep over the Earth. In the present study, the Solar-wind speed measured by Pioneer 7 is used to predict the contribution to Geomagnetic disturbance made by these long-lived Plasma Tongues.

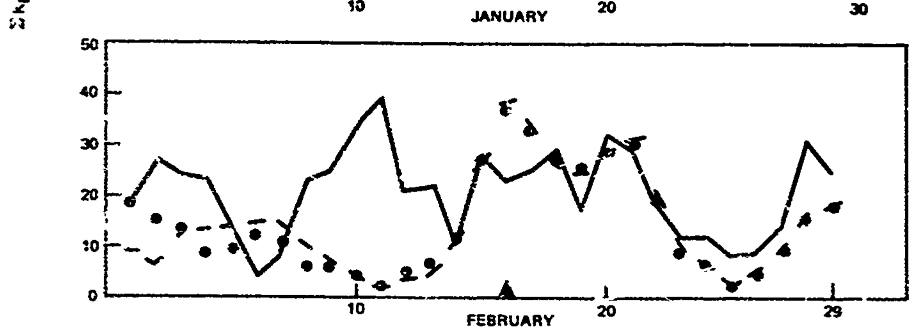

Figure 2 a. Comparison of Predicted and Actual ΣK_p

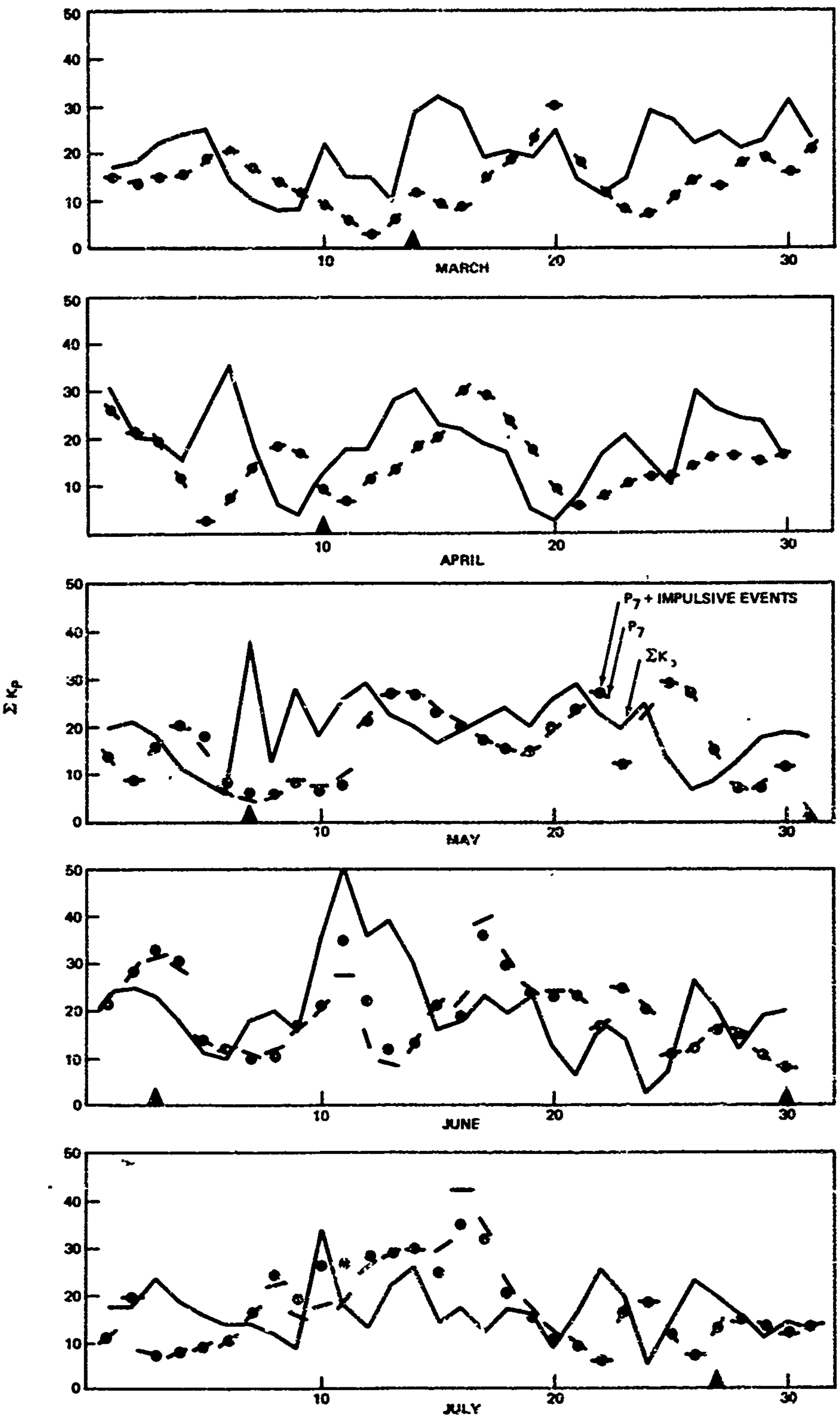
50
40
30
20
10
0
10
20
30
MARCH
APRIL
MAY
JUNE
JULY
ΣK_p
P_7 + IMPULSIVE EVENTS
P_7
ΣK_3

Figure 2b.

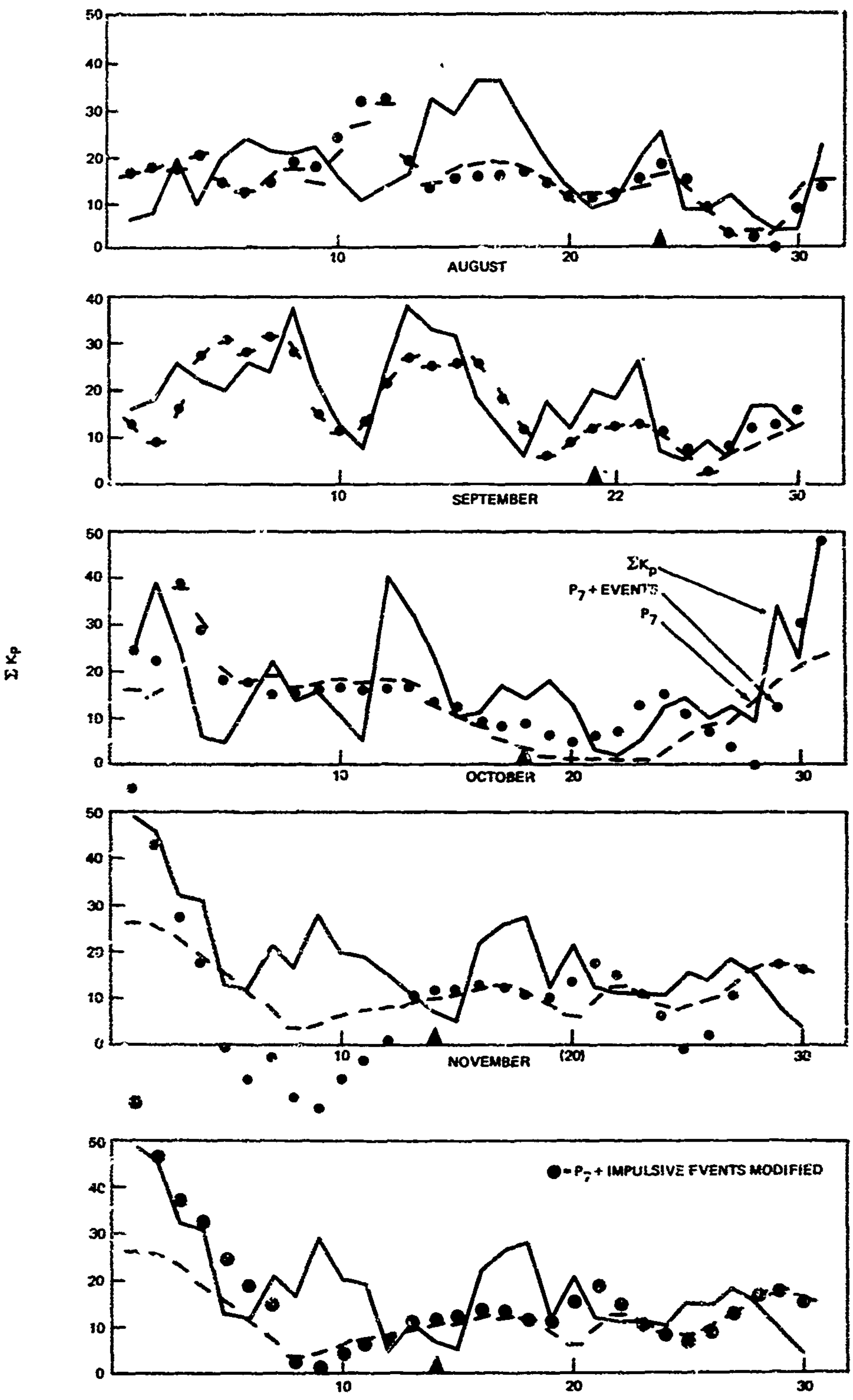
ΣK_p
AUGUST
SEPTEMBER
ΣK_p
P_7 + EVENTS
P_7
OCTOBER
NOVEMBER
● = P_7 + IMPULSIVE EVENTS MODIFIED
NOVEMBER (MODIFIED)

Figure 2c

THE MORPHOLOGY OF HIGH LATITUDE VLF EMISSIONS

by

A.R.W.Hughes, K.Bullough, T.R.Kaiser

Department of Physics,
University of Sheffield

The morphology of high latitude VLF emissions

A.R.W. Hughes, K. Bullough, T.R. Kaiser

Department of Physics,

University of Sheffield.

Abstract

Energetic particles (mainly KeV electrons) make an important contribution to the production of ionisation in the high latitude ionosphere. Studies of the emissions at VLF, LF and HF associated with these particles are essential for an understanding of the mechanisms and morphology of precipitation and thus, eventually, for the more successful prediction of ionospheric conditions at these latitudes.

The VLF experiment on the satellite Ariel III (circular orbit: altitude 550 km, inclination 80°) was designed to make a synoptic study of VLF phenomena above the ionosphere. The peak, mean and minimum signals at 3.2, 9.6 and 16 kHz are measured in each 28 second period ($\approx 2^{\circ}$) around the orbit. On-board tape-recording of this data and the high sensitivity ($\simeq 10^{-13}\gamma^2$/Hz) and wide dynamic range (75 dB) of the receiver make it possible to delineate a zone of emission above the auroral oval in both hemispheres at all magnetic local times.

This analysis is restricted to the period 1967 May, June, July. The locations of the zones of emission and associated particle precipitation in the north and south polar regions are related to the tilt of the earth's rotational axis towards the sun in the northern hemisphere summer. The zone maximum is displaced to lower invariant latitudes with increasing magnetic disturbance (K_p), the displacement being greatest at local noon and least at local midnight. ~~In the local evening~~ There is also a decrease in the relative frequency of occurrence of the more intense emissions ($>$ 65 dB above $10^{-15}\gamma^2$/Hz) for $K_p > 4$.

1. Introduction

Very low frequency wide band radio noise, known as 'hiss', is generated at auroral latitudes by energetic electrons, as has been established from simultaneous observations of energetic electrons and VLF radio waves on the satellite Injun 3. Gurnett and O'Brien (1964) and Gurnett (1966) found a good correlation between hiss and energetic electrons having an exponential folding energy (E_0) of between 3 and 4 KeV. Jørgensen (1968) demonstrated that the intensity and broad band spectrum of the hiss emission could be explained in terms of Cerenkov radiation from low energy (KeV) electrons.

Cerenkov radiation is generated by a charged particle moving through a magnetoplasma if the component of its longitudinal velocity in the wave normal direction equals the phase velocity of the wave. Thus Cerenkov radiation can only be produced at frequencies for which the refractive index is greater than one; this is the case for certain modes of propagation

in a magnetoplasma and includes low and very low frequency radio wave propagation in the whistler mode in the magnetosphere and ionosphere. Jørgensen (1968) showed, for example, that a frequency of 10 kHz may be generated at all altitudes up to 25,000 km, while 1 MHz can only be generated up to 1000 km; this altitude limitation is determined by the ambient plasma and the magnetic field strength such that for Cerenkov radiation in the dominant whistler mode the frequency lies below both the plasma frequency and the electron gyrofrequency.

An interesting feature of the Cerenkov mechanism is that the power generated is inversely proportional to the square root of the particle energy (McKenzie, 1963); thus it is lower energy electrons that are expected to make the greatest contribution at VLF. Since, as we descend in frequency, the Cerenkov condition is satisfied by electrons of lower energy we might expect a softer electron energy spectrum to be associated with a 'softer' VLF spectrum. Evidence of this is provided by the enhanced signals at 3.2 kHz observed in the local evening (Bullough et al, 1969a). Observations of auroral electrons made on the OGO-4 satellite (Hoffman 1968) indicate that the flux of the lower energy electrons may be greatly in excess of those at higher energies; specifically Hoffman gives examples of electron fluxes at 0.7 KeV which exceed those at 7.3 KeV by between 2 and 3 orders of magnitude.

From the above, we may expect the observations of high latitude VLF emissions, made on Ariel 3, to define regions of low energy electron fluxes; the proportion of these electrons precipitating into the upper atmosphere will depend on the pitch angle distribution and the loss cone. The wide global coverage obtained by the storage of data on Ariel 3, the large inclination orbit (80°) and the sensitivity of the receiver made it possible to define regions of VLF emissions at all magnetic local times. Since the whistler mode signals propagate along field lines (predominantly duct guiding) the VLF observations give a rather precise delineation, in invariant latitude, of the associated electron precipitation.

The results presented in this paper are based on an analysis of 80 days data from the 5th May 1967; in this period complete coverage in magnetic local time was obtained.

2. The Ariel III VLF equipment

The Ariel III satellite was launched on 1967 May 5 into a low altitude (500-600 km) orbit of high inclination (80°) and period 96 min. By means of a VLF receiver with loop aerial measurements of the peak, mean and minimum VLF magnetic field intensities are made at three frequencies (3.2, 9.6, 16 kHz) in 28 second periods ($\equiv 2^\circ$) around the orbit. At each frequency there is a wide-band (Δf = 1 kHz) channel; at 16 kHz there is also a narrower band (Δf = 100 Hz) channel. Measurements were stored on the satellite tape-recorder and world-wide coverage obtained. The receiver sensitivity is approximately $10^{-13}\gamma^2$/Hz. A detailed description of the equipment is given by Bullough et al (1968).

An outstanding feature of this experiment is that the essential information on VLF signal intensities and type of signal is obtained in a form which facilitates comparative studies with other geophysical disturbance phenomena such as particle fluxes, the visual aurora, magnetic storms, etc. (see e.g. Bullough et al (1969a,b)).

3. Profile of the high latitude hiss zone

Examples of traversals of the high latitude hiss zone are given by Bullough et al (1969a). Fig. (1) is reproduced from the latter paper and illustrates four traversals of the zone on a revolution passing close to the magnetic poles. The zone is usually sharply defined in latitudinal extent with a fairly flat frequency spectrum and at zone maximum the ratio of mean to minimum signal is characteristically less than 3 dB with the peak signal 10 to 15 dB higher. More recent analysis indicates that the electron bursts observed by Hoffman (1968) on the high latitude side of the auroral oval probably have their analogue in the increased ratios of peak/mean and mean/minimum VLF signals on the high latitude side of the hiss zone.

4. General morphology of the emissions

High latitude VLF emissions are commonly more intense in the evening hours, however the sensitivity of the Ariel III receiver made it possible to observe emissions at all magnetic local times and, in figures 2 and 3, the position of the high latitude zone is mapped in invariant latitude (Λ) and magnetic local time. The invariant latitude is defined by

$$\cos\Lambda = L^{-\frac{1}{2}}$$

where L is McIlwains L-parameter and is derived from the G.S.F.C. (1964) model of the earth's magnetic field, and the magnetic local time is that for the centred dipole approximation to the field. In these figures the position of the zone is defined as the position of the maximum signal level from the 16 kHz mean reading circuit. Analysis has been restricted to satellite passes reaching an invariant latitude of greater than 75° and, in this section, to periods when the planetary K-index (K_p) was equal to or less than 2+.

Referring to figure 2 (northern hemisphere) it may be noted that the lowest latitude (Λ_T) at which the zone maximum was observed is markedly dependent on magnetic local time. At noon $\Lambda_T = 75°$, while on the anti-solar side of the earth it is 67°; in the dawn-dusk meridian $\Lambda_T = 70°$. This general distribution is consistent with the view that auroral hiss is generated by particles which come from the tail of the magnetosphere, the asymmetry being due to field lines from the tail reaching lower latitudes on the anti-solar side of the earth. The VLF emission zone in the northern hemisphere is almost identical to the inner zone of high latitude disturbance phenomena identified by Hartz and Brice (1967).

Figure 3 is a similar plot for the southern hemisphere. In this case the noon/midnight asymmetry is not nearly as pronounced; Λ_T at midnight is the same as in the northern hemisphere (67°) but at noon is 70° (compared with 75° in the north). The difference between the hemispheres

may be attributed to the tilt of the earth's rotational axis around which its magnetic axis processes on a cone of half angle 11.5°. During the period of these observations the sun was in the northern hemisphere (declination varying from +16° to a maximum of +23°30' and back to +17°). Spreiter and Briggs (1962) predicted for theoretical studies that the effect of such an asymmetry would be to shift the position of the neutral points (these define the boundary, on the noon meridian, between the closed lines of force and those that enter the tail). In the northern hemisphere, the value of Λ_T (for this whole three month period) will correspond to a solar wind in a direction between 5° and 12° north of the magnetic dipole equator (solar declination minus 11.5°). From Spreiter and Briggs this would increase the magnetic latitude of the northern neutral point by some 1° to 2°. In the southern hemisphere, Λ_T will correspond to a solar wind direction of 35° (23.5° + 11.5°) north of the magnetic equator which, according to Spreiter and Briggs, decreases the latitude of the southern neutral point by 4°. This predicted N-S asymmetry of 5°-6° is thus in good agreement with the observed asymmetry of 5°. It may be noted (from figures 2 and 3) that there is no comparable asymmetry on the midnight and dawn-dusk meridians.

5. Variation of zone position and signal intensity with magnetic disturbance (K_p)

For this study, periods were selected which gave a reasonable range of K_p values. The data were split into the four magnetic local time ranges, 00 ± 03h, 12 ± 03h, 06 ± 03h, 18 ± 03h. Data points for both northern and southern hemispheres are shown in figure 4 with, in each case, a linear least squares fit (giving the invariant latitude of the zone maximum as a function of K_p). This analysis shows that there is a significant displacement of the mean position of the zone maximum to lower latitudes with increasing level of magnetic disturbance. The displacement ($\Delta\Lambda$) for unit increase in K_p (deduced from figure 4) may be summarised as follows;

MLT(±03h)	$\Delta\Lambda$ (north)	$\Delta\Lambda$ (south)
0000	- 0.7°	- 0.7°
1200	- 1.6°	- 1.9°
0600	- 1.0°	- 1.3°
1800	- 1.0°	- 1.7°

These figures may be a trifle low, particularly at local noon, since the relative proportion of data points obtained decreases progressively for invariant latitudes above 75° (see first paragraph of §4). It may be noted that the displacement of the zone maximum at local noon is significantly greater than at local midnight.

The signal intensity, when plotted as a function of K_p, exhibits considerable scatter with a tendency for a fall in the relative frequency of occurrence of the more intense emissions (> 65 dB above $10^{-15}\gamma^2/Hz$) when K_p exceeds 4. This behaviour is consistent with that of other high latitude disturbance phenomena such as the radio aurora (Bullough (1961))

where, in the inner zone, a close correlation with the local K-index and an anti-correlation with the K_p index was found. Thus radio-auroral activity observed in Terre Adelie was found to move from the inner to the outer zone with increasing K_p*. This behaviour is in accord with more recent studies by Krassovsky (1968) who has found evidence of an anticorrelation between the occurrence of strong aurora and of a strong ring current effect in a geomagnetic storm. Studies of the more detailed temporal and spatial (substorm) variations in the medium and high latitude emissions during magnetic storms are in progress (Bullough et al (1969b,c)).

A significant feature of high latitude hiss is a well-defined minimum in its intensity at 0500 to 0600 MLT such that the maximum observed intensity is about 55 dB above $10^{-15}\gamma^2/Hz$ compared to signal intensities which may be in excess of 70 dB in the late evening. There is a related variation of the flux and energy spectrum of KeV electrons around the auroral oval (Hartz and Brice 1967). Thus the wave and particle observations are again consistent with the Cerenkov hypothesis. The fairly well-defined upper limit to the VLF signal intensity, which is a function of magnetic local time around the aurorae oval, would imply a corresponding upper limit to the KeV electron fluxes.

As more detailed studies of the above features continue (Hughes et al (1969)) the need for a self-consistent system of coordinates, such as that proposed by Kilfoyle and Jacka (1968) has become increasingly apparent. This is especially so for invariant latitudes in excess of 80°, where the conventional "invariant latitude/magnetic local time" grid for presentation and organisation of the observations is no longer adequate. This is because the "auroral pole", which lies at the geometric centre of the invariant latitude contours is displaced about 3° and 5° from the centred-dipole geomagnetic pole in the northern and southern polar caps respectively.

Conclusions

The Ariel III observations of VLF emissions are yielding a great deal of new information on the morphology of disturbance phenomena at high latitudes. Such observations are essential to an understanding of the mechanisms giving rise to energetic particles at both high and medium latitudes which, in turn, should lead to a better prediction of particle effects in the ionosphere.

A more detailed study of wave-particle relationships will be possible on the UK4 satellite (launch date: 1971 July) which will carry an integrated payload consisting of ELF/VLF, LF/HF and particle experiments from the Universities of Sheffield, Manchester and Iowa.

---

* It should be noted that the K_p index is derived from observations of magnetic disturbance at stations located almost entirely at medium latitudes.

References

Bullough, K., 1961, 'Radio-echo observations of the aurora in Terre Adelie'. Annales de Geophysique 17(2), 195-230.

Bullough, K., Hughes, A.R.W., Hudson, T., Hickinson, D., Broomhead, P., Tomlinson, A., 1968, 'The Sheffield University VLF experiment on the satellite Ariel 3'. J. Sci. Instrum. (Series 2) 1, 77-85.

Bullough, K., Hughes, A.R.W. and Kaiser, T.R., 1969a, 'VLF observations on Ariel III'. Proc. Roy. Soc. A (in press).

Bullough, K., Hughes, A.R.W. and Kaiser, T.R., 1969b, 'Satellite evidence for the generation of VLF emissions at medium latitude by the transverse resonance instability'. Plan. and Space Science 17, 363-374.

Bullough, K., Hughes, A.R.W. and Kaiser, T.R., 1969c, in preparation.

Gurnett, D.A., O'Brien, B.J., 1964, 'High latitude studies with satellite Injun 3, 5, very low frequency electromagnetic radiation'. J. Geophys. Res. 69, 65-89.

Gurnett, D.A., 1966, 'A satellite study of VLF hiss'. J. Geophys. Res. 71, 5599-5615.

Hartz, T.R. and Brice, N.M., 1967, 'The general pattern of auroral particle precipitation'. Planet. Space Sci. 15, 301-329.

Hoffman, R.A., 1968, 'Low energy electron precipitation at high latitudes'. J. Geophys. Res. 74, 2425-2451.

Hughes, A.R.W., Bullough, K. and Kaiser, T.R., 1969, in preparation.

Jørgensen, T.S., 1968, 'Interpretation of Auroral Hiss Measured on OGO 2 and at Byrd Station in terms of Incoherent Cerenkov Radiation'. J. Geophys. Res. 73, 1055-1070.

Kilfoyle, B.P., Jacka, F., 1968, 'Geomagnetic L Coordinates', Nature 220, 773-775.

Krassovsky, M.I., 1968, 'Auroras'. Planet Space Sci. 16, 47-59.

McKenzie, J.F., 1963, 'Cerenkov Radiation in a magneto-ionic medium ...' Proc. Roy.Soc. A. 255, 585-606.

Spreiter, J.R. and Briggs, B.R., 1962, 'Theoretical determination of the form of the boundary of the solar corpuscular stream produced by interaction with the magnetic dipole field of the earth'. J. Geophys. Res. 67, 37-51.

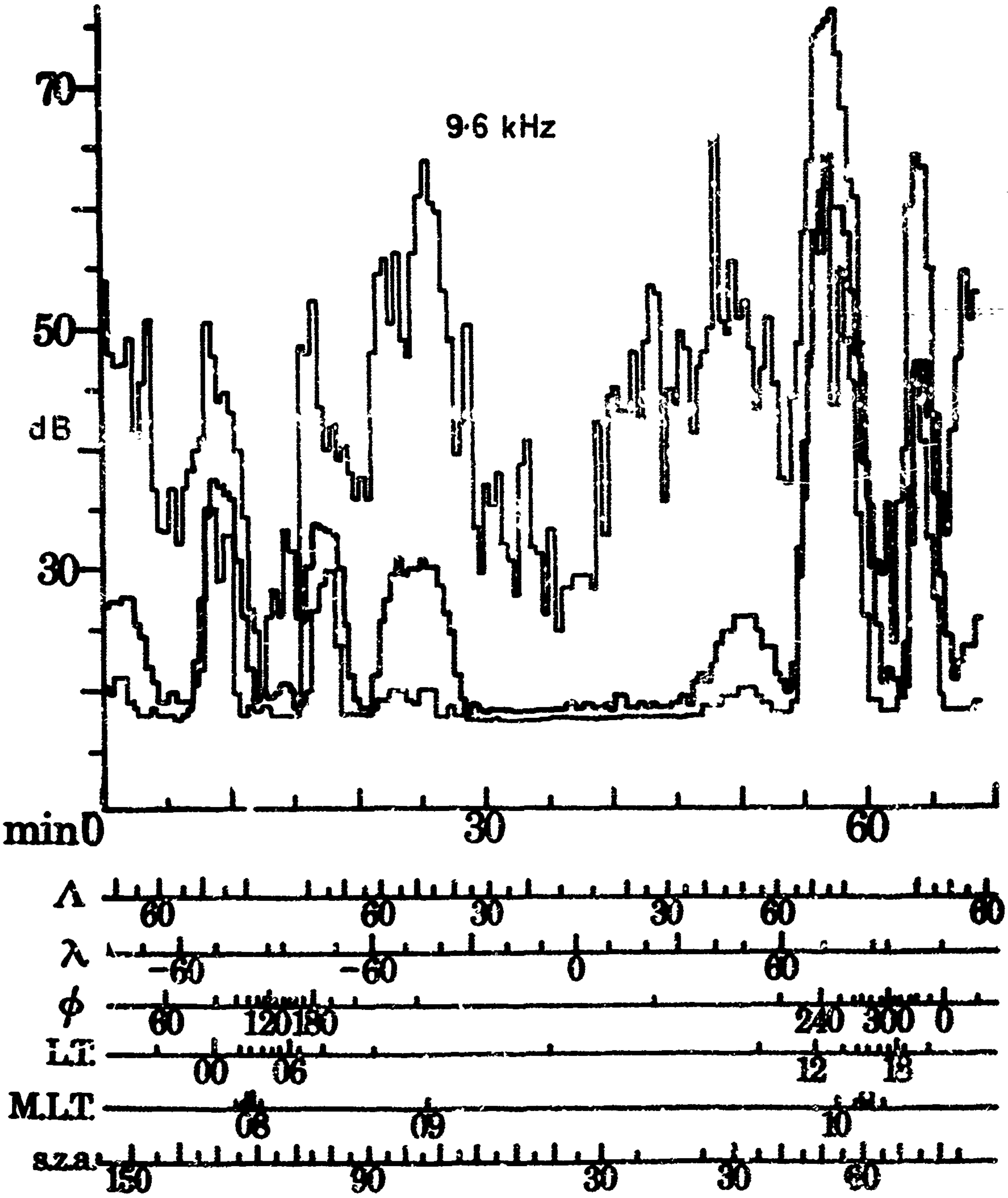

Figure 1. The high latitude hiss zone; four traversals on a revolution passing close to the magnetic poles, 14 July 1967, 18.57 to 20.06 U.T., 9.6 kHz. Ordinate: dB above $10^{-15}\gamma^2/Hz$ (the mean signal output has a thicker line) Abscissae: min, minutes along the orbit; Λ, invariant latitude; λ, geographic longitude; φ, geographic latitude; LT, local time; MLT, magnetic local time; SZA, solar zenith angle at the satellite.

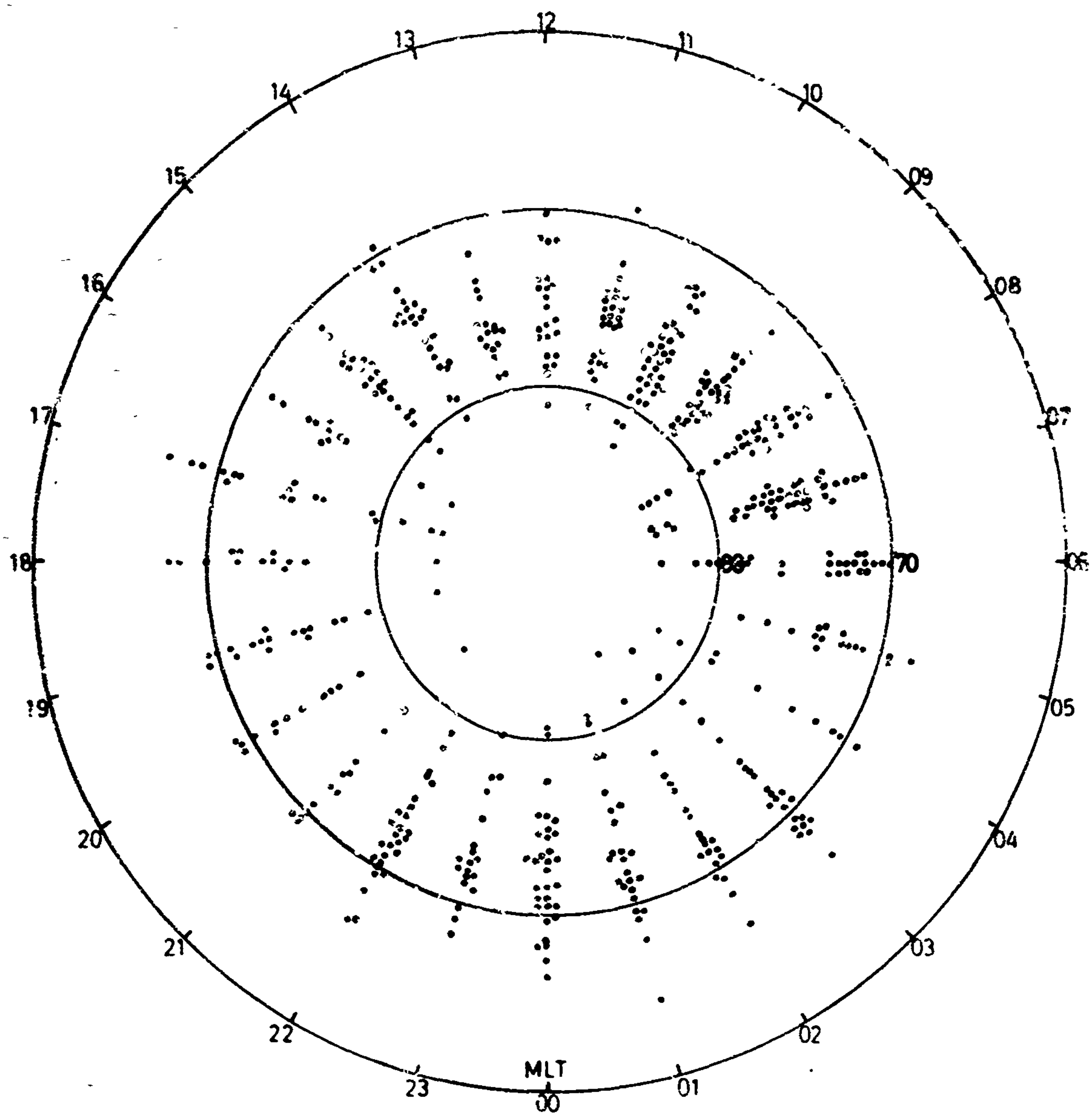

Figure 2. The location of the maximum of the high latitude zone of emission (northern hemisphere) plotted in invariant latitude and magnetic local time.

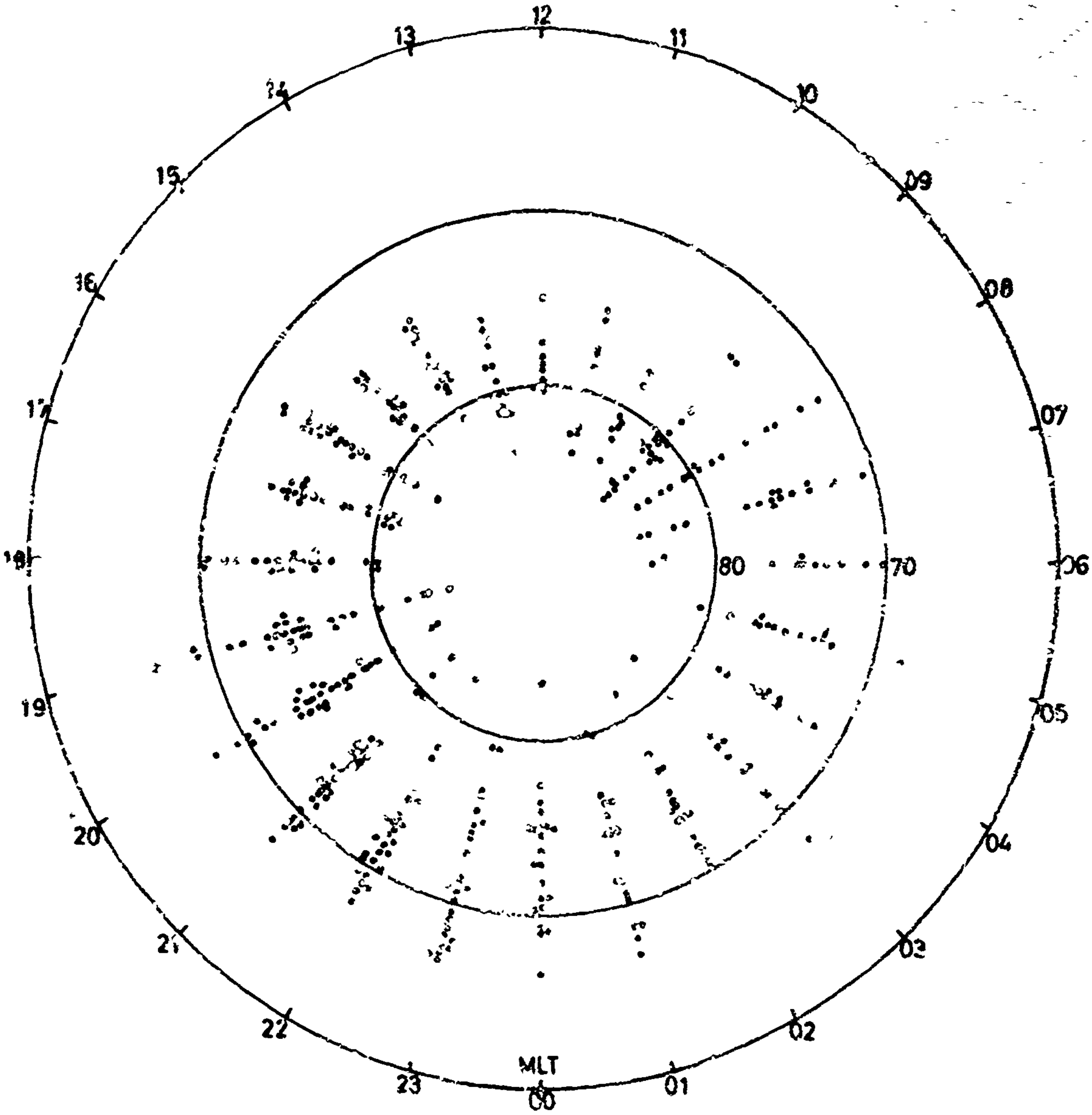

Figure 3. The location of the maximum of the high latitude zone of emission (southern hemisphere) plotted in invariant latitude and magnetic local time.

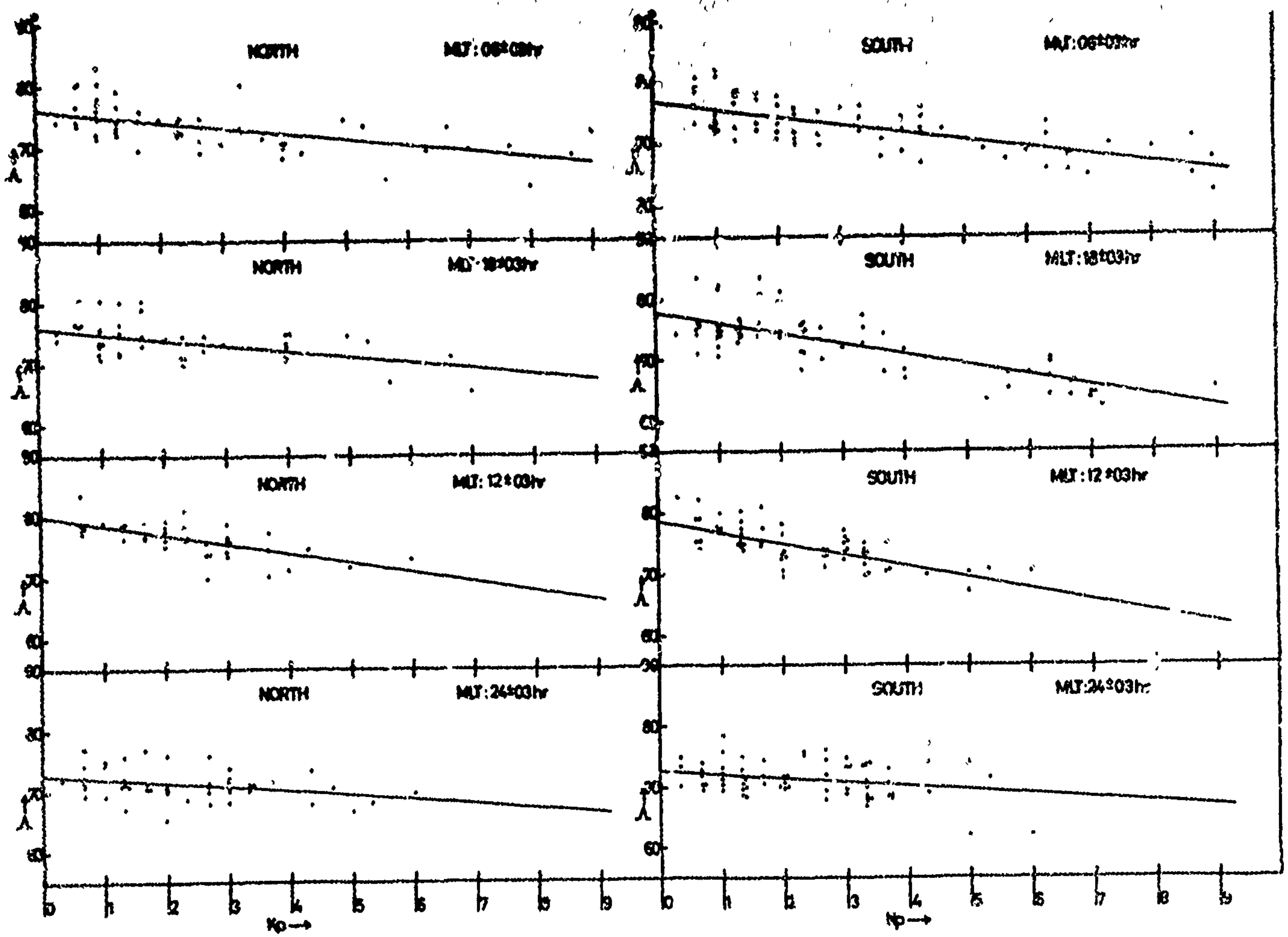

Figure 4. The invariant latitude (Λ) of the maximum of the high latitude hiss zone as a function of magnetic disturbance (K_p) for various periods of magnetic local time (MLT).

USE OF BACKSCATTER MEASUREMENTS TO IMPROVE HF COMMUNICATION PREDICTIONS

by

R.R.Bartholomew

Stanford Research Institute
Menlo Park, California 94025, USA

ABSTRACT

This is the first of a series of three papers being presented to demonstrate a new technique for predicting Maximum Usable Frequency (MUF) in real time.

A comparison of MUF's predicted by the ESSA PARLAY computer program with observations on three paths in the northern hemisphere demonstrates the need for better prediction methods. Past studies have shown that the MUF for a communication path can be predicted by using backscatter soundings. It is now possible to generate three-dimensional maps of ionospheric parameters from measurements of the remote ionosphere made by using backscatter sounding techniques. Examples of maps of penetration frequency, layer height, and skip distance are presented. Use of a map generated from a single backscatter sounding station to predict the MUF's for a number of differently oriented communication paths is explained.

USE OF BACKSCATTER MEASUREMENTS TO IMPROVE HF COMMUNICATION PREDICTIONS

by

R. R. Bartholomew
Stanford Research Institute

This paper is the first of three being presented at this meeting to describe the work we are doing at Stanford Research Institute (SRI) on a technique for obtaining a three-dimensional map of ionospheric parameters in real time. Such a map can be used to predict maximum usable frequency (MUF) or other propagation parameters.

Let me begin by discussing the problem of long-term statistical predictions. It is not necessary for me to go into much detail, since I am sure most of us recognize the drawbacks to monthly median predictions. However, to define the problem clearly, let us look at my first slide (Fig. 1). This slide shows a comparison of maximum observed frequency (MOF) versus the predicted MUF on a 7500-km east-west path. The predictions were graphically derived from the old CRPL monthly predictions. Admittedly, the new prediction program, PARLAY, developed by Lucas and Haydon at ESSA, is superior to the old one, but this slide serves to illustrate the problem of relying on monthly medians. Although, for this particular path, the medians are not in good agreement, let us ignore the medians for now and observe the spread of individual observations. We easily see how great the spread is from day to day. Other comparisons of this sort show similar results, even when the medians are in fairly good agreement. It is this problem of the large day-to-day variations in propagation conditions that needs to be resolved. Long-term statistical predictions such as monthly medians cannot solve this problem. Only short-term predictions, and ideally real-time monitoring of the ionosphere with real-time predictions of propagation conditions, are capable of solving it.

One technique that has been proved successful is CURTS.[1] The CURTS system operates by measuring, in real time, each of the propagation factors determining the quality of a circuit. With this information, the prediction system gives a quantitative indication of how well a circuit should perform. This system successfully performed on a network in the Pacific. CURTS requires, however, that there be oblique-incidence sounders at each end of each circuit to be controlled. What do we do, then, about circuits that do not have sounders at each end of the path? We think we have a solution in the form of a technique using backscatter sounding.

Past experiments have demonstrated that the MUF on a particular path can be predicted by using backscatter measurements.[2] This technique requires, of course, that a backscatter sounder be situated at one end of the path or the other. If it is possible to measure the ionosphere over a path, then why not use the backscatter sounder to measure the ionosphere over a large area and prepare a three-dimensional map of ionospheric parameters? This map can then be used to predict MUF. We at SRI have been participating for several years in a program to develop techniques for obtaining a three-dimensional map of the ionosphere in real time by using backscatter sounding. This program has been divided into two basic areas of study.

The first area is the development of techniques for using backscatter soundings to measure the state of the ionosphere at points remote from the transmitter. The development of these techniques requires the analysis and correlation of data from backscatter, oblique-incidence, and vertical-incidence soundings.

The second area of study is analysis of digital backscatter data with the goal of determining optimum methods of data sampling, recording, and analysis. Initially, effort was directed toward determining whether digitally recorded backscatter data could be used to achieve the ultimate objective, that of obtaining a three-dimensional map of the ionosphere in real time. If this could be done, or if, alternatively, a method could be developed for recording only the parameter of interest, the aim would be to determine the minimum data required from the sounder to provide the necessary information.

These two efforts have been concurrent and intermixed--sampling techniques are tested with techniques for transforming backscatter data into useful ionospheric parameters.

The data that we are using in our program were collected by using a Granger Associates (G/A) step-frequency sounder transmitter and a G/A receiver. A steerable antenna with a nominal beamwidth of 12 degrees was used. The backscatter soundings were made by using four pulses per channel, over a frequency range of 2 to 32 MHz. The data were recorded in digital form on magnetic tapes after analog-to-digital conversion. The data from the converter were preprocessed in a PDP-8 computer. The average of the four pulses on each channel was then recorded. Three parameters were recorded: time delay, frequency, and amplitude, the latter being recorded over a dynamic range of 64 levels.

---

[1] R. F. Daly, T. I. Dayharsh, K. D. Felperin, B. C. Tupper, and D. R. MacQuivey, "CURTS Phase II Automatic Frequency Selection System--Status and Progress," Status Report 1, SRI Project 5757 (December 1966).

[2] R. Silberstein, "The Use of Sweep-Frequency Backscatter Data for Determining Oblique-Incidence Ionospheric Characteristics," J. Geophys. Res., Vol. 63, pp. 335-351 (June 1958).

Maps of ionospheric parameters are obtained as follows:

(1) The digital data tapes are processed to recover the backscatter signal from background noise and interference.

(2) The signal is then processed to determine the leading edge of the ground backscatter trace.

(3) The leading edge of the ground backscatter trace is transformed into the desired ionospheric parameters as a function of ground distance from the transmitter.

(4) A contour map of this desired ionospheric parameter is prepared.

All of these steps are done by a digital computer.

We are not, at this stage, operating in real time but are only attempting to establish the feasibility of the processing and transformation techniques. We believe that, when these techniques have been perfected, the solution of the problem of compiling a real-time operating system will be only a matter of time and effort.

The next series of slides that I want to show you demonstrates some of the results to date. The first slide (Fig. 2) is a contour map of skip distance. This was a first crude attempt at mapping and was done manually. The conversion was done by assuming that skip distance and minimum path are equivalent and using a simple backscatter equation for finding minimum path length.[3]

The second slide (Fig. 3) shows contour maps of penetration frequency. Here, as in the previous slide, the backscatter sounder was located at the origin of the polar coordinate system. These maps cover one quadrant with a range of nearly 1500 km. Unlike the previous slide, the map was prepared entirely by computer. The conversion was done by using the assumption of equivalence of skip distance and minimum path, but in this case a quasi-parabolic model of the ionosphere was used.[4]

With such a map we can predict propagation conditions over a large area and for paths of various orientation. We can use a map to predict the skip distance of a particular frequency, or we can use a map to predict the MUF on a path. We can even determine ionospheric tilts from these maps, thus getting information on non-great-circle propagation.

Although the map that I have shown you covers only one quadrant, there is no reason why the backscatter sounder could not monitor over 360 degrees. In this way, a few sounders could provide information on propagation conditions for a large area. Two, or at the most three, sounders could monitor the entire continental United States. With these maps the communicators would have real-time information on the state of the ionosphere and would be in a better position to make their frequency selections. My co-workers and I believe that this can be, and will be, a very valuable tool for communications.

In this paper I have presented only a general description of a method for obtaining ionospheric maps to assist the communicator in determining propagation conditions.

In the following paper, Mr. Harry N. Shaver will describe some techniques that are used to preprocess the digital tapes to recover the signal.

Following his paper, Mrs. Elaine Hatfield will describe the techniques used to determine the leading edge of the ground backscatter trace and to transform the leading edge into ionospheric parameters.

---

[3]A. M. Peterson, "The Mechanism of F-Layer Propagated Backscatter Echoes," J. Geophys. Res., Vol. 56, pp. 221-237 (June 1951).

[4]T. A. Croft and H. Hoogasian, "Exact Ray Calculations in a Quasi-Parabolic Ionosphere with no Magnetic Field," Radio Science, Vol. 3, No. 1, pp. 69-79 (January 1968).

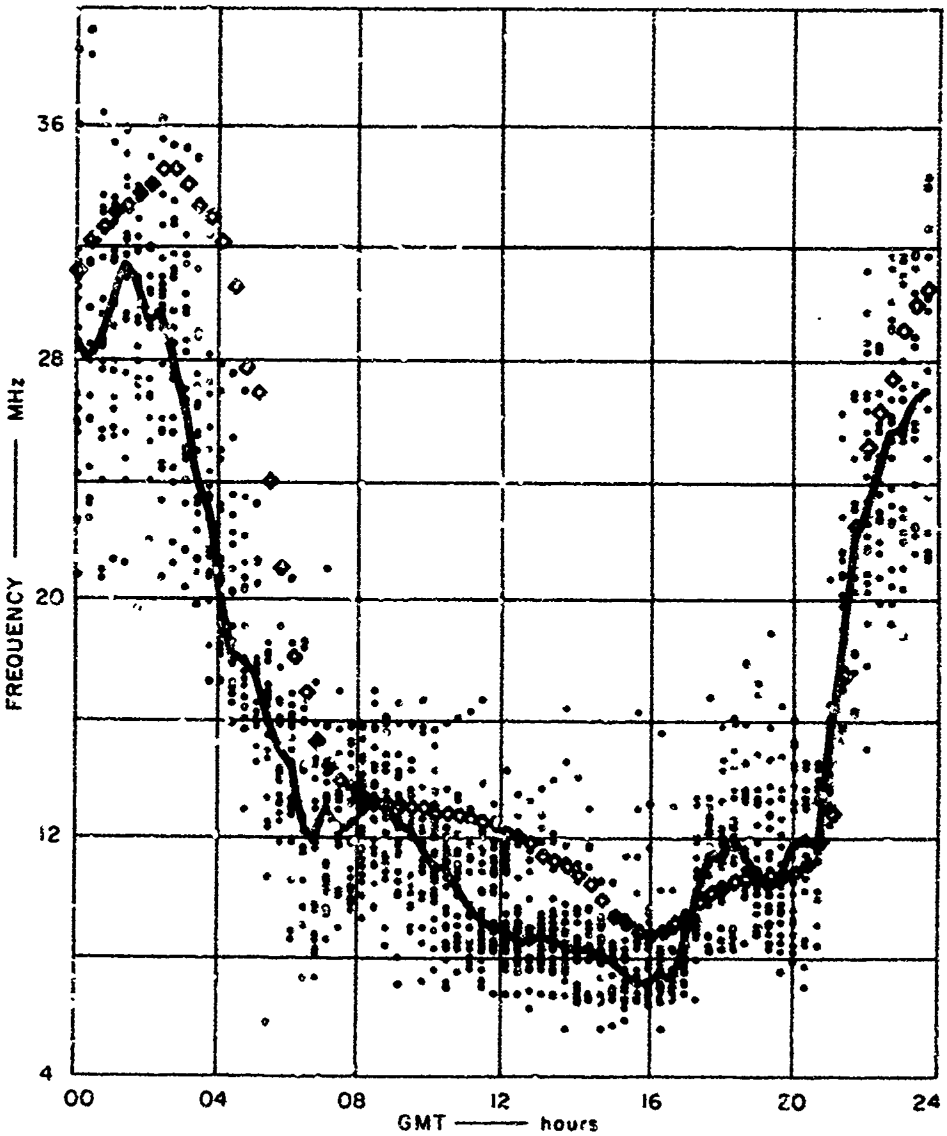

Fig. 1 Comparison of CRPL Predicted MUF, MOF, and Median MOF

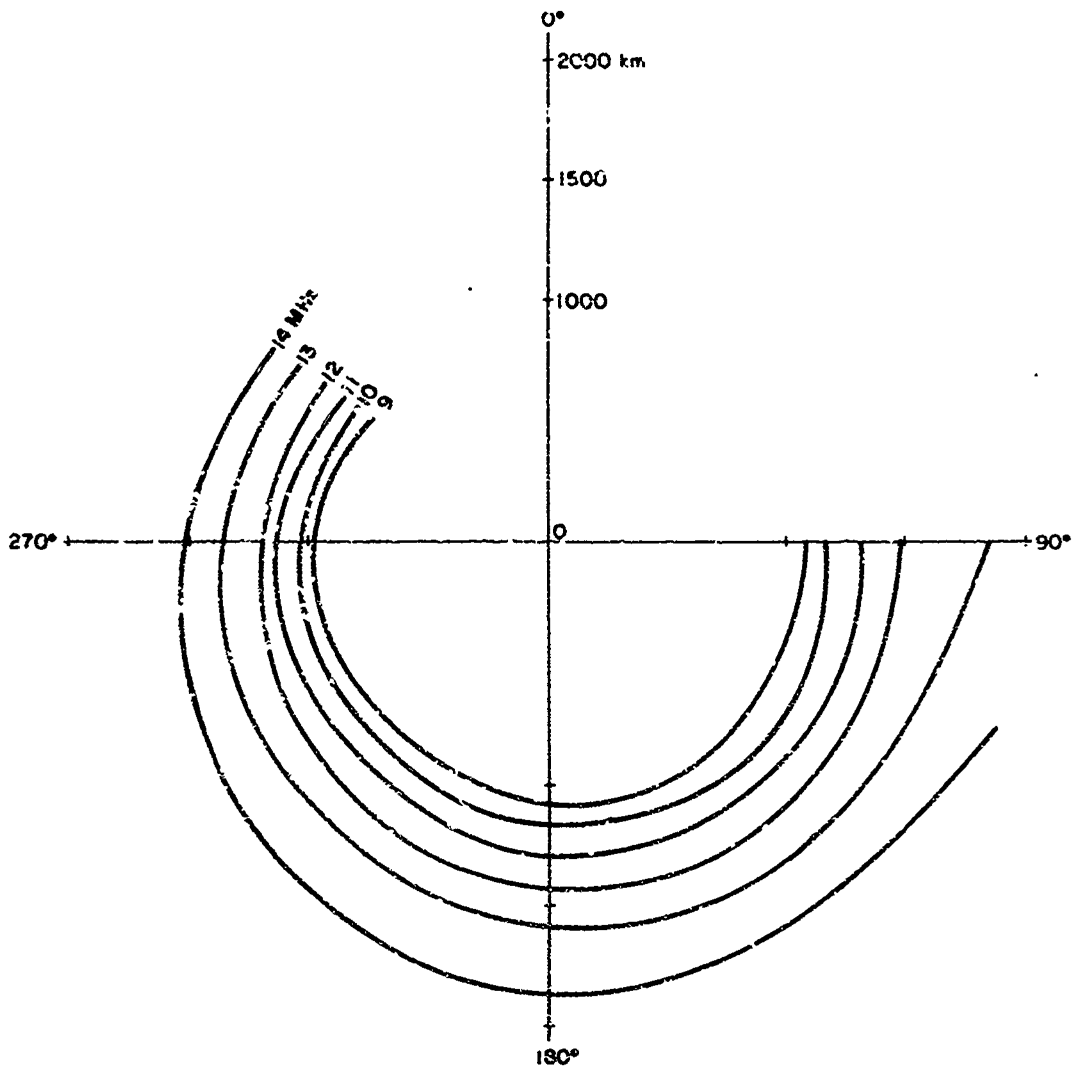

Fig. 2 Polar Diagram of Skip Distance

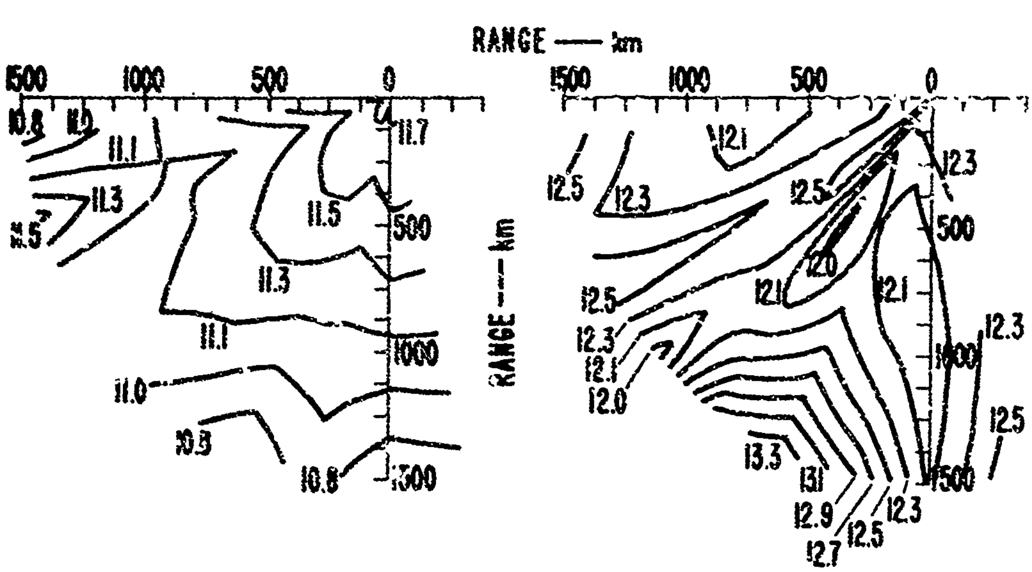

Fig. 3 Contour Maps of Critical Frequency

SIGNAL PROCESSING TECHNIQUES FOR BACKSCATTER IONOGRAMS

by

H.N.Shaver

Stanford Research Institute
Menlo Park, California 94025, USA

15

ABSTRACT

The usefulness of ground backscatter returns for estimating existing ionospheric parameters at a distance has provided the impetus for an investigation of appropriate techniques for ionogram processing. Signal processing techniques for estimating desired parameters from digitally recorded sweep-frequency backscatter returns are considered. The techniques presented include the currently used time-domain processing and alternative techniques based on frequency-domain processing. Results obtained by using various techniques are compared. System implementations of the techniques for nearly real-time processing are described and discussed.

SIGNAL PROCESSING TECHNIQUES FOR BACKSCATTER IONOGRAMS

by

H. N. Shaver
Stanford Research Institute

I BACKSCATTER IONOGRAM PROCESSING

The objective of the initial step in our analysis of ionospheric backscatter data is to form estimates of the times of arrival of the ionospherically propagated signals. The raw data are, in this case, the digitally recorded output of a Granger/Associates (G/A) sounder receiver. The G/A sounder is a step-frequency pulse sounder, and for the backscatter sounding application, a 700-μs pulse is transmitted. The receiver provides a logarithmic envelope-detected signal to the digital recording system. For each frequency channel, the received signal amplitude is sampled at a rate of 10,000 samples per second, quantized into one of 64 possible levels, and recorded over a 30-ms time interval.

The processing of these raw data to the point where estimates of the time of arrival of the ionospherically propagated signal are made has been designated preprocessing. The preprocessed data are subsequently analyzed to determine overhead parameters and parameters of the distant ionosphere.*

A simplified block diagram illustrating the major operations performed within the preprocessing program is shown in Fig. 1. The features of the preprocessing program, as well as some features that have been considered and rejected, are the subject of this paper. We will first consider the more conventional time-domain approach and then some preliminary work on a frequency-domain approach.

II TIME-DOMAIN TECHNIQUES FOR PREPROCESSING

The first operation performed in the time-domain preprocessing is the estimation of the time of arrival of the ground wave. Since the distance between the transmitter and the receiver is known, the estimate enables us to adjust the ionospheric signal returns to the time of pulse transmission.

The time of arrival of the ground wave is estimated in the following way. The raw data (log amplitude) are summed across all channels for the first 50 time indexes. The average sum, the maximum sum, and the time index of the maximum sum are determined from the data. An interpolation is initiated to find the time delay, preceding the time delay of the maximum sum, at which the sum is equal to one-half the difference between the maximum sum and the average sum. This time delay is the estimate of the time of arrival of the ground wave and is used both for the definition of the noise window and in the adjustment of the time index of each individual channel.

The remaining processing is applied on each individual channel. Within each channel, the signal-plus-noise samples are converted from log to linear amplitude and smoothed with respect to time delay--a process that corresponds to filtering. The purpose of the digital filtering is to enhance the signal in the presence of noise. The impulse response of the digital filter is approximately matched to the transmitted signal. The thresholding operation is designed to separate signal and noise. The technique used here is to estimate the noise level in a channel and to increase that level by a factor corresponding to the input threshold parameter. This quantity is the noise-based threshold. Smoothed sample values that are greater than the threshold are accepted as signal, and those less than the threshold are rejected as noise.

Following the thresholding operation, the next processing step is to estimate the times of arrival of signal. For a given channel, the time indexes of up to a specified maximum number of leading edges are computed, starting after the arrival of the ground wave. The time index of a leading edge is defined as the time in an interval of positive signal slope when the signal is above threshold and when the incremental signal amplitude from sample to sample is a maximum.

A question that has been considered in detail is the desirability of having the presence of signal in one channel at a specific time delay influence the decision as to the presence of signal in another channel and at a specific time delay.

In our investigation of alternative techniques, we have considered and ultimately rejected a form of cross-channel smoothing. The cross-channel smoothing resulted in a channel signal value (at each specific time delay) comprising the weighted sum of the signal values of the original

---

*Related topics are treated in two companion papers.[1,2]

[1] R. K. Bartholomew, "Use of Backscatter Measurements to Improve HF Communication Predictions," presented at the XV-th Technical Symposium of the Avionics Panel's Electromagnetic Wave Propagation Committee of the Advisory Group for Aerospace Research and Development of NATO, St. Jovite, Quebec, Canada, 2-5 September 1969.

[2] V. E. Hatfield, "Derivation of Ionospheric Parameters from Backscatter Data," presented at the above symposium.

channel, of the two adjacent lower channels, and of the two adjacent higher channels. The effective weighting coefficients were 1, 2, 3, 2, and 1. In all cases, the same time-delay smoothing was applied.

Examples of ionograms processed by using the cross-channel smoothing algorithm and by using the algorithm with no cross-channel interaction are shown in Figs. 2 and 3. The ionograms show signals detected as leading edges (estimates of points of maximum rate of change in time intervals where the signal rate of change is positive and the signal is above threshold). In both algorithms, the maximum number of leading edges to be found per channel was specified as six. In Figs. 2 and 3, the time delays have not been adjusted to the time of arrival of the ground wave, which may be clearly seen at a time delay of approximately 2.5 ms.

In the illustrations using the cross-channel smoothing algorithm, the region of the ionogram representing the ground backscatter trace has become somewhat distorted and horizontally stratified because of the cross-channel smoothing. It seems that this is due to the wide variation in signal strength that may be present from channel to channel. One might consider a form of signal-level normalization and a more complex smoothing algorithm to overcome some of the presumed bad effects of the cross-channel smoothing. A more complex smoothing algorithm might, for example, permit a variation in time delay as a function of frequency within the cross-channel smoothing. Although these and other possibilities have not been investigated, we have chosen, at least temporarily, to eliminate cross-channel interaction. This approach prevents the possible elimination of desired signal, results in simplification of the preprocessing algorithms, and retains the alternative of applying a form of cross-channel processing at a later stage.

III FREQUENCY-DOMAIN TECHNIQUES FOR PREPROCESSING

Some preliminary results of backscatter-ionogram preprocessing using an entirely new approach will now be presented. The approach has been made possible by recent advances[3,4] in the formulation of algorithms to compute the discrete, finite-time, Fourier transform. These advances have resulted in what is now known as the fast Fourier transform.

A. The Basis for Frequency-Domain Ionogram Processing

Ionogram processing in the frequency domain has evolved in a series of steps, some of which will be described. The basis for the processing lies with a frequency-domain interpretation of a single-channel amplitude record, or ampligram. An example of one such ampligram is given in Fig. 4. The amplitude in this figure is in a logarithmic form. The first arriving pulse is the ground wave, and the second pulse is reflected from the ionosphere (in this case a ground backscatter return). There may be additional returns, but in some cases they will be too weak to be distinguished, especially on a linear scale. The important point is that there are at least two pulses separated by a time interval that is of direct interest in the ionogram processing. The signal contains a sinusoid with a fundamental frequency whose period corresponds to the desired interval, and is rich in harmonics (although not every harmonic may be present).

To illustrate the frequency content of ampligrams, estimates of the power spectra (the squared envelope of the Fourier transform) of two ampligrams are shown in Fig. 5. For these particular examples, the first 256 sample values (25.6 ms) of the ampligram were converted to linear amplitude and smoothed in time delay; all sample values less than the threshold were set equal to the threshold value; and the Fourier transform was applied. In the frequency domain, sample values occur every 39.06 Hz, the reciprocal of the length of the time record (0.0256 s). In each of the examples, a series of spectral peaks appears, which we contend are related to the interpulse interval on the ampligrams.

We reiterate then, that the basis for our frequency-domain approach is the fact that two or more pulses are present on the ampligram, the first arriving pulse being the ground wave, signifying a zero time reference. Further, an important parameter in our analysis is the interpulse interval; this quantity is related to the peaks in the frequency-domain representation of the signal.

B. Period Processing from Spectral Peaks

The fact that the series of peaks in the frequency-domain representation of the ampligram is related to the interpulse interval can be simply demonstrated. Suppose that for each channel we take the Fourier transform of the ampligram, compute the squared envelope of the samples, and find the frequencies of all of the peaks in the spectral representation up to 1000 Hz. For each of these frequencies we then take its reciprocal to find the period of the sinusoid, and we plot the times corresponding to the periods as a function of sounder-channel frequency. Two examples of this processing are shown in Fig. 6. For these examples, both time and frequency (cross-channel)

---

[3] J. W. Cooley and J. W. Tukey, "An Algorithm for the Machine Calculation of Complex Fourier Series," Math. of Comput., Vol. 19, pp. 297-301 (April 1965).

[4] IEEE Trans. on Audio and Electroacoustics, "Special Issue on Fast Fourier Transform and Its Application to Digital Filtering and Spectral Analysis," Vol. AV-15, No. 2, pp. 43-117 (June 1967).

smoothing were applied to the ampligrams, and only the first 25.6 ms of data were used. In one case the data were in linear form, and in the other they were in log form.

Another point that is clearly illustrated in the examples is that at small delays, variations in the traces are fairly well defined (note particularly the traces at frequencies below 10 MHz), whereas for large delays there is a complete lack of detail in trace variation. This difference in definition can be explained as follows. In the power spectral estimate we have actually computed quantities related to the powers in narrow frequency bands. These bands are uniform in width, and we say that all of the energy occurs at frequencies in the centers of the bands. For the examples we have shown in Fig. 6, the center frequencies are given by

$$f_n = n\left(\frac{1}{0.0256}\right) = n(39.06) \quad ; \quad n = 0, \pm 1, \pm 2, \ldots, \pm 128 \quad ,$$

and the bandwidth of the narrow frequency band is 39.06 Hz. Suppose there are spectral peaks in the bands designated by n = 3 and n = 10. The actual frequency peaks may lie anywhere in the range given by

$$97.7 \le f \le 136.7 \quad ; \quad n = 3$$

$$371.1 \le f \le 410.2 \quad ; \quad n = 10 \quad .$$

If we now take the reciprocals of the frequencies at the band edges, we find that the ranges of the time delays that we have chosen to represent by the reciprocals of the center frequencies are given by:

$$7.31 \le \tau \le 10.24 \quad ; \quad n = 3$$

$$2.44 \le \tau \le 2.69 \quad ; \quad n = 10 \quad ,$$

where the time delay, τ, is in milliseconds. From this illustration we see that the uncertainty in the frequency of a peak, an uncertainty that is uniform with respect to frequency, results in an uncertainty of time delay that is nonuniform with respect to time.

One way to decrease the uncertainty in time delay is simply to decrease the uncertainty in frequency. To achieve this, we must improve the frequency resolution in the spectral analysis or, equivalently, take a longer time record. The raw data are recorded as 300 time samples representing a 30-ms interval. In the frequency-domain analysis we have been using the first 25.6 ms of data. Consider now the use of 102.4 ms (1024 sample points) of data. As we have stated, the data interval is only 30 ms long, so what we have chosen to do is to fill in the remaining interval (72.4 ms long) with samples having a value of zero. Several applications of this approach have given results that seem encouraging. Two examples of the results of this type of processing are shown in Fig. 7. As we have indicated, the data interval is 102.4 ms, and the frequency resolution is on the order of 10 Hz. For these examples, time smoothing was eliminated; however, frequency smoothing was applied to the ampligrams. As before, in one case the data were in linear form, and in the other they were in log form.

With some imagination, and perhaps with the aid of an ionogram processed by the use of conventional time-domain techniques, one may attach significance to the apparent traces shown in Figs. 6 and 7. We can define a one-hop vertical-incidence trace, a backscatter trace, and a multiplicity of traces with delays less than these traces. If we examine the additional traces in more detail, we see that they have delays of one-half, one-third, one-fourth, and so on, of the dominant longer-time-delay trace (either the one-hop vertical-incidence trace or the ground-backscatter trace). These additional traces are, in fact, due to the harmonic content of the ampligram. We will next address ourselves to the question of how we might utilize those harmonics to define more precisely the time delay of the dominant trace.

C. Harmonic Combinations

As we have illustrated, the spectral analysis of an ampligram will generally reveal a series of peaks corresponding to the frequency bands that contain the fundamental and the harmonics. Let us call these frequency bands f_1, f_2, f_3, ... If we consider the true fundamental frequency, f_o, we know that

$$f_1 - \frac{1}{2T} \le f_o \le f_1 + \frac{1}{2T} \quad .$$

where T is the length of the time record. Similarly, we know (assuming that we can determine the harmonic number of a particular peak) that

$$f_n - \frac{1}{2T} \le n f_0 \le f_n + \frac{1}{2T} \quad ,$$

or, equivalently,

$$\frac{f_n}{n} - \frac{1}{2nT} \le f_0 \le \frac{f_n}{n} + \frac{1}{2nT} \tag{1}$$

The interpulse interval, τ, is the reciprocal of the true fundamental frequency; it is bounded as follows:

$$\frac{n}{f_n + \frac{1}{2T}} \le \tau = \frac{1}{f_0} \le \frac{n}{f_n - \frac{1}{2T}} \quad . \tag{2}$$

Thus we see from Eqs. (1) and (2) that if we know the harmonic number, n, and if it is greater than one, we can decrease the uncertainty in our knowledge of both the fundamental frequency and its period.

To illustrate, suppose we process an ecologram by using the time record length of 25.6 ms, as in the previous section. The frequency bands are thus 39.06 Hz wide. Suppose further that the true fundamental frequency is 100 Hz, corresponding to a time delay of 10 ms. Assume that the spectral analysis reveals peaks at the fundamental, the fourth, and the ninth harmonic frequencies. Table I illustrates the decrease in the time-delay uncertainty as the harmonics are used to define it.

Table I

THE DECREASE IN TIME-DELAY UNCERTAINTY

THROUGH THE USE OF KNOWN HARMONICS

Harmonic Number	Frequency Band of Spectral Peak (Hz)	Computed Time-Delay Uncertainty (ms)
1	$97.7 \le f \le 136.7$	$7.31 \le \tau \le 10.2$
4	$371.1 \le f \le 410.2$	$9.75 \le \tau \le 10.78$
9	$878.9 \le f \le 918.0$	$9.80 \le \tau \le 10.24$

One problem that we encounter is that we do not know the harmonic number associated with each of the peaks. If they are regularly spaced, we can attempt to guess the harmonic number. Suppose there is a series of N peaks with center frequencies f_{pi}, $i = 1, \ldots, N$. Define a function

$$g(f_{pi},\tau) = \begin{cases} 1 \quad , & \dfrac{k}{f_{pi} + \frac{1}{2T}} \le \tau \le \dfrac{k}{f_{pi} - \frac{1}{2T}} \\ 0 \quad , & \text{otherwise} \end{cases} \quad , \tag{3}$$

where k is our best guess of the harmonic number for that peak. Define a new function

$$G(\tau) = \sum_{i=1}^{N} g(f_{pi},\tau) \quad , \tag{4}$$

that represents the harmonic reinforcement in the time domain. Two examples of this particular approach are shown in Fig. 8. The results are quite encouraging because the leading edge of a backscatter trace seems to be defined quite well.

As one might imagine, there are cases where it is difficult to guess the harmonic number associated with a particular spectral peak. To circumvent this difficulty, we have considered an alternative, which seems to provide a satisfactory solution.

D. <u>Some Preliminary Results</u>

As an alternative to the selection of a specific harmonic number to associate with a spectral peak, consider now the use of a range of harmonic numbers. In Eq. (3) then, k is a set of values, say 1, 2, ..., K, where K may be determined from the maximum time delay of interest. For a maximum time delay of 20.0 ms and a frequency resolution of 39.06 Hz in spectral analysis, two examples of the nonzero regions of $g(f_{pi},\tau)$ associated with spectral peaks are given in Table II. As given in

Table II

EXAMPLES OF THE NONZERO INTERVALS OF $g(f_{pi},\tau)$

Frequency of Spectral Peak (Hz)	Harmonic Number	Range of Possible Time Delay (ms)
351.6	1	2.69-3.01
	2	5.39-6.02
	3	8.08-9.04
	4	10.78-12.05
	5	13.47-15.06
	6	16.17-18.07
	7	18.86-21.08
390.6	1	2.44-2.69
	2	4.88-5.39
	3	7.31-8.08
	4	9.75-10.78
	5	12.19-13.47
	6	14.63-16.17
	7	17.07-18.86
	8	19.50-21.56

Eq. (4), the quantity $G(\tau)$ should be large at those values of τ for which there is reinforcement due to the presence of harmonics.

With a limitation on time delay of 30 ms, a 25.6-ms ampligram, and only those spectral peaks less than 3000 Hz being chosen, Fig. 9 gives two examples of the quantity $G(\tau)$. The ampligrams used for these examples contain no time or frequency smoothing or any thresholding operation. The raw data have, however, been converted into linear amplitude.

In these examples, the linear trend in the data at low time delays is very evident. Low time delays correspond to high frequencies, and within a specified range of frequencies they have fewer possible harmonics. If we now remove the linear trend by defining a new function,

$$H(\tau) = G(\tau) - \tau \quad ,$$

the results are as shown in Figs. 10, 11, and 12. Here we have included the results for the processing of both the raw data (directly from the data tape) and that raw data converted into linear amplitude.

We find the results illustrated here very encouraging. The predominant peaks seem indicative of desired signal. There remain, however, many aspects of the processing that need further investigation. For example, the differences between the results from the processing of the logarithmic data and those from the processing of the linear data, the correction to remove the linear trend in the data, and the use of longer time records (even though they may artifically be partly filled with zeros) need to be investigated further.

E. Some Implications of Frequency-Domain Processing

One might ask why we are concerned with frequency-domain processing, since we have techniques for the time-domain processing of the data. The primary reason for this concern is that we would like to evaluate ways of improving the estimates of those parameters that are required in subsequent stages of the backscatter processing. A secondary reason is that we would like to reduce the complexity of the processing. Although we have introduced several new processing steps, we have eliminated the smoothing operation, the ground-wave time-of-arrival computation, and the noise and threshold computation.

Perhaps one of the most important possibilities of the frequency-domain approach lies in a potential real-time implementation. Special-purpose computers can perform the Fourier transform very quickly. If one of these devices were operated directly with the sounder receiver, followed by a device to select the spectral peaks, the quantity of data to be recorded or stored for further processing might be reduced by a factor of 10. This assumes something less than 30 spectral peaks per channel rather than 300 sample values. The large quantity of data that must be recorded at a sounder receiver has been recognized as a problem for a long time. Frequency-domain processing may eventually contribute to the solution of that problem.

Significant steps have been taken in the evolution of frequency-domain processing techniques; however, as we have indicated, several aspects of the problem have not been resolved and are currently being investigated. The potential value of the processing technique remains to be verified as its development continues.

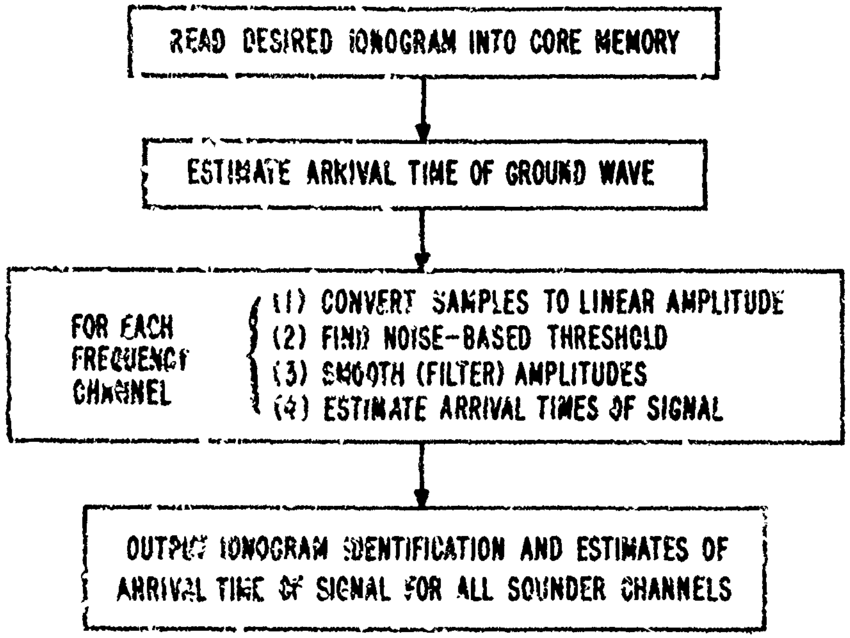

Fig. 1 Major Operations Performed Within the Preprocessing Program

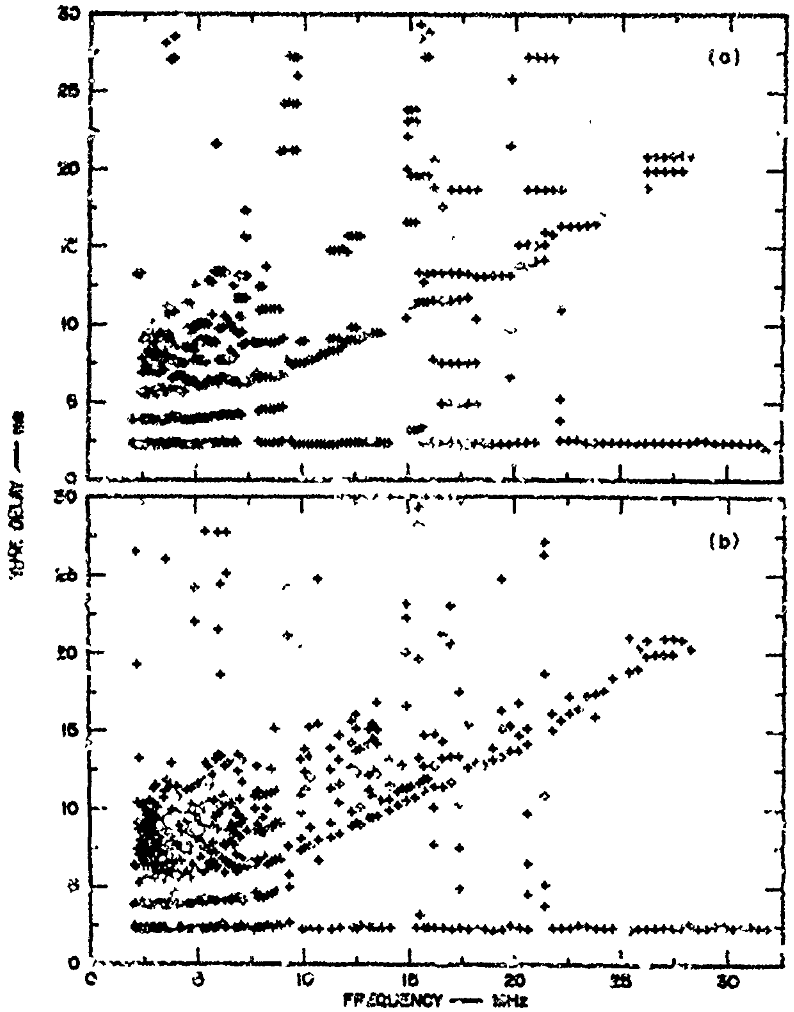

Fig. 2 Examples of Leading-Edge Ionogram Preprocessing for Antenna 24

(a) With Cross-Channel Smoothing
(b) Without Cross-Channel Smoothing

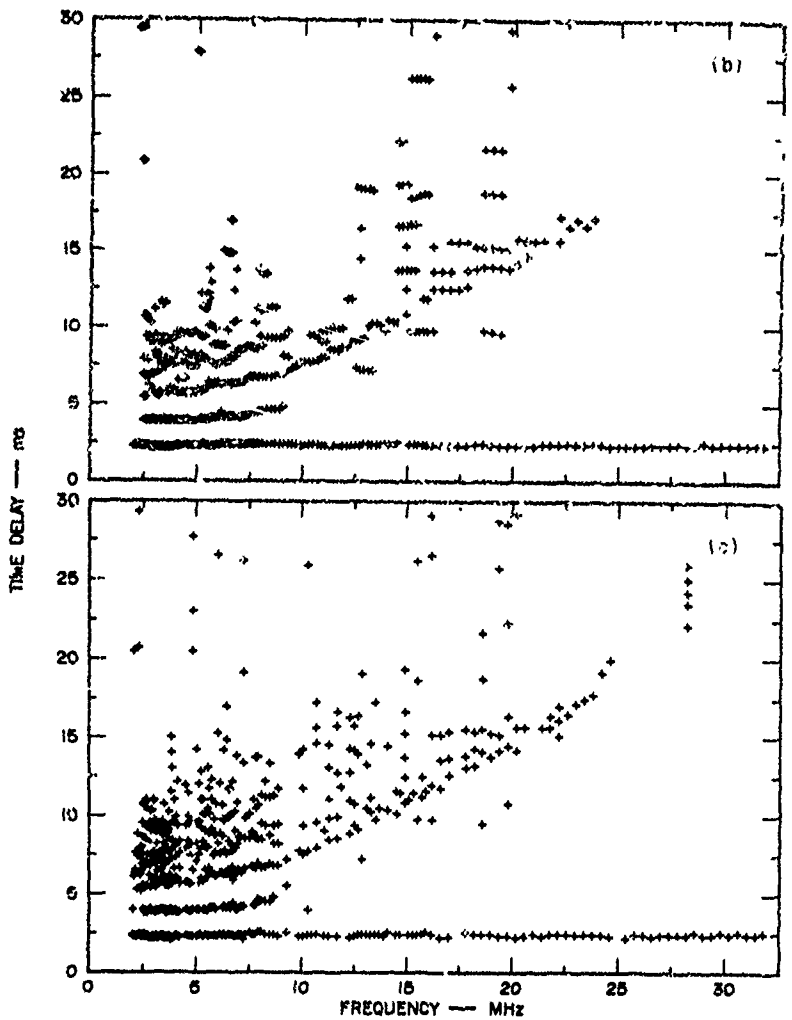

Fig. 3 Examples of Leading-Edge Ionogram Preprocessing for Antenna 25

(a) With Cross-Channel Smoothing
(b) Without Cross-Channel Smoothing

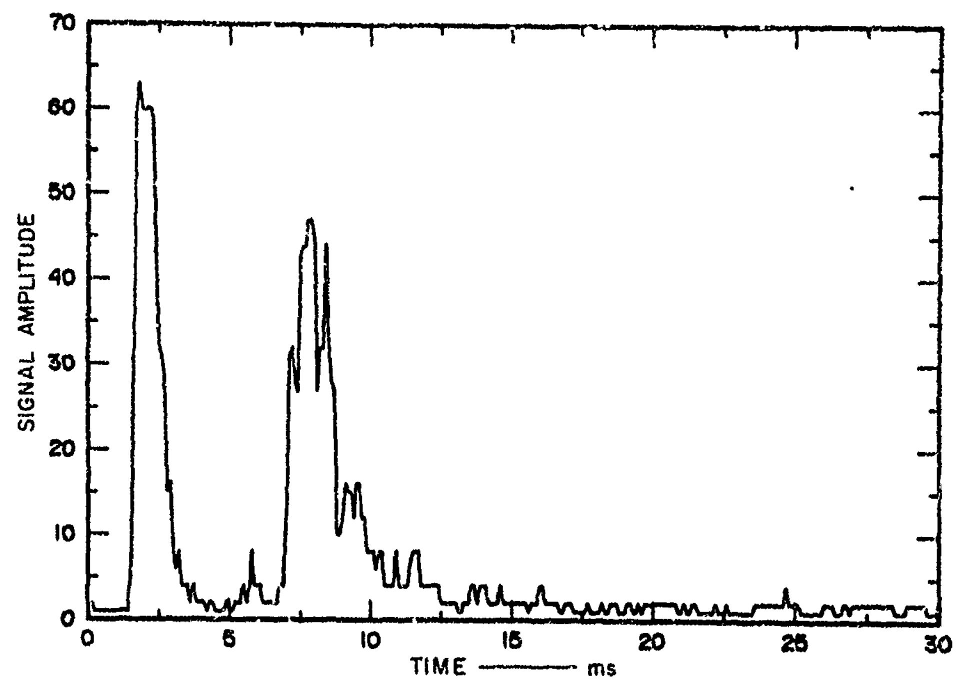

Fig. 4 Single-Channel Amplitude Record

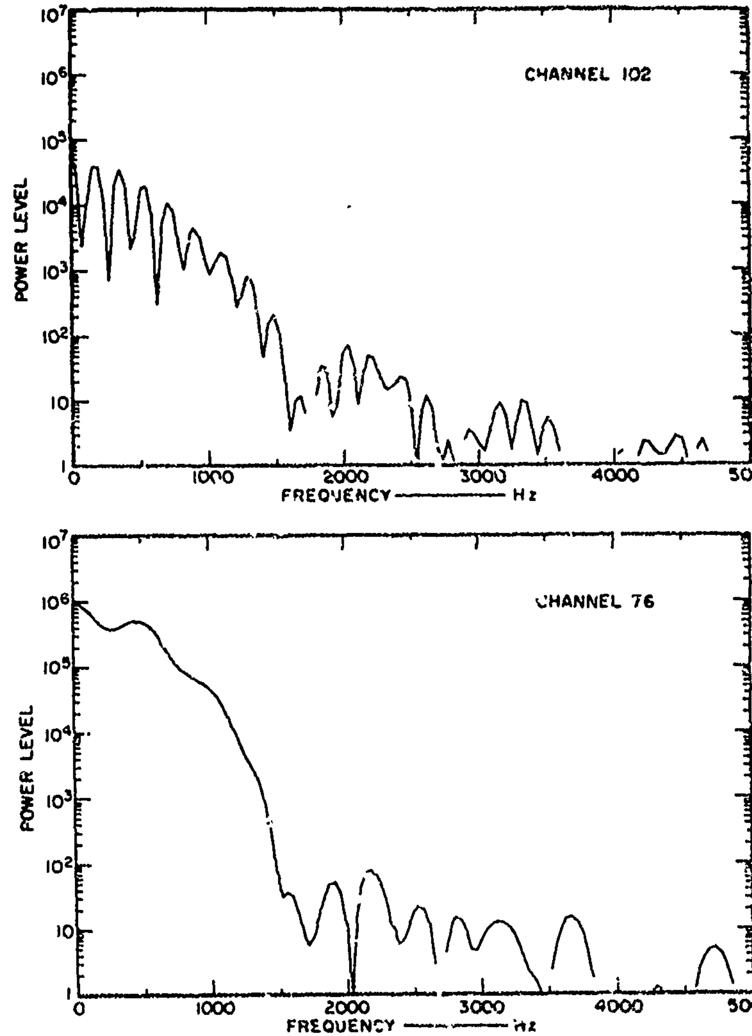

Fig. 5 Two Illustrations of the Frequency Content of Ampligrams

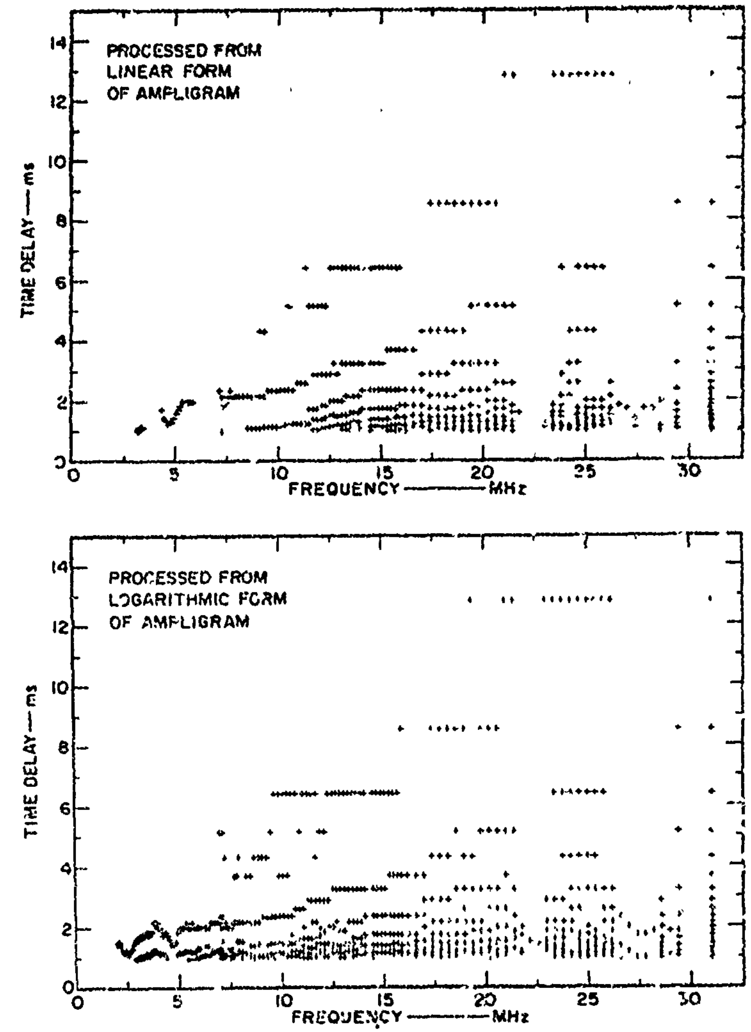

Fig. 6 Examples of Processing Using Spectral Peaks and 256 Sample Points per Ampligram

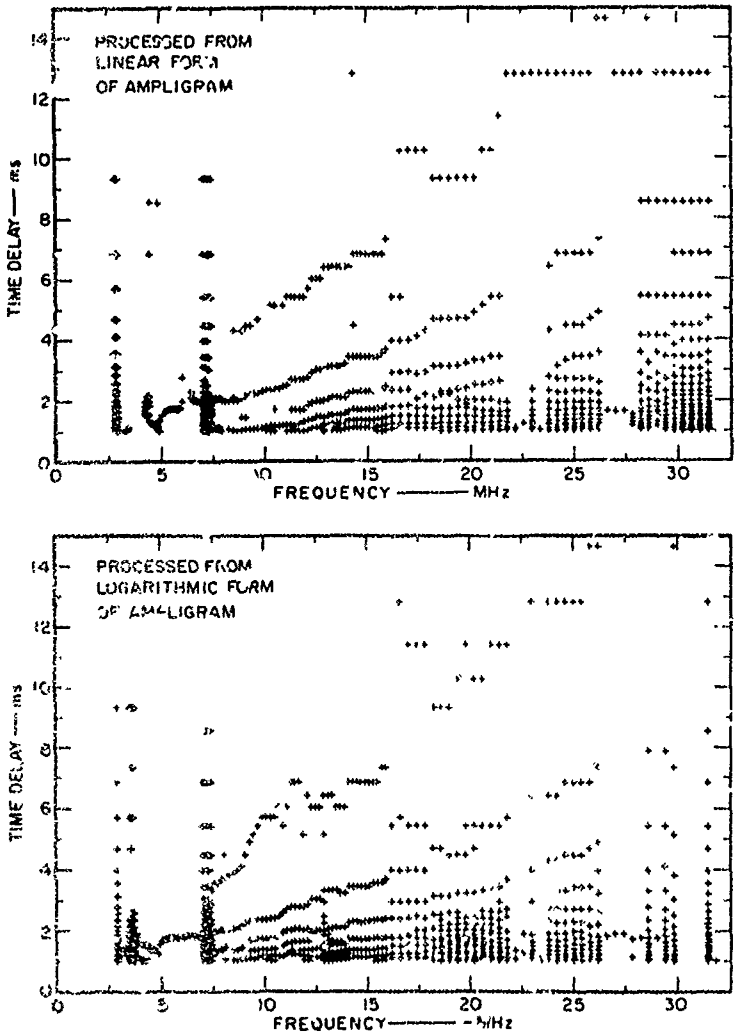

Fig. 7 Examples of Processing Using Spectral Peaks and 1024 Sample Points per Ampligram

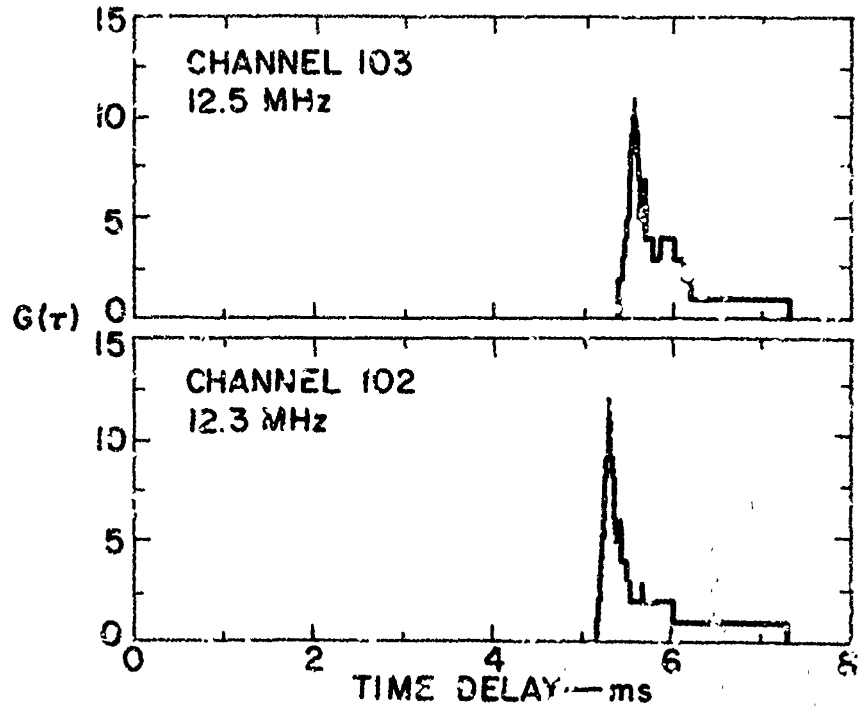

Fig. 8 Examples of Harmonic Reinforcement in Time-Delay Estimation Using Best-Guess Harmonic Numbers

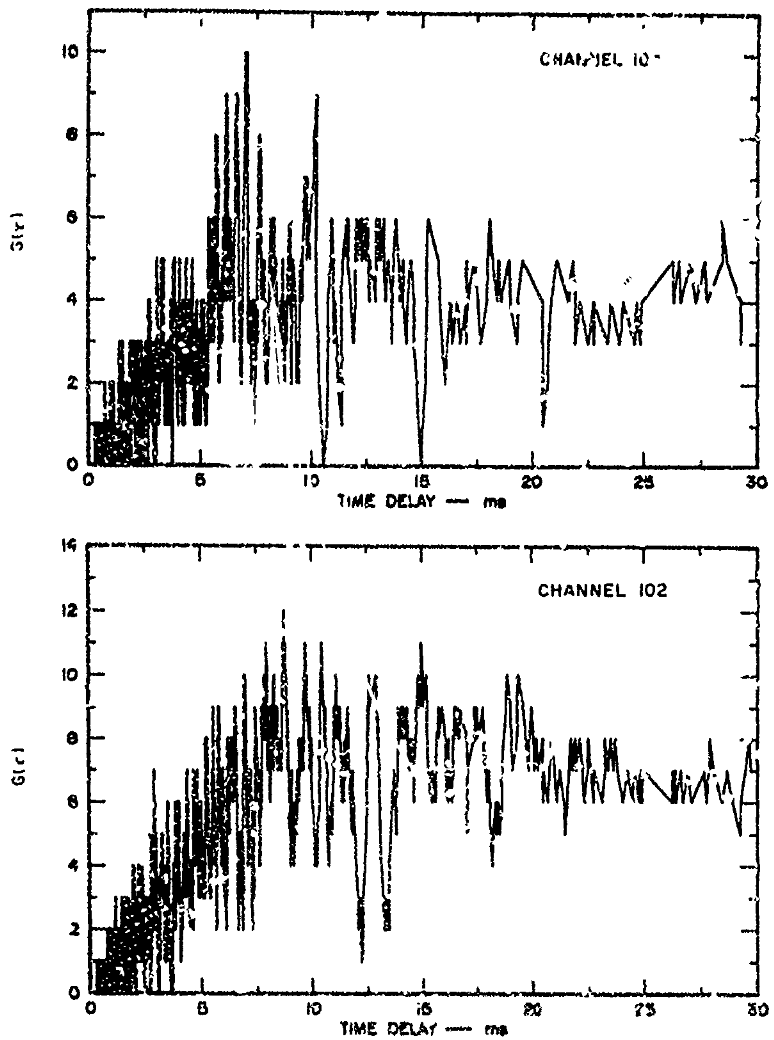

Fig. 9 Examples of Harmonic Reinforcement in Time-Delay Estimation Using a Range of Possible Harmonic Numbers

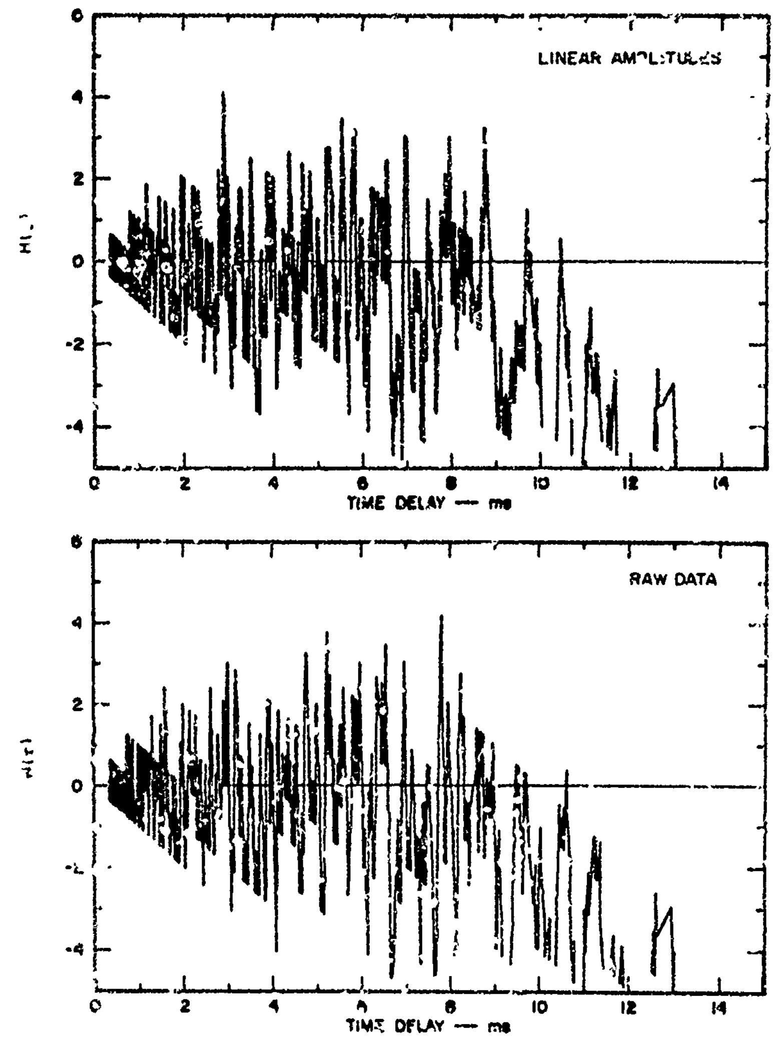

Fig. 10 Examples of Frequency-Domain Processing for Channel 102

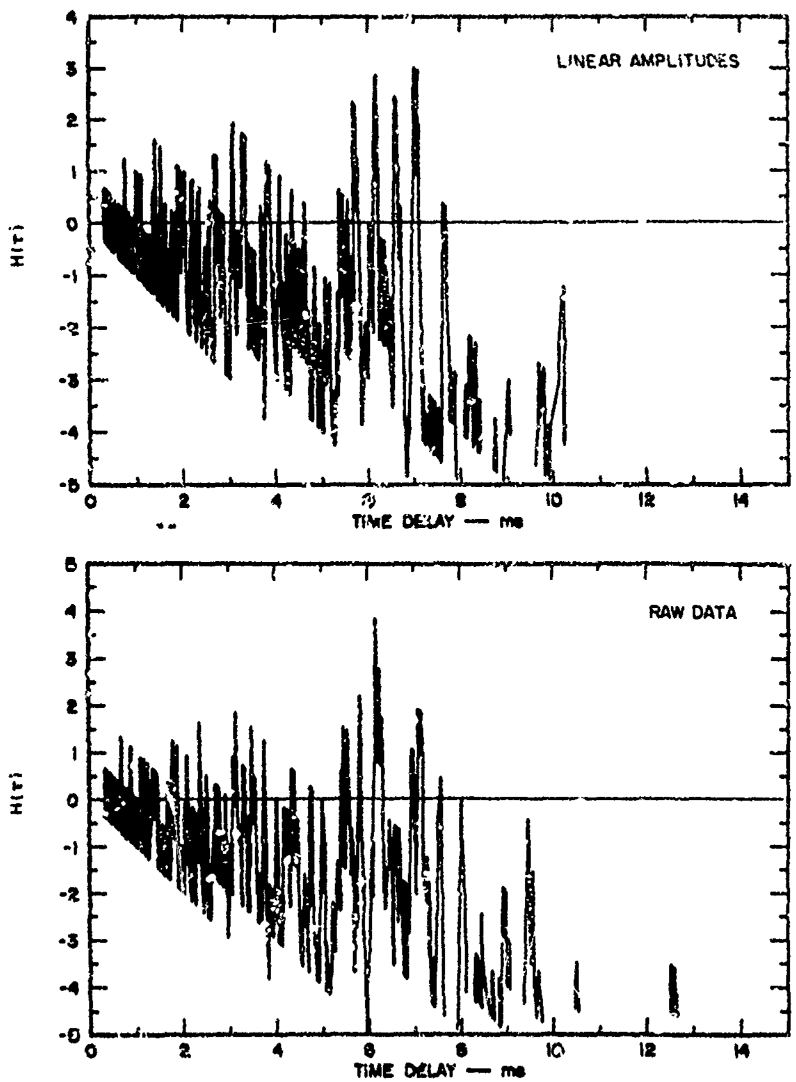

Fig. 11 Examples of Frequency-Domain Processing for Channel 103

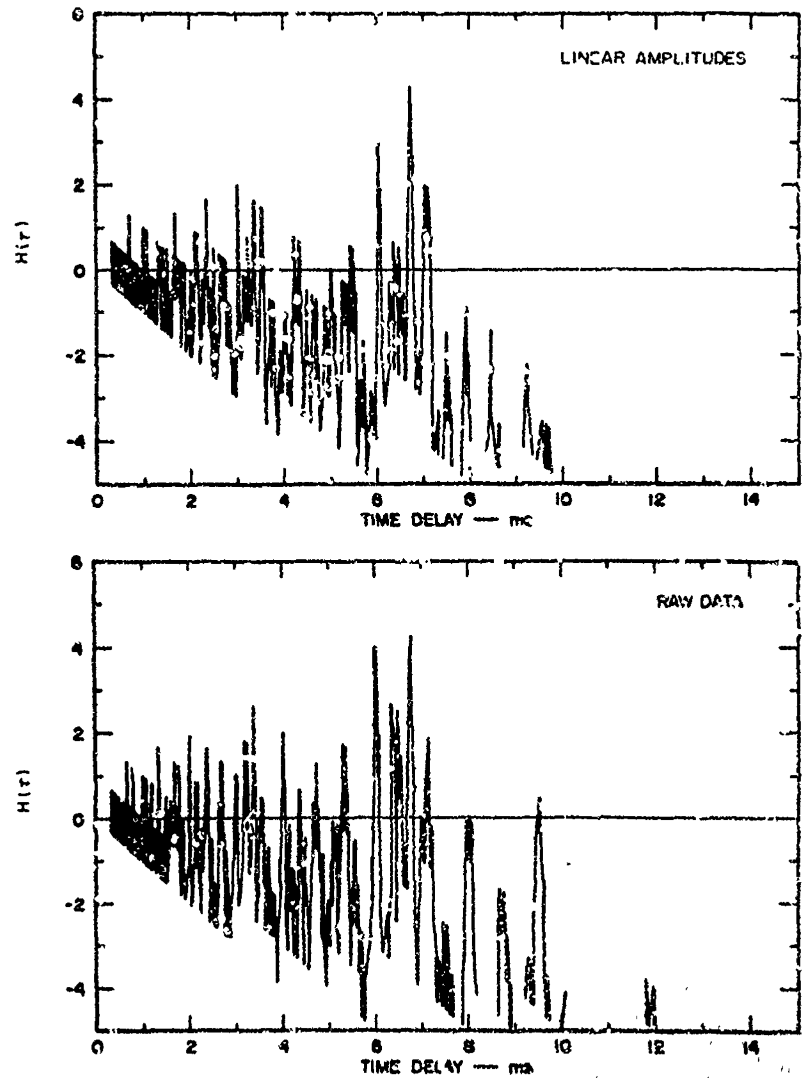

Fig. 12 Examples of Frequency-Domain Processing for Channel 104

DERIVATION OF IONOSPHERIC PARAMETERS FROM BACKSCATTER DATA

by

V.R. Hatfield

Stanford Research Institute
Menlo Park, California 94025, USA

ABSTRACT

A computer program has been developed to transform backscatter data into an ionospheric map.

To construct such a map, ionograms recorded from nine narrow-beam antennas over an azimuthal range of 108° were used. From the ionograms, time delay and amplitude as a function of frequency were derived and translated into ionospheric parameters. These parameters were related directly to the minimum time delay pulse by using theoretical equations. By assuming a "quasi-parabolic" model, the corresponding ray equations may be used. The parameters, the height of the bottom of the layer, H_0, the layer semi-thickness, y, and the critical frequency, f_c, may be varied to arrive at a solution of the minimum time-delay equation. It was found possible to fix two of these parameters and solve for the third. For the fixed parameters, vertical-incidence parameters directly overhead were used; the third parameter was generated from the backscatter trace. To obtain the overhead parameters, a new program was generated to extract them from the vertical-incidence portion of the backscatter ionogram. A satisfactory technique for deriving these parameters was developed.

Contour maps were made from critical frequency as a function of range and azimuth, using a polynominal fit. Representative maps are presented.

DERIVATION OF IONOSPHERIC PARAMETERS FROM BACKSCATTER DATA

by

V. E. Hatfield
Stanford Research Institute

I DESCRIPTION OF THE PROBLEM

It is useful to map the ionosphere over as much of the earth as possible, from a single location, using a sounder transmitter-receiver. Backscatter returns on a sweep-frequency ionogram offer a possible means for doing this, since oblique transmitted signals at certain frequencies are reflected by the ionosphere, reach the earth, scatter, and return by the same path (Fig. 1). Some of the signals may reach a distance of from 300 to 3000 km, depending on the ionosphere. The returning signals can be recorded on a sounder as an ionogram (Fig. 2). The information recorded is the time of arrival minus the signal start time (time delay) and the strength of the signal or amplitude. Both the time delay and the amplitude are affected by the ionospheric path through which the signal travels; thus the problem is to infer what the ionosphere is like by observing the time delay and amplitude of returning signals.

The data we are using are digitized amplitude as a function of time delay and frequency. Therefore more detailed information is available than can be obtained from the black-and-white film ionogram, as seen in Fig. 2, but the data are similar.

For this experiment we have ionograms from nine narrow-beam (about 12°) antennas, all located at approximately the same place but spaced evenly over an azimuthal range of 108°. The transmitter is located nearby.

II THEORETICAL CONSIDERATIONS

A. Choice of Model Ionosphere

To map the ionosphere from the ionograms, it is necessary to know the relationship between time delay and amplitude on the ionogram, and the distance, height, and electron density in the ionosphere. Several theoretical models exist that establish this relationship between group time or time delay and a model ionosphere. For this particular problem, a simple model that takes into account the curvature of the earth is needed. Only the F2 layer has been considered, since most of the backscatter comes from this layer. Figure 3 shows theoretical backscatter minimum-time-delay curves for the following five models, all with no field and uniform ionosphere:

(1) Flat ionosphere--parabolic distribution, flat earth[1]*

(2) Flat ionosphere--parabolic distribution, curved earth[2]

(3) Curved ionosphere--parabolic distribution, curved earth[3]

(4) Curved ionosphere--quasi-parabolic distribution, curved earth[4]

(5) Curved ionosphere--constant height of reflection, curved earth.[5]

The differences caused by an inaccurate model become quite large at the higher frequencies in which we are the most interested, since the backscatter returns at these frequencies have been reflected from the ionosphere at a greater distance. Therefore it seemed necessary to use as the model ionosphere either the parabolic ionosphere with curved earth or the quasi-parabolic ionosphere. The quasi-parabolic ionosphere was chosen, since exact equations for ray-path parameters exist, while the parabolic ionosphere requires approximation.

The quasi-parabolic equation for group path (or time delay) is

$$P' = 2\left\{r_b \sin\alpha - r_o \sin\beta_o + \frac{1}{A}\left[- r_b \sin\alpha - \frac{B}{4\sqrt{A}} \ln \frac{B^2 - 4AC}{(2Ar_b + B + 2r_b\sqrt{A}\sin\alpha)^2}\right]\right\} ,$$

where

$$A = 1 - 1/F^2 + [r_b/(Fy_m)]^2$$

$$B = (-2\, r_m r_b^2)/(F^2\, y_m^2)$$

$$C = \cdot\, [r_m B/2 + r_b^2 \cos^2\alpha]$$

---

*References are listed at the end of the paper.

r_m = height of maximum electron density measured from center of earth = $r_o + h_o + y_m$

h_o = height of bottom of layer measured from the ground

r_b = height of bottom of layer measured from center of earth = $r_o + h_o$

r_c = radius of earth

y_m = semithickness of the layer

β_o = take-off angle

α = 90° − angle of incidence with the layer

$F = f/f_c$ = ratio of transmitted frequency to critical frequency of layer.

B. Examination of Unknown Parameters

The unknown ionospheric parameters in the equation are r_m, f_c, and h_o. These are the parameters we will try to map from the backscatter data. The take-off angle, β_o, is also an unknown (the angle of incidence with the layer is a function of β_o); however, if only one angle is considered—the angle of minimum delay—this variable may be eliminated.

The equation for group time was solved for minimum time delay by taking the derivative with respect to sin α, rewriting P′ in terms of sin α, and taking the derivative. The result is:

$$\frac{\partial P'}{\partial \sin\alpha} = 0 = 2r_b\left[1 - \frac{1}{A}\right] - \frac{2r_b \sin\alpha}{\sqrt{\left[\frac{r_o}{r_b}\right]^2 - \cos^2\alpha}} + \frac{B}{A^{3/2}}\left[\frac{\sqrt{A} + \frac{B}{2\sqrt{A}\, r_b}}{\left[\sqrt{A} + \frac{B}{2\sqrt{A}\, r_b}\right]^2 - \sin^2\alpha}\right] .$$

This equation may be solved iteratively for α, given any set of ionospheric parameters. The angles for minimum group path or time delay may then be substituted in Eq. (1), and the result is minimum group path or minimum time delay. The theoretical minimum time delay may then be compared with the minimum time delay on the ionogram.

The minimum time delay on the ionogram is relatively easy to find, since generally there is focusing of rays at the minimum, making the signal stronger there. A typical backscatter signal is given in Fig. 4, showing the original data and the smoothed data. The minimum delay we are using is the maximum positive derivative of the linear smoothed data.

If the minimum delay from the ionogram is substituted into Eq. (1), there are three unknowns. To obtain a solution, two of the parameters must be assumed. It was decided to run some test cases on a ray-tracing program[3] to determine which parameter affected the backscatter curve the most. A variety of gradients were chosen to show change in height of maximum electron density, in critical frequency, and in layer semithickness.[6] Both height of maximum and critical frequency seemed to affect the backscatter curve more than layer semithickness, so it was decided to hold layer semithickness constant and to vary the other two parameters. The semithickness of the layer overhead at vertical incidence is assumed to be available, so this has been used as the constant value. The computer programs have been written to allow a known polynominal variation in height of the bottom of the layer, while solving for critical frequency. However, a decision as to what variation to use for the height has not been made, so the overhead values of height of the bottom have been used and held constant. These values have been used in the contours of critical frequency that have been constructed from the backscatter data.

C. Error in Method of Representing a Tilt

The equations we have chosen to use represent a uniform concentric ionosphere, while the real world from which the data were collected is far from this. The assumption essential to these equations is that, for the portion of the signal ray path within the F2 layer, the ionosphere is considered to be uniform. If the ionosphere is actually tilted, this approximation will produce an error. A few cases were tested to see what kind of an error this will be. A basic F2 layer overhead was assumed to be parabolic, with parameters h_o = 250 km, f_c = 6.5 MHz, and y_m = 80 km. Three critical-frequency gradients were assumed. Changes in critical frequency of ±1, −1, and −3 MHz per 1000 km were calculated. Simulated ionograms of minimum time delay are shown in Fig. 5. The lines were calculated by the approximate method, using the quasi-parabolic equation. The points were calculated by an incremental-step ray-tracing program.[7] Table I shows the errors that would be made in the calculation of critical frequency if the points on Fig. 5 were used as actual data points and calculations were made using the quasi-parabolic equation. As would be expected, the largest variations occur at the greatest distances or for the largest gradients.

Table I

ERROR IN CALCULATED CRITICAL FREQUENCY*

Gradient (MHz/1000 km)	Distance (km)	Actual Minus Calculated Values (MHz)
+1.0	311	+0.007
	461	+0.006
	737	-0.003
	1023	-0.014
	1474	+0 322
-1.0	279	+0.001
	389	-0.001
	600	-0.010
	845	-0.021
	1209	-0.061
-3.0	375	+0.075
	358	+0.128

*$h_o = 250$, $y_m = 30$, $f_c = 6.5$.

III PROGRAM FOR TRANSFORMING BACKSCATTER DATA INTO AN IONOSPHERIC MAP

A. Introduction

The transformation program is presently arranged in four separate programs. The first program, PREPROS,[8] takes the digitized amplitude, smooths the data, and calculates leading edges of all the signals. The second program, OVERHED,[9] calculates vertical-incidence parameters from the leading edges in the vertical-incidence portion of the ionogram. The third program, PRDCTFC,[8] makes the critical-frequency transformations from the backscatter trace. The fourth program produces a contour map using the transformed-frequencies from nine antennas.

A brief description of both OVERHED and PRDCTFC is presented in this section. A flow chart of the critical-frequency transformation program, PRDCTFC, is shown in Fig. 6.

B. Critical-Frequency Transformation Program (PRDCTFC)

Overhead parameters from Program OVERHED and leading-edge points (from PREPROS) are read in (Subroutine DATARED). If a variation in layer height is desired, this variation is read in at this point.

Some of the data points are eliminated by a mask in Subroutine DATALIM. The cone-shaped mask is based on the vertical-incidence parameters generated by using two easily calculated backscatter equations, the first for flat earth, which generally underestimates time delay, and the second for curved earth with constant height of reflection, which generally overestimates time delay (Fig. 3).

The remaining points are then submitted to the quasi-parabolic equation for minimum time delay. The solution of the equation is accomplished by a triple iteration to determine a critical frequency and a distance to the point of reflection. To keep the iteration time low, the points from the ionogram are processed in sequence, so that the changes in parameters with each new point will be small.

The iteration is initiated with an estimate of distance; minimum and maximum values for reflection distance are calculated (Subroutine DMAXMIN); and Subroutine ITERATE is called to determine the distance to the reflection point. Subroutine ITERATE requires a function whose solution is zero, an upper and lower estimate of the unknown, and a specified accuracy. The method used for solution is a combination secant and half method.

For each estimate of distance, h_o may be calculated from the equation for variation in layer height; a variation in layer semithickness could also be calculated here. Constants involving h_o are calculated. The critical frequency is estimated by first calculating minimum and maximum values for it and then calling Subroutine ITERATE at a second level to determine the exact value.

For each estimate of critical frequency, constants are calculated; estimates of minimum and maximum values for the angle of incidence at the layer for minimum time delay are calculated; and Subroutine ITERATE is called at the third level to determine α.

The result of each complete iteration is a critical frequency at a corresponding distance. These will be the data points for the contour map.

Before the contour map is made, the data points are further screened, and a polynomial is fit to the data. The first screening occurs within the quasi-parabolic solution loop: If more than one data point occurs at a frequency on the ionogram, the point giving the most likely critical frequency is kept; the most likely critical frequency is chosen by keeping a running average of accepted critical frequencies. The point nearest the average is kept.

The data are then fit to a polynomial. Beginning with a linear fit, the order of the polynomial is increased until a satisfactory standard error of estimate is reached; up to seventh order is allowed. With each fitting, a second screening of points occurs; points lying outside of a normal distance from the fitted polynomial are eliminated.

The final polynomials from each of nine antennas are used in the contour program, and a contour map is drawn.

Figure 7 shows the vertical-incidence curve fit, the final backscatter data points chosen, and the backscatter minimum-time-delay curve generated from the calculated polynomial.

C. Program for Determining Overhead Parameters (OVERHED)

Leading-edge points from Program PREPROS and the critical frequency from the last time computed (or a rough estimate) are input to the program. A rough calculation of h_o from first- and second-hop data points is made. The estimate of critical frequency and h_o are used as guides in choosing a set of data points from the first-hop vertical-incidence data. The equation for time delay (or virtual height) at vertical incidence in a parabolic layer is then fit by least squares to the data points:

$$h = \frac{y_m}{2} \frac{f}{f_c} \ln \left[\frac{f_c + f}{f_c - f}\right] + h_o \quad ,$$

where

h = virtual height

f = operating frequency

y_m = layer semithickness

f_c = critical frequency of the layer

h_o = height of bottom of the layer.

The equation is solved for the unknowns of y_m, f_c, and h_o by least squares. For each value of f_c, an analytical determination of h_o and y_m may be made. The value of critical frequency is found by iterating.

The final result is checked against all the data. If all the necessary criteria are met, the values are accepted; otherwise they are rejected. Figure 8 shows results of estimates made over a 4.5-hour period. The calculated critical frequencies are compared with critical frequencies from a nearby vertical-incidence station.

IV RESULTS

Figure 9 shows contours generated from these programs, using the digitized backscatter data from nine antennas It has been difficult to check our results, because of a lack of vertical-incidence data at the time the data were taken, but data from the one station that was available within the observation area and the one just outside the area agreed quite well. We expect to have more vertical-incidence data available in the future for checking.

REFERENCES

1. A. M. Peterson, "The Mechanism of F-Layer Propagated Backscatter Echos," J. Geophys. Res., Vol. 56, pp. 221-237 (June 1951).

2. D. L. Nielson, "Ray-Path Equations for an Ionized Layer with a Horizontal Gradient," Radio Science, Vol. 3, No. 1, pp. 101-109 (January 1968).

3. H. F. Bates, "The Height of F-Layer Irregularities in the Arctic Ionosphere," J. Geophys. Res., Vol. 64, No. 9, pp. 1257-1265 (September 1959).

4. T. A. Croft and H. Hoogasian, "Exact Ray Calculations in a Quasi-Parabolic Ionosphere with No Magnetic Field," Radio Science, Vol. 3, No. 1, pp. 69-79 (January 1968).

5. E. M. Kreitzberg, "An Interpretation of Ground Backscatter Records Using Curves Synthesized from Vertical-Incidence Ionograms," Research Memorandum, Contract NObsr-87615, Stanford Research Institute, Menlo Park, California (February 1966), p. 4.

6. R. R. Bartholomew, "Backscatter Data Analysis," Quarterly Progress Report 3, Contract DAAB03-67-C-0099, Stanford Research Institute, Menlo Park, California (August 1967).

7. T. A. Croft, "A Fast, Versatile Ray-Tracing Program for IBM 7090 Digital Computers," SEL Report No. 63-107, Stanford University, Stanford, California (1963).

8. R. R. Bartholomew, V. E. Hatfield, J. B. Lomax, G. H. Smith, "Some Further Results of Backscatter Data Analysis," Final Report, Contract DAAB03-67-C-0099, Stanford Research Institute, Menlo Park, California (June 1968).

9. R. R. Bartholomew et al., "Backscatter Data Analysis," Quarterly Report 4, Contract DAAB03-68-C-0373 Stanford Research Institute, Menlo Park, California (May 1969).

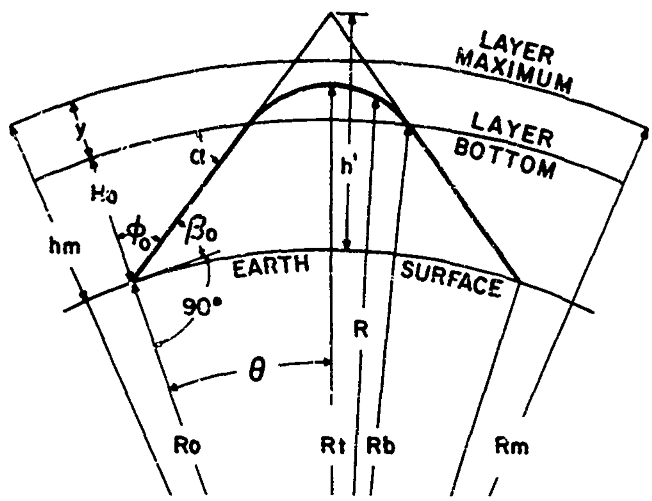

Fig. 1 Backscatter Ray-Path Geometry

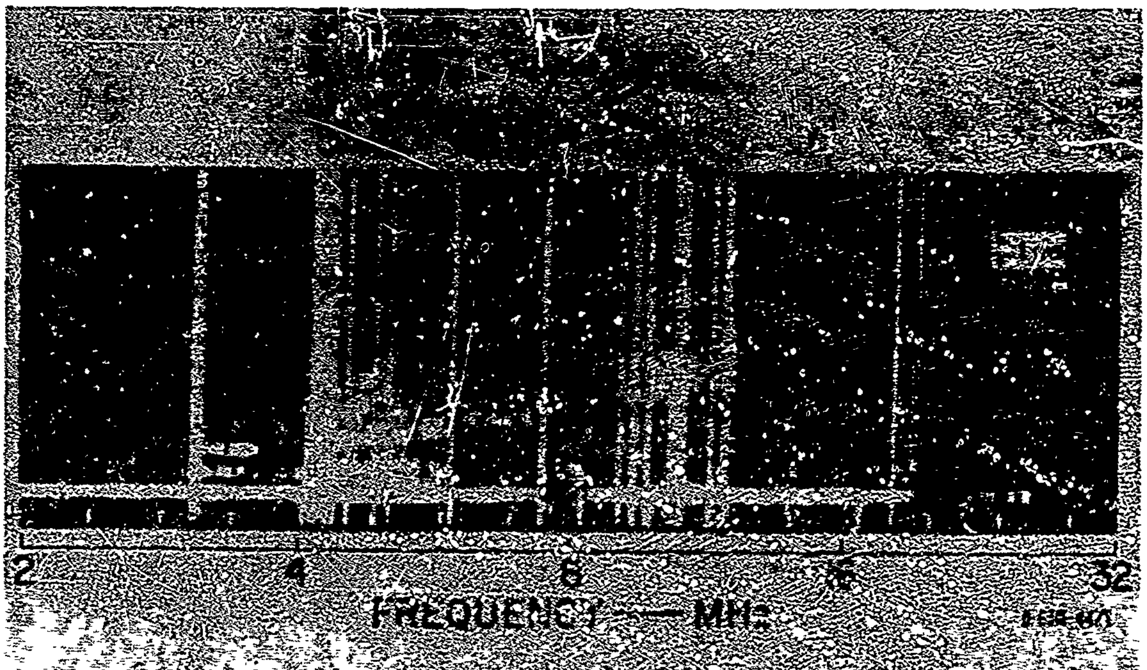

Fig. 2 Backscatter Film Ionogram

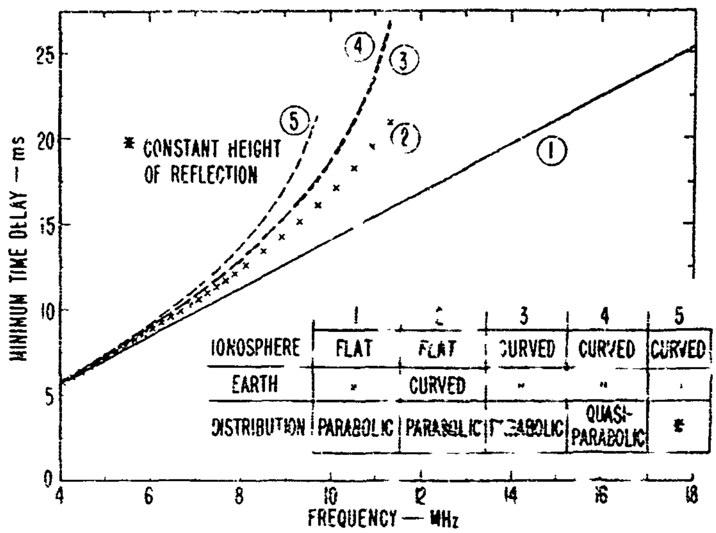

Fig. 3 Comparison of Theoretical Minimum-Time-Delay Traces

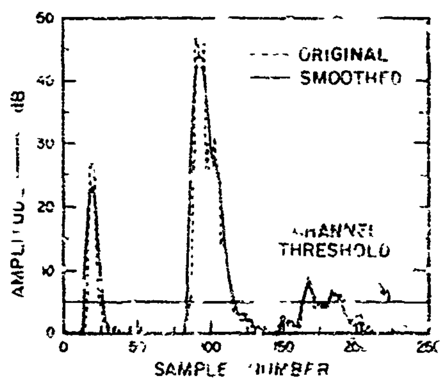

Fig. 4 Example of Original and Smoothed Data Showing Ground-Wave and Backscatter Signal

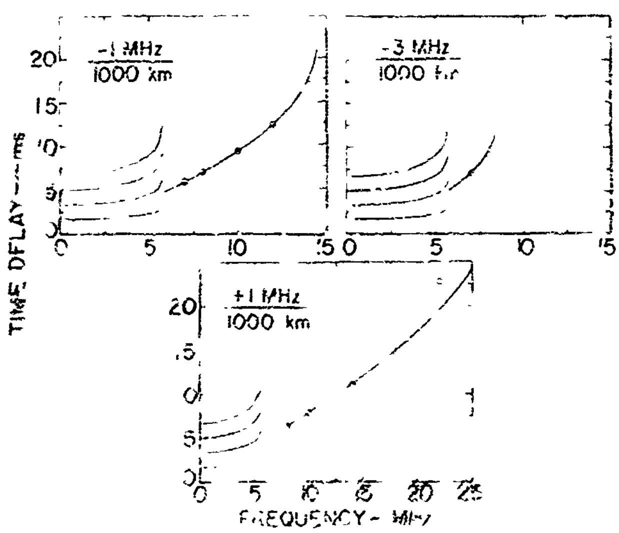

Fig. 5 Simulated Backscatter Ionograms for Tilted Ionospheres

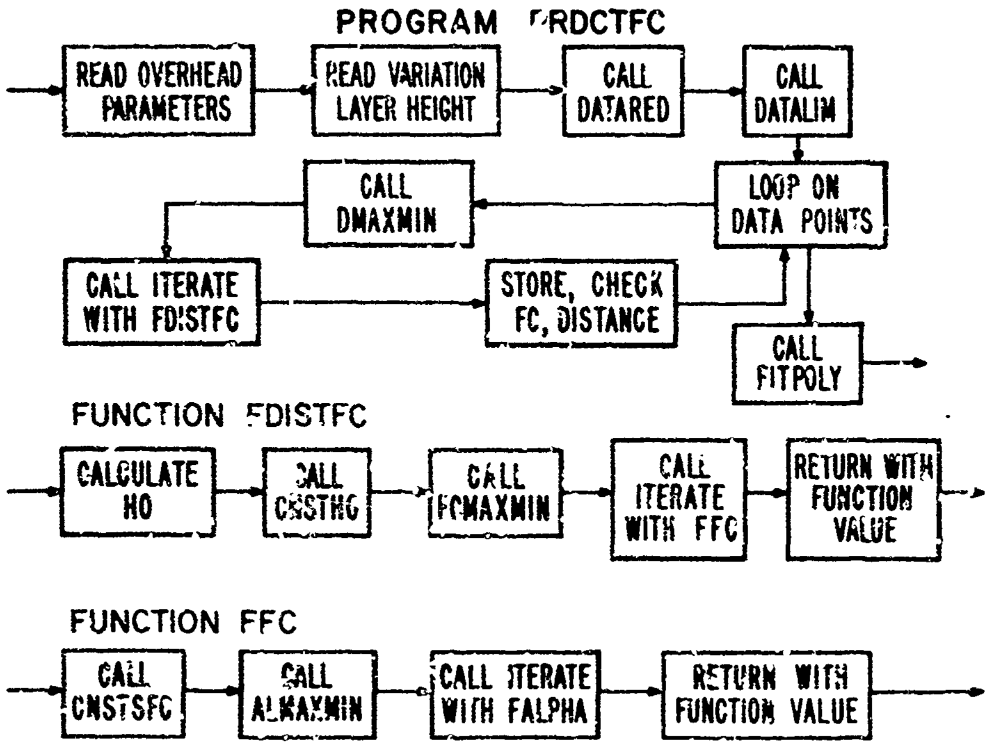

Fig. 6 Flow Chart for Critical-Frequency Transformation Program

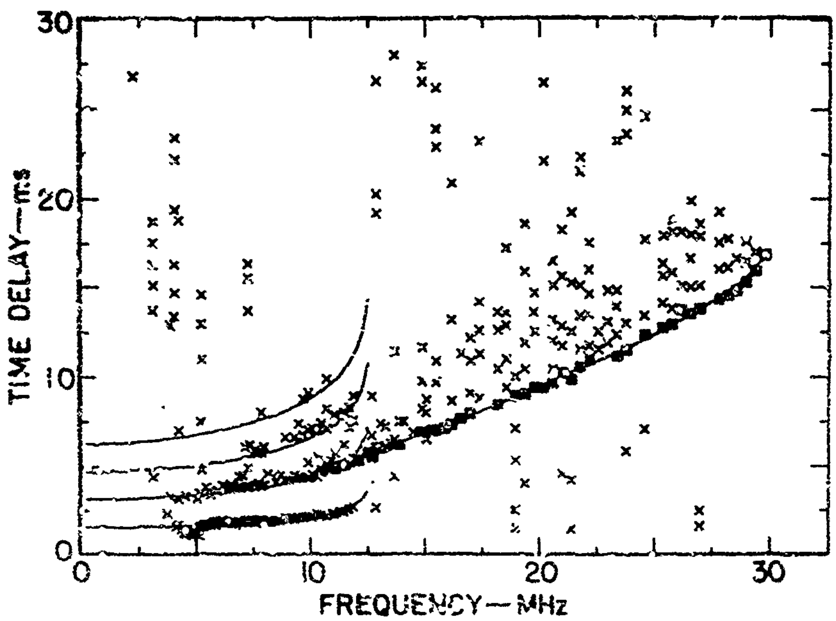

Fig. 7 Sample Ionogram Showing Leading-Edge Data Points, Accepted Points, and Vertical-Incidence and Backscatter Fitted Curves

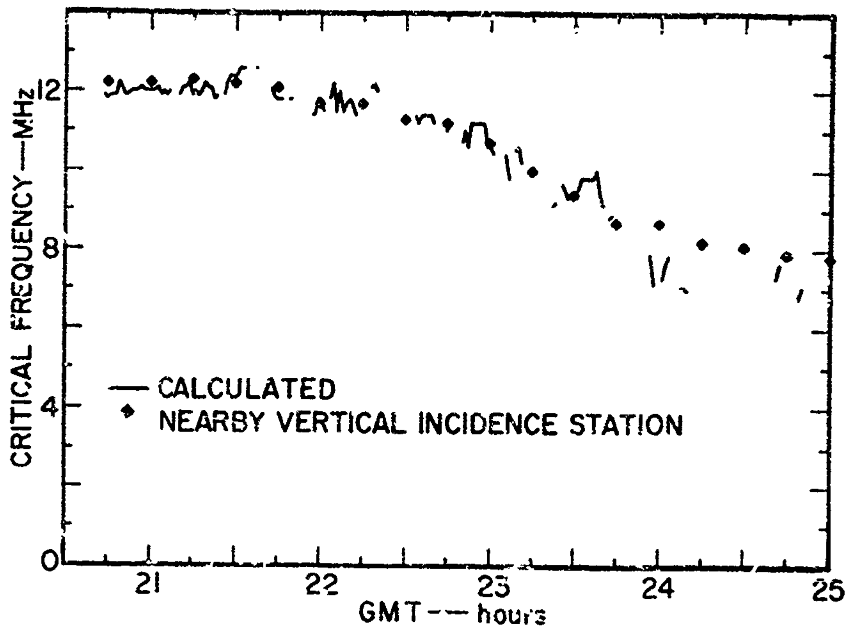

Fig. 8 Vertical-Incidence Critical Frequencies Derived from Digital Backscatter Ionograms

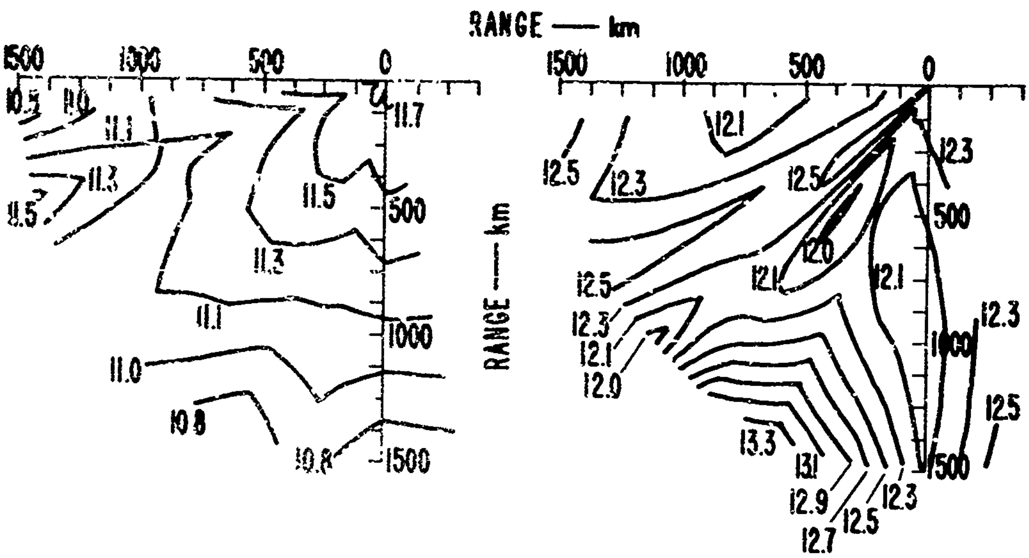

Fig. 9 Calculated Critical-Frequency Contours from Antennas 14-22

(a) 1 February 1968, 20:40 GMT
(b) 2 February 1968, 15:50 GMT

IONOSPHERIC MAPPING BY BACKSCATTER

by

J. C. Blair, R. D. Hunsucker and L. H. Tveten

Institute for Telecommunication Sciences
Environmental Science Services Administration
Boulder, Colorado 80302 U.S.A.

SUMMARY

Recent ionospheric mapping results obtained using a narrow-beam HF scan radar at the Institute for Telecommunication Sciences of the ESSA Research Laboratories at Boulder, Colorado are presented. These include skip distance contour maps at several different frequencies for a midlatitude location. Also given is a technique for obtaining ionospheric plasma frequency as a function of virtual height values from remote backscatter measurements. This technique yielded a 5 percent mean algebraic error and a standard deviation of 11 percent when compared to vertical ionosonde data during nondisturbed periods. Using HF Doppler backscatter and spectral separation techniques, ground features such as coastlines may also be mapped.

IONOSPHERIC MAPPING BY BACKSCATTER

J. C. Blair, R. D. Hunsucker and L. H. Tveten
Institute for Telecommunication Sciences
Environmental Science Services Administration
Boulder, Colorado 80302 U.S.A.

1. INTRODUCTION

The potential usefulness of backscatter for remotely sensing the state of the ionosphere has long been recognized. In its early development, this technique was considered valuable for finding skip distances in many directions from a single location. Considerable work was done in the 1950's and early 60's by Shearman (1956), Silberstein (1958), and others, who showed relationships between propagation conditions and backscatter returns. In spite of promising results reported from these experiments, little if any use has been made of the backscatter technique in monitoring communication circuits for frequency selection.

Earlier backscatter installations suffered from such inadequacies as low power, inability to measure Doppler shifts, and lack of directivity. At ITS we have found that narrow-beam scanning antennas used with high frequency backscatter make it possible to map skip distances and plasma frequencies as a function of virtual height.

2. SCANNING ANTENNAS

Two scanning arrays are used. One, called the azimuth array, has a fan-shaped pattern narrow in azimuth and wide in elevation and is scanned over a sector of azimuth. The other, called the elevation array, has a fan-shaped pattern wide in azimuth and narrow in elevation and is scanned over a sector in elevation. The scan system for the ITS high-resolution HF receiving array is located at the ITS Table Mountain field site north of Boulder, Colorado.

The arrays are shown in figure 1. The 500-ft mast contains the 10 log periodic antennas that, together with their ground images, make up the elevation array aperture. The azimuth array is made up of 25 log periodics spaced 17.67 m apart. Its aperture is 1392 ft and the effective aperture of the elevation array is 1000 ft. Each of the array element outputs is fed into its own preamplifier-converter circuit and then combined with the others to form a narrow beam that can be steered over a sector. A broad front end allows tuning by the choice of local oscillator frequency only. The local oscillator is an electronically controlled frequency synthesizer by which frequency can be changed in less than a millisecond. The beam is formed and steered with mechanically driven phase-shift capacitors operating on the local oscillator frequency for a second conversion in the individual converters.

The azimuth array scans a total sector of 90° with a 3° beamwidth when operated at 12 MHz. Both the sector and beamwidth decrease with frequency. A horizontal beamwidth of 1.4° and a total sector of 40° are obtained at 25 MHz. The vertical antenna has a beamwidth of 4.2° and scans from 3° to 52° at 12 MHz; at 25 MHz, the beamwidth is 2.0° and the scan sector includes 1.5 to 22°. More complex descriptions of this instrumentation and observations of various ionospheric phenomena have been reported by Hunsucker and Tveten (1967), Tveten and Hunsucker (1969), and Hunsucker (1969).

Figure 2 is an example of an azimuth-elevation backscatter record. The azimuth sweep as a function of backscatter delay is on the left; the variation between elevation angle and backscatter delay is on the right. The two antenna systems are scanned simultaneously at 1/12 scan per second. The record shown was made at 15.7 MHz. The azimuth sweep covers the range of 81.3° to 146.7°; boresight azimuth is 114°. The lobe pattern of the rhombic transmitting antenna is evident in the azimuth scan record.

The azimuth array is useful for skip-distance mapping and the elevation records can be used to map plasma frequency versus virtual height.

3. SKIP-DISTANCE MAPPING

The concept of determining skip-distance from high frequency backscatter is now quite old. Silberstein (1958) used sweep frequency backscatter with rhombic antennas to estimate maximum usable frequencies over a specific 2400 km path which was simultaneously

observed with an oblique sweep frequency sounder to measure the MUF's directly. This path was also sounded at the midpoint by a vertical incidence sounder. The significant result of this study was that the MUF's could be estimated from backscatter with a median error of 0.5% with 90% of the errors falling between -3.9 and +6.8%. This was more accurate and with less dispersion than by the conventional application of transmission curves to the midpoint vertical ionogram.

Backscatter skip distance mapping with a high resolution scan system plots path lengths at different azimuths for given MUF values instead of determining MUF's at specific path lengths. Only relatively crude estimates of reflection height are necessary since the rate of change of ground range with reflection height at a constant delay is approximately unity over the ranges of interest. Ground range estimates are also relatively insensitive to path asymmetries caused by ionospheric tilts of normal magnitudes.

In a plot of skip distance versus azimuth at a given frequency the question of error in azimuth position may also arise. On simple one-hop paths such as these it is only rarely that azimuth deviations exceed one degree. Even over a 3600 km-path this figure would result in an error of about 60 km. Shorter paths and smaller deviations will result in proportionately smaller errors. At very short ranges (< 700 km) the errors increase because the minimum delay signal no longer very closely approximates the skip distance (Hunsucker, 1969), and the rate of change of ground range with reflection height at a constant delay rapidly increases requiring more precision in knowledge of reflection height. However, these ranges near the sounder location are often not of great interest anyway.

Thus, over most of the ranges of interest (~ 700 km -3000 km) the errors in skip distance maps are not more than a few tens of kilometers - an accuracy quite adequate for many applications.

Figure 3 shows a skip-distance map for five different frequencies that was made with the high-resolution arrays and backscatter transmissions at 0753 MST, Feb. 17, 1967 (Tveten and Hunsucker, 1969). The azimuth and elevation versus backscatter delay are traced for clarity. The elevation records are useful in establishing the general propagation mode structure and the effective reflection heights for determining the ground range. There is obviously considerable variation in the skip ranges with azimuth. It is not yet certain that all the areas receiving the signal are included in ranges greater than those indicated by the appropriate skip-distance contours, but it is reasonably certain that the ranges beyond the indicated skip-distance contours do receive the signal. Thus, high-resolution backscatter measurements could be useful in determining area ground coverage for telecommunication systems.

4. PLASMA FREQUENCY MAPPING

Using the elevation scan data, one can determine plasma frequency as a function of virtual height for the distant ionosphere. To illustrate the technique, we find from figure 2 that a backscatter delay of 10 ms corresponds to an elevation angle of about 17°. Figure 4 shows a transmission curve similar to the one developed by Smith (1939), except that this one is parametric in ionospheric path delay time instead of ground range. To use this curve, one determines the intersection of elevation angle and delay time. With a delay of 10 ms and an elevation angle of 17°, the intersection occurs at a virtual height of about 265 km and a sec ϕ value of about 2.6. Dividing the operating frequency of 15.7 MHz by 2.6 as required by the secant law results in a plasma frequency of 6 MHz at a virtual height of 265 km. In this manner, by using many points on the elevation-angle delay record, one could generate a vertical incidence F-layer trace similar to that seen on an ionogram, assuming the ionosphere to be uniform over the range involved.

Given the virtual height and delay time, it is simple to calculate the ground range to the point on the earth's surface under the ionospheric point calculated. Given backscatter delay time-elevation angle records on different frequencies, one can determine vertical profiles of frequencies versus virtual height at different ranges from an observing point. The above calculations must assume at least local ionospheric concentricity to be valid.

5. ACCURACY OF THE TECHNIQUE

5.1 Tests of Accuracy

The accuracy to which plasma frequency can be measured by the backscatter technique was tested by a vertical sounder. For the backscatter plasma frequency measurements, we

used the high-resolution receiving antenna system. The illuminated azimuthal sector was limited by use of a rhombic transmitting antenna. The vertical sounder was located at Ponca City, Oklahoma. Plasma frequency versus height was measured from the elevation-angle scan records at ranges corresponding to the sounder location and at times the sounder was running by using a computer program solution of the transmission equations. About 240 plasma frequency versus height measurements, made over a period of about a year, were checked against those measured with the sounder.

Comparison of the data showed a 5 percent mean algebraic error and a standard deviation of about 11 percent for quiet ionospheric periods. The algebraic error can be corrected by a modification in the scaling technique. Corresponding figures for disturbed periods were considerably higher.

5.2 Sources of Error

The accuracy of the backscatter plasma frequency mapping described is dependent upon the magnitude of ionospheric ionization gradients. These gradients can cause plasma frequency estimates to be applied at the wrong heights and the wrong ranges. Errors are most serious for plasma frequencies near the critical frequency at long ranges. Besides an effective pure tilt effect, ionospheric gradients can generate an asymmetry in the ionospheric part of the ray path before and after reflection; however, this is probably not too serious a problem. For an F region reflection the ray is in the strongly ray deviating part of the ionosphere for perhaps 200 km in range. Even with a fairly strong critical frequency gradient of 1 kHz/km there would be only a 200 kHz differential across this range interval.

What is needed to improve the backscatter plasma frequency mapping is the measurement of another parameter besides elevation angle and delay time to explicitly define the virtual ray path geometry involved.

A parameter which fulfills this requirement is ground range. Thus the tilt problem can be corrected for, at least partly, by measuring delays and elevation angles from fixed targets of known range. One such target is a coastline where the land-sea interface can be identified by Doppler techniques (Blair et al., 1969).

The record in figure 5 shows how this technique was used to map the southeast United States coastline. The high-resolution azimuth array was steered slowly through its sector while receiving and coherently detecting backscatter from pulsed transmissions that illuminated the earth's surface at long ranges The coherent signals were processed through a multiple-range-gate spectrum analyzer and the non-Doppler shifted ground scatter components (excluding the Doppler-shifted sea scatter) were used to brighten a range-azimuth oscilloscope display. The dotted line shows the position of the coastline as it would transform to this display with an ionospheric height of 270 km. The correspondence is quite good. Figure 6 shows the same display with all backscatter components.

6. POSSIBILITIES OF BACKSCATTER MAPPING TECHNIQUES

If plasma frequencies versus virtual heights could be measured for a number of azimuths as well as ranges, a map of the information could be used for real-time-frequency-selection for HF communication circuits over a wide area regardless of whether the backscatter sounder were located at a communications terminal. Such maps would of course also be of great value in ionospheric studies.

The restriction of the azimuth sector over which a given elevation-angle-versus-backscatter-delay measurement is made constitutes one of the difficult problems to be overcome in real-time plasma frequency mapping. This restriction is necessary to detect ionospheric geographic variations. Either a narrow azimuth transmitting beam or a narrow receiving beam would be suitable. It may be possible to apply a Mills cross correlating technique to obtain a pencil beam that can be scanned over both a sector in elevation angle and a sector in azimuth.

7. REFERENCES

Blair, J. C., L. L. Melanson, and L. H. Tveten (1969), "HF ionospheric radar ground-scatter map showing land-sea boundaries by a spectral-separation technique," Electron. Letters, vol. 5, No. 4, 75-76.

Hunsucker, R. D. and L. H. Tveten (1967), "Large traveling disturbances observed at mid-latitudes utilizing the high resolution HF backscatter technique," J. Atmosph. Terr. Phys., 29, 909-916.

Hunsucker, Robert Dudley (1969), "Remote sensing of the mid-latitude ionosphere with a narrow-beam high-frequency radar," PhD Dissertation, Electrical Engineering Department, University of Colorado, Boulder, Colorado.

Shearman, E. D. R. (1956), "The technique of ionospheric investigation using ground backscatter," Proc. IEE., 103B, 210-221.

Silberstein, R. (1954), "Sweep-frequency backscatter-some observations and deductions," IRE Trans. Ant. Prop., AP-2, 56-63.

Silberstein, R. (1958), "The use of sweep-frequency backscatter data for determining oblique-incidence ionospheric characteristics," J. Geophys. Res., 63, No. 2, 335-351.

Smith, Newbern (1939), "The relation of radio sky-wave transmission to ionospheric measurements," Proc. IRE, 27, No. 5, 332-347.

Tveten, Lowell H. and Robert D. Hunsucker (1969), "Remote sensing of the terrestrial environment with an HF radio high-resolution azimuth and elevation scan system," Proc. IRE, 57, No. 4, 487-495.

Figure 1. High resolution azimuth and elevation scan arrays at ESSA Table Mountain Field Station.

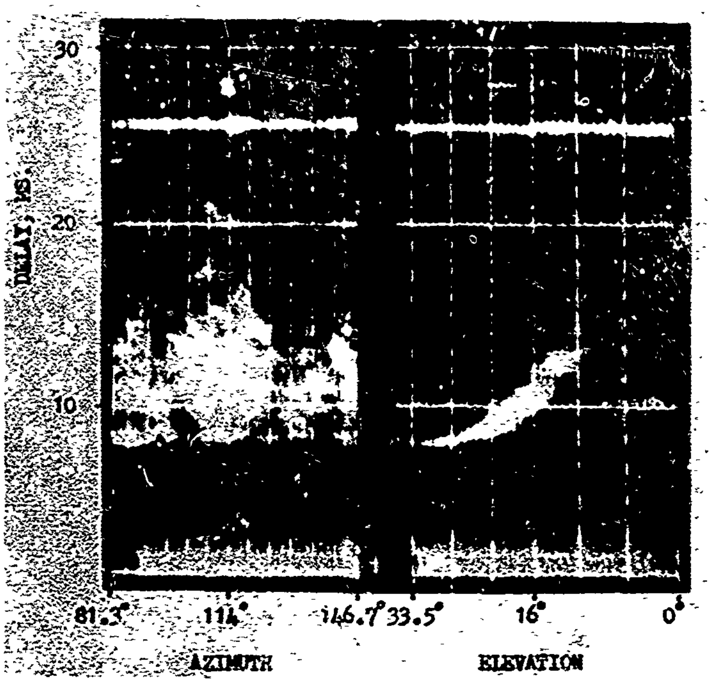

Figure 2. Simultaneous azimuth and elevation angle vs. delay display of HF backscatter.

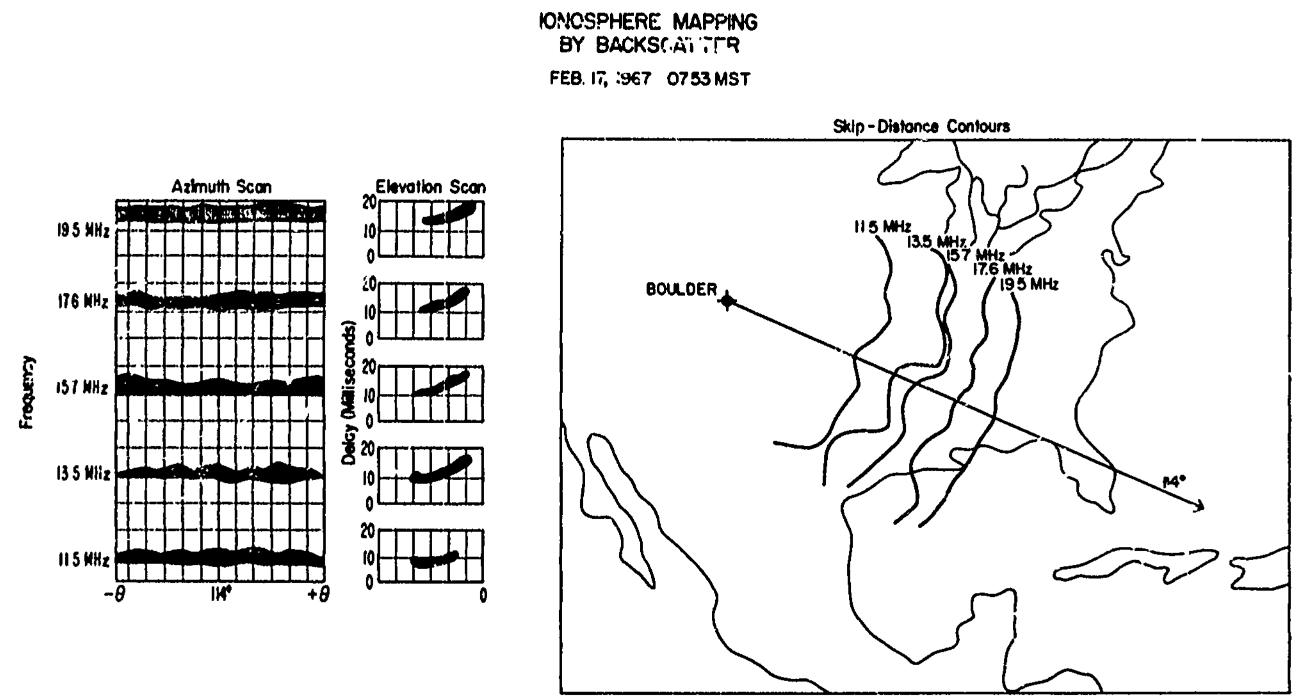

Figure 3. Ionosphere mapping by backscatter.

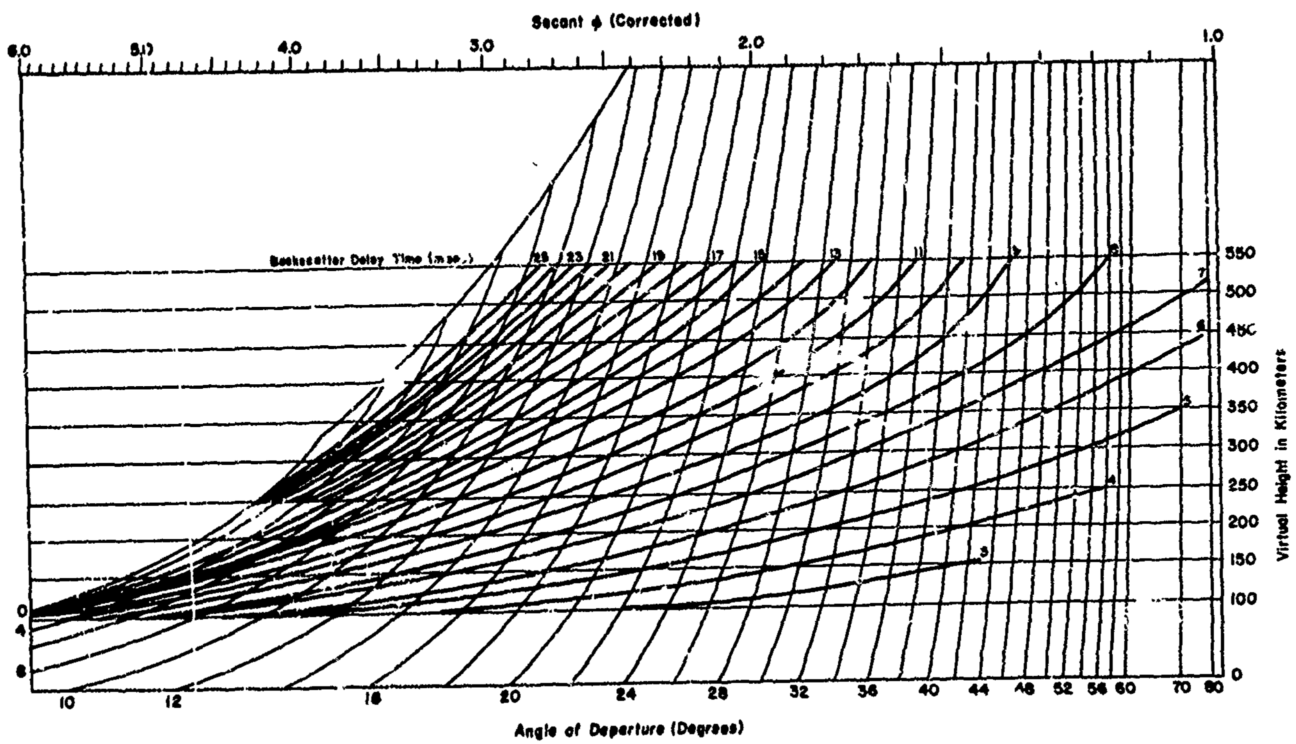

Figure 4. Smith transmission curve parametric in slant range backscatter path delay.

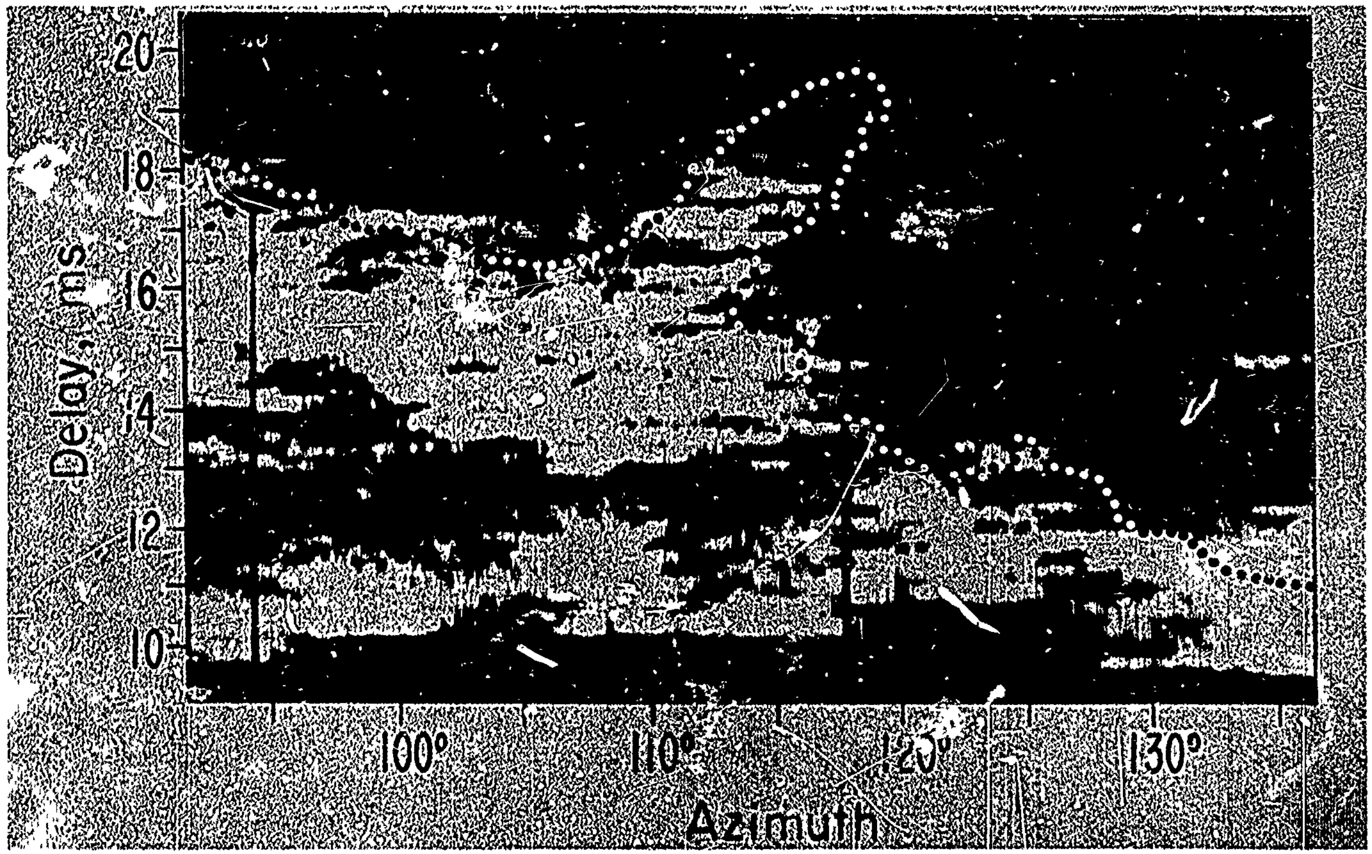

Figure 5. Comparison of delay vs. azimuth map of the southeastern United States with backscatter filtered to remove sea scatter Doppler components.

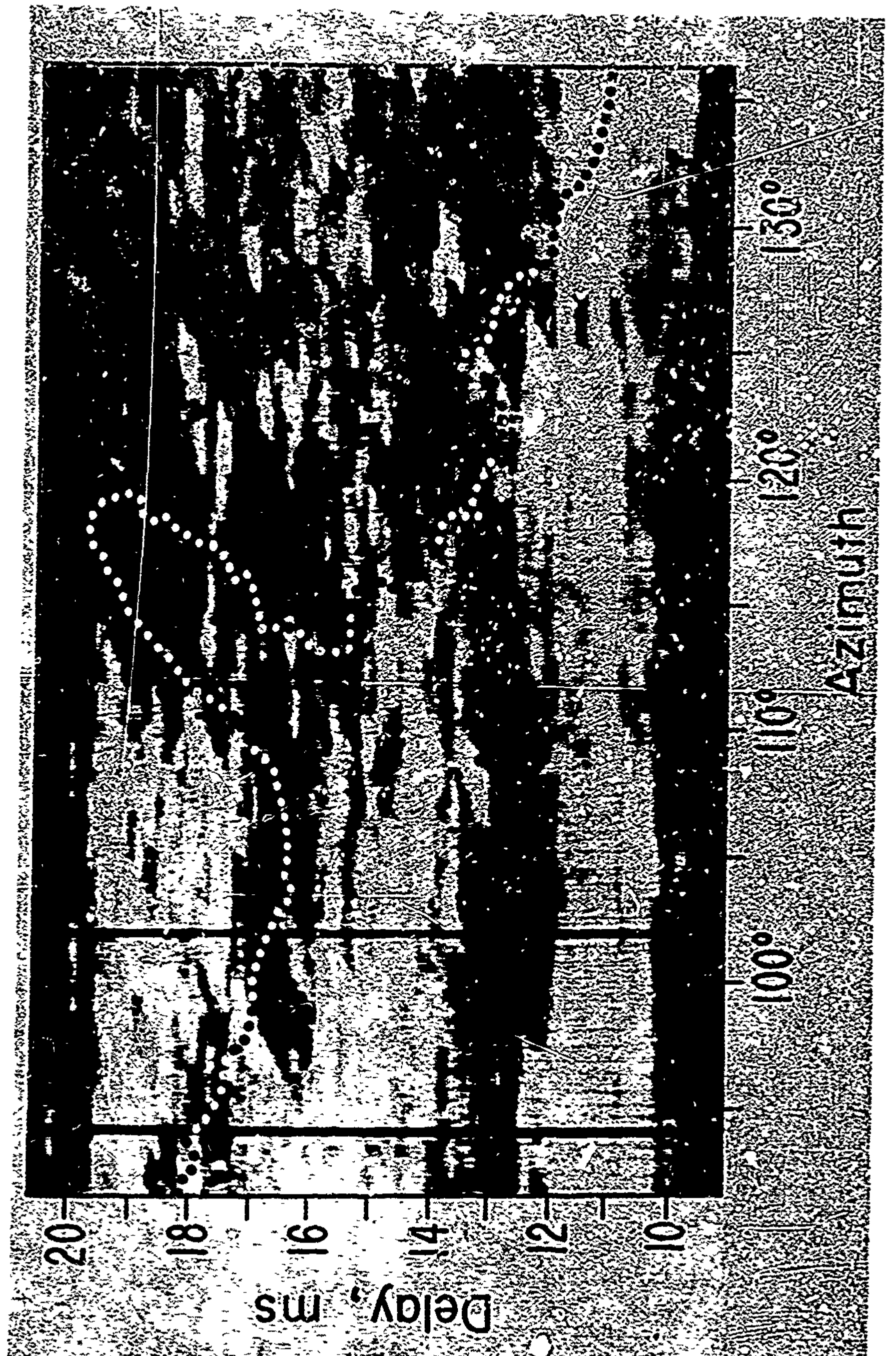

Figure 6. Same as Figure 5 with no Doppler components removed.

HF-RTW PROPAGATION STUDY: PREDICTION SCHEME AND SYNOPTIC BEHAVIOUR

by

C.A.Moo

Avco Corporation/Space Systems Division,
Lowell Industrial Park,
Lowell, Massachusetts 01851, USA

ABSTRACT

Results of a year's observations of the amplitude variations of pulsed-CW around-the-world (RTW) transmissions on selected frequencies from Manila at 320° azimuth are described. For scheduling monitoring time and frequencies, a prediction scheme based on the RTW propagation model of Fenwick (1963), was developed. The model involves earth-ionosphere reflections in the daylight hemisphere and ionosphere-ionosphere reflections in the dark hemisphere, with propagation possible when the transmitter is in the daylight. Using ESSA world maps of MUF (4000 km) F2, along the great-circle path, the scheme selected as the RTW MUF at a given time the lesser of the following quantities: the least MUF (4000) F2 value in the dayside (multihop MUF), and twice the least MUF (4000) F2 value in the night-side (ionosphere-ionosphere MUF, Grossi and Langworthy (1966)).

Amplitude measurements were made by range sampling the RTW-delayed echoes during half-minute pulsing periods every half hour, on several frequencies. The diurnal variation of signal amplitudes establishes the key role of sunrise and sunset tilts in RTW propagation, and validates the propagation model. The maximum frequencies observed were consistently above the predicted MUFs, the latter corresponding more nearly to the frequencies for optimum RTW signal levels. The disparity between predicted and observed MUFs may reflect the well known limits of the MUF maps employed in the predictions.

Introduction

During a one-year period in 1967-68 an experimental study of the propagation of high-frequency (HF) radio waves around the world (RTW) was carried out from stations near Manila, Philippines, radiating in the direction of 320° azimuth and receiving at the complimentary 140° azimuth. The purpose of the program was to monitor the amplitude and the spectral properties of the received signals, using pulsed and phase-stable CW transmissions, respectively. Detert and Moo (1968) displayed some of the unusual Doppler effects observed. In order to specify frequencies for the RTW investigation, procedures were developed for the prediction of usable frequencies during the day. This paper describes the prediction scheme used and its relationship with the synoptic behavior of the RTW signal amplitudes observed in the experiment.

RTW Propagation Mode

The phenomenon that HF radio waves can often propagate around the world one or more times has been known for many years. The first sufficiently systematic investigation was done by Hess (1948, 1949, 1952). He found that the RTW pulse echoes had attenuations of as little as 5 db per circulation. This was substantiated later by Luscombe (1957) and Isted (1958). Hess (1948) further indicated that pulses suffered very little distortion under multiple circulations, apparently not exhibiting multipath distortion that is experienced for signals propagated by the usual ionosphere-ground hop modes. Isted (1958) concluded from this characteristic, which he also observed, that the usual earth-ionosphere-earth hops were not involved.

Since 1961, Fenwick and Villard at Stanford University have carried out intensive studies for the purpose of defining the mechanism of RTW propagation modes. From measurements of time variations of MUF, LUF, optimum azimuth, time delay and pulse dispersion they developed a propagation model which substantially explains the observed features of RTW phenomena. Fenwick (1963) concluded that the dominant mode is a low-angle earth-ionosphere-earth hop mode, primarily in the sunlit hemisphere, plus an ionosphere-ionosphere (iono-iono) "tilt" mode in the dark hemisphere. The importance of iono-iono reflections (Fenwick and Villard, 1963) was shown experimentally by the existence of time periods when westbound transmissions from Okinawa were readily audible in Guam to the east but inaudible in Europe, all stations being generally along the same great circle. This result is readily explained by F-layer tilts present at these times; these tilts allow the launching of a tilt-supported mode along the underside of the F-layer, passing over the European receiving sites, and the RTW signals become audible at the receiver at Guam when deflected into the multihop mode by the sunset tilt.

The dominant RTW propagation mode suggested by the Stanford studies, then, is a configuration of classical earth-ionosphere-earth hops in the daylight hemisphere, and an ionosphere-ionosphere trapped mode in the nighttime hemisphere. Launching of the energy into the iono-iono mode is thought to be a consequence of horizontal gradients, or tilts, in the electron density profile during the hours of sunrise. Energy in this mode would be returned to earth by gradients associated with sunset.

Figure 1 shows a sketch of the dominant RTW mode for east-to-west propagation. Notice that because of the orientation of the sunrise and sunset tilts, propagation around the world is possible only when the transmitter and receiver pair are in daylight. Also, the shallow angle iono-iono rays induced by the sunset tilt through the night ionosphere allow RTW transmission at frequencies in excess of those possible by ordinary multihop propagation. This mixed propagation mode was used as the basis for predicting the RTW MUF, along selected azimuths, for scheduling purposes in the RTW experiment.

Prediction Scheme

In order to predict accurately the frequencies which will be able to sustain RTW propagation as a function of time of day, it is necessary to know the propagation modes, critical frequencies, tilts, and effective absorption index along the path. Since measured values of these parameters are not available, it is usual to employ predicted median ionospheric conditions expected for any given time of day, season, and sunspot number, such as the Ionospheric Predictions published by ESSA/ITSA three months in advance.

If we assume that RTW propagation is by multihop all along a chosen great circle path, then a reasonable estimate for the MUF for RTW propagation would be the minimum MUF

(4000 km) value along the great circle. Employing the more probable assumption that the dominant RTW mode is a combined day multihop plus night-iono-iono mode, it is necessary to develop a technique of prediction which will yield higher MUF (RTW) values than those obtainable with the total multihop assumption. In this case (and excluding absorption) the time and frequency availability will depend on three factors: the multihop MUF in the day path, the iono-iono MUF in the night path, and the orientation of tilts. Since the role of sunrise and sunset tilts is to launch and extract, respectively, HF radiowaves in the iono-iono mode during the east-to-west propagation of the RTW signals it is expected that RTW in the combined mode will be available only at those times when the transmitter is in the day hemisphere. That is, when in proceeding by earth-ionosphere-earth reflections to the positively oriented day-night tilt the iono-iono mode is launched into the night ionosphere. When the energy reaches the night-day tilt at the sunset line, it is deflected into the multihop mode again, and travels by earth-iono hops to the receiver. The MUF (RTW) value for any time when the transmitter is in the day zone may thus be defined as the minimum of the multihop MUF and the iono-iono MUF values along the path.

The multihop-MUF value should always be less than the iono-iono MUF value. Grossi and Langworthy (1966) have deduced from ray tracing through model ionospheres that iono-iono modes can propagate at frequencies up to roughly twice the multihop MUF (4000 km) value for a given path segment. With this observation, the following procedure was used for generating MUF (RTW) predictions for the RTW experiment, using the Ionospheric Predictions MUF (4000 km) maps published by ESSA.

1. On the MUF (4000 km) map for a given universal time, construct the great circle for the desired azimuth through Manila and across the ionospheric 300 km twilight line. (Sunrise and sunset times in the ionosphere as a function of latitude have been computed by Colin and Myers (1966), among others.) Figure 2 shows an example for April 1967 00 UT, of the 320-degree great circle through Manila, and the 300 km twilight line.

2. On the day portion of the great circle, 4000 km east of the sunrise line, read the minimum value of MUF (4000 km). The reason for using the MUF (4000 km) value 4000 km into the day side from the sunrise line is that illumination of the sunrise tilt is controlled, not by MUF (4000 km) values directly below the tilt, but by multihop values one-half to one hop distance away from the sunrise line.

3. For the night part of the great circle, obtain the minimum value of MUF (4000 km) and multiply it by two.

4. The lesser of the values of (2) and (3) is the MUF (RTW) value for the given time.

5. Repeat the procedure in (1) through (4) for different universal times to generate RTW (MUF) values during the day.

Figure 3 shows the variation with time of MUF (RTW) on a great circle azimuth of 320°, for January 1967. The upper curve gives values predicted by using the technique given above, while the lower curve shows MUF values obtained when assuming only multihop modes around the world. Notice that the former has higher frequency values at all times, and that the iono-iono plus multihop mode propagation, for frequencies greater than 10 MHz, is possible some 10 hours before purely multihop modes. Figure 4 shows the predicted MUF (RTW) values for RTW monitoring in 1967-68 on three azimuths, providing for a 20-degree azimuthal sector about the main boresight azimuth, 320° (140°), of the RTW experimental system. In practice, it was found that the predicted MUF (RTW) value was determined by the day multihop MUF (item 2 above).

Using the RTW MUF values predicted by the scheme described above, radio frequencies were scheduled for RTW CW monitoring. Since the frequencies which were available were few in number, no attempt was made to determine the actual maximum observable RTW frequency. Thus the relationship between the RTW MOF and the predicted MUF was not examined. The frequencies assigned (up to four) were picked near the predicted MUF values in the 20° sector about 320° azimuth at Manila. On all these frequencies RTW propagation was observed. However, the actual maximum observable RTW frequencies appear to be higher than those predicted. At least one reason for this is that the prediction scheme involves the use of ESSA MUF maps and these are well known to be conservative, generally predicting MUF (4000 km) values well below those actually observed.

RTW Amplitude Variations

The RTW experimental transmitter and receiver complex was located near Manila, Philippine Islands. CW transmissions of 20 kw power were beamed along a 320° azimuth by a low angle horizontal rhombic antenna. The receiver inputs were connected to a narrow-beam vertical array antenna directed at the complimentary 140° azimuth for monitoring RTW returns. RTW amplitude measurements were made by range sampling the RTW-delayed echoes (about 138 ms delay) during half-minute pulsing periods every half hour, on several frequencies. Each pulsing period consisted of 20 seconds of 5 pps pulses for measuring signal amplitude, followed by 10 seconds of no transmission for measuring noise level.

Figure 5 shows examples of the mean diurnal variation of RTW signal-to-noise ratio (SNR) on 22.0 MHz for August 1967 and on 20.5 MHz for September 1967. The arrows SR and SS indicate the time of ground sunrise and ground sunset, respectively, at Manila. The vertical bars show the average algebraic deviation from the mean of the data for the time of day. The most striking aspect of the variations is the control exercised by the sun in turning on and turning off the RTW signal level, a behavior which validates the propagation model used in making predictions of RTW MUF.

Figure 6 shows the RTW SNR on a single frequency for each of the months in which RTW monitoring was performed. Solar control is also generally evident. The freqeuncy chosen for display each month, from up to four in number, was one onwhich the SNR was generally largest during the day. Comparison with the predicted MUF (RTW) graphs in Figure 4 shows that the predicted MUFs more nearly corresponds to the frequencies for optimum RTW signal levels. Because of the small number of channels monitored in the RTW experiment the MOFs and the exact frequencies for highest SNRs could not be determined.

Conclusions

The diurnal variations of RTW signal levels have validated the RTW propagation model on which predictions of RTW MUFs were based. The fact that frequencies higher than predicted were frequently observed may reflect the well known conservative nature of the MUF (4000 km) maps used in making predictions. The presence of other ionospheric tilts, other than sunrise and sunset, could, of course, contribute to the higher frequencies observed. but these tilts are perhaps not large enough, nor systematic enough, to explain the observed higher frequencies.

ACKNOWLEDGMENT

The work reported in this paper was supported by the Rome Air Development Center of the United States Air Force, under Contract Nos. AF30(602)-3895 and F30602-67-C-0016.

REFERENCES

Colin, L., and M. A. Myers, "Computed Times of Sunrise and Sunset in the Ionosphere", NASA Technical Memorandum X-1233, Ames Research Center, Moffett Field, Calif. (1966).

Detert, D. G., and C. A. Moo, "Doppler Effects of Atmospheric Disturbances on HF Radio Propagation", Proc. AGARD EPC Symposium on Phase and Frequency Instability in EM Wave Propagation, Ankara, Turkey, (October 1967).

Fenwick, R. B., "Round-the-World High-Frequency Propagation", Rept. SEL-63-019 (TR No. 71), Contract Nonr-225 (64), NR 088 019, Stanford Electronics Laboratories, Stanford, Calif. (April 1963).

Fenwick, R. B., and O. G. Villard, Jr., "A Test of the Importance of Ionosphere-Ionosphere Reflections in Long Distance and Around-the-World High-Frequency Propagation", J. Geophys. Res., 68, 5659-5666 (1963).

Grossi, H. D., and B. M. Langworthy, "Geometric Optics Investigation of HF and VHF Guided Propagation in the Ionospheric Whispering Gallery", Radio Science, 1, 877-886 (1966).

Hess, H. A., "Investigations of High-Frequency Echoes", Proc. IRE, 36, 981-992 (1948); 37, 986-989 (1949); 40, 1065-1068 (1952).

Isted, G. A., "Round-the-World Echoes", Marconi Rev., 21, 173-183 (1958).

Luscombe, G. W., "Delayed Signals in Ionospheric Forward-Scatter Communication", Nature, 180, 138 (1957).

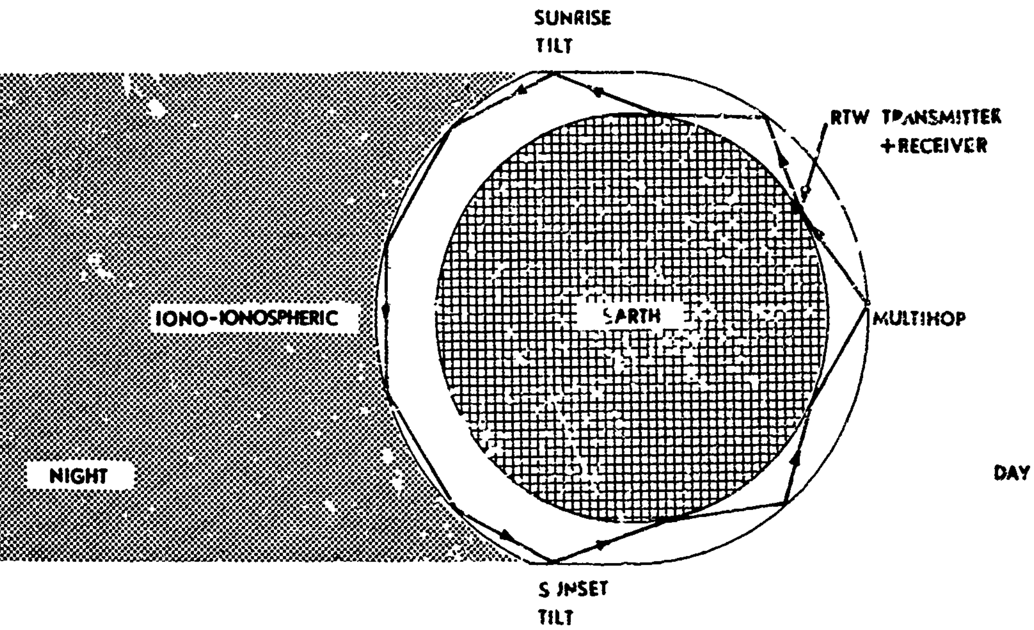

Figure 1: Sketch of dominant RTW propagation mode

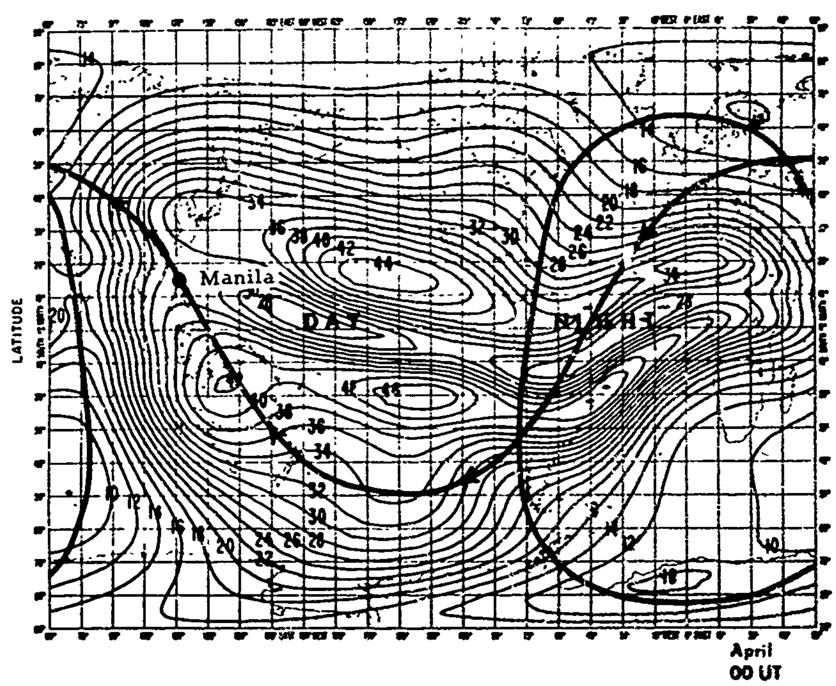

Figure 2: 320° great circle path through Manila and twilight line on MUF (4000 km) map.

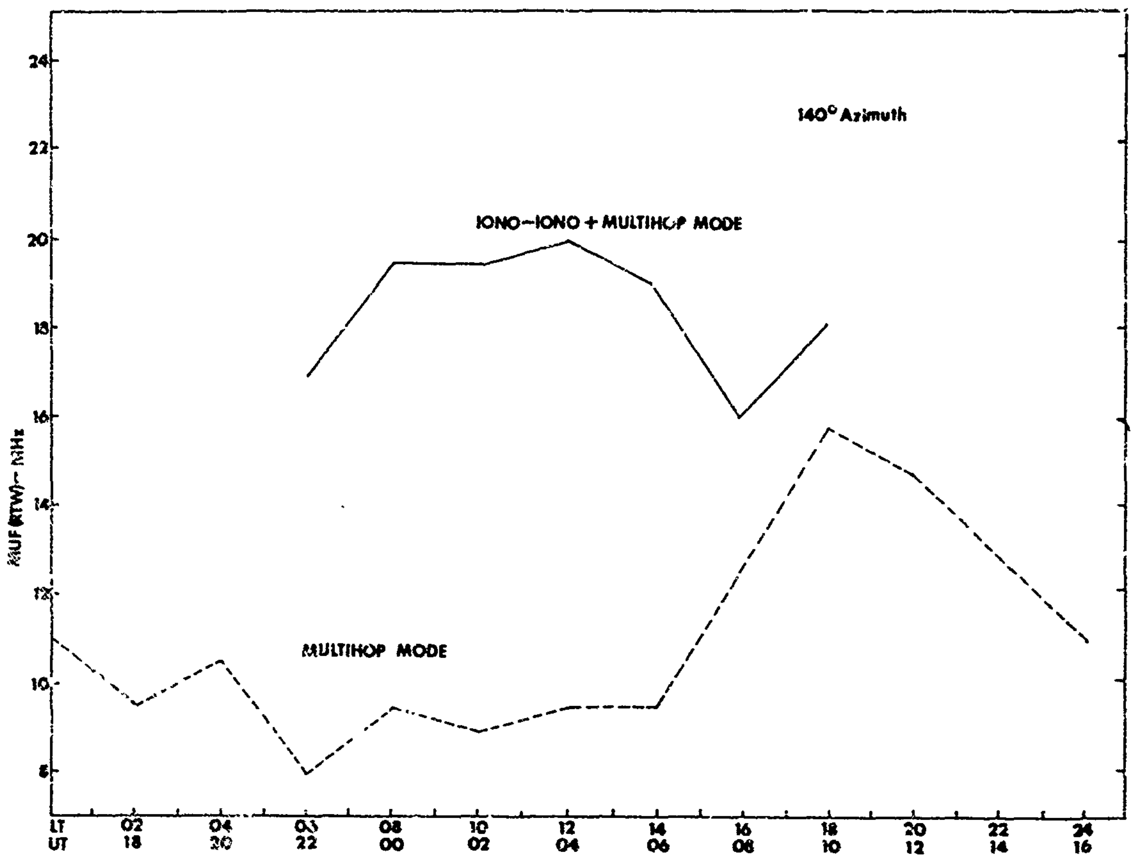

Figure 3: RTW predicted frequencies, January 1967, Manila

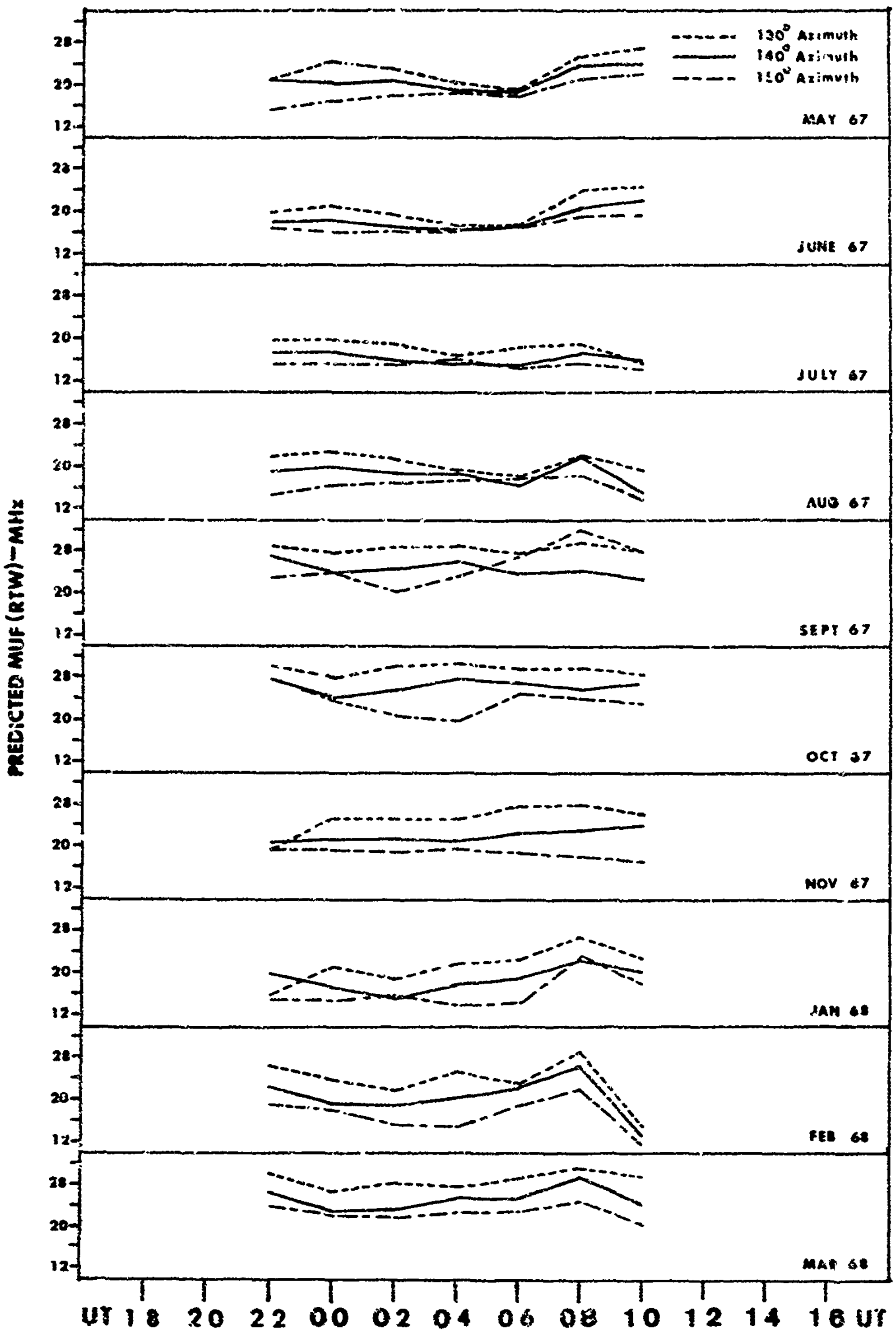

Figure 4: Predicted MUF (RTW), 1967-68, for Manila.

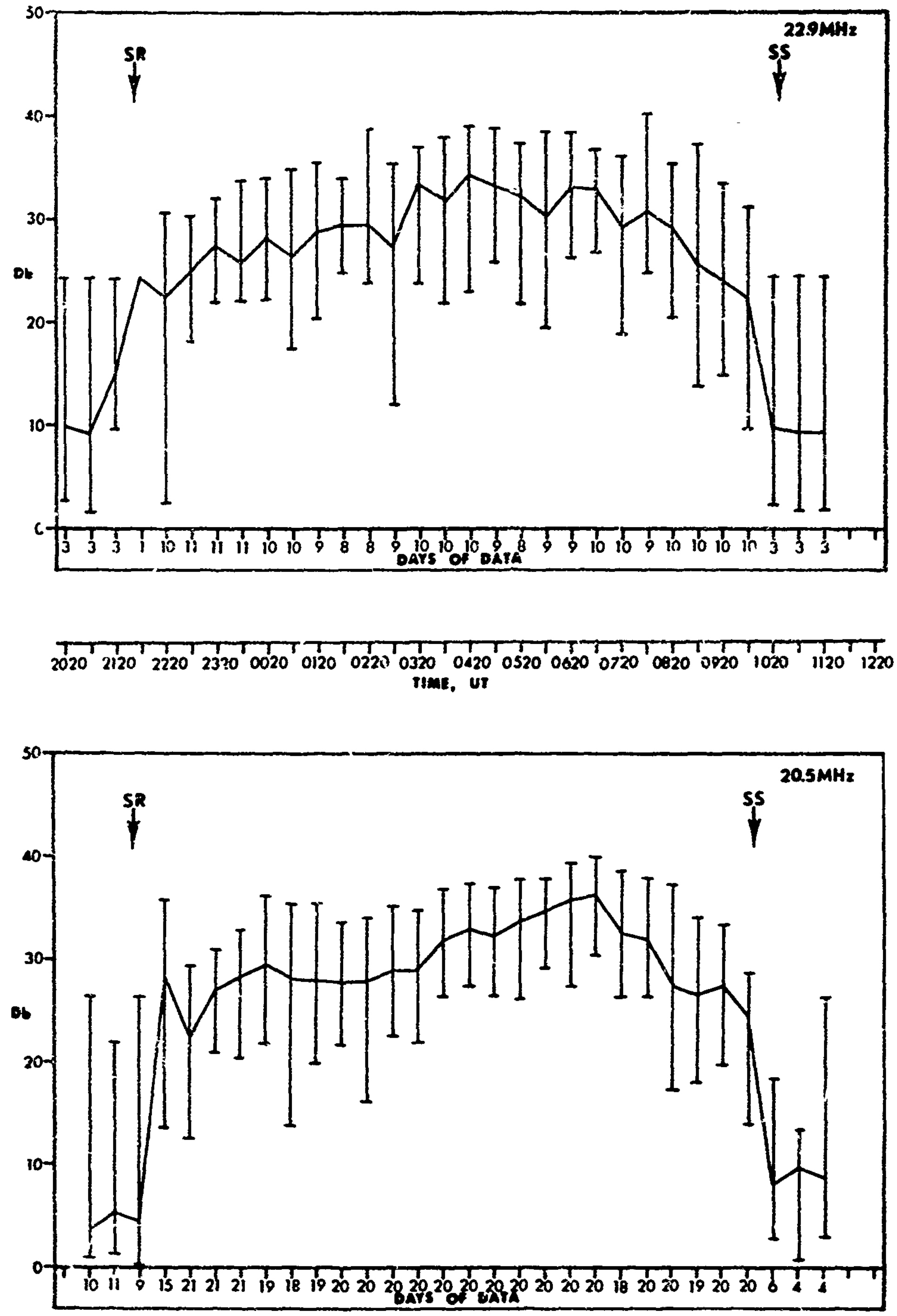

Figure 5: Mean RTW SNR in August 1967 (22.9 MHz), and in September 1967 (20.5 MHz). SR and SS indicate time of ground sunrise and sunset, respectively, at Manila.

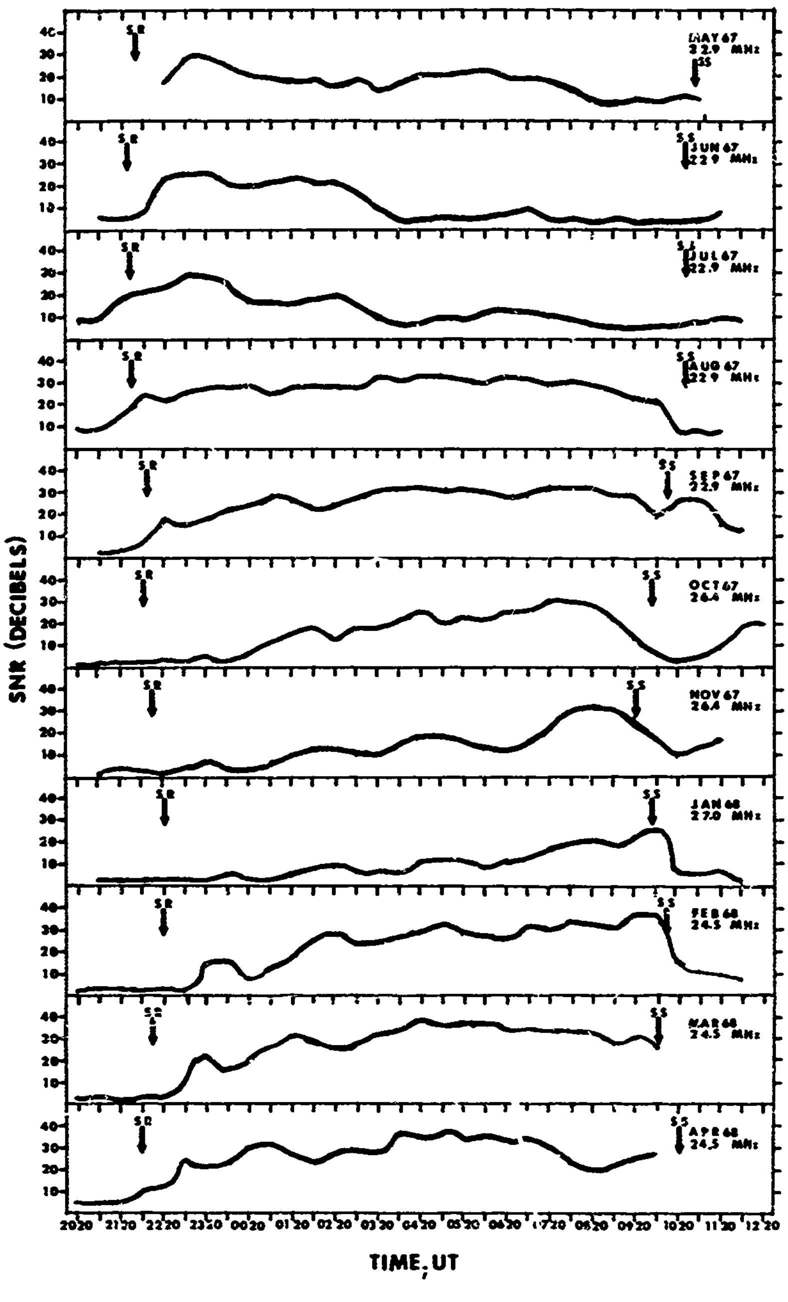

Figure 6: Mean RTW SNR on most optimum frequency observed each month, 1967-68.

THE USE OF SATELLITE DATA FOR PREDICTION PURPOSES

by

W.R.Piggott

Radio and Space Research Station, Ditton Park,
Slough, Bucks, UK

ABSTRACT

Analyses of satellite data developed at R.S.R.S. for prediction purposes are discussed. Data from the circular orbit satellites, Alouette I and Ariel III are used, the former primarily for delineating rapid changes in foF2 with position, the latter primarily to explore the probable characteristics of the ionosphere in regions where ground based observations are not available. The data disclose some new ionospheric phenomena and can be used to give rules for extrapolating into zones where little or no data are available. Surprisingly large differences are found between the N and S hemisphere at corresponding seasons. An analysis has been made of ridges of ionisation and it is shown that the tilts associated with these can enable oblique incidence reflections to follow the ridges as they move about. Equivalent ridges can be computed at the most probable position and used for HF predictions. This makes large differences in the predictions for certain times and zones. The data can also be used to estimate the probable importance of new observing sites.

Introduction

The object of this paper is to present some data on the properties of the F layer obtained mainly from Ariel III and Alouette I satellites and show how they can be used for improving predictions. Only a small sample of the data available has, at present, been studied, and fuller evidence for the statements made below will be presented elsewhere.

Ground-based sounding data describe the properties of about a quarter of the area of the ionosphere. A wider sample might indicate new relations or even new phenomena at present regarded as random discrepancies between observations and should also indicate where new observations are most likely to be worthwhile.

At first sight, satellite data appear very unpromising material for prediction purposes. The number of samples of reliable data available is usually too small to use without developing new procedures. The topside sounders have been mainly limited to real time data covering, in more detail, zones where there are already ground-based data, and the data obtained often lack the critical parameters - foF2 or fxF2 and the height of maximum density hmF2. However, they can give useful information about the statistical properties of ridges, e.g. by using Eccles (1967) technique and show the range of heights over which the electron density is simply related to that at hmF2.

Probe data can be readily recorded with a simple tape recorder on the satellite but must be extrapolated in height for practical applications. Our investigations show that this problem can be solved at least partially for a satellite in a near circular orbit, at about 550 km altitude, but the difficulties increase rapidly with altitude. The main difficulty arises because the relation between the plasma frequency at the satellite, fs, and the critical frequency, foF2, depends on the difference between the height of the satellite, hs, and of the level of maximum electron density, hmF2, i.e. hs-hmF2, which is not known in the unmonitored areas.

We are indebted to Professor J. Sayers of Birmingham University for permission to use his electron density and electron temperature measurements made on the UK/US satellite Ariel III. The electron density data are believed to be reliable to ±10%, the electron temperatures drift in time slowly and are much too high. Temperature differences over a few days are reliable and this is all that is needed for our purposes. The equipment in this satellite has been described by Wager (1968), Mackenzie and Sayers (1966) and Wilson and Garside (1968).

At this stage in the analyses we shall be mainly concerned with the properties of fs and the rules which can be deduced from them. Some deductions about foF2 will be presented but the extent, in space and time, for which the conversion can be accurately made is not as yet shown. As the longitudinal perturbations for most hours of magnetically quiet days agreed remarkably well with the predictions of wind theory the appropriate comparisons will be drawn at an early stage.

Ariel III orbit

Ariel III is in a polar orbit and covers the latitude range 81°N to 81°S; successive orbits are spaced almost exactly 24° apart in longitude, so that 15 orbits are completed each day apart from a slip of about 2° in longitude (9 minutes in LMT), between corresponding orbits on successive days. The same LMT at the equator is repeated, within 3 minutes, after exactly 80 days for reversed path and 160 days for corresponding path. Data for either 7 or 6 days in succession will be within ±30 minutes of a given hour.

The height of the satellite has varied between about 500 km and 610 km and the apogee returns to the same latitude, having completed a cycle, in 112 days. To a first approximation, comparisons at constant LMT between solstices or equinoxes can be made without correction for changing satellite height and apogee but this is important in exact analysis.

It is convenient to divide the orbit into four overlapping sectors:-

(a) 70°S to 70°N
(b) 70°N to 70°S
(c) Above 56°N
(d) Above 56°S

These have been mapped separately, using different projection schemes for (a) (b) and for (c) (d). Only data from sectors (a)(b) will be discussed in this paper.

In practice the desired data was only recorded for a maximum of 12 out of the 15 orbits each day and was sometimes interrupted to allow real time data and playback to occur. Thus in general between 60% and 70% of the orbits for any day provided usable data. Reasonably full coverage was obtained for the periods May-December 1967 (days 126-355 in 1967), January-February (days 7-37), and March-April (days 83-105) in 1968.

Experimental procedure

It is fundamental to an investigation where so many factors can alter to throw the data into a form which holds as many factors constant as possible. This is relatively easy with satellite data since both the LMT and height of the satellite do not change significantly for corresponding points at constant latitude in successive orbits over a day. There can be large day-to-day changes so that it is convenient to map the ionosphere for units of one day in U.T. For each latitude longitude changes are shown at constant LMT. This also has great advantages when comparing with theory since attention can be concentrated on longitudinal perturbations of the F layer structure rather than the much more difficult problem of explaining its exact form. Permanent and semi-permanent features of the longitudinal modulation can then readily be recognised.

The original Ariel III data for each day was spread over a number of tapes from different sources, some delayed by up to six months relative to the main batch. Thus a major sorting job was needed to put the data into usable form with the data sorted by date and time. This was successfully solved.

The 70°S to 70°N and 70°N to 70°S maps are printed by the computer on a rectangular graticule of latitude and longitude with scales of 12° of latitude and 40° of longitude to an inch. Contours at 1 MHz intervals are added by hand and the intervals colour coded. As the data are incomplete, contouring cannot be easily done by computer methods. An example is shown in Figure 1 together with the LMT variation with latitude relative to the mean LMT of the equator. For an orbit in the opposite direction the sign of the correction is reversed but the magnitude is unaltered. At the equator the LMT for the Northbound and Southbound maps are exactly 12 hours apart; at latitude ±56°, where the time shift is one hour, the LMT's are separated by 10 or 14 hours respectively. The correction is important when comparing Northbound and Southbound maps or Northern and Southern hemisphere phenomena at latitudes greater than about 40°.

The electron density, N, at the satellite can vary from between about 3.10^3 to about 10^6 electrons per cc, an inconvenient range for tabulating, so these were converted to plasma frequencies fs using the usual relation

$$fs^2 = 8.05.10^{-5}N$$

where fs is in MHz. The equipment saturates at fs = 9.6 MHz and is nonlinear above about fs = 9.3 MHz. This is a serious limitation at certain hours and seasons, preventing analysis over considerable ranges of latitude and longitude.

Ground-based observations suggest that, at near constant LMT, contours of constant fs should follow the dip latitudes to a first approximation. This can be tested conveniently by preparing an overlay of dip latitude on the scale of the maps (dip latitude = $\tan^{-1}(\frac{1}{2}\tan \text{dip})$), Fig. 2. In the majority of examples the expected result is not found, the most obvious structures being often North-South instead of East-West. Even when the structures near the equator look similar to the dip latitude curves they are usually shifted East or West relative to them by about ±30° in longitude, depending on time of day and season. Comparisons in other coordinate systems (L shells, magnetic longitude, constant B, etc.) have also been made using the same technique.

General features of the maps of fs

Comparison of maps for different days shows:-

(a) The variation of fs with longitude in the Southern hemisphere is very large in amplitude often 3:1 and shows one main maximum and minimum.

(b) The corresponding variation of fs with longitude in the Northern hemisphere usually shows two maxima and two minima, normally with different amplitudes.

(c) For magnetically quiet days, the longitude of these maxima and minima are, to a first approximation, independent of season but vary with LMT and latitude.

(d) At latitudes South of about 40°S the perturbation moves with LMT or probably more accurately with magnetic time, through 360° of longitude in 24 hours and the phase also varies with latitude.

(e) At night the maxima at different latitudes can often be followed from the Southern hemisphere across the equator to link up with one of the maxima in the Northern hemisphere. This is present with a seasonal shift at both solstices.

(f) The average values of fs over all longitudes often vary rapidly with magnetic activity. Care has been taken to allow for this when comparing data taken at different epochs.

(g) A feature of many maps is the presence of semi-permanent 'fingers' of abnormal ionisation affecting a single orbit only; these are discussed in more detail below.

(h) Certain zones appear to have abnormally large or small values of fs for long periods of time. These are linked with the magnetic field disposition over the world, e.g. there is a high over the South Atlantic anomaly.

(i) Considerable changes are often seen between magnetically quiet and disturbed days. Most commonly, in the latter, the standard longitude perturbation is shifted considerably or replaced by a completely different pattern and particular orbits often show extended ranges of latitude where fs is abnormal.

Some theoretical considerations

Most of the variations of fs with longitude for magnetically quiet days, described above are closely similar to those predicted by Kohl, King and Eccles (1968) in a theory of wind effects on ionisation in the F region. The wind pushes the ionisation up or down the field lines to heights with differing loss rates.

The theory gives an electron distribution as a function of time of day and height for a given epoch which is dependent on proper assumptions about scale height, loss rates and ion production. It is conceivable that these are not correct or that additional processes are present not included in the theory. Those could change the shape of the electron distribution with height but are unlikely to change the positions of the extreme values at a given latitude when these are mainly determined by the geometry of the magnetic field. In fact both the calculated and observed positions do not vary much with model, though the absolute values are very sensitive to the assumptions made and seldom fit the observed data. We are particularly interested in whether the theory predicts maxima and minima at the correct longitudes and gives the right form for the longitude changes, but we can disregard differences in absolute value.

Wind perturbation depends on both the declination of the magnetic field and the angle of dip, both of which vary with position. To obtain a theoretical description of the longitude perturbation the electron distributions are computed at a number of different longitudes adopting the same wind system and basic assumptions but putting in the local dip and declination. To a first approximation this should give the longitude perturbation for the latitude involved, which may be compared with the experimental observations, Fig. 3. In this figure the computed values of fs have been multiplied by a constant factor.

A mass plot of the positions of the maxima in the North against LMT for all days with Kp $\leqslant$ 12, Fig. 4, looks extremely complex but if plotted against the theoretical positions of the maxima, Fig. 5, is in remarkable agreement bearing in mind that the longitudes are only sampled at 24° and 30° intervals in the two parameters and some longitudes are missing in the experimental study and day-to-day changes in mean fs can shift the position of the maxima.

The corresponding pattern for 55°S is also in fair agreement with the theory, though height changes with longitude are more important in this case.

The principal cause of the difference between North and South can be readily understood by reference to Fig. 6 which shows, as an example, the relative positions of magnetic latitudes 70°S and 70°N and geographic latitudes ±70°. In the South there is one zone where the magnetic latitude is at lower latitudes than the geographic, in the North two. The wind interaction with the magnetic field depends on the difference in latitude and on the wind direction.

It should be noted that, while the longitude variations of hm are not, in general, in phase with those of fs and foF2, the difference seldom alters the relative position of the extreme values of fs and foF2 significantly. Thus the difference between the shape of the fs curves with longitude at constant latitude and those predicted for foF2 shows where the latter are likely to be incorrect.

Large scale changes in fs with longitude

Even a superficial inspection of the maps shows that the maxima and minima of fs at each latitude move systematically with LMT. The detail of the movement is, however, complex, particularly in the North where there are usually two maxima and two minima at each LMT. We first examine the variations with LMT and season found in the South.

A typical diurnal variation of the position of maxima and minima in fs for 55°S is shown in Fig. 7. This is based mainly on days 126-206 but with a number of hours confirmed from days 260-350. Most discrepancies between the two periods appear to be random and due to changes in magnetic activity. The positions of extreme values near 0600 and 1800 LMT do not, in general, repeat at all seasons.

The main feature is a fairly smooth trend in longitude with LMT, or possibly more accurately with magnetic time. The maxima and minima are spaced 180° apart e.g. for the period 2000-0300 LMT the medians of 45 samples are maximum at 120°W, minimum at 60°E, both ±5°. A pattern of this type could be described as maxima and minima at different longitudes which occur at constant U.T. Similar results are obtained at 35°S but with a phase shift of about 40° to the west i.e. nearly 3 hours earlier in U.T. For the Northern hemisphere the variation at first sight appears much more complex, but as we have seen, this fits with the theoretical predictions rather well (Figs. 4 and 5).

At night the latitude variation of fs is fairly simple and perturbations associated with the equatorial anomaly are relatively small. Thus we might expect to see the effect of the moving factor as a ridge of abnormally high values of fs. This is, in fact, found at certain hours. Figure 8 shows that the ridge is essentially at the same place at the same LMT after 160 days approximately.

The minima in the longitude perturbation of fs are rather more sensitive to other factors than are the maxima and are more commonly found in the longitude zones where the magnetic latitude was less than the geographic latitude. Near the equator clear minima are only observed in the longitude zone where the dip equator is North of the geographic, i.e. the equatorial zone behaves as if it was mainly influenced by Southern Hemisphere longitude perturbation. One might have expected this from the much larger amplitude of the longitude perturbation in this hemisphere.

At low latitudes a striking feature is that the equatorial anomaly is usually not equally developed at different longitudes for the same LMT. The combination of this effect with those due to moving maxima makes the situation complex and further work is needed to clarify the phenomena.

<u>Some characteristics of fingers</u>

A striking feature of many maps of fs is the presence of one or two orbits which show a completely different latitude variation of fs than the orbits on each side of them, Fig. 9. The anomaly sometimes lasts for several days, the corresponding orbit being affected throughout the period; sometimes it is only present for one day. In general, abnormal zones seen on Northbound orbits are not markedly abnormal when seen approximately 12 hours later in LMT on Southbound and vice versa. Changes of more than 3:1 in plasma frequency in 24° longitude have been observed at particular latitudes. A closer examination of the data shows that the phenomenon is very common when smaller changes are allowed and, in fact, adjacent orbits often show differences of 10% or more.

At this stage we shall consider only a sample of the more prominent fingers. For these the abnormality can be positive, negative or mixed, in the last case the latitudes of reversal change from day-to-day. The number of fingers increases, on the average, with magnetic activity but in large storms the life of most fingers is short. Some at least of these events are due to large scale changes in time lasting for only one or two hours but affecting a wide range of latitude. At some hours the position of fingers appears to be linked with the travelling maxima or minima, positive deviations being found on the same orbit during the time when the maximum is near that orbit and similarly for the minimum. This shows up as an apparently static finger for periods of up to two weeks (two hours LMT).

Cases of much wider anomalies have been observed, but most of these are associated with the moving large scale perturbations mentioned above or with localised storm effects in large magnetic storms. Further analysis must await a full description of these anomalies. Thus we restrict this study of fingers strictly to those less than about 48° wide and consider mainly longitude zones where the large scale perturbations are varying slowly with longitude and ignore abnormalities smaller than 12° in latitude.

We first examine the shape of the fingers. The length of the finger is defined as the range of latitudes where fs differs significantly from that for adjacent orbits, ignoring any saturation effect or temporary equality where the sign of the perturbation reverses.

Since our orbits are 24° apart in longitude, a finger 24° long could be circular in shape if placed at the equator where 1° longitude is equal to 1° latitude. At higher latitudes, where such short fingers are mostly found, it is elongated in the meridian. A sample of 50 maps, mostly daytime, was examined for fingers and 158 found, a rather larger number than normal. Their distribution with length in degrees of latitude is shown in Fig. 10. While we have less discrimination at the equator than at higher latitudes some tests with ground stations suggest that the width does not vary much with latitude. This would suggest that the modal finger is about twice as long as it is broad and the median between three and four times as long as its width in longitude. The change in fs between orbits can be more than a factor of 3. Analysis of day-to-day changes shows that differences of about 20% are very common. In the comparisons made so far either foF2 or hmF2 has been markedly abnormal when a finger crossed an ionospheric station.

The reality of the fingers at low latitudes can be checked readily by observations at ground stations in the following manner. Consider two stations the same distance from the magnetic equator and within about 15° from it on the same side. The equatorial anomaly ridge will cross these stations twice a day, causing peaks in the diurnal variation of foF2. Statistically very similar behaviour is found at different stations in a given longitude zone (Eccles and King 1969). One would thus expect a day-to-day correlation in the times of peak foF2 at stations in the same zone and at the same magnetic latitude. If fingers are present, the time of maximum will usually be perturbed. Thus a correlation between times of maximum foF2 is a good test of the presence of fingers. A typical example using data for one month is shown in Fig. 11. The stations Bogota and Paramaribo are separated by about 19° in longitude and no correlation in the times of maximum is found. This is true for other samples, though in a stormy month the disturbed days may show a systematic shift in time relative to the quiet, giving a weak apparent correlation. The range of times found correspond to changes from an undeveloped (single peak) structure to a fully developed double peak structure.

The variability of fs in this zone is consistent with the lack of correlation of foF2 peak time seen.

Application to predictions

In order to use the satellite data for predictions it is first necessary to deduce foF2, and if possible hmF2 from the data and also to find whether the samples used were representative, e.g. whether they were abnormally quiet or abnormally disturbed. The techniques explored are discussed briefly below.

In outline, the procedure adopted to see whether foF2 could be deduced was as follows:-

(a) The plasma frequency fs was mapped for each day on latitude:longitude graticules using the Ariel III tape recorded data.

(b) The apparent position of ground stations as seen by the satellite was deduced by following a line of force from hmF2 to hs. In practice extreme values of hs-hmF2 were used to show the range of positions possible for each station.

(c) The relations between fs and foF2 and also the appropriate value of hmF2 (deduced from M3000F2 data) were found; where fs did not vary rapidly with position, interpolation of fs in longitude was allowed between orbits.

(d) This analysis showed that foF2 and fs were linearly related:-

$$foF2 = a + bfs$$

where a and b vary with latitude, longitude, time of day, season and solar and magnetic activity. On quiet days, the correlation between foF2 and fs was usually very good, Fig. 12. Thus, most features in the maps of fs were reproduced in foF2 but with a scale factor which could vary slowly with position.

(e) The relation between fs and Te was examined as a function of position. This showed that where a close negative correlation between fs and Te existed the correlation between fs and foF2 was similarly good but the converse was not necessarily true.

(f) The fs maps were compared with longitude variations of fs and foF2 for selected latitudes and months deduced from theory, and found to agree well in shape but not in amplitude. The maxima and minima returned to the same longitudes usually reappeared for the same LMT, i.e. after 80, 160 and 240 days except sometimes for times near 0600 and 1800 LMT.

Using this result, the data from two or three stations well separated in longitude could be used to calibrate the longitude variation of the relation

$$foF2 = a + bfs$$

The test (e) could then be used t check whether the interpolation was likely to be reliable.

Conversely, of course, the relations between fs and Te were also used to select areas where the extrapolation was likely to be simple.

It is interesting to note that the range of values of fs and foF2 were usually several times the scatter of the points about the line of best fit, showing that the fs perturbations were good indices of perturbations in foF2 for quiet days. This was confirmed by other tests.

The main problems in current predictions are:

(a) Extrapolation to zones where no observations are available, in particular to the ocean areas.

(b) Treatment of moving ridges of ionisation.

(c) Effect of ionospheric storm.

At present, gaps are often filled by using data from stations in the opposite hemisphere, moving them so as to be at corresponding geographic and magnetic positions and allowing for seasonal changes. This can never be done accurately as the magnetic field is very different in the two hemispheres. The moving maxima discussed above also introduce a serious source of error; it is not possible to match them in time and, at the same time, match positions. Thus the current methods of predicting either foF2 or M3000F2 (hmF2) or both cannot be reliable.

This analysis, however, suggests that other factors are also present, for example, at many hours the median values of fs at each latitude are very different for Northern or Southern hemispheres, Fig. 13. Similar behaviour is found for the largest values, Fig. 14. The general relation with magnetic field can be clearly seen from the relative positions of the lines and magnetic latitude curves but the travelling ridges seen at the higher latitudes do not match and it is clear that fs is above 8 MHz in the southern hemisphere for roughly the same areas as it is above 4 MHz for the corresponding season in the North. Both magnetic and solar conditions are reasonably similar for this comparison.

Our data suggest that a more reliable extrapolation can be obtained using the fs maps with some support from theoretical longitude changes given by wind theory to identify the latitude of extreme conditions.

As stated above, the procedure is to calibrate the conversion relation:-

$$foF2 = a + bfs$$

with the aid of ground based stations in widely separated longitude zones.

A further approximation is possible by identifying the zones where fs and foF2 are abnormally high or low. Particularly at low latitudes, there can be seen on the maps but have not as yet been studied.

It is possible to extrapolate from fs to foF2 using the satellite data directly. This gives a particular sample for a specific hour. To make a proper assessment of average conditions the peculiarities of the sample have to be considered and corrected. However it appears more profitable to proceed indirectly, finding the main factors which determine the longitude effect at quiet and disturbed epochs and use these to extrapolate from the zones where adequate observations exist. Both methods are being used but at present we prefer the second as it appears more reliable, simpler and less sensitive to distortion from fingers.

While most of the well known storm effects can be identified on the maps, a striking feature of many storm perturbed maps is the presence of local zones of abnormal behaviour, some zones being very perturbed for more than 12 hours while others are affected to a minor extent only. The identification of the abnormal zones may be important in the future.

Satellite data have particular advantages for investigating the behaviour of moving ridges of ionisation, particularly at high latitudes where these can change position very rapidly. In general, a ground-based station only detects such structures when close to the station, though in some cases e.g. when they give polar spurs, oblique reflection to the sounder is possible. Thus a highly misleading impression is obtained both of the regularity with which a ridge is present in a given zone and its critical frequency. Such ridges are usually efficient reflectors at oblique incidence since the curvature of the levels of reflection allows skew ray paths to be used. Typically, a ridge moving within ±500 km from the midpoint of an oblique path will be as effective as if it was placed at the midpoint so far as reflection is concerned. The zone over Scandinavia has been examined for this phenomenon and should give reflection in this mode at about 2-3 times the normal MUF for about 95% of nights in winter at high sunspot number. Reflection of this type has been reported by Möller from studies of pulse transmissions, Sodankyla-Lindau (2000 km approximately) and an examination of these data shows that the expected regularity is, in fact, found. We are indebted to Professor W. Dieminger and Dr. Möller for access to these data.

The very steep gradients of electron density at low latitudes disclosed by satellite observations, particularly those from Alouette, are important for ray tracing problems but less important in conventional prediction mapping. In practice the oblique wave follows the ridge of ionisation so that the path goes skew to take advantage of the greatest densities present. Thus the conventional maps, which show the equatorial anomaly badly stretched in latitude, represent fairly the range of latitudes over which the large values are effective. Our data on large East-West gradients, however, suggest that off great circle propagation may be more important and effective MUFs higher than at present predicted.

Preliminary results suggest that current methods can often be 20-30% wrong in foF2 over ocean areas, probably worse in the Southern hemisphere and in zones where ridges are not properly included are probably wrong by a factor up to three.

An example of a comparison between values of foF2 predicted by ESSA and values deduced from satellite data for a zone where ground stations are abnormally numerous is shown in Fig. 15. This shows good agreement where stations are available but some discrepancies over the ocean areas.

Acknowledgements

The work described in this paper was carried out at the Radio and Space Research Station of the Science Research Council and is published with the permission of the Director.

Referenoes

Eccles, D. 1967, Journ. Atm. Terr. Phys. 29, p. 1337-1344 A quick method of using topside ionograms for ionospheric investigations

Eccles, D. and King, J. W. 1969, Proc. I.E.E.E. 57, p. 1012-1018 A review of topside sounder studies of the equatorial ionosphere

Kohl, H., King, J. W. and Eccles, D. 1968, Journ. Atm. Terr. Phys. 30, p. 1733-1744 Some effects of neutral air winds on the ionospheric F layer

Mackenzie, E. D. and Sayers, J. 1966, Planet. and Space Sci. 14, p. 731-740 A radio frequency electron density probe for rocket investigation of the ionosphere

Wager, J. H. 1968, Radio and Elect. Eng. 35, 55 The University of Birmingham Electron Density and Temperature experiments on the Ariel 3 satellite

Wilson, J. W. G. and Garside, G. 1968, Planet. Space Sci. 16, 257 A new technique for measuring electron temperature in the ionosphere

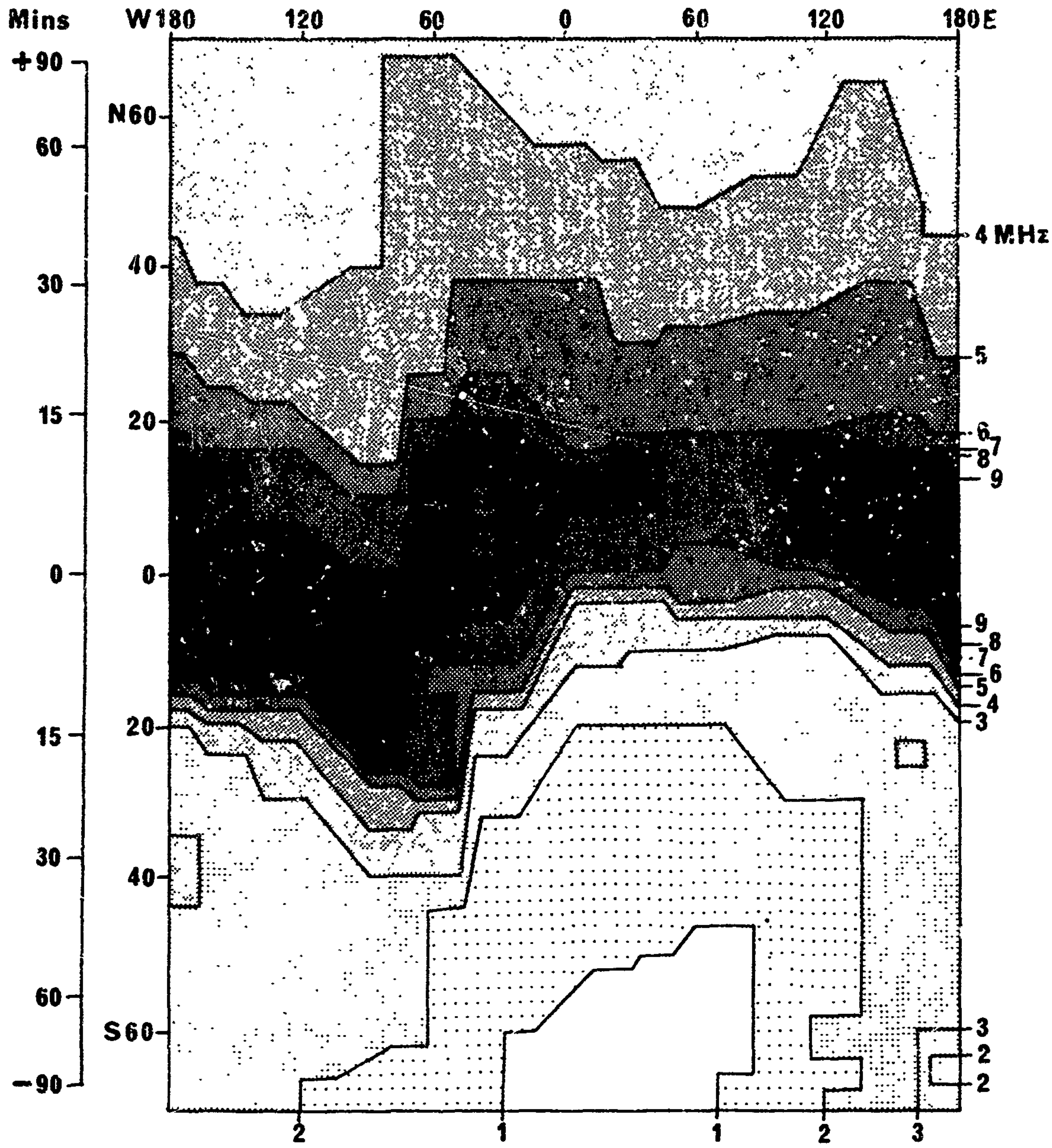

Figure 1 Map of fs for Day 208, 27 July 1967. Southbound LMT at equator 2000 $\Sigma kp = 9$. The L.H. scale shows the time shift in minutes relative to the equator.

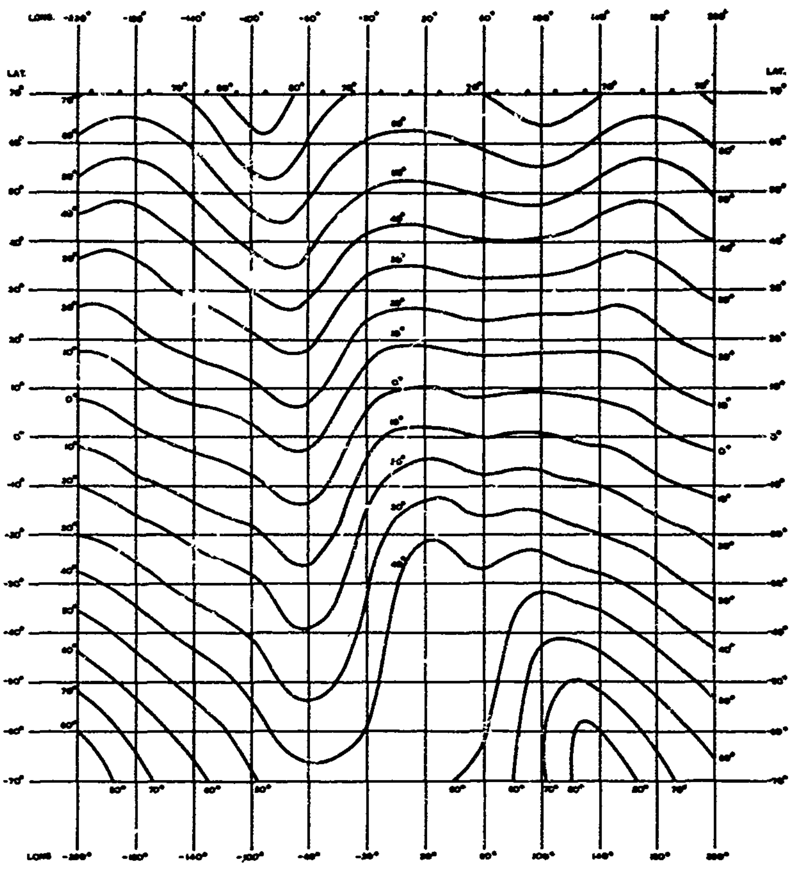

Figure 2 Dip latitude map

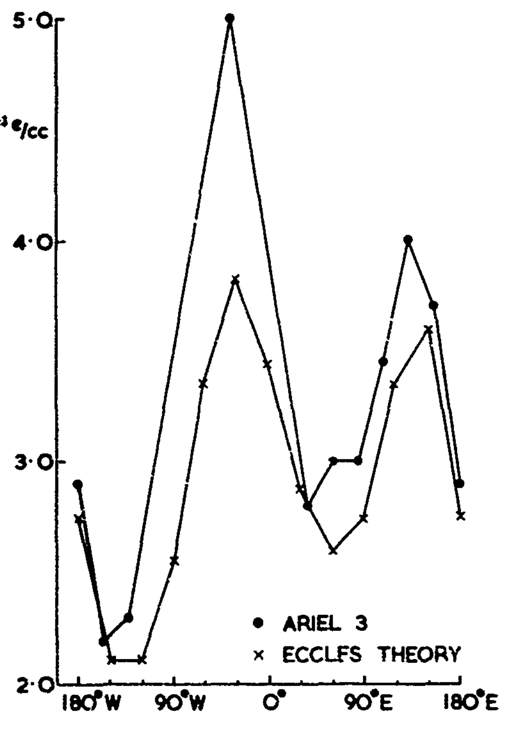

Figure 3 Comparison of observed and theoretical longitude variations of electron density at the satellite for 0600 LMT June at 50°N. The theoretical values have been multiplied by a constant factor at all longitudes.

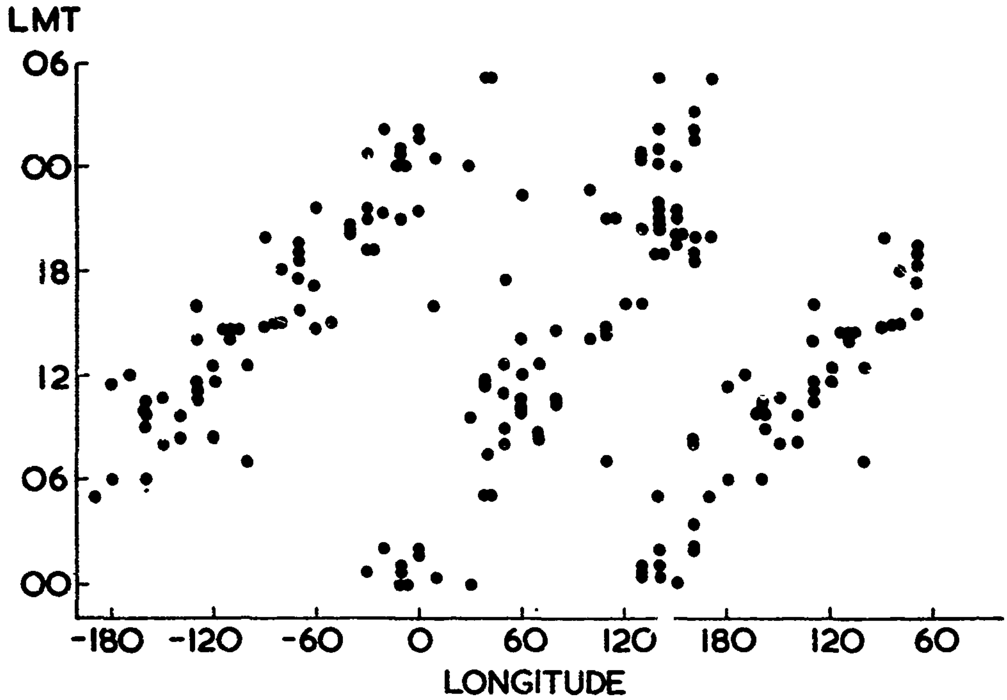

Figure 4 Variation of the longitude of maxima for 55°N with LMT for quiet days ($\Sigma kp \leq 12$), 1967.

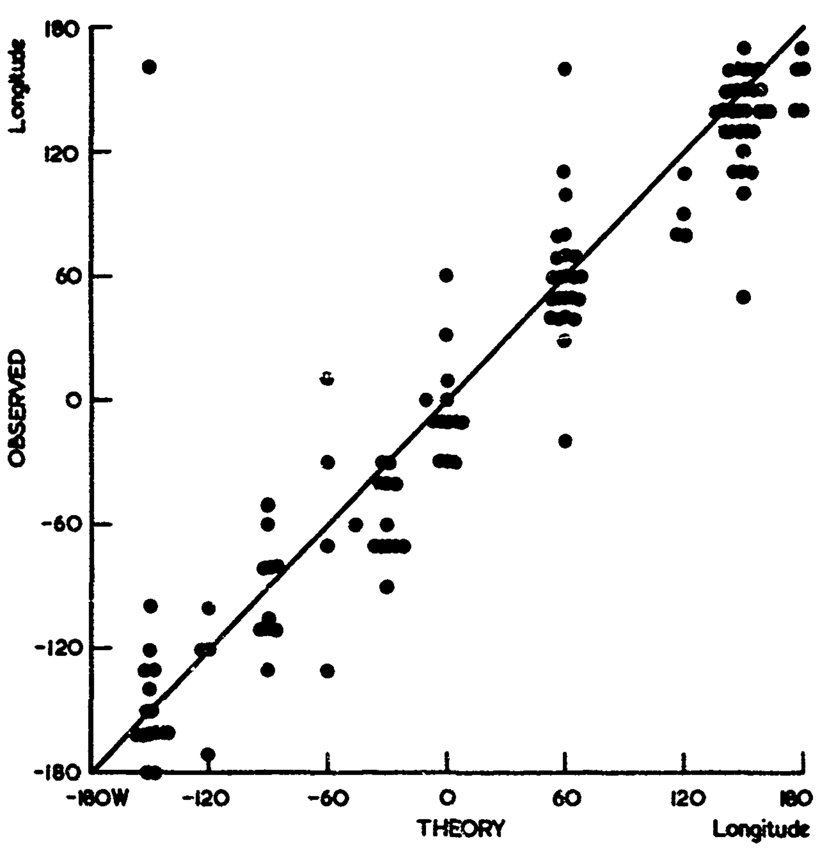

Figure 5 Comparison of observed and theoretical longitudes of maxima for 55°N, for data shown in Fig. 4.

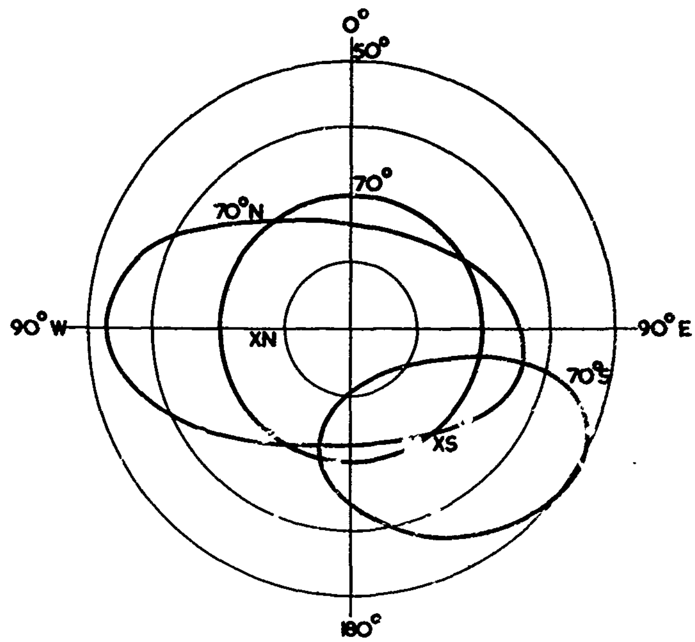

Figure 6 Polar projection map showing relative position of the magnetic and geographic latitudes 70°N and 70°S and the dip poles. Note that conditions are more extreme in the Southern hemisphere.

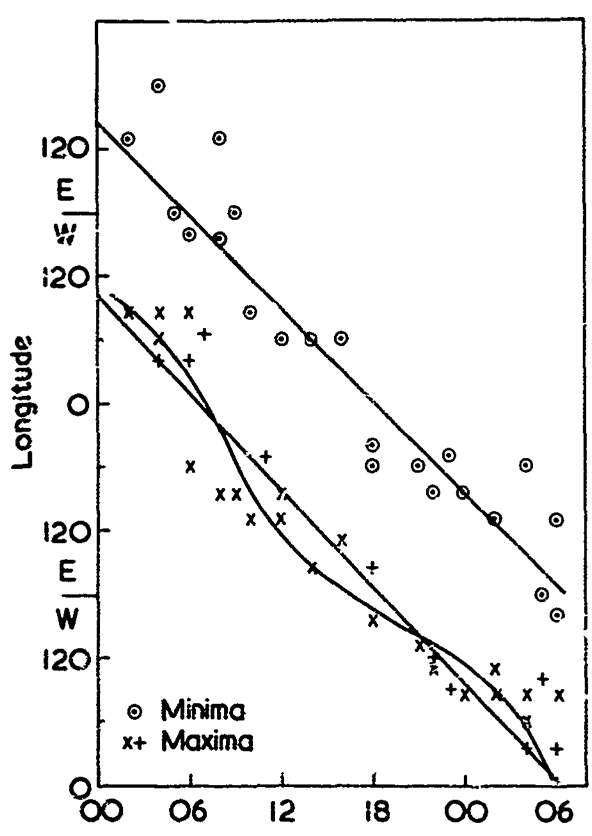

Figure 7 Variation of the longitude of maxima and minima of fs for 55°S with LMT. The lines show the expected variation for extremes constant in U.T. The curve shows the expected variation for maxima moving linearly in magnetic time.

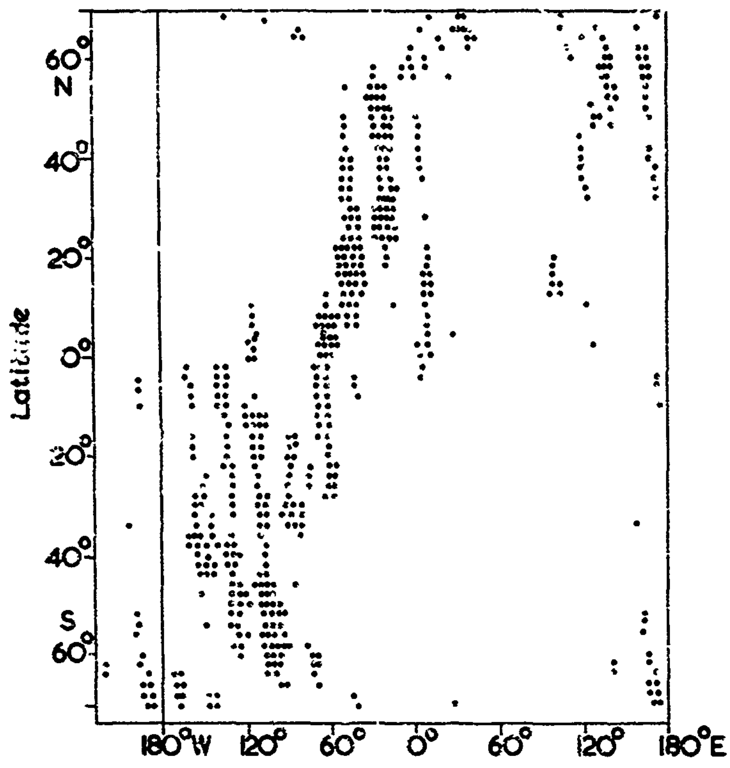

(a) Days 182-188 June 2330 LMT kp 15

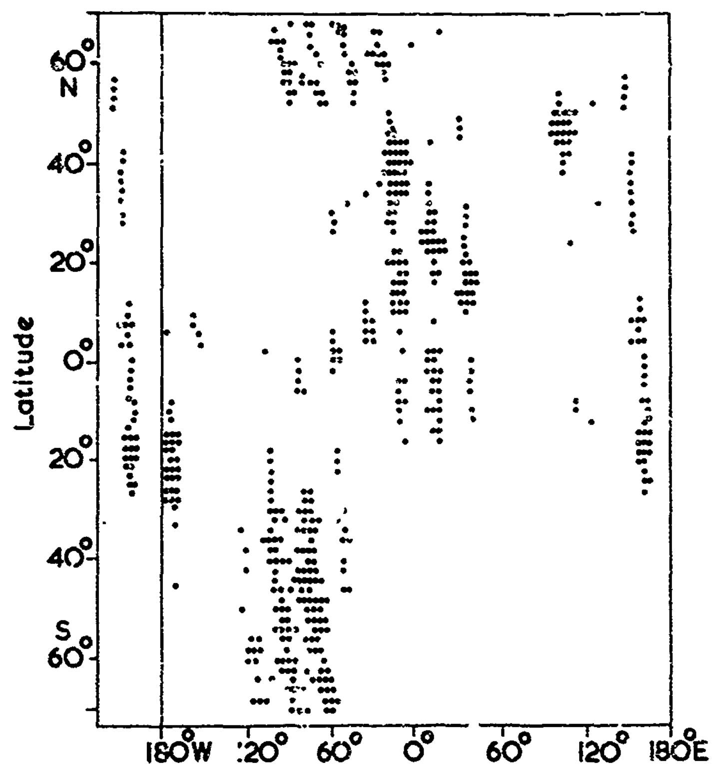

(b) Days 343-349 Dec. 2310 LMT kp 12

Figure 8 Comparison of positions of maxima at different latitudes near midnight summer and winter

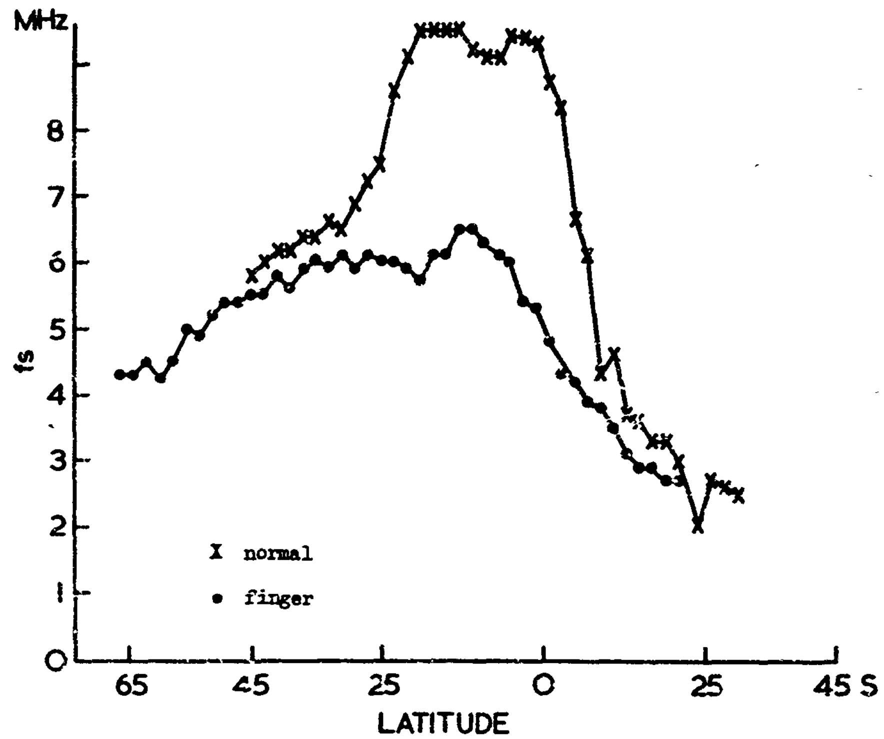

Figure 9 Negative finger near 30°E at 1815 LMT on day 140 20 May 1967. The normal pattern shows two peaks near the magnetic equator, only one is shown as the other is scarcely distinguishable from it. Only a single low maximum is seen on the abnormal orbit

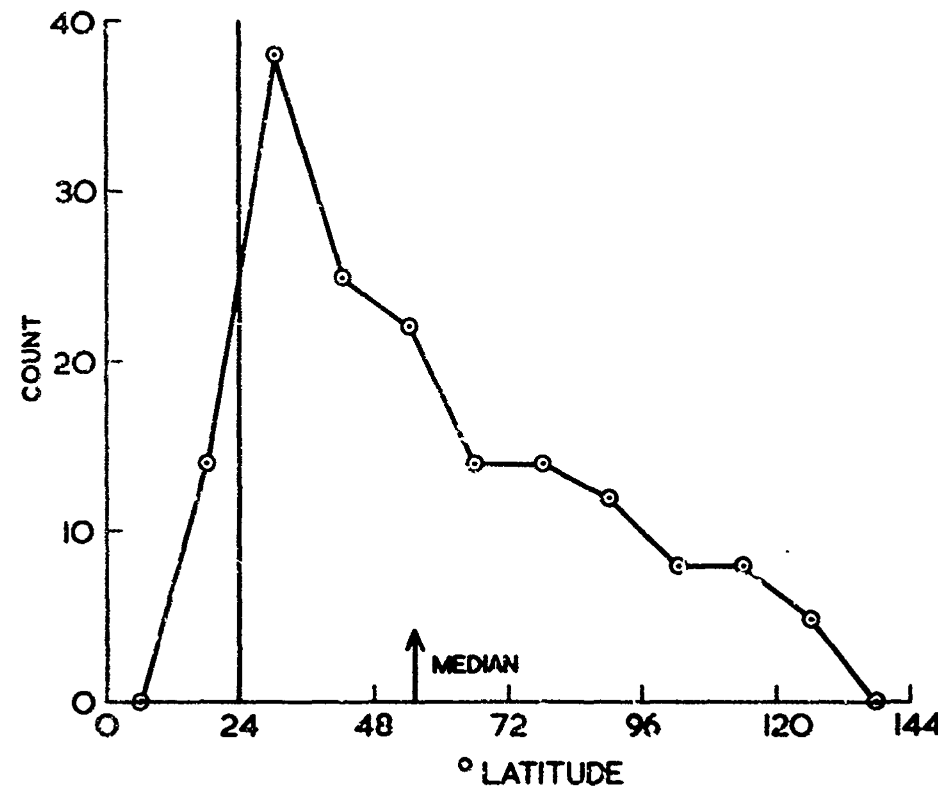

Figure 10 Distribution of length of fingers in latitude, random sample of 158 daytime fingers.

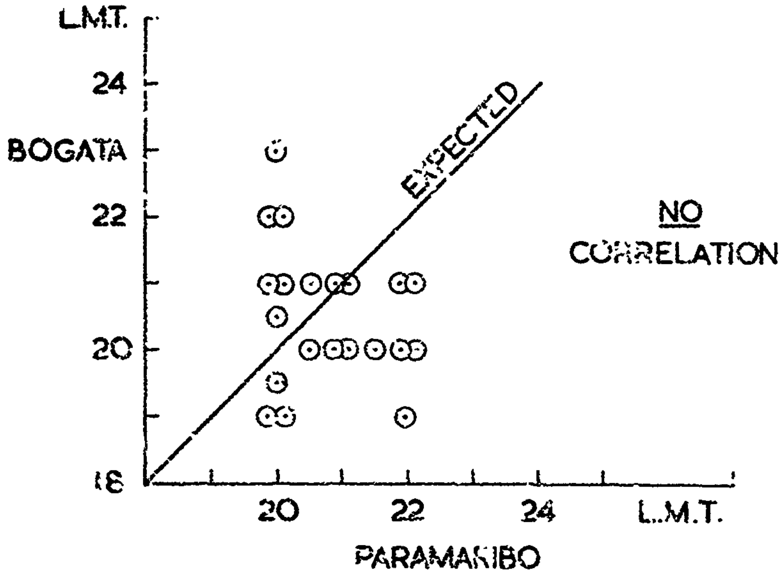

Figure 11 Relation between times of maxima of foF2 at two closely spaced stations, Bogota and Paramaribo 5°N, 74°W and 55°W respectively.

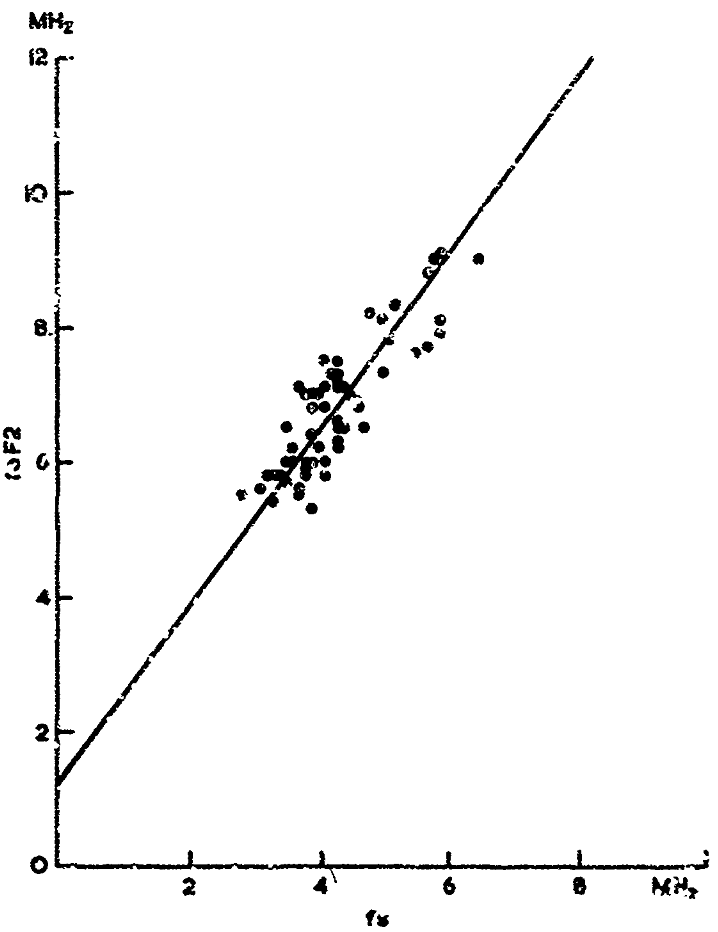

$foF2 = a.fs + b$

Figure 12 Relation between foF2 and fs near noon June 1967 using all stations between 20°N and 6[illegible]°N. Most of the scatter is due to changes in a, b, with longitude, for this sample [illegible] foF2 varied little with latitude.

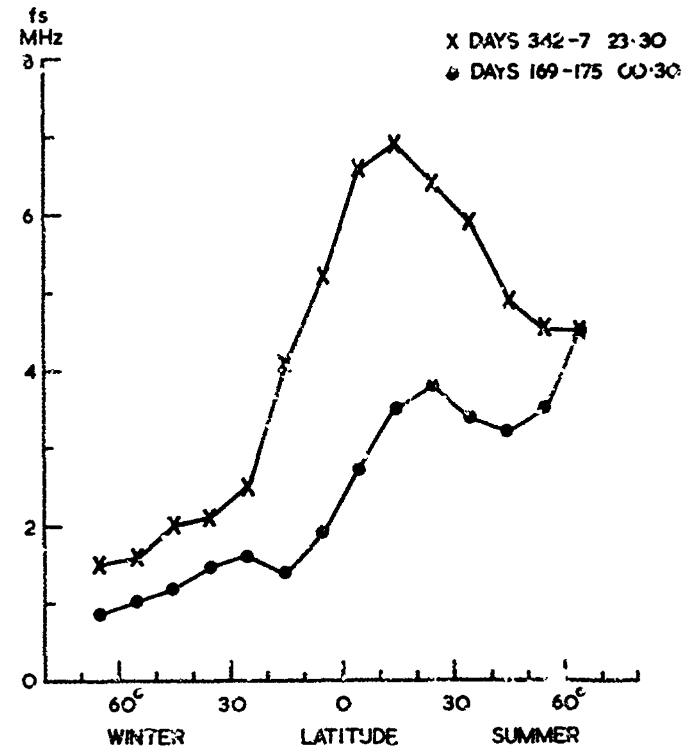

Figure 13 Variation of median fs for all longitudes with latitude in Winter and Summer
At this hour the Southern hemisphere shows higher values of fs than the Northern hemisphere.

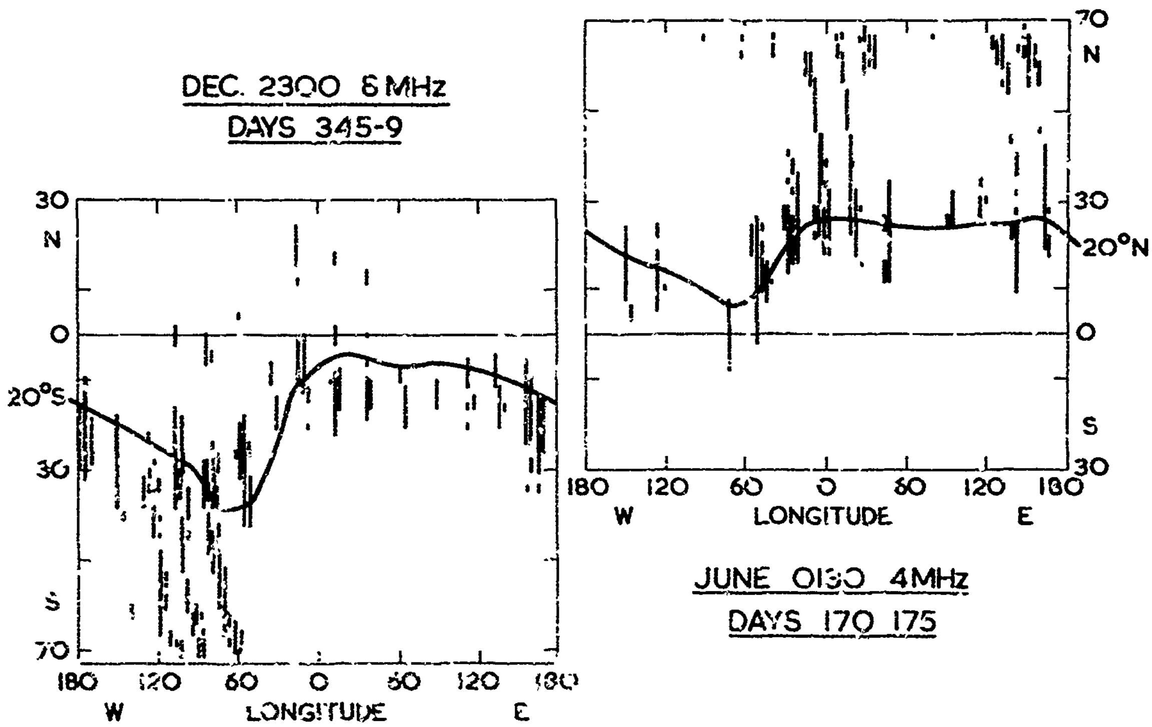

Figure 14 Position of high values of fs in Northern and Southern hemisphere local summer near midnight. Note 8 MHz is exceeded in the South as often as 4 MHz in North and relative displacement of the maxima at higher latitudes.

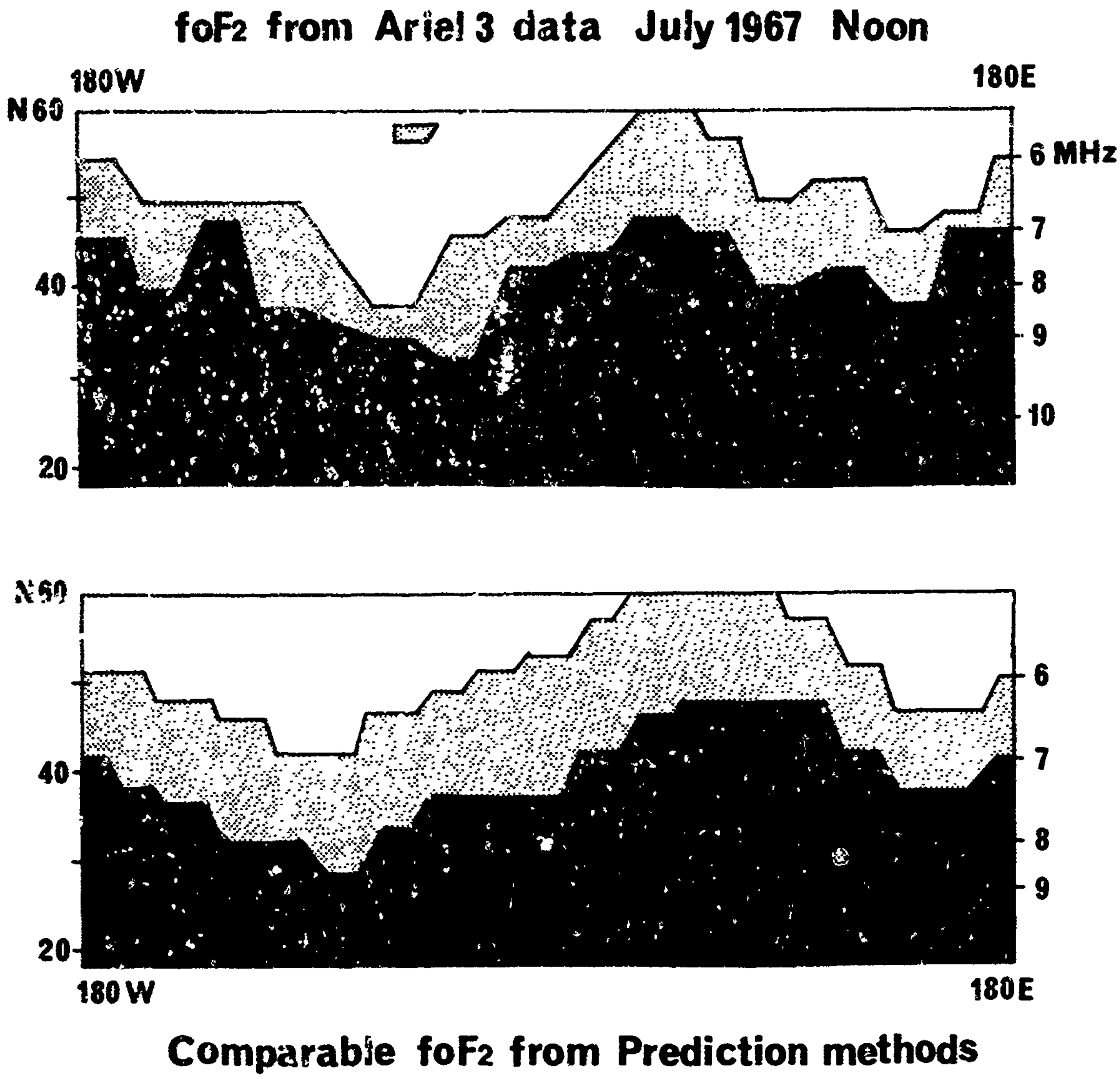

Figure 15 Comparison of foF2 predicted by ESSA and Ariel III data using first approximation as given by data in Fig. 12. The next approximation tends to increase the differences observed.

MONITORING MULTI-FREQUENCY MODE DELAY OVER LONG DISTANCES FOR IONOSPHERIC FREQUENCY SELECTION

by

H.J. Albrecht

Dept. of Telecommunications,
Forschungsinstitut für Hochfrequenzphysik
5321 Werthhoven, nr. Bonn,
Federal Republic of Germany

This work was sponsored by the Ministry of Defence, Federal Republic of Germany, under Research Contract No. T-833-1-203

SUMMARY

With particular reference to those ionospheric predictions requiring a large short-term accuracy, purely statistical methods, such as CURTS and similar systems, exist alongside with those considering at least some ionospheric parameters. These systems generally analyse the trend indicated by ionospheric parameters and use the result in calculation procedures. This paper describes a method of monitoring mode delay along the path of interest with the use of transmissions at one end on several frequencies in the HF-range. Mode delay measurements are simultaneously carried out on all frequencies. A comparison of such data with the average long term behaviour of the path then indicates the trend of short-term characteristics along the ionospheric path.

Methods of path analysis such as path diagrams, ground effects, etc. may then be employed similar to those described by the author several years ago.

The method as a whole renders itself to all applications of modern short-term predictions and automatic selection of optimum operating frequencies. In addition it is far more inexpensive than a complete oblique-incidence sounding system.

Following a general description of the system mentioned, experimental results are given for a path between locations in the United States of America and the Federal Republic of Germany, using time standard transmissions.

MONITORING MULTI-FREQUENCY MODE DELAY OVER LONG DISTANCES FOR IONOSPHERIC FREQUENCY SELECTION

by

H.J. Albrecht

1. Introduction

Although the technological development in the field of telecommunications now offers other systems for world-wide traffic, such as satellites, the classical use of the high frequency range continues to be important. One of the major aspects is the extension and modernisation of transmission systems with particular reference to modern requirements of channel capacity and link reliability.

During the last decade, original methods of forecasting ionospheric propagation conditions have gained from progress made in electronic instrumentation as well as in the application of computers. Examples are oblique incident sounding [1] and more statistical prediction systems, such as CRUFT [2]. Also to be mentioned is the ADAPTICOM system [3] and related methods of making the most favourable use of certain frequencies for given paths and channel requirements. Such a development has led to a considerable improvement in short-term predictions of channel usefulness while ionospheric parameters are not always taken into account. The combination with some computer facility enables optimum frequencies to be selected for a certain path. Although such installations are nowadays well distributed, they are still somewhat elaborate; thus their employment is not very popular with mobile or temporary communication networks, and whenever expenses are a major factor.

This paper deals with a reliable and efficient, yet relatively inexpensive and simple system of monitoring ionospheric characteristics with a short-term resolution adequate for automatic selection of optimum operating frequencies. Time signals emitted by several time-signal transmitters are utilized as references. In this respect the system may in principle be considered similar to a monitoring system used with the author's work in long-distance propagation more than a decade ago, when such transmissions were utilized as constant signal sources [4, 5, 6]. Progress made in equipment technology now allows the other constant parameter, the sequence of time pulses, to be employed on a general basis.

2. Mode-Delay System of Monitoring Ionospheric Parameters

2.1 General Description

As already mentioned, the system uses signals transmitted by standard transmitting stations. According to the particular path taken by signals, they experience different propagation delays. For this monitoring system, at least two time signal stations should be available. One should be located within a distance of the order of 1 000 kilometers from the observation point, while the great circle distance to the other station should amount to several thousand kilometers. The simultaneous reception of both signals, possibly on more than one standard frequency, then permits the determination of relative time delays on a continuous basis.

The distribution of standard transmitters in all parts of the world practically permits to select paths in all possible directions at a variety of great circle distances, in addition to multi-frequency emissions, from almost any observational point on earth [7]. Although this fact may be disadvantageous as far as time-signal selectivity is concerned, it permits a system based on monitoring time signals to be universal and versatile.

Depending upon the distance of time-signal sources selected with respect to the observation point, the time taken by signals and in particular its change are a direct indication of the path travelled. Characteristics averaged over certain periods may be considered responsible for the average mode-delay behaviour, if normally one mode is supposed to be representative at anyone instant.

For each path, possible modes may be determined on the basis of total great circle distance, and ionospheric characteristics (altitude, inclination, maximum usable frequency, etc.) with appropriate mode-delay values. Such a standard path may be covered by propagation in the chordal-hop fashion or by multiple hops. The first-mentioned mode category had been verified by the author more than twelve years ago as being mainly responsible for long-distance propagation of antipodal character [4, 5, 8]. In this case, inclinations in the appropriate layer, situated within certain distance ranges from either end of the path (at "tilt points") cause the ray to be propagated along chords with reference to the layer surrounding the earth, thus avoiding ground reflections over the path distance,

for which the chordal-hop mode is valid. In the case of multiple hops, propagation makes use of reflections at ionospheric layers as well as at the ground.

In practice, chordal-hop modes as well as modes making use of multiple hops between the two ends of a great circle path are possible in a well-defined or combined form. For a certain path and for standard characteristics the value of time delay experienced by the signal are a direct indication of the type of mode. Therefore, the change in time delay may be used to estimate variations in the mode structure. Depending upon the sequence or continuity of time delay measurements, this system may also be utilized to detect and evaluate short-term variations of mode characteristics along the path. In the last-mentioned case, it is possible to determine short-term changes of ionospheric layer characteristics in geographic regions touched by the path used for analysis. These mode delay characteristics may be monitored by means of signal observations or by automatic equipment. A relatively simple computer device may be utilized to compare actual mode delay characteristics with the standard one, thus permitting to automatically select optimum working frequencies by the use of resultant error values.

2.2 Standard Path to Signal Source

The above-mentioned standard path may be found by evaluating ionospheric characteristics predicted on a monthly basis by appropriate prediction services; ground characteristics have to be taken into account as well. For each particular case path diagrams may be established. These diagrams are plots of critical frequency, maximum usable frequency, effective height of ionospheric layers vs. distance from one end of the path. Diagrams of the type described were successfully used to achieve long-distance analysis in HF propagation work [4, 6]. They allow the important ionospheric characteristics to be surveyed without difficulty. A similar purpose is achieved by mode plots of the kind described by F. Kift [9] who also considered values of mode delay in graphical representations of conditions along selected paths; variations were of the long-term type.

A suitable method of extracting the necessary information on ionospheric characteristics from monthly predictions will be discussed in some more detail below, as well as the basis of taking ground characteristics into account. The last-mentioned parameter can also be shown on path diagrams with reference to the distance measured from one end of the path.

The geometric conditions for a standard path between observational point and signal source may generally be determined from nomographs, an example being published herewith as fig. 1. In this case, a horizontal line may be drawn from the appropriate value of the great circle distance/hop on the left-hand scale to the layer height to be considered and a vertical line through the intersection will then meet diagonal lines being typical frequencies of time signal transmissions, here shown as frequencies of minimum MUF, if the appropriate time signal is to be received. A horizontal line between the intersection with any of the diagonal lines indicates on the right-hand scale the minimum frequency of vertical incidence, representing the critical frequency required for such an MUF to exist. Radiation angles are also shown. The nomograph described is intended to allow conditions to be estimated. The concept of using apparent layer heights throughout is recommended if angles of arrival cannot be determined with adequate accuracy, and this difficulty may be assumed to exist in the majority of cases. Changes in near-field conditions of antennae and variable ground reflection characteristics in the antenna environment have usually been the main reasons for discarding angle-of-arrival measurements for analytical work in HF propagation.

Values of "corrected sec Φ_0" [10] have been utilized for the nomograph. For this application as well as other calculations it has been found useful to express the correction factor "L" by

$$L \simeq 1 + 0.01\, D\,(1+D) \qquad (1)$$

where D = distance in megameters.

2.3 Ground Characteristics

Electrical characteristics of the earth's surface affect the behaviour of the signal propagated over long distances if ground reflections are to be taken into account, viz. in the absence of chordal-hop propagation. Average ground characteristics may be used to determine the appropriate effects upon standard data for the purpose of the work being discussed in this paper. Essential parameters are ground conductivity, dielectric constant, and roughness of the surface. The two first-mentioned variables have to be known in order to determine the reflection coefficient by means of the Fresnel equations for vertical or horizontal polarization, respectively. The third variable is important if the ground roughness approaches the order of magnitude of the wavelength. In general, the consideration of ground conductivity and dielectric constant is sufficient for the standard path if ground parameters have to be taken into account at all.

Using a relationship determined on a statistical basis between relative dielectric constant ε_r, ground conductivity σ (in mho/m), and ground temperature t

$$\varepsilon_r \simeq 180\, k \sqrt{\sigma}\, e^{-0.01\, t} \qquad (2)$$

(0.5 < k < 1.5, depending on ground type)

as published some time ago [11], a world-map of ground conductivity may be employed to estimate both parameters. Such a world-map was established in 1967, together with maps showing the regional and seasonal changes of parameters caused by long-term climatic conditions [12].

2.4 Ionospheric Characteristics of Standard Path

The all important ionospheric characteristics along a standard path may be taken from monthly prediction charts, an example being the Ionospheric Predictions issued on a monthly basis by Environmental Science Services Administration, US-Department of Commerce. Details on ionospheric predictions and on all general aspects of ionospheric research and propagation may be found in K. Davies' book [13]. The steps now to be described may refer to the first portion of this monthly prediction presenting the predicted coefficients of numerical map functions as well as to the geographical maps:

Following the division of the entire great circle into sections of 500 km the values of MUF ZERO F2 as well as MUF [4000] F2 are taken for each of the representative points between sections, e.g. at 0, 500, 1000 km etc. from the observational point. Also, the gyro-frequency is determined for these points using an appropriate world-map [13]. Values of the MUF for 3000 km as well as f_oF_2 may directly be determined from the data indicated. Assuming also that the MUF factor $M(3000)F_2$ depends on height and to a very minor degree on f_oF_2 [14], average values of layer height may be estimated for each point.

The critical frequency of the E-layer is supposed to obey the following relationship

$$f_o E = 3.2 \sqrt[4]{1 + 0.008\,R} \quad \sqrt[4]{\cos X} \tag{3}$$

(R = sunspot number, X = solar zenith angle)

according to [13]. The critical frequency of the F_1-layer may also be expressed by an appropriate formula [13]

$$f_o E = 4.3\ (1 + 0.0023\,R) \sqrt[5]{\cos X} \tag{4}$$

In addition, changes of the height determined along the path may, up to a certain degree, be used to indicate a tilt condition of the F_2-layer. The difference between two consecutive height values, divided by 500, may be applied as a useful tilt parameter. Relatively large values in the appropriate positive or negative direction within 2000 km from either end of the path indicate the presence of tilt points in the layer; these inclined layer portions may be responsible for chordal-hop propagation along the path considered.

2.5 Mode Delay and its Short-Term Variation

Another nomograph has been developed in order to determine the relationship between great circle distance, number of hops, great circle distance/hop, layer heights, and half the signal-path length per hop for both multiple hops and chordal hops, as well as the time taken by the signal in milliseconds. The nomograph is shown on fig. 2. Diagonal lines from the upper left-hand corner to the lower right-hand corner indicate the relationship between the number of hops on the left-hand scale and a great-circle distance per hop on the bottom scale. A vertical line from the value of the great circle distance per hop to the appropriate parameter curve for the layer height considered with single or multiple, or chordal hops, and a horizontal line from that intersection to the right-hand scale yield half the signal-path length per hop. Now using this scale as an ordinary nomogram together with the number of hops on the left-hand scale and the centre vertical line, the milliseconds of time delay may directly be read off this centre scale. For this purpose a straight edge is to be used between the value of half the signal path per hop and the number of hops. Again, this nomograph only enables approximate data to be obtained. To allow a better resolution of parameters and therefore a better analysis of changes in the mode delay, range-limited graphs may be used, an example being shown in fig. 3. Obviously, data referring to all possible conditions along one particular path have to be calculated accurately for actual analysis.

Using only the geometrical conditions given by great circle distance as well as average layer heights, a mode delay scale may be developed for each particular great circle path. For the example of an observational point at the Research Establishment at Werthhoven, nr. Bonn, Germany, and a time signal transmitter WWV at its location prior to the 1st December 1966 with a great circle distance of 6400 km the Table I has been computed for typical conditions experienced, viz. an F_2-layer at 270 km and the E-layer at 110 km. The mode-delay values in the last column permit the tendency to be determined for each type of variation. Relatively low values suggest chordal-hop propagation with a high probability, if E-layer MUF does not permit three E-layer hops. Values generally agree with a previously published verification of predominant chordal-hop modes for round-the-world signals [15]. There is some ambiguity in some values, inasmuch as certain mode delay values may be obtained by several combinations, usually involving E-layer reflections. On the other hand, ionospheric characteristics permit a relatively easy selection between values of equal mode-delay. A sudden increase of mode delay to a value indicative

of E-layer reflections might be interpreted as the occurrence of sporadic E-reflections. Such a mode-delay scale should be established for each path, prior to analysis.

TABLE I

EXAMPLE OF A MODE-DELAY SCALE
FOR GREAT-CIRCLE DISTANCE OF 6400 km

Model Type	F 2 - Tilt Points from either end at (km)	F 2-Layer Height Indication (km)	Time Taken by Signal (m sec)
3 E-Layer Reflections	-	-	21.61
Chordal-Hop	1600	270	21.74
Chordal-Hop	1600	300	21.86
4 E-Layer Reflections	-	-	21.87
2 E-Layer-, 1 F_2-Layer Reflection	-	270	21.9
2 E-Layer-, 1 F_2-Layer Reflection	-	300	22.0
2 F_2-Layer Reflections	-	270	22.07
Chordal-Hop	1070	270	22.07
1 E-Layer-, 2 F_2-Layer Reflections	-	270	22.15
2 F_2-Layer Reflections	-	300	22.16
Chordal-Hop	1070	300	22.17
1 E-Layer-, 2 F_2-Layer Reflections	-	300	22.27
3 F_2-Layer Reflections	-	270	22.42
3 F_2-Layer Reflections	-	300	22.62

2.6 Processing of Resultant Data

As indicated in the general description of this system of monitoring mode delay, the multi-frequency measurement of these layer characteristics is the main objective, together with its further use for the selection of optimum working frequencies. The nomograph shown on fig. 1 may be used in connection with the ionospheric data derived from prediction charts discussed under 2.4 and the main nomograph shown in fig. 2,as well as an auxiliary chart of the type shown in fig. 3 may be employed to determine the standard path characteristics for each month. All short-term variations observed may then be evaluated with reference to these standard characteristics. Charts like Table I are utilized to interprete the mode delay observed on each frequency in terms of the actual propagation path experienced by the time signal. This interpretation,as, for instance, in the case of an increase in the mode delay and the appropriate changes in layer structure,can be used as input data to frequency selection facilities.

3. Some General Results

3.1 Criteria of Path Selection

With an observational point located at Werthhoven nr. Bonn in the Federal Republic of Germany, and simultaneous reception of time signal transmitters MSF located at Rugby, United Kingdom, and WWV, in its location prior to the 1st December 1966 (Beltsville, Md., USA) and its location thereafter (Fort Collins, Colo., USA) appropriate paths may be considered representative of the North-Atlantic area. In this particular case a statistical analysis over long periods of time may be used to compare a path under quiet ionospheric conditions with one crossing the aurora ring. Fig. 4 depicts an appropriate portion of the great-circle map. The conditions mentioned under 2.1 are satisfied by this path selection.

Some attention has to be paid to the probability of mutual interference of different time signals received on identical frequencies. In this respect, the use of 5, 10, 15, 20, 25 MHz by different time-signal services is extremely disadvantageous. It may here be suggested that one service per continent would be adequate for all applications of standard signals.

3.2 General Path Characteristics

Using a concept mentioned under 2.2, 2.3 and 2.4, the general path characteristics were obtained from prediction charts issued by ESSA [16] for the months of October and November 1966 as well as the selected periods in January and March 1967 and during the first quarter of 1969. In this particular case, and if only a relatively small number of hops is to be considered with multiple hop propagation, the ground characteristics may be neglected provided that only mode delay measurements without field strength considerations are of interest. In general, however, the propagation path with the least number of ground reflection points may be supposed to be the probable predominant path due to the general loss in signal strength at each ground reflection [6]. For the great-circle path indicated above, values outlined under 2.4 may now be determined. This together with a scale like Table I then leads to the type of mode to be taken into account at each hour during an average day in the particular month.

3.3 Brief Description of Equipment

The receiving equipment used comprises separate high-stability crystal-locked receivers for each of the five frequencies, 5, 10, 15, 20, and 25 MHz. The antenna is of the rhombic type. The use of a load resistance provides for a unidirectional characteristics. For the purpose of investigations described in this paper, sensitivity requirements are not critical. Thus particular attention was paid to a steady check on stability in order to eliminate effects upon delay time.

3.4 Analysis of Measured Data

In order to obtain a first indication of the usefulness of the monitoring system described in this paper, signal observations were made using oscillographic display and photographic evaluation. Such signal observations were conducted at suitable intervals. In each case, attention was paid to the objective of multi-frequency mode delay measurements, i.e. beside the reference signal of MSF at relatively short time delay, WWV signals were utilized at a maximum number of frequencies, the optimum being 5, 10, 15, 20, and 25 MHz. This procedure allows relative time delays to be used even if the reference signal in Europe supplied by MSF could not be detected in this or the other case.

Two methods of general evaluation are now possible: each relative time-delay value measured between, for instance, 15 and 20 MHz, may be compared to the appropriate standard value determined from characteristics extracted from ionospheric prediction charts; secondly, the fluctuation in such relative mode-delay values observed, also within very short intervals of perhaps two minutes, may be evaluated to yield an estimate on circuit stability. In both cases, a statistical analysis may be used to obtain a general relationship between the presence of short-term variations and predicted hourly variations. These data may thus be used to draw conclusions upon the general effectiveness of changes caused by the occurrence of sporadic E-layer or irregularities in ionospheric layers coinciding with magnetic disturbances and similar effects. Fluctuations observed within very short intervals indicate drifts and other irregularities.

The main purpose may, however, be achieved by analyzing the data obtained with particular reference to the tendency in mode changes, because this allows conclusions to be drawn upon the short-term characteristics in the ionospheric regions touched by the great circle path concerned.

3.5 General Results Obtained on Sample Paths

Observed simultaneous, multi-frequency mode-delay data show a general tendency of increasing delay time with decreasing frequency when the entire path is in day-light, viz. between 1200 and 1500 GMT. This is in accordance with standard characteristics, inasmuch as during this period propagation on 10 and 15 MHz is supported by a constant E-layer with MUF conditions generally allowing four hops or at least two E-layer reflections and one F2-layer reflection for the WWV path prior to 1st December 1966, whereas transmissions on 20 and 25 MHz are of the chordal-hop type, thus yielding a lower value of mode delay.

In detail typical deviations of this average behaviour is the increase in mode-delay time for 20 and 25 MHz and the disappearance of such transmissions. This change indicates an increase in E-layer ionization and its occurrence in unexpected regions, most likely by a sporadic E-layer, such that the mode behaviour resembles that on lower frequencies. The signal may also disappear with blanketing by a regular or sporadic E-layer. Such change in path characteristics can easily be recognized and monitored; its evaluation and interpretation as above permits very reliable short-term predictions of path behaviour.

Another parameter of major interest is the mode stability which is generally connected to path stability. Multi-frequency mode-delay measurements as described in this paper allow this parameter to be observed continuously by means of evaluating short intervals, of, e.g., four minutes. and even less, if jitter characteristics of a path are to be monitored for digital data transmissions. Important indications are contained in the mode-delay trend as a function of frequency, as well as the maximum deviation obtained on anyone frequency. Performing this analysis for the periods of October and November 1966, the trend was found to agree with the average one, i.e. increasing delay

time with decreasing frequency. Selecting 15 and 20 MHz as representative frequencies differences in mode delay of up to 1.8 msec and 1.5 msec, respectively, were obtained in 4-min intervals. On 15 MHz, the occurrence of such sudden changes in mode delay in each case coincided with a theoretically possible path making use of two E-layer- and one F2-layer reflection on that frequency, thus suggesting that the path was generally maintained by regular and sporadic E-layer reflections, while the sudden disappearance of the sporadic E-layer at a certain reflection point caused an F2-layer reflection with a consequential increase in mode-delay. The variations on 20 MHz may be interpreted as indicating a change from chordal-hop propagation to the multihop-F2-layer mode, in which case a sudden change in tilt condition should have been the cause.

In general, it should be emphasized that signals displayed well-defined single-path propagation for the period prior to 1st December 1966. After the change in location of WWV, multipath effects have a much more pronounced influence upon the oscillographic evaluation. This observation is in agreement with the fact that the path now crosses the polar region (see fig. 4). An appropriate statistical analysis is to be published at a later date.

For each observation, the tendency in the change of a layer structure can be determined from change in the mode delay as has been shown in Table I. This value can then be used to instantaneously correct frequency adjustments and transmitting and receiving equipment of any telecommunication link in the HF range.

4. Conclusions

The monitoring system for multi-frequency mode-delay described in this paper provides a reliably method of short-term predictions for representative paths from any observational point on earth. An automatic and continuous comparison with standard path characteristic results in error signals which are directly applicable to systems selecting optimum working frequencies.

Acknowledgements

The author gratefully acknowledges the work done by Mr. H.J. Schumacher in construction, maintainance, and operation of the equipment as well as the assistance rendered by Miss I. Drolshagen, Miss M. Faßbender, and Mr. H. Reppermund in data evaluation and preparation of the manuscript.

References

[1] Cox, J.W., Davies, K. — Oblique incidence pulse transmission, Wireless Eng., Vol. 32, p. 35 (1955)

[2] Daly, R.F., Felperin, K.D., Dayharsh, T.I., Tupper, B.C. — CURTS Phase II Automatic Frequency Selection System - Signal Processing, Application, and Evaluation, Stanford Research Institute, May 1967

[3] Goldberg, B. — 300 kHz - 30 MHz MF/HF, IEEE Trans. on Communication Technology, Vol. COM-14, No. 6, pp. 767-784, December 1966

[4] Albrecht, H.J. — Investigations on Great-Circle Propagation Between Eastern Australia and Western Europe, Geofisica Pura e Applicata, Vol. 38, pp.169-180 (1957)

[5] Albrecht, H.J. — Further Studies on the Chordal-Hop Theory of Ionospheric Long-Range Propagation, Archiv, Met.Geoph.Biokl., Ser.A, 11, pp.383-391 (1959)

[6] Albrecht, H.J. — Analysis of Ionospheric Paths in Long-Range Propagation, Indian Journ. of Meteorology and Geophysics, Vol.11, No.1, January 1960

[7] Morgan, A.H. — Distribution of Standard Frequency and Time Signals, Proc.IEEE, Vol. 55, No. 6, June 1967

[8] Banks, P.M. — Measurements of Antipodal High-Frequency Radio Signals, Journ.of Geoph. Res., Vol. 70, No. 3, pp. 625-638, February 1965

[9] Kift, F. — The Propagation of High-Frequency Radio Waves to Long Distances, Proc. IEEE. Vol. 107, pp. 127-140, 1960

[10] Wieder, B. — Some Results of a Sweep-Frequency Propagation experiment over a 1100 km East-West Path, J.Geophys.Res., Vol.60, p. 395

[11] Albrecht, H.J. — On the relationship between electrical ground parameters, Proc.IEEE, Vol.53, p. 544 (1965)

[12] Albrecht, H.J. — On the Geographical Distribution of Electrical Ground Parameters and its Possible Effects on Navigational Systems, EPC/AGARD Symposium, Ankara, Turkey, October 1967

[13] Davies, K. — Ionospheric Radio Propagation, NBS Monograph 80 (1965)

[14] Becker, W. — Der Übertragungsfaktor M(3000)F2 und seine Abhängigkeit von den verschiedenen ionosphärischen Parametern, Kleinheubacher Berichte, Bd.11, S. 67-70, 1966 (U.R.S.I. National Convention Germany, 1965)

[15] Albrecht, H.J. — Applying the Chordal-Hop Theory of Ionospheric Long-Range Propagation to Echo-Signal Delay, Proc. IRE, pp. 356-357, January 1961

[16] Ionospheric Predictions — Environmental Science Services Administration (ESSA), US Department of Commerce, Boulder, Colo., USA

MUF - Conditions

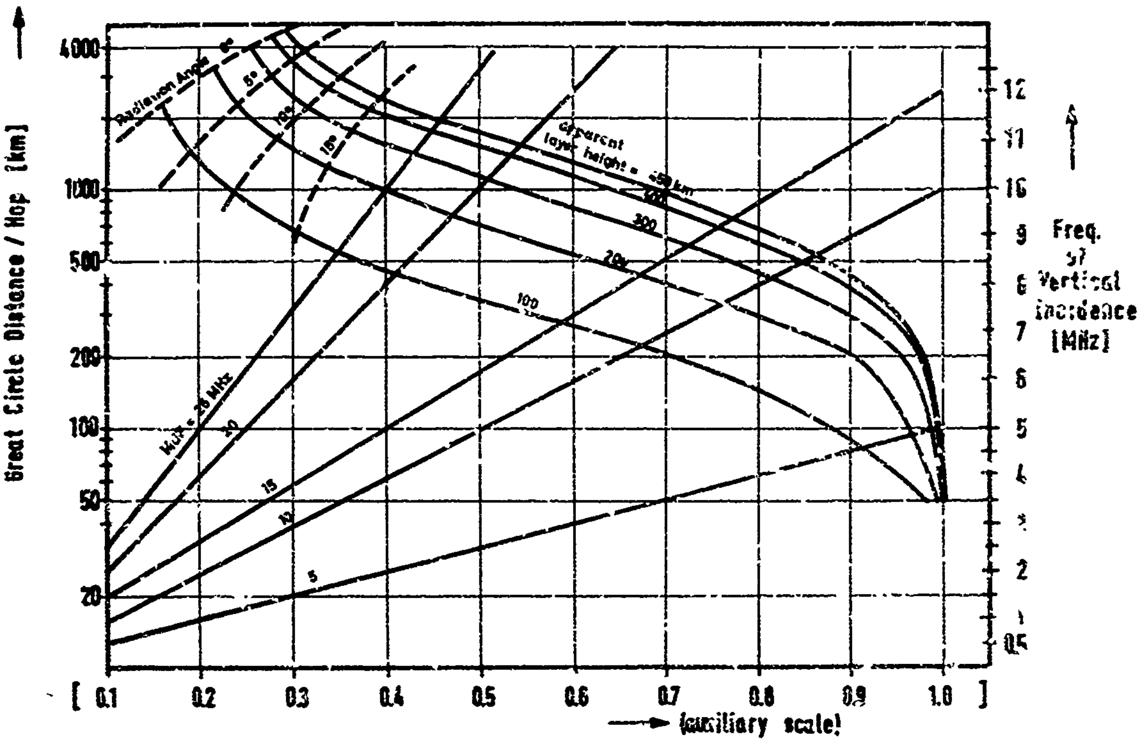

FIGURE 1

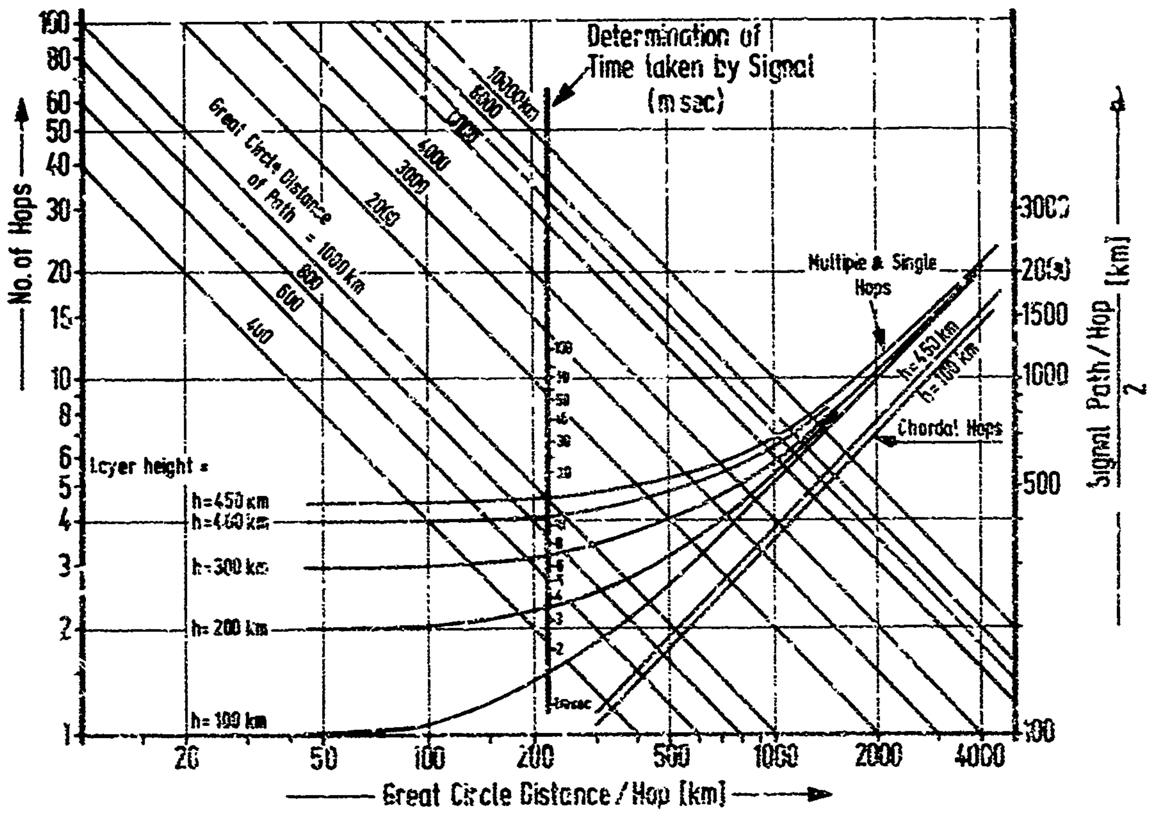

FIGURE 2

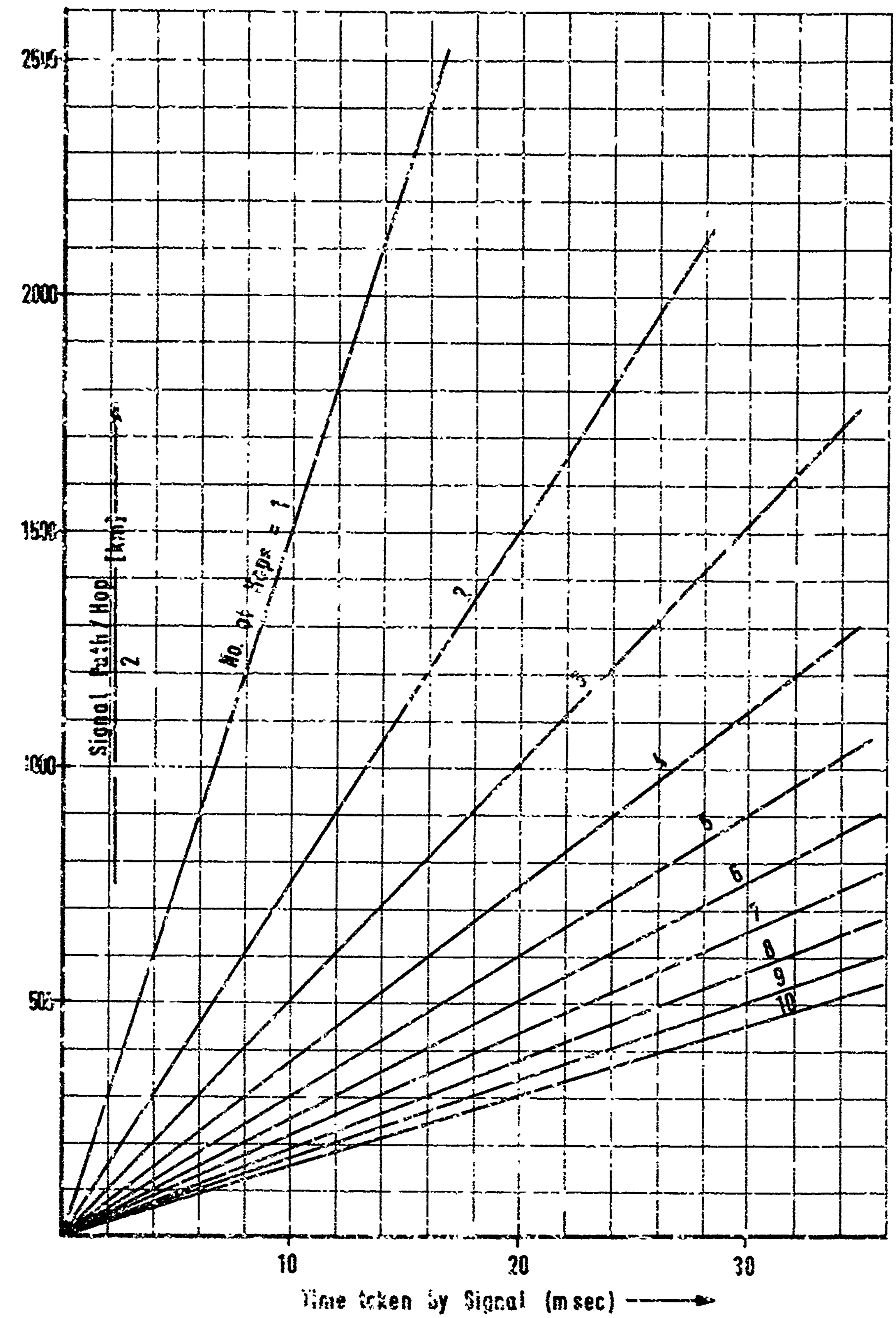

2500
2000
1500
1000
500
10
20
30
Signal Path/Hop (km)
2
No. of Hops = 1
2
3
4
5
6
7
8
9
10
Time taken by Signal (m sec)

FIGURE 3

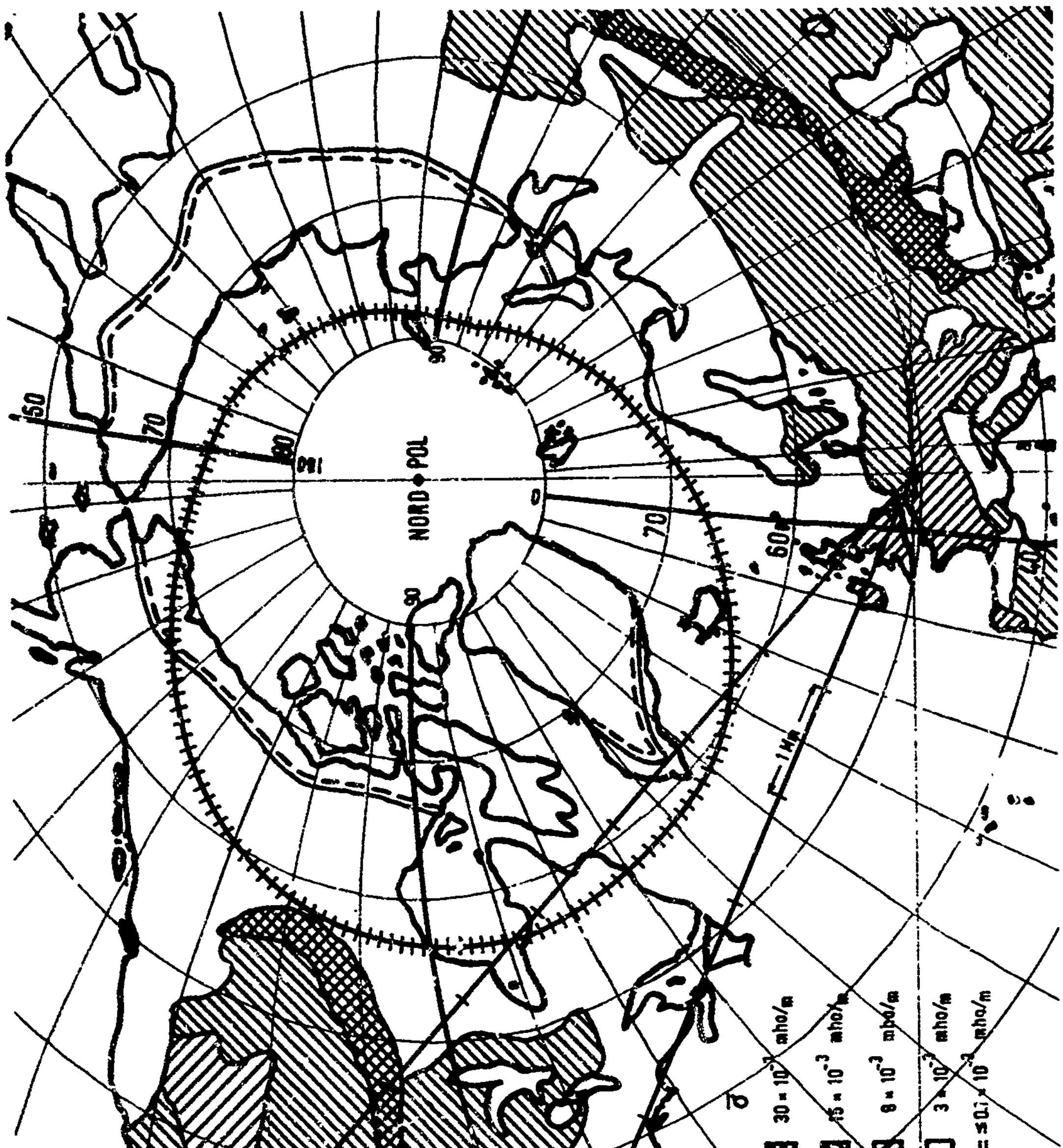
NORD POL
σ
30 × 10^-3 mho/m
15 × 10^-3 mho/m
8 × 10^-3 mho/m
3 × 10^-3 mho/m
≤ 0.1 × 10^-3 mho/m
150
70
80
180
0
90
70
60
40

FIGURE 4

SHORT-TERM PREDICTION OF HF COMMUNICATION CIRCUIT PERFORMANCE

by

J. W. Ames, R. D. Egan, G. F. MacGinitie

Granger Associates, Palo Alto, California

SUMMARY

Short-term prediction of oblique ionospheric HF communication circuit optimum working frequency and quality can materially aid frequency management and reduce spectrum congestion. Real-time prediction of these quantities has been implemented with a small digital processor. Ionosphere support (MOF, LOF) and multipath up to 80 minutes in the future are estimated using a linear prediction process based on oblique sounder measurements. The means, variances, and covariances of the variables necessary to the prediction process are stored as Fourier coefficients of diurnal variation. This provides smoothing of the random fluctuations between measurements for adjacent periods, and in addition saves storage space relative to the alternative of storing averages for each prediction increment. The coefficients themselves are updated in a manner similar to the formation of running averages.

The processor accepts either analog (video), or digital data from up to 15 sounder paths. Provision is also made for accepting measured interference or noise from selected communication frequencies to provide a direct estimate of signal-to-noise ratio. The ionosphere forecasts are combined with the signal-to-noise ratio to rank the assigned frequencies in order of expected utility during the prediction period.

SHORT-TERM PREDICTION OF HF COMMUNICATION CIRCUIT PERFORMANCE

J. W. Ames, R. D. Egan, G. F. MacGinitie[1]

Granger Associates, Palo Alto, California

INTRODUCTION.

This paper will describe some previously unreported details of the ionogram reading and short-term prediction processes used in an HF-radio short term reliability prediction and frequency management system called the "Path Predictor". The ionospheric sounder parameters and the basic linear prediction process are described in [1] and will be mentioned here only briefly for reference. Ionograms are created by a step-frequency pulse sounder operating at 20 pulses-per-second with 2 pulses-per-channel and 40 linearly spaced channels-per-octave. The Path Predictor has been implemented both for short and long pulse soundings (100 μs and 1 ms). The current Path Predictors (Granger Associates Model 9077-3), require that ionograms be in the form of a video signal from a sounder receiver. Addition of a pre-processing unit to remote receivers would allow operation with several such remote receivers via teleprinter lines.

The predictor determines the Lowest Observed Frequency (LOF), Maximum Observed Frequency (MOF), and multipath parameters from the video ionogram and predicts these quantities for 80 minutes in the future. If a Frequency Usage Monitoring Equipment (FUME)[2] has been included in a particular system, the Path Predictor combines current communication channel interference information with ionosphere predictions to predict communication channel quality and issue suggestions for timely frequency changes to maintain a high degree of circuit performance.

The major items of equipment are a sounder receiver, an interface unit, a FUME receiver programmed to periodically measure signal level on a number of arbitrarily chosen channels, and a small general purpose digital computer[3]. Input commands and predictor output are via standard teleprinters.

IONOGRAM ENCODING.

The video output of the sounder receiver, figure 1, is sampled by the digital processor acting as an analog-to-digital converter. Sounder channel output consisting of background noise and interference is sampled for 5 ms before the received pulse is expected. A threshold just above 95 percent of the samples taken during the noise measurement period is then computed. This noise threshold establishes what might be termed an amplitude window above which the signal must extend to be considered a possible ionospheric echo. The sample interval is 33 μsec for both signal and noise measurements when the sounding pulses are 100 μsec. Longer sample intervals and narrower receiver bandwidths are used for longer pulses.

A time window is established, as shown in figure 2, to logically discriminate against spurious signal indications and to assist in mode separation when short pulse ionograms are being received. Pulse amplitudes which exceed the noise threshold are entered numerically in the cells of figure 2, each column of which represents signal samples taken during one 10 ms signal reception period. The two pulses on each frequency are considered together by marking the existence of a possible echo only when 10 out of the 12 elements that define a time window contain signals. This process is repeated with the time window delayed by successive sample intervals until it reaches the end of the 10 ms signal acceptance period. When short pulse ionograms are being received, the time window will normally separate several distinct pulses. For simple path prediction these multiple echoes are combined to yield a single effective value of pulse duration. The modes can be separately processed, however. This has been done for encoding of vertical incidence ionograms.

(1) J. W. Ames and G. F. MacGinitie are Research Engineers in the Granger Associates Systems Research Division, of which R. D. Egan is the General Manager.

(2) Melpar, Inc.

(3) Digital Equipment Corp. Model PDP-8

To further guard against spurious responses, and to separate modes when that is appropriate, a third window, this time in the frequency domain, requires signal detection on 5 out of 8 adjacent sounder channels with time overlap of at least two sample intervals.

Received signals passing this series of tests are reduced to two digital ionograms. One is a list showing the peak pulse amplitude on each channel and the other is a list showing total pulse duration on each channel. The amplitude ionogram is also coded to indicate channels containing no detected signals but unusually strong interference. This information is used later in the processing to permit amplitude interpolation over such channels.

Logical signal processing employing the above time and frequency windows greatly simplifies the determination of Maximum Observed Frequency and Lowest Observed Frequency (MOF and LOF) from the resulting ionogram since virtually all spurious signals are removed. The MOF and LOF can be defined simply as the highest and lowest channels containing identified signals.

MEAN VALUE CALCULATION.

Prediction of the ionosphere parameters, MOF and LOF, is by the linear process indicated in equations 1 and 2 and is more fully described in reference [1]. Predictions are made for each of the following eight 10 minute periods and are renewed every 10 minutes.

$$\hat{x}(t+T) = \bar{x}(t+T) + \left[x(t) - \bar{x}(t) \right] \rho(t,T) \qquad (1)$$

$$\hat{\sigma}(t+T) = \sigma(t+T) \sqrt{1 - \rho^2(t,T)} \qquad (2)$$

$\bar{x}(t)$ = mean values at time t (of MOF or LOF)

$\sigma(t)$ = standard deviation at t

$\rho(t,T)$ = autocorrelation at t for delay T

$\hat{}$ = predicted value.

In earlier methods of prediction, the means and variances, $\bar{x}$, σ, and ρ, were up-dated by the running average technique, with the averages for each 10 minute interval independent of all the others. With this technique, random variability in the input data resulted in unavoidable growth of irregularities in the diurnal curves of the long-term functions. As an example, the dotted curves of figure 3 are the result of averaging over approximately one month's data. The variations from smooth curves detracted from the utility of short-term predictions by introducing large fluctuations in the estimation of the time remaining before a frequency was expected to fail. For example, a current ionogram might have a MOF practically equal to the previous one, but there might be a sharp decrease in the mean MOF between two adjacent future times, possibly coupled with a jump in the standard deviation. This could cause the estimate of time remaining before MOF failure on some frequency to drop from 70 minutes to 30 minutes in one 10 minute period.

The alternating variations in adjacent mean values of MOF and LOF and the short-period fluctuations of variance and covariance appear to have no physical significance. These irregularities have therefore been eliminated by converting the long-term data to a limited number of Fourier coefficients from which the desired values are found as needed. The solid MOF curves in figure 3 show the results of this procedure where eight harmonics are retained for the mean values and four are retained for the standard deviation.

Equation 3 illustrates the usual method of deriving Fourier coefficients from a set of data with a 24-hour period of 144 10 minute increments. Equation 4 shows the process used in the Path Predictor for renewing the Fourier coefficients each time a new ionogram is received. The value of ϵ is chosen to allow the Fourier coefficients to follow long-term ionosphere changes with a time constant of approximately 11 days.

Conventional Fourier coefficient equation:

$$a_n = \frac{2}{T} \sum_{t=1}^{T} x(t) \bullet \cos\left(\frac{2\pi nt}{T}\right) \qquad (3)$$

"Running Average" Fourier coefficient equation:

$$a_n \text{ (NEW)} = a_n \text{ (OLD)} + \epsilon \frac{2}{T} \left[x(t) - \bar{x}(t) \right] \cos\left(\frac{2\pi nt}{T}\right) \tag{4}$$

$\epsilon = 0.0944$

$T = 144$

Converting the diurnal variations of the long-term data to Fourier coefficients not only improves the prediction quality, but also substantially reduces the required amount of computer memory capacity. Table 1 shows the ionosphere data storage requirements for a single path for the case in which all data is stored separately and also for 2 degrees of data compression. The first step in reducing the data storage requirements consists of approximating the autocorrelation function by a decaying exponential (as described in reference [1]). This reduces the storage requirement from 2,880 words to 664. Converting the diurnal variations of all of these items to Fourier coefficients further reduces the storage requirement to 70 words per path.

Item	Simple Storage	Autocorrelation Delay Approximated By Exponential	Diurnal Variation Reduced To Fourier Coefficients
$\overline{LOF}(t)$	144	144	17
$\overline{MOF}(t)$	144	144	17
$\sigma MOF(t)$	144	144	9
$\sigma LOF(t)$	144	144	9
$\rho MOF(t, 10)$	144		
$\rho MOF(t, 20)$	144		
•	•	144	9
•	•		
•	•		
$\rho MOF(t, 80)$	144		
$\rho LOF(t, 10)$	144		
$\rho LOF(t, 20)$	144		
•	•	144	9
•	•		
•	•		
$\rho LOF(t, 80)$	144		
Total	2880	664	70

Units are Words of Computer Memory

TABLE 1. STORAGE REQUIRED FOR HISTORICAL DATA, 3 VERSIONS

CIRCUIT QUALITY PREDICTION.

The prediction of total circuit quality is based upon three factors: propagation support, multipath (MP), and signal-to-noise ratio (SNR).

Propagation support is predicted directly as the probability that a particular channel will lie between the LOF and MOF, which are assumed to be normally distributed about the predicted means with the predicted standard deviations (equations 1 and 2). This process is fully described in reference [1] and is illustrated in figure 4, which shows a situation in which the presently observed MOF is about 3 MHz below the long-term average curve. The MOF prediction for 10 minutes in the figure is very close to the presently

observed value and has a relatively small standard deviation. The predictions for times farther in the future are relatively closer to the long-term average curve and the standard deviation has increased. In the data from which this example was taken the observed LOF was so near to the corresponding average value that the prediction follows the diurnal curve. Figure 5 shows the variations in the probability of ionospheric support at several discrete frequencies calculated from the predictions of the previous figure. The probability for support at 12 MHz is seen to be decreasing because of the decreasing predicted MOF and the increasing predicted variance. The support probability at 6 and 3 MHz increases because of the decreasing predicted LOF. If no multipath or interference data were available, these curves could be used to decide when to change operating frequency. One might, for example, decide to change frequency whenever some other frequency is predicted to be 10% better than the present one within the next 20 minutes. The Path Predictor, however, also considers the effects of multipath and interference.

The effects of multipath upon communication are predicted indirectly. The presently observed ionogram is idealized as shown in figure 6, with the LOF and MOF as described previously. The frequency at which pulse stretching is a maximum is termed the MPF (Multipath Frequency) and in the idealization all frequencies below that are regarded as having an equal amount of multipath stretching while frequencies between the MPF and MOF have multipath linearly decreasing to zero at the MOF. The prediction of multipath (MP) at a future time is then made by simply translating this idealized ionogram in frequency to match the MOF predicted for the future time.

$$MP(f, t+T) = MP\left(f \times \frac{MOF(t)}{\widehat{MOF}(t+T)}, t\right) \tag{5}$$

Consider, for example, a frequency between the MPF and MOF. If the MOF is predicted to increase, then equation 5 predicts that the multipath at the frequency in question will also increase.

The signal-to-noise ratio predictions consist of estimates of the values that would be achieved currently if the communication system were to operate on each of its assigned channels. These estimates are derived from a smoothed version of the amplitude ionogram and of interference measurements made on specific assigned communication channels by the FUME receiver.

Unlike the probability of ionospheric support, the effects of multipath and signal-to-noise ratio are not directly representable on an 0-to-1 scale, which is convenient for ranking frequencies in order of desirability. If, however, we establish a performance threshold, such as receiving a standard length 45-bit word without error, the effects of multipath and signal-to-noise ratio can be stated on a 0-to-1 scale as the probability of meeting this requirement. An overall quality estimate is then conveniently formed by multiplying the three factors.

Each individual quality factor has the form

$$Q = Pr\Big[\text{no error in 45 bits}\Big] = (1 - p_e)^{45} \approx e^{-45p_e} \tag{6}$$

where $Pr\Big[\;\Big]$ = Probability of the event in the brackets

p_e = bit error probability

e = base of natural logarithms

(The approximation follows from the definition of e).

The bit error probability, p_e, can be calculated in a single equation including both signal-to-noise ratio and multipath. These effects have been separated for programming convenience by calculating an irreducible error rate for each factor acting alone. The computations are further simplified to equations 7 and 8 which are exponential approximations to previously calculated curves describing these effects, reference [2].

$$p_e(MP) = \frac{1}{4}\sqrt[3]{\frac{\text{multipath spread}}{\text{baud length}}} \tag{7}$$

$$p_e(SNR) = 10^{-\frac{1}{11}(SNR(db) + 2)} \tag{8}$$

$p_e(\ )$ = component of binary error probability due to effect in brackets

MP = multipath

SNR = signal-to-noise ratio

Any lack of absolute accuracy introduced by these approximations should have only a small effect on the total performance of the predictor since it is sensitive only to relatively large differences between channels in predicted total quality. Since it is inconvenient to make a signal-to-noise ratio measurement on the channel currently in use by the communication system, its component of quality due to signal-to-noise ratio is arbitrarily set to 0.99. If a separate signal analyzing device were available to measure operating channel SNR, its output could easily be supplied to the Path Predictor.

The third component of overall quality is, of course, the probability of ionospheric support, which can be used directly since it is already in the form of a number varying from 0-to-1.

FREQUENCY SELECTION.

An overall quality figure consisting of the product of the above 3 factors is calculated for each available frequency for each 10 minute interval from 10 to 80 minutes in the future (Table 2). This array of numbers, the size of which depends upon the number of frequency channels available to the communication system, is the basic output of the Path Predictor. Presented this way, however, it probably would not be helpful to ordinary communication system operating personnel. A separate computer subroutine applies decision criteria to this array to derive a recommendation for specific system operation orders. An example of a simple decision rule is to order a frequency change whenever the quality predicted on some channel exceeds that on the currently operating channel by more than 10 percent within 20 minutes of the present time. This situation is illustrated by the hypothetical quality prediction array of Table 2 which illustrates an exaggerated version of the usual nighttime decrease of MOF. Two frequencies, 10.3 and 6.7 MHz, are shown as they would appear if significant interference were being received on these channels at the time of the prediction.

		Future (Minutes)							
	Channel Frequency MHz	10	20	30	40	50	60	70	80
		Estimated Channel Quality							
	3.3	.18	.21	.24	.27	.30	.33	.36	.39
	4.5	.48	.50	.53	.55	.57	.60	.63	.65
	5.2	.67	.71	.73	.75	.77	.79	.81	.83
	6.7	.20	.21	.23	.24	.25	.27	.28	.30
	6.8	.91	.92	.93	.94	.95	.96	.97	.98
Alternate Frequency →	9.2	.98	.98	.98	.98	.98	.98	.98	.98
	10.3	.60	.56	.52	.47	.42	.35	.30	.25
Present Frequency →	12.3	.90	.80	.71	.63	.53	.47	.41	.30
	14.7	.79	.68	.58	.47	.36	.25	.10	0
	17.5	.35	.30	.22	.12	.02	0	0	0
	20.9	0	0	0	0	0	0	0	0

TABLE 2. CHANNEL QUALITY PREDICTION ARRAY (SIMULATED DATA)

The technical control operator has the option of following the frequency change order without question, or of requesting a display of all or part of the quality array from which he can form his own opinion of the best response. If there are a large number of assigned frequencies, it may be advantageous to request the array ordered not by frequency but by predicted quality at a specific time, such as 20 minutes.

CONCLUSION.

The Path Predictor system described here considers automatically all factors of critical importance to the usual radio system. Other factors such as doppler shift and diversity correlation could easily be included if they were especially important to a particular communication system, and if sensors were provided for their measurement. Similarly, rapidly disseminated warnings of ionospheric disturbances based on solar observation can be incorporated when available.

At its minimum utilization the Path Predictor will give technical control operators timely reminders of routine frequency changes and instructions for coping with at least some kinds of unusual conditions. As experience is gained with predictor systems, and as communication equipment becomes more adapted to fully electrical control, the direct execution of frequency change commands without operator intervention will be a distinct possibility. Technical control personnel can then monitor the operation of the system and consider improvements to its strategy without the burdens of routine frequency management.

REFERENCES

1) Ames, John W., and Egan, Raymond D., "Digital Recording and Short-Term Prediction of Oblique Ionospheric Propagation", IEEE Transactions on Antennas and Propagation, Volume AP-15, No. 3, May, 1967, pp. 382 - 389.

2) Sifford, B. M., et al., "HF Time and Frequency Dispersion Effects", TR No. 4, Contract DA36-039-SC-90859, Stanford Research Institute, AD 610330.

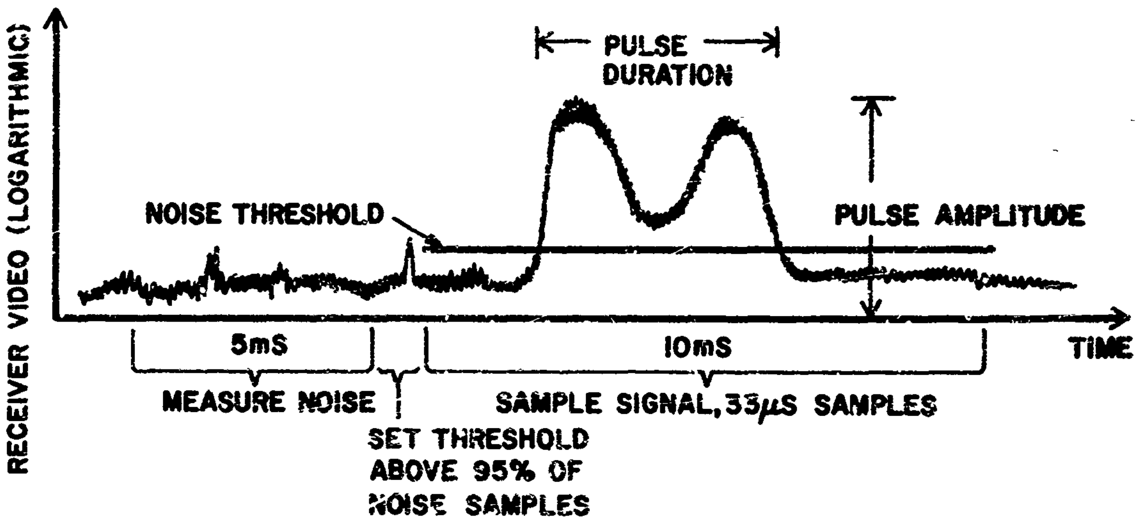

Figure 1. Video Measurements

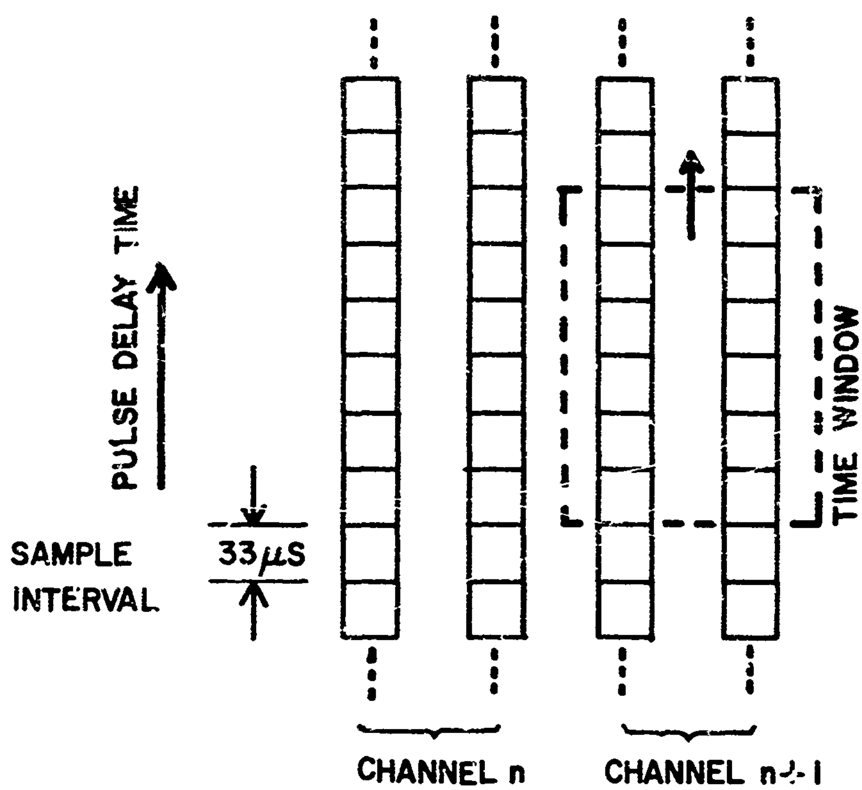

1) TRANSMITTER SENDS 2 PULSES PER CHANNEL.

2) SIGNAL DETECTION REQUIRES 10 OUT OF 12 ELEMENTS IN TIME WINDOW ABOVE NOISE THRESHOLD.

3) MODE DETECTION REQUIRES SIGNAL DETECTION WITH OVERLAP OF AT LEAST 2 SAMPLE INTERVALS ON 5 OUT OF 8 ADJACENT CHANNELS.

Figure 2. Signal and Mode Recognition Logic

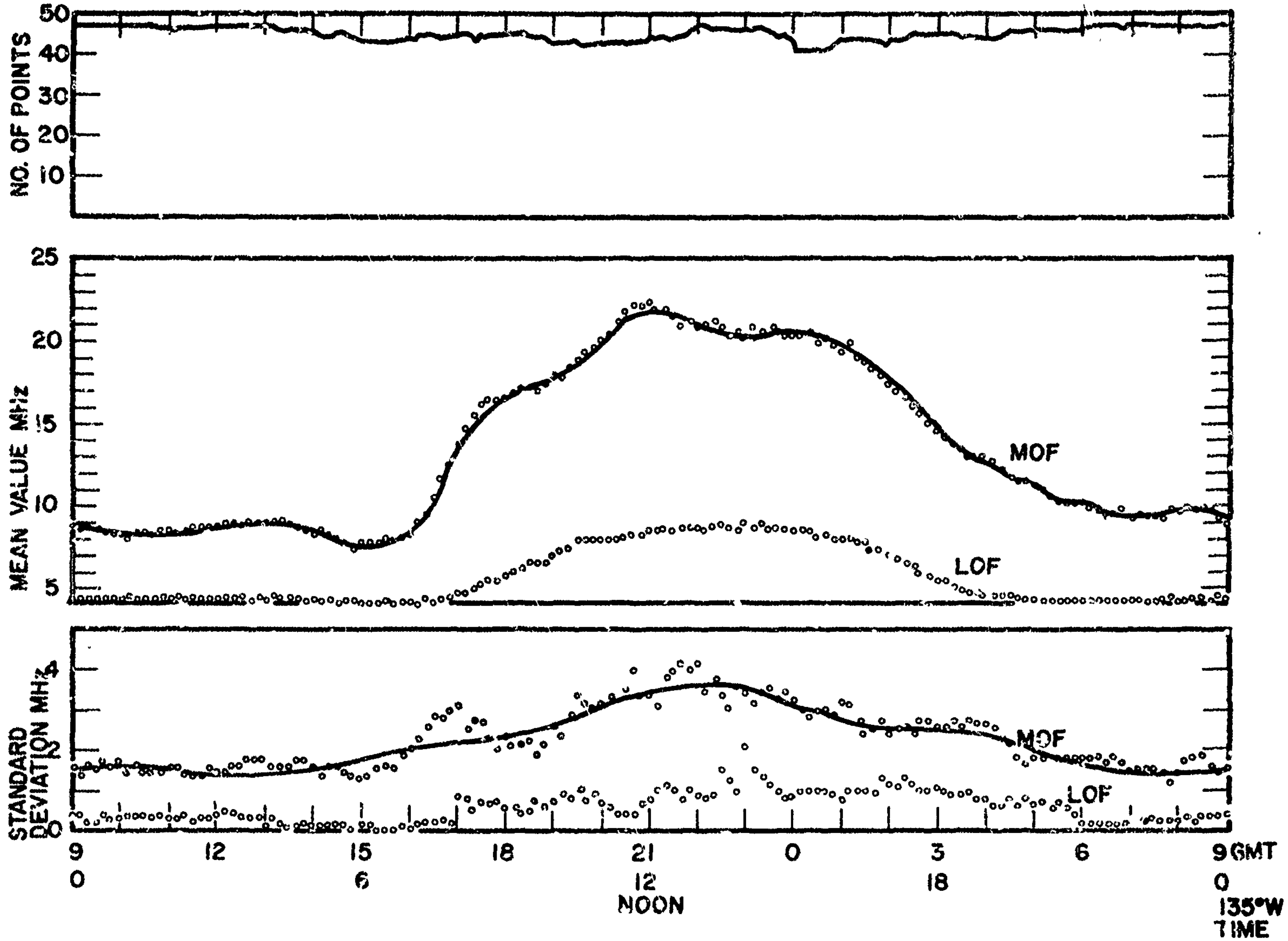

Figure 3. MOF, LOF Diurnal Var'ation

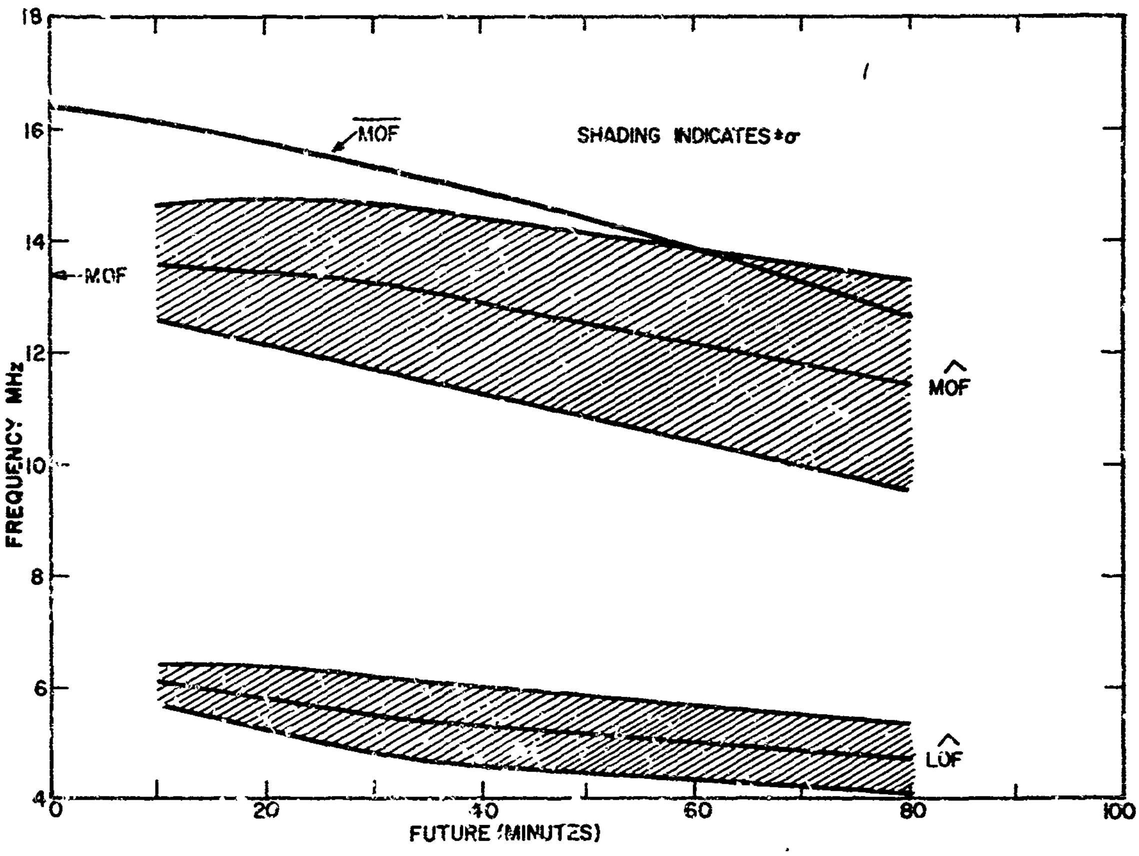

Figure 4. MOF, LOF Predictions

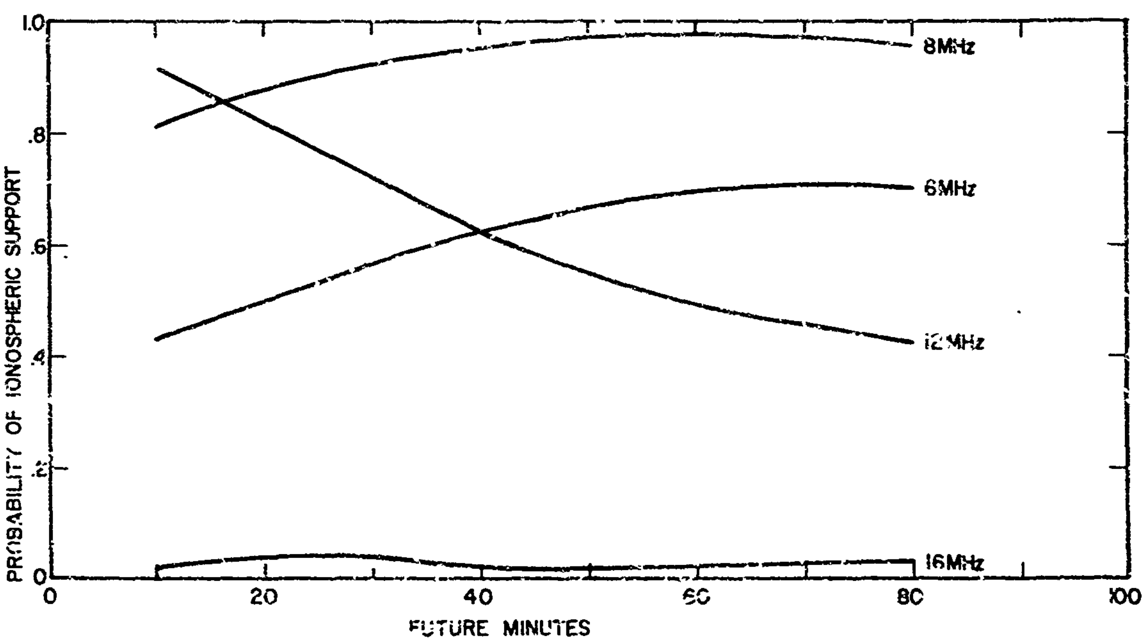

Figure 5. Ionosphere Support Decision Curves

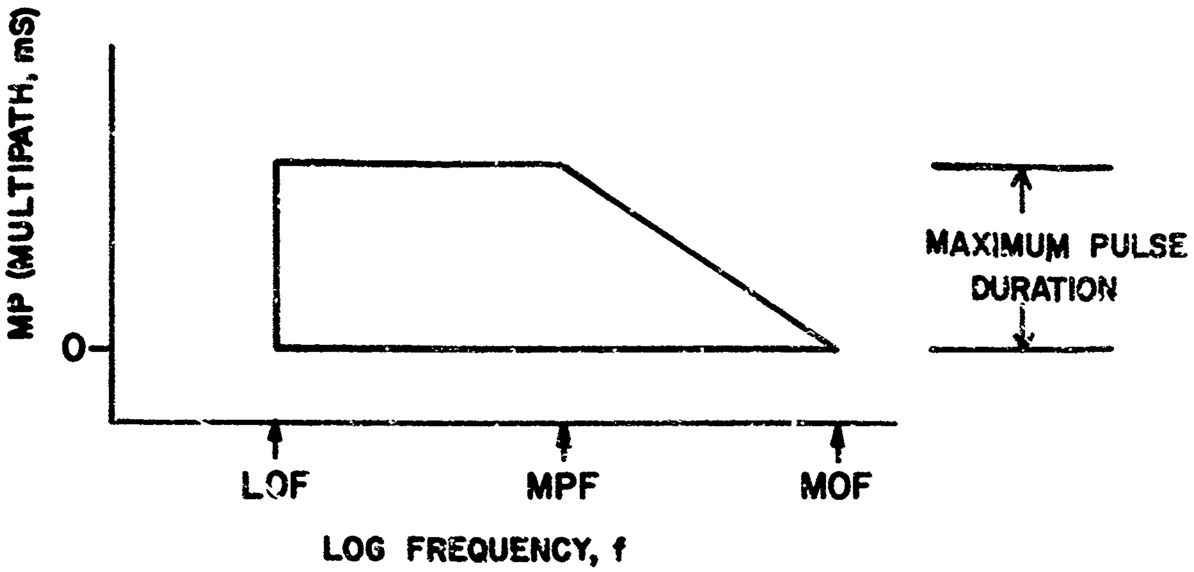

Figure 6. Idealization of Current Ionogram (t + 0) for Prediction of Multipath at t + T.

VARIATION OF IONOSPHERIC ABSORPTION AT WIDELY SPACED STATIONS

by

T.B. Jones and W. Keenliside

Department of Physics, University of Leicester, UK

ABSTRACT

The possibility of predicting ionospheric absorption changes on one propagation path from measurements made on another is discussed. Vertical and oblique incidence absorption measurements are available for a number of European stations and these have been examined for similarities in absorption variations for the period January - December 1966. During the equinox and winter seasons the absorption changes were found to be well correlated for paths with mid point separations of less than 600 km, although the degree of correlation decreases with increasing separation. In summer the correlation is not as clearly defined and for path mid point separation of more than 300 km, the correlation is not significant.

Care has been taken to distinguish between the general seasonal trend and the day to day fluctuation in absorption.

A Comparison of the Ionospheric Absorption of H.F. Radio Waves propagated over widely spaced paths

Introduction

The possibility of predicting ionospheric absorption changes on one propagation path from measurements made on another is of interest in the design and operation of H.F. communications circuits. Correlation studies of the ionospheric absorption measured at widely spaced locations have been reported by Rawer (1951), and Beynon and Davies (1954), although these investigations were restricted to vertical incidence propagation. In the present study the noon absorption values for a number of oblique incidence paths have been employed in addition to measurements at vertical incidence. The frequencies and path lengths have been selected so that all the reflection levels occur in the upper D or lower E-regions of the ionosphere and propagation is by the one hop mode in all cases.

The absorption data has been subjected to a statistical investigation of the degree of correlation between pairs of circuits and this has been expressed in terms of the conventional correlation coefficient (r). Noon values only have been considered but an attempt has been made to separate the long and short term variations for each of the three seasons i.e Summer, Equinox and Winter The correlation between the absorption variations on any two circuits is found to depend on season and on the separation of the mid-points of the path considered.

Method of Analysis

The correlation between any two sets of variables x_1, x_2, x_3 .... and y_1, y_2, y_3 .... can be expressed in terms of the correlation coefficient r defined as

$$r = \frac{\frac{1}{n}\sum (x-\bar{x})(y-\bar{y})}{Gx\ Gy}$$

Where n is the number of pairs of x and y considered, $\bar{x}$ and $\bar{y}$ are the respective arithmetic means and Gx and Gy are the standard deviations of all the values of x and y respectively. The significance of any correlation test will depend on the size of the sample taken and throughout the present study the significance of the coefficients have been established by means of the well known "t" test.

Noon absorption values have been reported for a number of oblique incidence paths in Western Europe for the period January to December 1966. In particular, measurements were made on the 2.61 MHz transmissions from Norddeich Radio (W. Germany) received at Leicester, Lindau and Neustrelitz and on the 2.775 MHz transmission of Kiel Radio received at Neustrelitz Vertical incidence observations for this period on frequencies of 1.725 and 2.0 MHz have been published by the Ionospheric Institute at Freiburg. Details of these six transmission paths and their equivalent vertical frequencies are given in Table 1.

The correlation coefficient has been evaluated for the circuits taken in pairs, thus every separation of path mid-point obtainable from the original six sets of observations was considered. It was possible to form fifteen pairs from the data available as indicated in Table 1, which lists the pairs of circuits in order of increasing separation of the path mid-points

Measurements were available for at least 20 days per month throughout the year, and the data were divided into three periods corresponding to Winter (January and February), Equinox (March and April) and Summer (May to August). Since the absorption is known to exhibit anomalies in Winter, a second Winter period comprising the three months October to December was also included in the correlation studies.

Daily Values

The correlation of the daily noon values of absorption was first examined and no attempt was made to separate long term changes from short term fluctuations. The results for the fifteen pairs of paths in Table 1 are presented in Table 2 which lists the correlation coefficients for each month in addition to the four periods referred to above. In Figure 1 the correlation coefficients are displayed as a function of the separation of the path mid-points. A high correlation is obtained during the Equinox months, the correlation coefficient decreasing with increasing separation of the path mid-points. In Winter the correlation coefficient is also fairly high for separations of up to 400 km. but for distances greater than this there is a rapid decrease in r. The summer period is particularly interesting since no correlation is evident between any of the absorption results and the separation of the path mid-points is of little significance.

The very high correlation during Equinox is not unexpected since large changes occur in the seasonal variation of absorption at this time The high correlation would seem to be a direct result of these seasonal effects which would produce similar changes in all the paths considered.

Long Period Variations

In order to test the influence of long term changes on the correlation coefficients, seven day running means of the daily values were determined for the Summer, Equinox and Winter periods. The running means were subjected to the same correlation analysis as the daily values in the previous section and the results are given in Table 3. The correlation coefficients are displayed as a function of the path mid-point separation in Figure 2.

The equinox data now yield exceptionally high coefficients with values of $r \simeq 0.7$ even for displacements of 700 km. in the path mid-points. There is a slight decrease in r with increasing distance but a high degree of correlation exists between all pairs of data. The two Winter periods indicate a high correlation for small separations of the path mid-points although the rapid decrease of r with increasing distance evident in the January-February data does not occur in the second Winter period. The absorption changes during the summer months are not correlated.

Short Term Fluctuations

In view of the marked differences between the daily and running mean results, an attempt was made to correlated the short term changes. For this investigation the differences between each daily value of absorption and the corresponding seven day running mean were subjected to the correlation analysis. The values of r for the fifteen pairs of paths for each month and the Summer, Equinox and Winter periods are tabulated in Table 4. The correlation coefficients are plotted as a function of the path mid-point separation in Figure 3. The coefficients for the equinox months are now smaller than those obtained with the daily and running mean data, indicating that the high values for these cases were to a large extent due to the marked seasonal changes and not to short term influences. The correlation coefficients of the difference values during Winter are greater than both daily and running mean results. This suggests that during this period, short term changes take place which simultaneously influence all the paths. In Winter, intervals of anomalously high absorption occur which normally persist for a few days and which Thomas (1962) has shown, can extend over a sufficiently large area to affect all the paths considered in the present investigation. No correlation is evident in the summer period and the values of r are less than those obtained using the daily and seven day running mean data.

Summary

The similarity of the absorption variations on the circuits considered is dependent on season and on the separation of the path mid-points. The correlation between daily values is influenced by long term seasonal changes, although short term fluctuations can also give high correlation coefficients for the Winter months. During periods when absorption variations are well correlated the correlation decreases with increasing separation of the path mid-points.

In Winter, the correlation coefficients are high for both daily, running mean, and difference values. There is a decrease in r with increasing path midpoint separation and this is especially noticeable in the case of the running mean results. The difference values give the best correlation for all separations indicating that all the paths are influenced by short term changes as for example, during the periods of anamalously high Winter absorption. The highest correlation coefficients are obtained for the Equinox data which also decrease with increasing distance between path midpoints. It is evident from a comparison of the running mean and difference values that the similar variations of the daily values of absorption on all the paths is due to the influence of the large seasonal changes in absorption which take place during these months.

No correlation was evident between any of the circuits in Summer and no systematic changes with path midpoint separation could be detected. This conclusion is in agreement with the earlier work of Rawer (1951) for vertical incidence absorption. Piggott (1955) suggests that the low correlation between absorption measured at spaced stations is a consequence of the different experimental techniques employed since the results will therefore include experimental errors of varying magnitudes. It seems unlikely that this is the sole cause of the low correlation unless the errors were in excess of the absorption changes during the period considered. It is perhaps worth noting however, that the day-to-day absorption changes are smaller in Summer than at any other time and therefore random errors are likely to produce low correlation coefficients for this period. During Equinox and Winter large changes in absorption occur which will dominate the fluctuations introduced by inaccuracies in the measurements. The regular decrease of the correlation coefficient with increasing separation of the path midpoints would not be obtained if the observations were contaminated by large experimental errors.

An attempt was made to investigate the dependence of the correlation coefficients on the difference in the equivalent vertical frequencies of the circuits. This difference is given as $\Delta f \cos i$ in Table 1. A systematic change in the correlation coefficient with $\Delta f \cos i$ could not be detected in any of the data considered. It was therefore concluded that, provided the reflection levels occur in the same general height range and that one hop modes only are considered, the separation of the path midpoints rather than the separation of reflection levels ($\Delta f \cos i$) controls the degree of correlation between any two circuits during the Winter and Equinox periods.

It seems possible to relate the absorption changes on one circuit to those on another for the Equinox and Winter periods. The degree of correlation differs for long term and short term changes and the coefficient decreases with increasing distance between the path mid-points. For the Summber months however, no correlation is evident on any of the paths considered.

References

Beynon W.J.G. and Davies K. "Simultaneous Ionospheric Absorption measurements at widely separated stations." J. Atmos. Terr. Phys., 1954, 5, 273

Piggott W.R. "On the variation of ionospheric absorption at different stations" J. Atmos. Terr. Phys. 1955, 7, 244.

Rawer K. "Comparison of Ionospheric Absorption measurements carried out at two European stations" J. Atmos. Terr. Phys. 1951, 2, 38.

Thomas L. "The Winter Anomaly in Ionospheric Absorption" J. Atmos. Terr. Phys. 1962. 23, 301.

TABLE 1

Pairs of Stations for which Noon Absorption Values have been Correlated

	PATH	f (MHz)	path (km)	f Cos i	PATH	f (MHz)	path (km)	f Cos i	Separations of Path Midpt.	Δf Cos i
1	Freiburg (Vertical)	2·050	0	2·05	Freiburg (Vertical)	1·725	0	1·725	0	0·325
2	Norddeich - Neustrelitz	2·614	395	1·20	Kiel - Neustrelitz	2·775	220	1·900	110	0·70
3	Norddeich - Lindau	2·614	295	1·45	Norddeich - Neustrelitz	2·614	395	1·200	147	0·25
4	Norddeich - Lindau	2·614	295	1·45	Kiel - Neustrelitz	2·775	220	1·900	245	0·45
5	Norddeich - Lindau	2·614	295	1·45	Norddeich - Leicester	2·614	550	0·894	350	0·56
6	Norddeich - Neustrelitz	2·614	395	1·20	Norddeich - Leicester	2·614	550	0·894	420	0·31
7	Kiel - Neustrelitz	2·775	220	1·90	Norddeich - Leicester	2·614	550	0·894	440	1·01
8	Freiburg (Vertical)	2·050	0	2·05	Norddeich - Lindau	2·614	295	1·450	543	0·60
9	Freiburg (")	1·725	0	1·725	Norddeich - Lindau	2·614	295	1·450	543	0·275
10	Freiburg (")	2·050	0	2·05	Norddeich - Leicester	2·614	550	0·894	620	1·16
11	Freiburg (")	1·725	0	1·725	Norddeich - Leicester	2·614	550	0·894	620	0·831
12	Freiburg (")	2·050	0	2·05	Norddeich - Neustrelitz	2·614	395	1·200	665	0·85
13	Freiburg (")	1·725	0	1·725	Norddeich - Neustrelitz	2·614	395	1·200	665	0·53
14	Freiburg (")	2·050	0	2·05	Kiel - Neustrelitz	2·775	220	1·900	727	0·15
15	Freiburg (")	1·725	0	1·725	Kiel - Neustrelitz	2·775	220	1·900	727	0·175

TABLE 2

Correlation Coefficient for the Daily Values of Noon Absorption
for the Different Paths During 1966

Ref. No.	Correlation coefficient r for various months and seasons															
	Jan.	Feb.	Mar.	Apr.	May	June	July	Aug.	Sep.	Oct.	Nov.	Dec.	Jan.-Feb.	Mar.-Apr.	May-Aug.	Oct.-Dec.
1	.70	.78	.69	.78	.43	.30	.50	.29	.66	.65	.34	.62	.74	.81	.35	.68
2	.90	.79	.74	.55	-.01	-.04	.19	-.03	.85	.56	.69	.42	.75	.72	.02	.58
3	.78	.77	.92	.56	-.19	.11	-.10	.04	.78	.49	.76	.35	.78	.56	-.06	.64
4	.76	.87	.79	.41	.37	.03	.39	.74	.36	.66	.83	.63	.67	.74	.40	.82
5	.78	.64	.88	.59	.22	.02	.15	.29	.70	.68	.76	.62	.67	.67	.19	.71
6	.82	.67	.72	.51	-.12	.07	.12	.32	.67	.48	.78	.51	.69	.56	. 0	.54
7	.73	.51	.87	.63	.02	.23	.39	.12	.50	.53	.62	.46	.56	.69	.22	.59
8	.66	.23	.56	.44	-.22	.20	.22	.09	-.09	.42	-.18	.39	.49	.50	-.02	.41
9	.58	.35	.73	.48	-.05	-.17	.24	-.02	.15	.58	.33	.33	.48	.64	.05	.58
10	.55	.28	.60	.30	-.15	.08	.17	.12	.02	.61	.32	.56	.45	.45	.10	.44
11	.59	.42	.72	.36	-.05	.27	.20	.15	.24	.71	.40	.64	.53	.55	.18	.57
12	.43	.29	.58	.26	-.11	.13	.12	.15	.10	.30	-.09	-.10	.39	.53	.48	.22
13	.42	.33	.67	.13	.38	.10	.06	.49	.34	.42	.12	.16	.38	.57	.32	.40
14	.41	.15	.49	.06	-.08	.44	.15	.36	-.01	.62	-.09	.55	.21	.19	. 1	.57
15	.35	.26	.73	-.06	-.07	.34	.34	.11	.27	.63	.36	.62	.22	.56	.26	.69

TABLE 3

Correlation Coefficient for the Seven Day Running Means of the Daily Values of Noon Absorption During 1966

Ref. No.	Correlation coefficient r for various seasons			
	Jan.-Feb.	Mar.-Apr.	May-Aug.	Oct.-Dec.
1	.85	.94	.46	.76
2	.53	.90	.11	.68
3	.74	.92	.12	.78
4	.24	.92	.44	.86
5	.71	.87	.38	.82
6	.57	.91	.41	.70
7	.61	.82	.26	.77
8	.47	.71	.01	.43
9	.41	.80	.06	.73
10	.24	.74	.26	.54
11	.31	.78	.31	.71
12	.12	.69	.44	.48
13	.24	.74	.60	.66
14	-.16	.65	.31	.70
15	-.07	.72	.37	.88

TABLE 4

Correlation Coefficient for the Deviations of the Daily Values from the Seven Day Running Means During 1966

Ref. No.	Correlation coefficient r for various months and seasons															
	Jan.	Feb.	Mar.	Apr.	May	June	July	Aug.	Sep.	Oct.	Nov.	Dec.	Jan.-Feb.	Mar.-Apr.	May-Aug.	Oct.-Dec.
1	.75	.53	.27	.47	.20	.15	.58	.38	-	.22	.54	.84	.62	.37	.28	.49
2	.93	.83	.31	.22	.31	-.11	-.29	.19	-	.24	.52	.45	.84	.62	.07	.43
3	.87	.71	.92	.41	-.19	.19	-.27	-.10	-	.31	.58	.22	.78	.81	-.15	.37
4	.85	.90	.81	.28	.36	.16	.41	.58	-	.76	.54	.68	.86	.63	.30	.68
5	.54	.71	.75	.34	.11	.12	-.06	.30	-	.46	.46	.53	.78	.62	.14	.49
6	.52	.72	.78	.20	.21	.01	.05	.11	-	.52	.50	.61	.76	.60	.11	.56
7	.79	.55	.60	.27	.05	.22	.12	.14	-	.26	.43	.50	.73	[illegible]	.18	.46
8	.69	-.03	.22	.21	.34	.39	-.01	.05	-	.25	.40	.52	.42	.23	-.13	.39
9	.63	.46	.34	.36	.22	-.52	-.06	-.04	-	.46	.37	.42	.56	.30	.05	.41
10	.67	.19	.38	.05	.02	.16	.02	.11	-	.22	.12	.48	.46	.26	.12	.28
11	.61	.34	.31	.14	-.09	.01	-.13	.06	-	.44	.26	.34	.53	.26	-.06	.32
12	.58	.06	.34	.37	-.28	.40	-.24	-.02	-	-.04	-.04	-.16	.41	.33	-.08	-.19
13	.55	.37	.32	-.09	-.31	.11	-.15	.30	-	.29	.06	-.13	.45	.15	-.09	.16
14	.65	-.11	.21	-.09	-.12	.14	.07	.45	-	.01	.33	.54	.35	.04	.15	.31
15	.43	.37	.14	.05	.15	-.09	-.14	.31	-	.63	.17	.38	.46	.03	.11	.40

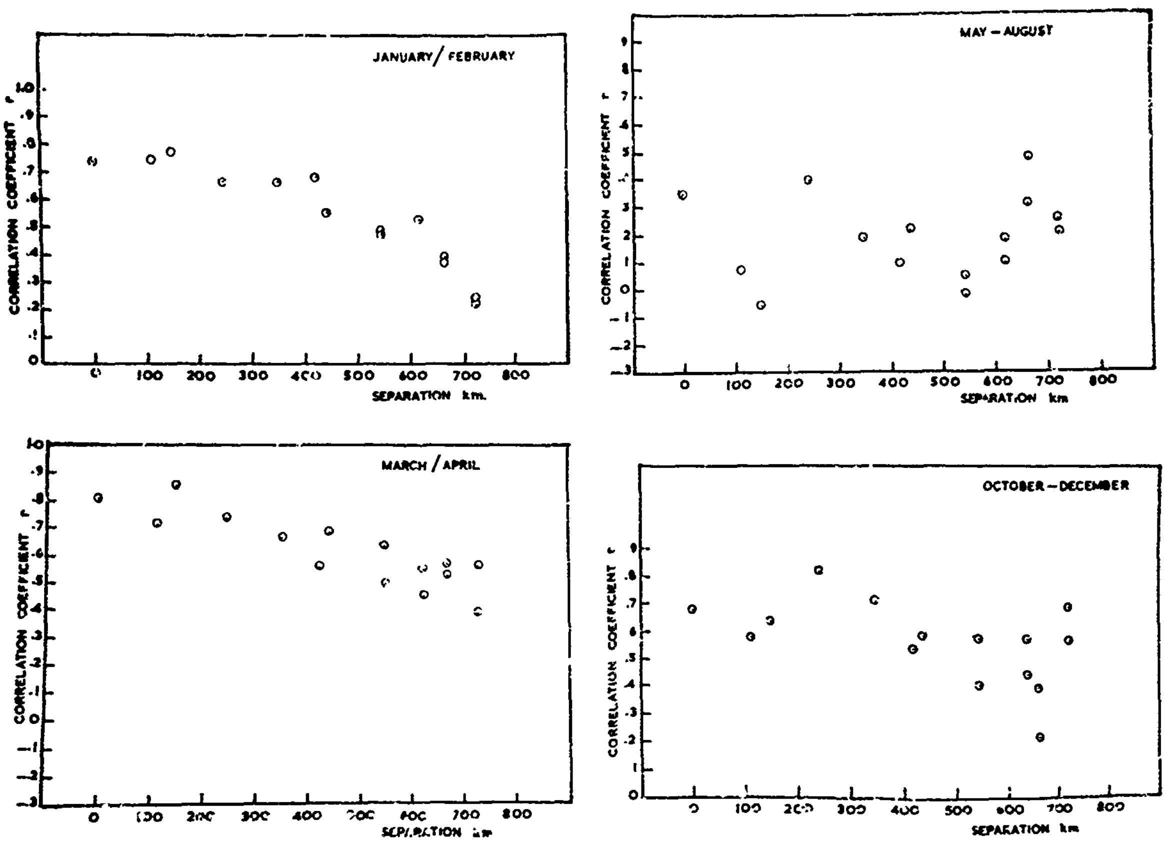

Fig. 1 Variation of the correlation coefficient of daily absorption values with station separation for 1966

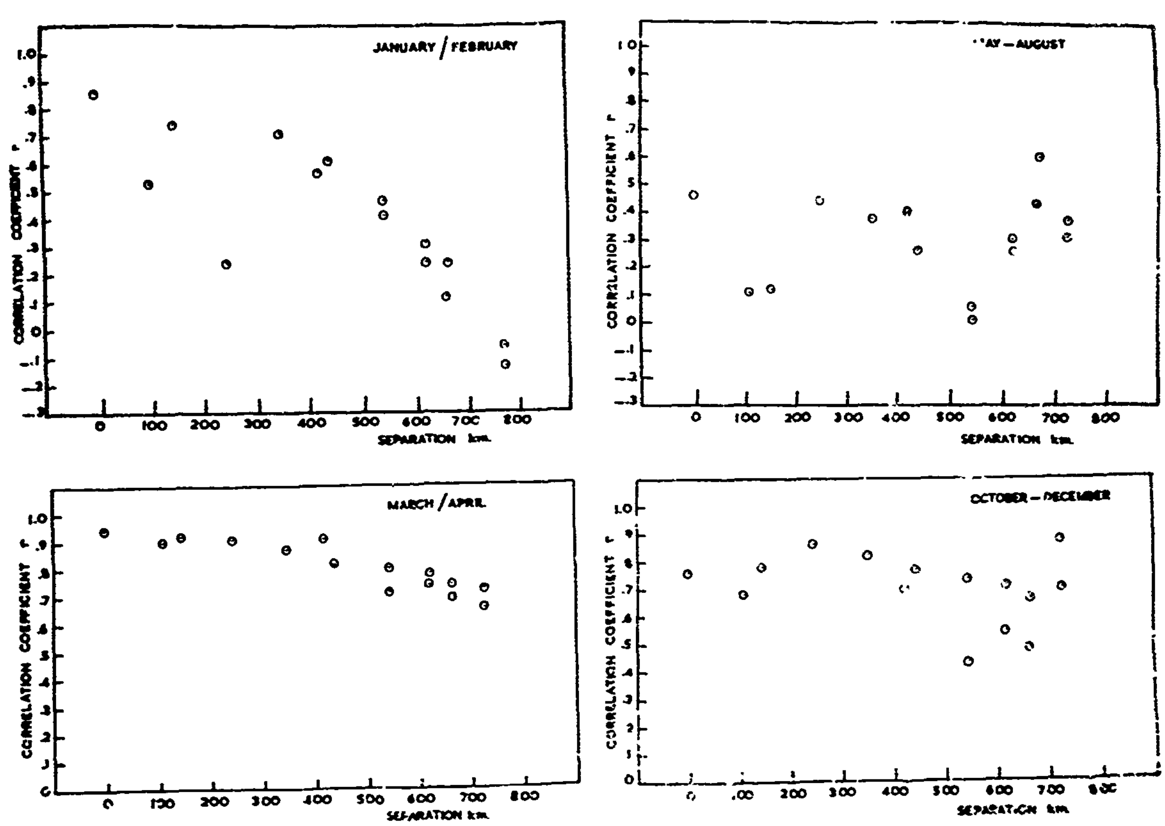

Fig. 2 Variation of the correlation coefficient of running mean absorption values with station separation for 1966

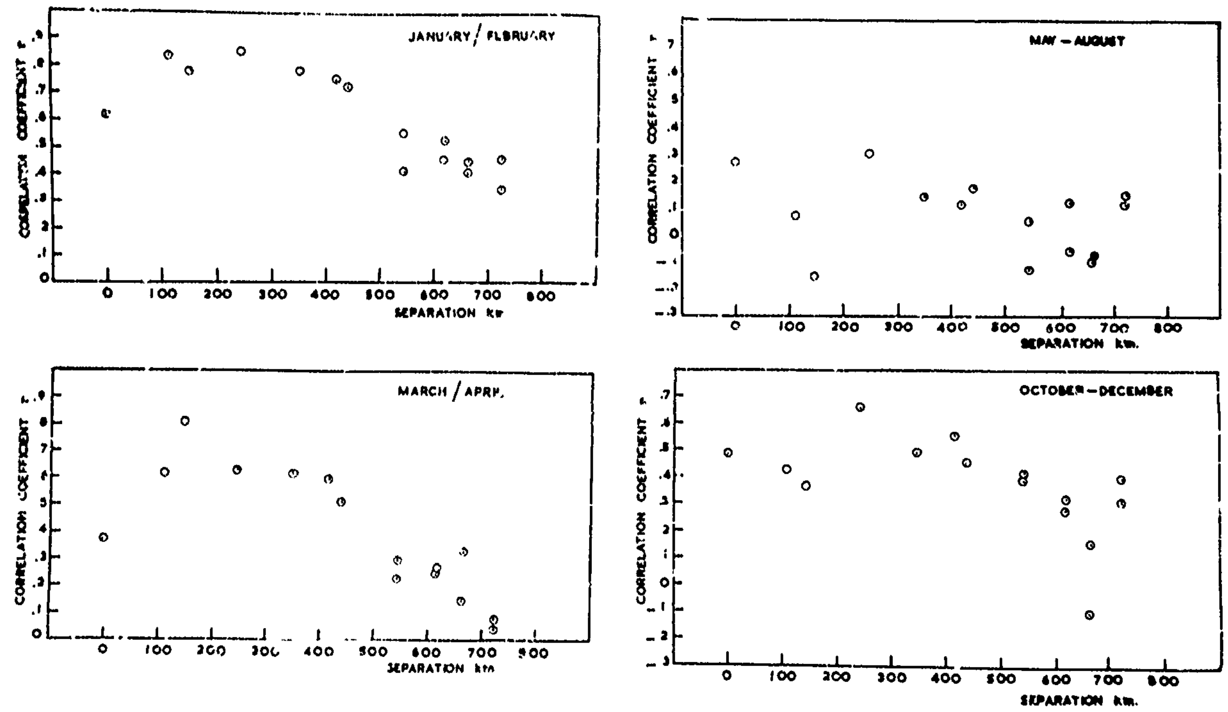

Fig.3 Variation of the correlation coefficient of the "difference" absorption values with station separation for 1966

POSITIVE PHASES AND DISTURBANCES OF THE IONOSPHERIC WAVE PROPAGATION IN COMPARISON WITH SOLAR-TERRESTRIAL EVENTS

by

B. Beckmann

Research Institute of the
Fernmeldetechnisches Zentralamt Darmstadt

SUMMARY

Positive phases, that is, abnormally wide transmission frequency ranges (MUF - LUF) with abnormally high field strengths usually indicate the presence of active centres on the sun. A decrease of the radio propagation quality from above-normal values may be considered as an indication of imminent disturbances. In some cases, the decrease is confined to the range between "above-normal" and approximately "normal" in spite of magnetic disturbance and solar activity while substantial local drops of the critical frequency foF2 (night minimum) are to be observed. During a 27-days repetition period the decrease in the above-normal range may initiate a sequence of recurrent disturbances, that is, local drops may develop into world-wide disturbances. These ionospheric observations can be evaluated for forecasting by means of an extrapolation in time. During the course of this changing sequence of positive phases and disturbances the following average results regarding the nature of solar-terrestrial relations can be obtained from superimposed epochs:

1) The frequency propability of local drops of the night-time critical frequency of the F-layer in mid-latitudes reaches up to 20% and varies with the geomagnetic activity, whereas in times of world-wide radio disturbances the figure is 100%.

2) Positive phases may be followed by a decrease in the above-normal range of the propagation quality which can be accompanied by moderate geomagnetic activity, moderately growing solar activity (flares, solar radio events etc.), local drops of the critical frequency and modulations of the cosmic rays.

3) If, simultaneously, the flux of the solar 10 cm-radiation changes in that it either rises or declines steadily while there is a strong increase in the flare activity, a world-wide radio disturbance can be expected to follow after 3 or 4 days. If, however, the 10 cm-radiation and flare activity which increase during the formation of the positive phase will also show a downward tendency when the positive phase begins to decline then the probability is greater that there will be no world-wide radio disturbance. During the subsequent magnetic activity the cosmic ray intensity will increase.

4) The upward tendency of the cosmic ray intensity occurring due to eruptive centres on the eastern side of the sun will be weakende or will turn into a downward tendency, respectivively, if these centres are situated in the central zone or on the western side.

5) During the disturbance the Forbush effect is often found to be accompanied by an increase in the ionospheric absorption.

6) Superimposed epochs from 30 solar rotations (1965-1967) of the ionospheric propagation quality, the geomagnetic acitivity and the cosmic ray intensity indicated a relatively rigid course which was probably attributable to the interplanetary magnetic field of the sun. The above mentioned components run almost parallel with one another and were particularly pronounced around the 9th, the 16th and the 23rd day of the rotation. The maximum intensity of the disturbances occurred around the 9th day with the following peaks decreasing.

Positive Phases and Disturbances of the Ionospheric Wave Propagation in Comparison with Solar-terrestrial Events

by

B. Beckmann+

Research Institute of the Fernmeldetechnisches Zentralamt Darmstadt

The transmission frequency range can be used for the definition of world-wide ionospheric propagation situations as has been described in former papers among others in a lecture held by my colleague, Mr. Ochs, at the Symposium of the Ionospheric Research Committee AGARD AVIONICS PANEL in Naples, Italy [1]. In that case the ionospheric propagation parameters quasi-MUF, LUF and mean logarithmic field strength $\bar{F}$ were combined in a "band characteristic figure":

$$BK = (MUF - LUF + 1). \bar{F}.$$

If the ratio of the time average $\overline{BK}$ of a day and a night period, respectively, related to the respective propagation path to the corresponding running mean of preceding 27 days (= 1 solar rotation) $\overline{BK}_{rot}$ is formed, one obtains the relative band characteristic figure

$$BK_r = \frac{\overline{BK}}{\overline{BK}_{rot}}$$

Positive phases are then defined by $BK_r > 1$ and disturbances by $BK < 1$ if $BK_r = 1$ corresponds to the normal conditions related to the 27-day average. Since it has been customary in earlier years to characterize the propagation conditions by means of a scale from useless to excellent (= better than average), it is also possible to express the relative band characteristic figure in this kind of scale if the parameters MUF, LUF and $\bar{F}$ of the transmission frequency range are observed and $BK_r = 1$ is adapted to the normal value of the respective scale. The American quality scale, which will be used in the following, runs from G = 1 (useless) to 9 (excellent) with G = 6 as normal value. The quality figure of the ionospheric propagation thus is $G = 6 \cdot BK_r$. It describes within certain limits the variation of the mean field strength of the transmission frequency range which is controlled by the MUF and LUF variations [2].

Fig. 1 shows as an example the transmission frequency range for USA (circuit Frankfurt - New York) for June 1967 as monthly median values according to observations and prediction calculations. The frequency is plotted on the ordinate and the daytime on the abscissa. The dots represent the observations. Their thickness is a measure for the field strength and their number in a square of 1.5 h and 1 MHz a measure for the frequency. The curves of constant field strength are taken from the calculated prediction. The transmission frequency range is at the lower end limited by the ionospheric absorption and at the upper end by the ionospheric refraction including scatter due to irregularities of the ionosphere. The field strength rises from both limits and has its maximum about in the middle. The transmission frequency range shows changes which exceed the permanently existing statistical fluctuations. In the case of disturbances it shrinks with decreasing field strengths and in the case of positive phases it extends with increasing field strengths above its normal value. This is - as described - also expressed in the quality figure which is the product of the transmission frequency range in MHz and the mean field strength. For this examples are given in Fig. 2 [2].

Fig. 2a shows the diurnal variations of the transmission frequency ranges represented together with solar-terrestrial events which cause the disturbances and/or run parallel with them. In lines 7 to 9 the following is drawn in according to transmission frequency range observations made by the radio-monitoring station at the overseas radio receiving station Lüchow for the directions USA (east coast), South America and East Asia in 1 1/2 - hour intervals for several days (29. August to 1 September, 1966, first line, at the top):

a) MOF and LOF++ = border of the dashed areas, [published in ESSA Solar-Geophysical-Data].

b) mean field strengths of the observed ranges, scale in S-values from "white" (lowest field strength) over increasing dashing to filled up (highest field strength),

+ Chief of Research Group D 33 "Ionosphere"

++ MOF = Maximum Observed Frequency
LOF = Lowest Observed Frequency

c) band characteristic figures (solid curve) calculated as product of the transmission frequency range in MHz (enlarged by 1) and the mean field strength (S-values) for characterizing the respective ionospheric propagation quality (scale 0 to 150),

d) quality figure G calculated by reference to a running normal value and adaption to the international quality scale of the propagation forecast (averages for daytime period, night-time period and the whole day = arrows left 12.00 hours, right 00.00 hours, right 12.00 hours, G = 6 normal value) [published in the daily ursigram].

A normal transmission frequency range can be seen on 29 August. But an earth-magnetic activity (second line) starts (Three-Hour Bartels Indices from Wingst with Sudden Storm Commencement, SSC). There is flare activity on the sun, especially strong at 06.00 GMT (fourth line arrows pointing in upward direction) and accompanying bursts (third line, vertical bars and arrows, respectively, overall range 50 MHz to 10 GHz for burst and drift types) as well as a ionospheric consequence SID's (Sudden Ionospheric Disturbances) known as "Mögel-Dellinger-effect" in radio propagation (fifth line). Some increases in radiation in the X-ray range measured by satellites are entered under the SID's. The critical frequencies of the F2-layer of the ionospheric station Lindau++ (solid curve) are to be found in the 6th line just like those of station Kiruna (crosses for 6 hourly values). The letter B means that all reflections in the ionogram of the Swedish station Kiruna, which is situated in the auroral zone, disappear due to a strong increase in absorption called blackout. On 30 August a strong deterioration of the radio propagation in the direction USA follows (shrinking of the transmission frequency range, decrease of the quality figure from 6 to 2, low field strengths, see 7th line). South America and East Asia are not affected to the same extent (8th and 9th line). Here the quality figure decreases only to 4. Parallel is a decrease of the critical frequencies of the stations Lindau and Kiruna (6th line) in the night from 30 to 31 August with blackouts in Kiruna. During the time from 31 August to 1 September the propagation quality becomes normal again although the magnetic activity continues as does the solar activity. The variation in field strength of the coastal radio station Norddeich on 2.6 MHz (DAN-scale in dB), measured in Darmstadt and Lindau (10th line at the bottom of the Fig.) indicates also in our latitudes - after a temporary decrease - an increase of the absorption after the beginning of the disturbance.

Fig. 2a 1 shows in the time from 30 August to 1 September a decreasing chromospheric plage density on the eastern side, an increasing one in the central zone and on the western side, that means, sharply limited active region moves from East to West with the solar rotation. As can be seen in Fig. 2a 2, on the 29th, that is one day before the disturbance, there is a spot group with the developing stages G,C,I in CMP with a noise intensity in the cm-range of $62 \cdot 10^4\,{}^oK$ and meter wave bursts (strip localization). The flux of the 10 cm-radiation, measured in Ottawa decreases in the time from 29 Aug. to 1 September from $\Phi = 130$ to $\Phi = 118 \cdot 10^{-22} W/m^2$ Hz. The diagram of the flares (Fig. 2a3) shows on the 29th flares on the eastern side (- 5d), in the central zone $\pm$ 30° and on the western side (+ 5d) from 30 Aug. to 1 Sept. follow flares in the central zone.

Fig. 2b shows an example for the development of a positive phase instead of a world-wide ionospheric disturbance, however, with a local drop of the critical frequency accompanied by earth-magnetic activity (25 to 28 September 1966, on 26/27 CMP of a large bright plage area, bipolar spot group). The succession of disturbances by positive phases can frequently be observed in the 27-day recurrence tendency. Fig. 2b 1 shows that here, too, is a decrease of the plage density on the eastern side and that on the 27th a very bright plage area is in CMP where the decrease of the ionospheric propagation quality and the local drop in the critical frequency begins. As can be seen in Fig. 2b 2 in this area exist bipolar spot groups (β configuration) in the Brunner development stages C and A with a noise source of $44 \cdot 10^{4o}K$. Meter-wave bursts are widely distributed over the central zone and the western side. The flux of the 10 cm-radiation of Ottawa decreases during this time from $\Phi = 125$ to $\Phi = 103$. Only a few subflares were observed.

An interesting disturbance period began after a positive phase on 13 March, 1966 as is shown by Fig. 2c. It is a very strong disturbance on 14 March with a very strong magnetic activity. The 15th was practically normal again. The sun shows - as can be seen in Fig. 2c 1 - only a few plages at the eastern limb (3+) with increased corona emission of the green line and in the central zone (2+). Fig. 2c 2 shows formation of spots in the plage area on the western side with high noise radiation intensity ($33 \cdot 10^{4o}K$) and meter-wave bursts, also in CMP. The 10 cm - flux from Ottawa increased up to 16 March from $\Phi = 84$ to $\Phi = 102$. In Fig. 2c 3 flares can be seen in the plage area on the eastern side which advance to the CMP between 15 and 19 March.

++Max-Planck-Institut für Aeronomie, Institut für Ionosphären-Physik, Lindau/Harz

The following conclusions can be drawn from the course of the ionospheric propagation quality:

Positive phases mostly announce the existence of active regions on the sun. A decrease of the propagation quality from above-normal values may indicate approaching disturbances. In some cases the decrease remains limited to the range from "above-normal" to about "normal" despite magnetic and solar activities whereas local drops of the critical frequency foF2 (night minimum) can be observed (as is the case in Fig. 2b). In the 27-day recurrence the drop in the above-normal range can initiate a series of repeated disturbances while regional drops of foF2 can in the following solar rotations develop into world-wide disturbances. Positive phases can in successive rotations be succeeded by disturbances and vice versa.

These purely ionospheric and propagation-type observations can be evaluated in forecasts by means of an extrapolation in time, which can also be effected with the aid of autocorrelation. This has always been a help for the forecast if other information on solar-terrestrial influences does not lead to clear results. In this paper I want to deal with the solar terrestrial events around world-wide ionospheric disturbances and positive phases [3] .

From the quality figures of the ionospheric propagation (direction USA), which were explained with the aid of Figs. 1 and 2, key-days (in the Figures designated as zero-day) for disturbances and positive phases were formed, and then - according to the method of the superimposed epochs - in the interval of $\pm$ 8 days around this zero-day the course of the ionospheric propagation quality in comparison with other geophysical and solar parameters was examined. Fig. 3 shows the course of the propagation quality (G) with earth-magnetic activity (Ap) for collectives of disturbances from the years 1963 - 1965 and positive phases for 1963 - 1966. The size of the collectives+ is in Fig. 3 noted after the years. The earth-magnetic activity, which is plotted in the opposite direction and expressed by the planetary daily-value Ap, shows in rough outline a similar course as the quality figure of the ionospheric propagation. On the average of the years $Ap \approx 26$ were obtained. In the individual case the behaviour is very different. Of 21 strong disturbances of the collective I ($G \leq 3$) of the years 1963 - 1966, 6 had an $Ap < 30$, 8 an Ap between 30 and 50 and 7 an $Ap > 50$. Of the 58 moderate disturbances of the collective II 43 had an $Ap < 30$ and 15 an $Ap > 30$. An Ap = 50 was exceeded only in one case. Of 1460 days of the years 1963 to 1966 earth-magnetic activities K_W++ = 5 occurred on 101 days without having any connection with a ionospheric propagation disturbance.

It may be pointed out that in the normal and above-normal range (G = 6) variations of positive phases occur between the 3rd to the 5th day before the key-day (positive phases 6th to 7th and 1st to 2nd day). They are also expressed by a slight increase of Ap as can be seen even more distinctly in other collectives of times of higher solar activity which are to be discussed later on. In Figs. 8a and 9, which will be discussed later, the same variation of the positive phases can be recognized in 3 different collectives from the years 1966/63 and 1967 so that this course of the ionospheric propagation quality is shown by a total of 6 collectives from 59 disturbances. In the case of strong positive phases in the lower part of Fig. 3 the very steep rise of the quality figure before the key-day is connected with a decrease of the magnetic activity (Magcalme state $A_k \approx 4$) whereas two days after the key-day at decreasing quality figure a temporary magnetic activity is observed. The decreasing propagation quality, however, remains after the key-day always in the above-normal range ($G > 6$). As described above in radio traffic no world-wide disturbance is observed in 90% of the cases, but local drops of the night-time critical frequencies may be observed on ionospheric stations (see Fig. 2).

Let us now in Fig. 4 consider the behaviour of the local drops in the night-time critical frequencies around the key-day of the world-wide disturbances according to measurements made by the ionospheric station Lindau. The frequency P of the drops of $foF2_{min}$ is on the key-day 100%, before and after the key-day approx. 20% (dashed curve), i.e. approx. 20% of the drops occur without world-wide disturbance. The solid curve of the F2-critical frequency ($foF2_{min}$) gives an idea of the size of the drops. In addition to a pronounced minimum on the key-day there are two less pronounced minima before and after the key-day. The minimum 3 to 5 days before the key-day falls in the time of the minimum of the above-mentioned modulation of G in the range of the positive phases. In the frequency P it is not pronounced, i.e. it was caused only by few disturbances. In the case of very high world-wide positive phases we observe shortly before the key-day a minimum of the frequency of drops P coinciding with the Magcalme state and before and after the key-day we see two distinct maxima, i.e. here, too, we have characteristic differences in comparison with the disturbance collective. The first coincides - as we will see - with a flare activity, the second with the magnetic activity noticed in Fig. 3.

+I collective of strong disturbances, II moderate disturbances,

++K_W = characteristic of the Observatory Wingst

Let us now examine the course of the solar activity represented by the solar radiation on 2800 MHz (Φ). Fig. 5a shows that the disturbances generally do not occur in the maximum of Φ. In 1963 and 1966 they occur at decreasing, in 1965 at increasing intensity of Φ. In 1964 no characteristic variation can be recognized since the curve has a very flat horizontal shape. In the case of positive phases, on the other hand, there is a very pronounced maximum of the noise radiation shortly before the key-day, which is a characteristic difference as against the disturbances.

While the flux of the solar 10 cm-radiation in 1963 to 1965 in Fig. 5a on the average was steadily between -8 and +8 days around the key-day, there is already in 1966 an indication of a maximum at -4 to -5 days which becomes more pronounced with increasing solar activity in 1967 as is shown by Fig. 5b. Remarkable in comparison to the - also drawn in - mean course of the ionospheric propagation quality $\bar{G}$ and the earth-magnetic activity $\bar{Ap}$ is the fact that the variation in the "above-normal" range, which in Fig. 3 and also in Figs. 8a and 9 occurs at little solar activity (sun spot minimum) between the third and the fifth day, in this case at stronger solar activity moves closer to the key-day (-2 days).

Among 21 strong ionospheric propagation disturbances of the years 1963 to 1966, 7 showed no characteristics of increasing activity in the central zone (flares or remarkable development of spot groups with attendant phenomena). Three were accompanied by flares in the eastern or western zones. Among the 112 strong and moderate disturbances, which altogether occurred, 36 showed no activity in the central zone. Within the whole collective the activity showed different characteristics. It was not always possible to assign the most pronounced activities to strong disturbances. Some of them appeared so weakly that an assignment as probable cause of disturbance was not possible until later. In order to obtain clearer results in this case, the integrated activity in certain zones of the sun, namely in the central zone (± 30°) and the eastern and western zones situated outside of it, were in addition to the asignment of discrete centers of activity, which all are as effects of eddies in the sun plasma connected with one another through magnetic fields, included in the consideration of the disturbance.

We now consider in Fig. 5c as measure for the solar activity the mean distribution of the chromospheric plage brightness, which shows a certain positive correlation to the size of the plages around disturbance days and positive phases defined according to the ionospheric propagation quality G. The investigations were made separately for the central zone (± 30°), for the eastern side and the western side. The solid curve Σ in the upper part of the Fig. shows the relative course of the summed plage brightness for the total disk, the dashed curve E shows the course of the plage brightness on the eastern side in the case of disturbances. At the beginning of the disturbance Σ rises steeply from small values (up to - 2 days) with periodic pulsations with a duration of 3 to 4 days. At -5 days the dashed E-curve begins already to rise until + 1 day. The following two pulsations run parallel with the sum curve. The difference between the sum curve Σ and the E-curve is negative before the disturbance. This means that after the disturbance the brightness increases in the central zone and on the western side whereas the eastern side dominates up to the key-day (advance of active areas).

In the case of the positive phase the variation is basically different. Except the solid curve, which here again represents the overall brightness, the sum brightness in the central zone and on the western side, which shows a similar variation, is in this case represented by a dashed curve. The two curves show maxima at about - 5 and + 5 days and a sharp minimum at the key-day. As can be seen from the difference of the two curves, there is a certain increase of the eastern-side brightness around the key-day.

We now examine the flare activity in Fig. 6, which is represented by the number of flares with an importance $\geq$ 1+. It is distinguished between the flare activity in the central zone ± 30° around the central meridian (Fl_z) and the flare activity outside of it on the eastern and the western side (Fl_E and Fl_W). The upper curve of the hatched areas represents the total number of flares $Fl = Fl_E + Fl_z + Fl_W$, the lower curve the sum of the flares in the central zone Fl_z and on the western side Fl_W. The hatched area thus is a measure for the number of flares on the eastern side. If it is zero, all flares are situated in the central zone and on the western side. With decreasing width of the hatched area the flare activity shifts to the central zone and to the western side. In 1963 the maximum of the flare frequency is around the key-day at the beginning of the disturbance. In 1964 this maximum has declined, but a few days after the key-day a somewhat larger maximum can still be seen. For 1965 and 1966 the maximum is one day before and one day after the key-day, respectively. As far as it can be recognized, a shift of the flare-frequency to the central and to the western zone seems to be partly responsible for causing the disturbance. The strongest narrowing of the hatched area, which expresses this fact, is in 1963 3 to 5 days before the key-day, 1964 1 day, and in 1966 2 and 5 days before and at the key-day itself. In 1965 during the time of 2 days before the key-day to 1 day after the key-day only central-zone and western-zone flares in large numbers occurred.

In the collective of the positive phases there is a distinct difference with regard to the flare activity. The maximum is 2 days before the key-day, the narrowing of the hatched area already 5 to 6 days before the key-day, i.e. the shift of the activity into the central and the western zone. On the key-day the flare activity has a second minimum. Three days later it increases again, also in the central and western zones, somewhat later than the beginning of the observed moderate earth-magnetic activity.

What part plays the occurrence of flares in the case of disturbances? In the years 1963 to 1966 21 strong and 91 moderate disturbances were evaluated. Among the strong ones 43% were without flares, among the moderate 73%. In a period of +8 days around 112 disturbances from the years 1963 to 1966 63 flares ≥ 1+ occurred in the central zone, 65 on the eastern side and 126 on the western side. In the case of 20 strong positive phases in the same period 47 flares ≥ 1+ occurred in the central zone and 25 in each case on the eastern and on the western side. The large increase of the flares on the western side compared to the eastern side and the central zone is characteristic for disturbances, the symmetry in this regard for positive phases.

Fig. 7a shows the modulation of the daily means of the cosmic-ray intensity (neutron component, mean value of measurements made in Lindau+ and Kiel++ as compared to world wide and local ionospheric disturbances for the years 1963 - 1965. In the disturbance collective after the key-day the Forbush effect can be seen for all years, and for 1963 and 1965 a weaker pre-modulation 2 - 5 days before the key-day [4] . In 1964 this is only indicated as a point of inflection in the curve. With the start of the Forbush effect the world-wide ionospheric disturbance runs parallel. The local drops of $foF2_{min}$ having occurred before and after the key-day are less frequent in 1964 than in 1965, i.e. they increase with increasing solar activity. This is also the case in the pre-modulation of the cosmic rays. Fig. 7b shows the basically different behaviour of the cosmic rays in the case of world-wide positive phase in comparison to the variations of the frequency of local drops in the critical frequencies, which was already described in Fig. 4 and is once more entered in this Fig. There are two maxima for both curves, at 5 to 6 days before the key-day and at 2 to 4 days after the key-day, the latter at the geomagnetic activity which can be seen in Fig. 3.

The modulation of the cosmic rays increases with growing solar activity as can be seen in Fig. 8a by means of a disturbance collective (G ≦ 3) from the year 1966. The 7 strongest disturbances are here not represented by the curve of the daily means, but by their day-to-day difference quotient enlarged by the respective amplitude of the diurnal variation. d) are summed values of the neutron component of Kiel and Lindau, b) are summed values of ionization chambers and scintillators on the Predigtstuhl+++ The solid curve in c) is the ionospheric propagation quality G according to which the key-day is defined. It can be recognized that its course with respect to the positive phases at 6 - 7 days as well as 1 day before the key-day with the intermediate decrease at 3 - 5 days in the above-normal range (G > 6) is very similar to that in the minimum years of the solar activity in Fig. 3. The dashed curve is the earth-magnetic activity Ap, which shows an increase even at 4 days before the key-day. The shape of the curve under a) represents the variation of a receiving field strength at noon on 2.6 MHz (distance approx. 400 km), which can be considered as a measure of the absorption. It shows that the absorption increases shortly before and particularly after the beginning of the disturbance with characteristic variations, an effect, which was already earlier proved statistically. The cosmic rays show - with the exception of the Forbush effect on the key-day in the neutron component - like in the preceding Fig. 7a the mentioned pre-effect more pronounced at - 4 days, in the ionizing component at - 6 days. Both drops can be seen in both cases, the weaker ones are indicated by the decreasing steepness of the rising curve and by a beginning slight decrease, respectively. At -4 to -5 days the magnetic activity occurs. This is obviously a consequence of the positive phase on the -6th and -7th day. The decrease of the ionospheric propagation quality between -5 and -3 days connected with it here, too, occurs only in the above-normal range, i.e. no radio disturbance was observed.

The mean variation of the receiving field strength at noon F on 2.6 MHz (change of absorption in the case of disturbances) which in Fig. 8a (curve a) is represented by superimposed epochs of 7 strong disturbances from the year 1966, is in Fig. 8b for larger collectives of a maximum of 59 disturbances in the years from 1959 to 1961 statistically proved in the scale σ_T (4.5) which is proportional to F. The solid curve shows the variation for all measurement values with interpolation in the case of missing values, the dashed only for complete periods. N gives the distribution of the number of disturbance beginnings in the two collectives. Both curves run almost parallel.

+Max-Planck-Institut für Aeronomie, Institut für Stratosphärenphysik, Lindau/Harz (Max-Planck-Institute for Aeronomy, Institute for Stratospheric Physics, Lindau/Harz)

++Institut für Reine und Angewandte Kernphysik der Universitat Kiel (Institute for Pure and Applied Nuclear Physics of the University Kiel)

+++measuring station of the Fernmeldetechnisches Zentralamt (FTZ), Darmstadt

The decrease of the absorption in the time of 2 - 4 days before the key-day and the increase after the key-day is small on the average, but can appear more distinctly in individual cases.

The following Fig. 9 once more shows the pre-effect of the modulation of the cosmic rays in two disturbance collectives of different times from the years 1962 and 1963. a) shows the ionospheric propagation quality (G), which defines the key-day, together with the earth-magnetic activity Ap. b) shows the modulation of the neutron component in Lindau and on the Zugspitze in collective I and in Lindau and on the Hafelekar+ in collective II. c) shows the course of the corresponding amplitudes of the diurnal variation. In this case, too, it is possible to recognize in all curves the pronounced pre-effect of the cosmic rays and of the ionospheric propagation quality at 3-4 days before the beginning of the disturbance caused by the decrease of the daily means and the increase of the amplitude of the diurnal variation.

These modulation effects and anisotropies which distort the diurnal variation seem to be connected with the - in Fig. 6 described - shift of the flare activity from the eastern side to the central zone and to western side. Statistics on the flare activity from the rotations 1815 - 1823 (1966) indicated that a shift of the flare activity from the eastern side to the central zone and to the western side reduces the upward tendency of the daily means of the cosmic rays. This is shown in Fig. 10 for various measuring sets (U-values for 73 days with flares).

The U-values defined in Fig. 8a mainly describe the change in the steepness of the variation of the daily means and of the distortion occuring in the diurnal variation. From this it can be seen that on the average in the case of eastern-zone flares there is a relatively steep rise for the 4 measuring sets (Mes, N, I K 3, Sc) in the positive range; this rise levels off strongly in the case of central-zone flares and changes into a downward tendency in the case of western-zone flares. In the ionization chamber I K 5, which is only partly shielded, the downward tendency starts already in the case of eastern-zone flares. Only a part of the 73 flares processed in these statistics caused disturbances.

Fig. 11 shows for 1966 the course of solar radio events and of the occurrence of proton flares and of PCA's in the disturbance collective connected with them.

The drift-type IV, the continuum, has a maximum of the frequency one day before the disturbance and a smaller maximum 5 days before the disturbance. Bursts in the meter-wave range indicate a rise of the frequency before and during the disturbance. Proton-flares and PCA's, respectively, have a frequency peak at the beginning of the disturbance and a second smaller one 5 days before it. In the case of one positive phase the larger peak in type IV disappears before the key-day. The maxima at -5 and +2 days increase. The burst activity behaves in a corresponding manner. There are no data on proton-flares in this collective, which goes back to 1963.

In the following Fig. 12 there is in addition the result obtained by H. Wegener (head of the measuring station Predigtstuhl) from superimposed epochs of 30 solar rotations (1811 - 1840, 27/11/65 to 14/2/1968) for neutrons (top left), scintillation (bottom left) and mesons (top right) in comparison to the ionospheric propagation quality G (bottom right, solid curve) and earth magnetic activity A_k (dashed vurve, Observatory Wingst). There seems to be a stable basic component of the mean variation (drop some days after beginning, rise around end of rotation) due to a stable configuration of solar-interplanetary magnetic fi lds in sector structure which is superimposed by further activity events as is indicated by corresponding comparisons with G and A_k. The depression of the cosmic rays (~1%) in the middle part of the solar rotation is reflected by the deterioration of the mean ionospheric propagation quality in about the same part of the rotation. The geomagnetic activity, however, shows the average connection with the course of the disturbance individually around the 5th, 9th, 16th and 23rd day of the rotation. A decrease of the disturbance intensity can be recognized in A_k as well as in G (Bk). A particularly pronounced variation in comparison to the magnetic activity is shown by the meson component.

Fig. 13 shows the relative course of the earth-magnetic activity in the following sub-collectives: rot. 1811 - 1820 (27/11/65 - 23/8/66), rot. 1821 - 1830 (24/8/66 - 20/5/67), rot. 1831 - 1840 (21/5/67 - 14/2/68). It can be recognized how after the sun spot minimum in 1964/65 with growing solar activity the above-described stable configuration of the disturbances becomes increasingly pronounced with the characteristic decrease of the A_k maxima (downward directed scale) in the course of the rotation. In the corresponding sub-collectives of the ionospheric propagation quality and the cosmic rays there is a parallelism with respect to modulation depth and relative amplitude of the "fundamental wave" in the course of the rotation. In the sector structure of the interplanetary magnetic fields (Wilcox and Ness [5]), which was measured by the IMP in 1963, the smallest sector with about 4 days (the other 3 sectors had approx. 8 days) was at the beginning of the rotation. In Figs. 11 and 12 there are also 4 "sectors" - resulting from the earth-magnetic activity - with 4, 7, 7, 9 days, i.e. the smallest sector is here, too, at the beginning of the rotation. The distance of the described characteristic pre-modulations of the positive phases and the cosmic rays before the day of the disturbance (Figs. 3, 7, 8a, 9) was at 6 - 8 and 3 - 5 days, respectively. Since the most disturbances are caused by activity centres of the central zone, these centres appear approx. 7 days before at

+ Physikalisches Institut der Universität Innsbruck
(Institute for Physics of the University Innsbruck)

the eastern limb of the sun. The connections, which here most probably exist with the sector structure, still call for further investigations. In any case it is certain that during the formation of positive phases not only increased UV-radiation of active centres on the sun are involved, but that in many cases also corpuscular emission is observed (Fig. 6) [6] .

As a summary the following results can be derived from the superimposed epochs for the average behaviour of the respective parameters with respect to the ionospheric propagation quality:

1) The frequency of local drops of the night-time critical frequency of the F-layer in mid-latitudes outside times of world radio disturbances (100%) reaches up to 20% and varies with the geomagnetic activity.

2) Positive phases (abnormally wide transmission frequency range at high field strengths) may be followed by a decrease in the above-normal range which can be accompanied by moderate geomagnetic activity, moderately increasing solar activity (flares, solar radio events etc.), local drops of the critical frequency and modulations of the cosmic rays as was found out in 6 different disturbance collectives with a total of 59 disturbances.

3) If the flux of the solar 10 cm-radiation changes by either rising or declining steadily while there is a strong increase in the solar activity, a world-wide radio disturbance can be expected to follow after 3 or 4 days. If, however, the 10 cm - radiation and flare activity which increase during the formation of the positive phase will also show a downward tendency when the positive phase begins to decline (pre-modulation), then the probability is greater that there will be no world-wide radio disturbance. During the subsequent magnetic activity the cosmic ray intensity will increase.

4) The upward tendency of the cosmic ray intensity occurring due to eruptive centres on the eastern side of the sun will be weakened or will turn into a downward tendency, respectively, if these centres are situated in the central zone or on the western side.

5) During the disturbance an increase of the ionospheric absorption is on the average also found to occur after a preceding decrease.

6) Superimposed epochs from 30 solar rotations of the ionospheric propagation quality, the geomagnetic activity and the cosmic ray intensity indicate a relatively rigid course which was probably attributed to the interplanetary magnetic field of the sun. The above-mentioned components run almost parallel with one another and were particularly pronounced around the 9th, 16th and the 23rd day of the rotation. The maximum intensity of the disturbances occurred around the 9th day with the following peaks decreasing.

The method of the superimposed epochs shows the average behaviour of the considered parameters. These are in individual cases pronounced in a different way. It was soon found out that the effectiveness of individual indicators, which were derived from frequency statistics, and of the rules deduced from them vary with the time, e.g. in the course of the sun spot cycle. This is not surprising since always only single events are examined, but they influence one another and the combined effect of all factors has not yet been clarified sufficiently. For these reasons it is - similar as in meteorology - necessary to have critical "selection frequency statistics", i.e. different rules must be according to their starting position checked with respect to their simultaneous concurrence and be included in the assessment of the situation. For each forecast it is therefore necessary to consider the overall situation in detail. The synopsis comprises all important indicators including the 27-day recurrence tendency with its characteristic behaviour in the alternate play between positive phases and disturbances. An important principle in this connection is the sentence: "Similar situations produce similar effects", as long as events cannot be described by more accurate physical laws. The following is an example for this kind of synoptical approach in combination with the results of this paper:

1) If, after a maximum of the plage activity in the central zone and on the western side which is connected with a maximum of the cosmic ray intensity, at local drops of the critical frequency with moderate magnetic activity, rising solar 10 cm-radiation and ionospheric propagation quality, there is a beginning decline of the cosmic ray intensity and the plage activity, perhaps parallel with temporary slightly increasing flare and burst activity, a strong positive phase with very low earth-magnetic activity and strongly decreasing plage activity in the central zone and on the western side can be expected. If plage activity and cosmic ray intensity increase again, a variation (decrease with slight renewed increase) of the ionospheric propagation quality in the above-normal range with moderate magnetic activity and little flare and burst activity (no disturbance of the world-wide ionospheric propagation, only local drops of the critical frequency) follows 2 to 3 days after the maximum of the positive phase.

2) If after a positive phase of the ionospheric propagation quality at little plage activity of the total disk the plage activity on the eastern side increases and the cosmic ray intensity at moderate magnetic activity, perhaps accompanied by

slight flare and burst activity, shows a modulation (temporary drop of the daily mean value with disturbed diurnal variation at enlarged amplitude) parallel with a variation of the ionospheric propagation quality in the above-normal range, 3 or 4 days later after a stronger increase in the plage, flare and burst activities (possibly type IV) and a 10 cm-radiation, which may steadily vary either by rising or by declining, a world-wide radio disturbance occurs whose data can at short notice still be defined more exactly by means of the beginning magnetic storm and the Forbush effect of the cosmic rays as well as by the renewed beginning of the anisotropy effects in the diurnal variation of the cosmic rays.

In this case a synoptical consideration of all available parameters provides the best result. In view of the numerous aspects of the observations and all facts in connection with them it is desired for facilitate and to improve the evaluation of current solar-terrestrial influences by using electronic data processing systems.

R e f e r e n c e s

[1] Beckmann, B. 1954 Kennzeichnung und Vorhersage von Übertragungsbedingungen. (Characterizing and forecast of propagation conditions) Kleinheubacher Berichte 2, 113-12[illegible]

Beckmann, B. 1958 Variable World Days und Funkwetter im ersten Halbjahr des Internationalen Geophysikalischen Jahres. (Variable World Days and propagation conditions in the first half of the International Geophysical Year) Kleinheubacher Berichte 5, 167-170

Beckmann, B.; Ochs, A. 1960 Funkwetter im Internationalen Geophysikalischen Jahr. (Propagation conditions in the International Geophysical Year) Nachrichtentechn. Z. 13, 414-418

Ochs, A.; Beckmann, B. 1963 On the 27 day's recurrence tendency of radio propagation disturbance in the period of high solar activity. "The Effect of Disturbance of Solar Origin on Communications" p. 235-244 published by. G.J. Gassmann, Pergamon Press, London

Ochs, A.; Beckmann, B. 1961 Über die 27tägige Wiederholungsneidung von Funkstörungen in der Zeit hoher Sonnenaktivität. (On the 27-day recurrence tendency of radio disturbances during the time of high solar activity) Kleinheubacher Berichte 8, 115-123

Ochs, A.; Beckmann, B. 1969 Vorhersage für die ionosphärische Kurzwellenausbreitung. (Prediction of the ionospheric short-wave propagation) Jahrbuch des Elektrischen Fernmeldewesens 1969. 281-365.

[2] Beckmann, B. 1968 Einfluss der Ionosphäre auf die Kurzwellenausbreitung. (Influence of the ionosphere on short wave propagation) Rundfunktechnische Mitteilung 12, 156-168.

[3] Solar Geophysical Data 1963-1967 published by CRPL and ESSA

Annals of the IQSY, Vol. 2 Solar and Geophysical Events 1960-1965 compiled by J.V. Lincoln

Daily URSIGRAMS

[4]	Legrand, J.P.	1960	Les prébaisses de rayons cosmiques en périodes de maximum de l'activité solaire (avril 1957 - dézembre 1958). Ann. de Géophys. 16, 140-142
	Caroubalos, C.	1964	Contribution à l'étude de l'activité solaire en relation avec ses effets geophysiques. Ann. Astrophys. 27, 333
	Ehmert, A.	1951	Eine neue Variation der Kosmischen Ultra-Strahlung bei leichten magnetischen Störungen. (A new variation of the cosmic rays at slight magnetic disturbances) Kleinheubacher Berichte 1, 63-65
	Ehmert, A.	1954	Zur kosmischen Strahlung als geophysikalisches Problem. (On cosmic rays as a geophysical problem) Kleinheubacher Berichte 2, 161-166
	Ehmert, A.	1959	Die Intensitätsschwankungen der kosmischen Strahlung. (The variation in the intensity of cosmic rays) Kleinheubacher Berichte 6, 112-124.
	Kirsch, E.	1964	Die Anisotropien der Kosmischen Strahlung. (The anisotropies of the cosmic rays) Mitteilungen aus dem Max-Planck-Institut für Aeronomie Nr. 16
	Miller, H.J.	1968	Zur Modulation der kosmischen Strahlung. (On the modulation of cosmic rays) Mitteilungen aus dem Max-Planck-Institut für Aeronomie Nr. 33
[5]	Wilcox, J.M. Ness, N.F.	1965	A quasi-stationary corotating structure in the interplanetary medium J. Geophys. Res. 70, 5793-5805
[6]	Ma, J.C.	1965	Einfluss der erdmagnetischen Unruhe auf den brauchbaren Frequenzbereich im Kurzwellenverkehr am Rande der Nordlichtzone (Influence of the earth-magnetic activity on the usable frequency range in short-wave traffic at the border of the auroral zone) Mitteilungen aus dem Max-Planck-Institut für Aeronomie Nr. 24.

Captions

Fig. 1

Observations of transmission frequency range USA I (New York, Chatham, June 1967) and prediction.
Thickness of dots (4 steps) between approx. -10 to +10 dB is a measure for the field strength. Solid and dashed curves: field strength according to FTZ prediction, dotted curve: predicted standard MUF.

Fig. 2a

Radio disturbance at solar activity

line 1: date and number of day in the solar rotation

line 2: auroral observations in Enköping (Sweden), earth-magnetic index of Wingst (Hamburg) and Sodankylä (Finland, dashed), ▲ SSC riometer type.

line 3: observations of bursts and storms of the solar radio noise in frequency groups 1 - 7 (<50 MHz up to 10 000 MHz, burst and drift types)

line 4: flares of the importance 1-4 represented by length of arrows (subflares without arrow-head).
X-ray radiation according to satellite measurements (Å-range and intensity)
pfp proton-flare

line 5: SIDs (Sudden Ionospheric Disturbances), "Mögel-Dellinger-effects" (short-wave fade out)
importance = length of arrows pointing in downward direction

line 6: critical frequency of f2-layer (solid curve) and Es-layer (dashed) of station Lindau,
x = foF2 values of station Kiruna (Sweden)

line 7-9: observations of the transmission frequency range by the radio propagation monitoring station in the overseas radio receiving station in Lüchow for the directions USA (East Coast), South America and East Asia in 1 1/2 hour-intervals
a) MOF and LOF
b) mean field strengths of the observed transmission frequency range expressed in S-values according to dashed area: "white" 1.0 to 2.4, | 2.5 to 3.4, || 3.5 to 4.4, ||| 4.5 to 5.4 ■ 5.5 to 9.0
c) BK = band characteristic figure (solid curve), scale: 0-150
d) G = quality figure, scale 2.0 to 9.0

←—— at 12.00 GMT: mean value for daytime period
——→ at 00.00 GMT: mean value for night-time period
---→ at 12.00 GMT: mean value for the whole day

line 10: diurnal variation in field strength of the coastal station Norddeich, 2.6 MHz, measured in Darmstadt (solid curve) and in Lindau (stepped curve). Scale in dB. x, o = absorption values in Breisach (scales C and B) measured by means of vertical sounding.

Fig. 2a1

Behaviour of chromospheric plages based on observations of the Observatory McMath (daily shift of solar maps by 13° corresponding to the solar rotation) for the period from 29 August to 1 September, 1966 according to Fig. 2a;
figures at circles = brightness

Fig. 2a2

Behaviour of spot component and radio emissions of the sun for the period according to Fig. 2a on the basis of observations made by various observatories (letters with figures: Brunner scale and number of single spots, respectively curves = results from strip localization of burst sources in the meter-wave range; in the table: radio noise results from measurements of the cm-wave radiation;
$\frac{W}{m^2 Hz}$ = total flux; 10^4 °K intensity of discrete point sources
ST = station: P = Paris, N = NERA, S = Stanford, Sy = Sydney, B = Berlin, O = Ottawa).

Fig. 2a3

Observations of flares made by various observatories during the period according to Fig. 2a.

Fig. 2b

Positive phase at solar and earth-magnetic activity and locally disturbed ionosphere (drop of the night minimum of foF2).

Fig. 2b1

Behaviour of chromospheric plages based on observations by the Observatory McMath for the period from 25 to 28 September,

1966 according to Fig. 2b.

Fig. 2b2 Behaviour of spot component and radio emissions of the sun in the period according to Fig. 2b.

Fig. 2c Radio disturbance at solar activity at the eastern limb during the time from 13 to 16 March, 1966.

Fig. 2c1 Behaviour of chromospheric plages during the period from 13 to 16 March, 1966 according to Fig. 2c.

Fig. 2c2 Behaviour of spot component and radio emissions during the period according to Fig. 2c.

Fig. 2c3 Observations of flares made by various observatories during the period according to Fig. 2c.

Fig. 3 Mean variation of the ionospheric propagation quality $\overline{G}$ and of the corresponding earth-magnetic activity $\overline{Ap}$ for $\pm$ 8 days around disturbances (key-day 0, collective I strong disturbances, collective II moderate disturbances) and around positive phases from different years (1963 - 1966).

Fig. 4 Mean frequency (P) and values (foF2) of local drops of the night-time critical frequency at disturbances and positive phases according to the collectives and key-days of Fig. 3.

Fig. 5a Mean variation of the 10-cm flux Φ at disturbances and positive phases according to the collectives and key-days of Fig. 3.

Fig. 5b <u>top:</u> mean ionospheric propagation quality $\overline{G}$ for the disturbance collectives I (strong disturbances) and II (moderate disturbances) for 1967,
<u>bottom:</u> corresponding variation of earth-magnetic activity Ap in comparison to the mean variation of the 10-cm radiation for the collectives I + II (Φ, <u>middle</u> part of Fig.)

Fig. 5c Mean variation of the chromospheric plage brightness around disturbances and positive phases defined according to the ionospheric propagation quality, for the total disk Σ and for the eastern side E (central zone $\pm$ 30°).

Fig. 6 Mean variation of the flare activity (importance $\geq$ 1+) at disturbances and positive phases according to the collectives and key-days of Fig. 3. The frequency of the flares is distinguished for the central zone ($\pm$ 30° around CMP) Fl_x, western zone Fl_W and eastern zone Fl_E. The upper curve of the hatched area shows the sum of all flares Fl, the lower (Fl_x + Fl_E). The width of the hatched area corresponds to Fl_E.

Fig. 7a, b Mean variation of the neutron component of the cosmic rays (mean values from Lindau and Kiel) as compared to the frequency P of local drops of the night-time critical frequency of the F-layer (station Lindau) according to the collectives and key-days of Fig. 3.

Fig. 8a Diurnal variation of the cosmic ray intensity represented by $U = \text{sign}(T-T_v)(|T-T_v| + S)$ (T = daily mean of the current day, T_v = daily mean value of the preceding day, S = day amplitude = difference between second highest and second lowest 2-hour value) for the disturbance collective I of the year 1966. N = number of disturbance beginnings
a) variation in ionospheric absorption, represented by summed noon field strength of the coastal station Norddeich (DAN) on 2.6 MHz at a distance of 420 km (Darmstadt, FTZ)
b) variation of the summed values of the ionizing component ΣU_{Pr} of the measuring station Predigtstuhl of the FTZ (ionization chamber and scintillator)
c) variation of the ionospheric propagation quality G (solid curve) and of the earth-magnetic activity Ap (dashed curve)
d) variation of the summed values of the neutron component in Kiel and Lindau ΣU_{KL}

Fig. 8b Mean variation of ionospheric absorption for $\pm$ 5 days around the key-day 0 (beginning of disturbance), derived from superimposed epochs of disturbances from the years 1958 - 1961.

$\frac{G_T}{4.5}$ = relative noon field strength of the coastal station Norddeich (DAN) on 2.6 MHz measured at a distance of 420 km (FTZ, Darmstadt).
Key-days defined according to the ionospheric propagation quality G in the direction North America (USA)

N number of disturbance beginnings in both collectives (total of 54 disturbances)

Fig. 9

Mean variation of the modulation of the cosmic rays caused by solar influences for ± 5 days around the key-day for the disturbance collectives I (21 June, 1961 - 24 July, 1962) and II (6 April, 1962 - 5 April, 1963) each of them containing 11 strong disturbances of the ionospheric propagation.
a) mean variation of the ionospheric propagation quality G and of the earth-magnetic activity Ap
b) mean variation of the daily mean values of the neutron component in Lindau (Harz) (Li_I and Li_{II}) and on the Zugspitze (Zu_I), and the ionizing component on the Hafelekar (Ha_{II}).
c) S = mean amplitude of the diurnal variations of the neutron component (see definition in Fig. 8a).

Fig. 10

Concerning the modulation of the cosmic rays caused by solar activity centres (flare areas) in the central zone, eastern and western side; (definition of U see Fig. 8a)

N = neutron component in Lindau (Harz) (IQSY monitor) (telescope = 0.25 m^2, 10 cm Pb)
Mes = meson component in Kranzbach near Klais (1020 m above sea level)
ionization chamber 25 l (from all sides shielded with 5 cm Pb)
ionization chamber 50 l (only shielded at sides and bottom)
2 NaJ scintillators (∅ 5 inches, spectral range > 2.5 MeV)
I K 3, I K 5, Sc Predigtstuhl, (1614 m above sea level)

Fig. 11

Frequency of occurrence of radio-noise events (Ra % and proton flares (PFI and PCA, respectively) at 44 radio disturbances in the year 1966.

Fig. 12

Mean variation of 30 solar rotation (1965 - 1968) of the cosmic ray intensity (top left: neutron component, Lindau, bottom left: ionizing component Predigtstuhl, top right: meson component Kranzbach) in comparison to the earth-magnetic activity (A_K Wingst, bottom right, dashed curve) and the ionospheric propagation quality ($G = 6 \cdot BK_T$, bottom right: solid curve) for the direction North America (USA).

Fig. 13

Mean earth-magnetic variation (A_K) for the given solar rotations (subcollectives of Fig. 12, relative scale, length of left arrow = 3.5 A_K).

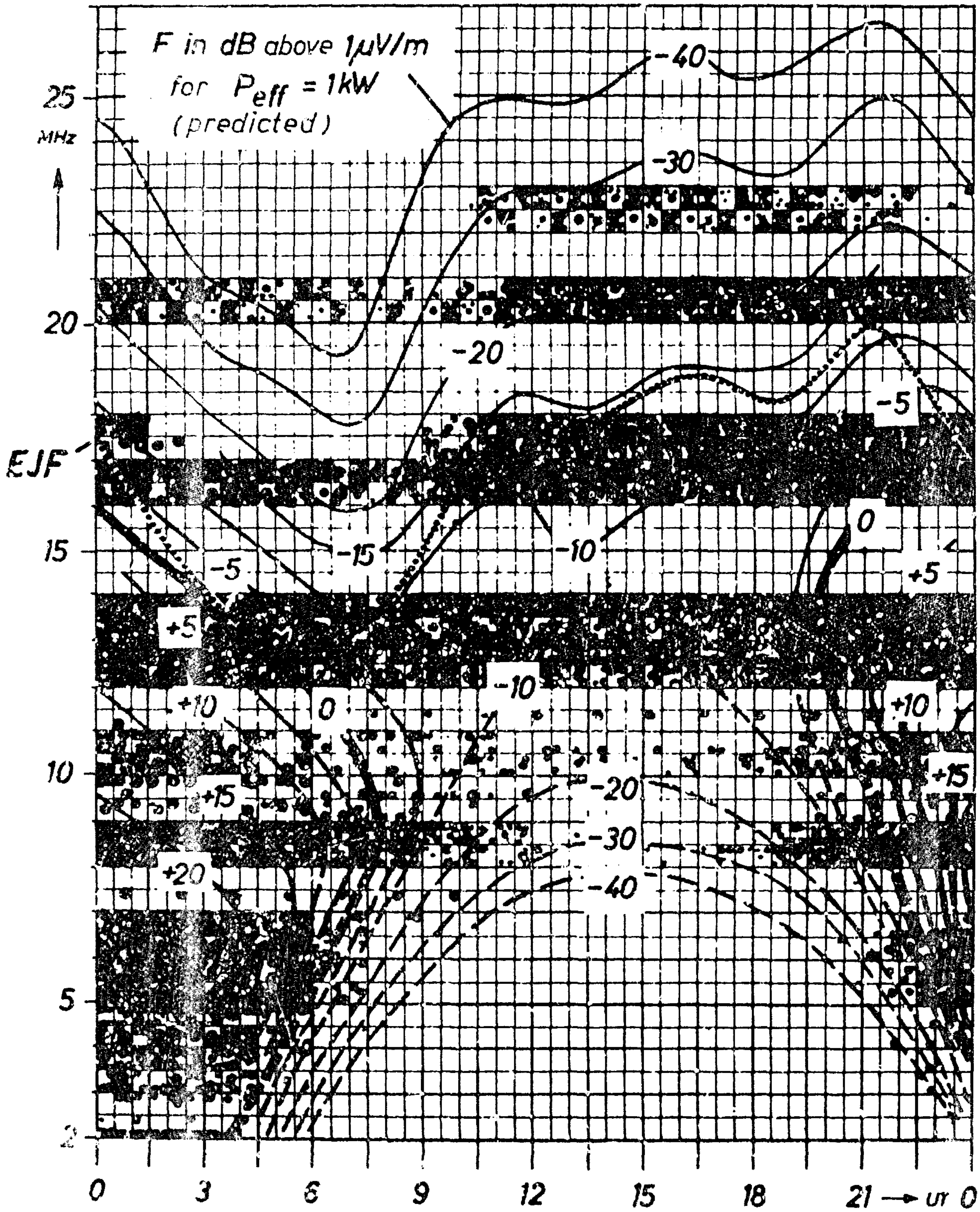
F in dB above 1μV/m
for P_{eff} = 1kW
(predicted)
MHz
EJF
-40
-30
-20
-15
-10
-5
0
+5
+10
+15
+20
25
20
15
10
5
2
0
3
6
9
12
15
18
21 → UT 0

FIGURE 1

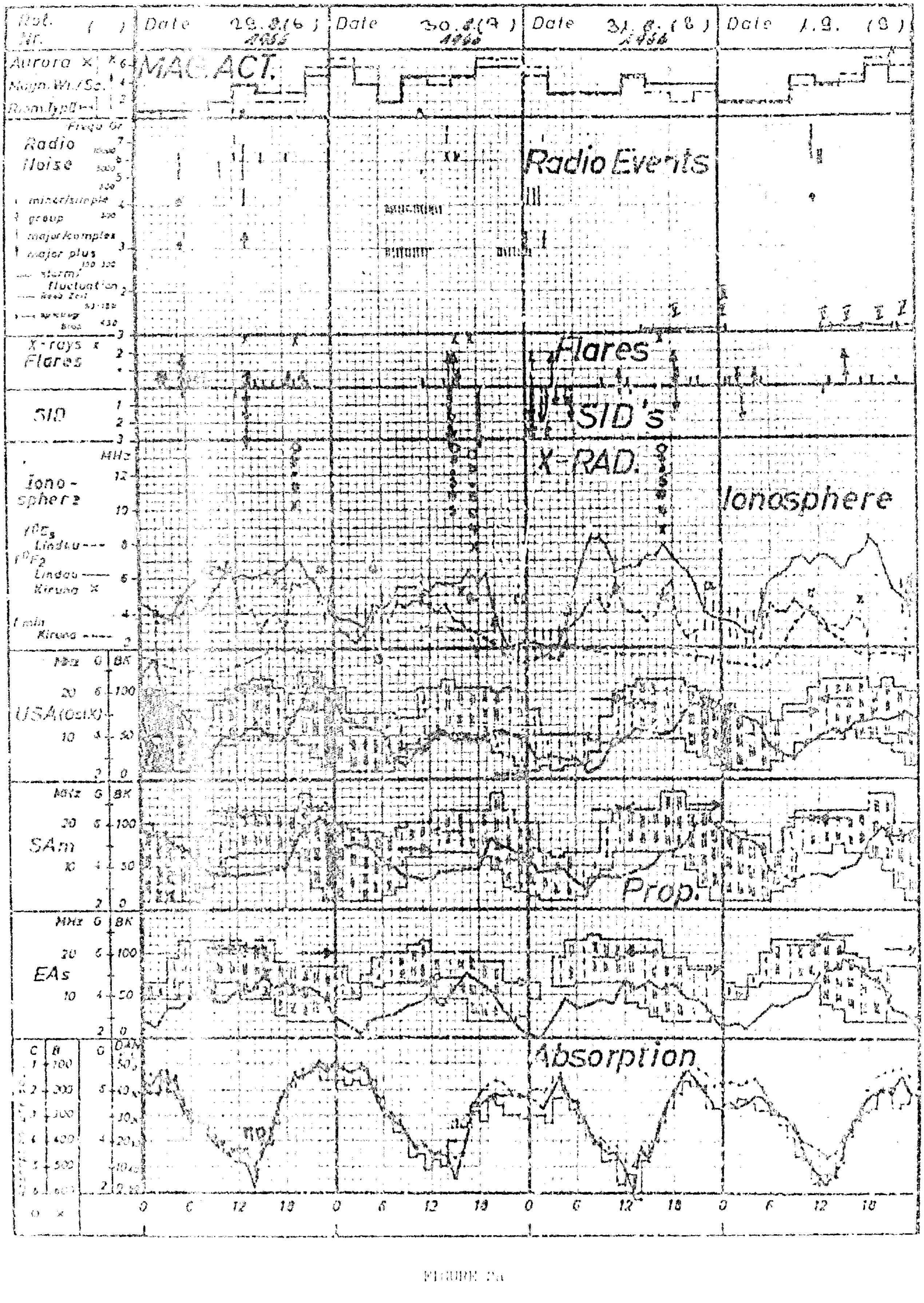
MAG. ACT.
Radio Events
Flares
SID's
X-RAD.
Ionosphere
Prop.
Absorption
Aurora
Radio Noise
X-rays
Flares
SID
Ionosphere
USA
SAm
EAs
MHz
BK
Date 29.8.
Date 30.8.
Date 31.8.
Date 1.9.

FIGURE 2a

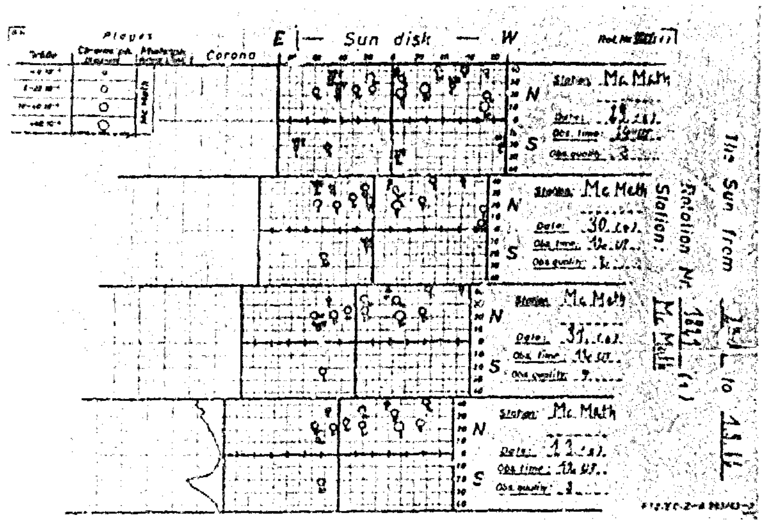

FIGURE 2a1

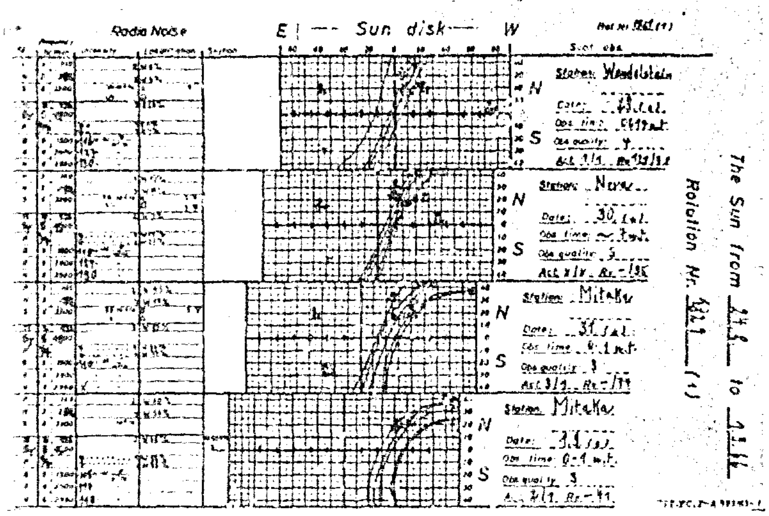

FIGURE 2a2

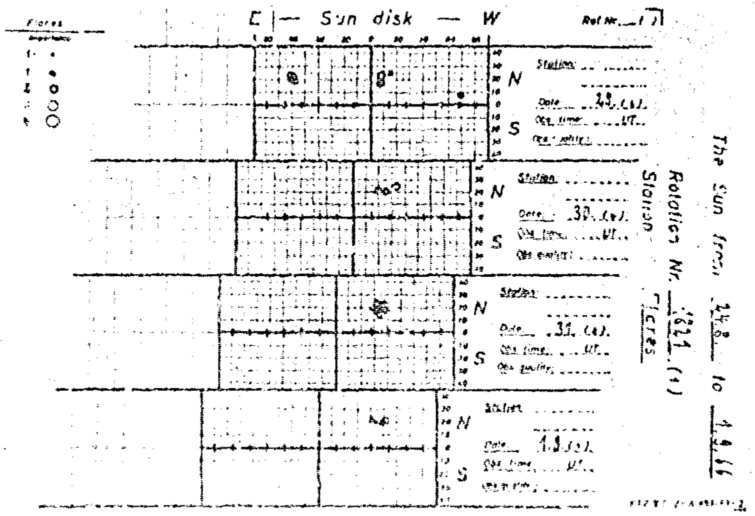

FIGURE 2a3

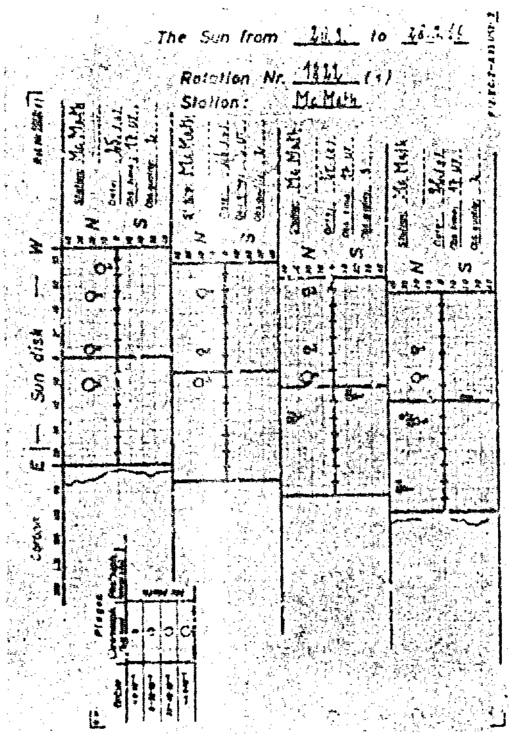

FIGURE 2b1

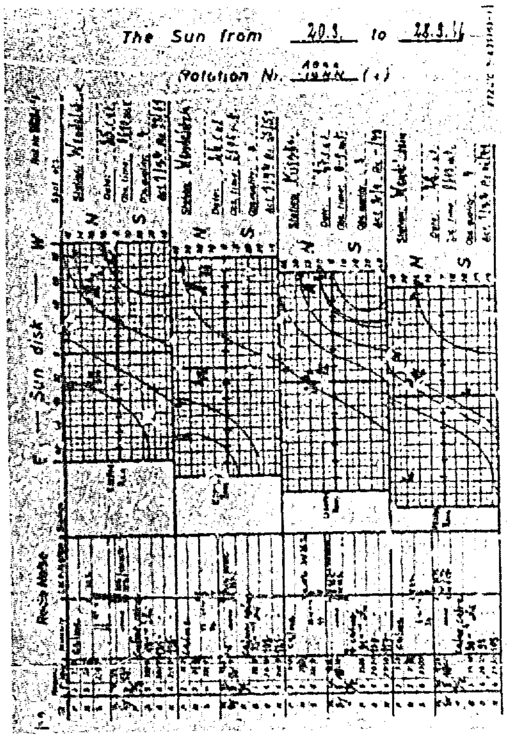

FIGURE 2b2

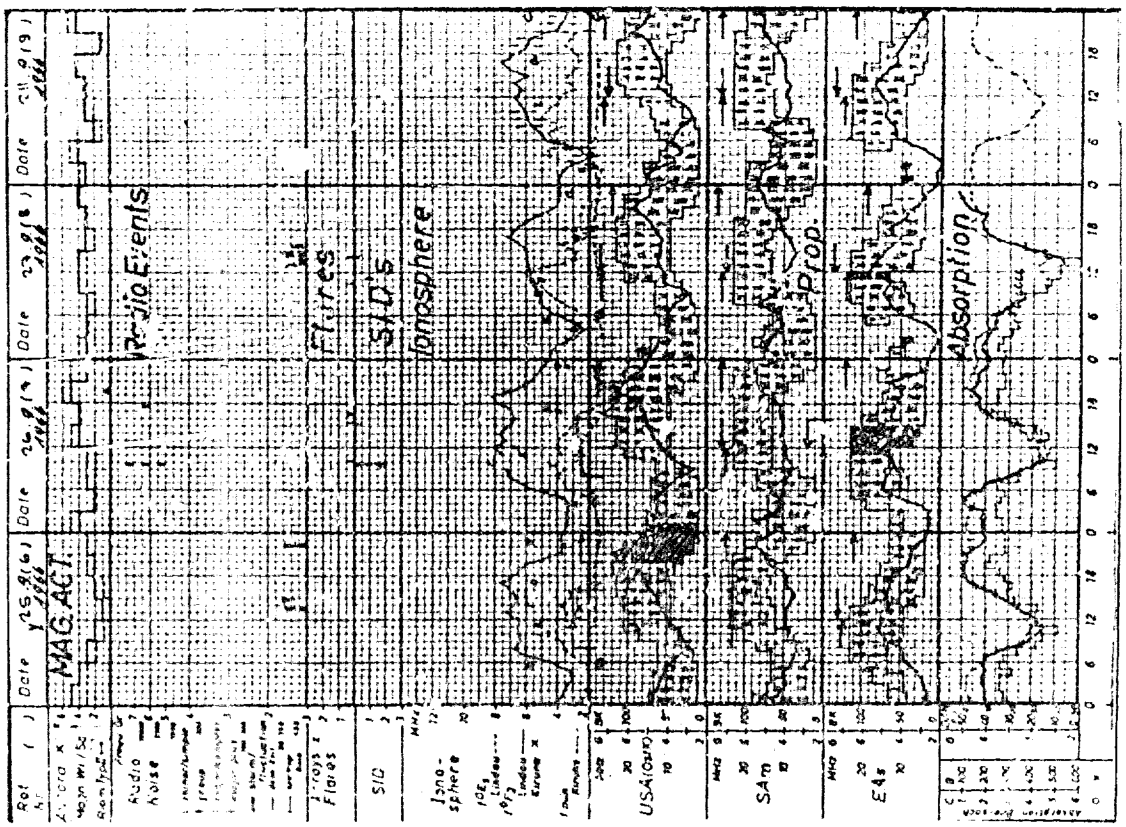

FIGURE 2b

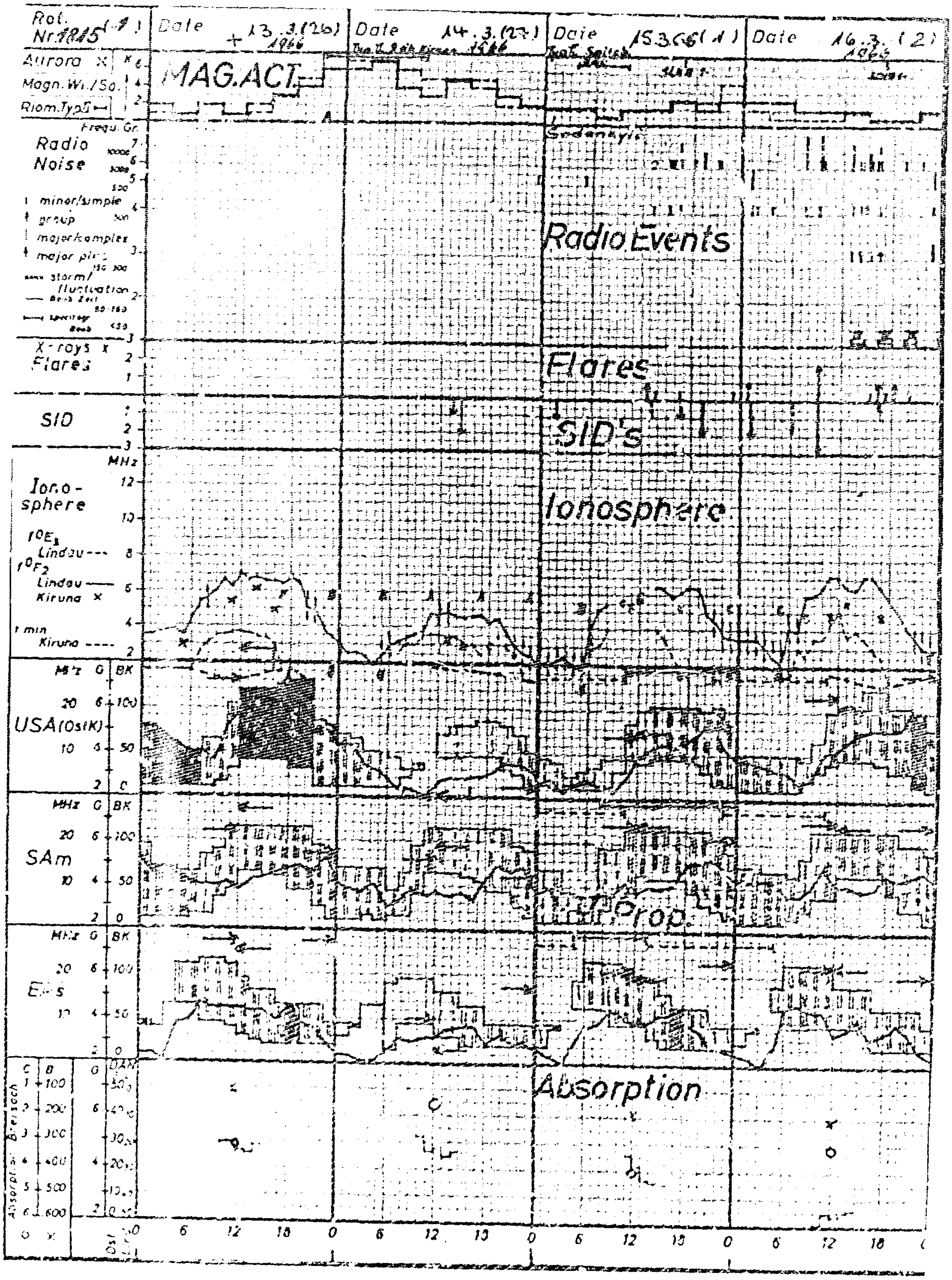
Rot. Nr. 1815
Date 13.3.(26) 1966
Date 14.3.(27) 1966
Date 15.3.66(1)
Date 16.3.(2) 1966
Aurora
Magn. Wi./So.
Riom. Typ II
MAG.ACT.
Radio Noise
Radio Events
X-rays
Flares
SID
SID's
Ionosphere
USA(OstK)
SAm
Prop.
Absorption

FIGURE 2c

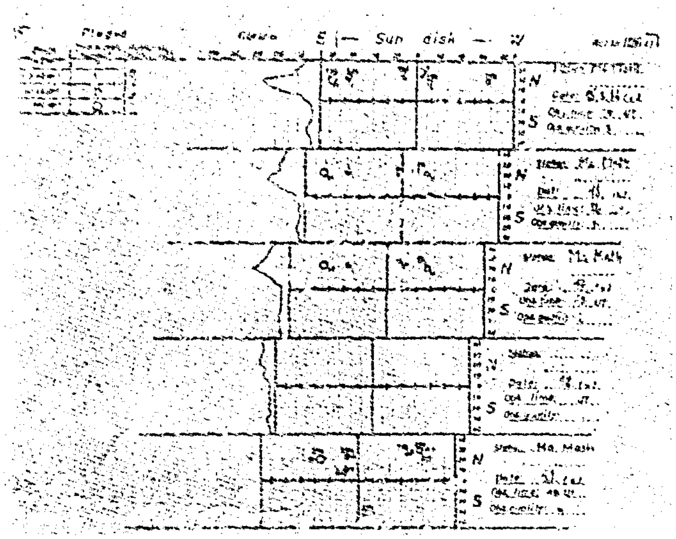

FIGURE 2c1

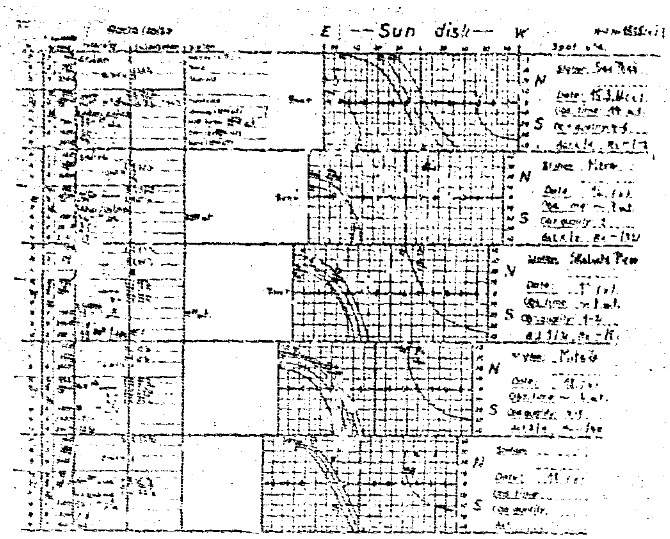

FIGURE 2c2

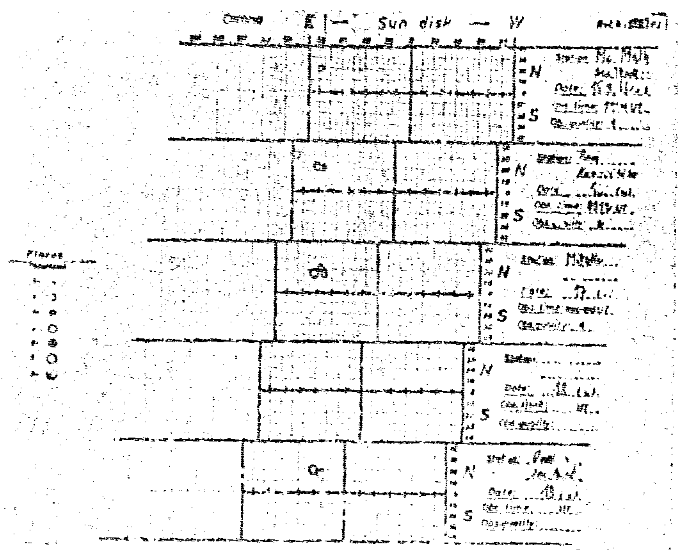

FIGURE 2c3

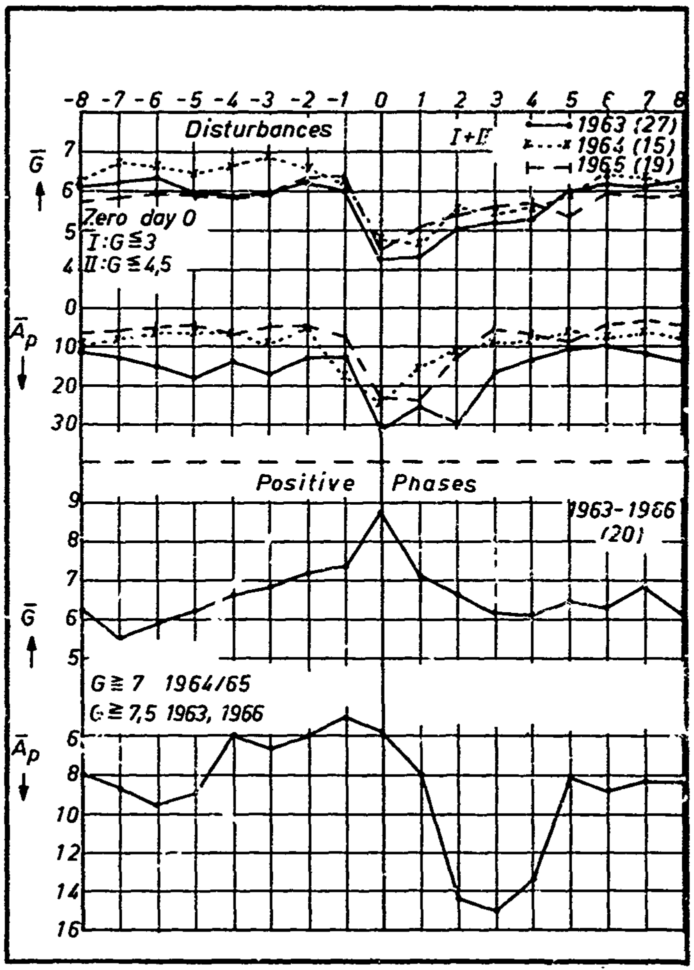

FIGURE 3

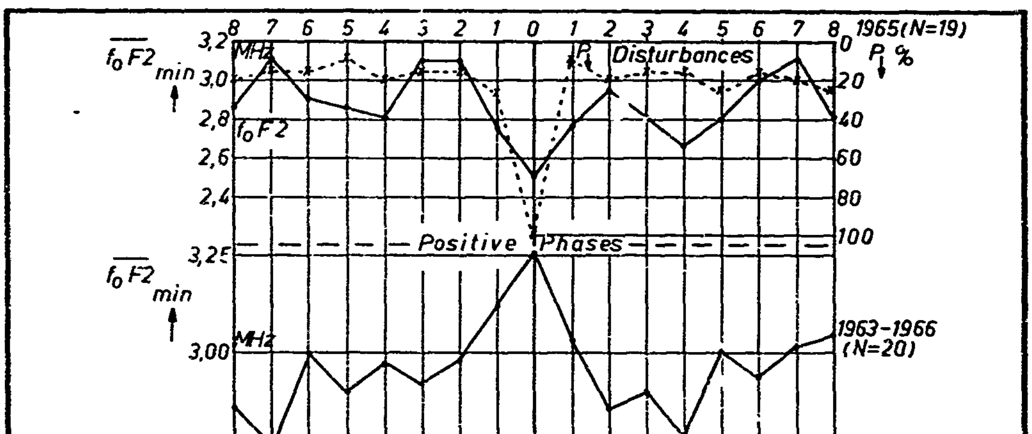

FIGURE 4

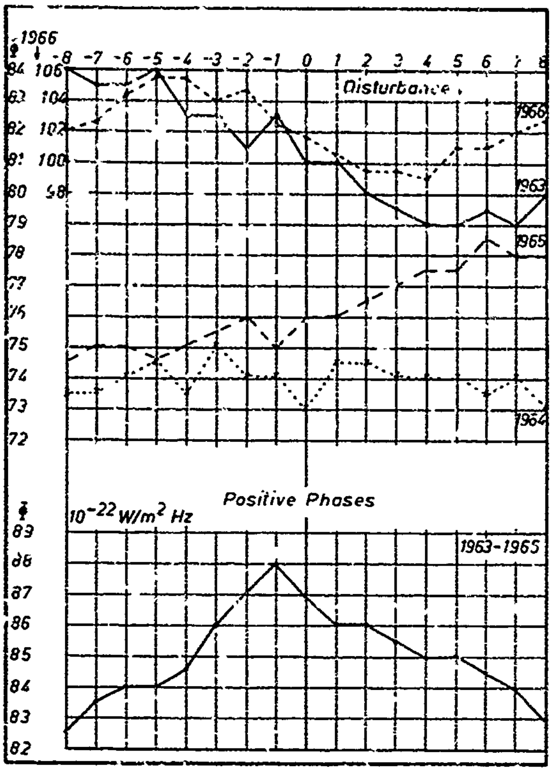

FIGURE 5a

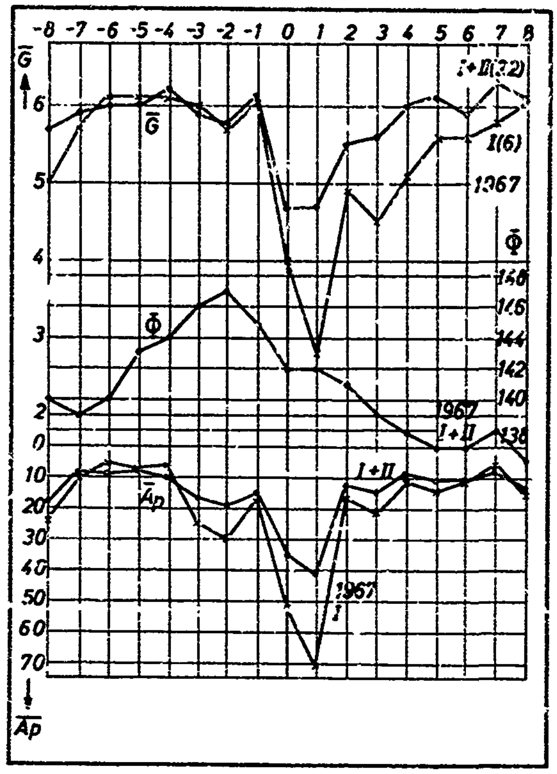

FIGURE 5b

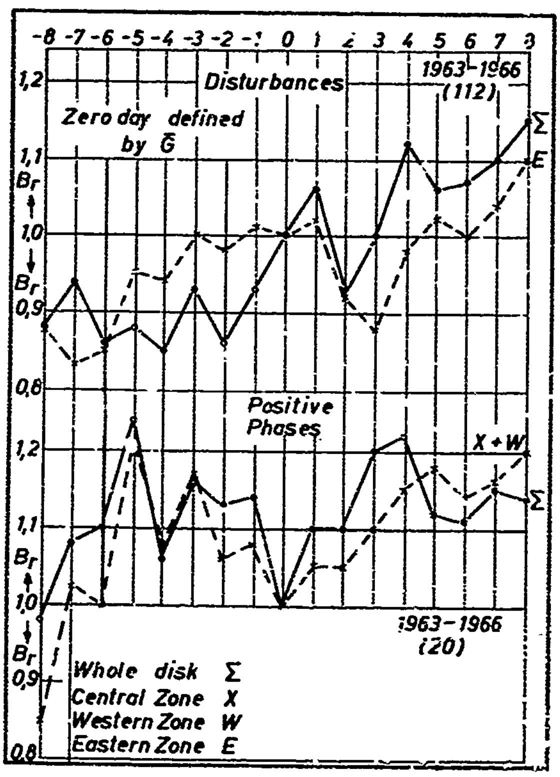

FIGURE 5c

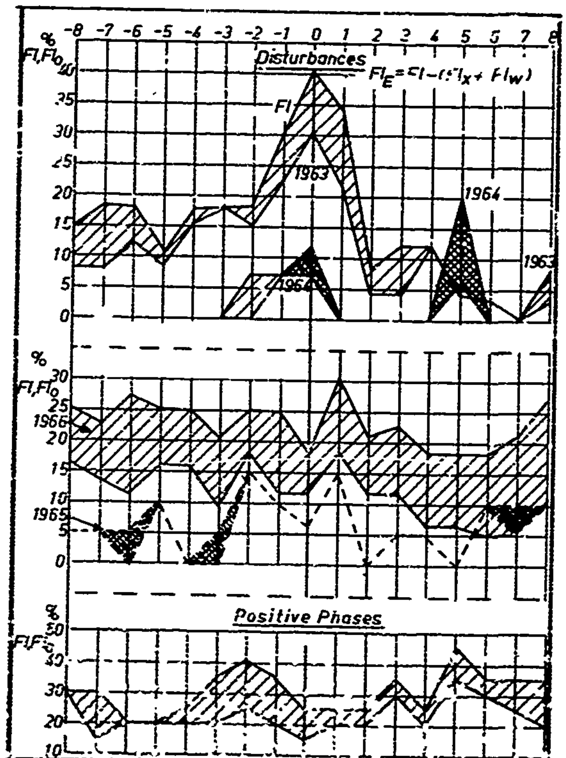

FIGURE 5

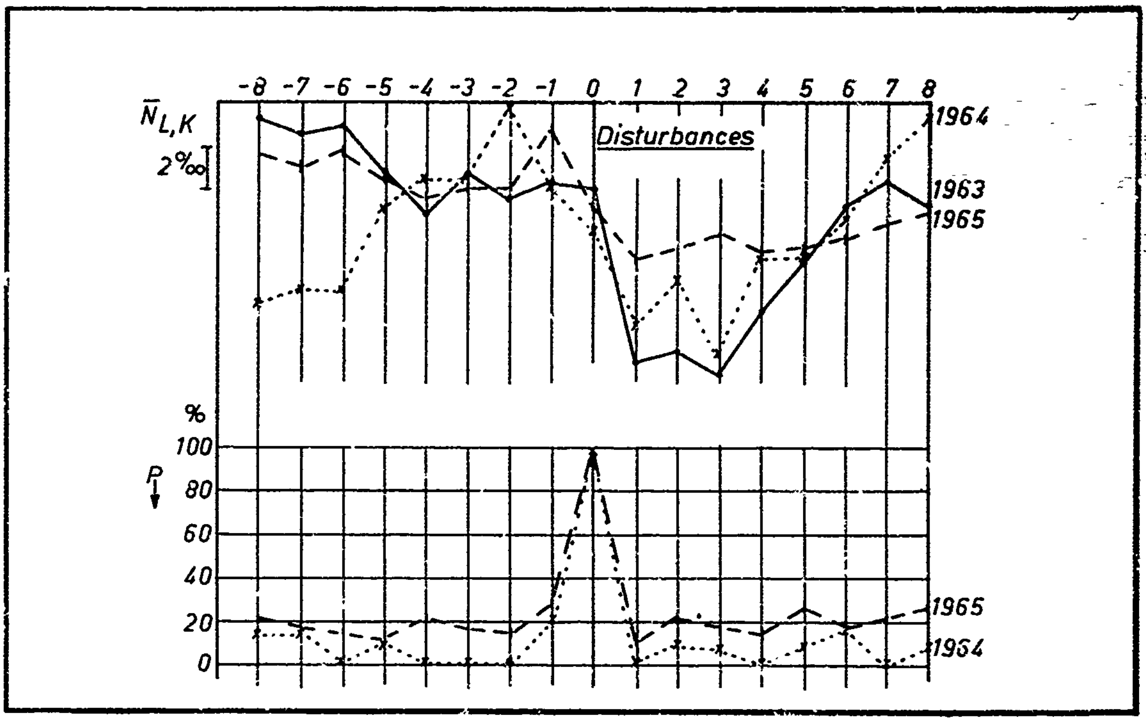

FIGURE 7a

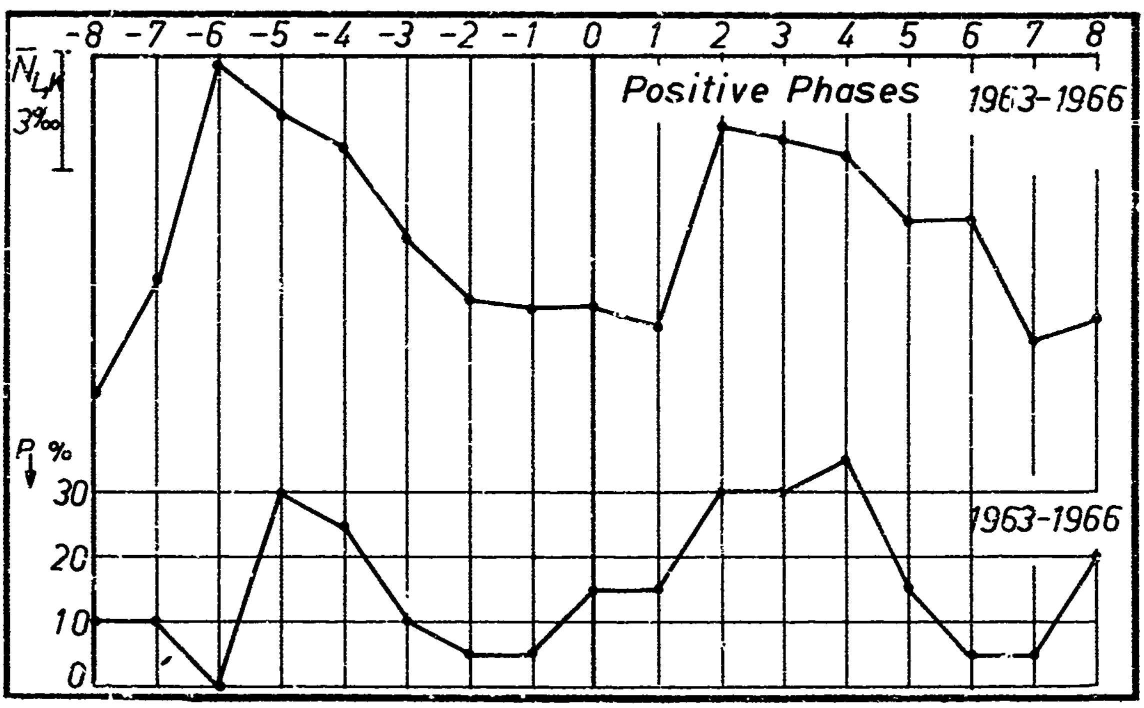

FIGURE 7b

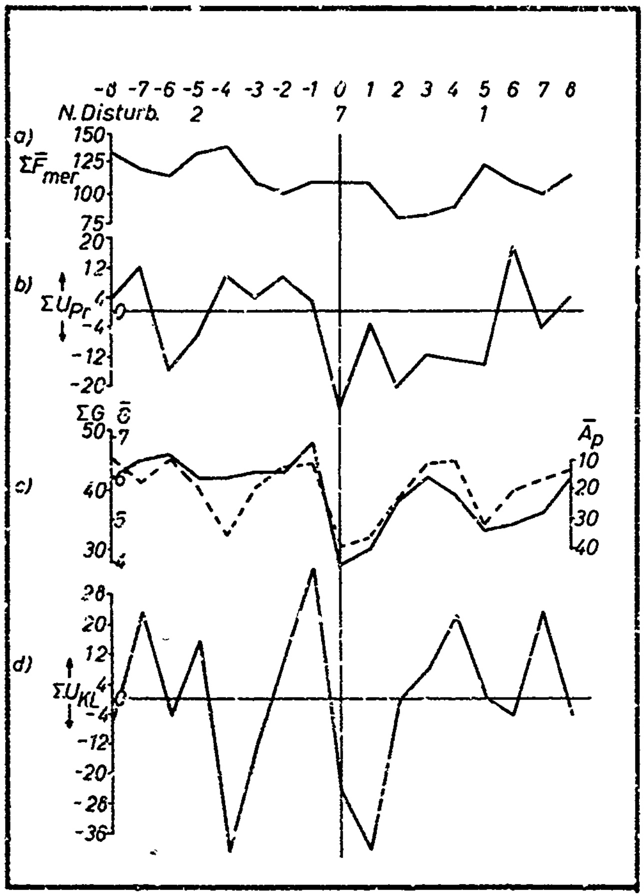

FIGURE 8a

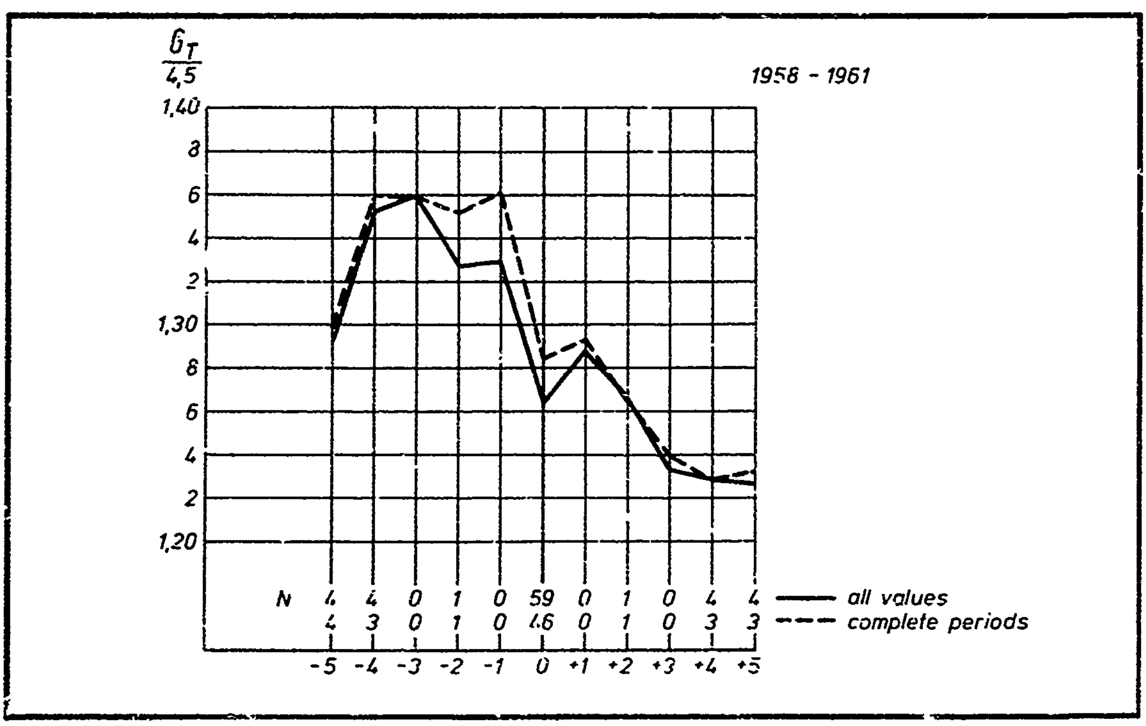

FIGURE 8b

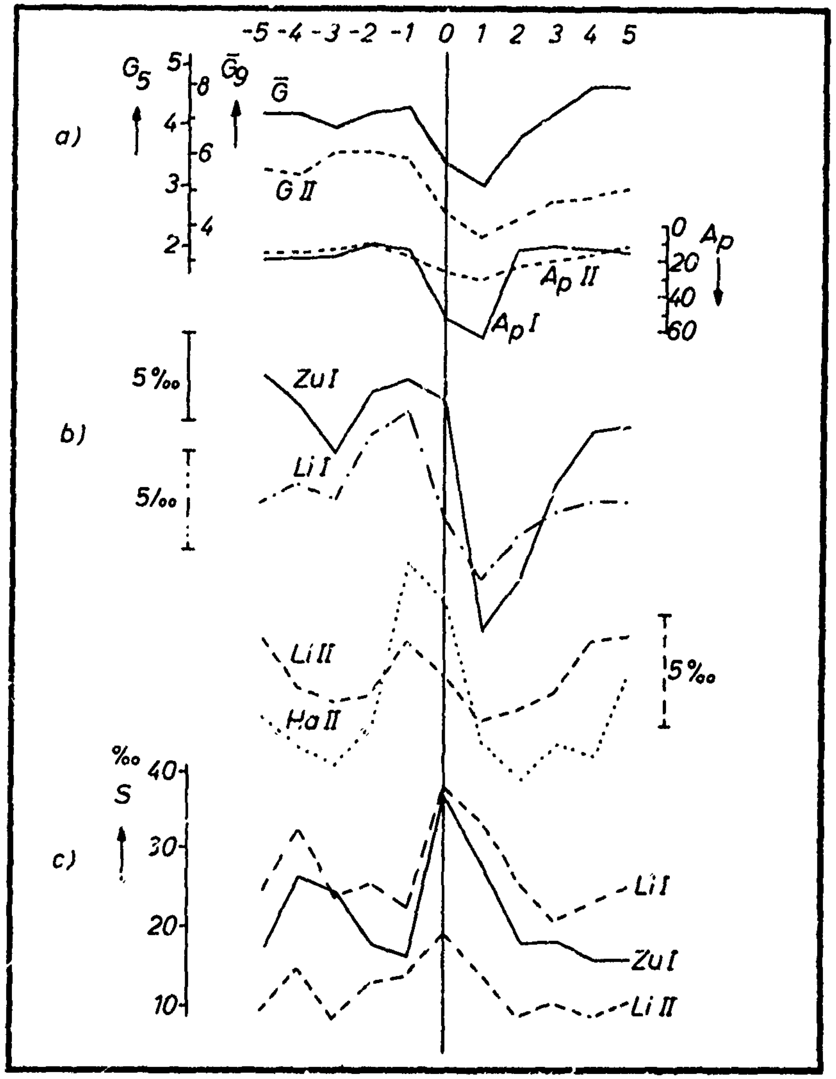

FIGURE 9

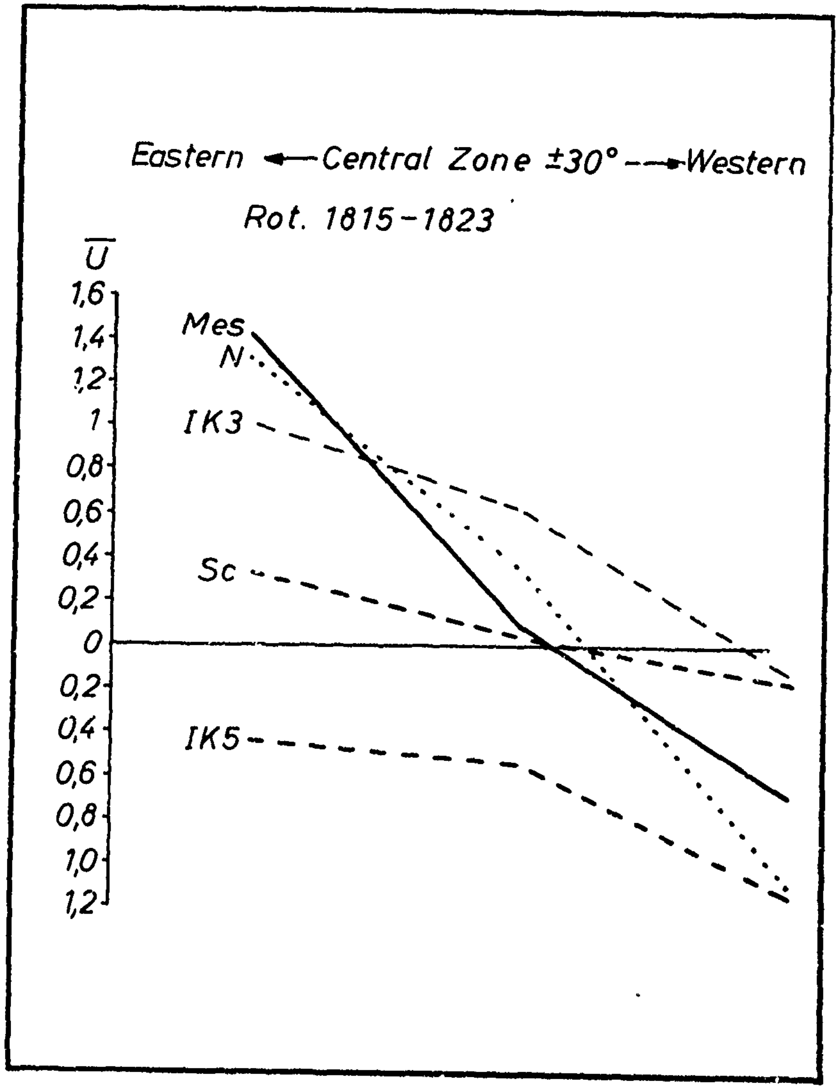

FIGURE 10

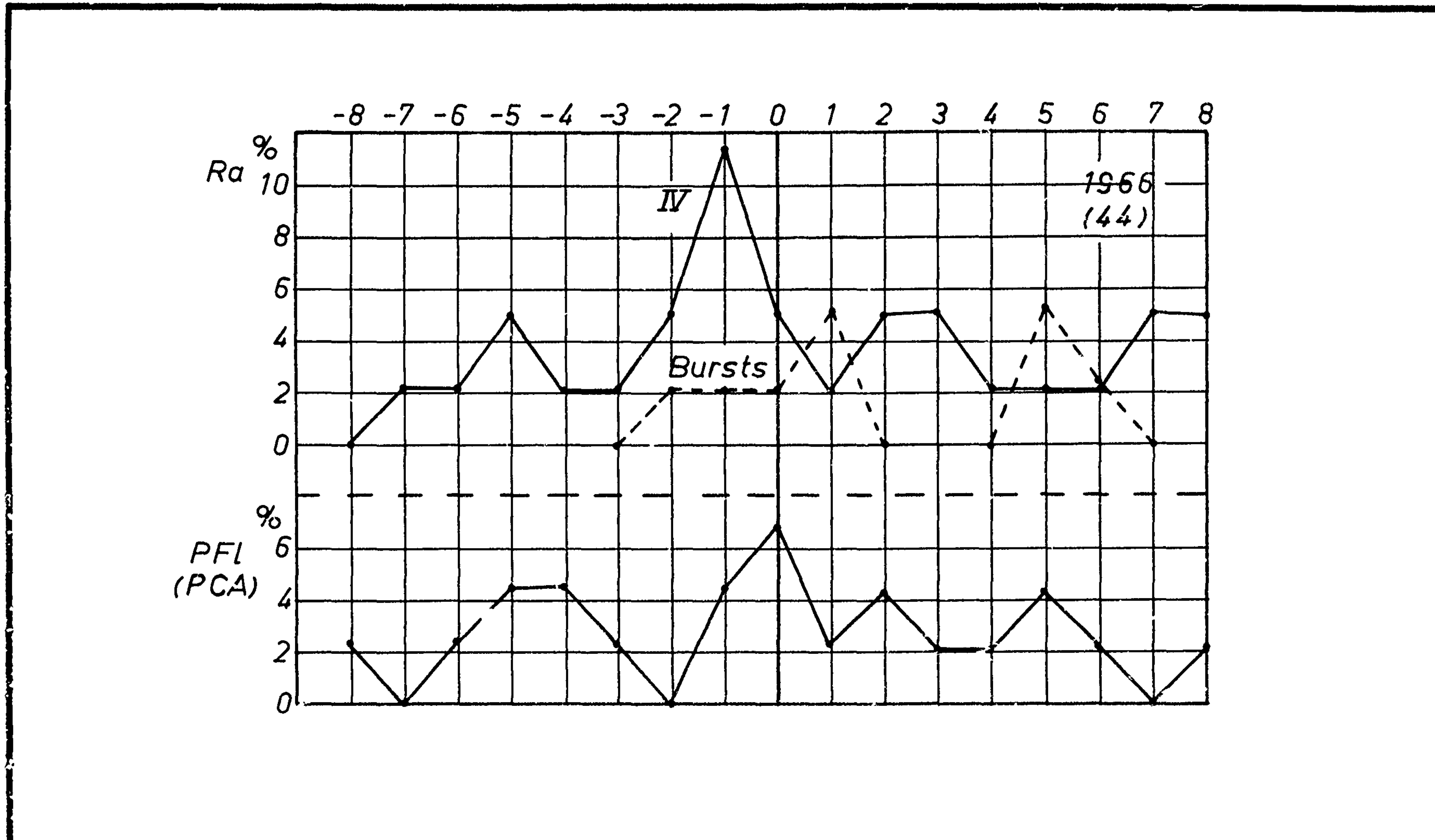
-8 -7 -6 -5 -4 -3 -2 -1 0 1 2 3 4 5 6 7 8
%
Ra
10
8
6
4
2
0
IV
Bursts
1966
(44)
%
PFL
(PCA)
6
4
2
0

FIGURE 11

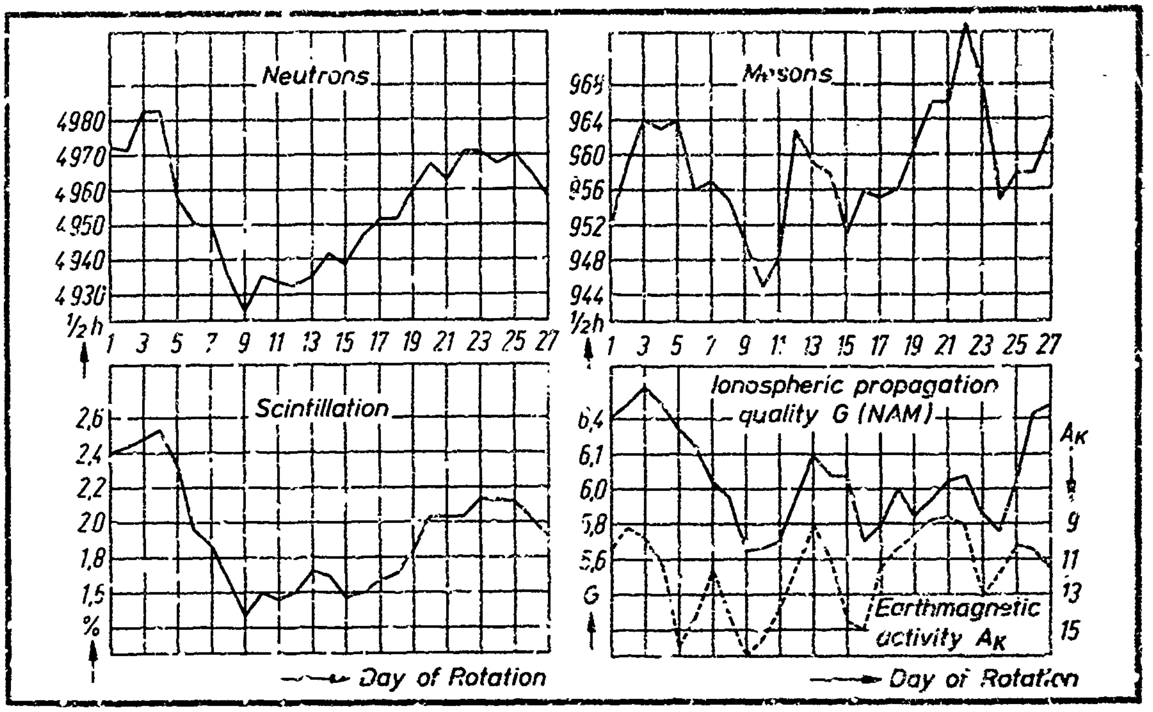

FIGURE 12

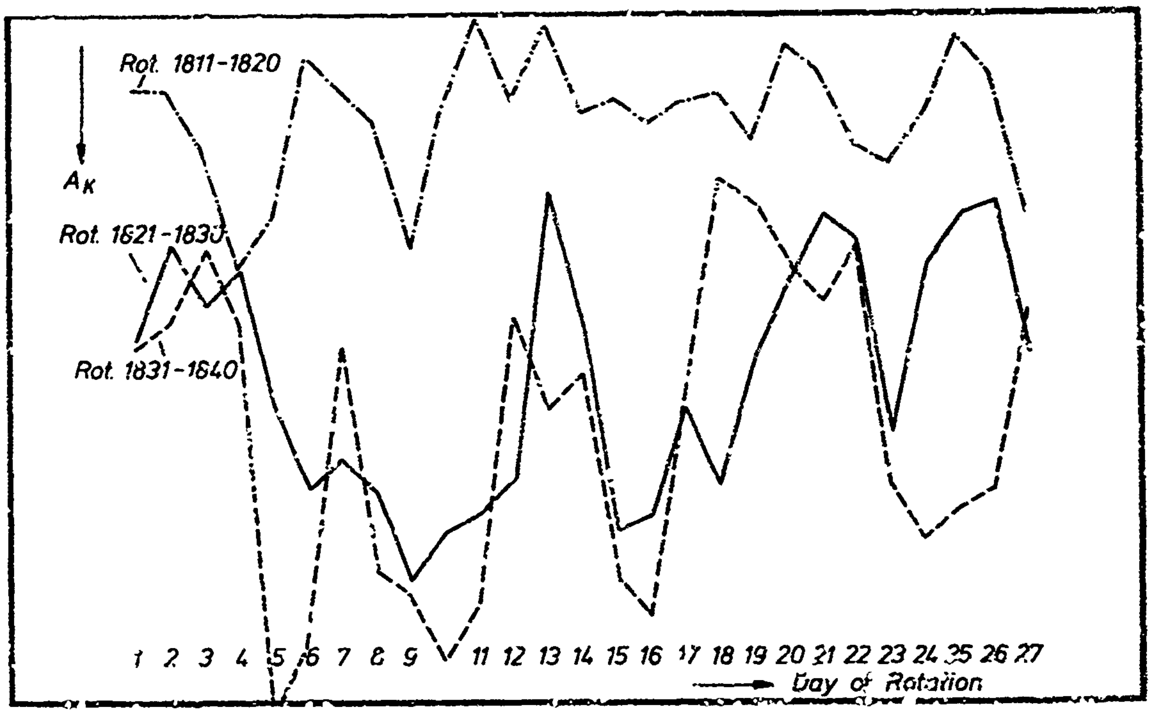

FIGURE 13

USAF SOLAR FORECAST FACILITY IONOSPHERIC SERVICES

by

Major T. D. Damon, USAF
4th Weather Wing
Ent Air Force Base
Colorado 80912

USAF Solar Forecast Facility Ionospheric Services

T. D. Damon*

Summary

Ionospheric services provided by the USAF Solar Forecast Center include rapid alerting of the onset of sudden ionospheric disturbances, and daily predictions of MUF and LUF for specific paths. Modern military communications systems allow rapid alerting of the onset of ionospheric disturbances, such as SWF, before the end of the disturbance, thus providing operationally useful information to the communicators. MUF and LUF forecasts are daily modifications of climatological predictions.

A group at Detachment 7, 4th Weather Wing, develops and improves forecasting techniques in response to military requirements. Efforts are being made to obtain more real-time VI sounder observations for use in day-to-day forecasting.

*Major, USAF, Technical Development Officer, Detachment 7, 4th Weather Wing, Ent Air Force Base, Colorado 80912.

Ionospheric services of the USAF Solar Forecast Facility fall into two categories: (1) rapid alerting of the onset of an ionospheric disturbance, and (2) prediction of MUF and LUF for specific paths.

Rapid Alerting: The real-time reporting capability of the solar observing network and communications network now enables us to warn communicators of the onset of a short wave fade (SWF) within minutes. In most cases of major SWF, the solar flare responsible for the fadeout is seen visually in H α a few minutes before the ionosphere responds. Thus we are often able to advise the communicator of such a disturbance before his circuits actually begin to fade significantly.

From optical observations alone it is not possible to tell conclusively whether a given solar flare will produce a SWF, but one of the first warnings we have of a possible SWF is the optical observation. Since SWF are produced by the X-rays from the flares, we have studied the optical characteristics of flares associated with 93 solar X-ray bursts observed by Explorers 33 and 35 from July 1966 to July 1968. Each event produced greater than ten-fold increase over background in the 2Å to 12Å band. Only 87 could be correlated with optical flares. The remaining six were apparently caused by flares occurring beyond the limb with X-rays emitted from the corona high above the flare region. Results are shown in Table 1. Note that the size (importance) of the flare is not particularly definitive since Importance 2 and 3 flares are relatively rare. However, the brightness of the flare is of considerable importance in determining the presence of X-rays. Also, large X-ray events appear to occur more frequently near the limb than near the center of the disk.

OPTICAL SOLAR FLARES RELATED TO X-RAY EVENTS

Jul 66 to Jul 68 (93 Total Events*)

Importance (Size)

	0	1	2	3	4
Number	10	45	24	8	0
Percent of Total	11	52	28	9	0

Brightness

	Faint	Normal	Brilliant
Number	1	30	56
Percent of Total	1	35	64

Optical Features

a) Two or more brilliant points 44 (51%)

b) Several eruptive centers 38 (44%)

c) a or b 61 (70%)

Solar Longitudinal Distribution

Increase in X-ray Flux	90E-30E	30E-30W	30W-90W	Beyond Limb
≥10X	33	28	25	6
≥20X	13	5	11	0
≥50X	3	1	4	0

*6 events not correlated with optical observations.

Table 1

Our forecasters use these statistics for a real-time evaluation of whether a SWF is likely to be associated with the optical flare. Additional data arrive at the Forecast Center almost immediately to help the forecaster decide whether a SWF is likely. Large microwave solar radio bursts indicate that the flare is very energetic and that hard X-ray emission is probable. Actual measurements of X-ray flux from Vela satellite sensors are most definitive. When the flux exceeds 10^{-3} ergs/cm^2 sec in the .5Å to 5Å sensors, we can be confident that a SWF is in progress.

The forecaster evaluates these optical, radio, and satellite observations and subjectively predicts the duration of the fadeout. He then telephones his prediction to the customers. The USAF weather communications system allows this entire sequence of events to take place within a few minutes.

For example, Eastern Test Range provides prime communications during Apollo flights. On March 12, 1969, during the Apollo IX mission, a major solar flare occurred, accompanied by an X-ray burst and a short-wave fadeout. The sequence of events is shown in Table 2. The importance of this service was pointed up by the actions taken by the NCS. On being notified of the onset of the solar flare, he switched high-priority circuits to a satellite and boosted one HF circuit to maximum power to send a message down range telling all stations to standby. Thus, when the SWF ended, all stations were still on frequency and communications were restored immediately. Without the information provided, the communicators would have begun "twirling knobs" in a fruitless attempt to restore communications and all stations would have been on different frequencies when the fadeout ended. Additional time would have been required to get back together.

SHORT WAVE FADEOUT OF 12 MARCH 1969

1735Z	FLARE BEGAN
1743Z	SFC NOTIFIED OF FLARE
1745Z	SFC ADVISED NCS - SWF JUST BEGINNING
1745-1752Z	ADDITIONAL DATA RECEIVED AT SFC
1752Z	PREDICTED RECOVERY BETWEEN 1815Z and 1820Z
1817Z	CIRCUITS RESTORED

Table 2

We also provide warnings of the occurrence of geomagnetic storms and solar proton (PCA) events. Since the ionospheric effects associated with these disturbances are more gradual in their onset, the forecasters have more time to react.

MUF-LUF Forecasts: In predicting MUF and LUF we use a three-step process:

1) Average MUF and LUF for a two-week period are predicted a week or so in advance.

2) Deviations from those average conditions are predicted for each hour, twenty-four hours in advance.

3) The twenty-four hour forecasts are revised as necessary.

Two-week average predictions are based on climatology. The monthly median predictions produced by ESSA are used in a computer program first developed by ESSA researchers and later modified somewhat. Since a marked discontinuity occurs in the ESSA predictions on the first of each month, the monthly median is used only for the middle two weeks, and two months are averaged to obtain a prediction for the last week of one month and the first week of the following month. These predictions are the first estimate. We modify them on the basis of our experience with the particular circuit, using propagation reports from the operator and path sounder data, where available. For example, we know that on certain long paths the median MUF predictions are too low, and the forecaster takes that into account in preparing the final two-week base-line predictions. A sample forecast is shown in Figure 1. The customers use these base-line predictions in setting up their operating schedules for the two-week period.

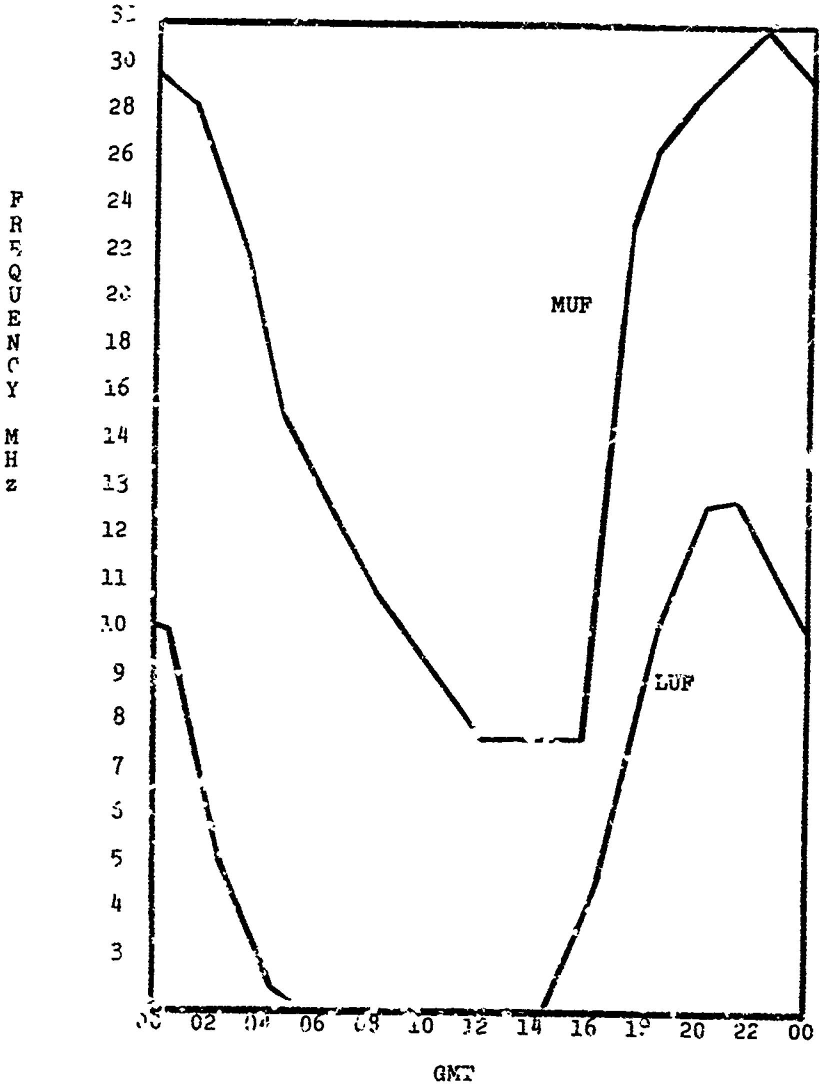

FORECAST FOR 9-22 Nov 68

CIRCUIT Hawaii to Southern California

Figure 1

The daily forecasts are essentially modifications or revisions of the two-week predictions. A sample is shown in Figure 2. The customers examine each daily forecast to determine whether it is necessary to adjust their operating schedule for that day. The forecasts are given as numbers of megahertz above or below the two-week base-line for each hour of the twenty-four. They are mainly subjective, based on all the data available at the Solar Forecast Center. Many "rules-of-thumb" have been developed. Some of them are well known and have been reported in the literature; e.g., the reduction in MUF during an iono-magnetic storm. Others, are newer and are still being evaluated; e.g., when the geomagnetic field is quiet and the 2800 MHz solar flux is at or above the 27-day running mean and is increasing, the MUF will increase by 10 to 20%; if this continues for two or three days, the MUF can increase by as much as 30%; the converse is not necessarily true.

FORECAST FOR Hawaii to Southern California

VALID DATE 18 Nov 68

LUF	0100-0300Z	+2
	0300-0500Z	+1
MUF	0000-0400Z	-2
	1500-1700Z	-1
	1800-0000Z	-3

Figure 2

Some of the most important data available to the forecaster for his daily forecasts comes from vertical incidence sounders. These data enable us to define the state of the ionosphere directly rather than through inferences from solar and geomagnetic data. From the international URSIGRAM data exchange and from various other sources, VI sounder observations reach the Solar Forecast Center daily. The percent deviation from the predicted median value is calculated for each observation. These deviations often form persistent synoptic patterns which the forecaster is able to analyze and follow for several days. Some patterns are associated with iono-magnetic storms while others cannot be associated with any solar or geomagnetic phenomena. Because they often persist for several days, we use these patterns in our routine forecasting, even when we do not understand their causes.

A technical development unit has recently been organized in 4th Weather Wing for improving our capability to provide ionospheric services. A major effort of this group is to examine the forecasting "rules-of-thumb" objectively so that the forecasting can be computerized. For example, we are calculating regression equations for predicting MUF during iono-magnetic storms using the average k indices for a preceeding period. This has been reported in the literature for foF2. We are applying the results to specific paths for which we make predictions.

As many of you are aware, Air Weather Service has been making a concerted effort to have hourly VI data from Europe and North America reported to the Solar Forecast Center in near real-time, i.e., every hour if possible. We are developing computer programs for handling these data directly from the communications circuits, making the necessary calculations, and displaying them in a format which is immediately useable by the forecaster.

We feel that future progress in ionospheric forecasting will be made when enough VI data are available in near real-time for mapping the ionosphere similiar to the way in which the troposphere and stratosphere are mapped for weather forecasting. This is not the entire answer to the forecasting problem; solar and geomagnetic information is also required. But direct observations of the ionosphere itself, available in near real-time, should be a great step forward in improving the state-of-the-art.

References: 1. Barghausen, A. F.; J.W. Finney; L. L. Proctor, and L. D. Schultz; Predicting Long Term Operational Parameters of High Frequency Sky-Wave Telecommunications Systems, ESSA Technical Report ERL 110-ITS78, May 1969.

2. ESSA Research Laboratories, Solar Geophysical Data, U.S. Dept of Commerce, 1967, 1968, 1969.

ADVANCED TELECOMMUNICATION FORECASTING TECHNIQUE

by

G. H. Stonehocker

Institute for Telecommunication Sciences

Environmental Science Services Administration

Research Laboratories

Boulder, Colorado U.S.A.

SUMMARY

Methods of evaluation of solar-geophysical data for objective, rather than subjective, short-term forecasting of ionospheric radio propagation have been assembled into a flexible system for computer application. Solar flare and solar radio noise burst data, with other solar-geophysical information, are used to forecast estimates of expected probability of occurrence, start time, end time and intensity of SWF-SID, PCA and geomagnetic (ionospheric) storms. Using these forecasts together with current observations of pertinent phenomena, hourly changes of attenuation and MUF are predicted for any location and any HF telecommunication circuit. A companion paper, "Operationally Oriented Telecommunication Forecast Service," by R. K. Salaman, discussed user access to the programs and automatic dissemination of data and forecasts. The programs are designed for rapid incorporation of new methods and data and for quick updating of subroutines as new information becomes available.

ADVANCED TELECOMMUNICATION

FORECASTING TECHNIQUE

by

G. H. Stonehocker

Institute for Telecommunication Sciences

Environmental Science Services Administration

Research Laboratories

Boulder, Colorado U.S.A.

1. INTRODUCTION

Short term forecasts for ionospheric radio propagation have been issued by different groups in several countries for a number of years. They are usually subjective, based on monitoring of changes in solar-geophysical variables and operation of selected radio circuits, and depend on the experience of the forecaster. He generally develops some rules of thumb for his subjective technique. Heavy reliance is usually placed on persistence, assuming that current conditions or trends will continue unless a change or disturbance can be foreseen. Such systems tend to be disturbance oriented. If communications for worldwide data exchange and dissemination of forecasts could be essentially instantaneous, a different forecast philosophy might emerge. Improvement is being made in communications, but considerable improvement in forecasting techniques is also needed.

A general system, using a computer to evaluate solar-induced events and their effects on the ionosphere and communications will be outlined, and applications to specific forecast problems will be discussed in detail. Although the system is an aid to the forecaster's memory and evaluates data rapidly, it is primarily the evaluation part of an automatic information retrieval and forecast system, discussed in a previous paper presented here by R. K. Salaman. This is mainly an adaptation of results already available in the literature to the computer, rather than a new basic study. However, the system is designed to be flexible, to permit ready incorporation of future advances. This is a preliminary effort, and improvements can be expected as research progresses on the many diffcult problems that now limit accuracy and reliability of forecasting.

2. THE SYSTEM

The basic philosophy of the system is a bootstrap detection-forecast approach. One detects and measures events, looks at the results, and forecasts trends until a later significant event is detected. This philosophy was implicit in previous subjective forecasting, which is now made more objective by modern computer techniques. The first part of the system makes an evaluation of solar geophysical events, such as solar flares, radio noise bursts at 10,000 MHz and 200 MHz type IV solar radio noise bursts, used singly or in combination (Sinno and Hakura, 1958). The probability of occurrence, beginning time, duration, and magnitude of the effects of these predictors are included in the file of current pertinent data. The general sequence of observed events usually begins with a solar flare, followed by a polar cap absorption, event in one or more hours, which is followed by a geomagnetic storm in one to three days.

The second part of the system determines how, in time and magnitude, the signal strength (LUF), stability, and MUF of an HF circuit will be affected by the disturbing event. The determination of stability is still under study. Figure 1 is a block diagram depicting the interrelated operations.

The evaluation is automatically made and filed each time a flare and/or other predictor is reported. Characteristics of observed events are compiled in this file also, which is instantly available to the second part accessed by subscribers desiring a forecast for a specific circuit. The

system is automatic. The forecaster only monitors the system, using the results to generate warnings for other purposes and inquiries. A detailed block diagram of the evaluation process is shown in figure 2, with typical radio burst data illustrated by figure 2a. Details of the circuit parameter calculations are indicated by the block diagram of figure 3.

3. SWF-SID PREDICTION

No attempt has been made to predict flares or SWF-SIDs in the system. We notify users immediately after flare, radio burst, or x-ray events are reported. A 24-hour estimate of probability of an SWF-SID is derived from the flare probability forecasts issued by the ESSA Space Disturbance Forecast Center. Given their probability of a flare a combination of probabilities is used as the probability of occurrence of an SWF-SID. Predicted SWF-SID characteristics that affect communications are signal attenuation, start time, end time, and the maximum attenuation expected during the interval. In the future, we plan to include an estimate of attenuation at any time during the SWF-SID interval by using an average shape of the local time variation of attenuation.

3.1. SWF-SID PROBABILITY PREDICTION

Gladys Harvey's (1964) data are used to derive estimates of probability of occurrence of an SWF-SID for each level of flare importance. The results are listed in table 1 as (SID) percent. This should be corrected for the cosine of the solar zenith angle (cos x) and frequency, the same as for attenuation, but this is not yet included in the system. We would like to use another indicator, solar x-ray observations, when the data are completely available in real time, but inclusion of this in the system requires further work.

To substitute for the x-ray data, we use observations of solar radio noise flux bursts at higher frequencies, say 8800 to 15,400 MHz which are reported almost in real time, and which are fairly well correlated with SWF-SID maximum attenuation and duration as reported by Harvey (1964) for 2800 MHz. The probability of occurrence of a SWF-SID estimated from the higher frequency solar radio noise bursts is derived from the logarithm of the energy in the burst (smoothed maximum intensity times duration) (Harvey 1964).

3.2. SWF-SID SIGNAL ATTENUATION AND DURATION PREDICTION

This section of the program is based on an unpublished study of average signal attenuation (dB) of WWV CW transmissions at 5 MHz from Ft. Collins, Colorado, recorded at White Sands, New Mexico. These well calibrated records were chosen from those available for many locations and frequencies. On these records, all attenuation maxima would be normalized to about the lower frequency limit of most HF operations. Also, at the midpoint of this one-hop path, the sun is nearly overheard for several hours around noon during the summer months and goes to low values of cos χ (large solar zenith angles) during winter days. Following Schwentek (1961), we shift the attenuation to other frequencies and locations simply by calculating the attenuation at the one-hop path midpoint, or at each control area for multihop paths. In the latter case, the combined value is used. In the future we will calculate attenuation for all hops.

The CW recordings were scaled by drawing the normal diurnal trend curve, and that for the SWF-SID event. The maximum attenuation is determined by the difference of the event and normal trend lines, using the daily calibration. Forty-six events in May, June, July and August during recent years for hours 1700 - 2100 Z(1000 - 1400 LT) were measured and the attenuation grouped by flare importance categories both for flares only and for flares with associated near 10,000 MHz radio noise bursts. (The results for the events with flares only are listed in table 1.) The attenuation associated with the radio bursts of the above study were plotted versus the logarithm of the (10,000 MHz) burst energy (see figure 4). A least squares fit to the points has a standard error of the residuals of 6.2 dB, and is indicated by the solid line of figure 4. The line actually used in the system computations is shown by the dotted line of figure 4, and is rotated slightly to coincide with the desired limits, determined by observed events, for the computations given by the equation:

$$\text{Attenuation, dB} = 11.333 \log \text{energy}, 10^{-22} \text{ Watts} - 3.333$$

The SWF-SID maximum attenuation is scaled to other frequencies from the basic subsolar point data for 5 MHz by using a $1/f^{2}$ relationship (Schwentek, 1961). The relationship was checked between 5 and 12 MHz for several other cases and was found to be less than 9 percent in error. The maximum subsolar point attenuation is also decreased by a cos χ factor, where χ is the sun's zenith angle at the one-hop path midpoint, or by the sum of the cos χ factors at the control areas for multi-hop paths.

If the normal operating signal-to-noise ratio (S/N) is known for the time in question, the usable S/N available during the maximum SWF-SID attenuation for a circuit is given by subtracting the SWF-SID attenuation from the normal S/N by the system. In our SWF-SID study, we found that the noise usually decreased about 10dB during the SWF-SID at midday, which agrees with a 13dB measurement of this effect in Southeast Asia in the morning for approximately the same cos X.

SID duration was plotted versus solar flare area corrected for foreshortening. A least squares fit was derived for the points, and values of duration for each level of flare importance were read from the curve. These values of SID duration are given for flares only in table 1, and the curve is shown in figure 5, with different groups of data indicated by the two symbols. When a 10,000 MHz radio burst accompanies a flare or occurs alone, its duration is used for the SWF-SID duration, as the correlation of the shape and duration of the burst profile seem to be very good.

4. PCA PREDICTION

Probability of PCA is taken as 25 percent less than the probability of a magnetic storm given by Hakura and Goh (1959), but current work may lead to revision of this value. A constant value of 7.5 dB attenuation, an average for 33 PCA events (D. K. Bailey 1964), is used for PCA attenuation. Much more work is needed in this area.

PCA events divide into two groups which have fast and slow particle travel speeds. The fast particle group tend to accompany flares with pre-flare noise bursts in the higher radio frequencies and whose travel time is a function of source flare solar longitude (Sinno, 1961, 1962). For a group of 15 (Sakura and Maeda, 1966), a least squares fit of the PCA start time after the time of flare (in hours) versus longitude is given by

Time (F-PCA) = 0.03L + 2.90 hours with a standard error of the residuals of 1.13 hours,

where L is the solar longitude in degrees of the source flare with signs of + for E and -for W. Few are indicated from extreme east longitudes. The start time of the slow particle PCA group seems to be independent of position of the source flare. Start time is a function of the particle trapping time and travel time from the sun, and is associated mainly with the post flare maximum 200-MHz type-IV radio noise bursts. Therefore, we can use an inverse relationship with the geomagnetic storm beginning time (which we can forecast with some degree of accuracy, see below) given by: Time (S-PCA) = 1.24t mag - 24.79 hours with a standard error of the residuals of 6 hours, where t is the forecast magnetic storm time in hours.

5. GEOMAGNETIC STORM PREDICTION

The geomagnetic (ionospheric) storm prediction is derived from several predictors: Flare, radio noise burst (post flare maximum time) at about 200 MHz, type IV radio burst occurrence, and reported PCA, each taken singly and in combination. The relations are based mainly on work of Sinno (1959) (1962), Sinno and Hakura (1958), Hakura and Goh (1959), Sakurai and Maeda (1961), Obayashi (1962), and McCracken and Palmeira (1960). Their relationships were used in an evaluation for each flare, radio noise burst, etc. as they are reported, of the probability of the event producing a geomagnetic storm. Sudden commencement (SC) type storms will be discussed in detail. No attempt is now made to include the prediction of recurrent-type geomagnetic storms, although data are being analyzed for this purpose. Until these can be added to the program, subjective use is made of this type of data by the forecaster.

5.1. PROBABILITY OF GEOMAGNETIC (IONOSPHERIC) STORM

The probability of a flare and/or post flare radio noise burst at 200 MHz producing a geomagnetic storm is taken from figure 4 of Sinno (1959) and programmed for the computer. This was done by quantizing his lower graph to the usual flare importance categories against the logarithm of the radio burst excess energy; the result is shown in figure 6. The extremes, of zero log burst energy or zero flare importance are used for flare or radio burst alone. The slope and zero log energy intercept for each flare importance curve were determined by graphical methods because of limitations to the accuracy of reading Sinno's graph. In this way, we obtain the constants A and B in the equation

$$P\ (MAG) = A\ e^{BE},$$

where E is $\log_{10}$ of the radio burst excess energy (the smoothed peak energy 10^{-22} Watts/meter^2/Hz times the duration) and P(MAG) is the probability of a geomagnetic (ionospheric) storm.

A slice through Sinno's positional dependence probability graph was made at 25° N and S latitude, giving a change in probability versus longitude function for north and south hemisphere flares as:

$$\Delta\ P(MAG)_N = A\ L_N^4 + B\ L_N^3 + C\ L_N^2 + D\ L_N + E$$

$$\Delta\ P(MAG)_S = F\ L_S^{10} + G\ L_S^{9} + H\ L_S^{8} + I\ L_S^{7} + J\ L_S^{6} + K\ L_S^{5} + M\ L_S^{4} + N\ L_S^{3} + P\ L_S^{2} + Q\ L_S + R,$$

where L_N is north longitude and L_S is south longitude in degrees, and A thru R are coefficients. The accuracy of a polynomical fit to these points is shown in figure 7 and the coefficients in table 2. Using the reported positional data, these functions are used to adjust the former flare importance versus energy values by as much as ± 20 percent.

5.2. TIME TO GEOMAGNETIC STORM

In the list of nine solar radio bursts (Sinno, 1959, fig.2) an apparent inverse relationship of the size (area under the curve of magnitude and duration) of the post-flare maximum of radio outburst at 200 MHz to the time of sudden commencement (SC) of the geomagnetic storm was noted. Therefore, by expanding the data to include all of the published 200 MHz burst profiles available, a mass plot of log energy versus time to SC, shown in figure 8, was made. The different symbols indicate two groups of data. The solid line shows the lease squares fit to the data, which was rotated slightly to better coincide with the known observed limits, to use in an operational system, as indicated by the dotted line. Although the standard error of the residuals is not smaller than 12 hours, this is considerably better than our previous forecast methods. The results are consistent with theories of the travel time from sun of the lower-energy trapped particles. The time to SC, for flares only, based on statistics developed from

Yoshida's (1965) study of geomagnetic storms and their source flares. Times are grouped by flare importance categories and are listed in table 1.

The time to geomagnetic storm SC is also obtained from slow type PCA start time when reported. This time function is obtained from a least squares fit to the data of figure 3 of Sinno (1962).

New satellite methods of obtaining the time to the geomagnetic storm SC by particle detection and solar wind speed variation are being studied by ESSA, and it is hoped they will provide a more accurate and reliable tool than the energy relation with particle flow from the sun.

5.3. INTENSITY OF GEOMAGNETIC STORM

In the list of nine solar radio burst profiles mentioned in 5.2., the intensity of the main phase decrease seemed a direct function of the excess energy of radio burst. A summary plot Figure 9, was made of 24 cases in two different groups of data, where this information was available. A combined graphical and least squares fit was made to determine the function.

$$\Delta H = 1.957 E^4 - 13.08 E^3 + 45.97 E^2 - 94.58 E + 118.34$$

where E is the logarithm of energy excess 10^{-22} Watts/meter^2 of the 200 MHz post flare maximum part of the type IV burst, and ΔH is the change in geomagnetic field in grammas. The curve is quantized into three categories of storm intensity at mid-latitude to derive the subsequent ionospheric storm change of MUF: 0-50 gamma - no storm; 50-100 gamma - small storm and greater than 100 gamma - large storm. In the 50-100 gamma portion of the curve the accuracy measured from the graph is about ± 30 gamma. Additional data might permit reduction of this uncertainty. The intensity of small and large magnetic storm categories for each flare importance category were obtained by grouping the data from Yoshida's listing of source flares. The probability of obtaining a large magnetic storm increased from 15 to about 50 percent in the importance 4 category and showed a longitude variation which has not yet been included in our system. These values are included in table 1.

5.4. MUF VARIATIONS

Given the starting time of an SC geomagnetic storm and the storm size, an estimate of MUF variations can be made for a propagation path. R. M. Davis (1963) determined the MUF change with storm size, season, and storm sudden commencement in local time for various latitude zones. Using his results, the change in hourly median MUF for the whole storm can be forecast 20 to 80 hours, in advance. When the storm actually begins, a forecast of MUF change is made for the next 6 hours, hour by hour, using other unpublished work by R. M. Davis (1968), based on an average for the past 12 hours of geomagnetic K figures. These forecasts of changes from previously predicted monthly median MUFs are compared with foF2 and MUF values obtained in real time over some known propagation paths as the storm progresses.

6.0 EVALUATION OF THE SYSTEM

A comparison of forecasts of the series of events (1950-1959), upon which the first part of the system was designed, with observation of the actual events observed subsequently is given in table 3. A similar comparison for another independent data sample for a later time period (June 1968), is presented in table 4. While these results are encouraging, considerable improvement would be desirable. However, the system has dynamic qualities that can only be tested while in full scale operation, rather than for selected sequences of events, Therefore, a test was made for the months of April thru July 1968, even though a limited number of PCA and magnetic storm events occurred in that interval. The following results and conclusions were reached.

SWF-SID

Probability of Occurrence	Error in Start time	Error in End time	Error in Intensity
Is too low, only 6% of 149 observed were predicted	4.7 min -0.8 min	16.6 min -9.7 min	Data not ready

PCA:

Probability of Occurrence	Error in Start time	Error in Intensity
Is about right, but didn't hit the one of the two that did occur.	-1 hr	+2.5 dB

Magnetic Storm:

Probability of Occurrence	Error in Start time	Error in Intensity
Within the ranges: >60% is right 30 - 60% is too high < 30% is about right	-3.9 hr	Data not ready

MUFs: No evaluation ready.

We intend to use a computer routine for automatic evaluation in the near future since there have been over 5,000 events processed since April 1968.

The probability scale used is; >60 percent, probably will happen; 30-60 percent, 50-50 chance; and <30 percent, probably will not occur.

7.0 Conclusions

A pilot computerized system for evaluation of solar-geophysical data and forecasting telecommunication system parameters, MUF and attenuation, has been described. Evaluation of some results obtained by the pilot system reveals limitations of the evaluation and prediction methods. Further research is needed to achieve substantial improvements in accuracy and reliability of short term prediction and evaluation techniques, and methods of applying them to practical problems. The computer programs are designed for rapid incorporation of new developments and updating subroutines whenever new information becomes available.

8.0 ACKNOWLEDGMENT

I thank D. N. Hatfield and H. E. Petrie, as well as the Space Disturbance Forecast Center, of ESSA for their cooperation and programming assistance in this work.

9.0 REFERENCES

Bailey, D. K. (1964), "Polar-cap absorption, "Planet. Space Sci. 12, p. 495.

Davis, R. M., Jr. (1963), Private communication.

Davis, R. M., Jr. (1968), "Short-term prediction of F2-Layer MUF from local magnetic activity." to be published.

McCracken and Palmeira (1960), "Comparison of solar cosmic rays injection including July 17, 1959 and May 4, 1960, "JGR 65 No. 9, p. 2673.

Obayashi, T. (1962) "Propagation of solar corpuscles and interplanetary fields," JGR 67 No. 5, p. 1723.

Hakura, Y. and T. Goh (1959), "Pre-SC polar cap ionospheric blackout and type IV solar radio outburst," J. Radio Res. Lab. 6, No. 28, p. 635.

Harvey, G. (1964), "Some relationships between 10. 7 cm solar noise bursts, flares, and SWF "Astrophys, J. 139, p. 16.

Sakurai, K. and H. Maeda (1961), "A relation between solar radio emission and low-energy solar cosmic rays, "JGR 66, No. 6, p. 1966,

Salaman, R. K. (1969), "Operationally oriented telecommunication forecast service, "NATO AGARD conference proceedings on Ionospheric Forecasting,

Schwentek, H., (1961) "Short Wave Fade outs, their modes and complete Characterization." JATP 23, p. 68.

Sinno, K. (1959), "Characteristics of solar outburst to excite geomagnetic storms." J. of Radio Res. Lab. 6, No. 25, p. 17.

Sinno, K. (1961), "Some Characteristics of Solar Corpuscular Radiations," J. of Radio Res. Lab. 8, No. 17, p. 21.

Sinno, K. (1962), "Characteristics of solar energetic particles which excite PC blackouts," J. Geomag. Geoelect. 13, p. 1.

Sinno, K. and Y. Hakura (1958), "On the relation of solar eruptions to geomagnetic and ionospheric disturbances: I. On the power spectrum of solar radio outbursts, "J. Radio Res. of Japan 12, p. 285.

Yoshida, S. (1965), "A new classification of geomagnetic storms and their source flares, " Scientific Report Geophysical Institute of the University of Alaska.

Table 1. Flare Effects by Flare Importance

FLARE IMP/ CODE	SID ATTN.	SID DUR.	A	B	#3 (MAG) % P	#1 (SID) % P	TIME MAGST HRS	% P LARGE MAGST
SF 0.1	007.4	0:17	12.7	0.3575	09.	000.	80	00
SN 0.2	010.5	0:19	14.9	0.3380	11.	001.	72	00
SB 0.3	020.0	0:21	15.8	0.3039	13.	005.	67	00
1F 0.7	008.0	0:24	20.5	0.2600	17.	002.	61	00
1N 1.0	018.0	0:28	24.6	0.2332	21.	012.	55	17
1B 1.3	025.0	0:31	27.3	0.2060	26.	027.	50	17
2F 1.7	012.0	0:37	34.0	0.1735	32.	005.	43	17
2N 2.0	025.0	0:45	38.7	0.1506	35.	052.	42	17
2B 2.3	032.0	0:54	43.1	0.1320	40.	079.	40	25
3F 2.7	015.0	1:06	47.6	0.1150	43.	014.	37	42
3N 3.0	030.0	1:18	52.9	0.1014	50.	093.	35	44
3B 3.3	040.0	1:32	55.8	0.0930	53.	100.	32	44
4F 3.7	018.0	1:40	59.7	0.0878	58.	016.	30	50
4N 4.0	035.0	2:06	63.5	0.0845	63.	095.	27	53
4B 4.3	045.0	2:15	71.2	0.0830	68.	100.	24	50

Table 2. Δ % P(MAG) Function Coefficients

North

A $-\ 0.233515 \times 10^{-5}$

B $-\ 0.144665 \times 10^{-3}$

C $-\ 0.132762 \times 10^{-1}$

E $+10.85569$

South

F $+\ 0.069896 \times 10^{-14}$

G $-\ 0.113596 \times 10^{-12}$

H $-\ 0.324247 \times 10^{-11}$

I $+\ 0.077023 \times 10^{-8}$

J $-\ 0.240946 \times 10^{-8}$

K $-\ 0.181181 \times 10^{-5}$

L $+\ 0.175752 \times 10^{-4}$

M $+\ 0.177842 \times 10^{-2}$

N $-\ 0.259017 \times 10^{-1}$

O $-\ 0.5659342$

P $+20.6743$

Table 3. First Evaluation Results
(Originating Data)

Based on 14 Sequences			% Correct
P (SWF)	Correct, 12 of 14 sequences		86%
P (PCA)	Correct, 10 of 13		77%
P (Mag Storm)	Correct, 14 of 14		100%
Magnitude of Mag Storm	Correct, 13 of 14		93%
SWF-SID Attenuation	Correct, 4 of 5		80%

(Program doesn't work on all paths yet so not properly tested.)

In cases given values are correct magnitude for further comparison when possible to program.

SWF-SID Duration	Max Error	Min Error	12 of 14
	+ 62 min	+ 3 min	
(20-40 min)	- 62 min	- 10 min	
Time to PCA	Max Error	Min Error	12 of 12
	+ 34 hr (+18)	+ 0.5 hr	
(1-40 hr)	- 18 hr	- 0.2 hr	
Time to Mag Storm	Max Error	Min Error	14 of 14
	+ 14 hr	+ 2 hr	
(20-72 hr)	- 16 hr	- 2 hr	

Table 4. First Independent Evaluation Results

Based on 11 Sequences			% Correct
P (SWF)	Correct, 1 of 11 sequences		9%
P (PCA)	Correct, 9 of 10		90%
P (Mag Storm)	Correct, 9 of 10		90%
Magnitude of Mag Storm	Correct, 5 of 5		100%

SWF-SID No path defined for analysis yet

SWF-SID Duration	Max Error	Min Error
	+ 10 min	0
	- 14 min	0

Time to PCA Only 1 observed PCA, but no time given (4 of 10 therefore forecasted greater than 75 hours)

Time to Mag Storm	Max Error	Min Error
	+ 34 hr	+ 8 hr
	- 0	- 0

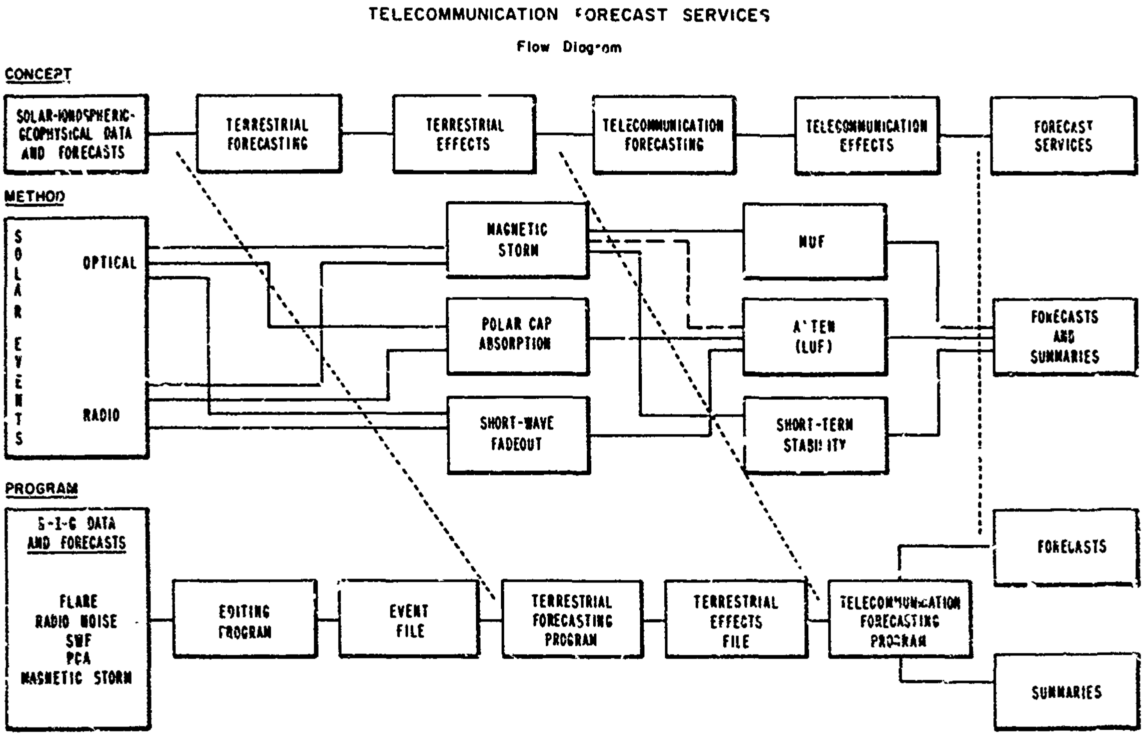

Fig.1 Overall system diagram

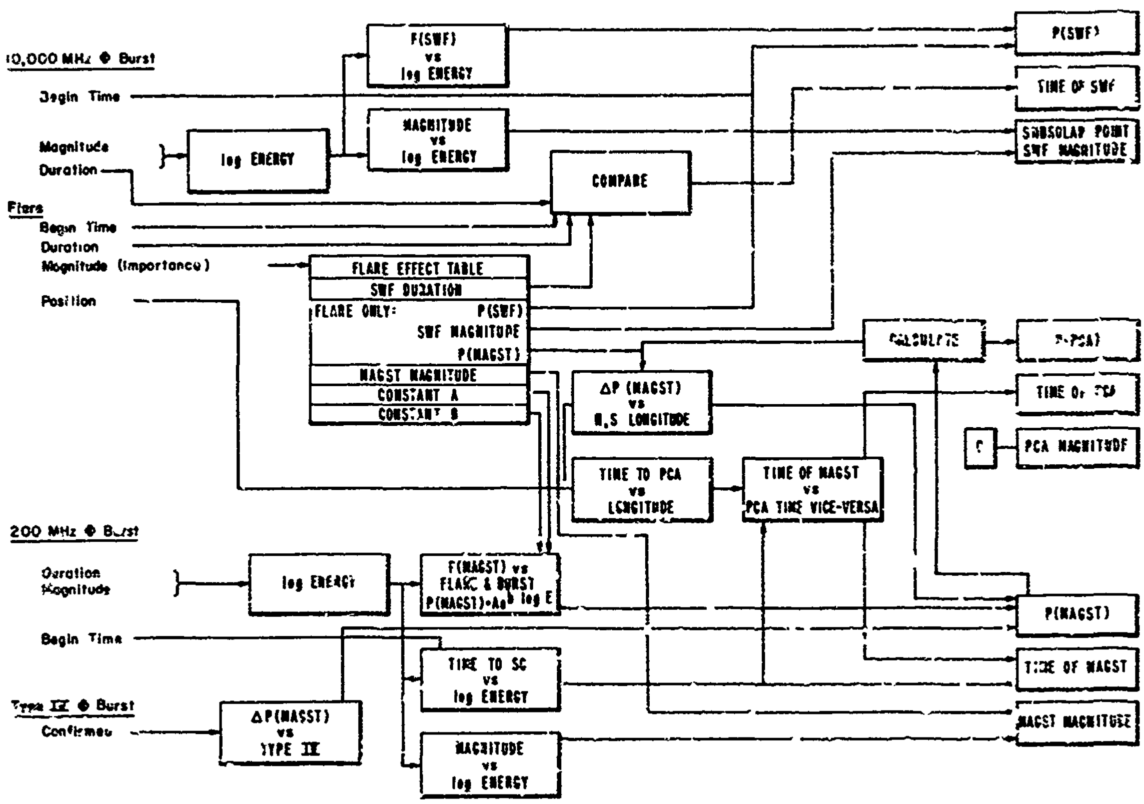

Fig.2 Part 1. Solar geophysical data evaluation diagram

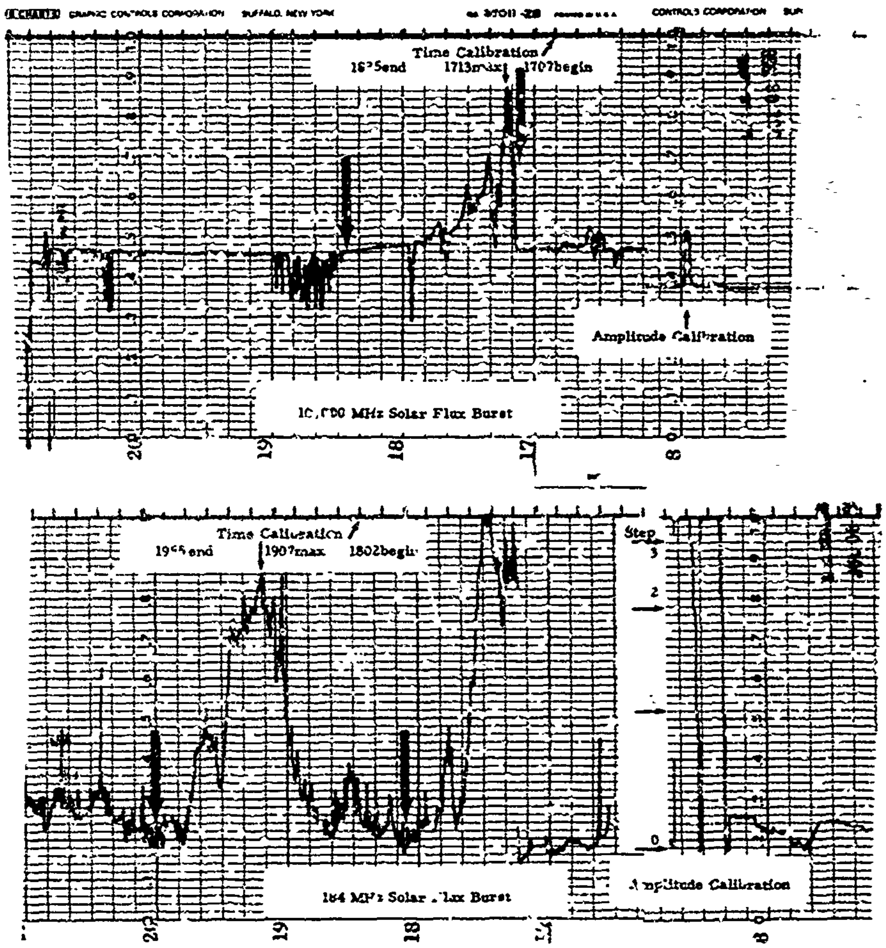

Fig.2a Typical solar radio noise burst data

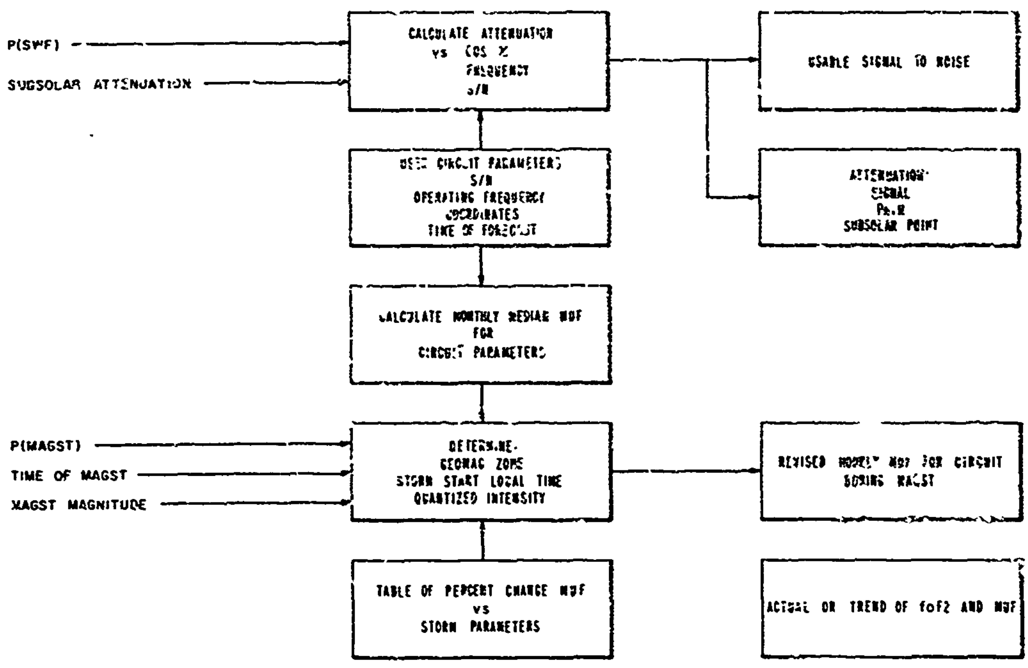

Fig.3 Part 2. Telecommunication parameter prediction diagram

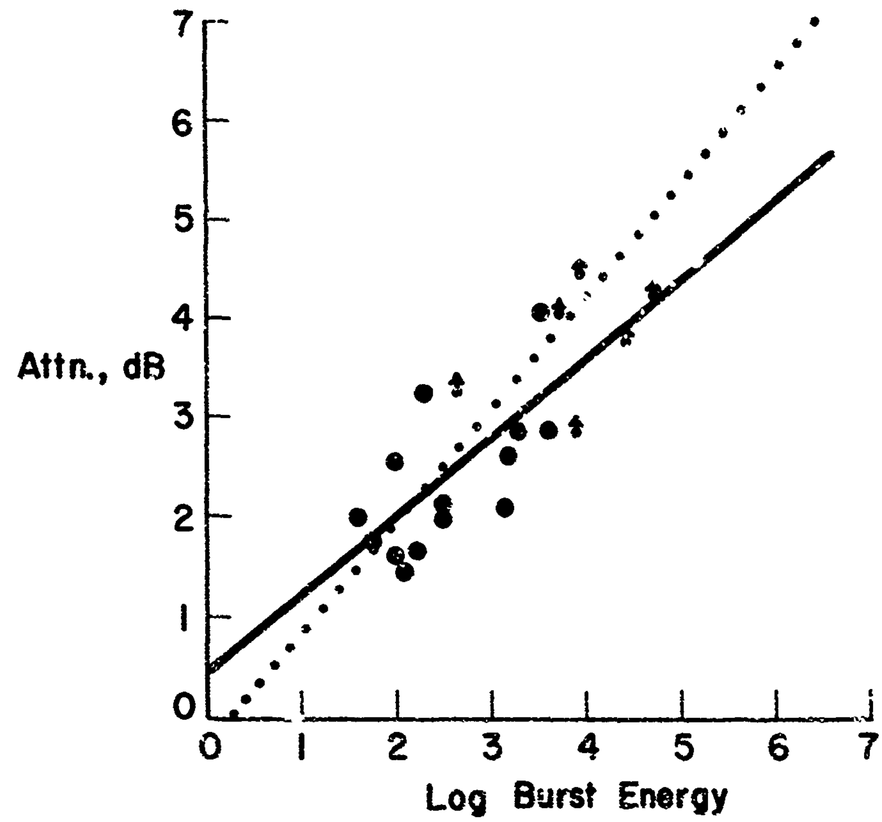

Fig.4 SWF-SID attenuation versus 10,000 MHz radio burst energy in 10^{-22} Watts/m^2

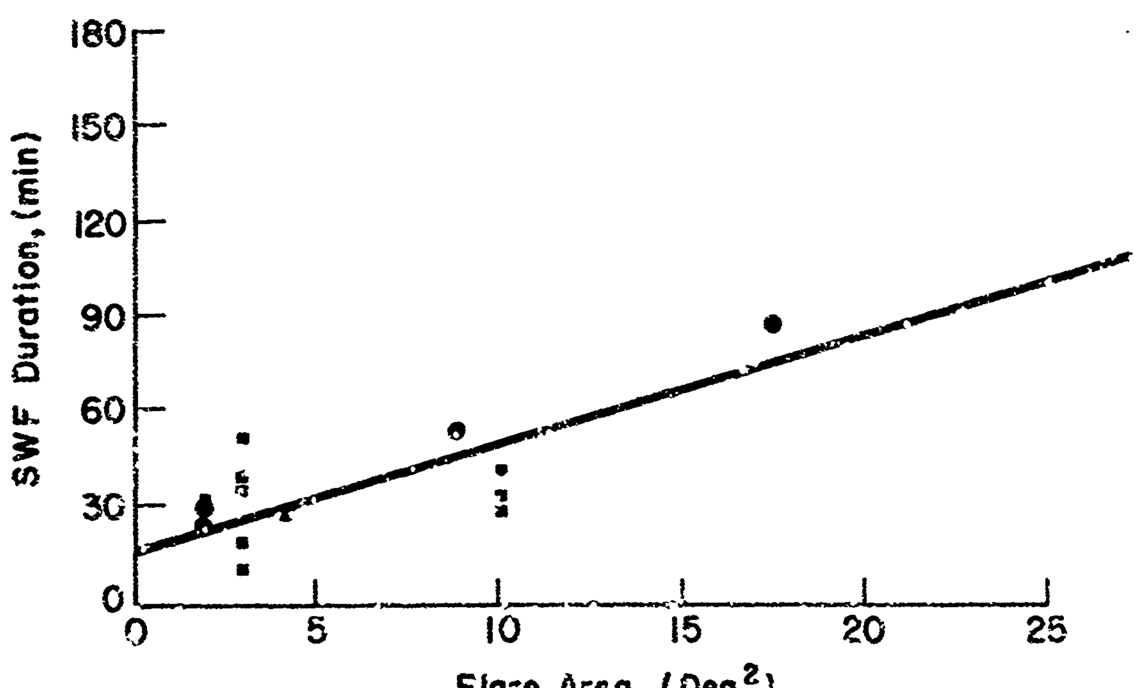

Fig.5 SWF-SID, duration versus flare area (importance)

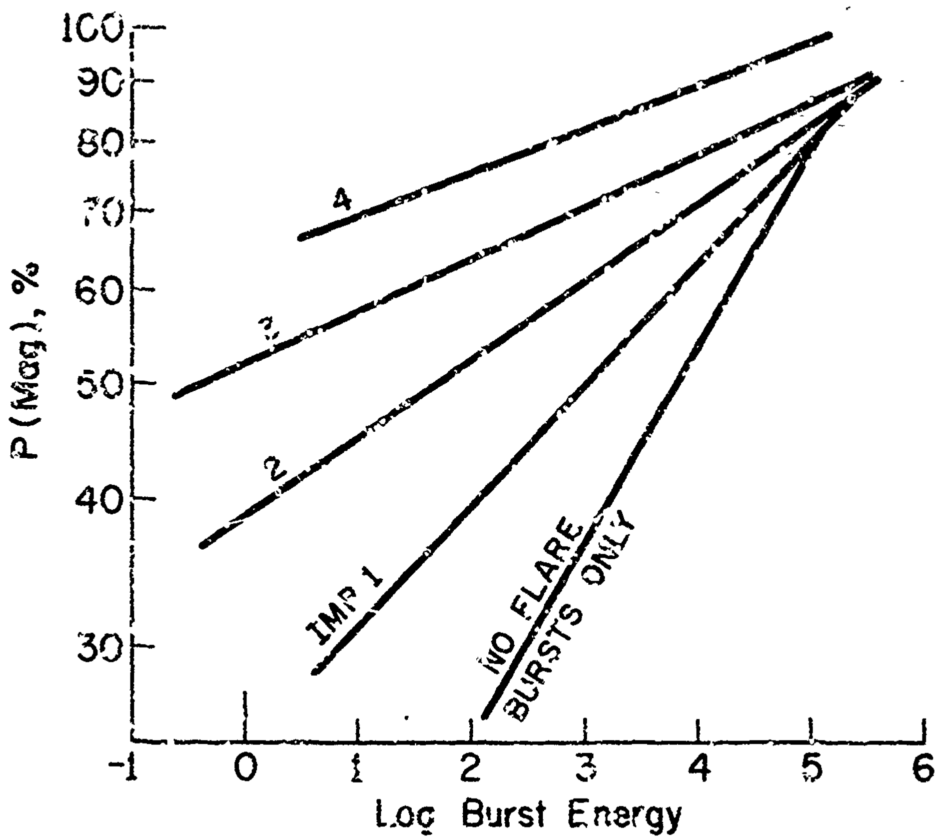

Fig.6 Probability of magnetic storm occurrence versus 290 MHz radio burst energy in 10^{-22} Watts/m^2

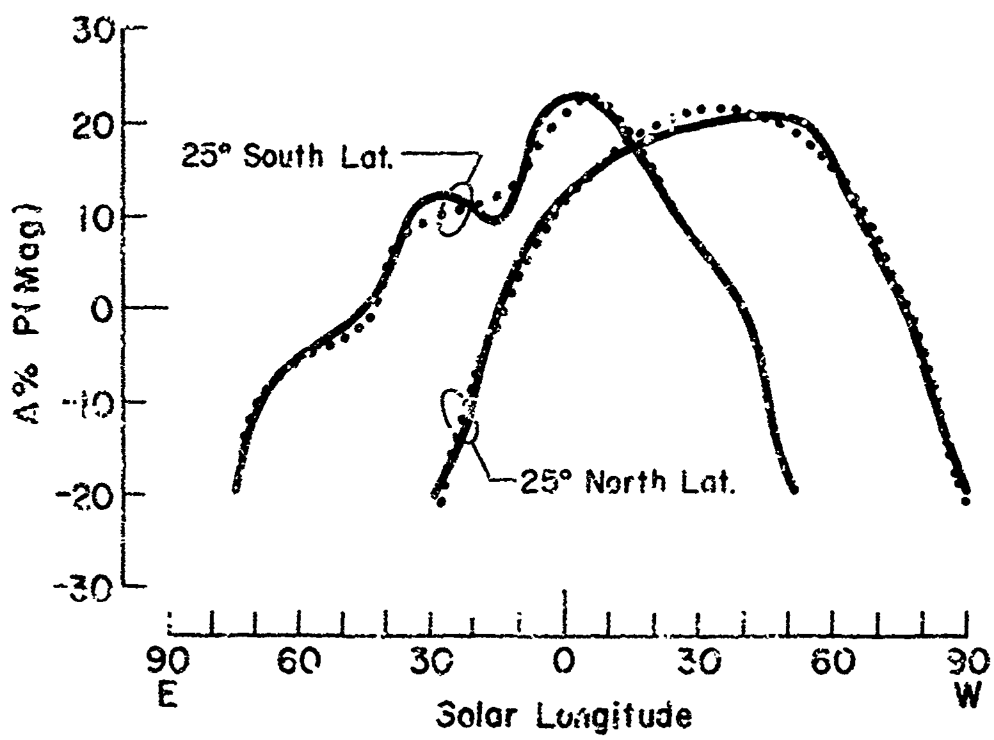

Fig.7 Change in probability of magnetic storm occurrence versus flare solar longitude

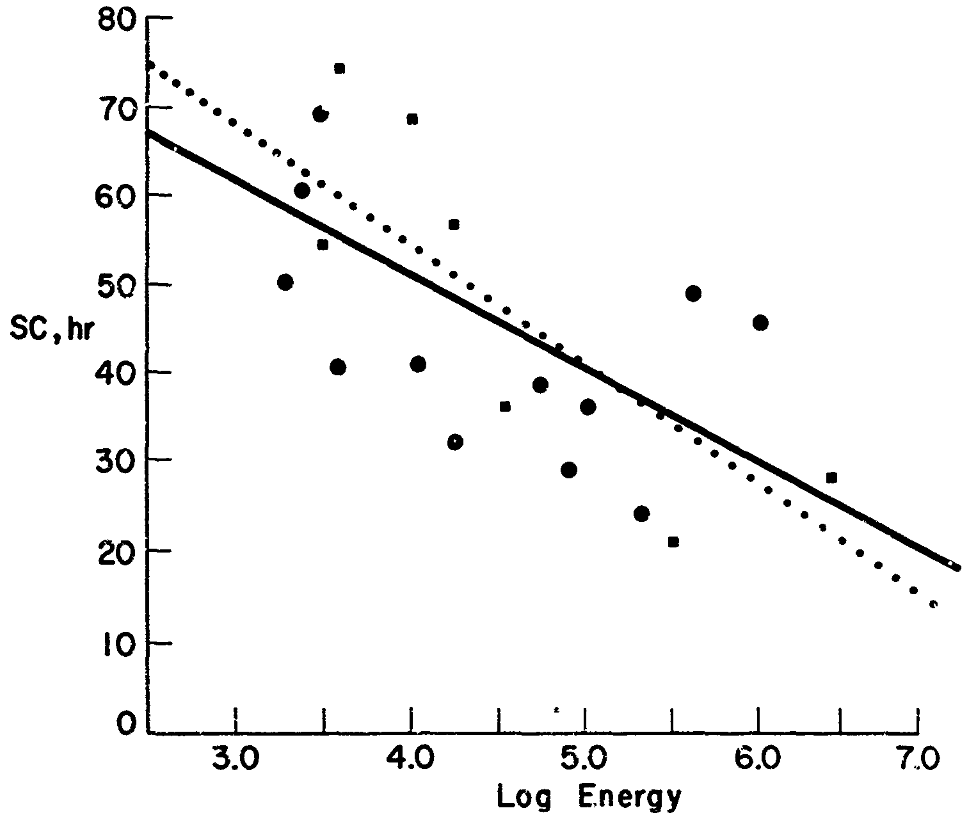

Fig.8 Time to sudden commencement versus 200 MHz radio burst energy in 10^{-22} Watts/m^2

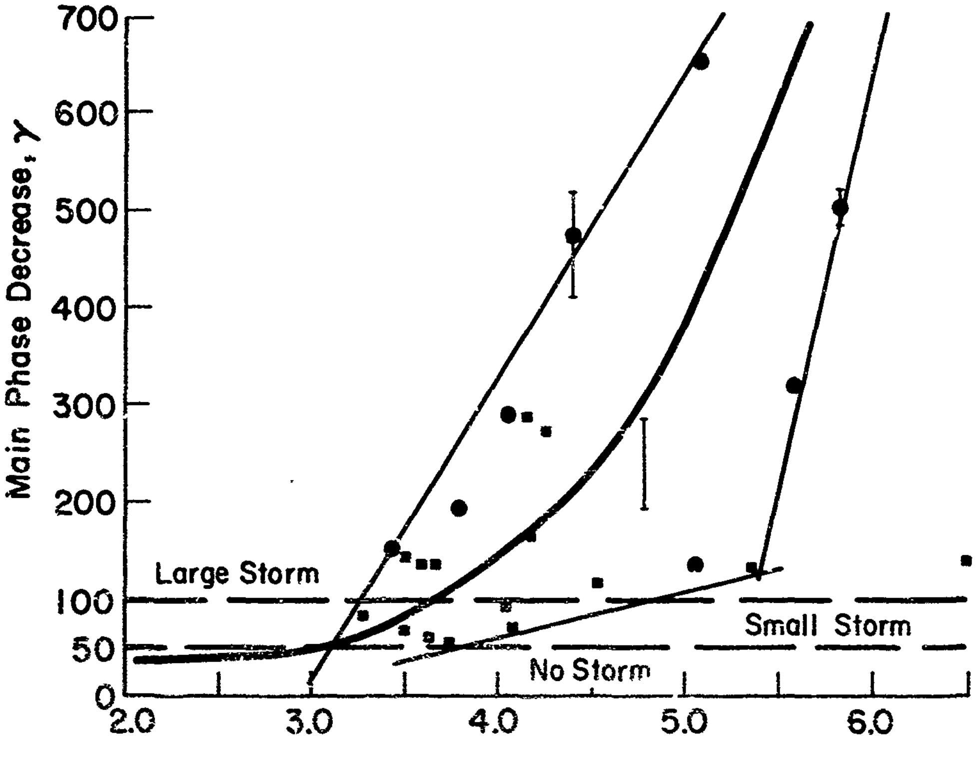

Fig.9 Main phase magnetic field decrease versus 200 MHz radio burst energy in 10^{-22} Watts/m^2

ON THE TIME DELAY BETWEEN SOLAR FLARES AND ASSOCIATED GEOMAGNETIC STORMS

by

F.E. Cook

Ionospheric Prediction Service Division, Commonwealth Bureau of Meteorology, Sydney.

SUMMARY

Preliminary examination of data on solar flares, active regions, and associated geomagnetic storms during the period July, 1957 to December, 1959 suggests a relationship between the areas of the corresponding calcium plages and the flare-storm delay times, the delay being greater for flares occurring in smaller plage regions. The relationship breaks down with plages of area greater than about 90×10^{-4} solar hemisphere, but smaller flare-associated regions may be identified within large plages in some cases.

ON THE TIME DELAY BETWEEN SOLAR FLARES AND ASSOCIATED GEOMAGNETIC STORMS

F.E. Cook *

Ionospheric Prediction Service Division
Commonwealth Bureau of Meteorology

1. INTRODUCTION

Disturbance warnings issued by the Ionospheric Prediction Service Division are based partly on the identification of precursors of geomagnetic storms, with some estimate of the probability of sudden ionospheric disturbances (SIDs) during solar flares. Two kinds, initially, of geomagnetic disturbances are recognized: those associated with long-lived features of the solar wind structure co-rotating with the sun and overtaking the earth at approximately 27-day intervals, and those associated with centres of activity which show rapid development of spot groups, magnetic complexity, strong coronal line emission when seen at the limb, strong radio emission especially at metre wavelengths, and major flare activity.

The active regions can of course be expected to modify the solar wind structure above them, resulting in the moderate disturbances associated with their central meridian passage. It is generally accepted however that many of the major sudden-commencement (SC) geomagnetic storms can be associated with major solar flares, especially those accompanied by strong type four radio outbursts. Several compilations of flare-storm relationships were published during or soon after the IGY-IGC period July 1957 to December 1959, directed mainly toward clarifying the relationship between solar activity and polar cap-absorption events (PCAs) but including geomagnetic storm relationships also, and reference is made here to compilations by Hakura and Goh (1), Thompson and Maxwell (2), Obayashi and Hakura (3), de Feiter et al. (4), Sinno (5, 9), Sarabhai and Pai (6), Maeda et al. (7), Haurwitz (8), Noyes (10), Bhargava and Natarajan (11), and Caroubalos (12).

It should be pointed out that not all workers in this field accept the idea of direct flare-storm relationship; the opposition point of view is summarized and reviewed by Bednarova-Novakova (13). However, if the association of SC storms with major flare events is accepted as a basis for forecasting their occurrence, and possibly their severity, there remains the problem of forecasting their starting times. It is not proposed to review this problem here, or to discuss the allied problem of forecasting the occurrence and starting times of PCAs, except to mention the possible relationship of delay time to the intensity of the radio outburst accompanying the flare (Caroubalos (12)), and a relationship suggested by Haurwitz (8) between the delay time and the level of geomagnetic activity before the storm. The purpose of this paper is to present evidence which might suggest another useful relationship, between the delay times and the areas of the calcium plage regions in which the flares occur. To be of any use for forecasting purposes, data must be available easily and quickly, and the calcium plage data (discussed below) are at present available through the daily ursigrams of the International Ursigram and World Days Service (IUWDS).

2. LIST OF FLARE-STORM EVENTS AND CALCIUM PLAGE AREAS (TABLE 1)

2.1 Selection of events

In compiling the list of flare-storm events in Table 1, the aim has been to include every significant event (Kp 5 or above, but including one disturbance with Kp 4) with a definite starting time and with which one or more solar flares could be reasonably associated according to the criteria mentioned in the introduction to this paper. References (1 to 12) are given to flare-storm associations already published, and where more than one flare meets the criteria they have all been listed and treated as separate flare-storm events.

* Disturbance Warning Section, and IUWDS Regional Warning Centre

2.2 The geomagnetic storm and flare data

The geomagnetic SCs and Kp indices have been published in the I.A.G.A. Bulletins and from time to time in other journals, e.g., Journal of Geophysical Research and the CRPL (now ESSA) F-series. The flare data have likewise appeared in the Quarterly Bulletin on Solar Activity of the I.A.U., and in the CRPL (ESSA) series, but reference has been made mainly to the McMath-Hulbert Observatory Working Lists of Flares, and to the IGY-IGC Calendar Record; these data are well known and need no further comment.

2.3 The calcium plage data

Calcium (K3) solar plage data have been made available by the McMath-Hulbert Observatory ever since the start of the IGY, and are still supplied within a few hours of observation and measurement through the IUWDS ursigrams (UPLAK code). The data are the daily areas (in units of 10^{-4} solar hemisphere), positions, and intensities of the plages, but it must be emphasised that they are not definitive data; they are preliminary, uncorrected data only, supplied rapidly in an effort to meet the need for a quick and general report of the calcium plages (F. Dodson Prince: private communication) and are therefore subject to large errors and scatter in day to day measurements. In particular, some regions will be found to contain more than one centre of activity producing separate sequences of flares but there can be no attempt, in the time available, to delineate separate regions within the one plage by recourse to H-alpha spectrograms, magnetograms, etc. Similar data from Mount Wilson Observatory (serial numbers preceded by WL) have been used in the table where McMath-Hulbert data were not available.

Where the flare time is some hours away from the time of plage observation, the plage areas timed to the nearest tenth of a day are given, and the area at flare time estimated by interpolation although the rate of change is certainly not always uniform even if the measurements are correct. In some cases, an attempt has been made to estimate what the area of a particular region was, at the time of flare, from earlier or later measurements made when the region was separate although at flare time it was merged with one or more others in a single plage. These "reconstituted" areas appear in Table 1 as follows:

(1) 1957 Aug 30 - Sep 02. The flare at 1337 UT Aug 30 occurred in a region which on Aug 29.6 was listed as WL215 (Mount Wilson data), position E28 N25, area 80 units. WL216 at E25 N15 was 57 units at that time. On Aug 30.6 these plages were combined and listed as WL216 only. Assuming that WL215 still accounted for 0.6 of the total area of the combined regions, its estimated area at flare time was 66 units. Similarly, separate areas of WL215 and WL216 have been estimated for Aug 31 and Sep 02.

(2) 1958 Feb 09. The flare at 2108 UT on 9 Feb 1958 occurred in a region which on Feb 06.6 was listed as McMath 4402, area 90 units or 0.36 of the total areas of 4400, 4402 and 4404, 250 units. On Feb 09.6, they were combined into one plage listed as 4404 with area 180 units, so again making the plausible assumption that 4402 still accounted for the same proportion of the total plage area, its area at flare time is estimated as 28. Both the total and the "reconstructed" areas are listed in the table and shown separately in the diagram.

(3) 1958 Oct 19. Plage 4819, area 50 units, comprised two regions of approximately equal area; areas of 50 and 25 are plotted separately in the diagram.

It is probable that many of the bigger plages, especially those shown "off scale" in the diagram, could be resolved into smaller ones, but as the aim has been to see what can be done with the data actually available from day to day, the process has not been carried further at this stage.

3. THE PLAGE AREA - DELAY TIME DIAGRAM (Fig. 1)

The estimated plages areas at flare time and the corresponding flare-storm delay times from Table 1 are plotted in Fig. 1. Where a storm is related to more than one flare, according to different investigators, the alternatives are shown, and in two cases (1957 Sep 21 and 1958 Jun 05) the same flare is related to two different storms. The "reconstructed" alternatives mentioned in Section 2 are also shown: the delay time of 28 hours for the storm of 1958 Feb 11 is shown against 180 units of area, and 70 units,

TABLE 1. MAGNETIC STORMS AND ASSOCIATED FLARES, INCLUDING ALTERNATIVES, WITH CORRESPONDING CALCIUM PLAGES, IGY-IGC.

Magnetic Storm			Flares					Calcium Plage				ΔT	
Date	Start	Kp max	Date	Start	Imp.	Long.	Lat.	McMath No.	Date	Area	Est. area at flare time	Flare-storm delay (hr.)	References and comments
1957													
Jul 02	0857	8	Jun 30	1140R	2	W01	N10	4039	Jun 30.6	40	40	45	flare time from radio event
Jul 05	0042	8	Jul 03	0830	3+	W42	N10	4039	Jul 03.5	70	66	40	3, 4, 5, 7, 8, 9, 10
									Jul 04.5	35			
Jul 19	1344	5	Jul 16	1742	1+	W28	S33	4061	Jul 16.5	12	12	68	4, 9
Jul 27	1959	4	Jul 24	1801	3	W27	S24	4070	Jul 24.5	55	55	74	3, 4, 5, 6, 7, 8, 9, 10
Aug 03	1557	6	Aug 01	0602	2	W05	N34	4086	Jul 31.5	(new)	10	58	8
									Aug 01.5	10			
" "	"	"	Aug 02	1432	1	E32	N26	4083	Aug 02.5	50	50	25	7
Aug 06	0508	6	Aug 03	1721	1	E17	N26	4083	Aug 03.5	50	50	60	7
" "	"		Aug 04	1827	1	W02	N26	4083	Aug 04.5	50	50	35	
Aug 09	1347	5	Aug 05	1930	1	W08	N26	4083	Aug 05.5	50	50	94	possibly relates to an earlier unlisted SC, masked by Aug 06 storm 7
" "	"	"	Aug 08	1116	2+	W57	N27	4083	Aug 08.5	50	50	26	
Aug 29	1920	7	Aug 28	<0913	3	E33	S31	4125	Aug 27.5	82	70	34	3, 4, 5, 7, 8, 9, 10
								WL214	Aug 29.6	54			Mt. Wilson plage
" "	"	"	Aug 28	2010	2+	E30	S28	"	" "	"	63	23	
Aug 31	1812	7	Aug 30	1337	1	W18	N25	WL215	(see text)		66	29	
" "	"	"	Aug 30	2213	-	-	-	-	-	-	-	20	4, 7 radio event, no optical obs.
Sep 02	0314	9	Aug 31	1257	3	W02	N25	WL215	(see text)		69	38	3, 4, 5, 7, 8, 9, 10
Sep 04	1300	9	Sep 02	1257	1+	W26	N10	WL216	(see text)		74	48	3, 4, 7, 10
" "	"	"	Sep 02	1313	2+	W36	S34	4125	Aug 02.6	60	60	48	5, 9
Sep 13	0046	9	Sep 11	<0236	3	W02	N13	4134	Aug 11.7	80	30	46	1, 3, 4, 5, 7, 8, 9, 10
Sep 14	0729	6	Sep 12	1510	2	W18	N11	WL228	Sep 12.9	57	57	40	

TABLE 1. (continued)

Magnetic Storm Date	Start	Kp max	Flares Date	Start	Imp.	Long.	Lat.	Calcium Plage McMath No.	Date	Area	Est. area at flare time	Δ T Flare-storm delay (hr.)	References and comments
1957													
Sep 21	1005	7	Sep 18	<1722	3+	E08	N23	4151	Sep 18.5	68	70	65	8
Sep 22	1344	8	Sep 20	2117	2	W14	N07	4152	Sep 19.7	35	43	40	7
" "	"	"	Sep 21	1330	3	W06	N10	4152	Sep 22.6	54	43	24	3, 4, 5, 6, 8, 9, 10
Sep 23	0255	9	" "	"	"	"	"	"	" "	"	48	37	7
Sep 29	0016	9	Sep 26	1907	3	E15	N22	4159	Sep 25.5	182	200	53	3, 4, 5, 7, 8, 9, 10
									Sep 26.5	195			
									Sep 27.5	220			
Oct 14	0440	6	Oct 13	<0534	2+	E40	N12	4186	Oct 12.5	86	82	23	
									Oct 13.5	80			
Oct 21	2241	7	Oct 20	1637	3+	W45	S26	4189	Oct 20.6	142	142	28	3, 4, 5, 6, 7, 8, 9, 10, 11
Nov 06	1821	7	Nov 05	<1205	2	W54	S24	4207	Nov 05.7	160	160	30	4, 7, 8
Nov 26	0155	7	Nov 24	0948	3	E37	S14	4263	Nov 24.6	83	83	41	4, 7, 8, 9, 11
Dec 31	0514	6	Dec 28	2229	2	W50	N25	4321	Dec 27.6	160	145	55	4, 7
								WL421	Dec 28.7	145			
1958													
Jan 20	2124	7	Jan 18	2253	1	W12	S11	4368	Jan 18.6	40	38	46	7
									Jan 19.6	32			
Feb 11	0125	9	Feb 09	2108	2+	W14	S12	4404	Feb 9.6	180	180	28	3, 4, 5, 6, 7, 8, 9, 12
" "	"	"	" "	"	"	"	"	"	" "	"	(70, see text)	26	
Mar 05	0537	7	Mar 03	<1005	3	E60	S15	WL563	Mar 03.7	114	114	43	4, 7, 11, 12
Mar 11	2316	7	Mar 11	<0030	1	E02	N11	WL571	Mar 9.8	80	83	23	
								4449	Mar 12.6	83			
Mar 14	1212	6	Mar 12	0024	2+	E02	N08	4449	" "	"	83	60	7, 12
Mar 17	0757	6	Mar 14	1454	2	W85	S21	4445	Mar 12.6	100	100	65	5, 7, 12 area doubtful, near limb
Mar 25	1540	6	Mar 23	0947	3+	E78	S14	4476	Mar 23.5	180	103	54	3, 4, 5, 7, 9, 10, 11, 12

TABLE 1. (continued)

Magnetic Storm			Flares					Calcium Plage				Δ T	
Date	Start	Kp max	Date	Start	Imp.	Long.	Lat.	McMath No.	Date	Area	Est. area at flare time	Flare-storm delay (hr.)	References and comments
1958													
									Mar 24.6	103			areas doubtful near limb
Jun 07	0046	8	Jun 04	0055	1	E74	N46	4597	Jun 4.6	20	20	72	
" "	"	"	Jun 04	<2147	2	W58	N14	4578	Jun 4.6	52	55	51	4, 5, 7, 9, 12
									Jun 5.5	60			
" "	"	"	Jun 05	0835	2+	W65	N15	"	" "	"	59	40	
" "	"	"	Jun 05	1656	2+	E66	S20	4598	Jun 5.5	40	40	32	3, 4
Jun 08	1728	6	" "	"	"	"	"	"	" "	"	40	73	7
Jun 28	0713	8	Jun 26	<0245	2+	E49	N10	4623	Jun 24.5	100	113	52	1, 7, 12
									Jun 26.5	130			
Jul 08	0748	9	Jul 07	0020	3+	W08	N25	4634	Jul 06.0	45	58	31	1, 2, 3, 4, 5, 7, 8, 9, 10, 11, 12
								WL763	Jul 07.7	75			
Jul 21	1617	7	Jul 19	1902	2+	E13	N23	4651	Jul 19.5	50	50	46	1, 4, 7, 8, 12
Jul 31	1520	5	Jul 29	<0259	3	W44	S14	4659	Jul 29.5	200	200	60	1, 2, 3, 5, 6, 7, 9, 10, 11, 12
Aug 17	0622	7	Aug 16	0425	3+	W50	S14	4686	Aug 15.8	80	90	26	2, 3, 4, 5, 7, 8, 9, 10, 12
									Aug 16.6	100			
Aug 22	0227	6	Aug 19	2118	2	E26	N18	4708	Aug 19.5	35	43	52	4, 5, 7, 8
			Aug 20	0042	2+	E15	N16	"	Aug 20.5	65		49	9
Aug 24	0140	5	Aug 22	1428	3	W10	N18	4708	Aug 22.5	64	64	35	2, 3, 4, 5, 7, 8, 9, 10, 11, 12
Aug 27	0303	7	Aug 26	0005	3	W54	N20	4708	Aug 25.5	70	80	27	1, 2, 3, 4, 5, 7, 8, 9, 10, 12
									Aug 26.5	90			
Sep 16	0930	5	Sep 14	0822	2+	W80	S10	4741	Sep 13.5	60	26	49	4, 7, 9, 12 area doubtful, near limb
									Sep 14.5	18			
Sep 25	0408	7	Sep 22	0738	2	W42	S19	4765	Sep 22.5	150	150	69	5, 9, 10, 12
" "	"	"	Sep 23	1024	2	W46	S19	4765	Sep 23.6	140	140	42	8

TABLE 1. (continued)

Magnetic Storm Date	Start	Kp max	Flares Date	Start	Imp.	Long.	Lat.	McMath No.	Calcium Plage Date	Area	Est. area at flare time	ΔT Flare-storm delay (hr.)	References and comments
1958													
Sep 25	0400	7	Sep 23	1334	1+	W43	N23	4754	Sep 23.6	55	55	38	
Oct 22	0315	6	Oct 19	0658	2+	W35	S17	4819	Oct 19.4	50	50	68	7, 8, 12
			" "	"	"	"	"	"	" "	See note	25	68	4819 two regions, approx equal area
Oct 24	0731	7	Oct 21	2318	2+	W22	S04	4826	Oct 21.6	45	51	56	1, 4, 7, 8, 9, 12
									Oct 22.8	62			
Dec 13	0001	6	Dec 11	1802	2	E00	S02	4913	Dec 11.8	85	85	30	4, 7
Dec 15	2022	4	Dec 12	1229	2+	W08	S03	4913	Dec 12.6	100	100	80	7, 9
1959													
Jan 09	1459	6	Jan 07	0215	2	W10	S16	4947	Jan 6.7	32	38	60	7
									Jan 7.8	48			
Feb 14	1142	6	Feb 12	<2301	3	E48	N13	5009	Feb 12.6	63	63	37	4, 7, 9, 11, 12
Mar 26	0842	8	Mar 24	0958	3	W77	N29	5054	Feb 24.5	30	-	47	8, 11, 12 near limb
Apr 09	1828	8	Apr 08	0905	3	E85	N27	5093	(No obs. CMP area,65)		-	33	4, 7, 8, 12 near limb
May 04	2021	6	May 02	2355	1	W48	N15	5120	May 2.6	35	33	44	7
									May 3.5	30			
May 11	2328	8	May 10	2102	3+	E47	N18	5148	May 10.5	190	190	26	2, 3, 4, 5, 7, 8, 9, 10, 11, 12
May 15	0703	6	May 13	0509	2+	E26	N22	5148	May 13.6	170	170	50	7, 9, 12
Jun 11	0909	6	(radio events, no optical data - possibly E limb flares)							-	-	-	4, 9, 12
Jul 11	1625	7	Jul 10	0206	3+	E60	N20	5269	Jul 09.5	40	40	38	2, 3, 4, 5, 7, 8, 9, 10, 11, 12
									Jul 10.5 (incl. in 5265)				
Jul 15	0803	9	Jul 13	1920	2	E48	S23	5273	Jul 13.5	70	64	3[illegible]	
									Jul 14.6	50			
			Jul 14	<0325	3+	E04	[illegible]	5265	Jul 14.5	120	120	29	2, 3, 4, 5, 7, 8, 9, 10, 11 region 5269 incl. in 5265
Jul 17	1638	9	Jul 16	2114	3+	W31	N16	5265	Jul 16.5	120	120	19	2, 3, 4, 5, 7, 9, 10, 11 region 5269 incl. in 5265

TABLE 1. (continued)

Magnetic Storm Date	Start	Kp max	Flares Date	Start	Imp.	Long.	Lat.	Calcium Plage McMath No.	Date	Area	Est. area at flare time	ΔT Flare-storm delay (hr.)	References and comments
1959													
Aug 16	0404	8	Aug 14	0040	2	E27	N11	5323	Aug 13.6	100	92	51	4, 7, 12 at least two regions
									Aug 14.6	80			
Aug 20	0412	6	Aug 17	2046	2	W27	N14	5323	Aug 17.7	60	60	55	two regions
" "	"	"	Aug 18	1014	3	W33	N12	5323	Aug 18.6	68	67	42	4, 5, 7, 9, 10, 11, 12 two regions
" "	"	"	Aug 18	1654	2+	E16	N05	5329	Aug 18.6	70	70	35	
Sep 03	1417	8	Aug 31	1850	1+	E11	N10	5344	Aug 30.7	24	24	67	7
								5344+ 5347	Aug 31.6	75			
" "	"	"	Sep 01	1910	1+	E90	N04	-	-	-	-	43	9 at limb
Sep 03	2159	8	Sep 01	1923	2+	E60	N12	5354	Sep 01.6	22	22	51	
Nov 27	2351	8	Nov 26	0923	2+	W17	S15	5467	Nov 26.7	45	45	38	7, 12
Nov 30	0653	6	Nov 28	2006	3	E31	N12	5476	Nov 28.7	170	170	35	7
Dec 05	0659	8	Dec 02	<1219	2+	W16	N07	5476	Dec 02.7	90	90	57	7, 12
Dec 23	1525	6	Dec 21	0043	2	W55	S05	5494	Dec 20.6	26	26	63	7, 12
									Dec 22.7	27			

while the delay of 68 hours for the storm of 1958 Oct 22 is shown against 50 and 25 units of area. The delay time of 94 hours for the storm of 1957 Aug 09 is related to the flare of 1900 UT Aug 05 by Maeda et al. (7) but it is probable that an earlier SC related to this flare was masked by the storm which began on Aug 06, and that the more likely relation for this storm is the flare at 1116 UT Aug 08.

4. DISCUSSION

The IGY-IGC period was chosen for this investigation because, as a result of the interest engendered at that time, many discussions and compilations of possible flare-storm relationships during this period have been published; those mentioned here are representative but are by no means the complete list. The forecasting of starting times of geomagnetic disturbances has remained the least satisfactory part of practical disturbance forecasting, and is a problem which has not been solved even with the aid of data from satellites. The relationship suggested by this analysis is presented as a new approach to this problem, and as a basis for further investigation.

The results tend to confirm that flare-storm delays are seldom less than a day or greater than about three days, and suggest that the areas of the active regions represented by the plages, being perhaps a measure of the solar magnetic fields available for driving the plasma (magnetic storm) clouds, can be directly related to the speed with which these clouds are propagated outwards from the sun.

From fig. 1 it is clear that this relationship breaks down in the case of very big plages, with areas more than about 9,000 millionths of the solar hemisphere, but the examples given in the description of the plage data in Section 2.3 above suggest that if the individual regions can be delineated, using perhaps coincident H-alpha spectrograms along the lines being developed for flare forecasting as part of the Solar Particle Alert Network programme (P. McIntosh, private communication), useful results might be achieved.

5. ACKNOWLEDGMENTS

This paper is part of the work of the Ionospheric Prediction Service Division, Commonwealth Bureau of Meteorology. The writer thanks Professor H. Dodson Prince and Miss E.R. Hedeman for their interest and for supplying spectroheliograms and tracings when this project was first suggested, and for their warnings about the fallibility of the calcium plage measurements.

References

1. Hakura, Y. and T. Goh.
Pre-SC polar cap ionospheric blackout and type IV solar radio outburst.
J. Radio Res. Lab., 6 (28) : 635-650 (1959).

2. Thompson, A.R. and A. Maxwell.
Solar radio bursts and cosmic rays.
Planet Space Sci., 2 (2/3) : 104-109 (1960).

3. Obayashi, T. and Y. Hakura.
Propagation of solar cosmic rays through interplanetary magnetic field.
J. Geophys. Res., 65 (10) : 3143-3148 (1960).

4. de Feiter, L., A.D. Fokker, H.P. Th. van Lohuizen and J. Roosen.
Solar radio events and geomagnetic storms.
Planet Space Sci., 2 (4) : 223-227 (1960).

5. Sinno, K.
Some characteristics of solar corpuscular radiations which excite abnormal ionization in the polar upper atmosphere.
J. Radio Res. Lab., 8 (35) : 17-28 (1961).

6. Sarabhai, V. and G.L. Pai.
Cosmic ray effects associated with polar cap absorption events.
J. Phys. Soc. Japan, 17 Suppl. A-2 : 286-289 (1962).

7. Maeda, H., T. Sakurai, U. Ondoh and M. Yamamato.
A study of solar-terrestrial relationships during the IGY and IGC.
Ann. Geophys., 18 (4) : 305-333 (1962).

8. Haurwitz, M W.
Dependence of interval between flare and associated SC storm on prestorm conditions.
J. Geophys. Res., 67 (7) : 2979-2982 (1961).

9. Sinno, K.
Characteristics of solar energetic particles which excite polar cap blackouts.
J. Geomagn. Geoelect., 13 (1, 2) : 1-10 (1961).

10. Noyes, J.C.
Solar active regions and solar cosmic rays.
J. Phys. Soc. Japan, 17 Suppl. A-2 : 275-280 (1962).

11. Bhargava, B.N. and R. Natarajan.
The remarkable sudden commencement of November 13, 1960 in the low and middle latitude magnetograms.
J. Atmos. Terrest. Phys., 29 (8) : 957-964 (1967).

12. Caroubalos, C.
Contribution a l'etude de l'activité solaire en relation avec ses effets géophysiques.
Ann. Astrophys., 27 (5) : 333-388 (1964).

13. Bednarova-Novakova, B.
Solar indicators of the origin of geomagnetic storms.
Geofysikalni Sbornik 14 : 477-501 (1966).

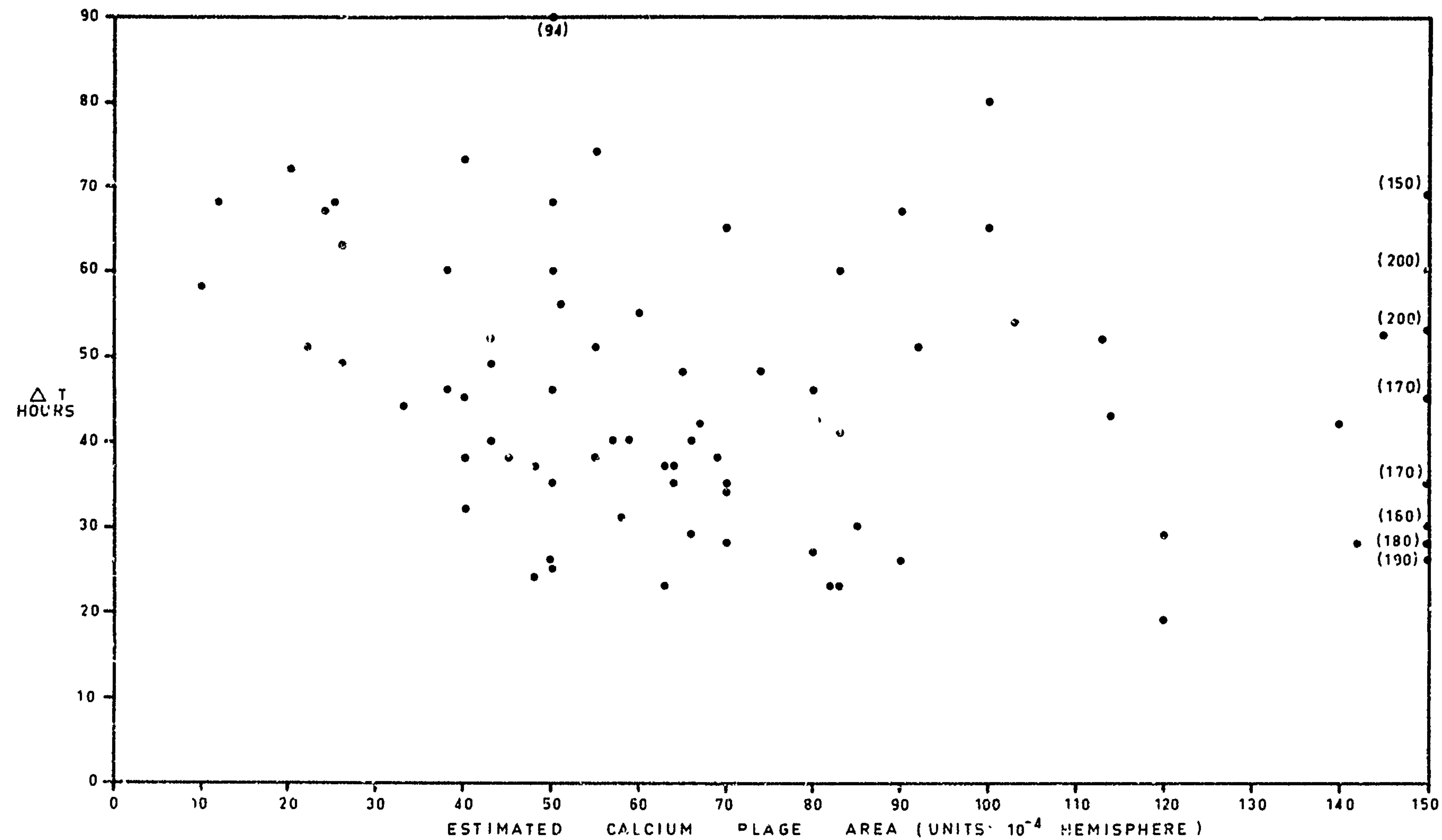

Fig. 1. Relation between flare-storm delay times and areas of corresponding calcium plages during IGY-IGC (data from Table 1).

FORECASTING HF ABSORPTION DURING POLAR-CAP-ABSORPTION EVENTS

by

Ming S. Wong

Air Force Cambridge Research Laboratories,
L. G. Hanscom Field, Bedford, Massachussetts 01730, USA

ABSTRACT

A method is described of using real-time riometer data for short-term prediction on the course of absorption during PCA events. From Thule and other riometer stations, data on past PCA events have been analyzed for prediction. As the absorption rises above a threshold (0.7 dB at 30 MHz) at a station, when an event begins, the incoming data points are projected ahead by prediction routines at the forecasting central. Integrated flux-intensity data on the solar radio burst at centimetric wavelengths (when there is identifiable association between the causative solar flare and the evolving PCA event) provide a useful estimate of the peak absorption for an event. For the period from this peak to noon the next day - during which absorption may decrease sharply during night hours and then rise to a second peak at noon, or it may decrease gradually if night hours do not occur at the station - the prediction is the least accurate. After this period, reasonable accuracy has been obtained: 10% or 1 dB RMS error (whichever is larger) for lead times up to one or two days in some cases. The predicted absorption values for the reporting riometer stations are fitted to models which - with consideration of solar zenith-angle dependence, and auroral-oval boundary - prescribe the distribution of absorption in the polar region, for vertical incidence and 30 MHz.

For conversion to lower frequencies of interest, we prescribe models of frequency dependence for the absorption, these models being based on theoretical calculations made for various electron-density and atmospheric-pressure profiles in the D-region - with consideration for latitudinal, seasonal, and solar-cycle variations. Departures from the inverse frequency-squared law, at the lower frequencies, are shown in the calculations. For conversion from vertical-incidence absorption to oblique-incidence values, for given propagation paths traversing the polar region, computer routines in use at the ESSA Laboratories (Boulder, Colorado) are adopted to estimate the likely propagation modes, and the corresponding angles of incidence in the D-region.

The reliability of transpolar v.l.f.-measurements as a method to forecast HF-propagation disturbances.

by

G. Lange-Hesse and K. Rinnert

Max-Planck-Institute for Aeronomy, Institute for Ionospheric Physics,
3411 Lindau/Harz uber Northeim, West Germany

SUMMARY

A three year period (1966 - 1968) of transpolar v.l.f.-propagation measurements (phase and amplitude) is analysed with regard to test the reliability of this method to detect the impact of solar protons (ejected from proton flares) in the polar lower ionosphere. This impact of solar protons causes the polar cap absorption events (PCA) of HF-radio waves. In most of the cases a PCA can be considered as a precursor event of ionospheric and geomagnetic storms.

The long distance v.l.f.-propagation is of such manner, that it is very reliable to detect the PCA on the v.l.f.-recordings during night-time but uncertain during day-time. The special day and night distribution over the polar cap is responsible that the reliability of the detection of PCA-events by v.l.f.-recordings is very high in winter and low in summer. Data are given about the reliability of the detection of a PCA by transpolar v.l.f.-measurements made in middle latitudes. In addition to this data are given about the reliability that a geomagnetic sudden commencement follows the PCA detected by v.l.f.-measurements.

Finally data are given about the reliability to give a prediction of the duration of the recovery phase of the PCA from the typically disturbed v.l.f.-recordings.

For more than 20 years it has been well known that a sudden decrease in F2-layer critical frequency is caused by geomagnetic disturbances. This effect occurs in middle latitudes and its magnitude is greatest at high latitudes (see e.g. APPLETON and PIGGOT, 1950, and LANGE-HESSE, 1953). This decrease of F2-layer critical frequency also occurs in the auroral zone, but there it is masked by a simultaneous increase of ionospheric absorption, called auroral zone absorption (AZA), which also is controlled by the degree of geomagnetic activity (see e.g. WELLS, 1947). The decrease in F2-layer critical frequency in middle latitudes and the increase of ionospheric absorption in the auroral zone cause a remarkable interference of HF radio waves propagation. Since both effects are controlled by the geomagnetic activity, there is a big interest for the users of HF radio wave propagation to predict geomagnetic disturbances.

The geomagnetic storms and the accompanying ionospheric disturbances are caused by plasma which is ejected from active centers on the sun and which enters the earth's atmosphere. Due to the earth magnetic field this plasma impact mainly takes place in the regions with geomagnetic latitudes of about ± 65 degrees. These are the auroral zones. After the ejection at the sun it takes about 24 to 48 hours up to the beginning of the disturbance of the atmosphere. To forecast such disturbances we need events which on the one hand are in good correlation with the impact of solar plasma in the earth's atmosphere and which, on the other hand, can be measured in advance.

Under some conditions the effects of high energetic protons (energy greater than 10 MeV) can do this. At times of high solar activity such solar protons are ejected by proton flares. High solar activity also means that there is an intensified ejection of plasma and therefore also stronger geomagnetic disturbances on the earth together with disturbances of HF radio wave propagation. These phenomena are closely connected with one another, but, in general, a plasma burst does not necessarily mean that protons are blown out, and vice versa. It is also possible that the earth is only hit by one species of particles, protons or plasma. Because of their high energy the protons travel with a much higher velocity than the plasma clouds and therefore reach the earth earlier. The protons hit the atmosphere in the polar caps and there change the ionospheric structure, especially in the lower regions down to 30-50 km. These particles neither cause geomagnetic disturbances nor can they be detected in middle latitudes. These proton events produce the well known PCA-effects (Polar cap absorption-event). [BAILEY, 1964] Strong attenuation of HF radio wave pro-

pagation is then observed within the polar cap but no effect is noticed in middle latitudes. Observations of strong HF-propagation disturbances in higher latitudes which later were identified as PCA-events were reported back to 1942 [LANGE-HESSE, 1963].

Rather simple methods to measure these PCA-events or to detect the impact of polar protons are riometer-measurements and the propagation of v.l.f.-radio waves in polar regions. Riometer-measurements have to be made in the polar cap whereas the v.l.f.-radio waves only have to cross the polar regions and can be received in middle latitudes. Therefore the last method seems more suitable. The following reduction are based on a three year period of measurements (1966 - 1969). These are v.l.f.-recordings in amplitude and phase of the transmitter NPG (18.6 kHz), Seattle/USA at Lindau/Harz, Germany and riometer-measurements on 27.6 MHz at Godhavn, Greenland. Figure 1 shows the propagation path NPG-Lindau across the polar cap. The riometer-station Godhavn is about in the middle of the path. The methods proved to have different sensitivities. The riometer shows the biggest effects with day-time conditions because at this time the electron density has much increased by photo-detachment. Contrarily, the v.l.f.-propagation is most affected at night-time conditions, when we have highly increased absorption. The two methods complement one another very well. [RINNERT, 1967] Considering the changing day-night conditions in the northern polar regions it follows that the summer months May-July offer good conditions for riometer measurements. V.l.f.-propagation is not essentially affected at this time. Whereas the observations by v.l.f.-propagation measurements are to be advised during the winter months, at this time the riometer shows nearly no effects. Figure 2 shows the change in the solar illumination along the great circle path NPG-Lindau. The lower border of each diagram corresponds to the receiving station Lindau and the upper border to the transmitter NPG, Seattle. The dashed lines mark the intersection of the propagation path with the zone of maximum aurora frequency (see Fig. 1). The different curves represent sunset or sunrise in different heights. The cross-hatched regions represent night-time.

Figure 3 shows an example of a PCA-event on the v.l.f.-recordings NPG-Lindau. The diurnal change in fieldstrength is very disturbed on Nov. 2/3, that is, the normal increase of the amplitude of the received signal at night-time does not take place. Sometimes these disturbed conditions can last up to 10 days. During the whole time the normal history of the phase is rather unaffected. At least, minor proton events clearly affect only night-time propagation. This fact may lead to an uncertainty in determining the beginning of an event. If a PCA-event starts during day-time condi-

tions on the transpolar v.l.f. propagation path, the absorption effect can be noticed not until night-time conditions occur. Due to the propagation path and season a delay of about half a day is possible which can be improved if one records several v.l.f. transmitters over transpolar paths. Figure 4 shows another example of solar proton effects on v.l.f. amplitude records in comparison with riometer records.

Figure 5 shows schematically all PCA-events observed during the three year observation period. The shaded regions represent times during which there are no usable recordings available (instrument trouble and so on). All effects recorded have been confirmed by other measuring methods (from May 1967 up to now) by satellite data (Explorer 34, Vela, Pioneer 9, OGO III). Otherwise, no considerable effect has been measured by any method which could not be seen on v.l.f. recordings. If there are sufficient night-time conditions on the propagation path, the control by v.l.f. is very reliable. In the table the probability of forecasting geomagnetic disturbances following these effects is shown.

Schedule

Total number of events	28
Kp $\geq$ 5o within the following 3 days (disturbed)	18
Kp $<$ 5o within the following 6 days (quiet)	10
ssc, within 24 - 48 hours after SPE	17
ssc, $\sum$Kp $\geq$ 30 within the following 5 days	11
ssc, $\sum$Kp $<$ 30 within the following 5 days	6

Starting with a total number of 28 observed proton events 18 were followed by geomagnetic storms, that is, Kp $\geq$ 5o within the three days after which the v.l.f. recordings began to show the absorption effect. In most cases a PCA is followed by a ssc, however, a ssc does not mean that the geomagnetic activity will reach a degree of Kp = 5o. $\sum$Kp stands for the sum of the eight Kp-values of one day. This is a measure of the mean diurnal geomagnetic activity. The relation disturbed-to-quiet conditions is 18 to 10 and that means that, with a certainty of 65 %, a PCA is followed by a magnetic storm. This is also the probability with which we can predict HF radio wave disturbances from transpolar v.l.f.-data.

Figure 6 shows the statistical connection of the degree of geomagnetic activity with the time after the occurence of PCAs. The number of days following the day the PCA had been observed on the v.l.f.-recordings is scaled on the abscissa whereas the sum of the 28 $\sum$Kp-values is scaled on the ordinate. Two days after the PCA one expects the geomagnetically most disturbed conditions, and these decrease in the course of 7 or 8 days. Also, on the second day after the onset of the PCA one can expect (with a probability of 65 %) the most disturbed conditions of HF-radio wave propagation. The impact of solar protons into the polar cap leads to an increase of the electron density at lower altitudes. This causes the high absorption in the v.l.f.-band, particularly at night-time. The absorption then reaches values of the day-time propagation. This effect lasts several days. [RINNERT, 1968] The reduction of the v.l.f.-effects observed reveals that the recovery is nearly proportional to the maximum absorption in db. Figure 7 shows the value of about 3 days per 10 db. This special value depends on frequency and propagation path.

Summary

HF radio propagation is essentially affected by the impact of solar plasma which leads to the geomagnetic disturbances. In the auroral zone, disturbances of HF radio wave propagation are most intense and decrease both towards the equator and towards the poles. Many such solar eruptions of plasma are connected with bursts of high-energy protons. These protons can reach the earth's atmosphere much earlier than the slower plasma and thus produce PCA-events in the polar caps. PCA-events can always be noticed by means of transpolar v.l.f. measurements if there are night-time conditions. Out of 28 PCA-events recorded during the years 1966 - 1968, 18 were followed by magnetic storms, i.e., plasma impacting into the earth's atmosphere. A magnetic disturbance and also a disturbance of HF radio wave propagation is most probable on the second day after the arrival of the protons. The proton event itself only affects the radio propagation within the polar caps. According to the intensity of the effect it can last several days up to about 10 days. There is a connection between the duration of the PCA-effect and the maximum absorption of the v.l.f. propagation.

References

APPLETON, E. V. and PIGGOT, R., 1950, Nature 165 p. 130

BAILEY, D.K., 1964, Planet. Space Sci. 12 p. 495

LANGE-HESSE, G., 1955, J. Atm. Terr. Phys. 7 p. 49

LANGE-HESSE, G., 1963, Naturwissenschaften 19 p. 605

RINNERT, K., 1967, Kleinheubacher Berichte 12 p. 261

RINNERT, K., 1968, Kleinheubacher Berichte 13, in preparation

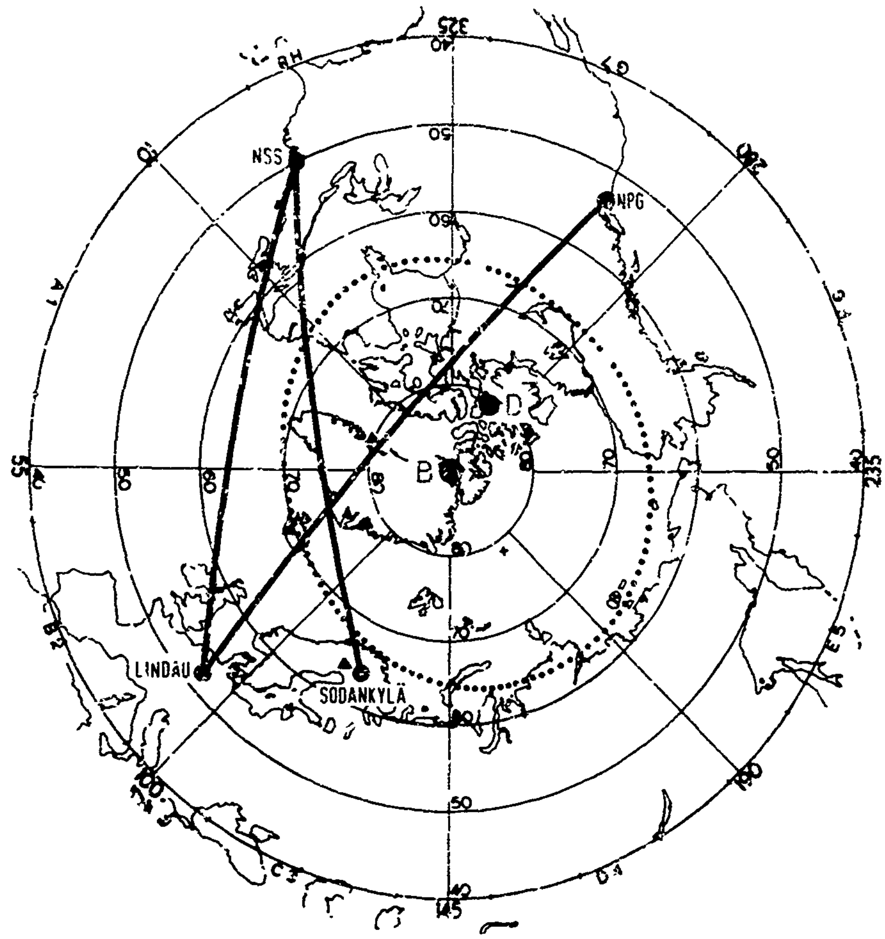

······ Maximum Auroral Region: θ = 22.5°

D = Magnetic Dip Pole

B = Magnetic Axis Pole

Fig. 1 Polar map with geomagnetic coordinates showing the transpolar propagation path NPG-Lindau. The black triangle in the middle of the path on the west coast of Greenland marks the Riometer-station Godhavn.

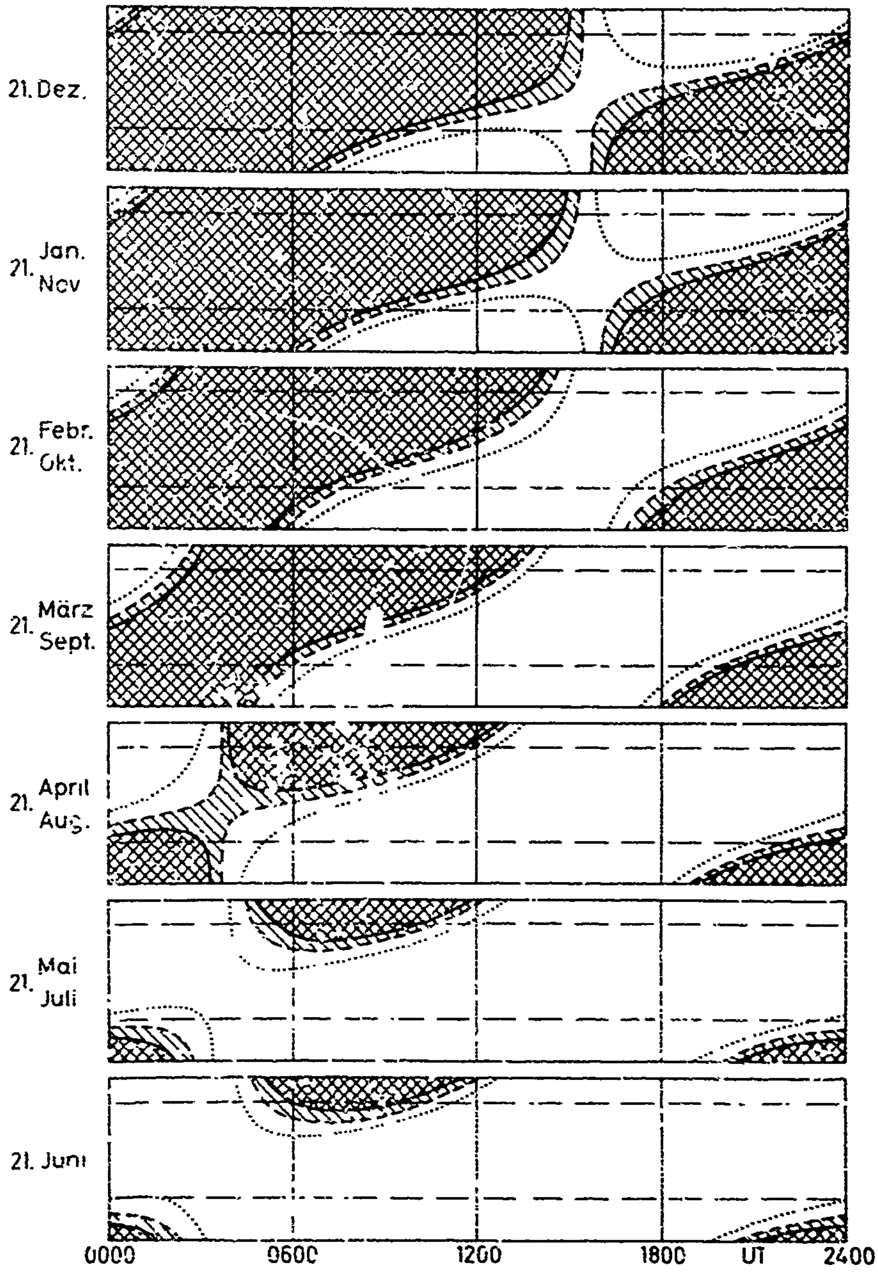

Fig. 2 Change of illumination along the great circle path from Fig. 1 between Seattle and Lindau. The lower border of each diagram corresponds to the receiving station at Lindau and the upper border to the transmitter. The different curves represent sunset and sunrise in different heights: ..... at ground, —— at 75 km and ----- also at 75 km but taking into account a screening-height of 30 km

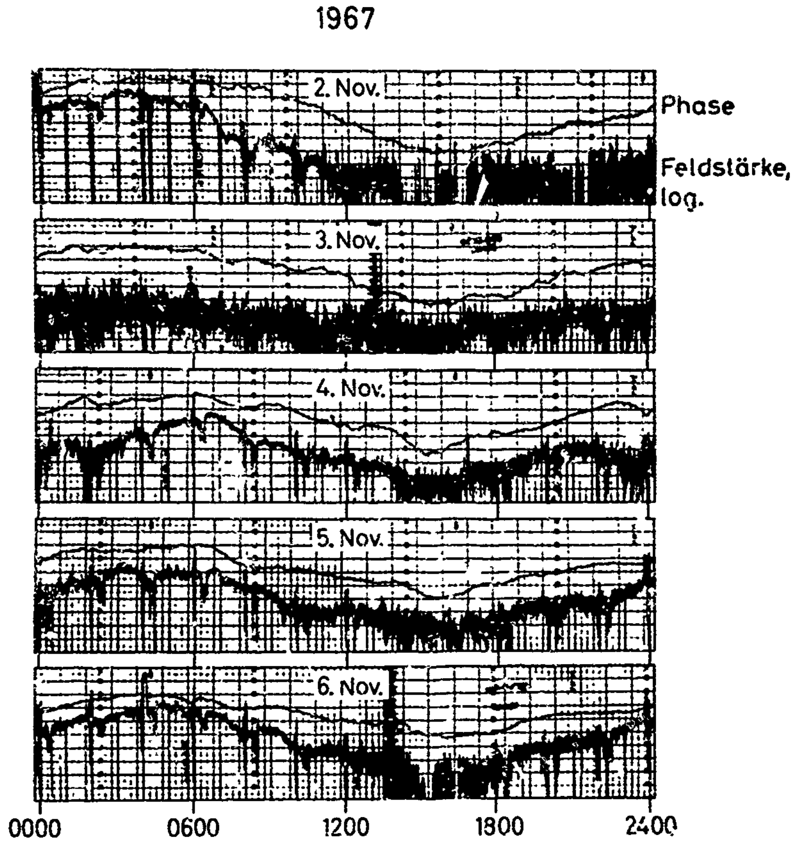

Fig. 3 Example of v.l.f. recordings NPG, 18.6 kHz made at Lindau disturbed by the PCA from Nov 2, 1967. The amplitude record is logarithmic with 50 db full scale whereas fullscale of the phase record corresponds to a time-delay of 100 μsec (360^o $\hat{=}$ 53,7 μsec at 18.6 kHz).

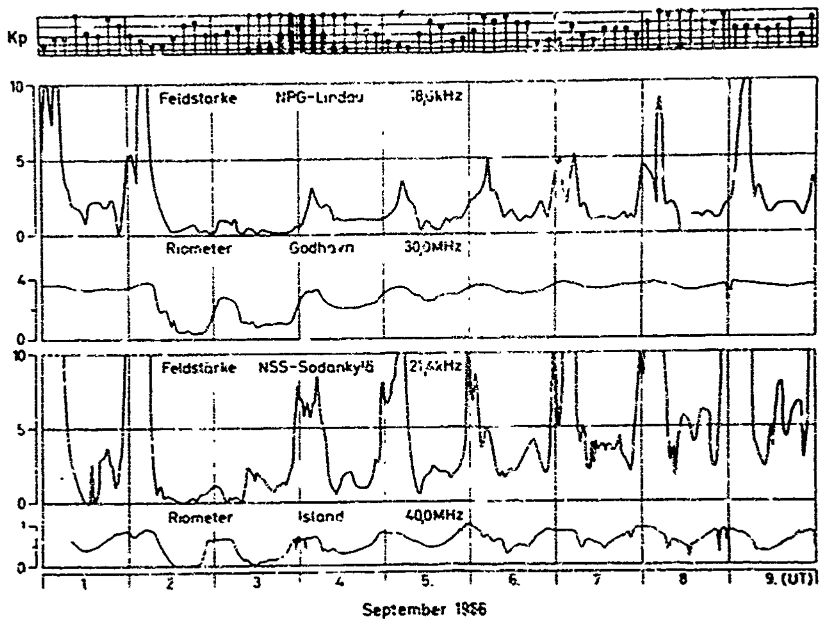

Fig. 4 Effect of the PCA-event from September 2, 1966 on transpolar v.l.f.-amplitude records in comparison with Riometer records.

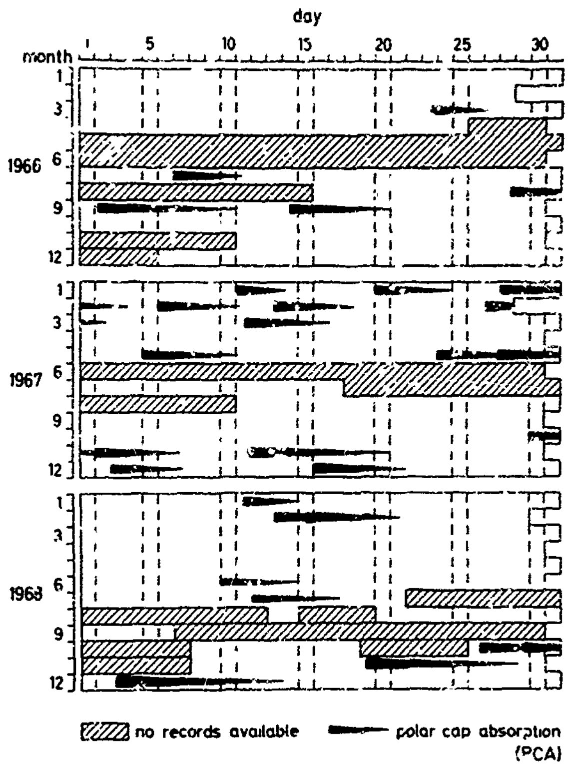

Fig. 5 Schedule of observed PCA-events during the tree years period 1966 to 1968.

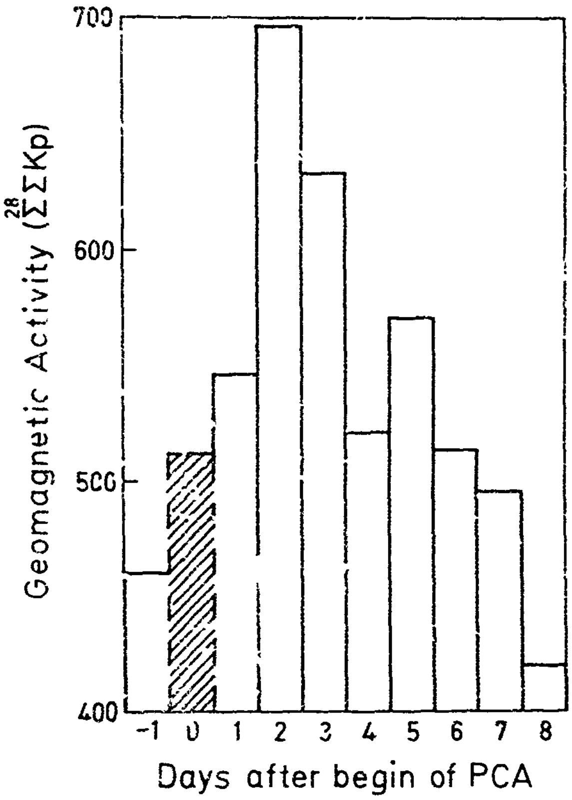

Fig. 6 Connection between the degree of geomagnetic activity and time after a PCA has been observed on the transpolar v.l.f.-records NPG-Lindau.

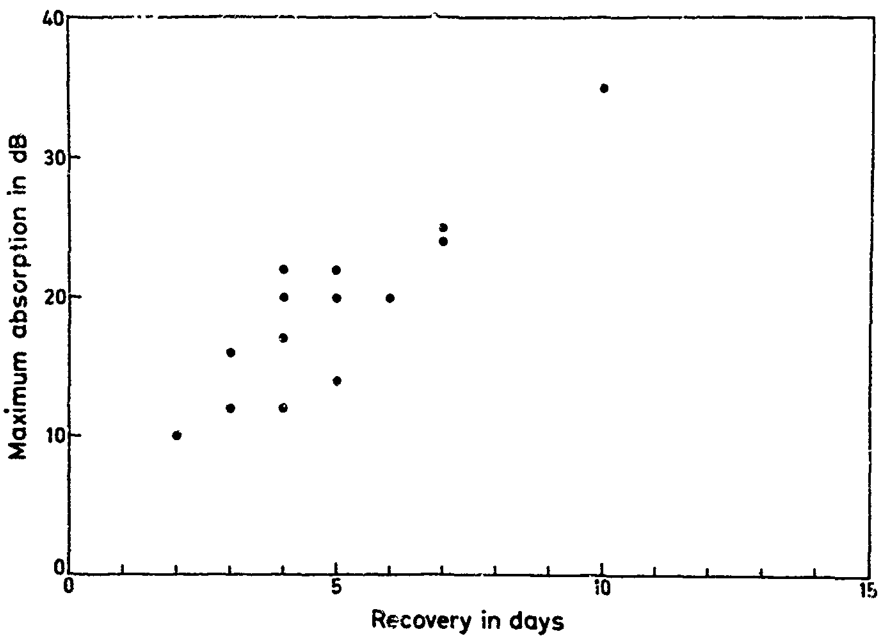

Fig. 7 Connection between the duration of recovery to normal propagation conditions and maximum absorption.

PREDICTION OF DAILY FLUCTUATION OF THE F-REGION PLASMA FREQUENCY

by

S. M. Bennett and A. B. Friedland
Avco Corporation/ Applied Technology Division
Lowell Industrial Park
Lowell, Massachusetts 01851

Prediction of Daily Fluctuation of the F-Region Plasma Frequency

by

S. M. Bennett and A. B. Friedland*
Avco Corporation/Applied Technology Division
Lowell Industrial Park
Lowell, Massachusetts 01851

SUMMARY

While the solar cycle variation of the foF2 is understood, seasonal and daily perturbations of the F-region plasma frequency occur without clear dependence upon solar-geophysical indices. Apart from the magnetic storm effect, the perturbations appear to be random in nature. We have attempted to relate daily fluctuations in foF2 to daily solar flux changes and the 3-hour global magnetic index K_p by statistical techniques. Multiple regression analysis of data obtained by 19 Northern Hemisphere vertical-incidence sounding stations during 1961 was performed. Hourly values of foF2, normalized to the station mean monthly value at each hour, solar flux at Ottawa normalized to the monthly mean value, and global K_p with a six hour lag, yielded statistically significant results for many periods studied. The most satisfactory intervals included a winter daytime relationship to the solar flux, and a summer daytime relationship with K_p. The nighttime results were generally less satisfactory, probably due to magnetic storm effects. Of particular significance to forecasting is a large monthly perturbation related to 27 day periodicities in the 10-cm solar flux (presumably related to the EUV output). Several other methods of forecasting foF2 on a daily basis are compared.

INTRODUCTION

Solar cycle, seasonal, diurnal, and geographical variations of the F-region plasma frequency (foF2) are well documented and at least partially understood, but the daily fluctuations of the foF2 recorded at individual vertical-incidence ionosondes during geomagnetically undisturbed periods are often considered to be a purely statistical phenomenon. Yet, in previous synoptic studies of the ionosphere during magnetic storms, we have occasionally observed that the pre-storm ionization levels are systematically different from their monthly median values. Since the reference levels utilized were derived from the monthly-hourly median measured foF2 at each station, the discrepancy could not be ascribed to any prediction scheme.

The solar-cycle relationship between sunspot number (or solar 10-cm radiowave flux) and the F-region plasma density suggests a saturation effect at the maximum of intense cycles, while there is a general absence of solar centers-of-activity during the solar sunspot minimum. However, the declining phase of a solar cycle often exhibits large percentage changes in solar energy flux, related to the 27-day synodic rotation period of major centers of solar activity. We chose to investigate the relationship between daily values of the 10-cm solar radiowave flux as measured at Ottawa, and the fluctuation of foF2 at a group of 19 stations in North America and Europe during a substantial portion of 1961. Only a small fraction of the computer processing output has been seriously studied, due to the usual time and funding restrictions. The initial results were encouraging, and this paper presents a summary of data for Washington, D. C.

REGRESSION ANALYSIS

The data were cast in the form of a regression equation,

$$X_1 = A_2X_2 + A_3X_3 + B$$

where

$$X_1 = \left[\frac{foF2_{obs} - foF2_{mean}}{foF2_{mean}}\right]$$

$$X_2 = \left[\frac{\phi_{obs} - \phi_{mean}}{\phi_{mean}}\right]$$

$$X_3 = K_p .$$

The monthly mean value of the solar flux (ϕ) observed at Ottawa was computed, and the daily fractional deviation X_2 utilized for all computations on the specified day. The foF2 mean is computed for each hour of the day over the month period, and the specific hour and day are selected for computation of the fractional deviation X_1. Also included in the computation was the planetary magnetic index K_p which was lagged by 6-hours to approximate the neutral air response to transient heating.

* now at American Science and Engineering, Inc., Cambridge, Massachusetts.

Figure 1 is a typical computer tabulated summary of the multiple-regression program. The mean value of variables 1 and 2 are essentially zero since they are normalized to the monthly mean, while the numerical average of the quantized values of K_p is not very meaningful mean for variable 3. The standard deviations are shown in the next column, and we shall eventually compare the standard deviation of the dependent variable with the standard error of the estimate. The regression coefficients A2 and A_3 and their standard errors S_{A_2} and S_{A_3} are shown along with the computed value of Student's-t distribution.[1] For the number of degrees of freedom resulting from the ordinary monthly sample of about 25 days, t-values of 2.06 and 2.80 imply that the probability that the regression coefficients being zero is 0.05 and 0.01 respectively. In this example, the probability that the regression coefficient A2 actually being zero is less than 2 percent (t-value of 2.452), while a t-value of -0.430 for the coefficient A_3 implies that zero is as satisfactory a value as that which has been computed. The lack of correlation with K_p in this example should not be mistaken for a general result. Rather significant correlations with K_p have been noted in this study. The standard error of the estimate is a measure of the dispersion of the data points X_1 about the regression line. In this instance the standard deviation of the raw data X_1 is 0.15746, while it is only 0.14104 with respect to the regression line. An analysis of the variance is also performed utilizing the F test to estimate the validity of the linear behavior of the data.[1] From tables of the distribution of F for 2 and 23 degrees of freedom, we find that for F of 3.42 and 5.66, the regression analysis is significant at the 5 percent and 1 percent levels respectively.

The effect of the linear regression program on the distributions is graphically presented in a histogram (note that the histogram of figure 2 is for a different station than that shown in figure 1). For convenience, the ordinal number 12 is selected as zero and the data are quantized in intervals of 0.05. The upper histogram is that of X_1, the fractional fluctuation of hourly values of foF2 about the monthly mean value, while the lower histogram displays the residuals about the regression line. Each asterisk represents a data point within the class interval, and the number in each class is at the top of each column. Also presented below each histogram is the percentage of quantized points in intervals of $\pm$ 0.05, $\pm$ 0.10 ... about the mean value. This is a measure of the dispersion of the points from the mean in the first histogram, and from the regression line in the second histogram. In this instance, a clearly superior organization of the data is obtained by the regression analysis; this is visually apparent, but is also manifest in a comparison of the standard deviation of X_1 (0.121) with the standard error of the estimate (0.080).

The regression coefficients derived for selected periods in 1961 for Washington, D. C., are summarized in figures 3, 4, 5. Since only a survey of the possible results was intended, not all hours of the day or months were processed. Values of the linear regression coefficients A_2 and A_3, corresponding to the dependence of the fluctuation of foF2 on variations in solar flux and on the planetary magnetic index, K_p, are plotted with error bars extending to one standard error.

The significance of the solar flux in day-to-day variations of foF2 should be evident from the figures. The dependence is most noticeable during the winter and equinoctal months, and weak or absent during the summer. A clear tendency exists in the case of K_p for positive correlation in winter and negative correlation in the summer with a transition at the equinox. The relative magnitude of the regression coefficients is misleading; while one expects a variation of $\pm$ 0.20 in the solar flux variable X_2 over a month, the X_3 ranges over the K_p values of 0 to 9. As a consequence, magnetic activity can be at least as important a contribution to the variability as the solar flux.

An interesting result is the correlation of foF2 with solar flux levels even during the nighttime hours. This is undoubtedly an indirect result of the changes in the previous day thermosphere temperature and electron density. At this juncture, it would be unwise to presume that this is a general result, or that any direct causal relation obtains.

We attempted to identify other potential geophysical variables of significance by plotting the residuals against such parameters as the sum of K_p and A_p for the previous 6, 12, 18, and 24 hours, resulting in reasonably significant subjective correlations, especially for the longer sums. We were not, however, able to treat this portion of the study in a quantitative manner as it would have required a major revision of the data merging program. A possible improvement in the computation of the mean value of foF2 would account for the seasonal trend in foF2 since this is related to day of the year and not to solar flux. A 30-day running predictor, based on observed data, might be a more satisfactory mean, and further reduce the residual scatter.

PREDICTION TECHNIQUES

While the establishment of a statistical correlation between solar and geophysical variables and variations in the F-region plasma frequency may result in more efficient prediction of daily-hourly values of foF2, it cannot be assumed that it is the only effective short-term prediction technique. For purposes of comparison, we tested several prediction methods and compared them with the ESSA/ITSA three-month advance predictions for Washington, D. C., for the first and last three (3) months of 1961. A total of 189 sample points for each curve of figure 6 was obtained by predicting foF2 every three (3) hours of every seventh day of the period considered. The cumulative percentage distribution of the percentage of the test points having percentage errors less than ϵ is a measure of the efficiency of the method considered. The most successful method is the monthly multiple regression, while the ESSA/ITSA advance predictions are the least successful. This is not surprising since the monthly regression

utilizes all of the data for the month to arrive at a prediction, and the average error is zero, but the ESSA/ITSA forecast may result in a systematic error due to errors in the predicted solar flux value and in the prediction coefficients. But the three-month in advance predictions are not expected to be accurate on a daily basis. Note that the three-day running mean is relatively satisfactory. This can be understood since the previous several days reflect, at least, the influence of the solar flux variation. The 30-day running mean is more satisfactory than the 15-day running mean, since it effectively averages over a whole solar rotation

CONCLUSION

The analysis reported in this paper suggests that, in addition to the solar cycle dependence of foF2, there is a daily relationship with the solar flux output as observed in the 10-cm radiowave emissions. One should not assume any necessarily direct causal relationship, especially at night; however, a correspondence of the daytime result with solar ionizing radiations such as EUV is likely. The period chosen for study was particularly fruitful since there were few major centers of solar activity and the solar flux exhibited marked 27 day cyclic tendencies. The search for correlations at other phases of a solar cycle may be clouded by the difficulty in isolating seasonal and secular trends. The residual data exhibit the largest errors during geomagnetically disturbed periods. Hence, it may be suggested that sorting of the data by geomagnetic activity indices prior to correlation analysis may yield more stable results during quiet times, and the geomagnetic storm effect reserved for separate study.

REFERENCES

1. Tables for Statisticians, H. Arkin and R. Cotton, Barnes & Noble, New York, 1963.

```
MULTIPLE REGRESSION...STATION  22 YEAR   1 MONTH   1 HOUR 1200

     SELECTION... 2

VARIABLE      MEAN        STANDARD       CORRELATION       REGRESSION     STD. ERROR      COMPUTED
  NO.                     DEVIATION       X VS Y           COEFFICIENT    OF REG.COEF.    T VALUE
   2       -0.00000       0.20280        0.50597          0.36840        0.15025         2.45201
   3        2.17923       1.46731       -0.26272         -0.00894        0.02077        -0.43037
DEPENDENT
   1        0.00195       0.15746

INTERCEPT                   0.02142

MULTIPLE CORRELATION        0.51181

STD. ERROR OF ESTIMATE      0.14104

                      ANALYSIS OF VARIANCE FOR THE REGRESSION

     SOURCE OF VARIATION          DEGREES        SUM OF          MEAN              F VALUE
                                 OF FREEDOM      SQUARES         SQUARES
ATTRIBUTABLE TO REGRESSION          2            0.16238         0.08119          4.08164
DEVIATION FROM REGRESSION          23            0.45749         0.01989
     TOTAL                         25             0.61987

RB(X,Y)=(SDX/SDY)*AI WHERE AI=REGRESSION COEFFICIENTS
RB(X(I),Y)=    0.47448  -0.08328

THE FOLLOWING ARE THE CORRELATION COEFFICIENTS FOR ALL COMBINATIONS OF X AND Y
       Y,X2       Y,X3      Y,X4
                  X2,X3     X2,X4
                            X3,X4
WHERE Y=X1
  0.50597   -0.26272     0.44013
            -0.37818     0.78042
                        -0.33081
```

Fig.1 Computer tabulation of regression analysis

```
DATA SCREENING PROBLEM     1  STATION  3 YEAR 1 MONTH  1 LOCAL HOUR 1200

SUMMARY STATISTICS FOR VARIABLE   1

TOTAL=  -0.070  AVERAGE= -0.002  STANDARD DEVIATION=  0.121  MINIMUM= -0.218  MAXIMUM=  0.253  DELTA= 0.0474

                                        HISTOGRAM   1

FREQUENCY   0   0   0   0   0   0   1   0   3   5  10   1   0   2   4   2   1   0   0   0   0   0   0
```

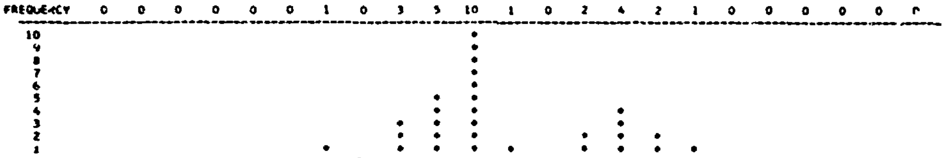

```
INTERVAL    1   2   3   4   5   6   7   8   9  10  11  12  13  14  15  16  17  18  19  20  21  22  23
CLASS
PERCENTAGE OF POINTS BETWEEN 0.0 AND .05 IS  37.93
PERCENTAGE OF POINTS BETWEEN 0.0 AND .10 IS  52.07
PERCENTAGE OF POINTS BETWEEN 0.0 AND .15 IS  85.21
PERCENTAGE OF POINTS BETWEEN 0.0 AND .20 IS  93.10
PERCENTAGE OF POINTS BETWEEN 0.0 AND .30 IS 100.00
PERCENTAGE OF POINTS BETWEEN 0.0 AND .40 IS 100.00
PERCENTAGE OF POINTS BETWEEN 0.0 AND .50 IS 100.00
```

```
DATA SCREENING PROBLEM     1  STATION  3 YEAR 1 MONTH  1 LOCAL HOUR 1200

SUMMARY STATISTICS FOR VARIABLE   7

TOTAL=  -0.000  AVERAGE= -0.000  STANDARD DEVIATION=  0.077  MINIMUM= -0.152  MAXIMUM=  0.163  DELTA= 0.0476

                                        HISTOGRAM   1
STANDARD ERROR OF ESTIMATE    0.08027

FREQUENCY   0   0   0   0   0   0   0   0   2   1   7  10   5   1   3   0   0   0   0   0   0   0   0
```

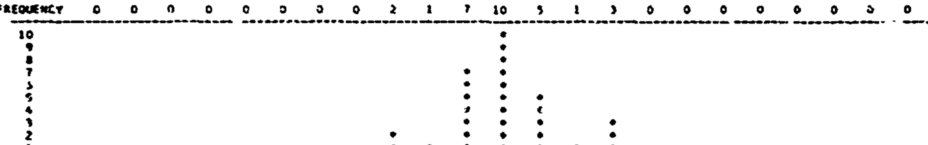

```
INTERVAL    1   2   3   4   5   6   7   8   9  10  11  12  13  14  15  16  17  18  19  20  21  22  23
CLASS
PERCENTAGE OF POINTS BETWEEN 0.0 AND .05 IS  75.86
PERCENTAGE OF POINTS BETWEEN 0.0 AND .10 IS  97.76
PERCENTAGE OF POINTS BETWEEN 0.0 AND .15 IS 100.00
PERCENTAGE OF POINTS BETWEEN 0.0 AND .20 IS 100.00
PERCENTAGE OF POINTS BETWEEN 0.0 AND .30 IS 100.00
PERCENTAGE OF POINTS BETWEEN 0.0 AND .40 IS 100.00
PERCENTAGE OF POINTS BETWEEN 0.0 AND .50 IS 100.00
```

Fig.2 Histograms of fractional deviation of variable X_1 (above) and of the residual (below)

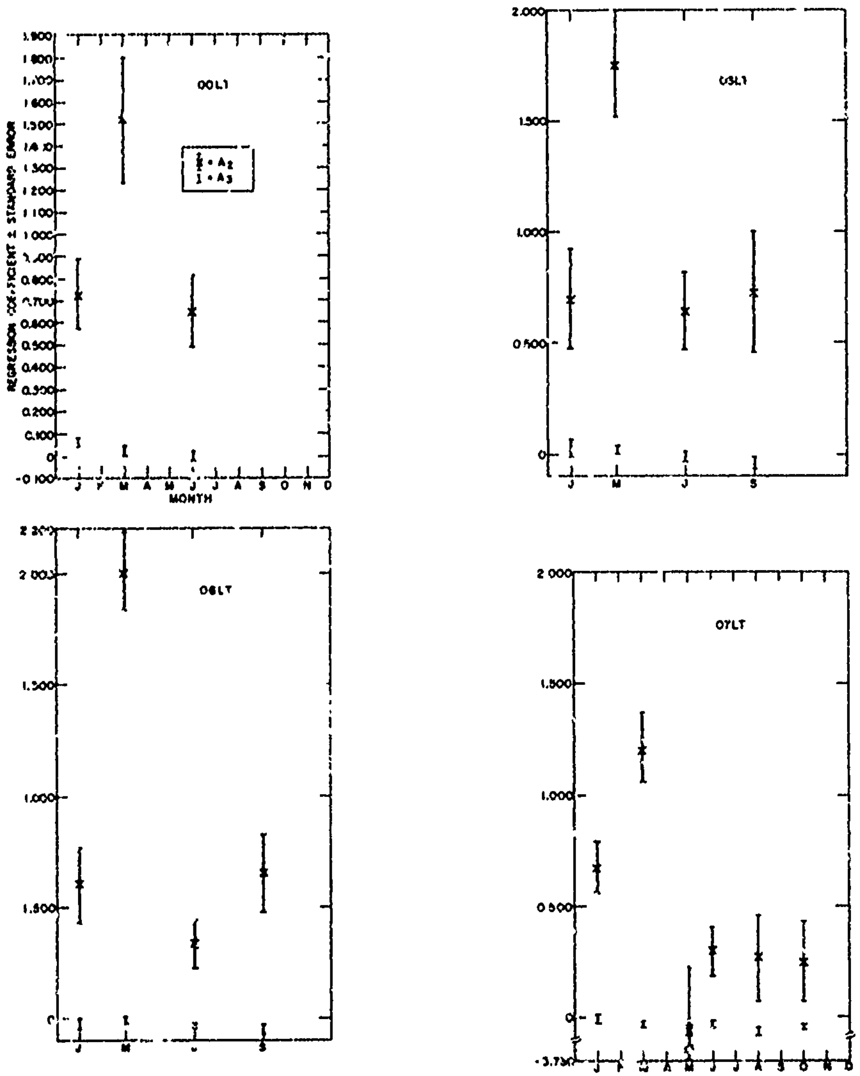

Fig.3 Regression coefficients for Washington, 1961

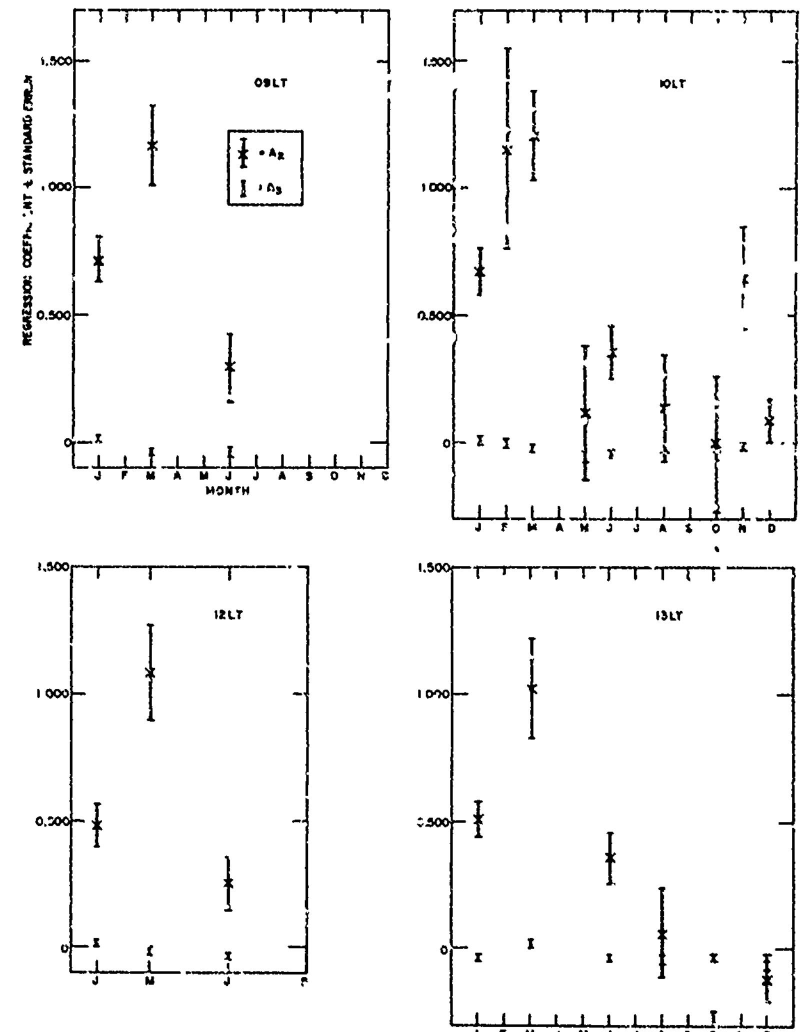

Fig.4 Regression coefficients for Washington, 1961

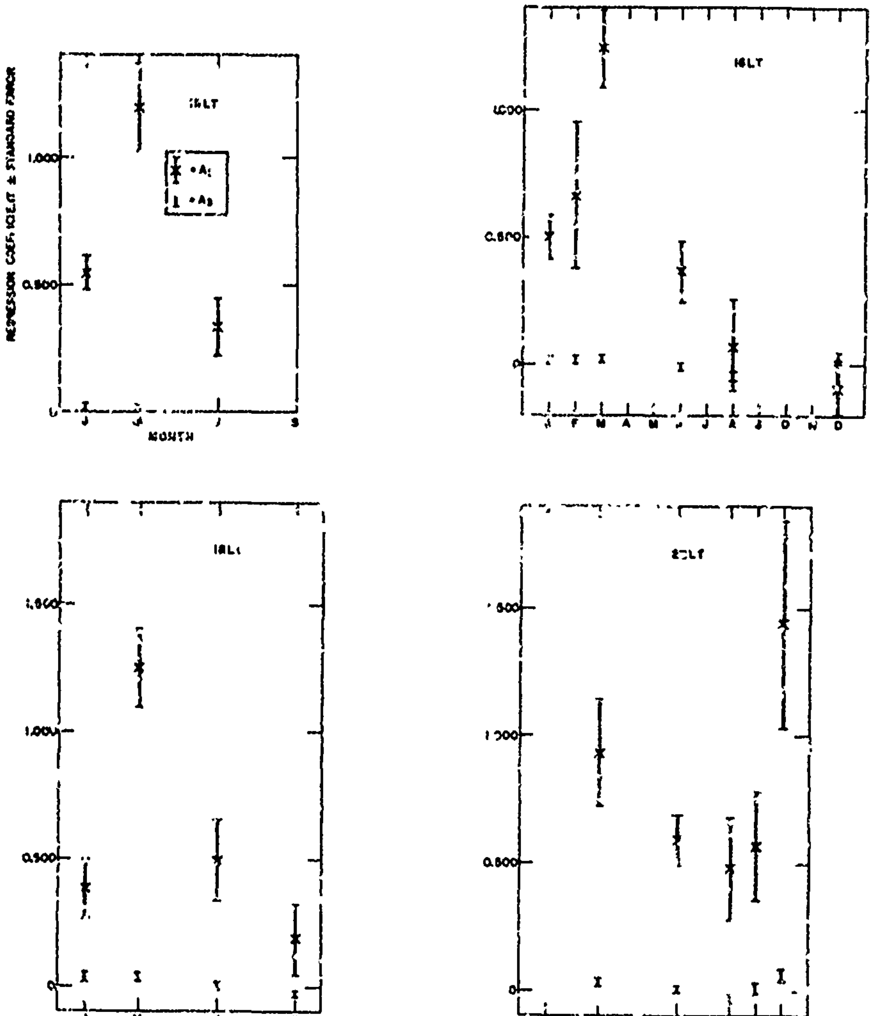

Fig.5 Regression coefficients for Washington, 196[illegible]

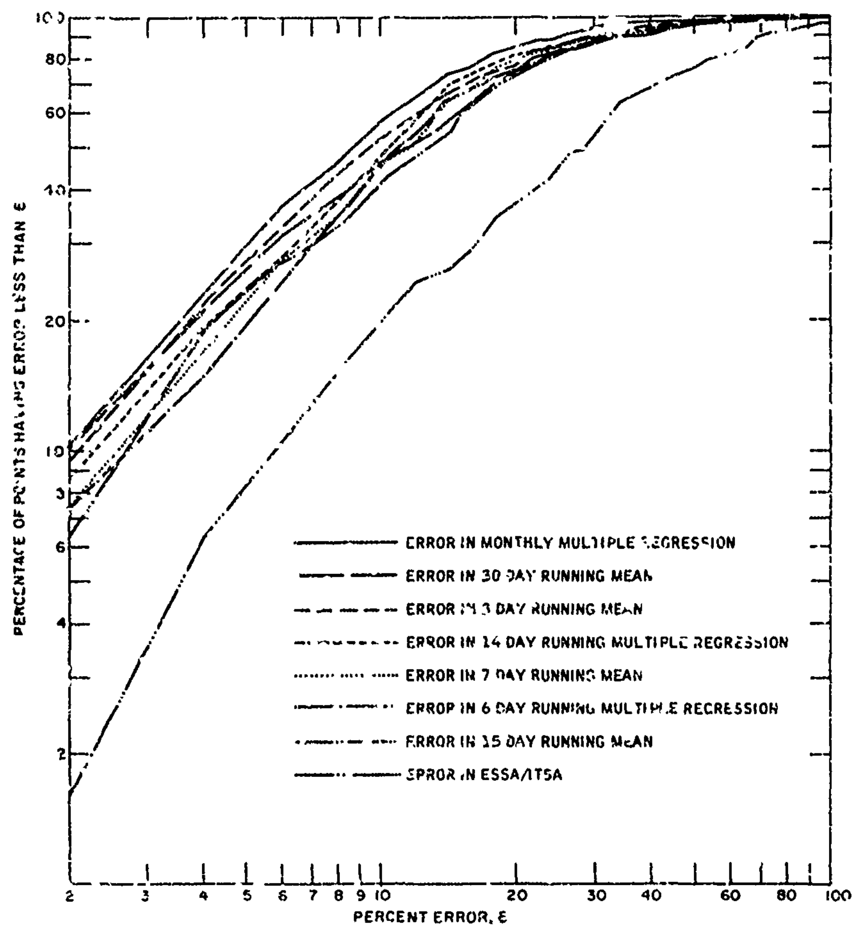

Fig.6 Cumulative distribution of errors in several prediction techniques

PRECURSOR EVENTS FOR POSSIBLE FORECASTING OF SPORADIC E AND INCREASED ABSORPTION

by

E. Harnischmacher and K. Rawer

Ionosphären-Institut, Breisach (Fed. Rep. of Germany)

ABSTRACT

Simultaneous records of the characteristic $f_t(E)$ at three stations have been digitalized with 24 readings per hour. The distances between stations were of the order of 300 km. (1) A straightforward cross-correlation analysis centered on noon gave a widespread spectrum covering the whole range almost from −1 to +1 for the correlation number with important day-by-day changes. Therefore the monthly median correlation is almost zero. (2) After filtering out the more persistent events those were selected which appeared at the three stations, and the apparent motion of the ionized "clouds" was determined. The "motion vectors" agree well with the monthly E-region drift statistics obtained independently by local observations with the D1-method. The conclusion is that sporadic E clouds seem to drift with the general circulation in the height range where they appear. As d1-data are known to depend largely on tidal influences, correlation of Es-appearance between pairs of stations is supposed to depend on the azimuth and the hour. This finding could, eventually, explain phenomena which have formerly been found with vhf propagation tests during an experimental campaign in Europe named "Volta". It could also be used for short term prediction of Es using a knowledge of E-region drifts.

In winter the same records show series of subsequent days where Es appears day-by-day at the same local hour plus one hour per day. Increased absorption mostly occurs at the end of such a sequence. This unexpected phenomenon could be used for short term predictions of increased ionospheric absorption, at least at subauroral latitudes in winter. Different possibilities of explanation of the new finding are discussed.

PRECURSOR EVENTS FOR POSSIBLE FORECASTING OF SPORADIC E AND INCREASED ABSORPTION

E. Harnischmacher and K. Rawer

A) POSSIBILITIES FOR PREDICTION OF SPORADIC E-APPEARANCE IN SPACE AND TIME

The well-known ionization of sporadic E has been demonstrated in many papers (f. e.: Rawer 1955, Smith 1957, Matsushita & Smith 1962). The large fluctuations in particular of the top-frequency FEs are mostly interpreted as preventing any chance of deatil prediction for sporadic E. Of course, statistical predictions are possible and are used in certain types of prediction systems, f. e. in that used by our group since 1943.

However, a new technique of continuous observation first introduced by Nakata (1953) and improved by Bibl (1954) seems to allow studies which have not been possible with the old observational technique based on quarterhourly ionograms. The following findings have been obtained with this technique usually called "recording of ionospheric characteristics", which is continuously applied at FREIBURG since 1957 and - also since many years - at DOURBES in Belgium and, for a certain time, at DARMSTADT Germany.

1) Some regularities concerning the diurnal appearance of sporadic E.

The behaviour of sporadic E characterized by fluctuation of the characteristics fEs is easily seen on records of the frequency range reflected from the whole E-region, as shown f.e. in fig. 1 presenting six consecutive days during June 1969. A quick overlook shows without going into the details that there is a certain regularity in the appearance of strong sporadic E in so far as certain columns appear when the diagrams are ordered by day after the h[illegible] The "columns" have a tendency to be inclined on the diagram so that their ascent is shifting from u. to day a time between 1/2 and one hour. This shifting has different sense for the morning and the afternoon maximum in the sense that the morning maximum is displaced towards later hours while the afternoon maximum is displaced towards earlier hours.

We have, many examples of this kind, and we feel that this is a very frequent case of quasi-periodicity with systematic time shifts.

As to periodicity we should yet state from fig 1 that, seen over all, some tendency for a roughly semi-diurnal maximum of appearance cannot be overlooked. This is more clearly seen from fig. 2 which is based upon the same type of records as shown in fig. 1. In the upper part we consider a sequence of seven days in July/August 1962. It appears clearly that sporadic E is more frequent in the evening and near sunrise while it is less important near noon and midnight.

The conclusion is that sporadic E at temperate latitudes has a tendency to appear with a quasi period of about 12h and that systematic phase shifts occur with periods of the order of a few days.

2) Comparison of the appearance of Es stations distant by a few hundred kilometers.

We have recordings of the same type for a few years obtained at the three stations DOURBES, GRUMSTADT (near Darmstadt) and FREIBURG. The distances between stations range from 200 to 350 km (fig. 6). The lower part of fig. 2 shows records obtained at two of these stations, DOURBES and FREIBURG, in June 1961 It is quite clear that the individual features, in particular quick changes, are often different at both stations. This is the reason why the direct correlation technique could not give a hopeful answer (Rawer, 1958). It is, however, seen that the gross features are quite similar at both stations so that one can quite well identify periods of enhanced sporadic E and even certain features with time constants of the order of one hour.

This is f.e. seen very well during the night of 25/26 June where blocks of rather short (quarterhourly) duration can be identified at both stations. It is important that this identification is obtained with time shifts of the order of 1...2h.

We have in our data many cases which are similar in character The time shift reveals a clear tendency of sporadic E to appear later at FREIBURG than at DOURBES. This means that the cause of the event could be displaced in a north-sorth direction with a velocity of the order of 50... 100 m/sec. It seems worthwhile to note that in a very early ionospheric paper ASCEENBRENNER (1939) from fixed frequency observations concluded that sporadic E had a motion from north to south.

A comparison between GRUMSTADT and FREIBURG which are distant by 210 dm, almost north-south, is shown in fig. 3 left. It appears here that the variations at both stations often have a great similarity, but at occasions it is difficult to identify the small short term features at both stations. In this case

the typical time difference is one hour which gives us an apparent displacement velocity of 58 m/sec. We have used these records (after smoothing for short term features) to determine an apparent drift vector in the triangle mentioned above.

An example is shown in fig. 3 right. The resulting apparent velocity goes to an azimuth of 150° with 60 m/sec. We have many examples in our record where these can really be used to deduce an apparent velocity vector for the sporadic E phenomenon.

In fig. 4 we have given the results of such determinations during the months of August and December 1966. The so determined polar coordinates of the drift vector are given as dots. The characteristic average behaviour of ionospheric drift in the E-region as determined at FREIBURG by the KRAUTKRAMER (1943) method is shown by cross-marked lines. It is quite striking that most dots are quite near to these lines, while they have been determined with a completely different technique and in different years.

Another set of observations has been obtained by Becker and his colleagues (1964) with 5 min-ionogram observations at 3 stations in northern Germany, the geometry of which is presented in fig. 6 also.

We have also used some of the data assembled during these experiments in order to determine apparent Es-drift vectors. An example including the identification of the most important features is shown in fig. 5. Apparently two different drift conditions seem to coexist here, one going towards 210° and ano another one going towards 30° of azimuth. Roughly semidiurnal periodicity appears.

The conclusion is that systematic sporadic E conditions over Europe are often displaced between stations in a way which is very similar in azimuth and speed to the fading drift as in the E-region.

3) A model explaining the observed features.

We feel that a provisional explanation could be obtained if the similarity with ionospheric drifts is taken as a serious feature of sporadic E. In this case the conditions for the production of sporadic E should be related with motions of "air masses", thus "going with the wind".

In fig. 6 we have tried to give an interpretation of some of our observations in terms of such motion. As there is a quasi-periodicity of the order of 12h, one could think that the Es motion follows a closed curve as it should be with tidal motions. The diameter of such a closed curve could be of the order of several hundred to 100 km. A first explanatory model has been given in fig. 6 and the corresponding "periodical clock" is shown aside, for a typical case observed with the triangle DOURBES - CRUMSTADT-FREIBURG. If such systematic motions of conditions needed for the production of Es do appear, they could explain the observed features viz. the meteorological character and the quasi-periodical behaviour of Es at the same time. If this hypothesis proves to be true, it could certainly be used for short term prediction of increased sporadic E.

1. At a given point from observations of other stations distant by a few 100 km,
2. for a given time by using the quase-periodicity at a set of stations.

B) POSSIBILITIES FOR PREDICTION OF INCREASED IONOSPHERIC ABSORPTION

With the same technique of characteristics recording we now also analyze the characteristic fmin identifying absorption in the lower ionosphere. While this work is in progress we have been looking for other absorption data. Our own noon-observations at FREIBURG using a multi-frequency A1-method will be discussed in a separate paper. On the other side a long series of A3-observations on an effective frequency of about 2 MHz has been made at LINDAU by SCHWENTEK (1958). These observations have the advantage of being made continuous during daylight hours. We have deduced from Schwentek's curves representative noon value avoiding SID-effects.

The dependence on solar activity has been studied with the superposed epochs method using relative minimum values of the Zurich sunspot number as reference.

1) Relation between ionospheric absorption and solar activity

Fig 7 obtained with the 1967 measurements shows that the observed absorption A has a minimum at the same time with sunspots. This is best seen by decomposing the A curve into a smoothed curve corresponding to a harmonic 27 days component (Δ A 1), and the rest (Δ A 2). For comparison in fig. 7 the corresponding curve of solar radio noise flux is given for 6 different frequencies. On frequencies higher than 1 GHz the variation is sensibly similar to that obtained with the sunspot numbers.

The first conclusion obtained from Δ A, is that absorption follows the 27 day period without delay. This is in agreement with earlier foundings of LANGEHESSE.

Now looking for the remaining component, ΔA_2, it appears that in 1967 there was a tendency for rather regular variations within a week, roughly, which variations appear also in the daily magnetic disturbance character, Σ Kp. There is, however, a time delay of a few days, two to four in the average. We have evidence that this consistent behaviour is related with the pattern of the solar wind existing during 1967.

The conclusion is that both, the magnetic disturbance character and the fluctuations of absorption, are related to this pattern, the effect on absorption being, however, delayed against that on the magnetic disturbance by a few days.

2) Seasonal variations of absorption.
With the A 3 - data of LINDAU the seasonal variation of absorption has been studied using monthly mean values for 6 years. The years have been chosen in a way to distinguish between sunspot maximum (1957 and 1961), average solar activity (1962 and 1967) and minimum solar activity (1964 and 1965). In fig. 8 it is seen that the seasonal variation is extremely small in years of maximum solar activity but it becomes more pronounced with decreasing sunspot number. During the solar minimum a clear variation with cos χ is obtained from March through October; during winter the now well-known winter anomaly of absorption (DIEMINGER) gives us higher values with a maximum in January much higher than the summer values. With average sunspot numbers some anomalies appear during summer where higher values are seen in May and September. The winter anomaly appears similar in ratio as before. It has been studied in detail by SCHWENTEK. However, for really great solar activity a "saturation" effect seems to be produced so that none of the variations mentioned before appears clearly, even the winter anomaly being reduced to a small increase only.

The conclusion is that solar maximum data must be considered separately and not be confused with absorption data obtained at lower solar activity. If one takes all data together, a clear seasonal effect might be smoothed out by the differences in behaviour obtained at different phases of the solar cycle.

3) Seasnoal effects in the relation between absorption and magnetic disturbance charatter.
In order to study this effects superposed epochs diagrams have been established month by month for the years 1962 through 1968. Amongst threse years two classes of solar activity have been distinguished, namely:
maximum activity (1966 through 1968),
low activity (1964 and 1965).
The diurnal sum of Kp has been used as indicator element, maxima of this disturbance figure being taken as reference. The corresponding mean variation of absorption is shown in the upper parts of fig. 9.

There appears a clear difference between summer and winter conditions. During the period March through August, the magnetic effect upon absorption is quite small. There is, however, a tendency in most months for absorption to increase after a maximum of Σ Kp. In winter a very large increase of absorption comes after a maximum of Σ Kp with a delay of about two to four days, as yet shown in fig. 7. Exceptionally strong effects are found in September and December. (It must, however, be stated that the magnetic disturbances also occur more often in September).

The conclusion is that a high sensitivity of absorption to the magnetic disturbance character exists, prefeventially in winter, with increased absorption a few days after the magnetic disturbance.

4) Solar radio noise flux effects.
With maxima of solar fulx on 169 MHz as observed at NANCAY a superposed epochs study has been made for winter months of the years 1966 and 1967 great solar activity. Fig. 10 shows that each curve for an individual month has a clear minimum almost coincident with the maximum of 169 MHz solar radio noise. Thus absorption and 169 MHz radio noise are inversely correlated. The lowest diagram shows the magnetic character to be only slightly related with 169 MHz noise but in the sense of a positive correlation.

References

Rawer, K.	1955	Geofis. pura e appl 32, 170-244
Smith, E. K.		Worldwide Occurrence of Sporadic E (NBS Circular 582)
Matsushita, S. and Smith, E. K.	1962	Ionospheric Sporadic E: Pergamon Press
Nakata, Y., Kan, M. and Uyeda, H.	1953	Rep. Ionosphere Res. Japan 7, 129-135
Bibl, K.	1956	J. Atmosph. Terr. Phys. 8, 295
Rawer, K.	1968	ESSA Rep. on 2. Es Symposium in Vail
Aschenbrenner, H.	1939	Diploma Thesis Techn. Hochschule Munchen
Krautkramer, J.	1943	Dtsch. Luftfahrtforsch. FB Nr. 1761
Becker, W.	1964	Kleinheubacher Berichte 9, 45
Klostermeyer, J.	1965	Kleinheubacher Berichte 10, 141
Schwentek, H.	1958	Archiv. elektr. Ubertragung 12, 301-308
	1963	J. Atmosph. Terr. Phys. 25, 733-736
	1965	Nachrichtentechn. Z. 18, 94-98
Langehesse, G.		Verbal communication
Dieminger, W.	1952	J. Atmosph. Terr. Phys. 2, 340-349

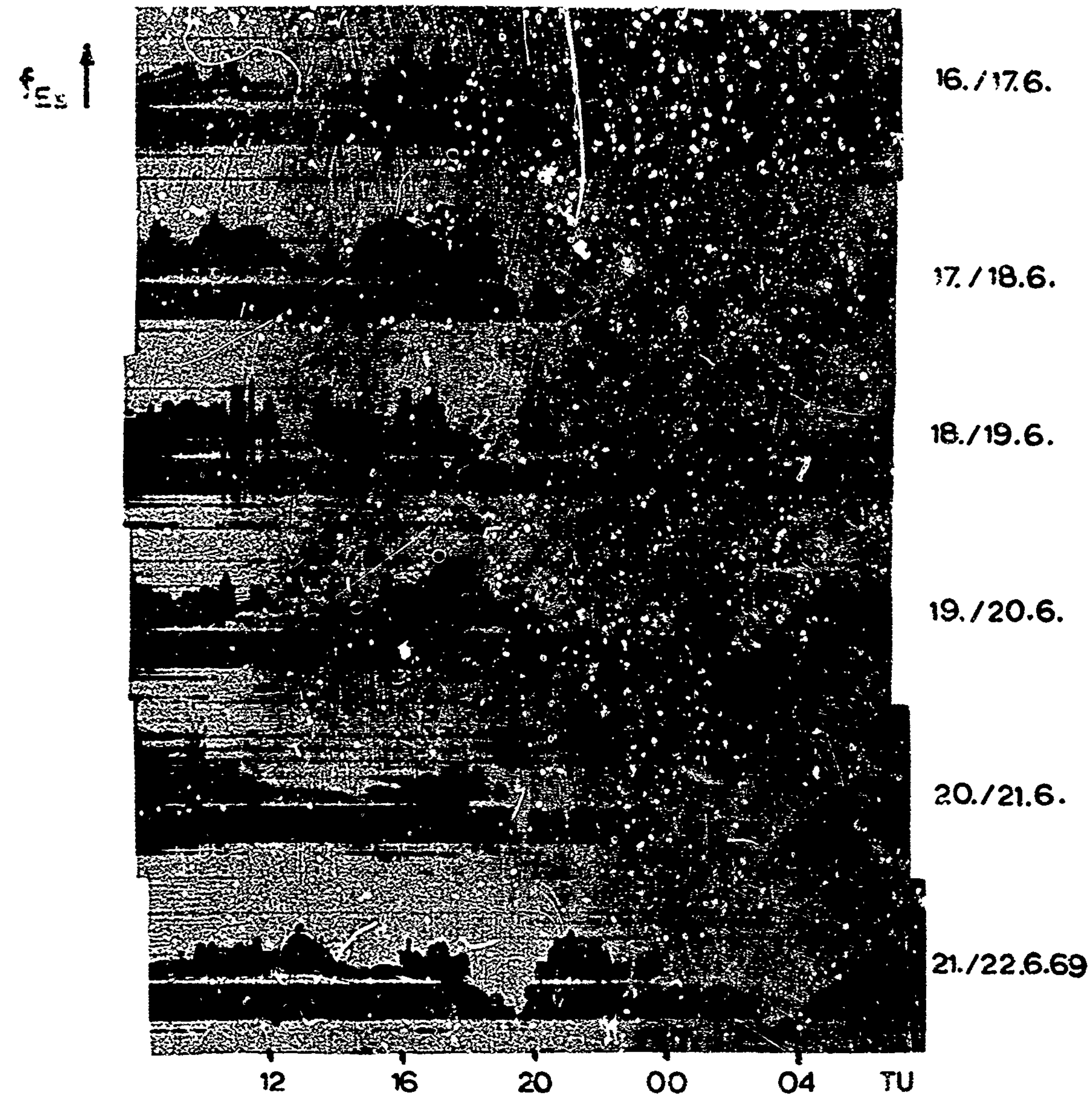

BREISACH

Figure 1

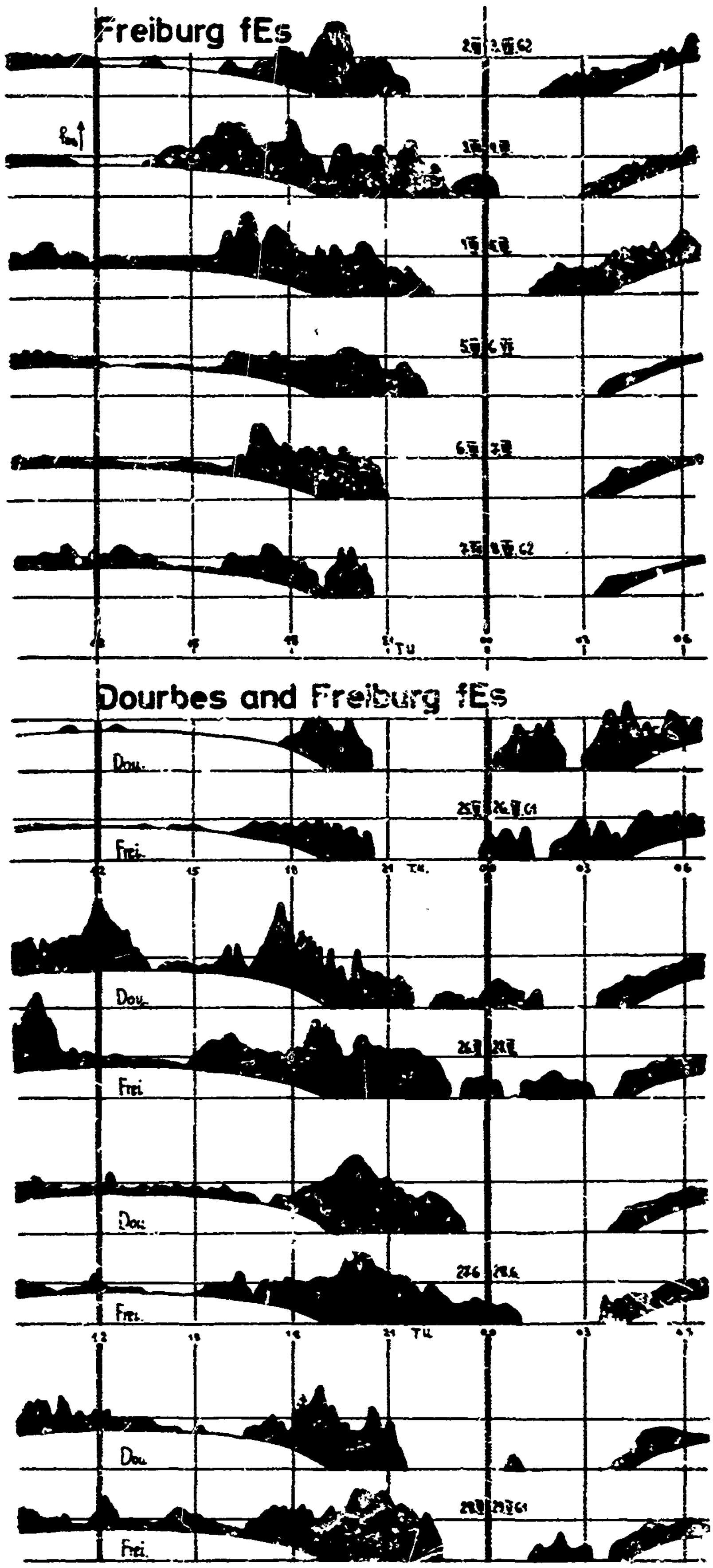

Figure 2

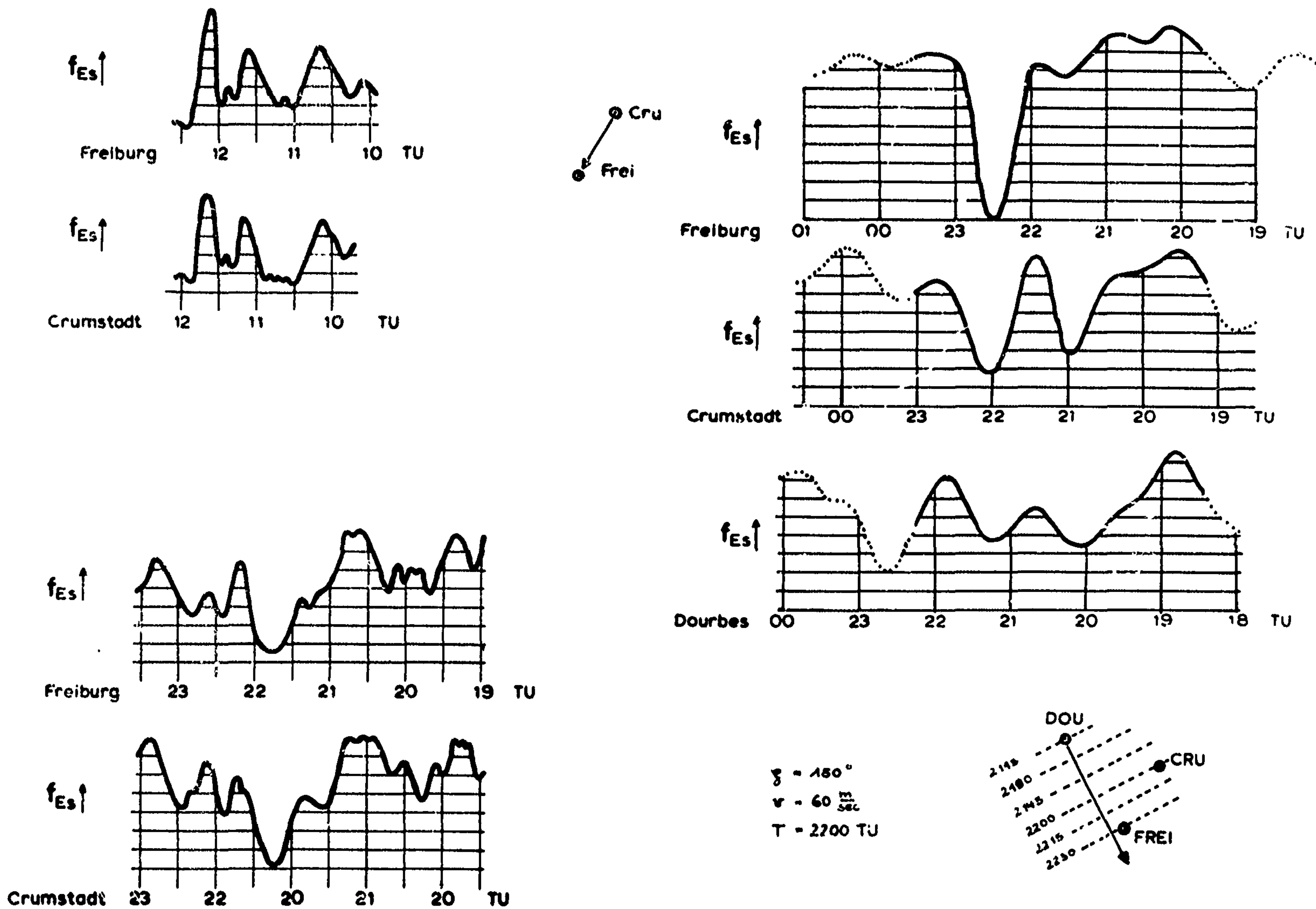

f_{Es}
Freiburg
12
11
10
TU
Crumstadt
Cru
Frei
Dourbes
00
01
23
22
21
20
19
18
DOU
CRU
FREI
γ = 150°
v = 60 m/sec
T = 2200 TU

Figure 3

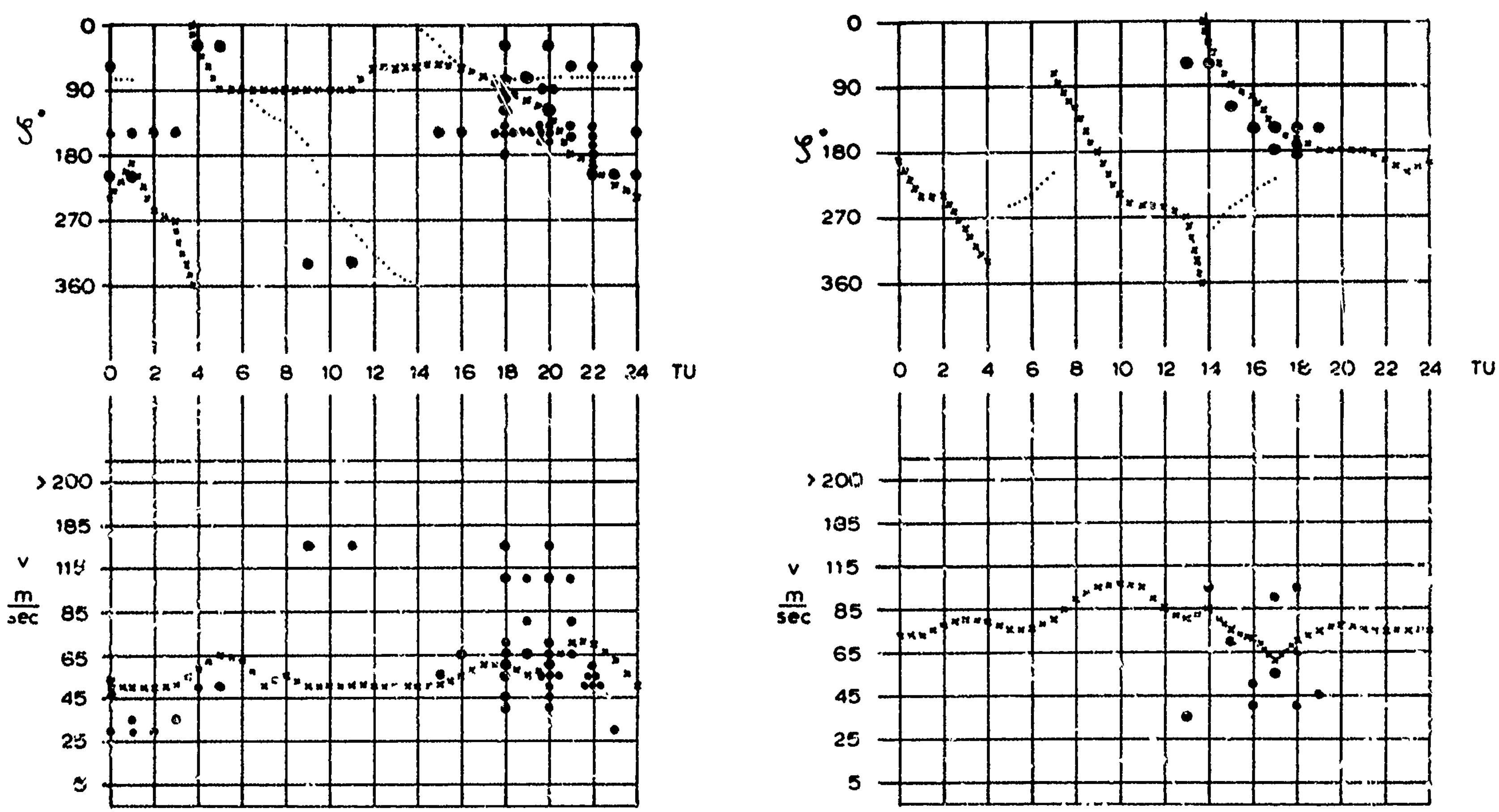

E Drift Freiburg VIII. 1956 -64 × × × max . . . sec max

"Es Patches" over Dourbes – Crumstadt – Freiburg VIII 1966

E Drift Freiburg XII. 1956 – 64 × × × max . . . sec max

"Es Patches" over Dourbes · Crumstadt – Freiburg XII. 1966

Figure 4

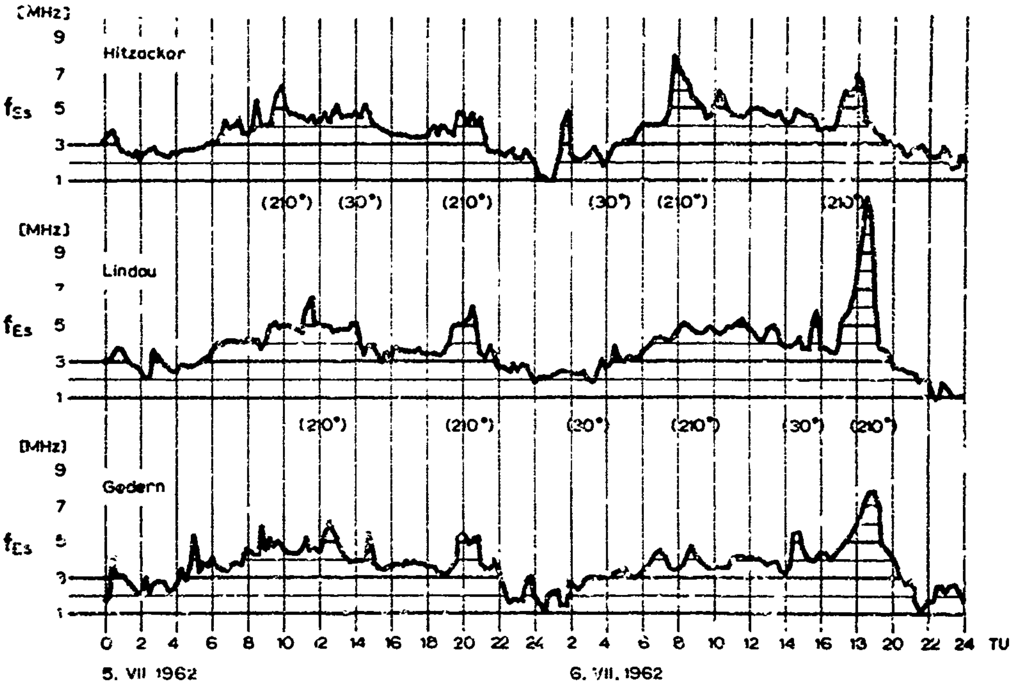

Figure 5

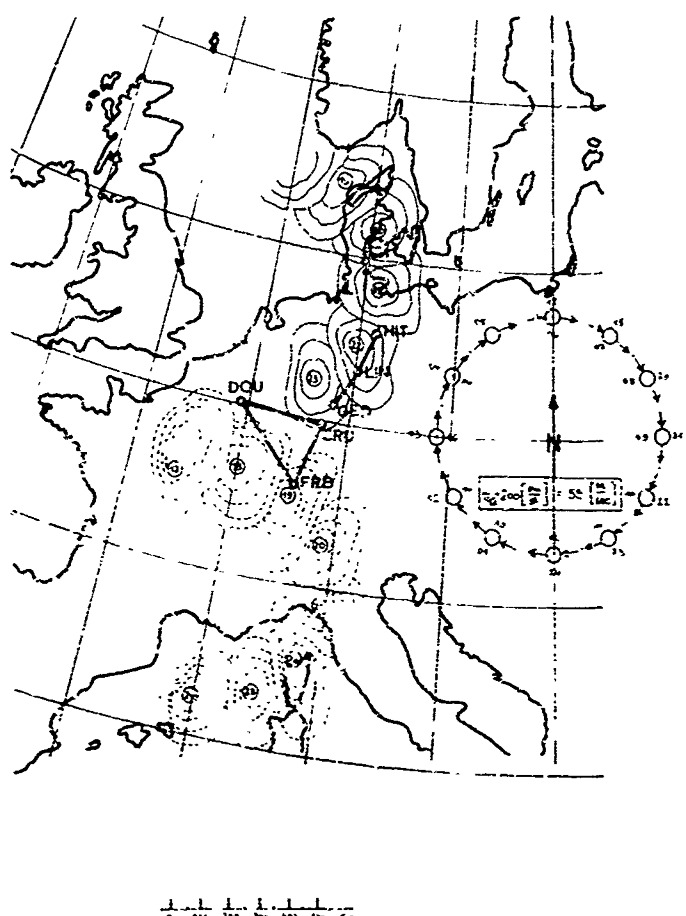

Figure 6

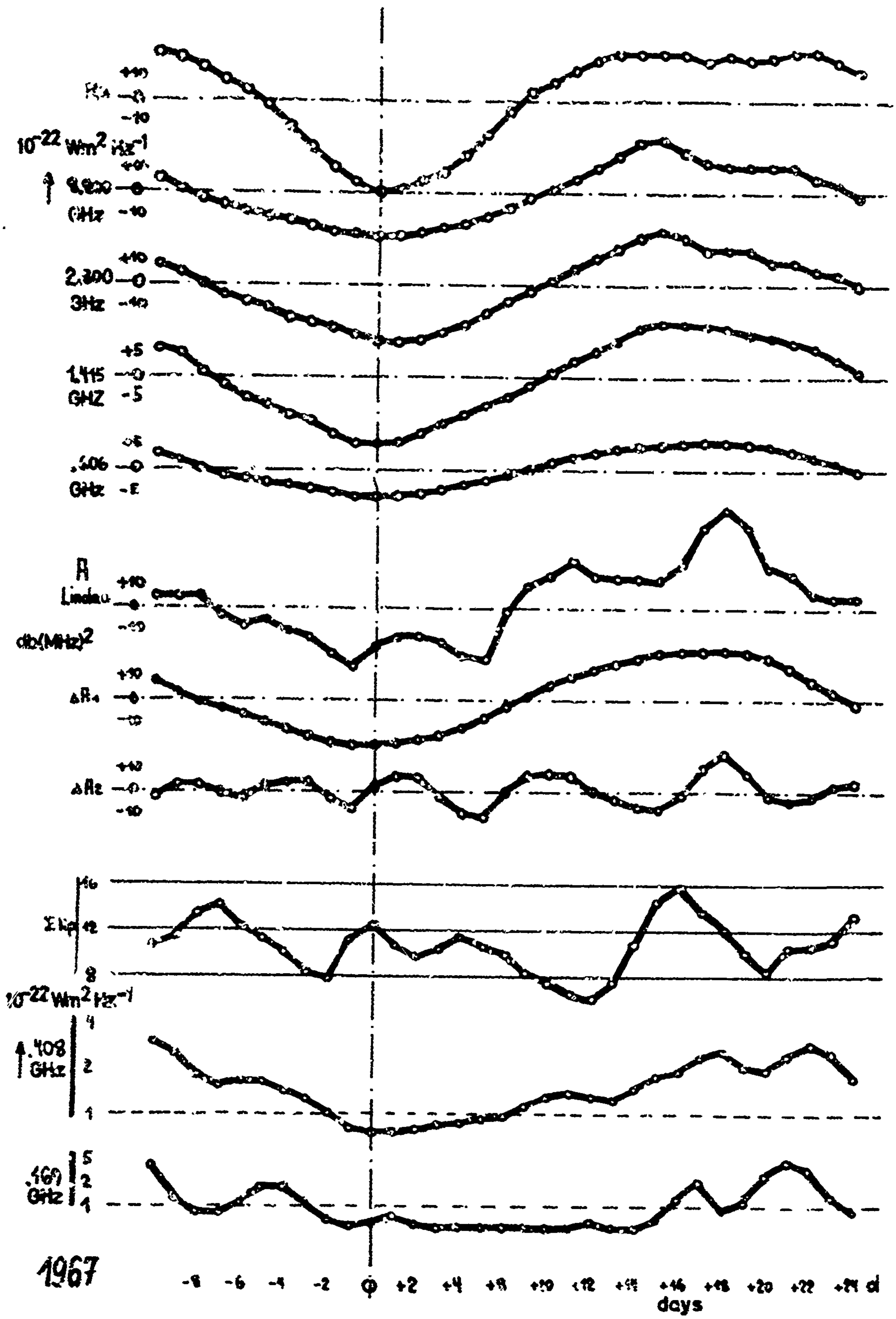
+10
R
0
-10
10^{-22} Wm^2 Hz^{-1}
GHz
2,800
GHz
+5
1,415
GHZ
-5
.406
GHz
R
Lindau
db(MHz)^2
ΔR
ΔR
ΣKp
12
8
10^{-22} Wm^2 Hz^{-1}
.408
GHz
4
2
1
.169
GHz
1967
-8
-6
-4
-2
0
+2
+4
+8
+10
+12
+14
+16
+18
+20
+22
+24
d
days

Figure 7

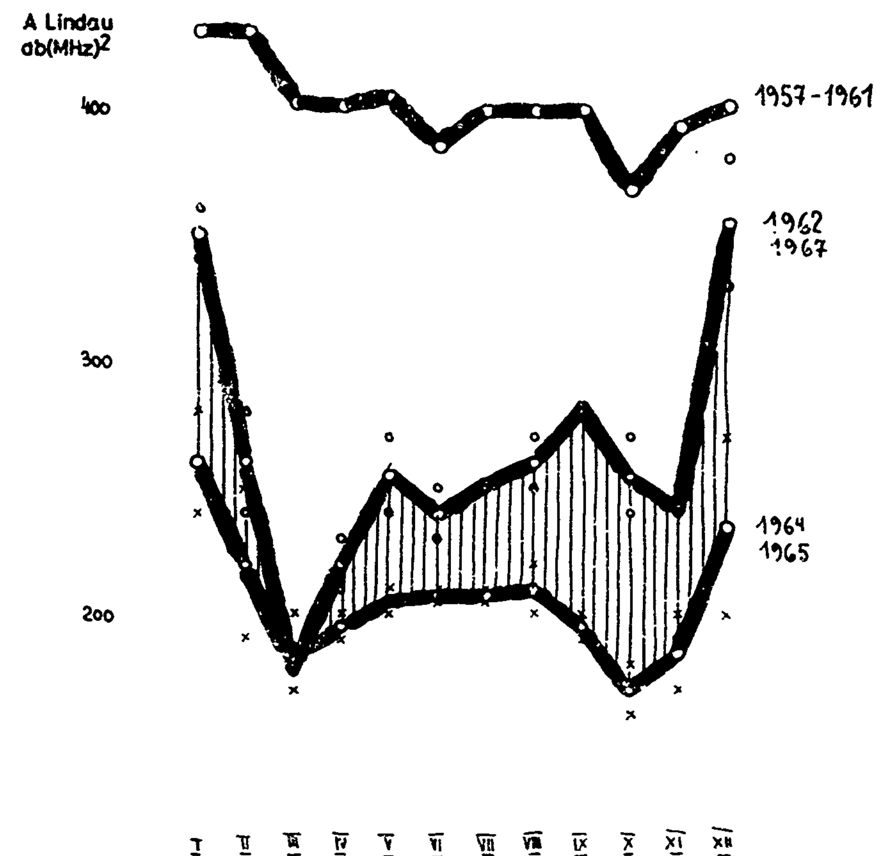

Figure 8

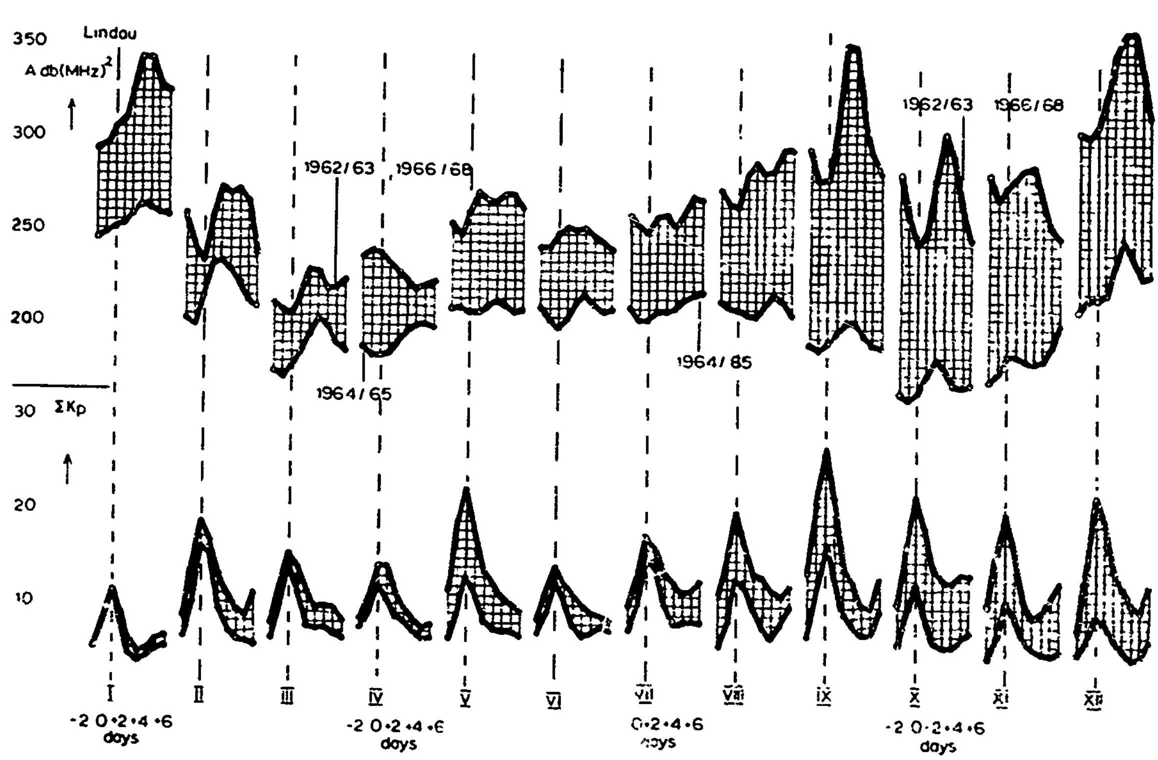

Figure 9

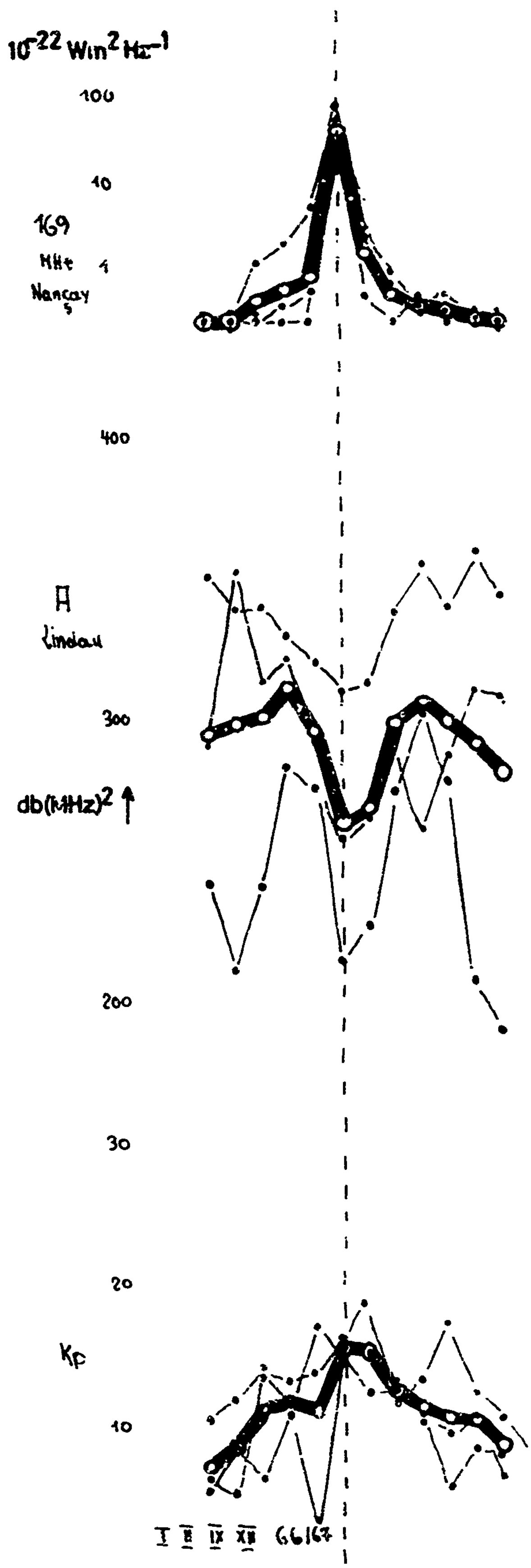

10^{-22} Wm^2 Hz^{-1}
100
10
169
MHz
1
Nançay
400
A
Lindau
300
db(MHz)^2 ↑
200
30
20
Kp
10
I II IX XII 66167

Figure 10

F-LAYER PROPAGATION CHANGES DURING MAGNETIC STORMS

by

A.H. Katz

Avco Corporation, Space Systems Division,
Lowell, Massachusetts 01851, USA

33

ABSTRACT

In order that an ionospheric forecasting system be applicable during magnetic storms, knowledge of the changes in height and critical frequency of the F-layer must be acquired. One possibility is to study MUF for a given range as a function of a magnetic index. The study of MUF will take into account both height and electron density changes. A second possibility is to study electron density profile changes during magnetic storms and by ray tracing through the disturbed and undisturbed ionosphere, the effects of ionospheric changes associated with magnetic storms can be determined.

I selected the second approach. Ray tracing was performed for both a 1 and 2 hop F propagation path using magnetically quiet and disturbed electron density profiles obtained from four locations along the 75°W meridian (Washington, Jamaica, Grand Bahama Island, and Bogota). The electron density profiles were obtained from a true height analysis using hourly ionograms for selected time periods. Each time period consisted of 3 to 4 days around a magnetic storm. The results are compared with those obtained by using the ionograms and transmission curves.

An example of the changes that occur is illustrated by the effect of a Sudden Commencement magnetic storm beginning at 1602 EST on 9 February 1962. Several hours later the height of the F-layer at Washington increased by 75 - 100 km and foF2 increased by 50% as compared to the previous magnetically quiet day. The effect of these two changes was to increase the MUF by 1 - 2 MHz (depending on ground range); whereas, if it was assumed that just the critical frequency changed the MUF would increase by 3 - 4 MHz (depending on ground range).

Ray tracing through various stages of other ionospheric disturbances (during several magnetic storms) and comparison with quiet day propagation path will demonstrate the effects of magnetic storms upon ionospheric forecasting systems and lead to a better understanding of how to make better use of the available frequency spectrum during magnetically disturbed times.

Introduction

For mid-latitude stations the majority of the propagation changes during disturbed conditions can be attributed to F region changes during magnetic storms. Much of the emphasis in discussing storm effects has been placed upon either statistical studies or synoptic mapping of ionospheric parameters such as foF2. Studies of this type neglect the height changes that occur during magnetic storms. Several workers (Becker, 1964; Thomas & Robbins, 1958) have investigated electron density profiles during magnetic storms for a single station and have shown that the largest height increases occur during the night hours. A multiple station analysis has been done by Rajaram and Rastogi (1968) although only for midday, and only average profiles were shown. A multiple station analysis by Somayajulu (1963) similar to the study discussed here was conducted for three severe magnetic storms in 1957-58. The height changes were typically observed on the first day of the storm, and an inverse correlation between height and electron density was seen. Because the study was limited to 1957-58 sunspot maximum, an additional multiple station analysis by this author was conducted for medium and low sunspot numbers.

A study of the latitudinal (75° W.) and diurnal variation of electron density changes during magnetic storms was performed. This involved true height analysis of hourly ionograms for 75° W. meridian ionosonde stations for several days surrounding the occurrence of magnetic storms. In order to evaluate the importance of storm induced electron density changes on HF propagation, ray tracings will be shown for several cases which illustrate the disturbed behavior. Profiles from Washington, Grand Bahama Island (GBI), Jamaica, and Bogota were used to produce the latitudinal versus height (two-dimensional) electron-density distribution necessary for the Snell's law ray tracing program.

Magnetic Storm Effects

Figure 1 shows a plot of hmF2 (height of foF2) and foF2 vs. EST for Washington, for four days in February 1963. A Sudden Commencement magnetic storm began at 1602 EST and had a maximum Kp value of 6 (8 February 1963 was one of the quietest days of 1963). The dashed line on the first day of the foF2 scale is the monthly median foF2 for that station. Shortly after the start of the storm an increase of 75-100 km in hmF2 and 1-2 MHz in foF2 was observed as compared to the previous quiet day. The increase in hmF2 was also observed at GBI and Jamaica, with the largest height change observed at Jamaica, although there was little change in electron density at this station. The daytime results at Washington show a decrease in electron density, GBI showed no change, and Jamaica showed an increase in foF2 during this period. Before discussing the results of the ray tracing, additional storm studies at Washington will be mentioned to indicate that the results just described are typical for magnetically disturbed periods. (Since only a limited amount of the results from this study can be shown here, we refer the interested reader to a more comprehensive report in preparation under the supporting contract.)

Figure 2 shows hmF2 and foF2 for Washington for five days in March 1961. A GC magnetic storm occurred at 1600 EST on 5 March 1961 with a maximum Kp of 7 at 1800 EST. A 100 km height increase in hmF2 was observed that night, with foF2 showing a very sharp decrease at 2000 EST. The foF2 remained high for several hours past the usual sunset decline and then dropped suddenly at 2000 EST, although in this case the height remained at its high value until sunrise. The daytime shows a decrease in foF2 with little height change being observed.

Figure 3 illustrates the effect of a June 1963 magnetic storm which began at 1200 EST with a maximum Kp of 7 occurring at 2100 EST. Note the height increase (25-50 km) beginning at 1400 EST and lasting throughout the night, with an increase in critical frequency ($\sim$ 3 MHz) between 1500-1900 EST. No decrease in foF2 is observed during the daytime following the storm.

Propagation Changes During Magnetic Storms

For illustrative purposes, ray tracings will be shown for 1200 EST and 2000 EST during the February 1963 magnetic storm. Selected elevation angles and frequencies were chosen and rays were traced for a one hop F mode (maximum range, 4000 km). The ground range as a function of take-off angle was plotted parametrically in frequency, and from these plots the MUF as a function of ground range was determined. Figure 4 shows the latitudinal profiles of plasma frequency (MHz) at 2000 EST for 8 and 9 February 1963. (hmF2 is shown by a dashed line). The transmitter is assumed to be located at 0 range, and the location of each

station as a function of range from the transmitter is indicated. The effect of the storm at this time is an increase in height 70 km - 100 km, with a 1.5 MHz increase at Washington and GBI but little change in plasma frequency at Jamaica and Bogota. It is interesting to note that the effect of the storm-induced height change was to make the disturbed ionosphere more concentric than the quiet ionosphere.

In order to evaluate the effect of height changes, the profiles at 2000 EST were artificially reduced in height by 70 km so as to approximate the height of the quiet ionosphere. Figure 5 shows the latitudinal profile at 2000 EST for 8 February 1963 and the artificially reduced layer height for 9 February 1963 at 2000 EST. Figure 6 shows the MUF as a function of ground range for the different nighttime ionospheres. The results for the disturbed day (9 February 1963) shows an increase of 1.5 MHz (at 1000 km range) to 3 MHz (at 3000 km range) over the quiet day value. When the same rays were traced through the artificially lowered disturbed profile, the MUF/range curve (indicated in the figure as A-9 February 1963) shows an increase of 3.5 MHz (at 1000 km range) to 5 MHz (at 3000 km range) over the quiet day observation. Thus, if only the foF2 changes were assumed to occur, then the predicted MUF would be an over estimate of 2 MHz (at 1000 km range) to 3 MHz (at 3000 km range).

To further illustrate this, if it is assumed that there is no change in the height of the ionosphere, the percentage deviation of disturbed MUF from quiet MUF can be related to the percentage deviation of quiet from disturbed values of foF2, that is:

$$(1) \qquad \frac{MUF_D - MUF_Q}{MUF_Q} = \frac{foF2_D - foF2_Q}{foF2_Q}$$

where

MUF_D is disturbed MUF

MUF_Q is quiet MUF

$foF2_D$ is disturbed foF2

$foF2_Q$ is quiet foF2

From Eq. (1), MUF_D can be related to known quantities.

$$(2) \qquad MUF_D = \frac{foF2_D - foF2_Q}{foF2_Q} \; MUF_Q + MUF_Q$$

In the first example, $foF2_Q = 2.50$ MHz, $foF2_D = 4.0$ MHz. The results for this approach are shown as the MUF-predicted curve in Figure 6, and, as observed, they agree rather well with the results obtained by artificially lowering the disturbed ionosphere. This indicates that if no height change is assumed, foF2 is a useful parameter in predicting MUF's during magnetic storms. This result is obvious, but as we have shown, height charges do occur, and therefore the effects of changes both in height and foF2 have to be considered.

It is important to realize that the actual ray tracing was performed through a two dimensional ionosphere in height and latitude. Thus, the effect of the small latitudinal gradient is included in the ray tracing results. In cases where large gradients occur, rays at particular takeoff angles may experience trapping or ducting to various extreme ranges in the ionosphere. This ducting is not a predictable effect, and since it does not exhibit a consistent or patterned behavior, it will not be discussed here.

As mentioned previously, the alternative to true height analysis in determining the effect of height changes on propagation conditions is to use the MUF (3000) and correlate this with magnetic indices. The MUF inherently contains hmF2 and foF2 changes. A transmission overlay for 1000, 2000, 3000, and 4000 km ranges was obtained for the Washington ionograms (Davies, 1969). Since the midpoint of all these paths is between Washington and GBI, and at this time Washington and GBI have the same electron density profile, the Washington ionogram was chosen to represent this path. The solid dot shows the results of the transmission curve for 8 February 1963 which agree very well at all ranges with the results obtained from ray

tracing. The asterisks are the results using the 9 February 1963 2000 EST ionograms, and these show agreement with ray tracings only at 1000 and 2000 km ranges, but an increasing error with increasing range: 1 MHz at 3000 km and 2 MHz at 4000 km.

A possible explanation of this behavior is that under the assumption of thick curved ionosphere the secant law is written as: $f_{ob} = fv \sec \phi_r$; (where f_{ob} is oblique frequency, fv is vertical frequency and ϕ_r is angle between continuation of unrefracted rays and radius vectors at reflection height h). For the thin, flat ionosphere the angle ϕ_o is independent of height of reflection, where in the thick curved ionosphere ϕ_r depends on level of reflection and thus on the particular electron density profile. The overlay of a thick ionosphere is constructed assuming that $\sec \phi_r = k\sec \phi_o$ where the k-factor is calculated for model ionospheres (Davies, 1969). Thus, the overlay for the corrected secant law when used with typical h'f profiles will produce equivalent results to ray tracing. However, when using disturbed ionograms the changes in h'f curves are not indicative of changes in disturbed N(h) profiles (Thomas and Robbins, 1958), and the results using a corrected secant law which are based upon model ionospheres are not applicable. Admittedly, the results shown are based on a very restricted sample of data, but the k factor is determined from model ionospheres and our results indicate that care must be exercised when using an overlay method based on model ionospheres to deduce MUF changes during disturbed conditions.

The second ionospheric change during a magnetic storm is a decrease in electron density with little change in height. Figure 7 shows the contours of plasma frequency for the disturbed day (10 February 1963) and quiet day (9 February 1963) for 1200 EST. At Washington and GBI the plasma frequency is decreased by 1.4 and 0.4 MHz, respectively. Figure 8 shows the MUF as a function of range for the one hop F mode during the period. The solid dots represent the results of a transmission overlay on the Washington ionogram for 8 February 1963. For the quiet midday ionogram the transmission overlay gives MUF values which agree rather well with those obtained from ray tracing.

The disturbed MUF is depressed 0.8 MHz at 1000 km range and 3.4 MHz at 3000 km range compared to the quiet day values. The MUF-predicted values, based on the percentage difference of the quiet foF2 from the disturbed foF2, agree rather well at long range (< 15 MHz at range > 2500 km) but are in error at short ranges. The letters W and G indicate the values of MUF obtained for a transmission overlay on the disturbed ionograms for Washington and Grand Bahama Island respectively. This was done because (see Figure 7) the effect of the storm on 10 February 1963 at 0000 EST is to make the ionosphere non-concentric between Washington and GBI, where the control points lie for the ranges of interest. At a range of 1500 km Washington is the control point and at 3000 km GBI is the control point. The transmission curve values for Washington are below the ray tracing values at all ranges; this could be due in part to the non-concentricity of the ionosphere between Washington and GBI. (If this were totally true then the overlay at Washington should be applicable at 1000 km range, where in fact we find a 2 MHz difference between the ray tracing and overlay values.) The values obtained using the GBI ionograms are close to actual values at close range, even though GBI is not the control point for these ranges. Whereas at long ranges where GBI should be the control point, the overlay MUF is 2-3 MHz in excess of the ray tracing values. This indicates that the use of h'f curves at Washington and GBI with simple transmission curves gives inconsistent results. Thus apart from knowledge of tilts obtained with electron density profiles at separate locations, the h'f changes at different locations are not related.

Summary

The occurrence of magnetic storms produces height and electron density changes, both of which affect propagation of hf radio waves. Thus knowledge of both height and electron density changes is required in order to predict propagation during storm conditions. Comparisons were made between MUF vs. range curves derived from Snell's law ray tracing and from a transmission overlay applied to a vertical-incidence control ionogram, in order to determine if h'f curves could provide useful information during disturbed conditions.

Because h'f changes during disturbed conditions are not simply related to electron density profiles, the two methods show dissimilar results, especially at long ranges. In addition, the overlay method does not take into account even small tilts in the ionosphere. It appears that even the use of a parameter such as MUF (3000), which appears to include both height and electron density changes, is suspect to errors due to the assumption made in using a transmission curve to obtain these values. Changes in foF2, when used as a parameter to deduce

changes in MUF's, ignore height changes that occur, and even if the height does not change appreciably (e.g., midday observation) the use of foF2 can lead to errors at small and intermediate ranges.

In order to know height as well as electron density changes electron density profiles are required, and at several locations, so as to obtain some knowledge of the tilts that are occurring. Because of the variability that occurs from storm to storm, a real-time sensing of the medium might be required to provide boundary values for the ionospheric model chosen during disturbed periods.

ACKNOWLEDGMENTS

I would like to thank Drs. Detert and Penndorf for many helpful discussions in the preparation of this report. This effort was sponsored by the Rome Air Development Center, Air Force Systems Command, under Contract F30602-67-C-0274.

REFERENCES

1. Becker, W., Real height analysis of an ionospheric storm, Electron Density Distribution in Ionosphere and Exosphere, E. Thomas, Ed. John Wiley & Sons, N.Y., 1964.

2. Davies, K., Ionospheric Radio Waves, Blaisdell Publishing Co., Mass., 1969.

3. Matsushita, S., A study of the morphology of ionospheric storms, J.G.R., V. 64, No. 3, 305-321, 1959.

4. Rajaram, G. and Rastogi, R. G., Abnormal electron density distributions over Huancayo on disturbed days of IGY/IGC. Ann. Geophys., J. 24, fax 4, 1045-1051, 1968.

5. Somayajulu, Y. V., Changes in the F region during magnetic storms, J.G.R., V. 68, No. 7, 1899-1922, 1963.

6. Thomas, J. O. and A. Robbins, "The electron distribution in the ionosphere over Slough: II - disturbed days", J. Atmos. Terrest. Phys., V. 13, No. 1/2, 131-139, 1958.

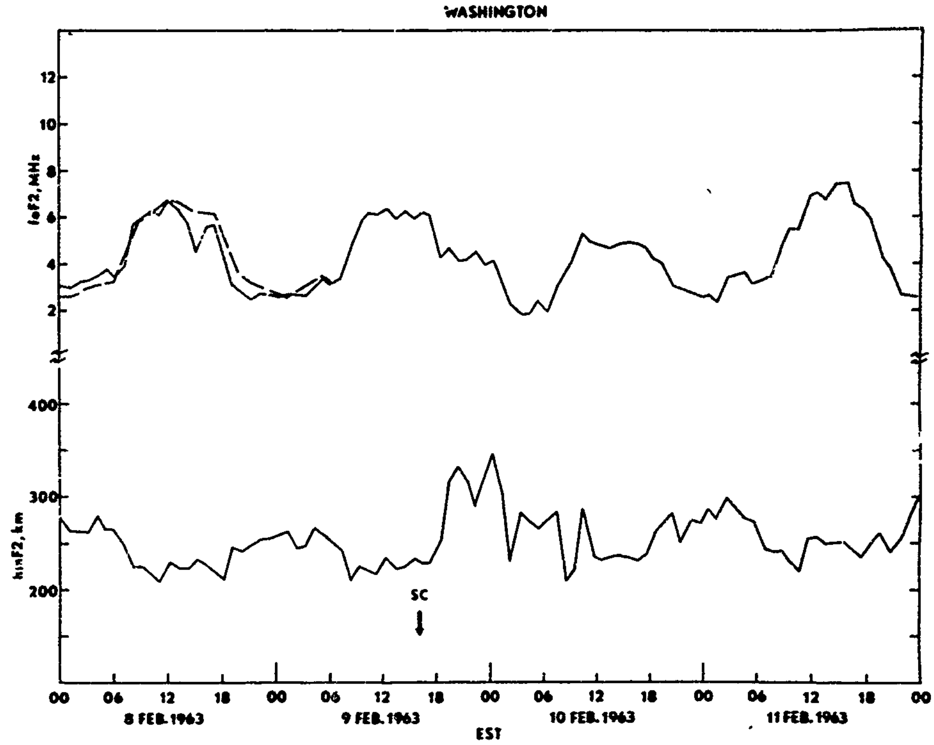

Figure 1: Hourly values of hmF2 and foF2 at Washington for 8-11 February 1963. A Sudden Commencement magnetic storm began at 1602 EST. The dashed line is monthly median foF2.

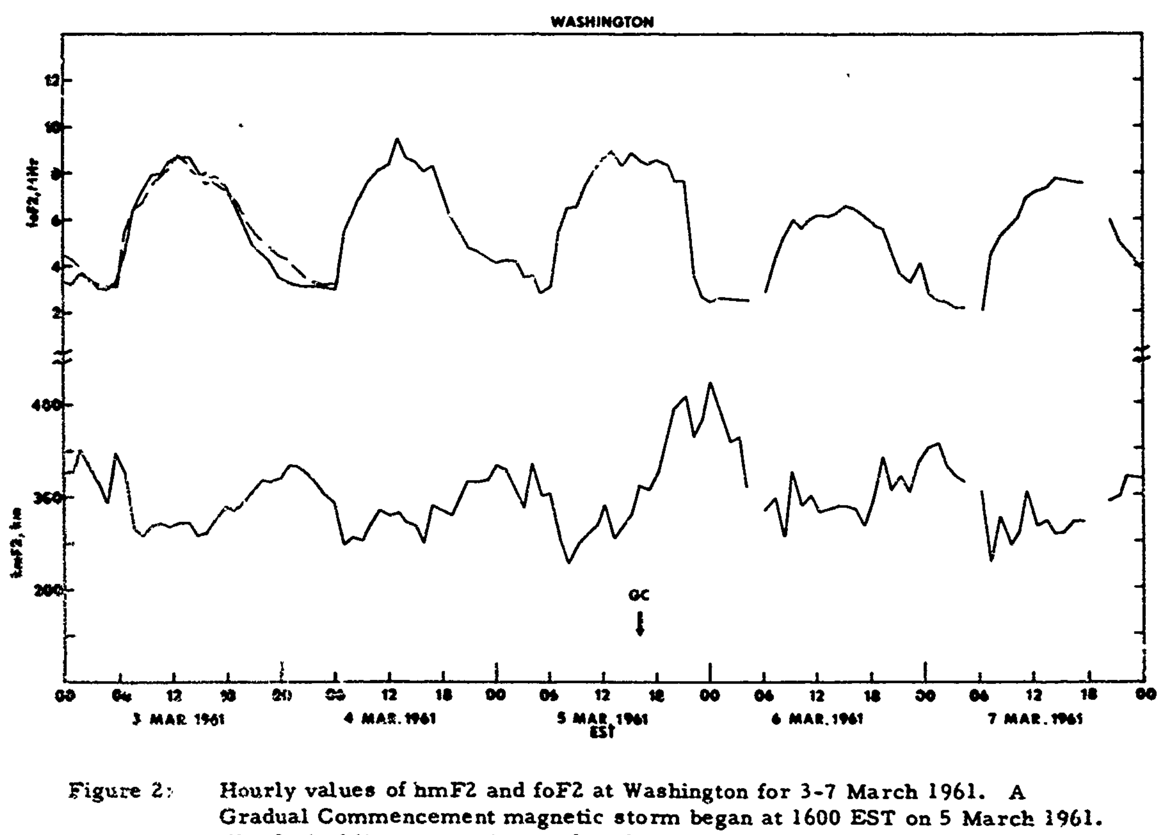

Figure 2: Hourly values of hmF2 and foF2 at Washington for 3-7 March 1961. A Gradual Commencement magnetic storm began at 1600 EST on 5 March 1961. The dashed line is monthly median foF2.

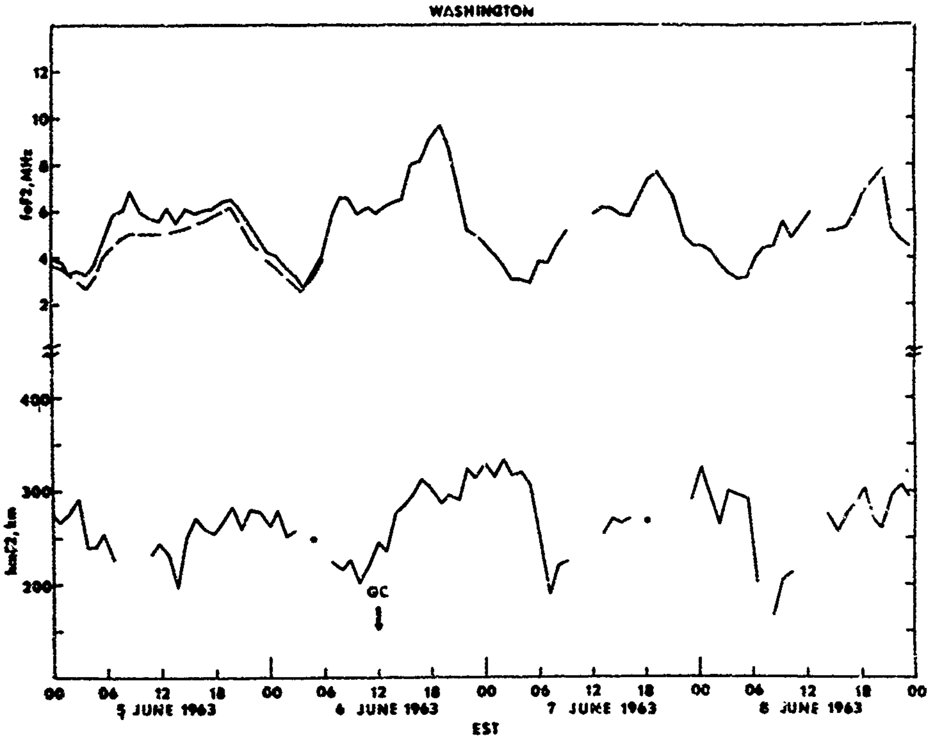

Figure 3: Hourly values of hmF2 and foF2 at Washington for 5-8 June 1963. A Gradual Commencement magnetic storm began at 1200 EST on 6 June 1963. The dashed line is monthly median foF2.

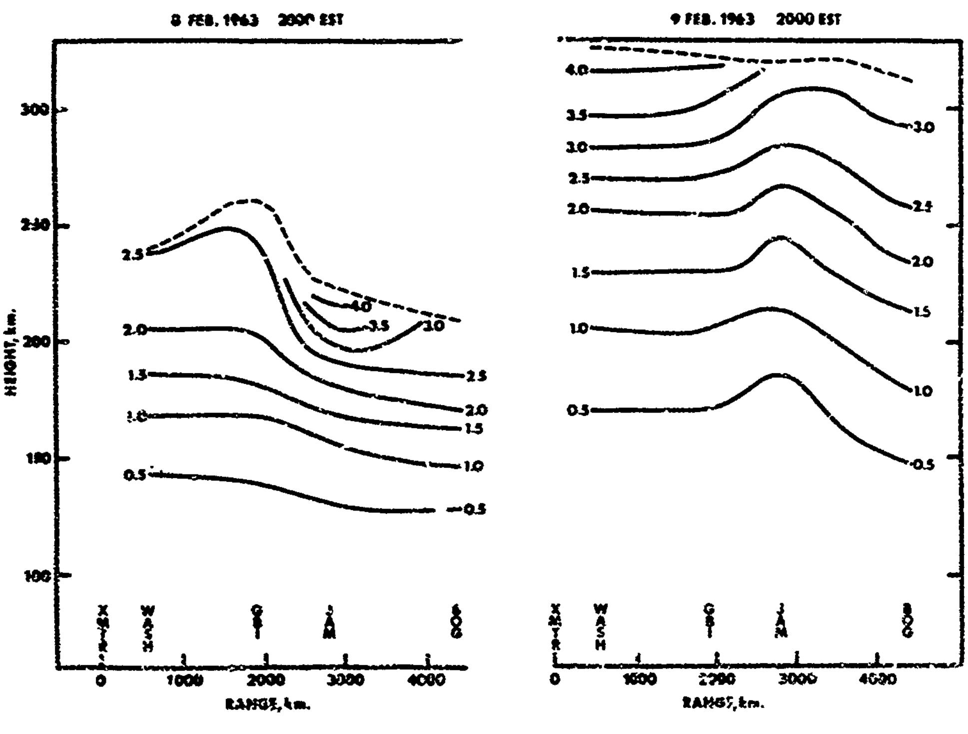

Figure 4: Latitudinal profiles of plasma frequency (MHz) for 8 and 9 February 1963 at 2000 EST. 9 February 1963 is the magnetically disturbed profile.

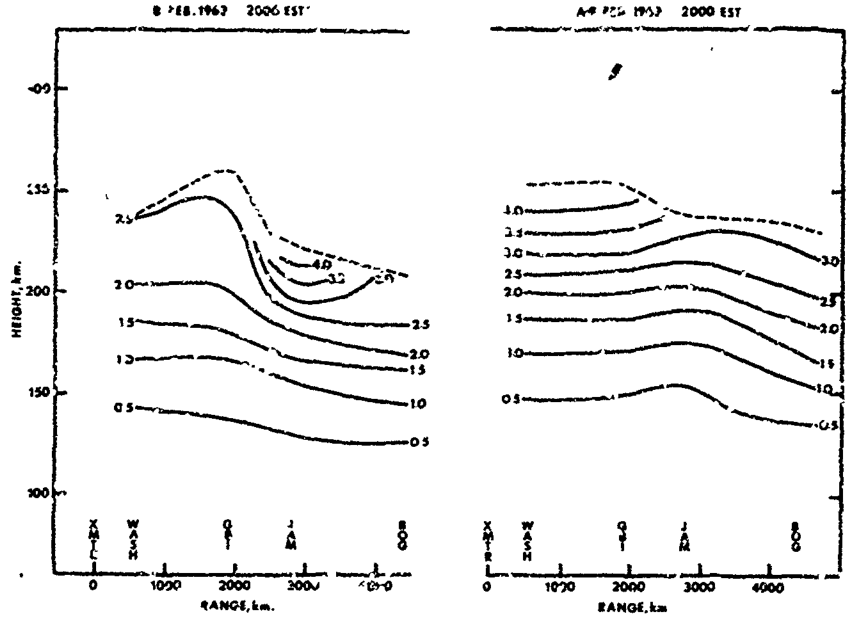

Figure 5: Latitudinal profiles of plasma frequency (MHz) for 8 and 9 February 1963 at 2000 EST. 9 February 1963 profile is adjusted to be approximately the same height as the 8 February 1963 profile.

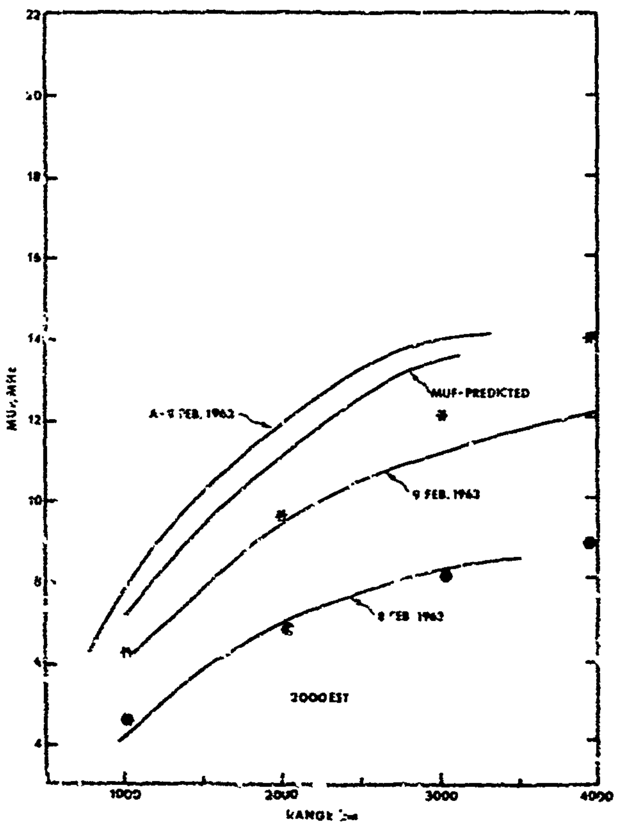

Figure 6: MUF (MHz) vs. range (km) for one hop F mode as determined by ray tracing through profiles shown in Figures 4 and 5. In addition, values of MUF obtained from predicted MUF and transmission overlay are also indicated. (Solid dots for 8 February 1963 and asterisks for 9 February 1963 transmission overlay values using Washington ionograms)

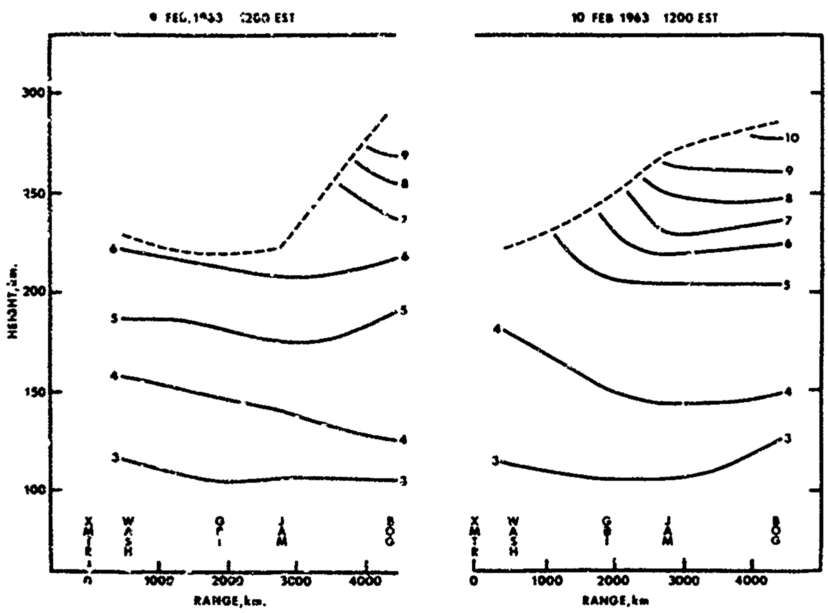

Figure 7: Latitudinal profiles of plasma frequency (MHz) for 9 and 10 February 1963 at 1200 EST. 10 February 1963 is the magnetically disturbed profile.

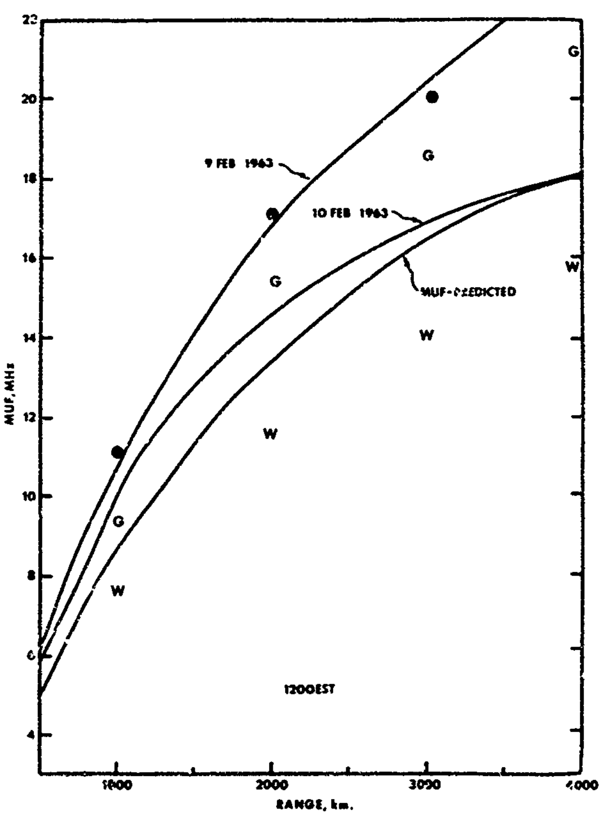

Figure 8: MUF (MHz) vs. range (km) for one hop F mode as determined by ray tracing through profiles shown in Figure 8. In addition predicted MUF and value of MUF obtained for transmission overlay are also indicated. (Solid dots for 9 February 1963 Washington ionograms and W and G for 10 February 1963 values using Washington and Grand Bahama Island ionograms, respectively.)

IONOSPHERIC FORECASTING: RELATED RESEARCH
CURRENTLY UNDERTAKEN AT
WEAPONS RESEARCH ESTABLISHMENT, SOUTH AUSTRALIA

by

R.F.Treharne*

AUSTRALIAN DEFENCE SCIENTIFIC SERVICE,
WEAPONS RESEARCH ESTABLISHMENT,
DEPARTMENT OF SUPPLY,
SOUTH AUSTRALIA

* Principal Officer, Ionospheric Studies Group

SUMMARY

A brief survey is made of research related to ionospheric forecasting currently undertaken by the Ionospheric Studies Group, Space Physics Wing, Weapons Research Establishment, South Australia. This research includes the comparison of the field strength of separate modes of propagation observed over a 1900 km path with a theoretical prediction programme including defocussing effects, the measurement of the distant equivalent vertical ionogram by ground backscatter techniques involving vertical triangulation, the prediction of ionograms and the prediction of anomalous transequatorial radio wave propagation.

INTRODUCTION

The Ionospheric Studies Group, Space Physics Wing, Weapons Research Establishment has a programme of research on radiowave propagation via the ionosphere which includes some work which is relevant to the problem of ionospheric forecasting. This work may be grouped under four headings, namely, prediction of skywave field strength, measurement of the distant ionosphere by ground backscatter techniques, the prediction of ionograms and the prediction of anomalous transequatorial radiowave propagation.

PREDICTION OF SKYWAVE FIELD STRENGTHS

A routine h.f. field strength prediction program is being developed in which the accent is on relative accuracy from point to point rather than on absolute accuracy. Even with modern digital computers the sophisticated ray tracing techniques necessary to give accuracy to within a few decibels are not economical in computer time. A single ray traced with moderate accuracy usually takes a minute or so. Thousands of rays are necessary for routine monthly predictions. For this reason analytic ray tracing of a model ionosphere is employed. Vertical incidence ionograms are reduced to the equivalent parabolic ionosphere by means of a well known technique due to Appleton & Beynon (1). The effect of the earth's magnetic field upon the layer shape is included after the manner of Shinn and Whale (2).

E and F hop distances are computed as a function of elevation angle for any derived parabolic ionosphere (multi layered). Both non-deviative and deviative contributions to the absorption over the path are calculated. It is found that the deviative contribution occurring in the E region is often most important, sometimes being greater in magnitude than the non-deviative D region contribution. It is also found to be desirable to include the effect of defocussing, particularly on daytime F region hops of distance 2000 to 3000 km.

The current absolute accuracy of the prediction technique is of the order of 10dB and it will probably not be possible to improve this significantly. The relative accuracy is thought to be better than 6dB.

Some results of a series of h.f. radio wave experiments over an 1894 km oblique path between St. Kilda, South Australia and Townsville, Queensland have been obtained (3). The path lies in a magnetic meridian. The experiments took place in the winter of 1957, both time delay-frequency and amplitude measurements being made at oblique and vertical incidence.

The vertical incidence amplitude measurements taken at the path mid-point are used in conjunction with a full ray trace computer program to establish that portion (80 - 100 km) of the electron density-height profile which was not directly available from profile reduction of the vertical ionograms. The D region electron density is shown to be rather low despite the prevailing medium to high sunspot numbers.

Under these conditions it is possible to demonstrate the inapplicability of the classical Q.L. approximation (4) to the calculation of the ionospheric attenuation of most of the oblique F modes. The oblique amplitude results obtained at 6.7, 9.2, 10.2 and 13.5 MHz on the 1F mode show a total change in field strength of the order of 15 dB between nighttime and mode cut-off. Ray tracing calculations for this mode indicate that the absorption decrement due to collision phenomena should lie between 4 and 6 dB. It is apparent that an additional attenuation mechanism was in operation. Because the field strength appeared to change in a linear fashion between nighttime and cut off, and because the magnitude of the change appeared to be relatively independent of frequency the additional mechanism has been associated directly with the phenomenon of cut-off.

Investigations of the geometry of the cut-off phenomenon (3) indicates that defocussing of the F2 region propagated modes occurs because of increased retardation of the rays as they pass through the underlying E and F1 layers. This defocussing is of order 10dB for a first order F2 mode and of order 4dB for a second order F2 mode over the path concerned.

Some field strength observations obtained on 6.7 MHz for the one and two hop F modes are shown in figure 1. There are times when the two hop mode is stronger than the single hop, an unexpected result.

The defocussing contribution taken together with the ray trace computed absorption is sufficient to account for the observed increase in attenuation of F modes between nighttime and cut-off. It is important to note that the total change in attenuation due to defocussing at cut-off may always be expected to be of the order of 10dB on low angle first order F modes. It is evident that any field strength prediction system that neglects this mechanism may often be in error by this amount even if properly based on accurate ionospheric data. It is considered possible that the defocussing mechanism discussed may provide theoretical justification, previously lacking, for the empirical lowest useful frequency predictions issued by the Australian Ionospheric Prediction Service.

THE MEASUREMENT OF THE DISTANT IONOSPHERE BY BACKSCATTER OBSERVATIONS

In this section is discussed a new technique of ionospheric measurement, which is included because of its importance to ionospheric forecasting.

The characteristics of the ionosphere which are needed for forecasting are usually measured by means of a number of vertical ionosondes. Each ionosonde gives information about the ionosphere immediately overhead. Ground backscatter techniques have been used in the past to study the skip distance appropriate to the distant ionosphere. A technique is used for measuring the apparent height of the distant ionosphere by means of the vertical triangulation of ground backscatter echoes.

The use of triangulation methods for locating the apparent sources of high frequency (h.f.) ground backscatter echoes was demonstrated in 1960 (5); a three-dimensional direction finder was used to observe the direction of arrival of the ground backscatter pulses from a h.f. radar transmitter. The locations of these apparent ground sources were determined relative to the observing point in terms of bearing and distance, the latter being calculated from the vertical triangle knowing the time delay, the approximate velocity of propagation and the angle of elevation. Also available from the vertical triangle was the apparent height of reflection from the ionosphere at the distant points, halfway to the ground scatter sources. From the apparent heights and the observed elevation angles, points on the apparent vertical ionogram at the distant point could be estimated.

A 1 kW pulse transmitter and low horizontal dipole aerial were used to illuminate, via the ionosphere, a variable zone of ground which was limited in azimuth primarily by the directivity of the transmitting aerial and by the propagation conditions; the zone was limited in distance at the near edges by the skip distance and less clearly at the far edges by the rays having the lowest useful angles of elevation; some of the energy backscattered from this illuminated zone travelled back via the ionosphere (primarily via the same mode as the forward path) and was received a few miles from the transmitter on a direction measuring instrument consisting of eight horizontal dipoles arrayed in two orthogonal arms each of two symmetrically disposed pairs of dipoles.

The ratio of the amplitudes of signals in the pairs of dipoles was displayed, for each arm in turn, with the aid of a twin channel receiver and a cathode ray oscilloscope. This display was brightened periodically for intervals of 20 microseconds at times which were delayed a measured interval from the trans-

mitted pulses so that a selected time-portion of the backscattered echo was examined in isolation. The direction angle, α, between the normal to the wavefront and the direction of the first aerial arm was calculated using the redundant equations for α in terms of the observed angles on the cathode ray tube trace, ψ^{+} and ψ^{-}, corresponding to the phase and antiphase connections:

$$\psi^{+} = \tan^{-1}(\cos((2\pi d/\lambda)(\cos\alpha))/\cos(2\pi Nd/\lambda)(\cos\alpha)))$$
$$\psi^{-} = \tan^{-1}(\sin((2\pi d/\lambda)(\cos\alpha))/\sin((2\pi Nd/\lambda)(\cos\alpha)),$$

where d was the spacing between the outer pairs of dipoles, N the ratio of the spacing of the inner pair to the outer pair and λ the operating wavelength.

The second direction angle, β, between the normal to the wavefront and the direction of the second aerial arm (at right angles to the first) was obtained from a second set of observations with aid of a pair of similar equations. The quadrantal sense of these observations was resolved using mixed phase and anti-phase connections.

The two direction angles α and β were converted to bearing, ϕ, and elevation, θ, using equations of the form:

$$\theta = \cos^{-1}(\cos^2\alpha + \cos^2\beta)^{\frac{1}{2}}$$
$$\phi = \tan^{-1}(\cos\beta/\cos\alpha)$$

It was necessary to confine the observations obtained with this instrument to moments when the wavefront presented to the aerial system was substantially plane and undistorted since the interpretation of the results was based on the assumption of a simple plane wavefront. The system was effective on waves of various polarisations provided the above wavefront conditions were met. Departures from undistorted wavefronts were indicated when the trace on the cathode ray tube formed an ellipse instead of a straight line. In practice, an arbitrary tolerance, which corresponded to an unwanted mode suppression of about 10dB, was placed on the degree of ellipticity permitted before readings were rejected.

The time delay at which the strobe was set was measured by means of a calibrated A-scan on a cathode ray tube display.

The backscatter returns were confined, by some combination of aerial directivity, propagation conditions, pulse-time strobing and wavefront selection, to an effective highlight which behaved as an apparently localised source. The direction of arrival of the returns gave the bearing, ϕ of the apparent highlight and its elevation angle, θ; its time delay, t, was given by the strobe setting. The mode of propagation was identified from considerations of the operating frequency, elevation angle and time delay. For a curved earth, concentric ionosphere model and with the assumption that the waves travelled the apparent path in a single hop with free-space velocity, and for an earth of radius 6370 kilometres, the apparent distance, D, and the apparent height, h, for a time delay, t (milliseconds) are given by the equations:

$$D = 222.5\tan^{-1}((75t\cos\theta)/(75t\sin\theta + 6370))$$
$$h = (75t\cos\theta/\sin(\tan^{-1}((75t\cos\theta)/(75t\sin\theta + 6370)))-6370$$

It is possible to convert the oblique path frequency, f, at which the backscatter observations of θ are made to an approximate equivalent vertical frequency, f_v, at the mid path distance, D/2, on a bearing, ϕ, using

$$f_v = f(1 - (6370\cos\theta)^2/(6370 + h_1)^2)^{\frac{1}{2}}$$

Here h_1 ought to be the true height of re[illegible]ction but an estimated height is usually of sufficient accuracy for the types of path considered since the earth radius (6370 km) is much larger than the true height of reflection and very much larger than the error in estimating this true height. The value of f_v so obtained may be regarded as corresponding to the measured apparent height, h. These values of h and f_v may be taken, within the assumptions considered, to be representative of the appropriate portions of the distant vertical ionogram, and may be used to modify the vertical ionogram at one end of the path to more closely represent the apparent vertical ionogram at the distant point.

In April, 1968, an improved version of this system (7) was installed at St. Kilda, South Australia. These improvements were made feasible by the development of good quality h.f. hybrid transformers for forming the sum and difference aerial polar diagrams and by the use of transistors and integrated circuits both for automating the wavefront discriminating process, and for fast aerial switching. Two transmitting systems were available, one using a 20kW pulse transmitter with vertical log periodic aerial having an azimuthal beamwidth* of 110 degrees and a second system using a 1kW transmitter with a 13 degree* sloping vee aerial. A block diagram of the system is shown in figure 2.

Additional ionospheric sounding equipment was used. This consisted of conventional ionospheric vertical sounders located at Salisbury, Woomera and Townsville (the latter kindly made available by the Australian Ionospheric Prediction Service Division) and forward oblique sounder between St. Kilda and Townsville.

Some observations were made, at various fixed frequencies, of the direction of arrival of ground backscatter returns using the 20kW transmitter, the broad transmitter aerial and the three-dimensional direction measuring receiving system. Signals of adequate strength were received on most occasions. A simple wavefront (as indicated by the automatic system) was observed rarely with this broad beam system, and even with fast, automatic switching between arms, it was not often possible to be sure that the effective high-light observed on one arm corresponded to the same high-light observed on the other arm. The best conditions for measuring the direction of arrival of the backscatter echoes appeared to be when looking in the direction of minimum skip distance, when the variation in skip distance with azimuth was greatest, the strobe being set to the time delay corresponding to the shortest skip distance. This can be explained in terms of the improvement in effective azimuthal directivity of the system provided by the combination of the time strobe and the ionospheric skip distance which excludes propagation except from the directions near the minimum skip distance.

The A-scan display observed was quite variable, with the pattern of echo clusters changing shape rapidly and with the apparent skip time shifting about a millisecond or more several times per second. At the same time the conventional time-delay/frequency backscatter ionograms were observed; these showed the expected general shape for the skip-time curve, but on careful examination a roughness of the leading edge of the record could be seen. This roughness corresponded to the time shifts seen on the A-scan with fixed frequency observation: it appears to be due to the complexity and the variability of the paths by which the backscatter is observed. This variability was attributed to irregularity in the ionosphere.

In May, 1968, observations were made using the 1kW transmitter and the narrow beam aerial for transmitting. Three dimensional direction finding measurements were relatively easy to make, particularly near midday when the measured bearings of the echoes remained within two degrees of the direction of fire of the transmitting aerials. See figure 3, which shows the points on the ground located as the source of ground backscattering, the area of the ionosphere involved (shaded), and the predicted contours of MUF for zero distance for midday, May, 1968. At other times when the direction of minimum skip distance and presumably the best direction for propagation moved out of the main beam of the transmitting array echoes were received from a variety of bearings in quick succession.

In figure 4 the block of results for the period 1200 to 1230 IK on 7th May, 1968, was plotted on the equivalent ionogram. The triangulated backscatter results for ordinary and extraordinary ray shown by dot-dash lines fall between the Salisbury (solid lines) and Townsville (dashed lines) ionograms for the same time. However, in figure 5 a similar set of results obtained two hours later shows, unexpectedly, a reverse gradient between the Salisbury ionogram and the Townsville ionogram. On the day concerned 7th

*beamwidth

May, 1968, there was a moderate degree of magnetic activity (magnetic index was 36).

The ionosphere at the remote point between St. Kilda and Townsville as observed by the triangulated backscatter appeared to have values which confirmed the reverse gradient. The predictions for this period suggest a gradient of the opposite sign to that actually recorded by the vertical ionograms and observed by the triangulated backscatter. In figure 6 is shown the variation with time of the vertical critical frequencies observed at Salisbury (near St. Kilda), Woomera, and Townsville, and the variation of the observed oblique MUF between Salisbury and Townsville for the day concerned. It is of interest to note that in the techniques described above the need to make very large h.f. aerials is avoided since: (a) observations of direction are made only at those instants of time when the ionospheric propagation conditions favour a single dominant mode of propagation; this means that simple wavefront conditions are approximated wherever direction measurements are taken and consequently that the design of the direction measuring instrument is greatly simplified and its size is greatly reduced, (b) irregularities in the ionosphere itself are made use of to provide the equivalent of a time dependent directional aerial system so that for brief intervals (which are detected by the wavefront testing mechanism on reception) the effective direction of observation is confined; the role of the directional transmitting aerial is to increase the productivity of the observing system rather than to confine the direction of observations by means of its beamwidth alone; consequently the need to make a transmitting aerial with a very narrow beam is avoided and an aerial with a modest directivity may be used instead.

THE PREDICTION OF VERTICAL IONOGRAMS

Usually vertical ionograms are observed and from them predictions of maximum usable frequency (MUF) are made. The reverse process, that of generating the ionogram from predicted MUF data, is difficult since much of the ionospheric detail, particularly that detail relating to the height of the lower parts of the ionosphere, is lost in the MUF prediction. Other data are used to fill this gap. Techniques for generating predicted ionograms have been studied (9).

The methods used were based on:

(a) predictions (10, 11) of extraordinary ray critical frequencies for propagation at zero ground distance via E, F1 and F2 regions. Ordinary ray critical frequencies were predicted when needed using the extraordinary values and the appropriate difference separating the ordinary and extraordinary values (12).

(b) world predictions of base height of F region, h'F, for average sunspot numbers (13).

(c) predictions of maximum height, hp, of F2 region, based on empirical relationships between hp, M(0)F2 and M(3000)F2 for the area involved. See figures 7 and 8.

(d) predictions of sunspot number (14).

(e) predictions (15) of types of E_s, and of vertical frequencies fE_s (maximum) and f_bE_s (blanketing) having probabilities of occurrence exceeding 30%.

(f) ionograms taken at a similar phase of the sunspot cycle near the locality for which predictions are required.

(g) ionograms taken twelve months earlier near the locality for which the predictions are required.

The predicted monthly median ionograms for each hour were sketched with height and frequency scales corresponding to those of the available past ionograms enlarged to approximately 8" x 10". A horizontal line representing the value of h'F was drawn to provide a guide to the "horizontal" part of the F region; vertical lines were drawn at the predicted critical frequencies f_oE, f_xE, f_oF1, f_xF1, f_oF2, f_xF2 to indicate the limiting values of each of the appropriate traces (emphasis was usually placed on the extraordinary ray values in the first instance). Observed ionograms from the previous year and those from a corresponding sunspot number were then projected onto the paper in turn and the actual ionograms were sketched in, including sporadic E traces. A mass plot of such traces was made, selecting traces about every five days (plus or minus a day or two if necessary to obtain clear records and to avoid magnetically disturbed days) during the appropriate month and hour. A representative ionogram was then traced off the mass plot using the ionogram traces and the guiding height and frequency median values. Solid lines were used to indicate traces whose heights were within the accuracy specified as "normal". Dotted lines were used to indicate limits of variation when the heights predicted were likely to exceed the normal limits. Dashed lines were used to indicate the E_s trace (which may or may not be present) having a probability of exceeding the limiting frequency shown of 30%. When the variations in the critical frequencies during the time block were excessive (e.g. a sunrise and sunset) the resultant uncertainty was indicated by using a cross hatched box to cover the range of variation within the time block.

An example of a mass-trace (figure 9) which was used to generate a predicted ionogram (figure 10) is given to illustrate the method. In the example chosen the frequency range was confined to 2.0 to 7.0 MHz. This range could be extended if desired. In the example shown f_oF2, f_xF2 and h_pF2 were outside the frequency range considered. Even so, it was necessary to indicate height tolerances above 6.0 MHz.

The predicted virtual height/frequency characteristic was shown for E, F1 and F2 layers as solid lines. (It related generally to the dominant magnetic ionic ray, usually the extraordinary ray at the higher frequencies and the ordinary ray at the lower frequencies). The predicted Es characteristic was shown as a dashed line at the predicted height. It indicated approximately its frequency extent, but where appropriate, the Es characteristic was considered to extend, at the same height, to somewhat higher frequencies than shown. Prohibited zones were shown as cross-hatched areas for which the ionospheric variability within the specified time block was so great as to preclude useful predictions. Sometimes the daily variations from the monthly medians or the variations in characteristic during the hour were so great that it was thought to be advisable to include limits of variations of the characteristic. These limits were shown as dotted lines.

The above system of predicting ionograms was applied in temperate latitudes and, within the limitations, which specifically exclude days when severe ionospheric storms are present, the heights had distributions which suggested the following accuracy limits:

NIGHT	F2	: ± 12%
	Es	: ± 5%
DAY	F2	: ± 15%
	Es	: ± 10%
	E	: ± 5%
	F1	: doubtful in summer; for equinoctial months and winter, about 15%.

As a result of some 12 months experience in temperate latitudes it appears that whilst frequency predictions are reasonably good the prediction of heights from readily available tabulated data is unsatisfactory. It is necessary to use previously recorded ionograms to obtain predictions of the height data required.

Finally, if representative predictions of electron distribution with height are required these may be obtained from the predicted ionograms by the usual methods.

TRANSEQUATORIAL RADIO WAVE PROPAGATION

Since 1946 there have been many reports of anomalous v.h.f. propagation over circuits up to 9000 km in length which cross the magnetic equator. The frequencies have been as high as 80 MHz and are usually in excess of any frequency which would normally be forecast to propagate over these distances. The majority of these observations have been obtained during the 1957-58 sunspot maximum period and since 1966. As an Australian contribution to the International Quiet Solar Year (1964-65), we commenced a research project on transequatorial propagation (t.e.p.) in 1964 in collaboration with the Radio Research Laboratories of the Japanese Ministry of Posts & Telecommunications and the United States Army Signal Corps Radio Propagation Agency at Okinawa (now the United States Army Strategic Communications Facility). Other organisations which are cooperating in the operation of equipment, or with data exchange, include the Ionospheric Prediction Service Division, the Royal Australian Navy, Townsville University College and the Stanford Research Institute (16, 17).

Stepped frequency pulse transmissions and fixed frequency transmissions are being used to obtain data on the characteristics of t.e.p., e.g., frequencies propagated, diurnal and seasonal variations, attenuation and fading and correlation with solar and geophysical phenomena. Regular transmissions at 20 minute intervals from a Granger 4 to 64 MHz oblique ionospheric sounder at Okinawa are being received at St. Kilda (South Australia) and at Townsville. The recording of these oblique ionograms at St. Kilda and Townsville commenced in February 1964 and September 1966 respectively. Typical results are given in figure 11 for March 1967 Okinawa to Townsville. Transmissions from Darwin on frequencies of 32.80, 48.45 and 72.65 MHz have been monitored at Yamagawa, Japan (18, 19), since August 1964. In addition, an f.m. broadcast transmission on 45.9 MHz of the Korean Broadcasting Service is being monitored at St. Kilda. It is hoped to continue operation of these circuits.

There appear to be two classes of t.e.p. (20); an afternoon enhancement providing reasonably steady signals up to approximately 50 MHz over the longer circuits and an anomalous nighttime phenomenon of signals with flutter fading propagating up to 80 MHz over shorter circuits approximately 4000 km to 5000 km in length. Although the mechanisms of propagation are still not clear it appears that they are different for the two classes of t.e.p. The 8000 km circuit from, Iri, South Korea to St. Kilda is an example of a long transequatorial path and the 45.9 MHz signals are received most frequently around 1400 hours local time. See figure 12 which, on the bottom histogram, indicates the percentage of days during March 1967 when a 45.9 MHz path was open from Iri to St. Kilda; on the middle histogram the median duration per day for each hour is shown and on the top histogram the weighted median duration per day for each hour has been calculated. Similarly the highest frequencies propagating over the 6900 km Okinawa to St. Kilda circuit occur during afternoon hours.
For both these circuits the activity peak at equinoxes is somewhat less during the June solstice. On the other hand, although propagation of the 48 and 72 MHz transmissions over the 5000 km Darwin to Yamagawa circuit is most frequent at equinoxes it is almost exclusively a nighttime phenomenon at this time of the year, starting at approximately 1900 hours. Reception is far less frequent at the solstices but, contrary to the situation for the longer circuits, this t.e.p. activity is greater during June than in December. The 5500 km Okinawa to Townsville circuit shows both classes of t.e.p. during equinox periods.

The increase in t.e.p. activity with increasing sunspot numbers, see figure 15, is most apparent for the data recorded at Yamagawa. The 48 and 72 MHz transmissions were first received in April and May 1965 respectively and over the following three years there was approximately a sixfold increase in the activity on these frequencies. The MOF's observed over the Okinawa to St. Kilda circuit, as well as the number of hours reception of frequencies greater than 30 MHz, have also increased significantly from sunspot minimum to maximum although not to the same extent as the activity on the shorter Darwin to Yamagawa circuit.

It is expected that these observations may be applied to the problem of forecasting the MUF of transequatorial radio circuits.

ACKNOWLEDGEMENTS

The work reported here arises from the joint efforts of my colleagues of the Ionospheric Studies Group.

REFERENCES

1. APPLETON, E.V. & BEYNON, W.J.G. — The application of ionospheric data to radio communication problems, Part I & II. Proc. Phys. Soc. 1940 and 1947. Vols 52 and 59 (Reproduced together in DSIR Special Rpt. No. 18, H.M.S.O., London 1948).

2. SHINN, D.H. & WHALE, H.A. — Group velocities & group heights from the magneto-ionic theory. Journ. Atmos. and Terres. Physics 1952, Vol. 2, No. 2, pp. 85 - 105.

3. GEORGE, P.L. — The attenuation of radio waves reflected from the ionosphere at oblique incidence. Abstracts of Technical Papers, 12th National Radio and Electronics Engineering Convention, Sydney, Institution of Radio and Electronics Engineers Australia, May 1969, p.66.

4. RATCLIFFE, J.A. — The magneto-ionic theory. Cambridge University Press, 1959, p.75.

5. WALIPHANT, R.G. — The control of F layer L.U.F. by the defocussing effect of the lower layer. NATO-EPC-AGARD Symposium on L.U.F. Leicester, England, July, 1966.

6. TREHARNE, R.F. — Triangulation of high frequency backscatter returns. Proc. I.R.E.E., Australia, vol. 29, No. 4, April, 1968 pp. 109 to 114.

7. TREHARNE, R.F. — Determination of the distant ionosphere - the triangulation of high frequency backscatter returns. Proc. I.R.E.E., Australia, Australian Electronics Communications, Vol. 30, No. 1, January 1969, pp. 25 to 27.

8. TREHARNE, R.F. The measurement of the height of the distant ionosphere by backscatter observations. Abstracts of Technical Papers, 12th National Radio and Electronics Engineering Convention, Sydney, Institution of Radio and Electronics Engineers Australia, May 1969, pp. 162 to 163.

9. TREHARNE, R.F. & SPOPAL, Jillian The prediction of vertical ionograms. Abstracts of Technical Papers, 12th National Radio and Electronics Engineering Convention, Sydney, Institution of Radio and Electronics Engineers Australia, May 1969, pp. 166 to 167.

10. Ionospheric predictions, Series B, Ionospheric Prediction Service Division, Aust.

11. Ionospheric predictions, Series C, IPS-C8, 1951. Ionospheric Prediction Service Division, Aust.

12. RAWER, K. The ionosphere, Frederick Ungar Publishing Co., New York, 1956.

13. DAVIES, K. Ionospheric Radio Propagation NBS Monograph 80, U.S. Dept. of Commerce, 1965.

14. Geophysical Data E.S.S.A., Boulder, Colorado, U.S.A.

15. SMITH, E.K. MATSUSHITA, S. Ionospheric Sporadic E Pergamon Press, Oxford, 1962.

16. McCUE, C.G. & FYFE, D.F. Transequatorial Propagation: Task Bridger introductory review. Proc. I.R.E.E., Australia, vol. 26, no. 1, January 1965, pp. 1 to 10.

17. FYFE, D.F. Oblique propagation experiments over transequatorial circuits. Paper presented at the 1965 Congress of the Australian and New Zealand Association for the Advancement of Science. Hobart, August 1965.

18. YAMAOKA, H., TAO, K., WATANABE, S., OCHI, F., WATANABE, C., TANOHATA, K., SAKAMOTO, T. The experimental results on the transequatorial propagation between Australia and Japan in the v.h.f. band. Institution of Elec. Comm., Engg., Japan. Rec Note A-P October 1966. (In Japanese).

19. KURIKI, I., ICHINOSE, N., KAINUMA, S., WATANABE, C., TANOHATA, K. Investigations of the transequatorial propagation mode in the v.h.f. band. Journal of Radio Research Labs., Japan, Vol. 15, p no. 80/81 September/October, 1968.

20. FYFE, D.F. Transequatorial propagation during half a sunspot cycle. Abstracts of Technical Papers, 12th National Radio and Electronics Engineering Convention, Sydney, Institution of Radio & Electronics Engineers, Australia, May 1969, p. 62.

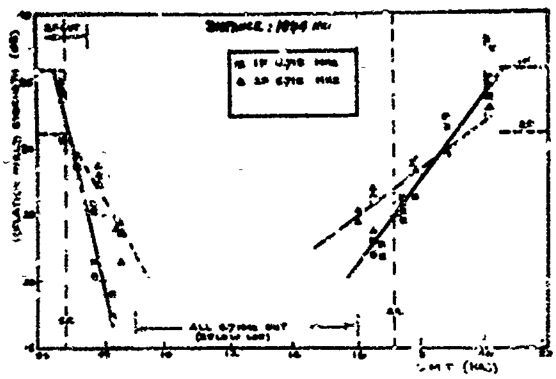

FIGURE 1. OBLIQUE AMPLITUDE RESULTS; 1F AND 2F MODES ON 6.115 MHz

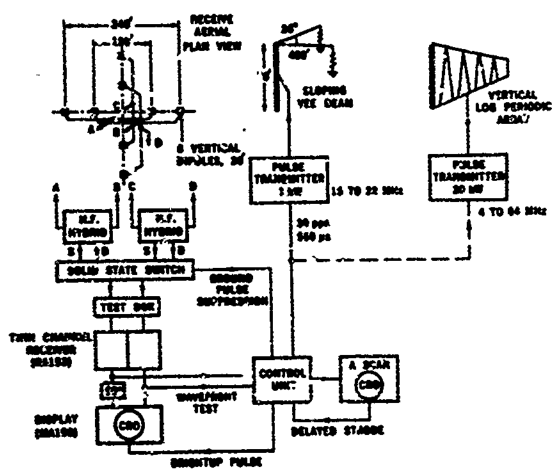

FIGURE 2. BLOCK DIAGRAM

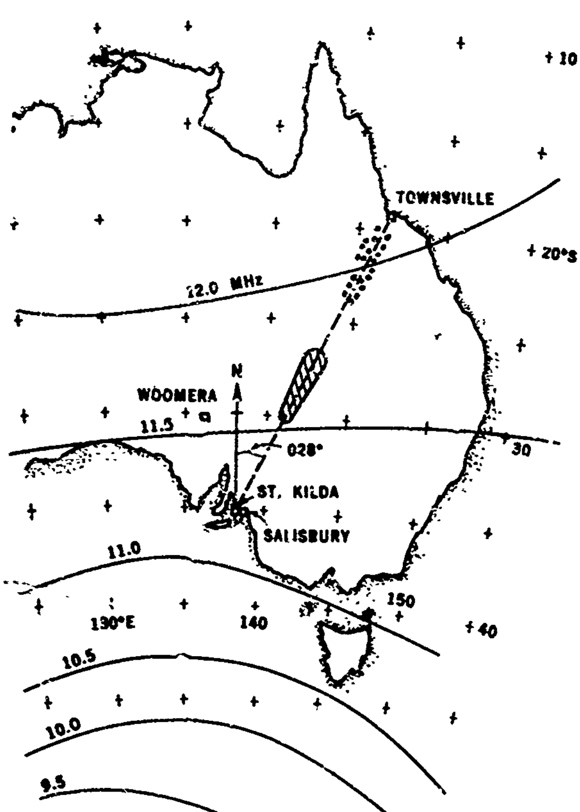

FIGURE 3. BACKSCATTER OBSERVATIONS

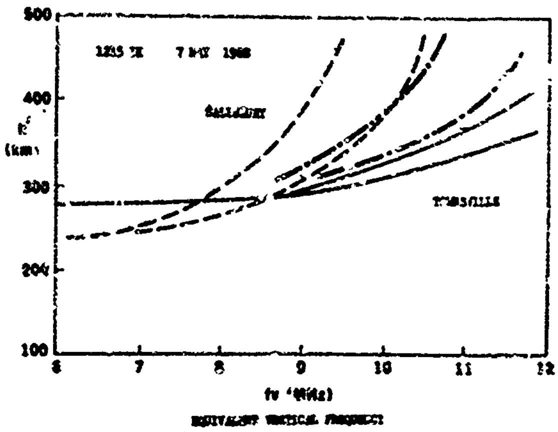

FIGURE 4. EQUIVALENT IONOGRAM

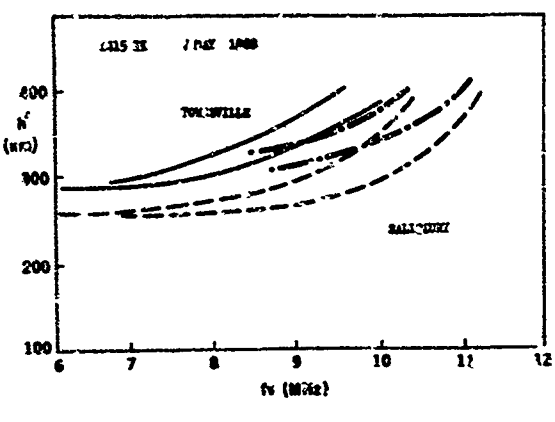

FIGURE 5. EQUIVALENT IONOGRAM

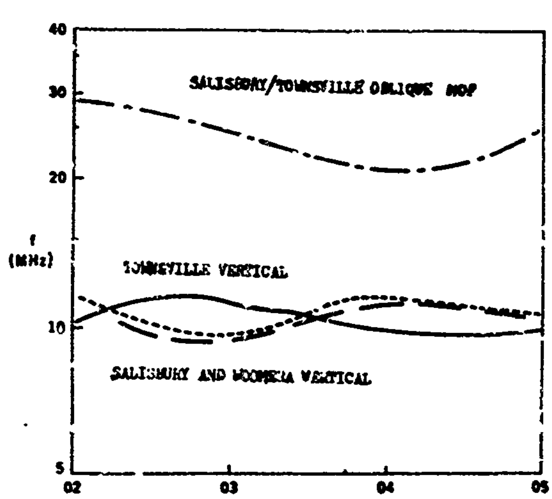

FIGURE 6. VERTICAL AND OBLIQUE FREQUENCIES

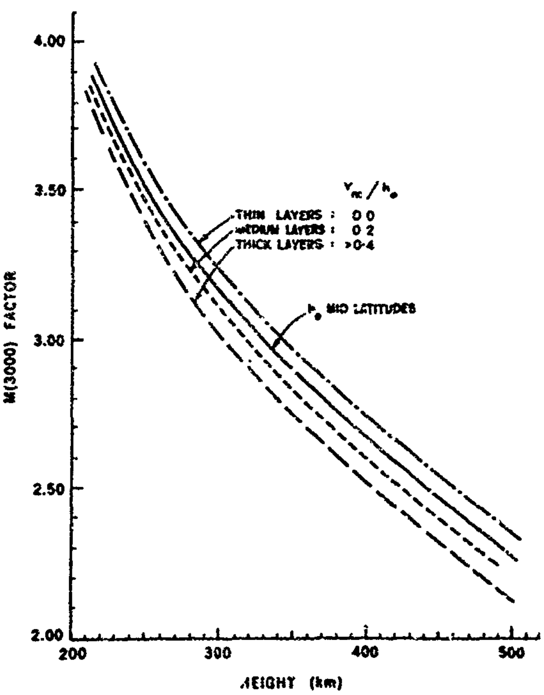

FIGURE 7. HEIGHTS FROM FREQUENCIES

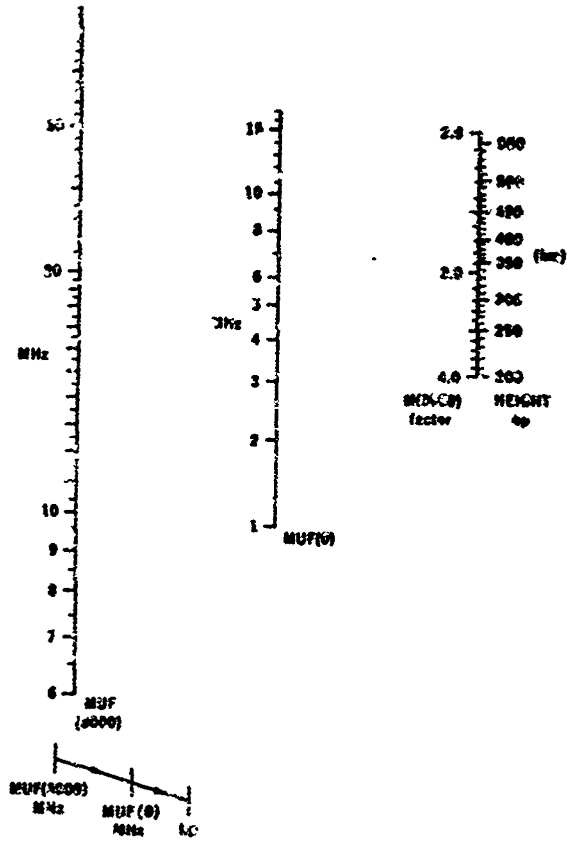

FIGURE 8. NOMOGRAM FOR CONVERTING FREQUENCIES TO HEIGHT

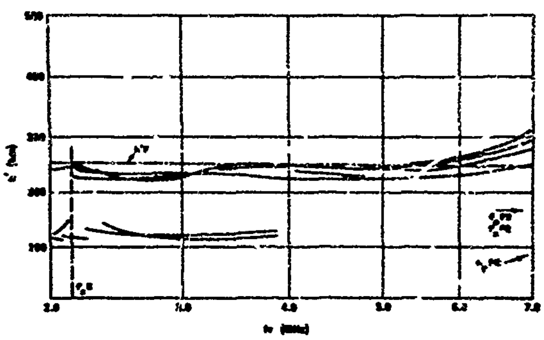

FIGURE 9. [illegible]

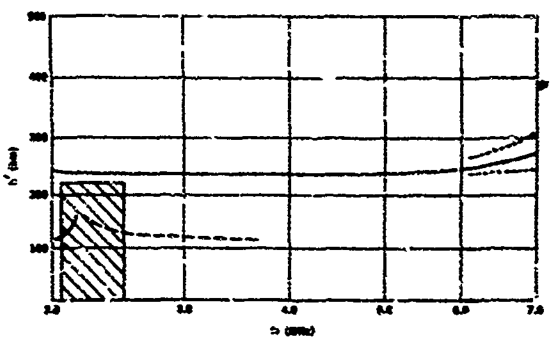

FIGURE 10. [illegible]

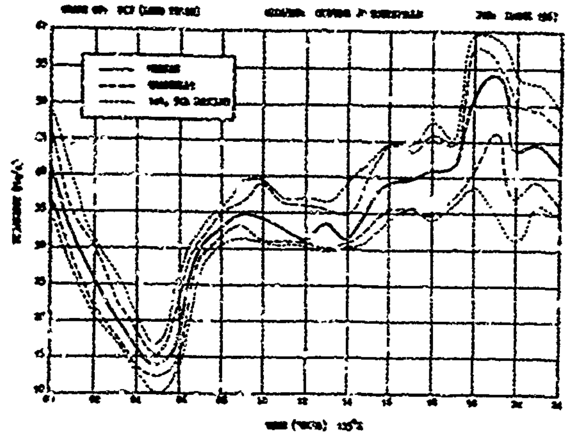

FIGURE 11.

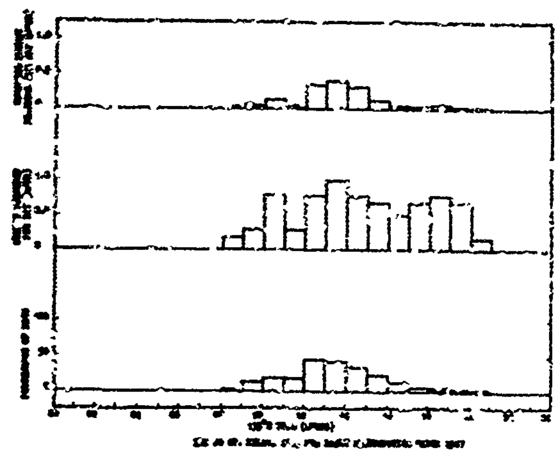

FIGURE 12.

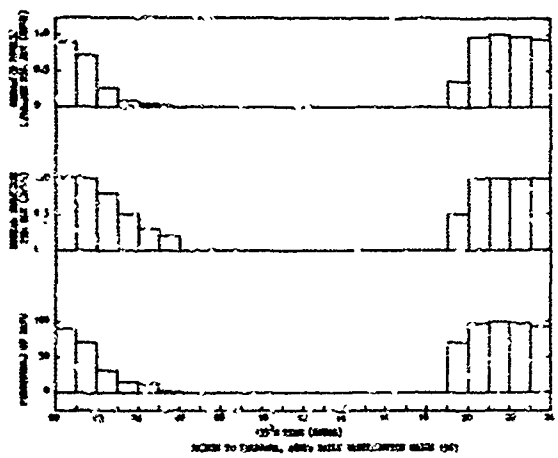

FIGURE 13.

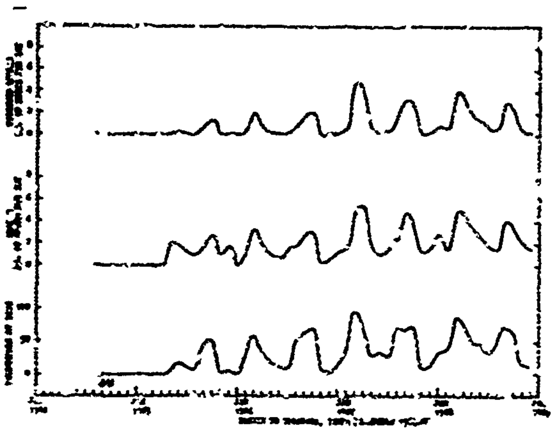

FIGURE 14.

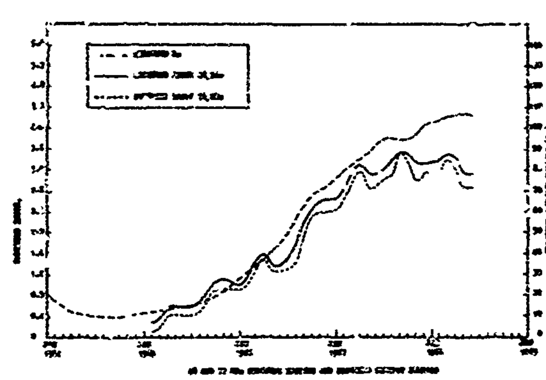

FIGURE 15.

THE VALUE OF IONOSPHERIC PREDICTIONS

By N. C. Gerson

Syracuse University Research Corporation

SUMMARY

As a strict management tool HF ionospheric predictions are useful in planning the frequency spectrum which may be available for a given path and date. The predictions offer some assistance in roughly defining the transmitter power requirements, distributing the station work load, etc. At the working level, however, the predictions usually have little impact. The decision to maintain or close a given circuit is made on the basis of existing propagation conditions, not on the basis of the predictions.

Insofar as the MUF program ITS 1968 is concerned its greatest asset seems to be its advertised computational convenience. As written it represents an unrefined program wasteful of computer time and memory. When employed it offers no assurance that the results obtained are the best possible or the cheapest for the effort involved. It contains a number of inherent deficiencies over and above those organic to the program. The predicted absorption seems too high particularly at the lower frequencies. Noise magnitudes are based upon the assumption of homogeneous isotropic noise distributions within arbitrarily defined geographic zones. Improvements possible today -- the inclusion of sporadic E, detail around sunrise and sunset, ionospheric relaxation after a solar flare, etc. -- are in a rudimentary state.

Within the U.S. a fair number of groups now run obstensibly the same ITS 1968 program for overlapping purposes in order to obtain precisely computed but inaccurate predictions. The need for continuing duplicative efforts seeking similar approximate predictions seems questionable. If predictions are required it is suggested they be obtained from one large national computational facility specifically designed for this purpose. Until costs are competitive present users will maintain their own prediction units.

1. INTRODUCTION

Ionospheric predictions were first devised for the HF communicator who needed guidance on the gross diurnal and seasonal variation of frequencies usable over given links. The procedure evolved for determining these frequencies was basically geometric. It utilized the secant law and an empirical linear relationship between the critical frequency and sunspot number. Initially a crude average critical frequency and average height at the reflection point were adopted. For determining absorption empirical coefficients were deduced. They were based on field strength recordings obtained from a relatively few transmitters whose radiated powers, frequencies and distance from the recording site varied widely.

Few changes in the basic approach to frequency predictions have occurred. The increase in the number of observing allowed greater confidence in the interpolations. More sophisticated computational techniques were introduced. With the machine calculation of MUFs the tedium of hand determinations was reduced. This method embodied more elaborate averaging methods without indicating whether or not they were needed.

Unfortunately the feedback between the communicator and predictionist always has been sluggish and weak. The communicator was restricted by a practical consideration -- only assigned frequencies irrespective of the prediction or forecast could be employed. A working circuit was retained despite a negative prognostication. Sometimes there were well grounded suspicions that the communicator did not examine the predictions. One indication may be mentioned of the weak impact of the predictions on operations in the U.S. MUFs obtained by computer (utilizing the ITS 1968 technique) and by the older hand method (utilizing geographical zones) may differ by 8 MHz over some paths (e.g., New York - Buenos Aires). It is doubtful whether the communicator, geared to practical circuits, really appreciated the difference or changed his operating procedures when the new results became available.

This paper attempts to assess the value of ionospheric predictions in general and those obtained with the ITS 1968 program in particular. It examines some programming deficiencies. It questions the necessity of the monthly coefficients, the need in the computations of refined reflection altitudes and the choice of constants for absorption. It compares MUF values obtained by different groups. It illustrates typical differences between predicted and observed operating frequencies over given paths. It suggests the inclusion in the predictions of additional features which seem feasible today: e.g., sporadic E data, noise as a function of azimuth, greater resolution around sunrise and sunset, and ionospheric recovery after sudden ionospheric disturbances. It also discusses the future of HF communications and the continuing need for ionospheric predictions.

2. THE ITS 1968 PROGRAM

The ITS 1968 Program represents one technique for calculating ionospherically supported radio frequencies which allow radio contact between two given ground locations. It furnishes hourly values of the monthly median propagation characteristics and implicitly contains similar values of ionospheric parameters for the path concerned. Since the Zurich sunspot number must be specified, the computations rest upon future predictions of the general solar activity.

As a whole the program loosely meets the general requirements of many distinct users whose needs and degree of sophistication vary considerably. The program is unduly large for its objectives. Few users fully understand the assumptions involved, the programming, or the properties and nuances of the program. In large part this ignorance may be attributed to a lack of clearly written and precise documentation.

The bulky and needlessly large program increases the computer time needed for a specified output. Some of the extra running time is utilized in redundantly calculating values needed at many levels of the program. Additional computer time is expended in undertaking logical decisions which later allow a choice of one or more (up to 11) incorporated output options. Since some output functions are divided arbitrarily among several subroutines great difficulty may be encountered in attempting to design an output peculiar to a given problem. Thus, ITS 1968 squanders computer time and demands an excessive reprogramming effort if particular outputs are to be accommodated.

The program is written in Fortran IV of Control Data Corp. This language is not completely compatible with many machines necessitating an appreciable reprogramming effort if another computer (e.g., IBM 7090, 7030, 7094, etc.) must be employed. Unfortunately this condition usually prevails. It may be argued that in reality any program is written around a particular computer by a programmer thoroughly familiar with that machine's idiosynchrosies. To some extent this comment is correct but reprogramming for commonly available computers could be much simplified if a more

representative language were utilized originally. It might be noted that even if correctly rewritten the program would still exceed the capacity of most computers.

For its employment ITS 1968 requires the use of an ITS monthly coefficient tape. This restriction seems unnecessary and for many purposes is undesirable. There are numerous occasions when data from alternative sources or from current observations are available. Nevertheless, no convenient means exist for utilizing these data as computer input even though they may be more pertinent to the problem considered. Employment of the numerical maps (which are derived from the ITS monthly coefficients) increases the computer time involved.

In summary ITS 1968 seems inaptly programmed leading to inefficient computer usage and operation. Mechanical programming shortcomings could be removed. More flexible input arrangements could be incorporated to allow the introduction of general or localized observational data, specified electron density gradients, and particular absorption coefficients (either as single points or as geographical maps). Subroutines could be self contained. The programming language could be more basic. Self contained outputs of a more extensive and flexible type could be provided.

Finally, since HF predictions will have continued utility, consideration should be given to a national computer wholly devoted to ionospheric and propagation predictions. Practically all interested users would have input and output terminals. The total savings in costs over the present fragmented efforts revolving around the first generation ITS 1968 program would be considerable. However, it must be recognized that to be utilized a computational facility must offer more efficient services and at a cheaper cost than the potential user himself could furnish. It is uncertain whether existing time shared computers for this purpose are truly competitive in either accuracy, output, flexibility or cost.

3. COMPUTATIONAL ACCURACIES

In the U.S. a fair number of groups have reprogrammed ITS 1968 for use on their own computers. A comparison was made to test the consistency of MUFs obstensibly derived from the same ITS 1968 program but run at different locations. MUFs for the same path, month and sunspot number were evaluated. The results reveal agreement mainly within 1.5 MHz for the middle latitude paths adopted for the study. Prior to this study discrepancies of tenths of MHz were expected. On a practical basis MUF accuracies to within 1 MHz seem sufficient for most purposes. Under these conditions it seems appropriate to inquire whether some refinements now included in the predictions are needed. For example, if an accuracy of 1 MHz in MUF over usual path lengths is acceptable, what accuracies are required in the value of the reflection height, particularly when the looseness in specifying the launch angle is considered?

4. COMPARISON: PREDICTION AND OBSERVATION

A comparison between the predicted and observed results for given paths typify some of the prediction deficiencies and illustrate the difficulties presented to the communicator. As one example 22 MHz backscatter observations from Puerto Rico (at distances of 1000, 3000 and 5000 km to the N, E, S, and W) were compared with MUFs computed for the same paths. The vertical beamwidth (25°) of the antenna ranged between launch angles of 5° - 30°. For the three ranges and reflection altitudes of 300 km and 500 km, the calculated launch angles are: for one hop -- 28° and 42°, 4° and 11°, and impossible: for two hops -- 48° and 61°, respectively. Predicted MUFs along the 12 paths for June and December 1959 are displayed in Figures 1 and 2, and the actual backscatter results in Tables I and II. One observation/15 minutes provided a total possible of 120 (124 in December)/hour. Half this number of occurrences corresponds to a realizable MUF. The radiated power was 1 kw and a 3 element Yag was used.

A number of agreements are found. For the 1000 km paths predicted MUFs did not attain 22 MHz in either month. Actual backscatter occurrences were all less than 50%. Hours when MUFs equalled or exceeded 22 MHz are underlined in Tables I and II. For the 3000 km path agreement between the predictions and observations may be considered as fair - good. In other cases distinct differences arise. June occurrences attained 50% only for a portion of the predicted hours. Actual open paths over 1000 km occur much less frequently than over 3000 km and mainly between 1800 - 2200 GMT; they may arise from Sporadic E.

It is possible that the poor comparison between observation and prediction arises from experimental parameters which introduced inefficiencies in the backscatter soundings. For example, the launch angles available were unsuitable for propagation to 1000 km and 5000 km. Agreement between the calculated and observed values in December seems even less favorable over all ranges than for June. Note that for the 1000 km path many more backscatter occurrences were found in June than December. The character of the predicted MUF curves, which do not include Es, imply an opposite conclusion.

A second study compared MUF predictions and observations over a forward oblique path from Washington to Bermuda where WWV at 20 MHz was received. An omnidirectional antenna and R390 receiver were utilized. The percentage of reception for each month of the year 1960 is graphed in Figure 3. A summary of the actual percentage of reception and MUF predictions obtained from (a) the ITS 1968 program, (b) the Canadian DRTE 1-1-3 method and (c) the Australian IPS technique is tabulated in Table III. The Table allows an inter-comparison among the different prediction techniques. Discrepancies are found between the computed and experimental results. Emissions were received 50% or more of the time between about 1200-2400-0100 GMT and frequently, forlonger periods in all months. All MUF predictions are pessimistic. Predictions of no openings are found for many months especially in summer. Predictions of openings are found for other months mainly between 1400-2200 GMT

The differences between the experimental and computed results seem serious. It would almost seem that the predictions cannot be that wrong. In this vein a number of possible explanations arise for the far greater than predicted reception. One includes the effect of side-scatter; e.g., reflection from a ground area simultaneously illuminated by both the transmitting and receiving antennas. This type of propagation occurs much more frequently than expected, but the effect is never included in the predictions. It can permit significant increases in the hours of reception beyond those indicated by the usual predictions particularly when an omnidirectional antenna is used. A second factor is the reception of other, non-WWV standard frequency recordings at 20 MHz. Several such transmitters are located in Europe. A third possibility is the reception of WWV 10 MHz with the generation of 20 MHz in the front end of the R390 receiver. Such a condition would provide a mixed record of WWV 10 MHz and 20 MHz reception that could not be reconciled with the 20 MHz MUF predictions. However, it is felt that the latter condition is of low probability. Also, the recordings which were analyzed contained the known WWV transmission cycle. The possibility of sidescatter, or indeed of ionospheric scatter in general has not been resolved. Obviously the intensity of these modes would be less than that for F_2 layer reflection. In any event, it should be noted that appreciable differences between the predictions and actuality do exist and that the comparison given here may not be too uncommon.

While the value of the predictions in frequency management, manpower and station management, HF radar design, etc. is not questioned, the utility of the predictions for operational circuits requires improvement. The existing deficiencies detract from the aura of the predictions and stigmatize the entire concept and use of the predictions as an operational tool.

5. IMMINENTLY POSSIBLE IMPROVEMENTS

Since the predictions serve a useful function, improvements in accuracy as well as new needed features should be incorporated. Imminently possible additions would include (but not be limited to) the following.

5.1 Sporadic E

Current attempts to include Sporadic E information are commendable but require accleration. Factors such as the Es occurrence, partial transparency, blanketing frequency, reflectivity etc. are required. The inclusion of recent Sporadic E data from high latitudes seems warranted. Both the U.S. and the U.S.S.R. now attempt to provide Es prediction techniques. An evaluation of the two methods seems desirable if their relative strengths and weaknesses are to be determined.

5.2 "Absorption" Loss

The extent to which the calculated path losses are useful in practice is uncertain. The "absorption" coefficients presently incorporated in the ITS 1968 program seem to be those empirically derived over 20 years ago. They were based on observations of field intensity recordings of a limited number of transmissions at distances ranging between 1600-15000 km.

If path losses serve a function it would seem that an improved data based could be obtained. Any new empirical coefficients should be redefined in terms of the various losses involved (inverse square, lower layer blanketing or cut off, and absorption) as a function of frequency, distance and time.

The ITS 1968 program seems to predict excessive absorption during the summer noon period. However, computations of field intensities pose special problems. The entire procedure and need may require reexamination. Perhaps all modes whose predicted intensities are within 5-10 db of the strongest mode should be furnished.

JUNE 1959

TABLE I

OBSERVED NUMBER OF 22 MHz CONTACTS
(Mayaguez, P. R.; Observations: 4/hr)

Time	1000 km*				3000 km*				5000 km*			
(GMT)	N	E	S	W	N	E	S	W	N	E	S	W
02	1	0	0	1	53	52	46	58	4	8	1	9
04	0	0	0	2	59	46	57	57	0	9	1	5
06	3	2	0	2	23	36	28	42	0	2	1	7
08	5	0	0	4	55	31	61	60	0	0	0	0
10	25	5	9	13	30	47	63	40	0	0	0	0
12	16	7	10	7	26	25	27	21	0	0	0	0
14	8	6	9	11	17	0	3	2	0	0	0	0
16	12	10	7	11	29	2	16	13	0	0	0	0
18	21	26	15	21	61	18	51	61	0	0	3	1
20	28	39	22	25	69	69	53	41	6	0	2	0
22	14	8	1	14	83	77	73	67	9	9	1	4
24	6	11	2	7	93	63	93	92	7	5	0	23

NOTE: *Predicted MUF occurrences are underlined.
Total possible backscatter contacts in any hour = 4 x 30 = 120.
By definition occurrences 50% or more of the time correspond to the MUF.

December 1959

TABLE II

OBSERVED NUMBER OF 22 MHz CONTACTS
(Mayaguez, P. R.; Observations: 4/hr)

Time	1000 km*				3000 km*				5000 km*			
(GMT)	N	E	S	W	N	E	S	W	N	E	S	W
02	0	0	0	0	3	28	44	39	0	0	0	1
04	0	0	0	2	0	0	8	0	0	0	0	0
06	0	0	0	0	0	0	4	3	0	0	0	0
08	0	0	0	0	18	0	43	37	0	0	0	0
10	0	0	0	0	28	35	38	28	0	0	0	0
12	0	0	0	0	7	25	2	20	0	0	0	0
14	3	0	0	2	8	18	13	30	0	2	0	1
16	0	0	4	6	30	29	11	46	1	0	0	2
18	0	3		2	62	66	58	68	1	0	1	1
20	0	2	0	0	58	50	59	56	0	7	0	8
22	0	1	1	0	27	35	51	55	0	5	9	13
24	0	0	1	0	5	35	53	50	0	0	0	4

*Predicted MUF occurrences are underlined.

NOTE: Total possible backscatter contacts in any hour = 4 x 31 = 124. By definition occurrences 50% or more of the time correspond to the MUF

TABLE IV

COMPARISON: PREDICTED VERSUS OBSERVED
(20 MHz, Washington-Bermuda)

HOURS OF SUPPORT (GMT)

Month (1960)	Sunspot Number	Observed*	Its 1963 Predicted	DRTE 1.1-3 Predicted**	IPS Predicted
Jan	129	1200-2400	1400-2200 (1F)	1500-2000	1400-2200
Feb	125	1100-2400-0200	1400-2200 (1F)	1400-2100	1400-2200
Mar	122	1100-2400-0500	1400-2200 (1F)	No support	(1800) #
Apr	120	1400-2400-0400	1400-2200 (1F)	No support	No support
May	117	1000-2400-0600	No support	No support	No support
Jun	114	0000-2400	No support	No support	No support
Jul	109	0000-2400	No support	No support	No support
Aug	102	1000-2400-0600	No support	No support	No support
Sep	98	1100-2400-0300	No support	No support	No support
Oct	93	1100-2400-0200	1400-2200 (1F)	(1900-2100)#	(1600)#
Nov	88	1100-2300	1400-2200 (1F)	No support	1400-2000
Dec	84	1200-2300	1400-2200 (1F)	(1600)#	(1500-1800)#

*Reception above noise level 50% or more of the time.
** F2 layer modes.
#Predicted MUF of 21 MHz.

5.3 SID Relaxation

The perturbing effects of SIDs on ionospheric propogation are well known. The dependence of the storminess on one ionospheric circuit (20 MHz, Washington-Bermuda) is illustrated in Figure 4. It would seem possible to deduce "average ionospheric recovery models" after typical SIDs as a function of the duration of fade out at a standard frequency, and to incorporate this model into the predictions. Thus, despite the lack of warning on the occurrence of a SID, the general behavioral pattern of the ionosphere on a circuit for several days after initiation of the SID may be predictable. While models dependent upon the SID intensity, solar zenith angle, frequency, etc. may be rudimentary at present the results may not be much worse than the general prediction inaccuracies now available.

5.4 Sunrise-Sunset Behavior

Vertical Thomson scatter and detailed circuit measurements allow the characteristics short term behavior of the ionosphere around sunrise and sunset to be determined. These data permit the deduction of empirical relationships for predicting ionospheric properties around the sunrise or sunset period.

6. FUTURE PREDICTION REQUIREMENTS

An assessment of the future value of HF predictions may be attempted. The character of long range global communications circuits is rapidly changing. Strongly competitive alternatives to long distance HF links already exist. Satellite communications systems are an accomplished fact and their expansion is inevitable (to perhaps a maximum density of one/4^{o} in equatorial orbits). Advances in cable technology allow their logical justifications as independent backup systems, particularly if wideband cables are considered. Present technology permits the establishment of cables in all oceans including the Arctic. These developments superficially indicate that HF ionospheric circuits with their attendant vagaries are outmoded. It is obvious that the cutting of a cable or the destruction of a satellite are readily possible by a determined group, and that the latter may be easier than the former. This aspect will not be considered here.

To some extent a conclusion that HF is being superceded is justified. Military users always will prefer a reliable to an unreliable circuit irrespective of cost. The professional communicator always has sought non-ionospheric circuits: the tropospheric, meteoric and ionospheric scatter circuits were developed under his aegis. Their fulfillment removed a dependence upon circuits subject to sudden catastropic outages. As another factor separate communications satellite systems soon will be within the grasp of all large and many moderately developed nations. Under circumstances where each national or military group has his own peculiar alternative system, the need for HF circuits would seem to dimish.

However, despite this expected trend by the military the HF ionosphere will not be so readily abandoned. It offers a great convenience. It will always remain as the poor man's communications link. Anyone can obtain a simple unsophisticated transmitter and receiver and establish an HF circuit. The published body of literature on HF link performance and MUF forecasts permit the needed frequencies for the path to be deduced to a greater or lesser extent. This approach has been taken by some newly developed nations and undoubtedly will be utilized by others. For these users predictions of future link performance will continue to be valuable.

Thus, even if military traffic is removed the HF ionosphere will continue to be well utilized. Commercial companies and governments have a large capital investment in equipment, trained manpower and ground installations. Operating and maintenance costs for HF equipment are low, the technical competence required is moderate and replacement costs are minimal. For future HF circuits closed loop sounders integral to the communications link offer a basis for minimizing outages. If long range global HF links are ever to be redesigned, grids of trunks (including antipodal trunks) together with rapid switching networks could materially improve innage of most if not all circuits.

Sounding systems incidentally also allow an entirely new approach to the use of the HF ionosphore by communicators. They offer a potential for abolishing the entire concept of frequency assignments. In these place would be sounders which would indicate the existing frequency openings between the major communications trunks. This procedure would permit communicators to employ actually available frequencies supported by the path. Transmitter powers would be maintained at the lowest level possible for circuit needs. Considerable potential for multiple use of the same frequency then becomes possible and unwanted signal interference should be reduced

The present method of frequency allocation is to a fair extent responsible for increasing the noise level. If communicators are restricted to assigned frequencies a not uncommon usage is the transmission of the same information on several channels to insure that at least one frequency will

be received. Aside from the fact that this procedure is wasteful of the freqvency spectrum, it increases the man-made noise level. Thus, it is found an increasing percentage of "noise" is RF interference produced by other emitters. In some areas the man-made noise level is the dominant noise encountered. A frequent tecnnique for overcoming the noise is the employment of higher powers. In essence, the frequency allocation system fasten a cycle of increased inteference, increased noise intensities, increased transmitter powers, etc.

In perspective HF ionospheric circuits always will exist and with them the need for some type of prediction seems appropriate to incorporate improvements at all levels for the HF predictions. It also seems imperitive to design more efficient procedures for utilization of the HF ionosphere.

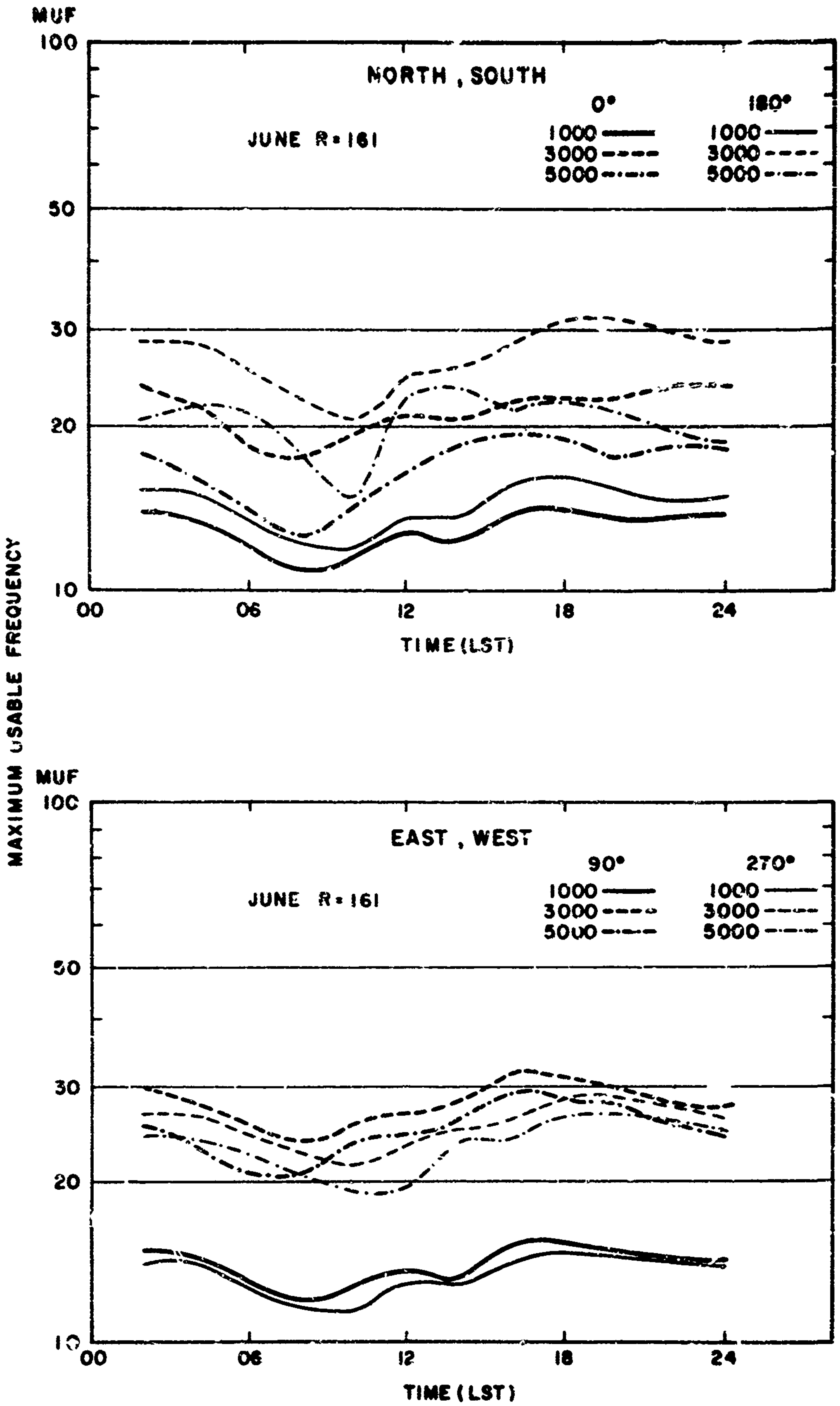

MUF
100
NORTH , SOUTH
0°
180°
JUNE R=161
1000
3000
5000
1000
3000
5000
50
30
20
10
00
06
12
18
24
TIME (LST)
MAXIMUM USABLE FREQUENCY
MUF
100
EAST , WEST
90°
270°
JUNE R=161
1000
3000
5000
1000
3000
5000
50
30
20
10
00
06
12
18
24
TIME (LST)

Figure 1

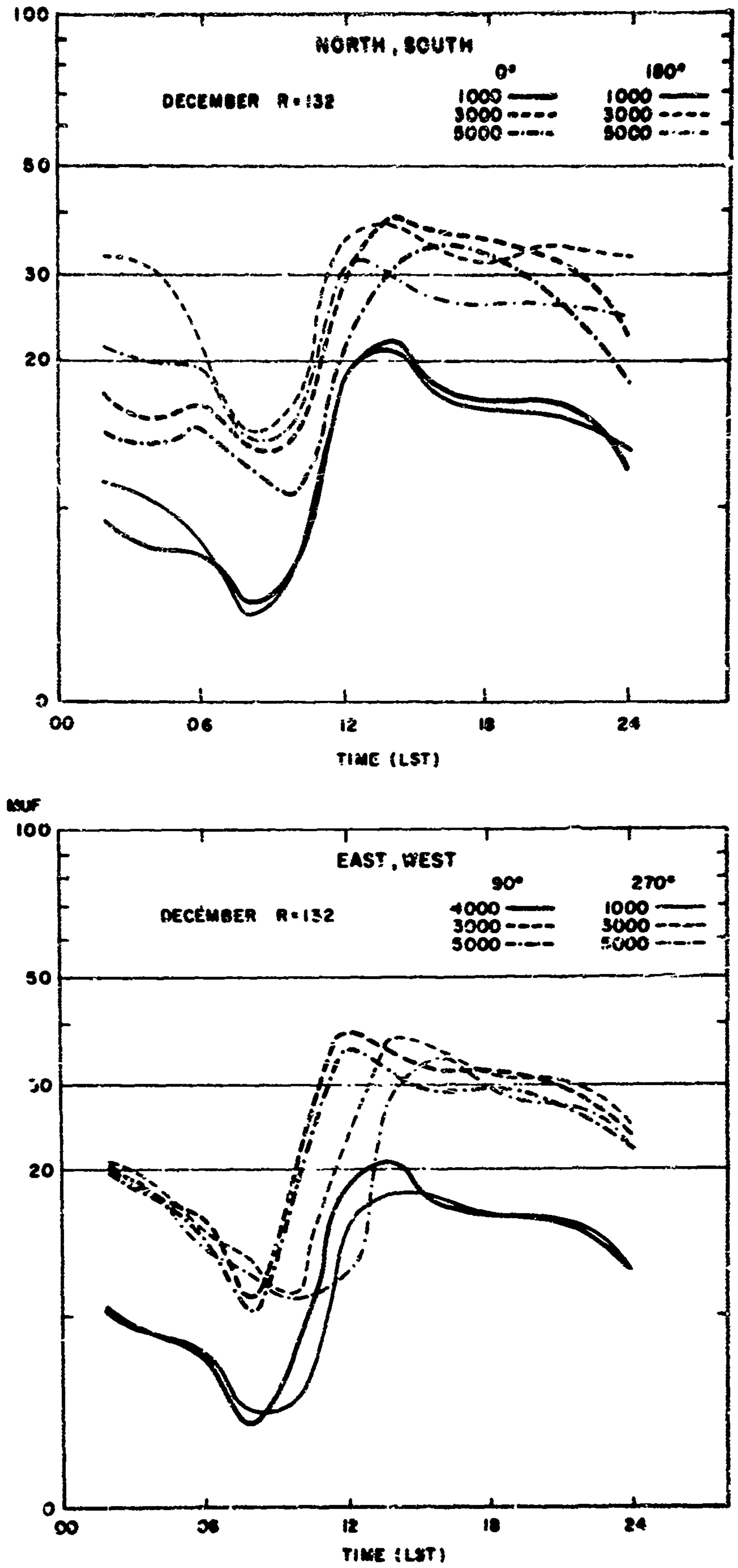

NORTH, SOUTH
DECEMBER R=132
0°
1000
3000
5000
180°
1000
3000
5000
100
50
30
20
0
00
06
12
18
24
TIME (LST)
MUF
EAST, WEST
DECEMBER R=132
90°
4000
3000
5000
270°
1000
3000
5000
100
50
30
20
0
00
06
12
18
24
TIME (LST)

Figure 2

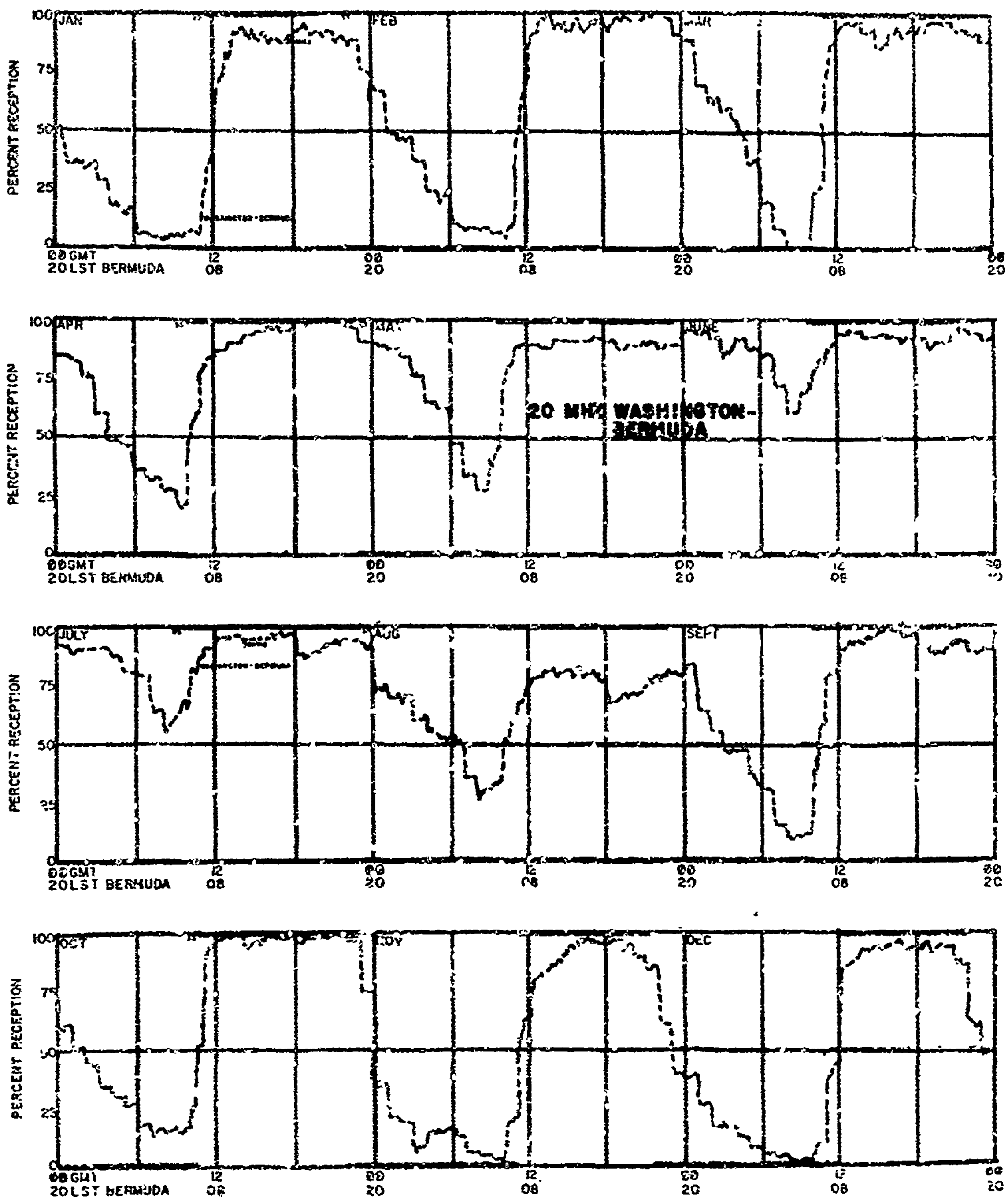
JAN
FEB
APR
JULY
SEPT
OCT
DEC
PERCENT RECEPTION
100
75
50
25
0
00GMT
20LST BERMUDA
12
08
00
20
20 MHz WASHINGTON-BERMUDA

Figure 3

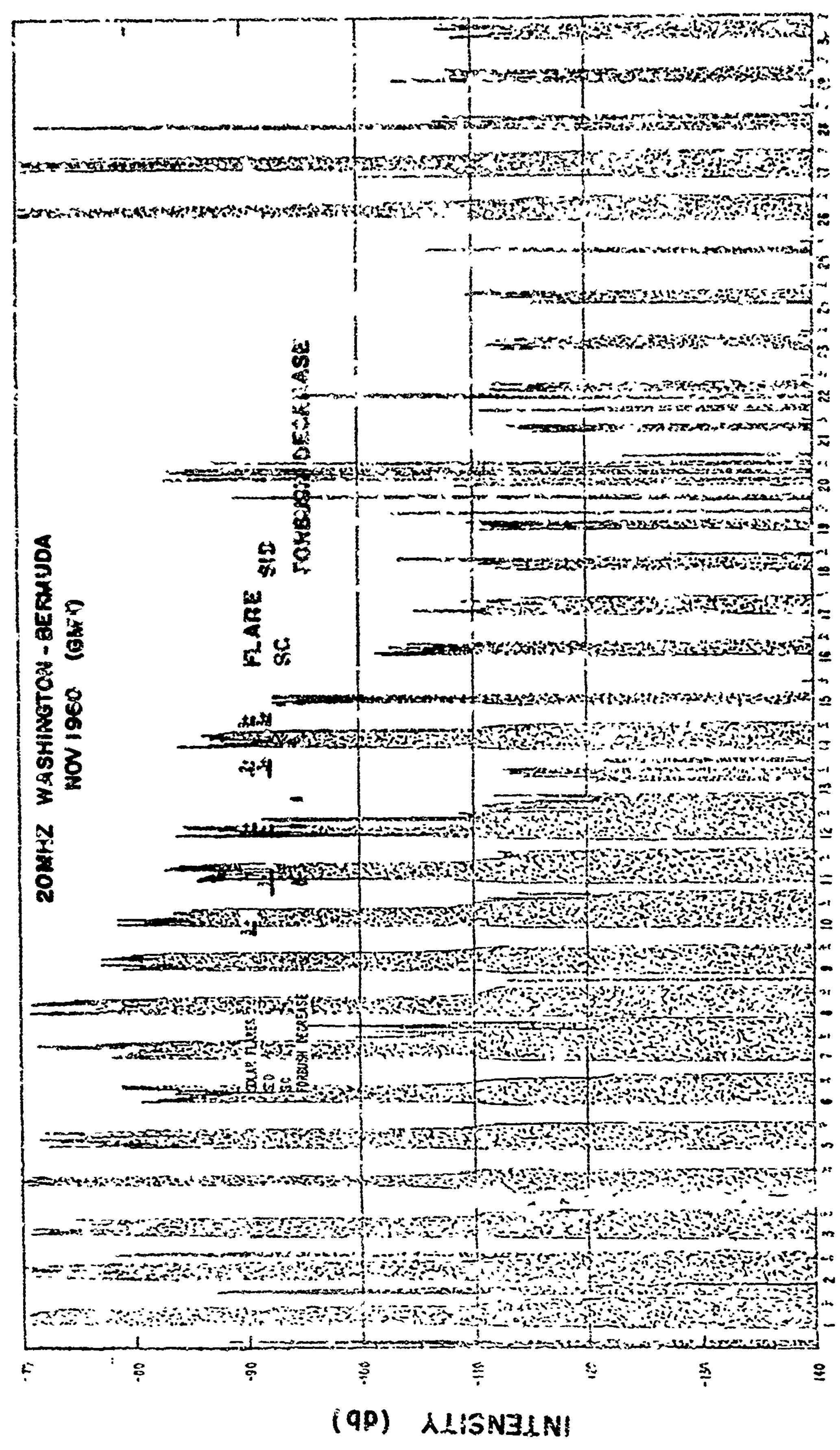
20MHZ WASHINGTON - BERMUDA
NOV 1960 (GMT)
FLARE
SC
SID
INTENSITY (db)

Figure 5

APPLICATION OF SHORT TERM PROPAGATION PREDICTIONS AND RADIO DISTURBANCE WARNINGS WITHIN THE CANADIAN FORCES COMMUNICATION SYSTEM

by

CAPTAIN D.A. REYNOLDS
CANADIAN ARMED FORCES

Footnote:
Staff Officer on the staff of the Headquarters Canadian Forces Communication System

SUMMARY

The Canadian Forces Communication System (CFCS) is responsible for the operation and maintenance of strategic communications to serve the needs of the Canadian Armed Forces.

This paper outlines the utilization of ionospheric information by communicators within CFCS and presents practical examples of the affects of ionospheric disturbances on actual HF radio circuits.

1. CANADIAN FORCES COMMUNICATION SYSTEM

In September 1964 as one step in the integration of the Canadian Armed Forces, the Chief of Defence Staff directed that a communication system called the Canadian Forces Communication System (CFCS) be organized to place under common management the former Canadian Army Signals System, the RCAF's Main Communication Relay Network, the RCAF's Military Aeronautical Communication System, plus certain of the Armed Forces special purpose communications and transmission systems. Although functional control of the former Naval Shore Communication System is exercised by CFCS HQ, Maritime Command retains command of a major relay on each coast.

CFCS was authorized as a formation with an integrated organization effective 1 April 1965. Initially it was organized into five Communication Groups, 17 Communication Squadrons and 67 Communication Detachments, with the Headquarters located at Victoria Island, Ottawa. The Commander CFCS was charged specifically with the operation and maintenance of strategic communications to meet the operational and administrative requirements of the Canadian Forces and emergency government communications within the resources allotted, and to the degree and standard established by, the Canadian Forces Headquarters.

One function of CFCS is to operate a network of HF and IF radio stations which serve trans-Atlantic, trans-Pacific and domestic fixed operational/administrative circuits. In addition, Aeronautical Stations located at Edmonton Alberta, Trenton Ontario, St. John's Newfoundland and Lahr Germany provide air-ground communications for Air Transport Command, Mobile Command, Training Command and the Department of Transport.

The motto shown on the CFCS Crest translates as "SWIFT and SURE". As indicated by this motto, one of the primary aims of CFCS is to pass common user narrative type traffic from the originator to the addressee(s) in the quickest possible time with the highest degree of accuracy. Although narrative type traffic can be handled and/or transmitted by various means, this paper deals only with the transmission of radio teletypewriter traffic (RATT) over fixed service circuits.

2. TYPICAL COMMUNICATIONS SYSTEM

Figure 2 depicts a typical HF communication system. For simplicity, this block diagram does not reveal in detail many of the technical improvements that have been made to HF communication systems over the past years. A modern communications system should include:

a. synthesized transmitters whose inherent qualities include frequency stability and rapid frequency changing;

b. transmitter antennae systems which provide not only transmission path versatility through different type antennae, different take-off angles and polarization, but also include use of diplexers for simultaneous transmission of intelligence on two different frequencies;

c. receive systems which include antennae and equipments for:

   (1) space diversity

   (2) frequency diversity

   (3) polar diversity

   (4) automatic switching for route selection and regenerative processing.

There are many different areas in a communication system through which a message, after translation into a telegraph code, must pass before it is radiated as electrostatic and electromagnetic fields of energy from the transmitter antennae. Furthermore, the small portion of that energy received at the receive antenna must be amplified, reshaped, checked and fed through the reverse process before being printed out on a page copy device. In amplification let us examine briefly the number of equipments involved within the different areas on a send path:

a. Communication Centre/Tape Relay Centre Areas

   (1) Transmitter-Distributor

   (2) Reperforator

   (3) Number Device

b. Secure Area

(1) Encyphering equipment

c. Facility Control Centre (FCC) Area

(1) Patching facility

(2) Error Detection Equipment (EDC)

(3) VFCT (for conversion from D.C. to tones)

d. Carrier Equipment Area (Commercial or military-owned carrier systems whether VHF microwave or audio lines)

e. Transmitter Site Area

(1) Tone conversion equipment (VFCT)

(2) Drive unit

(3) Amplifier

(4) Antennae system

f. Propagation Path

Between each of these internal areas are D.C. loops which themselves have to be adjusted for correct current or voltage levels. So it can be seen that each telegraph loop (D.C. or VFCT) and each piece of equipment is itself a source of distortion. The problem then for the system controller is to not only detect and identify the presence of distortion but also to establish whether the distortion is caused by equipment or disturbance in the ionosphere. It is evident that the areas portrayed as simple blocks on the diagram are in fact quite complex. The transmitter and receiver sites plus antennae farms are usually located many miles from the Communication Squadron's Headquarters. Other areas within the Headquarters itself may be widely dispersed and isolated from each other.

The most important facet of any communications system is its personnel. Well trained personnel in both the operator and technical fields are necessary to make a communications system function effectively. Technicians tend to become specialists within very narrow fields and become very proficient on a small number of highly specialized equipments. This is also to a certain extent true of the operators. Although an operator sent to a fixed communications terminal for a three-year posting may be confined to the Relay and Message Centres, he may well work in other fields on his next posting. In the military environment, personnel are being constantly changed about due to postings, courses etc. Thus at any one time in a communications system there is a mixture of personnel in different fields, each possessing various educational backgrounds, degrees of training and experience. Backing up these operators and technicians is a cadre of administrative, scientific, engineering and logistic personnel including, naturally, the ionospheric specialists.

The heart of the communications system is the Facility Control Centre (FCC). The FCC is responsible for the efficient utilization of its communications facilities and, in conjunction with other FCCs, for maintaining standards of efficiency commensurate with the Canadian Armed Forces communications requirements. The FCC is the hub through which all communications are fed, providing a common meeting ground between the two main groups involved in communications, operators and technicians.

The efficiency of the communications system is dependent upon the quality of the individual circuits comprising it. Evaluation of performance is the key to quality control. For normal or average propagation conditions, the Communications Research Centre (formerly DRTE) computer predictions, operator experience, and circuit historical performance have proven to be quite adequate. Although ionospheric oblique soundings would enhance any communications system, providing the soundings were carried out on a particular circuit's assigned frequencies, this device and its associated equipments, as part of the normal station complement, appear to be prohibitively expensive.

In addition to inherent quality control provided by EDC and VFCT diversity demodulation, the FCC Quality Controller is continually manually checking for:

a. distortion

b. signal strengths

c. interference

d. noise

e. fading

f. readability on those circuits not protected by EDC equipments.

3. SHORT TERM PROPAGATION FORECASTS AND WARNINGS

To assist in the day-to-day operation of all HF and LF circuits, the Department of Transport provides CFCS HQ with short-term weekly propagation figures obtained from the Telecommunications Disturbance Forecast Centre, Fort Belvoir, Va. These forecasts are transmitted to all Canadian Military radio stations and ships at sea. All Canadian Military fixed radio and aeronautical stations also monitor WWV (Fort Collins, Colorado) on a regular basis to obtain present propagation conditions and predictions for the next six hours. In addition, radio disturbance warnings are received from the Ionospheric Prediction Service Division, Sydney, Australia. These IPSO warinings are also forwarded by CFCS HQ to all Canadian Military radio stations.

When propagation conditions deteriorate due to an ionospheric disturbance, the Quality Controller in the FCC is limited as to what he can do to try and overcome the effect of the disturbance. He can change frequency, or, if operating a multi-channel system, reduce the number of channels and thus effectively increase channel power on the remaining channels. This task is particularly demanding if the Quality Controller is faced with engineering, at almost the same time, a large number of multi-channel circuits.

When a communication facility is faced with an ionospheric disturbance which may last for a considerable period, the operational staffs of the facility have a number of choices available to enable them to clear the traffic. These choices are:

a. Making use of LF circuits as primary traffic routes if they suffer less from the effects of the ionospheric disturbance.

b. Patching to commercial landlines, cables or combination landlines and tropospheric circuits.

c. Alternate routing traffic through other military or commercial agencies.

Short term ionospheric predictions provide a measure of comfort to the FCC Quality Controller. For example, suppose that a Quality Controller has been taking regular distortion measurements and the circuits appear to be within predetermined limits. It is then noted that one or two of the EDC-equipped circuits start to exhibit extensive RQ (repetition) periods. Is this caused by faulty equipment or poor propagation conditions? If the Quality Controller has at hand a propagation warning he will be prepared for poor propagation conditions, and have already notified his operational supervisors. Without a short term ionospheric warning, the Quality Controller must always opt for malfunctioning equipments or propagation path disturbance. If his assumption is incorrect it is inevitable that re-establishment of the service will be delayed.

4. EFFECTS OF DISTURBANCES ON LIVE TRAFFIC CIRCUITS

Figures 3A to 3J depict:

a. circuit availability figures for actual traffic circuits for three periods in Mar 69;

b. Department of Transport short term weekly propagation predictions (PROPRED) which originate from T.D.F.C. Fort Belvoir, Va.;

c. WWV hourly propagation conditions and forecasts; and

d. ionospheric disturbances based on IPSO warnings (Figure 4 is a copy of these IPSO warnings received from 28 Feb to 26 Mar 69).

Of the days plotted (Mar 12, 13, 16, 17, 18, 23, 24 and 25) the days immediately preceding and immediately following are also plotted to provide continuity. With exception of the trans-Atlantic circuits, reception at the western terminals of the circuits are depicted by solid lines, the eastern terminals by broken lines. The trans-Atlantic chart (fig 3A) shows reception at the Canadian terminals only. Figure 3A is a composite of a number of trans-Atlantic circuits; the path length of the longest circuit (represented by a broken line) is 1000 Km longer than the shortest path.

<u>Comments on Figures 3A to 3J</u>

a. Generally speaking, the western terminals were affected by the ionospheric disturbances several hours after the eastern terminals.

b. For Domestic Circuit #3 (fig 3F), it appears that reception at the western terminal, which is in the auroral zone, was less affected by the disturbances than the eastern terminal, which is located at a more southernly latitude.

c. During periods of ionospheric disturbances, the circuits showing the best results (fig 3H and 3J) were those of the longest paths.

d. With reference to the trans-Atlantic circuits, the longest path circuits appears to have suffered more from the disturbances than the shorter path circuits.

e. Domestic #4 (fig 3B), a short path circuit, over the years has consistently produced the best results of any domestic circuit. This circuit was severely affected by the disturbances.

f. With reference to Domestic Circuits #1, #2, #5 and #6 (figs 3C, 3E, 3G and 3D) there is a common terminal for the four circuits which is located in central Canada. This terminal appears to have been more severely affected by the disturbances than the other terminals located in either eastern or western Canada. Also the lower powered circuits running at power ratios 1:2 appear to have been less affected by the disturbances.

5. SUMMARY

Although many new and improved communication systems have been devised and are coming in to increasing use e.g., satellite communications, HF RATT still proves and will continue to prove to be an effective means of communication. Much of the effectiveness of a HF RATT system depends on high quality frequency predictions for normal or average propagation conditions, and short term ionospheric wariningy for those periods when propagation conditions are disturbed. Ionospheric scientists should not only be concerned with the compilation of information with which to prepare forecasts, but should be just as concerned to provide this information in plain, layman's terms and pass it to the user as quickly as possible.

Canadian Forces Communication System Badge

FIG 1

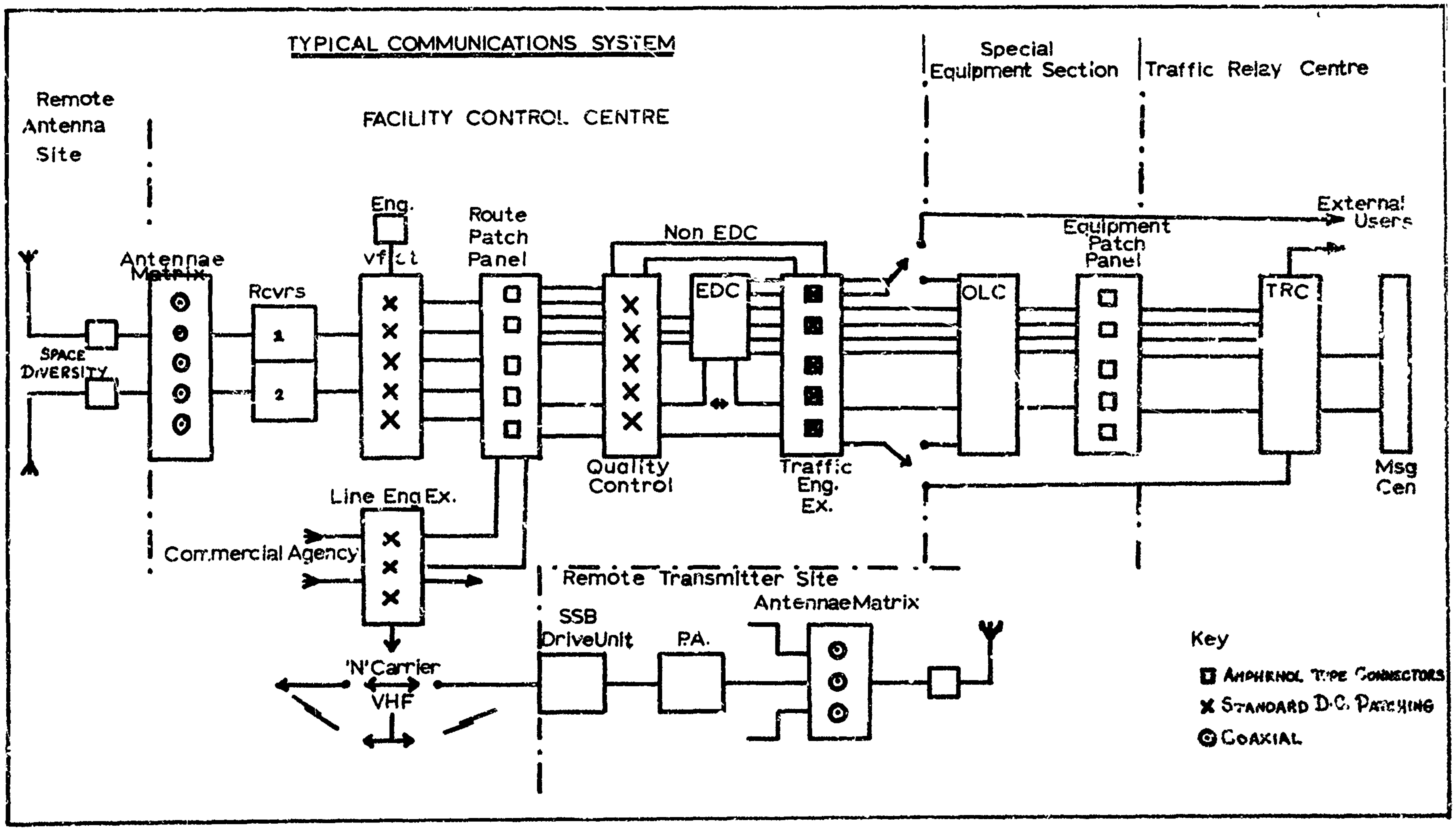
TYPICAL COMMUNICATIONS SYSTEM
Remote Antenna Site
FACILITY CONTROL CENTRE
Special Equipment Section
Traffic Relay Centre
SPACE DIVERSITY
Antennae Matrix
Rcvrs
1
2
Eng.
vf ct
Route Patch Panel
Non EDC
EDC
Quality Control
Traffic Eng. Ex.
OLC
Equipment Patch Panel
TRC
External Users
Msg Cen
Line Eng Ex.
Commercial Agency
'N' Carrier
VHF
Remote Transmitter Site
SSB DriveUnit
P.A.
AntennaeMatrix
Key
AMPHENOL TYPE CONNECTORS
STANDARD D.C. PATCHING
COAXIAL

FIG 2

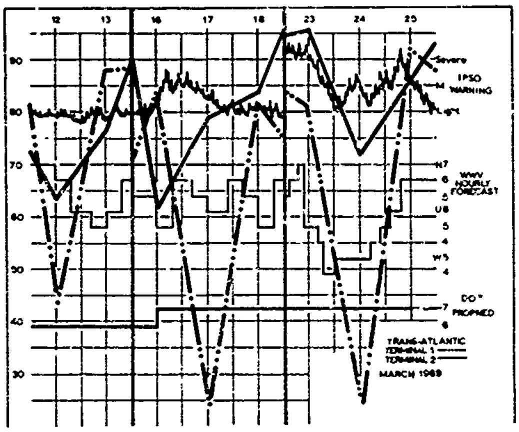

FIG 3A - TRANS-ATLANTIC

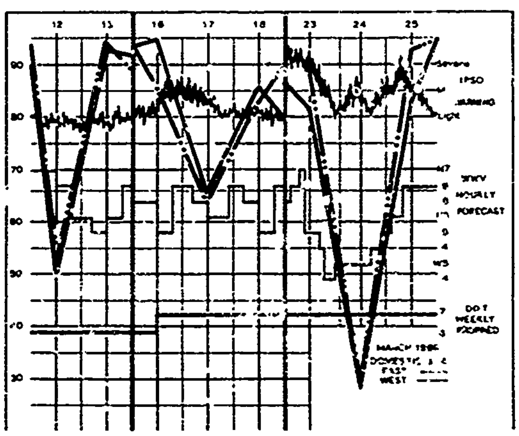

FIG 3B - DOMESTIC # 4

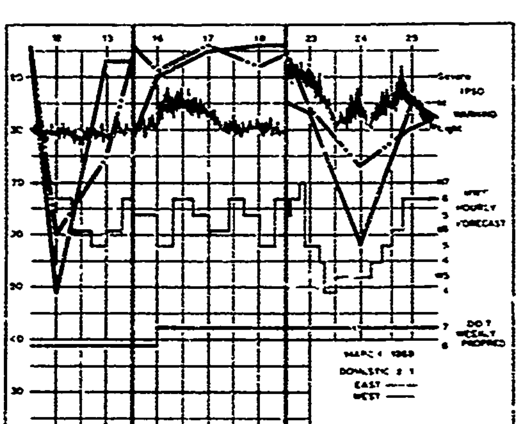

FIG 3C - DOMESTIC # 1

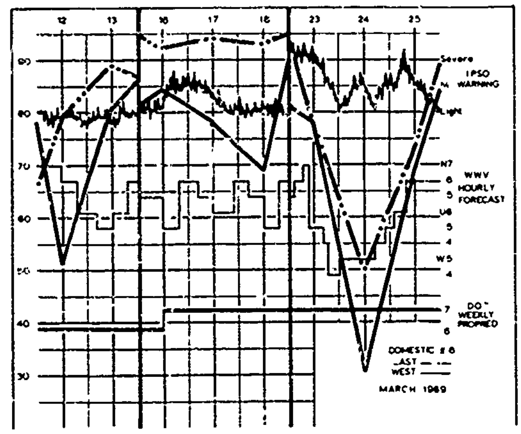

FIG 3D - DOMESTIC # 6

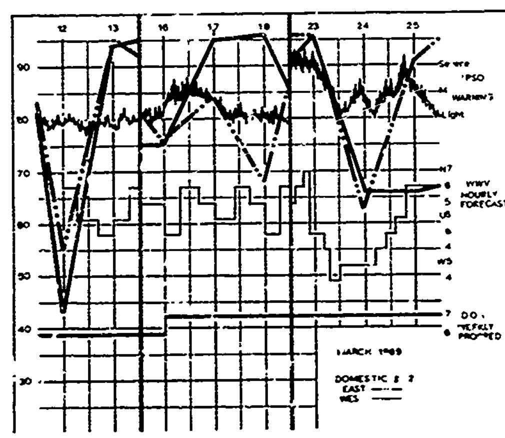

FIG 3E - DOMESTIC # 2

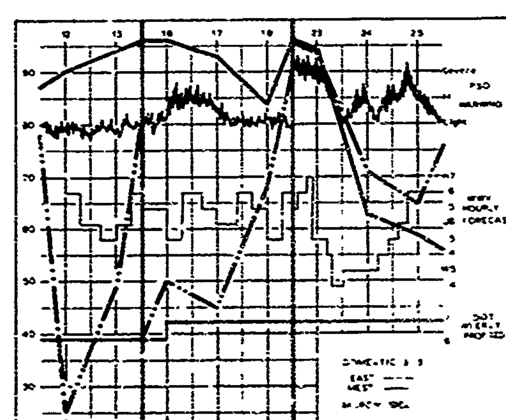

FIG 3F - DOMESTIC # 3

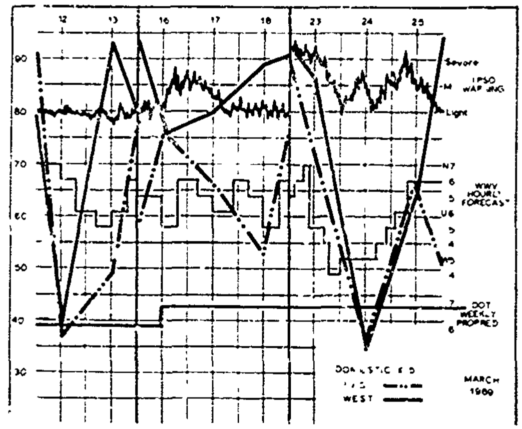

FIG 3G - DOMESTIC # 5

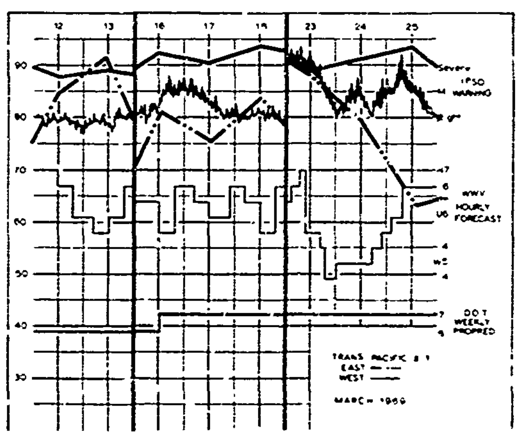

FIG 3H - TRANS-PACIFIC # 1

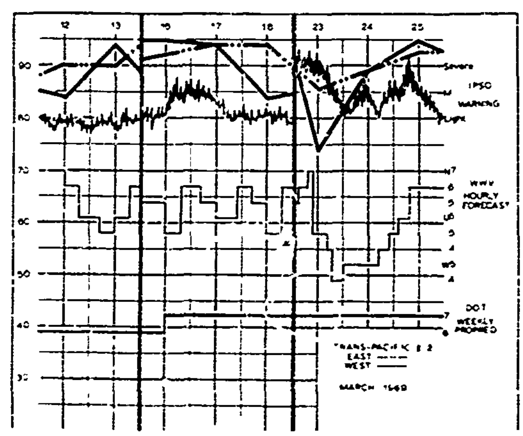

FIG 3J - TRANS-PACIFIC # 2

IPSO WARNINGS

1. IPSO WARNING NO. 11 280510Z FEB - Severe fadeout reported 271400Z associated with major flare near suns western edge. Active region is now about one day east of central meridian. Moderate to severe disturbance probable later to-day through Mar 1st following magnetic sudden commencement 0424Z. Probability of daylight fadeouts continues.

2. IPSO WARNING NO. 12 - Daylight fadeouts probable next few days but no indication yet of major magnetic disturbance. Minor fadeout reported 162336Z and slight magnetic disturbance in progress to-day (17 Mar).

3. IPSO WARNING NO. 13 MARCH 210205Z - Confirms severe fadeout 0147Z due to solar flare still in progress. Magnetic storm forecast will be sent when details are received.

4. IPSO WARNING NO. 14 MARCH 210620Z - Fadeouts ended about 0420Z. Moderate to severe magnetic storm expected Mar 22 -23. Very slight disturbance is in progress expected to continue in the meantime. Probability of daylight fadeouts continue.

5. IPSO WARNING NO. 15 232330Z MARCH - Confirms magnetic storm began suddenly 231825Z. Disturbance at present moderate but is expected to become severe later to-day and continue through 25 Mar. Major flare and fadeout occurred 211330Z with minor events 220644Z, 230200Z and 230500Z. Probability of daylight fadeout continues.

FIG 4

DISCUSSION OF OPERATIONAL FORECASTING PROBLEMS AND REQUIREMENTS OF THE CANADIAN FORCES AIR TRANSPORT COMMAND

By

R. P. Hypher

Defence Research Board, Air Transport Command Headquarters
Canadian Forces Base Trenton, Astra, Ontario

ABSTRACT

Long range communications carried out by either the Pilot or Radio Officer in Canadian military aircraft are demanding from a time point of view because of the competing requirements of Civil air control, weather forecasting and military command and control. Depending upon the area of operation, the reliability of HF communications will vary sufficiently to present a problem either in attempting to maintain flight safety or to meet the requirements of the military centralized control. Accurate forecasting on a reasonably short time basis would obviate the requirement for radio operators (and especially pilots) to waste much time in searching through the frequency spectrum. Problems of incompatibility also arise through the predicted best frequency and frequencies allocated by international agreement. This paper will discuss also some of the associated environmental problems that have arisen in Operational Research studies carried out at Air Transport Command.

DISCUSSION OF OPERATIONAL FORECASTING PROBLEMS AND REQUIREMENTS OF THE CANADIAN FORCES AIR TRANSPORT COMMAND

By

R. P. Hypher

Defence Research Board, Air Transport Command Headquarters
Canadian Forces Base Trenton, Astra, Ontario

Introduction

This paper is drawn from the results of an operational research attack on operational communications problems and therefore the data collected relates to the behaviour of a man-machine system, working in its normal environment. It differs widely from a laboratory-type experiment in that:

(a) no special instrumentation was used;
(b) careful control of variables was impossible; and,
(c) a rationale for all the variations in results was not attempted.

The conduct of the trials was, however, methodical and orderly even though we were looking for global answers to man-machine problems. The object in carrying out the studies was to answer in a limited time some specific operational questions. We were interested in studying command and control problems viewed from a wide spectrum of considerations: workload, timeliness, geographical location, mode of operation (i.e., voice versus CW), accuracy, pilot versus radio officer operated communications, ground handling times, relay effectiveness, etc. In order to answer these questions, we had to carry out comparative trials over given routes and under roughly similar conditions using radio officers and pilots, respectively. We have carried out data collection on some 200 transatlantic flights and some 21 global flights, altogether, covering two periods of four calendar months both totalling about 4,000 airframe flying hours.

The studies shed new light on many well-known problems, one of which was the effect of time wasted looking for a workable air-to-ground frequency. Therefore, emphasis will be placed on those items of interest that highlight this aspect of the problem. Certain background information needs to be described.

Profile of Air Transport Command Purposes

Because the military air transport fleet is not a civil airline, its raison d'être is to respond to military, quasi-military and civil emergencies. Because it may have to be used under militarily or politically fluid or disaster situations, there is a requirement for the centralized operational control body to have as reliable and fast communications as possible, air-ground-air, within the financial resources available. We do not have the resources to place powerful transmitters on all routes we might use, therefore we are forced to try and make the most efficient use of the few transmitter-receivers we have.

Equipment

Because the home of the Air Transport Command Headquarters (ATCHQ) is Trenton, we have a particular interest in the transmitter-and-receiver site located nearby so results will be given in this talk relating to this facility where applicable.

Within our aircraft we have in the case of the C-130 (Hercules), two 400-watt 618T SSB sets and in the CC-106 (Yukon), one 618T and one lower-power AM set type ARC 38; we also have VHF and UHF. The HF antennas on the Hercs are off-centre feed wires and on the Yukon the single fin-cap type. The presence of two transmitters does not mean necessarily that we have built in redundancy; we have in fact competing demands for communications which we shall discuss later.

Problems of Range

As you see, Canada is a long way from the areas in which her defence commitments lie, be they NATO or UN such as Cyprus and Kashmir, and even domestic such as the Arctic. This means in effect that whenever we consider the proper use of our long-range aircraft we are often speaking of distances of 5 000 km and greater. This means that for frequency prediction purposes we are, on any transatlantic flight, considering both single-hop and double-hop communications from whatever layer is at work in the ionosphere. For our Pacific, Australian, Indian, African and

TRANSMITTERS

Transmission	Quantity	Power (Watts)	Type	Use
SSB	3	10,000	RACAL	air-ground-air
	2	1,000	PALIK	weather and backup
	1	10,000	GPT 10	weather and backup
AM	5	500		backup
	3	4,000		

ANTENNAE

Quantity	Configuration
2	Discones (Omni-directional)
3	Fixed Log Periodic NE NW N
1	Rotatable Log Periodic
2	Nested Rhombics

Figure 1. Radio facilities at CFB Trenton

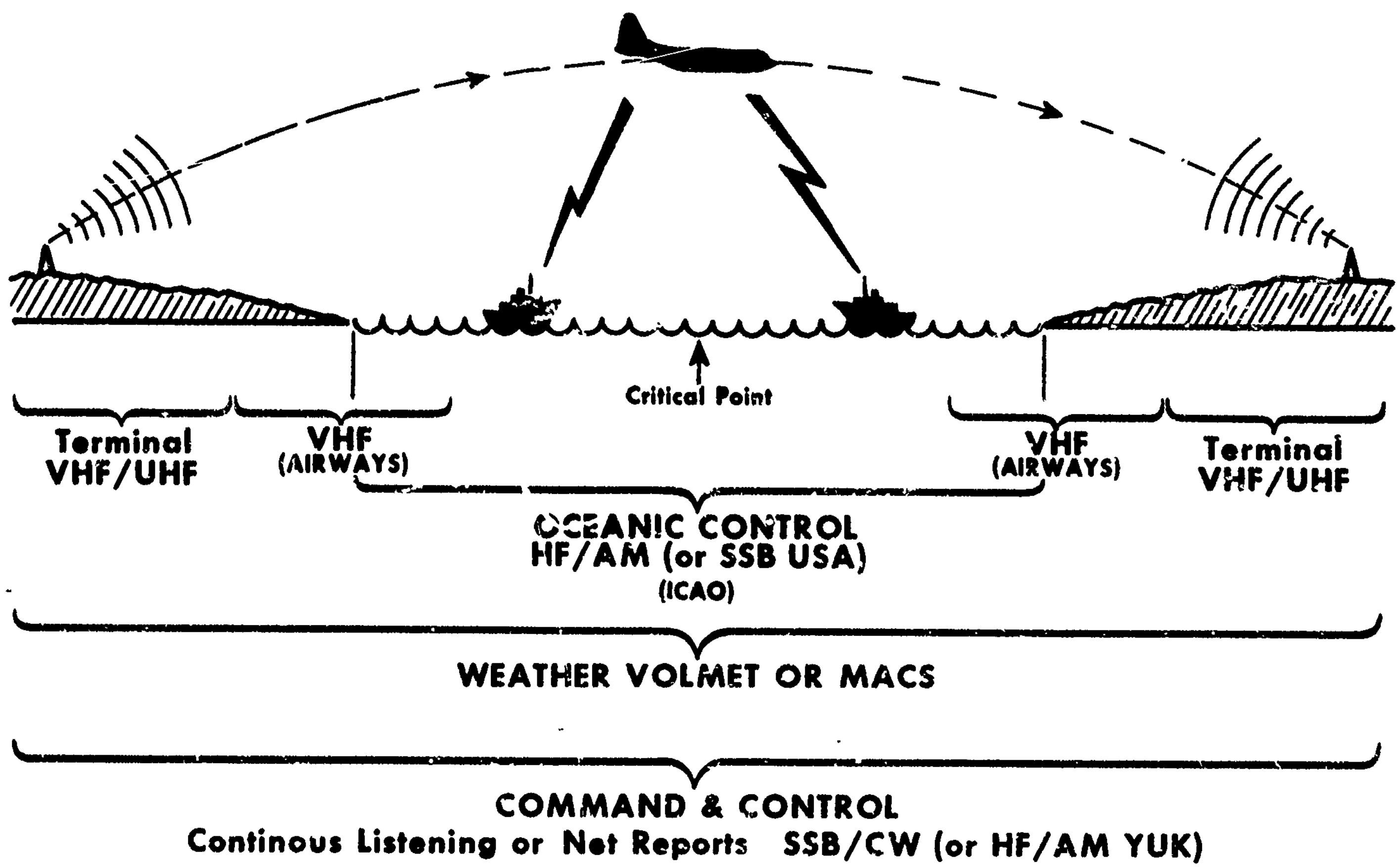

Figure 2. Schematic sketch of communications activity

South American flights we are, of course, speaking of multi-hop or high-angle wave communications.

A significant item to consider is that our problems relate to a moving platform in which those who draw up the frequency prediction tables or maps presumably consider not only the seasonal and diurnal frequency selection problems but the emergence and disappearance of reflection hops or control points as the platform approaches or recedes from the transmitter. Each reflection point is, of course, at a different time of day from the neighbouring one and, of course, the time of day on the moving platform bears little relationship to that at the first reflection point from the ground station except at commencement or termination of the trip. depending upon flight orientation east or west.

Communication Discipline

Because of the variability of reception when using HF, we have imposed on our crews a discipline and procedure in communicating which is intended to ensure (as best we can) in a practical way, that every effort is made to keep channels open with ATCHQ. We believe, in continuous monitoring by both the aircraft and the ground facility and also half hourly net reporting. Were HF more reliable, this would not be necessary; in fact there are many crews who would dearly love to have us relinquish our grip in this regard, however we are reluctant to do so for operational reasons.

Competitive Demands on Communication Time

The fact that a long-range transport aircraft is a moving radio platform under airways or oceanic control, means that continuous communications are also required between the civil control agency and the aircraft. This is a legal requirement for flight safety purposes. Over land this is usually VHF and over water HF, except for ocean weather ships which use VHF. In addition to this, there is an indispensable requirement for weather monitoring both behind the aircraft up to the critical point and ahead of it. Weather is broadcast regularly on HF voice and CW, at given times past the hour. Lastly, there is the requirement to monitor the VHF distress frequency. Because of the variety of requirements to communicate, the work of communicating even over long periods on ocean legs can be quite demanding of an operator's time. Some communications are scheduled, others relate to geographical position and others are random, hence the total communications scene demands both planning and close attention to timing.

Pilot-operated Communication

The problem of communication becomes more pressing when it is made the duty of pilots rather than radio officers because this is not their primary task. Although there are two pilots in the cockpit, the second pilot is obviously not there for the sole purpose of communication. Even though one pilot has control of the aircraft, the functions of the two pilots are interwoven from an airmanship point of view. (Excellent communications are a small consolation if a pilot fouls up the landing through inattention to airmanship!)

We have conducted a time study of two pilots on the transatlantic route Trenton to Lahr, South Germany, when it was made their task to tend to all communications. The results show that even under good conditions of weather, aircraft serviceability and communications condition, there is a tendency for one of the two pilots to become inordinately engrossed in communications planning and communications activity. Under conditions of poor weather, manual flying, noisy communications, the business of looking after communications and flying or co-operating in flying at the same time, can be extremely difficult and fatiguing, especially on slow turbo-prop aircraft which tend to fly through the weather and not above it.

As mentioned earlier, all the ATC aircraft are fitted with two HF transmitter-receivers. It can now be seen that with the continuous monitoring demands of ICAO and the military, plus periodic and frequent requirements to check weather on HF, two sets are normally a minimal requirement.

CW versus Voice

Regarding mode of communication, the trials showed that if voice was used until it was beginning to be unreadable, and then resort was made to CW, then traffic could often be read through the noise. We found, however, that the use of CW over voice was not a function of range from transmitter but more a function of communications condition. On transatlantic paths CW was resorted to 9 per cent of the time when voice failed. At times however, a radio officer will listen to CW weather broadcasts in preference to vice, if reception conditions are noisy. An interesting side is that when using the phonetic alphabet:

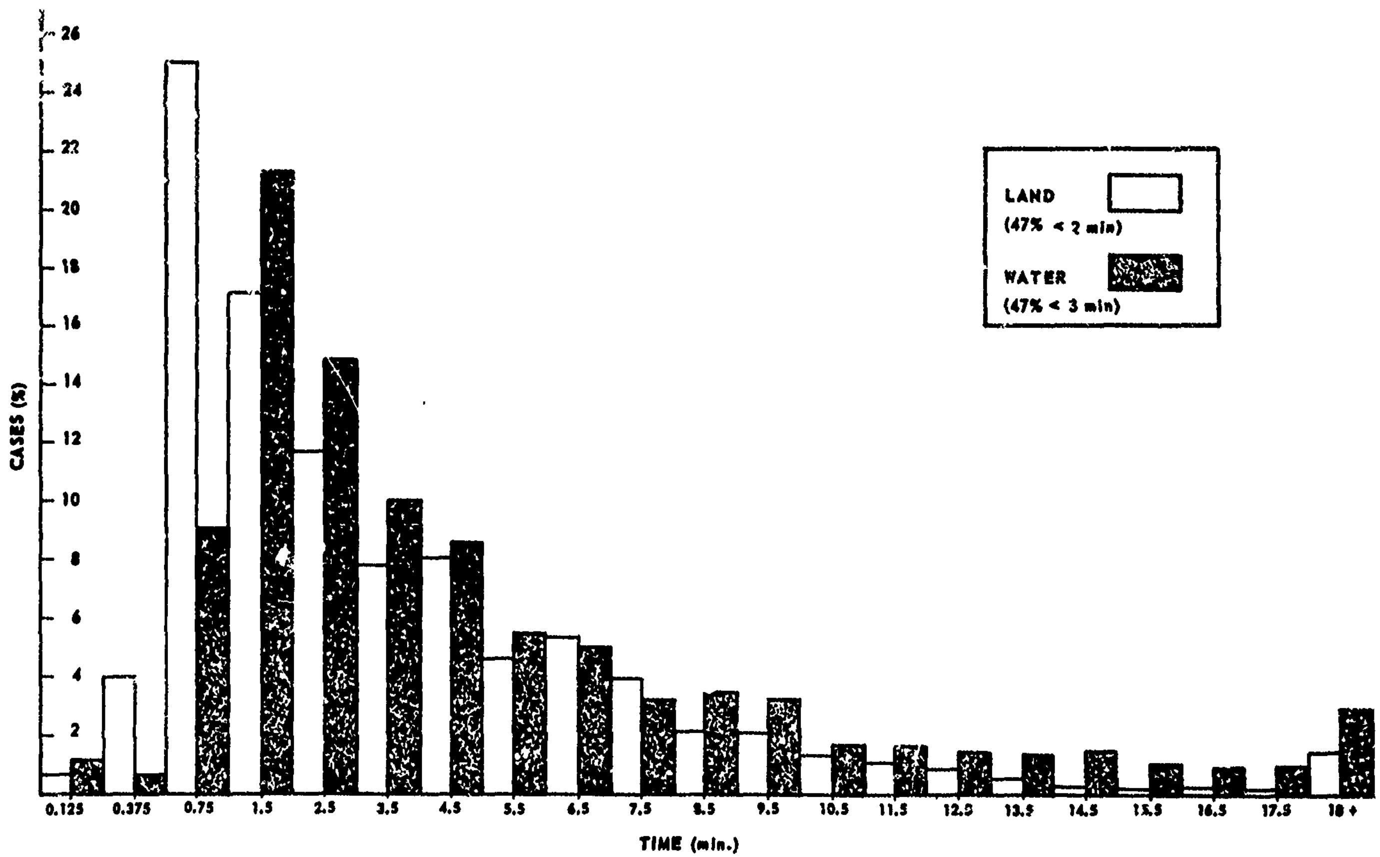

Figure 3. Distribution of listen-out periods over land and water. (Radio officers Yukon aircraft)

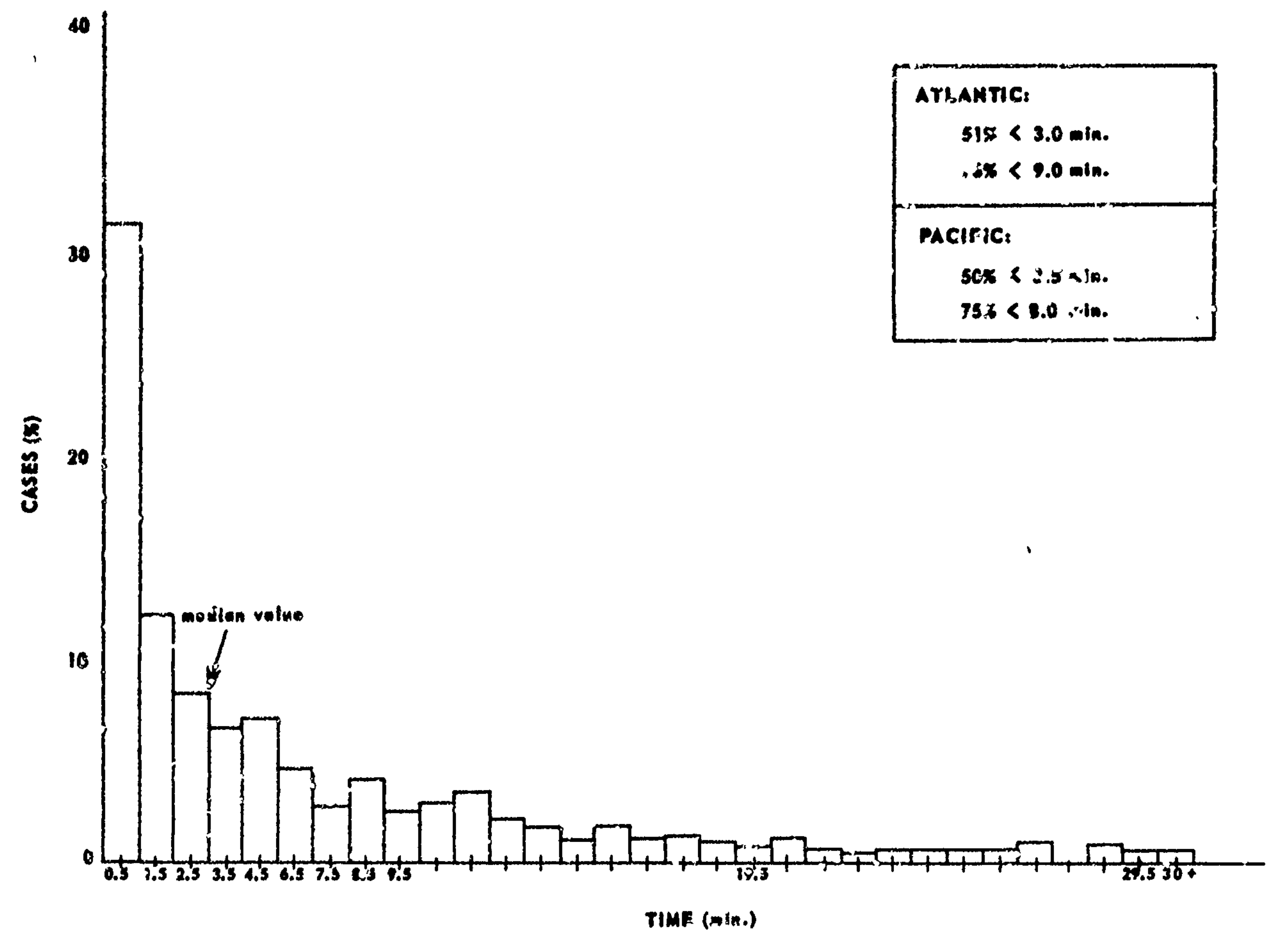

Figure 4. Distribution of workload periods where listen-out >4 minutes.
(Radio officers Yukon aircraft)

TYPE OF COMMUNICATION			%
1.	VHF / UHF	(Airways)	24
2.	MILITARY :	VOICE	24
		CW	7
3.	VOLMET	(Weather)	35
4.	HF ICAO	(Oceanic Control)	10
		Total	100

Figure 5. Per cent share of communications on transatlantic leg (approximation)

Area	CAPTAIN		FIRST OFFICER		Number of Pilots
	80% of interval less than	Median value	80% of interval less than	Median value	
Over Canada	3 min	1 min	2 min	30 sec	2
	1 min	40 sec			1
			30 sec	15 sec	1
Over Atlantic Ocean	6 min	1 min			1
			1.5 min	30 sec	1
Over Europe	1.5 min	20 sec			1
	1.3 min	30 sec	1 min	20 sec	2

Figure 6. Probability of obtaining intervals of a given length of time between pilot activities under good conditions (transatlantic route)

(a) the accuracy is approximately as high as CW; and,
(b) pilots are as accurate as radio officers.

This is quite contrary to expectations.

Variability of HF Communications

During the trials carried out last year, we found that if one measures the time attempting to communicate air-to-ground against the successful time communicating, it was in the following ratio: 0.37:1.0 on transatlantic legs. On Pacific and global flights it averaged at 0.50:1.0. In arriving at these figures we eliminated periods of severe communication black-out, therefore it is an operating figure. (It should be pointed out that most transmissions are short, 60 per cent are less than approximately 3 minutes). There is a certain problem involved in assessing the reliability of communications in this manner and that is the meaning of the words "attempt to communicate". Obviously this indicator could be invalid if an inordinate amount of time was spent on a useless frequency. Alternatively, if insufficient calling effort were made the readings would likewise be invalid. An enormous amount of common sense has to be employed in both attempting to communicate and defining it. Some attemps are met finally with success and others are not, some are met with success by speculative changing of frequency, and still further others are met with success on advisement by the receiving station that they are barely audible on that frequency and that they should change to another specified frequency. Clearly, professional communicators do not "flog a dead horse indefinitely", so if a call to a ground station produces no reply in reasonable time, the radio officer assumes it has not been heard and changes frequency. Occasionally the ground station is busy with another aircraft and cannot answer immediately or maybe it requires time to switch frequencies to reply. In Trenton we can monitor many more frequencies than any single communications operator can transmit on at any one time. Approximately one minute is needed to switch from a "receive" to "transmit" when frequency changes are made. We found that when pilots started carrying some of the HF communications load, they were switching so fast from one frequency to another that the ground operator could not keep up. Thus they were not as successful communicating as they should have been. Another measure of failure similar in nature to and drawn from the same sources as the time wasted trying to communicate, was occurrence frequency of trying to communicate versus the success frequency. This was similarly a variable from one operator to another but demonstrated a general trend. The results for analytical purposes had to be modified to take into account the difference between the number of times communications were desired compared to the number of times attemps were made to communicate. Latterly we have concentrated on measuring the success of communications by measuring the number of random messages sent to the aircraft against those received. It is interesting to note that both these rather crude empirical ways of approaching communications reliability, produce approximately the same results despite:

(a) the astronomical number of underlying variables; and,
(b) the fact that the trials were separated by one year.

In any event it is this type of measurement which is operationally meaningful. The problem then of measuring the reliability of communications from a man-machine point of view is not simple, but we believe we have made a first approximation. Because unreliability may be a function of impatience and fatigue, ("hope deferred maketh the heart sick") there is all the more reason why a busy operator, especially a pilot, requires some indication that ionospheric conditions are suitable for propagation.

Frequency Prediction Problems and Requirements

Now regarding the requirements and use of frequency prediction to improve our HF communications. It is believed we are up against very special problems in the long-range air-ground-air business. Because MUF and LUF frequency prediction is not synonymous with instantaneous sounding and a guaranteed workable channel, it has a limited use in its present form in the air-ground-air environment.

To obtain a certain perspective on this problem, let us review how radio officers operate.

(1) Experienced professional airborne communicators are cognisant of such items as diurnal variations in MUF and the general principles and problems of HF propagation.

(2) They are often in touch with the ground operator while communications conditions are changing or deteriorating and they both mutually experiment to keep in touch with one another.

	QUIET				NOISY
NOISE	0	1	2	3 4	5
					GOOD
READABILITY	ZERO	1	2	3 4	5
					GOOD
STRENGTH	ZERO	1	2	3 4	5

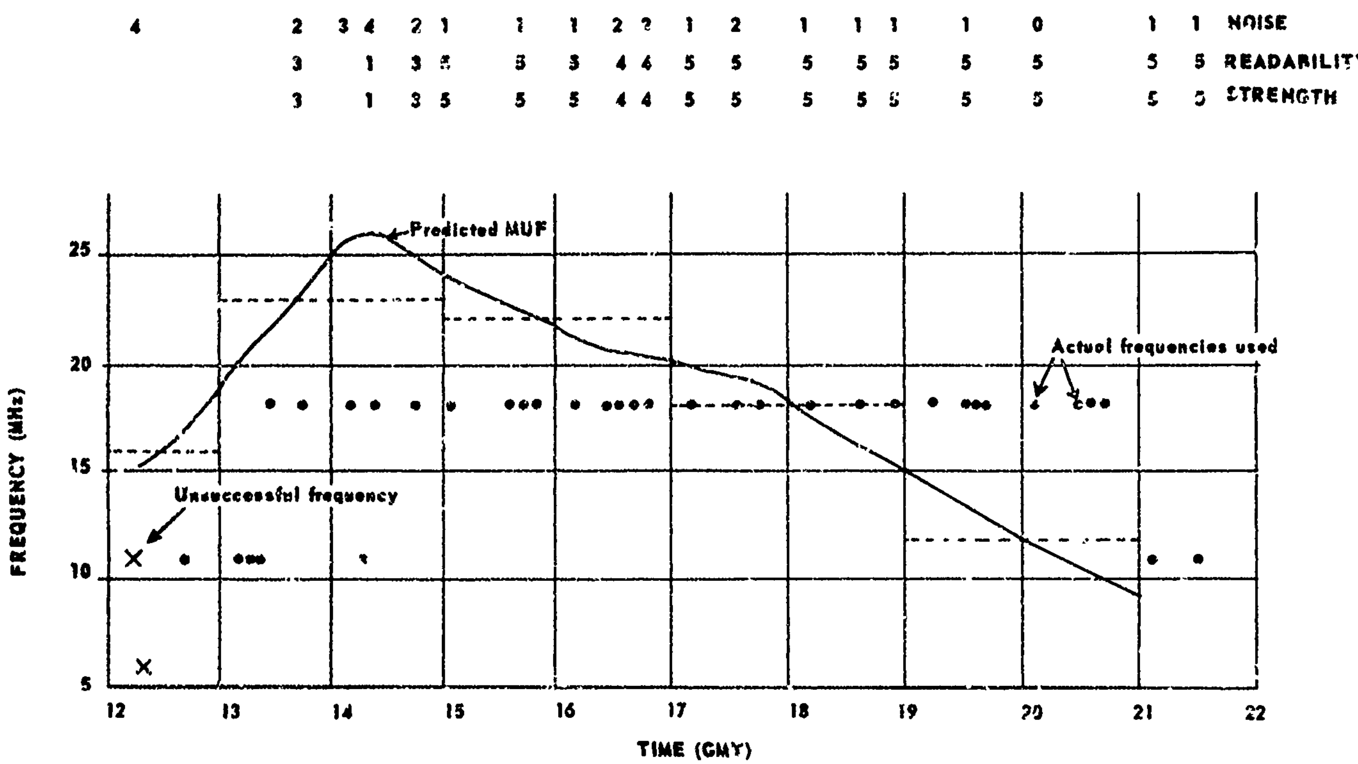

Figure 7. Sample of frequency used versus MUF predicted and communication conditions. East to west transatlantic (towards ground station)

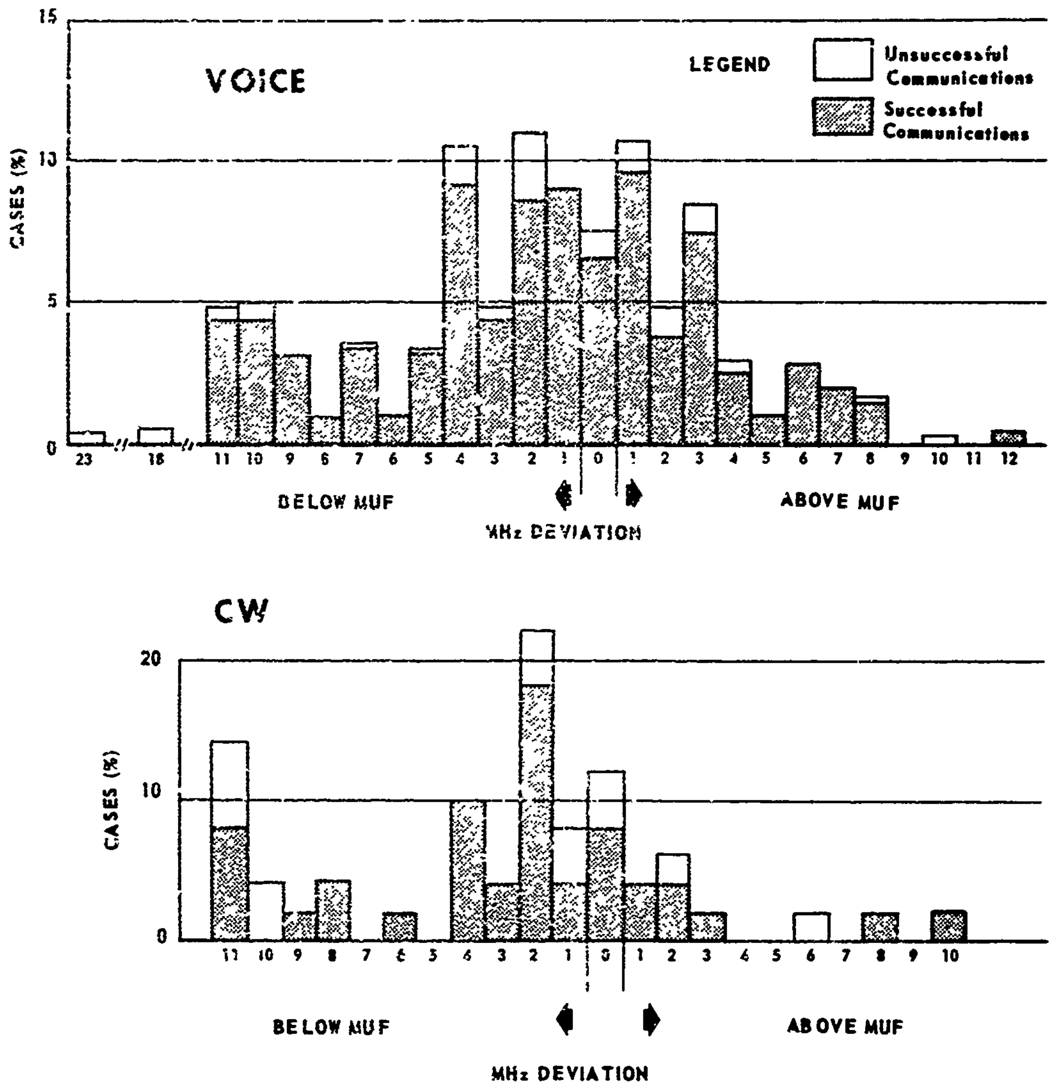

Figure 8. Successful and unsuccessful deviations from predicted MUF. (CFCS monthly prediction. Jan. 68).

(3) There are a limited number of frequencies that are assigned to the user and they can only select from among them.

(4) At best they will only refer to frequency prediction maps if available for the area they are in but are unlikely to go through a process working out an MUF if it involves overlays and nomograms. Working through the frequencies experimentally can be much quicker and more convincing.

It is no secret then, that radio officers are seldom seen consulting prediction charts even though frequency prediction tables are issued by our Canadian Forces Communications System (CFCS) based on monthly trend and relating to given transmitters and receivers. This is not a sign of disrespect so much as real time utility and it would appear that the variations in communications condition and usable frequency due to a host of local reasons, eclipse to some extent the data given in the tables which are based on monthly median or FOT values. What is really required we believe, is not a crude global estimate of MUF but something inexpensive of the variety of the Channel Evaluation and Calling (CHEC) system which permits one to know rapidly if a frequency is available in the first place and if so, what it is. Therefore, it would appear that much more research on ways to improve effectiveness and sensitivity of freqency prediction for long ranges and moving platforms is probably required. To illustrate my point, extracted data from radio officer logs show the use of HF frequencies in relation to those predicted.

Of course it must be remembered that during periods of heavy precipitation static and Polar Cap Absorption (PCA) all frequencies may be in difficulty. It must be added that frequency prediction tables remind one of weather forecasts in which the expectancy of heavy precipitation is said to be very low or "scattered" but the person who comes home from the annual picnic with his secretaries drenched is not going to display an enormous amount of faith in the person who said the probability was after all only 5 per cent.

In conclusion, then, the main requirement of frequency prediction for Air Transport Command is one in which we are looking for a means of reading directly:

(a) if a frequency exists; and,
(b) what it is.

Any system therefore that leaves the chore of trial and error to the operator, especially a pilot, is no better than what exists already.

A secondary but obvious deficiency about which little can be done, is the requirement for and ability to use higher frequencies.

Bibliography

1. Anon. Handbook for CRPL Ionospheric Predictions, U.S. Dep. Comm. Handbook 90, 1962.

2. Anon. Frequency Predictions (Trenton), CFCSHQ, 1968.

3. Anon. Ionospheric Predictions, U.S. Dep. Com. TO 11-499-70/TO 31-3-28-2, 1969.

4. Anon. Solar-geophysical Data. Descriptive text. U.S. Dep. Comm., Feb. 1969.

5. Anon. Solar-geophysical Data. Descriptive text. U.S. Dep. Comm. IER-FB-294 (Supplement) Feb. 1969.

6. Davies, K., Ionospheric Radio Propagation. U.S. Dep. Comm. 1965.

7. Davies, K., Magneto-ionic Theory of Radio Propagation. AGARD. Lecture series XXIX. I:1-91. 1968.

8. Deminger, W., Ionospheric Propagation of High-Frequency Radio Wave. AGARD. Lecture series XXIX. III:1-83. 1968.

COMMENTS ON THE NATURE OF HF IONOSPHERIC PREDICTIONS REQUIRED FOR USE IN THE DCA AND THE DCS

by

Samuel E. Probst
Chief, Radio Frequencies Branch,
Defense Communications Agency,
Washington, D. C. 20305

COMMENTS ON THE NATURE OF HF IONOSPHERIC PREDICTIONS REQUIRED FOR USE IN THE DCA AND THE DCS

BY
SAMUEL E. PROBST*

I am the Chief of the Radio Frequencies Branch in the Defense Communications Agency and a member of the Joint Frequency Panel of the U. S. Military Communications-Electronics Board and, in that capacity, I become directly involved in the frequency allocation and assignment process. I am not actually a user of the radio frequency spectrum, although, at meetings of this type, I tend generally to be categorized with the users. A few of the problems with which my office is regularly faced would be of interest to you and I would like to briefly outline a few of them now. The Defence Communications System (DCS), which is managed by the Defense Communications Agency (DCA), includes the largest high frequency (HF) radio network in the world. Almost all of the individual HF radio paths in the DCS operate on a bandwidth of 12 kHz and each transmission consists of four nominal voice channels of 3 kHz each. Typically, at least one of these 3 kHz voice channels will contain 16 channels of derived teletype. The other three channels will normally carry voice modulation or, possibly, one of these voice channels may be carrying a digital data stream.

The radio frequencies assigned to support these HF radio paths are obtained from the internationally allocated fixed bands. These fixed bands, as has been noted by previous speakers, are highly congested and, to an extent, disorganized. Experience has shown that it is very rarely atmospheric noise or local noise at the receiving site which limits the performance of our HF radio paths. On the contrary, it is almost always interfering signals on the assigned frequencies that limit the system performance. The assigned frequencies on the DCS HF radio paths constitute, within the U. S. Military, almost the total resource of relatively broadband, in terms of HF, frequency assignments. In each case where our operations are conducted on foreign soil, we have, of course, negotiated with each host country for the right to use these radio frequencies.

Within the U. S. Military, we are frequently faced with temporary requirements for operations which require the use of 12 kHz bandwidth frequencies. I shall note three examples.

The U. S. Strike Command, with headquarters in Florida, is responsible for any possible military activities in which the U. S. might become engaged at some future date in the Middle East, Africa south of the Sahara, and possibly in support of other major U. S. theater commanders. The Strike Command has at its disposal, some transportable communications capability which must be periodically exercised for purposes of personnel training and equipment checkout. It is the nature of the high frequency spectrum today that successful operation of long haul HF radio paths can only be effected by using frequencies which are in essentially continuous daily use at high power. The only such frequency resource available to the U. S. Military is that contained in those frequencies assigned to the radio paths of the DCS. When it is necessary to support these Strike exercises, my office is called upon to make frequencies from the DCS resource available for use in supporting the exercises. When supporting exercises of this nature, the frequencies are authorized for use in a manner that will not interfere with their normal use on the DCS radio paths to which they are assigned. For planning frequency support for exercises of this type, my office requires the ready availability of typical MUF-LUF type predictions. These predictions are used in selecting the frequencies which can be made available for exercise use without interfering with their normal assigned use.

There are other requirements which are even more difficult to support, however, because, due to their importance, they must have frequency resources made available on a primary rather than on a secondary basis. One example of this type of requirement is the military communications support provided to the Apollo program. Communications from land bases to the Apollo Range Instrumented Ships and the Apollo recovery forces are critical in nature and require high reliability. While these communications have been partially effected, and in the future will be primarily effected, through communications satellites, HF radio is still used and will continue to be used at least in a backup role. During Apollo missions, the frequencies made available to support these communications are given to Apollo on a primary basis and their use is denied to the HF radio paths of the DCS to which they are normally assigned. This effectively removes a significant part of the frequency resource available to the DCS. For obvious reasons, the selection of the frequencies to be made available for Apollo support must be done with great care if the remaining reliability of the DCS HF radio paths is to be preserved at reasonable levels. These DCS radio paths are also carrying, particularly across the Pacific, communications of critical importance to the U. S. Military. Again, my office requires detailed and accurate HF radio MUF-LUF predictions to aid in selecting the frequencies to be made available.

One further example can also be noted. The Defense Communications System does not include tactical communications and, in general, the DCA is not normally involved in supporting air-ground communications. The DCS is, however, responsible for providing all of the communications from the Commander-in-Chief through the Joint Chiefs of Staff down to the major Unified and Specified Commanders and their major subordinate commanders in the field. The Commander-in-Chief of the U. S. Armed Forces is, as you know, the President. The President travels rather frequently, and when he does so, communications

must be maintained with him at all times. Communications with the Presidential aircraft while in flight must be of the highest possible reliability. Here again, frequencies normally assigned to HF paths of the DCS are made available during the periods when the President is airborne and during certain periods when the Presidential aircraft is on the ground at locations outside the U. S. Again, when used for Presidential communications support, the frequency resources involved are denied to the DCS radio paths to which they are normally assigned. The most accurate possible MUF-LUF predictions are necessary for use in planning for this communications support. Naturally, the problem of providing both Presidential and Apollo support communications requirements are compounded when the President elects to be present aboard the prime Apollo recovery ship as happened on the Apollo 11 mission.

In addition to the special frequency support for exercises and operational requirements noted above, my office must also plan for frequencies required in the evolutionary development of the DCS. This involves both the periodic deactivation of existing facilities and the provision of frequency resources to support newly activated radio paths. Although HF radio is assuming a relatively less significant role in the DCS than it had a few years ago, and the number of HF facilities is being reduced as greater reliance is placed on satellites and broadband systems, including tropospheric scatter and underseas cables, a minimum essential HF network will be retained to provide the minimum necessary residual command and control communications to be relied upon in any eventuality. Also, transportable HF communications facilities will be retained and new ones may be procured to provide the capability to rapidly restore essential elements of the system. In the process of planning for the exercises and operations described above as well as in planning for the evolutionary development of the DCS, typical predictions of the MUF-LUF type are routinely utilized. These predictions are produced both for specific months and for the extremes of seasonal and solar cycle variations. For this purpose, my office utilizes the ITS 68 program at the present time and we are now in the process of converting to the ITS 69 program in our computer.

In addition to the MUF-LUF predictions, computer outputs listing the angles of arrival of the predominant modes and the reliability of the various modes are utilized to help in the design and selection of the appropriate antennas and to analyze failures of performance on some of the paths of the DCS. The predictions produced in our office are utilized in our office or are provided to system planners in the military departments responsible for operating the various portions of the DCS. Routine predictions of the MUF and the LUF for use by the operators in the DCS are produced by the Department of the Army Strategic Communications Command at Fort Huachuca, Arizona.

For maximum efficiency of system operation, a communications network such as the DCS, which is managed on a system basis, requires real time measurement and evaluation of system capability and automated or semiautomated control of the frequency selection process. Such a system has been researched, developed, and tested for the DCA by the Stanford Research Institute. This system, known as the Common User Radio Transmission Sounding (CURTS) System has been thoroughly proved and is capable of achieving higher reliability from an integrated HF communications network. Economic factors, however, have prevented the implementation of the CURTS System.

Lacking such an automated system, there are two levels of short term forecast information which are required. The system controller located at regional or area control centers requires a short term forecast which tells him which of the radio paths in the portion of the system he controls are going to be reliable and which are going to fail during the next forecast period. If this information were ideally available, it would be all the system controller would really need to know to enable him to control the routing and rerouting of traffic and the restoral of allocated circuits through the system. The operator on each radio trunk, on the other hand, really needs a forecast that will tell him whether or not communications can be maintained on his radio path during the next forecast period and, if so, on which of his assigned and available operating frequencies the maximum reliability can be obtained. Even if the CURTS System could be fully implemented, there would still be a requirement for short term forecasts. The computer logic which would control the utilization in real time of the frequency resource in the system would need to be modified during periods of propagation disturbance. It is not my intent to describe the CURTS System at this meeting as it has been extensively reported on before. For those who may be interested, I would refer you to the proceedings of the AGARD EPC Meeting at Finse, Norway, April 13-19, 1967 or you could write to me for a list of references to the CURTS reports.

In summary, we find a need for three different levels of future information on the phenomena of HF radio wave propagation within the DCS. Predictions of the type produced by the ITS 69 program for use in system planning and analysis of system performance and for use in the administrative management of the available HF frequency resource will continue to be required. Short term forecasts of propagation disturbances are required at two separate levels within the DCS. Predictions for the radio system operators should be designed to provide an indication of whether or not an individual radio path will support communications during the next forecast period and, if so, on which of its assigned complement of available frequencies. Forecasts for use by regional or area system controllers should provide an indication of which radio paths within the portion of the system controlled can be relied upon to provide reliable communications during the next forecast period.

One other level of information is required within the DCA but this is neither forecast nor prediction. To aid in post analysis and in daily staff briefings which attempt to explain system performance on the previous day or days, information on the extent and severity of observed propagation disturbances is required. This latter need is currently being satisfied quite nicely be the availability in our office of one of the remote teletype terminals (such as was displayed here on the table) by means of which we can telephone the computer at Boulder, Colorado and obtain summary information on observed disturbances.

* Chief, Radio Frequencies Branch, Defense Communications Agency, Washington, D. C. 20305

SHORT-TERM FORECASTING IN GERMANY

by

B. Beckmann

SUMMARY

Short term forecasting began in Germany around 1940 simultaneously at the Proving Ground (Department F) of the German Air Force at Rechlin (about 150 km North of Berlin) and at the Research Institute of the Deutsche Reichspost (Department Wave Propagation) at Munich. Later in 1942 an independent board was separated from the first mentioned Department F at Rechlin with the name "Zentralstelle für Funkberatung" at Bad Vöslau near Vienna. After 1945 this organization was one of the main bases of the later Max-Planck-Institute for Ionospheric Physics (Lindau/Harz). The main task of this institute was ionospheric research. Therefore the regular preparation of forecasts was discontinued. A smaller part of the "Zentralstelle für Funkberatung" was separated after 1945 and, in cooperation with the French Forces, organized the Service de Prévisions Ionosphérique Militaire (SPIM). The group of the German P.T.T. was reorganized within the Fernmeldetechnisches Zentralamt (FTZ) at Darmstadt and resumed its prediction and forecasting work in 1950.

Short-term Forecasting in Germany

by

B. Beckmann*)

Research Institute of the Fernmeldetechnisches Zentralamt

At the request of the Programme Committee I shall give you a report on the history of forecasting in Germany from the early 1940's to the present. At that time, there were two agencies in Germany which were concerned with short-term forecasting, namely Department F of the German Air Force Test Centre at Rechlin (150 km north of Berlin) and the Amt für Wellenausbreitung (Wave Propagation Department) of the Research Institute of the Deutsche Reichspost at München.

I. Radio Propagation Advisory Centre (1940-1945) [1]

To begin with, I would like to give you a survey of the work performed by Department F, which was in 1942 re-named "Zentralstelle für Funkberatung" (Radio Propagation Advisory Centre) and was working at Bad Vöslau near Vienna under the direction of Professor Dieminger, who has been so kind as to let me have some information for this report.

The knowledge of the propagation phenomena and the continuous observation of the ionosphere enabled the Radio Propagation Advisory Centre at Rechlin to issue advice on radio propagation matters to the military agencies. The latter requested the indication of a reliable frequency range to be used at a certain distance and time of the day. Now I would like to say some words about the normal conditions, because they are the basis for the prediction of disturbances. Since the critical frequencies of the F2 layer vary from day to day, it was necessary to consider the most unfavourable possibility for each time of day. Curves were determined therefrom by excluding considerably disturbed days. They were converted to the specific distance in the classical manner. Moreover, the normal E layer entered the calculation, the result of which was used to plot the so-called "blanketing curve". The upper envelope of the two critical frequency curves indicates the highest most reliable frequency. The well-known theory used at that time was applied to determine the lower absorption limit from the maximum decrement given by the equipment characteristics. The standard value required for this purpose, which furnishes mainly data on the ionization of the D layer, was taken from field strength measurements of the preceding two weeks. Thus, a lower usable absorption frequency limit which might have to be replaced by blanketing was obtained for every propagation mechanism.

As far as the regular two-weekly general advices with indications of usable frequency ranges for various distances and times of the day were concerned, this method was applied to all distances in question. These advices were distributed over the military communications network. Furthermore, d.f. warnings were issued the same way, i.e. the period was indicated during which the night effect was to be expected. In special cases individual advice was given, even with regard to the choice of the equipment.

In cases of disturbances the Radio Propagation Advisory Centre informed or warned the Armed Forces, if possible. A drop of field strength, the Mögel-Dellinger effect today known as sudden wave fade-out, allows only subsequent information to be given since it is not possible to forecast this effect with sufficient reliability. The time of occurrence could only be estimated by the 27-day recurrence tendency. It was not expected, but hoped nevertheless that a prediction of flares and consequently of the Mögel-Dellinger effects might be achieved by means of solar physics. The time during which a radio circuit faded-out was subsequently announced by the Radio Propagation Advisory Centre. These announcements were made in order to explain the fade-outs and to prevent unnecessary attempts to service the equipment.

There are better possibilities for the prediction of ionospheric storms which cause the worst disturbances of the radio traffic. It was well-known that ionospheric storms are caused by a corpuscular stream which needs about 20 to 30 hours to reach the earth from the sun and that the optimum observation of its start on the sun would allow a forecast for approximately 1 day in advance. Now, events had become known where about 24 hours later an ionospheric storm was caused by the corpuscles emitted by the sun simultaneously with a chromospheric eruption which in turn gave

*) Chief of Research Group D 33 "Ionosphere"

rise to a Mögel-Dellinger effect. However, these events were not so regular that they could be used as a basis for a forecast. Similar considerations applied to all other solar phenomena which had as yet been investigated in conjunction with disturbances of the ionosphere. It was thought that the fact that there are statistical relations is not sufficient for a forecast, where it is the individual case which matters. Even the 27-day recurrence tendency did not seem to be so clear that it alone could substantially contribute to the solution of the problem. An investigation performed by Bartels in 1943/1944 at the request of the Radio Propagation Advisory Centre was only successful in the case of weaker disturbances.

The several hours lead of the magnetic disturbances was considered as the best basis for forecasting disturbances. Here, the period available for forecasting is very short and it requires a smooth organisation in order that the radio warnings are issued so early as to reach the interested parties in good time. Experience gained during the war showed, however, that it is possible and that the benefits of such an arrangement are considerable. But some difficulties are even encountered in the case of forecasts based on magnetic phenomena. Although there are very clear correlations when comparing the development of the events at a later date, it is difficult if the further development of a magnetic disturbance shall be concluded fairly reliably from its initial stage. In this connection the fact that a rather active sunspot passes the central meridian at the same time or that there was a Mögel-Dellinger effect on the preceding day can be a valuable hint. During the war more than 70% of all warnings proved to be correct, this was partly to be attributed to the sure instinct and the great experience of the observers. The success achieved in the higher northern latitude was very good, the probability of making a lucky guess was even higher. In these regions the conditions are more favourable in so far as the greater number of disturbances allows more experience to be gathered and the development in time of the individual disturbances is very similar. In the auroral zone the corpuscles arrive between 2100 and 0200 h. In case of a simultaneous magnetic activity disturbed conditons must be expected in the second half of the night and the next morning. If the magnetic field remains quiet during this critical time, there will probably be normal conditions during the next day.

Bartels was of the opinion that these experiences are only true for moderate disturbances restricted to the auroral zone. As for more severe disturbances, Berkner indicated already in 1939 that they begin at the same time both in magnetic and ionospheric measurements.

The problem of occurrence of the sporadic E layer was studied. It is not considered possible to forecast it in the individual case, since its occurrence can only be predicted statistically. Harang stated that in the case of the Es ionization in the higher northern latitude, which is correlated with the geomagnetic activity, the geomagnetic disturbance and the Es begin at the same time. However, the opinion was held that, with the exception of the auroral zone, the forecast of Es was not so essential for normal radio traffic, because, apart from a possible blanketing, a deterioration of the propagation conditions by Es was generally not observed.

In the case of a magnetic storm a warning was given over the military communications network. This warning was issued as soon as a considerable deterioration of the propagation conditions could be ascertained or could be foreseen for the near future. Hence, the warning was given at short notice, possibly soon after the beginning of the disturbance. In very favourable cases solar observations, for instance the observation of the quick development of spots, enabled the forecasters to indicate the disturbance with a certain degree of probability. Admittedly, the cases were but rare, where the solar event causing the disturbance could be ascertained. As a rule one had to wait until the beginning of the magnetic storm indicated the beginning of the disturbance. Then a drop of the critical frequency was expected mainly during the following night. If the storm began during the day, it was possible to issue a warning for the night, i.e. some hours in advance. If it began during the night, the warning could only be issued at the beginning of the ionospheric disturbance. In the case of longer disturbances it was always worth-while.

The radio propagation monitoring station of the Radio Propagation Advisory Centre was equipped with the following:

1. Sweep-frequency ionosonde for the determination of the critical frequencies.

2. Magnetic field balance to measure the variations of the earth's field. The results of these measurements were used to obtain indices characterizing the disturbances.

3. Field strength measuring equipment and direction finders.

Observations were carried out continuously. The current knowledge of the ionospheric condition allowed warnings to be issued in the case of disturbances; moreover, field strength measurements were made in order to determine the absorption as well as deviations from the great circle bearings.

A special radio network available to the radio propagation monitoring station was also used to make radio tests and to check the advices. In addition oblique-angle pulse measurements with remote synchronization were performed on some paths in order to determine the propagation modes, etc. Every day all results of the measurements were passed on to the control centre at Voeslau. Special advisory centres were established in Norway and Finland, because the conditions existing in these regions were particularly difficult and departed from those prevailing in Central Europe.

The following scale was used to characterize the ionospheric conditions in the higher northern latitudes:

1. calm = normal conditions
2. moderate = foF2 below normal, but transmission possible via aurora - Es layer
3. disturbed = black-out

In the third case (black-out) absorption prevented the changing-over to lower frequencies as was done successfully in medium latitudes. In consideration of the changing conditions a very close co-operation of the radio stations and the ionospheric stations in the higher northern latitudes proved to be very successful. It was possible to increase the reliability of the radio traffic from 40% to 75%. The introduction of a special "advice for the aeronautical radio service" which was called for immediately before the start in the same way as the "meteorological route forecast" and which indicated the present ionospheric conditions and their anticipated development within the next few hours had turned out very well.

At the end of the war in 1945 the Radio Propagation Advisory Centre discontinued its work. After 1945 most of its staff joined the Max Planck Institut für Ionosphärenforschung at Lindau (Harz), which was only concerned with ionospheric research and did not take up the preparation of forecasts. Some of the members of the Radio Propagation Advisory Centre left and together with the French Armed Forces they established the Service des Prévisions Ionosphériques Militaire (SPIM).

II. Wave Propagation Department (1940-1945) [2]

Like the Radio Propagation Advisory Centre, the Wave Propagation Department was concerned with short-term forecasts. Thorough investigations into radio propagation phenomena were carried out by the Reichspostzentralamt (Reichspost Engineering Centre) and the Reichspost Forschungsanstalt (Reichspost Research Institute) for the world-wide commercial radio service as well as for broadcasting and other services under the care of the Deutsche Reichspost. In 1937 part of the Radio Department of the Institut für Schwingungsforschung (= Institute for the Study of Oscillations) was merged in the Deutsche Reichspost. On this occasion observation material dating back to 1932 became available to the Deutsche Reichspost. On 1 July, 1940 the department of the Reichspostzentralamt, which was responsible for investigations into radio propagation conditions, moved from Berlin to München. Dr. F. Vilbig was in charge of this department, the new designation of which was "Amt für Wellenausbreitung" (Wave Propagation Department). Based on the knowledge of the propagation phenomena gained in studies performed over many years and on the continuous observations of the ionospheric conditons the normal conditions were determined once a month and compared with the superimposed disturbances. Four ionospheric stations were set up approximately at the 11th meridian between $\sim 55^{\circ}$ and $\sim 42^{\circ}$ N. They operated on nearly the same fixed frequencies - which varied according to the season - with a pulse power of about 10 kW. The results of the measurements made on this network showed the dependence on latitude of the behaviour of the ionosphere under normal conditions and in the case of disturbances. Field strength measurements carried out at the same time indicated the attenuation behaviour of the ionosphere resulting from the D/E layer absorption near the LUF and from scatter losses and deviative absorption at higher frequencies near the F-MUF. Sweep-frequency measurements performed by the station at Herzogstand were made available by Zentralstelle für Ionosphärenforschung (Ionospheric Research Centre). Later on similar data were obtained from the Grafing station of the Wave Propagation Department. Moreover, field strength recordings of the operating frequencies carried out by the Deutsche Reichspost since 1928 were evaluated. Empirical conversion factors (M factors) were found by comparing the latter results with vertical soundings. Partly these factors were considerably higher than those derived theoretically from the ionograms and showed a dependence on power. They were evaluated for forecasting the times the operating frequencies could be used

during a month. In this connection the influence of the LUF was allowed for by the classical computation of the non-deviative absorption. The radio stations of the Deutsche Reichspost, the broadcast HF stations and other civil radio services were advised by telex, by telephone and in monthly discussions. There was also a close co-operation with the Radio Propagation Advisory Centre, for instance the supply of propagation data, of field strength measurement results, discussions, meetings, etc.

The short-term forecasts of disturbances, issued by the Wave Propagation Department, whenever required, i.e. in the case of forthcoming or existing disturbances, were made with following objective in mind: When working in the HF range it was, of course, not possible to avoid disturbances of the radio service, which were sometimes rather severe. However, the early recognition of the occurrence of a disturbance was of great importance, because the traffic could then be so handled as to allow for the forthcoming disturbance. If longer, serious disturbances were to be expected, a change-over to the LF transmitter could be made in good time. However, in the case of a minor disturbance, urgent telegrams could be transmitted before or one could wait until the disturbance was over. Hence, it was desirable to know the beginning of a disturbance and its probable duration. In brief, the importance of the so-called "radio weather" to the radio services was similar to that of the meteorological conditions to aviation, etc.

In order to be able to issue short-term forecasts the measuring station of the Wave Propagation Department at Bernried near München observed the propagation conditions all the day round. The station was equipped with the following:

1. Equipment for field strength measurements and recordings in the HF, MF and LF bands.

2. A pulse transmitter with manually tunable frequency for vertical soundings.

3. Frequency spectrum recorder.

4. Magnetic field balance for the vertical component.

As far as observed geomagnetic activities were concerned, there applied the same as was outlined in connection with the Radio Propagation Advisory Centre. The records taken by the Erdmagnetisches Observatorium (Geomagnetic Observatory) at Potsdam were also available for the subsequent evaluation of the magnetic activity. The current propagation observations furnished information about positive phases and disturbances, which formed the basis for estimating the development of the propagation conditions during one solar rotation and allowed corrections to be made at short notice, provided the tendency of the results of the observations carried out simultaneously in different directions and on several frequencies indicated the development earlier than it was noticed by the radio services. If the disturbances did not begin suddenly with a high intensity, there was a time difference of some hours according to the direction of propagation. Moreover, in the case of long waves an increase in the noon value of the field strength was sometimes observed 2 to 3 days before a disturbance. In some cases one could also observe a decrease of the night value, but here the time until the beginning of the disturbance was shorter. When the pulse transmitter was used for observation purposes, attention was also paid to the height of the F layer which decreases shortly before the disturbance and increases again with the beginning of the disturbance.

In addition, the results of photospheric solar observations and of measurements of the weak component of the cosmic rays were evaluated Unlike today, at that time there was no solar observatory in Germany equipped with a spectro-helioscope or being able to use it for the continuous observation of the sun. The performance of the solar observation depended very much on the weather, i.e. there were times where bad sight prevented the observation of the sun. Attempts were made to compensate to a certain degree for these deficiencies by making additional records of the weak component of the cosmic rays. These ideas were expressed by J. Zirkler, who had observed that the increases in radiation exceeding the statistical variations recurred with the multiple of the solar rotation. In some cases, a geomagnetic disturbance with secondary ionospheric phenomena took place during the next day. So far as statistics could be prepared with the data then available, there seemed to be an accumulation of these effects three to four days prior to the beginning of the disturbance. However, they were even experienced during calm periods. Zirkler was of the opinion that these effects were due to the weak component of the cosmic rays and that this component was emitted from the sun. According to

literature available at that time, it could also be modulation effects of the general galactic radiation caused by solar influences. Special attention was paid to the ring-current effect (Forbush effect). There were also changes in the diurnal variations. Today, both possibilities, i.e. solar radiation components and modulation effects in the diurnal variations, have been proved. In order to be able to measure as weak radiation components as possible use was made of a bottom-shielded ionization chamber proposed by Zirkler. However, radioactive influences were also possible. All the effects mentioned above were recorded globally. For this reason, the use of these effects gave frequently rise to overwarnings.

At that time the opinion was held that it was better to put up with overwarnings than with an unannounced disturbance, because, when considering it from the point of view of meteorology it is better to take the umbrella than to get wet.

In order to avoid overwarnings and to achieve a higher probability of lucky hits, the forecast was based on all geo- and astrophysical indicators available at that moment to clarify the overall situation. In the declining part of the sun spot cycle No. 17 (minimum in 1944) it was mainly the recurrence tendency which allowed rather successful forecasts to be made.

III. Radio Propagation Prediction Service of the Fernmeldetechnisches Zentralamt (1950 to date) [3]

In 1950 the Fernmeldetechnisches Zentralamt (Telecommunication Engineering Centre) resumed the preparation of short-term forecasts, which the Wave Propagation Department had discontinued at the end of the war. Since that time the following has been done by the Radio Propagation Prediction Service:

1) Establishment of an Ursigram service.

2) Regular daily and weekly forecasts with the help of quality figures.

3) Continuation of the trials concerning the application of the results of cosmic ray measurements.

4) Systematic observations of the transmission frequency range and derivation of an objective quality figure used to objectively define disturbances as a function of time and intensity.

5) Expansion of the development tendency into situation synoptics of all parameters on the lines of the "selection frequency statistics" used in meteorology.

6) Participation in the International Ursigram and World Days Service as Regional Warning Centre during the IGY and the IQSY.

7) Application of solar predictions.

8) Inclusion of additional information in the forecasts.

Re 1)
In 1950 the Deutsche Bundespost began to collect the most essential topical data made available by geophysical and astrophysical institutes and to pass them on to interested parties. In this way access was obtained to the results of the latest measurements and observations, which could be used for studies and for the preparation of short-term forecasts. This exchange of data was the reason for the establishment of a "Arbeitsgemeinschaft Ionosphäre" (Working Group for Ionospheric Studies), whose members are representatives of the German institutes and of the Fernmeldetechnisches Zentralamt. According to the statute the Fernmeldetechnisches Zentralamt was entrusted with the work of the secretariat which is responsible for the Ursigram service. This latter service which had already been recommended by the URSI some years before and which was first taken up in France, has since been performed together with the URSI along the lines recommended by the CCIR. At the beginning, the data were encoded by means of a code developed on consultation with the institutes. In 1952 this code was modified in co-operation with the other European Ursigram Centres, i.e. with the Paris Centre and NERA, and adopted as European Ursigram code. The French, Dutch and German PTT Administrations worked together in the preparation and distribution of the Ursigrams, which comprised the results of solar and geophysical observations carried out in France, the Netherlands, Austria and Germany. In the attempt to turn the Ursigram service into a world-wide service, the observation data attained in the United States of America

were passed on to the Centres by telegram or airmail. Up to the taking over of a post in the IFRB at Geneva in 1955, Herr Dipl.-Ing. W. Menzel, the first secretary of the "Working Group for Ionospheric Studies" devoted much time to the establishment of the Ursigram service. In 1956 the Ursigram Committee of the URSI combined the regional Ursigram Services existing in the USA, Japan and Europe to form a world-wide international Ursigram service. Agreement was reached on a uniform layout of the contents and a uniform code to be used for the Ursigrams. After the fusion of the Ursigram service with the World Days Service, which had been set up at the same time and in which the Fernmeldetechnisches Zentralamt at Darmstadt participated as Regional Warning Centre (RWC) during the IGY, the Fernmeldetechnisches Zentralamt became a Regional Warning Centre of the IUWDS. In the course of time the Prediction Service of the Fernmeldetechnisches Zentralamt could thus gain access to a growing number of global solar and geophysical measurement and observation data, the quality of which improved very much with the progress made in research and the technical possibilities of measurement so that the forecasts could be based on more reliable information.

Re 2)
Contrary to the former method where a forecast was only issued if required, i.e. in the event of forthcoming disturbances, propagation conditions are now forecast for each day, even if there are normal conditions. According to the former method a forthcoming disturbance was announced in plain language, but today quality figures are used to characterize the radio propagation conditions in daily and weekly forecasts. In this way, every Friday the day and night conditions for the overseas traffic to USA, South America and East Asia as well as for the European traffic are forecast by quality figures for 10 days in advance, i.e. with three days' overlapping. As far as the European traffic is concerned, the night conditions are indicated separately for high frequencies where the influence of the MUF prevails and for low frequencies where the influence of the LUF prevails. Quality figure 6 stands for the normal conditions which correspond more or less to the transmission frequency range shown in the monthly prediction. For quality figures greater than six an expansion of the transmission frequency range with growing field strengths is to be expected whereas quality figures below 6 indicate the narrowing of the transmission frequency range with decreasing field strengths.In the case of the 10-day forecasts, the so-called weekly forecasts, for the first seven days the events observed on the sun are evaluated with respect to those observed during the preceding solar rotation. Thus, allowance is made for the behaviour of new and changed centres of solar activity. These weekly forecasts are currently corrected by daily forecasts. Up to 31 March, 1969, they were issued twice a day, i.e. in the morning for the day and the following night and in the afternoon for the night and the following day. These periods correspond with the geographical position of the radio paths and thus with the utilization of the day and night frequencies. Contrary to the weekly forecasts, in which day and night conditions are each expressed by one quality figure, the daily forecasts comprise two quality figures for each period of time. The first quality figure characterizes the propagation conditions at the beginning of the forecasting period and the second indicates the approximate quality at the end of the period, i.e. the comparison of the two figures indicates the development tendency. It should be mentioned that a description of the propagation conditions existing during the preceding week (review) is attached to the weekly forecast.

Re 3)
Since the assumption that in the event of flares the sun can cause a substantial increase of the cosmic ray intensity proved true after 1945, measurements of the cosmic rays have been continued and the measuring equipment has been improved in the course of time. For instance, the great effects of 19 November, 1949 and of 23 February, 1956 were measured by means of the equipment available to the Fernmeldetechnisches Zentralamt on the Predigtstuhl and on the Zugspitze. These data were published together with the related ionospheric phenomena. Since that time special interest has been taken in the polar cap absorption effect discovered by D. K. Baily. However, when it became apparent that in our latitudes the GeV effects to be measured on the ground do not occur very often, efforts have been made to observe the polar cap absorption by recording high-latitude VLF propagation as proposed by Lange-Hesse. As for cosmic rays, the more frequent modulation effects seem to be of interest to the forecaster. In addition to the Forbush effect, the changes in the diurnal variations, which are interpreted as anisotropy effect, and the modulations with the solar rotation, confirmed by the great eruption on 23 February, 1956, furnish further information for forecasting purposes. I need not explain it in detail, because it will be dealt with in my second paper.

Re 4)
As early as 1943 the Norddeich coast station prepared regional statistics of the propagation conditions as a function of frequency, which lead to systematic observations of the transmission frequency range. The results of these observations were used to derive an objective quality figure indicating a functional relation between the mean field strength and the quasi MOF and LOF. At first, the observations of the transmission frequency range were carried out by the Radio Monitoring Service. Later on, the method was improved by a Radio Propagation Observation Station, which was set up especially for this purpose and which is now partof the Overseas Radio Receiving Station at Lüchow. Thus it has been possible to distinguish between the world-wide propagation conditions and those measured locally by an ionospheric station.

Re 5)
It proved more and more useful to take not only individual events as prediction indicators, but additionally to prepare a synoptic of the development tendency of the different prediction parameters, to use it according to "selection frequency statistics" and to work according to the sentence "similar situations yield similar effects", which is applied in meteorology, as long as the physical interrelations are not sufficiently explained.

Re 6)
The participation in the International Ursigram and World Days Service as Regional Warning Centre during the IGY and the IQSY enlarged the knowledge of solar terrestrial influences and their world-wide effects and increased the activity of the co-operating scientific institutes in this field. This activity has been very valuable for the forecasters. The fact that the RWC did not work around the clock and that it was closed on Sundays and holidays sometimes proved to be disadvantageous for the preparation of the daily advices. Although the Ursigrams could be passed on via other channels, the advice and the daily forecasts had to be issued some days in advance. For this reason the probability of lucky hits of the forecasts varied from 75% to less than 50%.

Re 7)
During the IQSY solar observatories began with short-term solar predictions in the form of the solactivity Alert; long-term forecasts, i.e. monthly forecasts were made by Dodson, Michard and Giovanelli. After the IQSY Sveska and Simon continued to improve the methods of solar predictions in conjunction with the proton flare project. The objective of these improved methods is to forecast individual flares.

Ionospheric forecasts have been considerably improved and facilitated by the fact that today similar forecasts are also regularly issued by solar observatories which concentrated formerly on scientific studies and supported the ionospheric forecast services only by furnishing observation data.

Re 8)
In the first half of 1950's attempts were already made to enlarge the contents of the forecasts by adding quality figures, which indicate approximately the mean variation of field strength. At first it was tried to add the percentage variation of the MUF and LUF of the individual periods to the daily forecasts. On consultation with the operational services these trials were discontinued after it was found that an extrapolation in time for the 12-hour forecasting period was not accurate enough. With effect from 1 April, 1969 the development tendency of the upper and lower limits (MUF and LUF) of the transmission frequency range has been indicated relatively, i.e. it is stated whether it is positive or negative with respect to the monthly prediction. Moreover, the contents of the forecast is now explained in plain language and the daily forecasts are only issued once a day. Corrections are published if there are unexpected changes of the solar terrestrial events or the development tendency of the propagation quality. However, this is only possible during office hours between 0630 to 1545 GMT, but not on Saturdays, Sundays and holidays.

Bibliography

[1] Plendl, H., Dieminger, W., Rawer, K. — Die Ionosphäre und ihre Bedeutung für den Funkdienst der Truppe (The Ionosphere and its Importance to the Radio Services of the Armed Forces).
Lecture held on the occasion of a training course for Air Force communication engineers in spring 1942.

Dieminger, W. — Ionosphäre (Ionosphere)
FIAT Rev. of German Science 1939-1946
17 Geophysik, 93-163

Bartels, J. — Erdmagnetismus II (Geomagnetism II)
FIAT Rev of German Science 1939-1946
17 Geophysik, 39-91

[2] Beckmann, B. Menzel, W., Vilbig, F. — Über die praktische Bedeutung der Ionosphärenforschung für den Funkdienst (On the Practical Importance of Ionospheric Research to the Radio Services).
Telegraphen-, Fernsprech-, Funk- und Fernseh-Technik, TFT 29 (1940), 106-117.

Vilbig, F., Beckmann, B., Menzel, W. — Die Wellenausbreitungsforschung mit besonderer Berücksichtigung der Aufgaben und Ziele des Amtes für Wellenausbreitung der Forschungsanstalt der Deutschen Reichspost (Wave Propagation Research with due Regard to the Responsibilities and Objectives of the Wave Propagation Department of the Deutsche Reichspost Research Institute).
Postarchiv 71 (1943), 35-117.

Zirkler, J. — Solare Korpuskularstrahlung, weiche Komponente der Höhenstrahlung (Solar Corpuscular Radiation, Weak Component of Cosmic Rays).
Geophys. 18 (1943), 126.

Biermann, L., Meyer, B., Temasvary, St. — Über eine frühe Beobachtung solarer Höhenstrahlung (On an Early Observation of Solar Cosmic Rays).
Naturwissensch. 51 (1964), 34-36.

Zirkler, J. — Das Solar Cosmic Event vom 9. September [illegible] (The Solar Cosmic Event of 9 September, 19[illegible]).
Naturwissensch. 52 (1965), 389-390.

Beckmann, B. — Messungen der Wellenausbreitung, Elektronenemission, Elektronenbewegung und Hochfrequenztechnik (Measurements of Wave Propagation, Electron Emission, Electron Movement and HF Technique).
FIAT Rev. of German Science 1939-1946, 16, 143-167.

[3] Beckmann, B., Menzel, W. — Funkwetterprognose (Prediction of Radio Propagation Conditions).
Jahrb. des elektrischen Fernmeldewesens 1954/55, 186-216.

Beckmann, B., Ochs, A. — Vorhersage für die ionosphärische Kurzwellen-Ausbreitung (Prediction of Ionospheric Short-wave Propagation).
Jahrbuch des elektrischen Fernmeldewesens 1969, 281

Müller, R., Augustin, O., Menzel, W., Ehmert, A., Gelow, H., Sittkus, A., Dieminger, W., Geisweid, K.H., Bartels, J. — Solare und terrestrische Beobachtungen während des Mögel-Dellinger-Effektes (SID) am 19. November 1949 (Solar and Terrestrial Observations during the Mögel-Dellinger Effect (SID) on 19 November, 1949).
Journ. Atm. Terr. Phys. 1 (1950), 37-48.

Beckmann, B., Dietrich, P., Salow, H.	Über den Einfluß der solaren Ultrastrahlung auf die Funkwetterlage am 23. Februar 1956 (On the Influence of Solar Cosmic Rays on the Radio Propagation Conditions on 23 February, 1956). Nachrichtentechn. Z. 10 (1957), 329-334.
I.U.W.D.S.	International Ursigram and World Days Service. Synoptic Codes for Solar and Geophysical Data Second Revised Edition 1969. Published by the IUWDS Secretariat, Boulder, Colorado

IONOSPHERIC FORECAST REQUIREMENTS OF THE OMEGA NAVIGATION SYSTEM

by

V.R.Noonkester and E.R.Swanson

Naval Electronics Laboratory Center
San Diego, California 92152

SUMMARY

The Omega Navigation System which will be implemented by the early 1970's is expected to have a root-mean-square position error of about one nautical mile. This small error can be attained if good skywave corrections and good forecasts of solar and ionospheric activity are available. Reliable sunspot number forecasts will be needed at least one year ahead because the sunspot number is used to compute the skywave corrections which require about one year for computation, printing, and distribution. Thus, poor estimates of sunspot number create position errors which persist for the life of the associated skywave correction tables. Reliable forecasts of SID's and PCA's are needed so that Omega navigators can be warned of expected poor navigation conditions. SID and PCA forecasts must be made at least one day ahead so that they can be distributed by radio messages. These Omega forecast requirements are discussed relative to application and user response.

IONOSPHERIC FORECAST REQUIREMENTS OF THE OMEGA NAVIGATION SYSTEM

V. R. Noonkester*

E. R. Swanson*

I. INTRODUCTION

The United States Navy has developed a world-wide navigation system called the Omega Navigation System.[1] The Omega system uses very-low-frequency (vlf) radio waves and can provide a geographic position fix anywhere at any time aboard an airplane, a land vehicle, an ocean vessel, or submerged submarine. The root-mean-square fix error is expected to be about one nautical mile.[2,3] Anyone of any nationality will be able to use the navigation system by securing an Omega radio receiver with appropriate charts and tables. Omega has been approved for implementation and the eight stations necessary for global coverage will be installed and operating at full design power of 10 kW in the early 1970's. Presently, four stations are providing useful navigation information over an area of approximately fifty million square miles.

This paper will discuss the basic principles of the Omega system and some sources of error in a position fix. The ionospheric forecast needs of the system will then be discussed relative to the time regime of information dissemination and the expected response of Omega users to ionospheric forecasts.

II. THE OMEGA NAVIGATION SYSTEM

Omega operates in the vlf radio band between 10 and 14 kHz. Transmissions of about one second duration are time-shared by various transmitting stations within a ten-second commutation pattern at 10.2 kHz (figure 1). Coherence is achieved by using several atomic frequency standards at each station, together with appropriate control procedures, so that all stations may be held to an agreed international time base. Accordingly, each station is a source of precise time and a "master-slave" distinction such as used in Loran is not made. Although the system can be used for range-range navigation, the system is normally used in the hyperbolic mode in which phase differences are measured between signals received from various pairs of transmitters. Hyperbolic geometry is employed primarily because it eliminates the need for precise time at the navigation receivers. One feature of the hyperbolic configuration is that lines of constant phase difference will repeat every one-half carrier wavelength along the great circle between the transmitters (baseline) and at slightly greater distances elsewhere. Because it is inherently impossible to measure the integral cycle differences between Omega signals from two transmitters at one frequency, the fix provided is ambiguous by multiples of one-half the wavelength, or eight miles at 10.2 kHz. The ambiguity is not normally significant because measurements are made continuously and hence the various integral cycle differences (lanes) can simply be counted as they are traversed. In the event of short outages, normal dead reckoning or other navigational information can be used to resolve the lane ambiguity. If conventional techniques for lane resolution fail, the Omega system provides a method to determine the approximate position.[4] Each Omega transmitter will transmit pulses of vlf wave packets at 10.2, 11.33 and 13.6 kHz as shown in figure 1. By obtaining the phase difference between two pairs of transmitters at each frequency a unique position can be obtained within an area of over ten thousand square kilometers. This is possible because each frequency has a set of hyperbolic lines of slightly different lane width within which only one common hyperbolic line can satisfy the phase difference measurements of all frequencies. This signal format also provides a method of station identification because the pulses have a slightly different duration.

III. OMEGA FIX ERROR SOURCES

Very-low-frequency radio waves propagate in the earth-ionospheric waveguide. The phase velocity is a function of the surface conductivity and the distribution of conductivity in the ionosphere. The ionospheric conductivity is a function of the time of day, season, sunspot number, and geomagnetic conditions. Ionospheric disturbances can alter the ionospheric conductivity considerably. An Omega user is provided with corrections to the phase difference measurements which will account for the difference between the standard phase velocity used to prepare the navigation charts and the phase velocity expected at a particular location and time.[5] These tabulated corrections are called skywave corrections and are functions of the time of day, season, sunspot number, geographic region and transmitters being monitored. The presence of highly predictable phenomena such as solar eclipses might also be indicated in future tables. Techniques are constantly being evaluated for improving the skywave corrections.

If any part of the waveguide deviates from the assumed waveguide, the phase beyond that point will depart from that predicted and will cause position fix errors. Sources of waveguide perturbations causing Omega fix errors include sudden ionospheric disturbances (SID's), polar cap absorption events (PCA's), and errors in the predicted long-term sunspot number (R).

Although Omega-fix errors can be caused by errors in predicting the phase velocity over one or more vlf paths, the following examples of the effect of SID's and PCA's on Omega propagation and position error are given for a single path for simplicity.

The effect of SID's on an Omega position fix is illustrated in figures 2 and 3. Figure 2 shows a decrease of at least 30 μs in the propagation time of the 10.2 kHz signal from Trinidad to Forestport, New York, by a flare which began at 1615 GMT on September 29, 1968. The propagation time returned to normal in about 1½ hours.

With normal hyperbolic geometry, a 30 μs decrease at Forestport would indicate that Forestport moved about 3 nautical miles (5.5 km) closer to Trinidad. Receivers making phase difference measurements for transmissions from these Omega transmitters at other locations would note an apparent position change during the flare. The magnitude and direction of this change depends on the location of the receiver and the effect of the flare on the phase velocity along the vlf paths to the receiver. However, some position error may be introduced by the flare at most locations.

*Physicist at Naval Electronics Laboratory Center, San Diego, California 92152

A type of solar flare activity which seriously degrades Omega navigation is the "M" type event as illustrated in figure 3. Figure 3 shows that the propagation time from Trinidad to Forestport, New York gradually decreased nearly 20 μs below normal about 2 hours after the solar x-radiation started increasing at 1056 GMT on April 10, 1969. The propagation time remained abnormal for about 12 hours and did not return to normal until after sunset. This abnormal propagation was associated with a class 3 flare having excess x-radiation for over 8 hours. Although rare, such events are significant primarily because of their extended duration.

A more persistent and a more serious condition which can degrade Omega navigation is the polar cap absorption event or PCA. Figure 4 shows that the propagation time from the Norway Omega station to Hawaii decreased almost 60 μs within a day of the PCA commencement at 0900 GMT on June 9, 1968, and did not return to normal for about 13 days. A 60 μs decrease in propagation time at Hawaii would indicate that Hawaii apparently moved about 6 nautical miles (11 km) closer to Norway.

The rate of change in the propagation time during the onset of a PCA on November 18, 1968 is shown in figure 5 for the Norway to Hawaii path. The maximum decrease in propagation time was about 80 μs and was attained in about 3 hours after the onset at 1050 GMT. The apparent motion of Hawaii toward Norway was about 3 nautical miles (5.5 km) per hour immediately after the onset for a total change of about 8 nautical miles (15 km). Erroneous position changes of these magnitudes must be made known to Omega navigators by appropriate communications.

Another source of error is long-range prediction of average sunspot activity. Omega skywave corrections are determined from both theoretical and empirical considerations and include a variation of phase velocity with sunspot number R. The dependence on R has been deduced by regression analysis. The Omega phase velocity, relative to the speed of light, has been found to increase by about 2×10^{-6} per unit R during the day and 3 to 4×10^{-6} per unit R at night. Although the changes in the relative velocity per unit R are small, the effects may be appreciable. Predictions of the maximum R may be in error by as much as 50 to 100 units. The relative velocity used in producing worldwide skywave corrections could thus be in error by as much as 4×10^{-4} which would cause errors on typical paths (3 to 6 thousand kilometers) of about 0.6 nautical miles (1.1 km) while errors over long paths could exceed one nautical mile (1.9 km).

Skywave correction tables will have a useful life from one and three years, depending on the rate of change of R. Allowing time for modifications in the prediction model, computation, publication, and dissemination of the correction tables, R must be predicted one to two years ahead. Errors of the magnitude given above are probably sufficient to cause the tables to be recomputed and republished at considerable effort and expense.

The effect of more typical skywave correction errors is readily evaluated. If the coverage area for a particular station pair is approximated by the circle for which the baseline is a diameter and plane geometry is assumed, the root-mean-square difference in propagation distance between the stations throughout the coverage area is about 0.58 times the baseline. In the implemented system, the baselines or distances between stations, ordinarily paired in hyperbolic geometry, will be almost 10 thousand kilometers. Hence, typical measurements in the implemented system will have a root-mean-square propagation pathlength difference ε of about 5 thousand kilometers. For expected geometry, the error contribution from sunspot number uncertainty will be approximately $\varepsilon \times 10^{-3} \times \delta R$ nautical miles where δR is the prediction error in R. Because the nominal system accuracy is about one nautical mile, an uncertainty of 65 in the sunspot number will cause a typical degradation in the Omega-fix accuracy of about 5 percent.

More stringent demands are placed on the prediction of sunspot activity in the use of Omega for time dissemination. Omega may have a capability of disseminating epoch with an accuracy on the order of 1 to 5 μs[4,6] when the epoch determination is made by averaging signals from several stations. In this case, the average propagation pathlength, not the typical pathlength difference, is important. Because several stations would be used, the average pathlength would be about 6 to 9 thousand kilometers causing the timing uncertainty to be about (0.04 to 0.1) δR microseconds. Thus, if time dissemination is to be accurate to 1 μs, for example, δR must be less than about 10R units.

The need for forecasts of SID's, PCA's and R will be discussed in the next section relative to the time delay in data transmission and the expected attitude of the Omega users to forecast or alert messages.

IV. OPERATIONAL OMEGA FORECAST REQUIREMENTS

The elements which control the operational Omega forecast requirements are the time delay of forecast dissemination, the ease of use by the Omega user, and the proven reliability of the forecasts. Unless sufficient time is available to make computations, tabulate, or create messages in response to an ionospheric forecast, a forecast is obviously of no use to the Omega navigator. Unless the special forecast messages are relatively simple to apply, the Omega navigator may make mistakes or be discouraged in applying them. An Omega navigator will undoubtedly ignore forecasts if, after exerting effort to use them for a period, he finds the forecasts are reliable only about one-half the time. These elements place rather stringent conditions on operational Omega forecasts of ionospheric perturbations.

The types of messages generally available for an Omega forecast are: 1) the skywave correction publications, 2) letters, 3) radio or teletype messages, and 4) real-time messages. Skywave correction tabulations presently require about one year from initiation to complete distribution. These publications require considerable computer and printing time and are delivered to Omega recipients by regular mail delivery. Letters and radio or teletype messages would contain forecasts of short-term disturbances. Letters can usually be used if one to two weeks were available before the expected ionospheric disturbance while radio or teletype messages can be used if a one to two day forecast is made. Real-time messages using a warning code are not expected to relay any detailed forecasts unless special formats are developed. The warning code is not expected to convey more disturbance information than to alert Omega users that an ionospheric disturbance is in progress. Table 1 shows the type of forecasts required relative to the forecast lead time and the method of information distribution.

Table 1. The lead time and forecast distribution method for major elements influencing Omega navigation

Required	Forecast Lead Time	Method of Forecast Distribution
1. Sunspot number R	1 to 2 years	Publication
2. Solar flare events (SID's, PCA's, etc.)	1 to 2 days	Radio message
3. Existing ionospheric disturbance	- - - - - - - -	Alerts by Omega warning code

Because of the one to two year lead time to publish and disseminate the skywave corrections, forecasts of R are required up to two years ahead. If reasonable errors are made in the R forecast they would not be obvious to the Omega navigator. It would be difficult to revise the skywave corrections after solar observations verify that errors in the sunspot number prediction have been made and better predictions are available.

Ionospheric forecasts of SID's and PCA's would probably be relayed to Omega navigators by radio messages because these disturbances are not expected to be forecast more than one or two days ahead. Until forecast techniques improve, letters will probably have little use in relaying forecasts.

For PCA's and SID's of high probability, messages are expected to provide general statements on the expected position errors, to give the probability level, and to give their probable magnitude and duration. These probability forecasts could be used by an Omega navigator to avoid obtaining a position fix during an SID, to avoid polar Omega paths during PCA's if possible or to make use of other navigation techniques available during the forecast period.

Probability forecasts on ionospheric disturbances are likely to be used only if the Omega user has found them to be reliable. Thus, the Omega system forecast message center is likely to avoid sending forecasts on ionospheric disturbances unless the forecast is based on proven techniques and the probability level is high that an event will occur which will influence Omega transmissions. An Omega navigator may not always be able to determine if a disturbance is in progress unless a special alert is transmitted to him. Real-time alerts to the Omega users may also increase their confidence in the forecasts which are based on proven techniques.

V. OTHER POSSIBLE OMEGA FUNCTIONS

The previous sections have discussed the ionospheric forecast needs of the basic Omega system to be implemented in the early 1970's. Some special applications using Omega are also being considered. Oceanographic surveys will profit from Omega navigation although it is not always essential to have accurate fix information available when the survey is being conducted. It may be essential to reconstruct an accurate track of a ship several months after completion of a survey. Although this application does not require ionospheric forecasting it can profit from confirmation of ionospheric conditions during the survey. To satisfy this requirement detailed records from a data collection agency are needed. This agency could presumably work as an adjunct to the forecasting center.

Other systems are being investigated which use remote receivers that telemeter basic phase information from Omega signals to a central point where the receiver position is determined. The Omega Position Location Experiment (OPLE) and Position Location And Communications Experiment (PLACE) being conducted by NASA are examples.[7,8]

The development of a central computing facility with an extensive telemetering network could provide many useful functions. For example, if the central computer is provided immediate data from a geophysical and solar data collection agency, substantial data can be evaluated and synthesized in real time and can be used to produce global propagation predictions in real time. A navigation system using real-time propagation predictions would be more accurate than ordinary Omega. The same computer could also produce an up-to-date history of geophysical conditions which would also be valuable for ionospheric forecasting.

Because each Omega station will constantly monitor transmissions from all other stations continuously, the Omega system may provide its own system for detecting the presence of ionospheric disturbances. This self-supporting detection has not received intensive examination. If an Omega ionospheric disturbance detection system is developed, the disturbance information would be available to anyone having appropriate Omega radio receivers.

VI. CONCLUSIONS

The Omega Navigation System needs good forecasts of the sunspot number at least one year ahead and if reliable probability forecasts of sudden ionospheric disturbances or polar cap absorption events could be provided at least one day ahead, utility should be enhanced. These lead-time requirements result from the methods available to calculate and disseminate the skywave correction manual and the time required to disseminate radio messages to Omega users. A major problem will be to select those forecasts of ionospheric disturbances which will have the greatest probability of success so that Omega navigators will learn to respect and respond to the forecasts.

A system to alert all Omega users of on-going disturbances should further enhance system utility. Messages to the Omega system at the commencement and termination of disturbances from scattered worldwide sensors would aid the Omega system to determine if alerts should be transmitted over the Omega warning channel.

REFERENCES

1. Swanson, E. R., and M. L. Tibbals, "The Omega Navigation System," NAVIGATION, vol 12, No. 1, Spring 1965, pp 24-35. (Also available in French: "Le Système Mondial de Navigation Omega," Navigation: Revue Technique de Navigation Maritime Aérienne et Spatiale, vol 13, pp. 255-271, Juillet 1965.)

2. Tibbals, M. L., and D. P. Heritage, Accuracy of the Omega Navigation System Navy Electronics Laboratory Report 1185, October 1963.

3. Swanson, E. R., and W. E. Davis, Omega in the Atlantic (1963-1965) - In-port measurements from HMS VIDAL and HR. MS. SNELLIUS on Oceanographic Survey NAVADO, Navy Electronics Laboratory Report 1350, January 1966.

4. Swanson, E. R., Omega Lane Resolution: Phase Measurements at two Very Low Frequencies, Navy Electronics Laboratory Report 1305, August 1965.

5. U. S. Naval Oceanographic Office, Omega Skywave Correction Tables, H. O. Publication No. 224 (100-C and 200-C series). Current edition.

6. Swanson, E. R., "Time Dissemination Effects Caused by Instabilities of the Medium." Paper presented at XIIIth AGARD-NATO Symposium, Ankara, 1967. To be published in the Proceedings.

7. Laughlin, C., et al., Description of Experimental Omega Position Location Equipment (OPLE), Goddard Space Flight Center Report X-731-66-20, January 1966.

8. Laughlin, C. R., et al., Place Experiment Description, Goddard Space Flight CEnter Report X-733-67-577, November 1967.

START — TRANSMISSION INTERVAL — 10 SECONDS — START — ETC.

STATION	0.9	1.0	1.1	1.2	1.1	0.9	1.2	1.0	0.9
1	10.2	13.6	11.33	f_1 →					10.2
2	f_2 →	10.2	13.6	11.33	f_2 →				
3		f_3 →	10.2	13.6	11.33	f_3 →			
4			f_4 →	10.2	13.6	11.33	f_4 →		
5				f_5 →	10.2	13.6	11.33	f_5 →	
6					f_6 →	10.2	13.6	11.33	f_6 →
7	11.33					f_7 →	10.2	13.6	11.33
8	13.6	11.33					f_8 →	10.2	13.6

0.2 SEC

Figure 1. The Omega Navigation System signal format. The frequencies are in kHz.

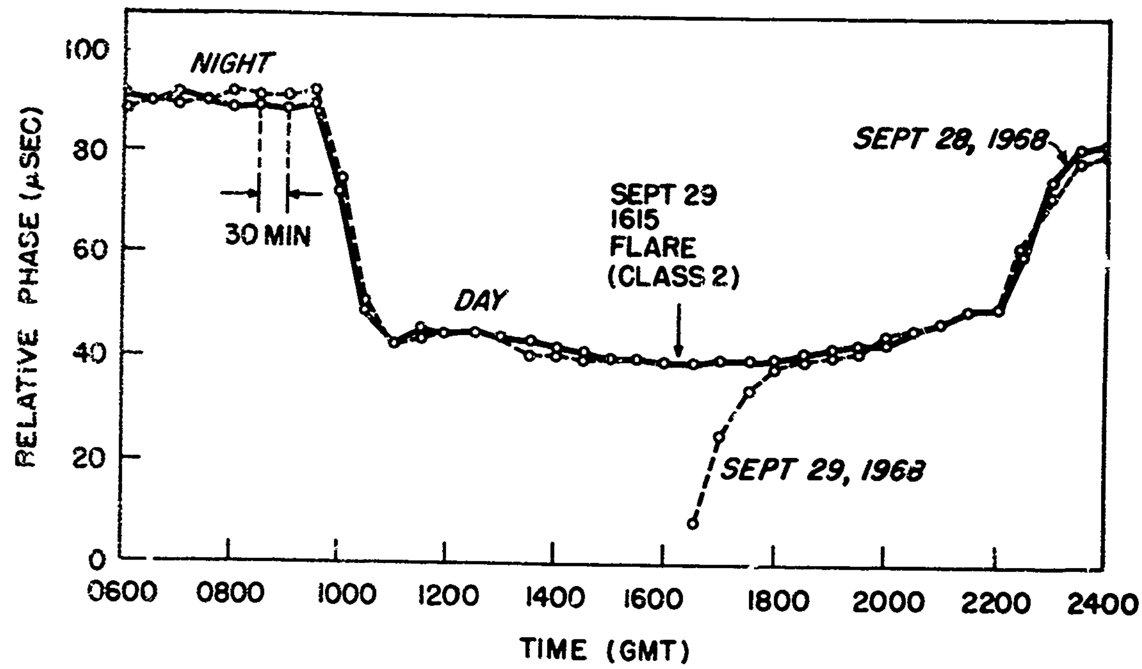

Figure 2. The relative phase of 10.2 kHz signals transmitted from Trinidad to Forestport, New York, on September 28 and 29, 1968. The effect of a class 2 flare at 1615 GMT on September 29 is shown. The undisturbed day on September 28 is shown for comparison.

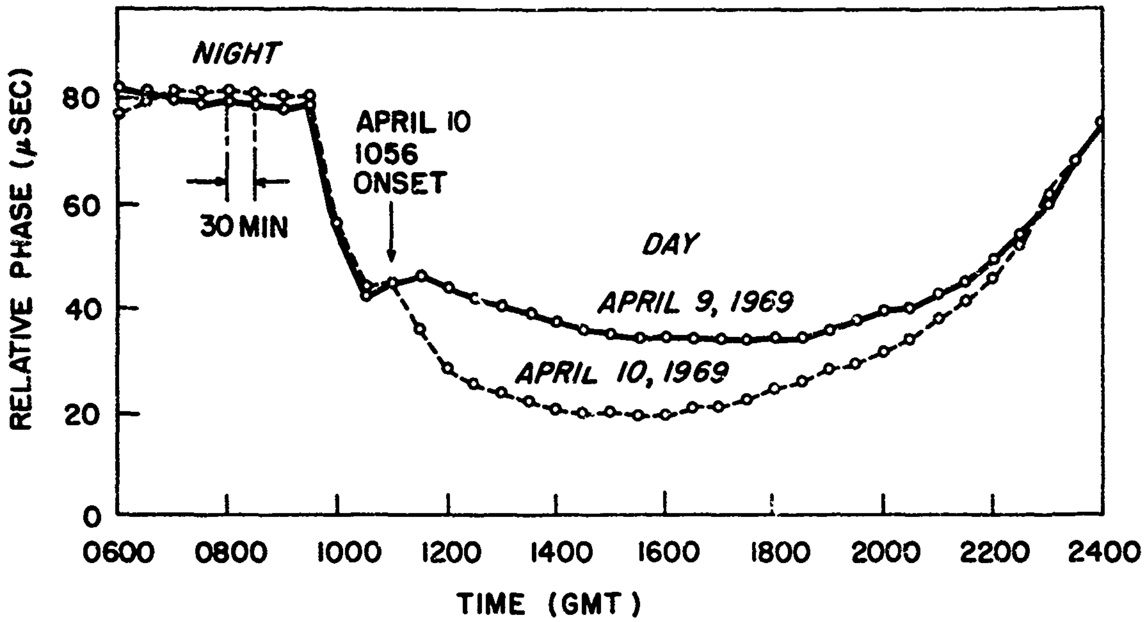

Figure 3. The relative phase of 10.2 kHz signals transmitted from Trinidad to Forestport, New York, on April 9 and 10, 1969. The effect of a "M" type event commencing at 1056 GMT on April 10 is shown. The event was associated with a class 3 flare having excessive x-radiation for over 8 hours. The undisturbed day on April 9 is shown for comparison.

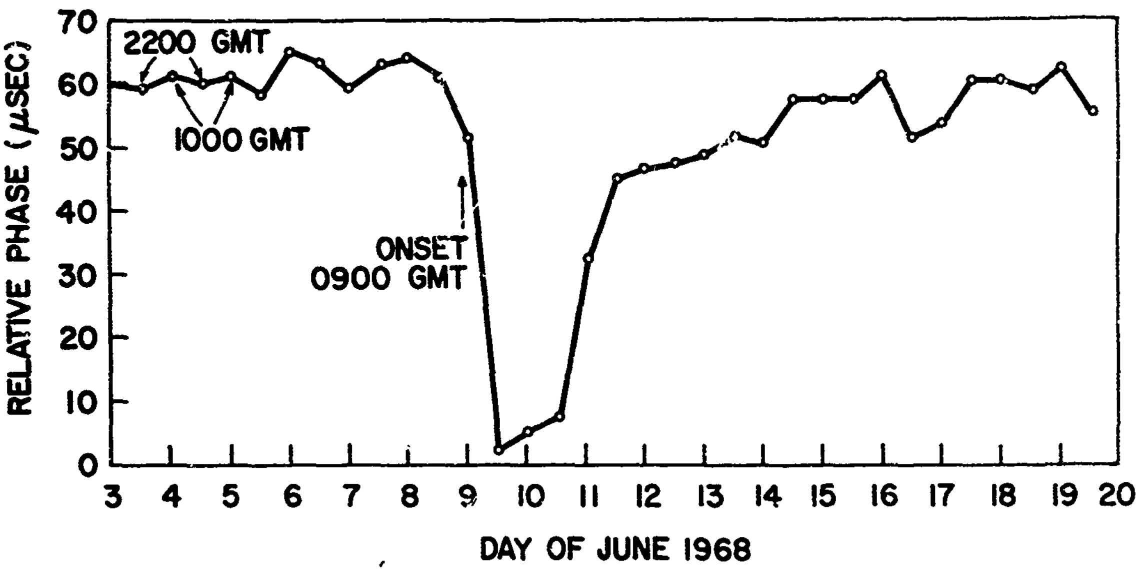

Figure 4. The relative phase of 10.2 kHz signals transmitted from Norway to Hawaii during a PCA event commencing June 9, 1968 at 0900 GMT. The normal relative phase was about 60 μs for 1000 and 2200 GMT during this period.

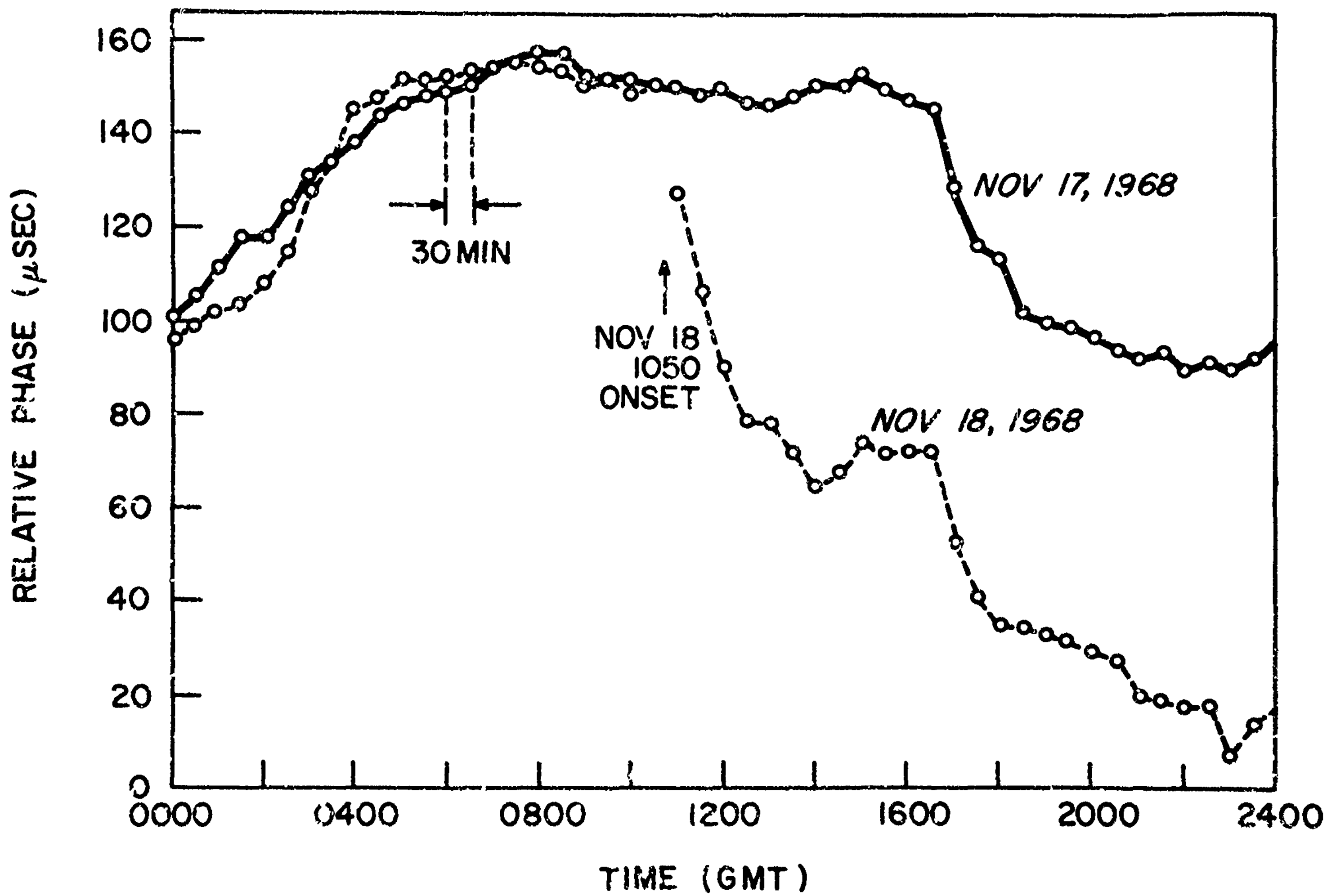

Figure 5. The relative phase of 10.2 kHz signals transmitted from Norway to Hawaii during a PCA event which started about 1050 GMT on November 18, 1968. The undisturbed day on November 17, 1968 is shown for comparison.

A MANUAL IONOSPHERIC PREDICTION METHOD USED FOR SYSTEM PLANNING

by

L.W. Barclay

The Marconi Company Limited,
Research Laboratories,
Great Baddow, Essex,
England

SUMMARY

Ionospheric predictions are prepared by the Marconi Company primarily for communications system planning to meet customers' requirements. For this purpose both frequency and signal-to-noise ratio predictions are required at extreme ionospheric conditions. Frequencies are now predicted using the C.C.I.R. Atlas, Report 340. Signal field strengths on selected frequencies are predicted by Piggott's technique and are then referred to the noise field strengths from C.C.I.R. Report 322 to give signal-to-noise ratios. This way of showing the expected service is more useful for circuit planning purposes than methods which indicate the LUF.

A MANUAL IONOSPHERIC PREDICTION METHOD USED FOR SYSTEM PLANNING

L.W. Barclay
The Marconi Company Limited,
Research Laboratories,
Great Baddow, Essex,
England.

1. INTRODUCTION

Ionospheric predictions are used by The Marconi Company in the process of planning H.F. communications and broadcasting installations. The estimated cost of a new installation depends in part on the lowest required frequency, and hence on the antenna size and the mast height, and on the transmitter power. These requirements may be predicted and the equipment specified accordingly. From the predictions a complement of frequency allocations may also be suggested so that application for use of the frequencies and the specification of tuned antennas may proceed before the equipment is installed.

Predictions are made by a manual system and the processes and presentations have remained essentially unchanged for about 8 years. During this time the need for predicted information has apparently been met and, if it is permissible to judge from the absence of complaints, the predictions have been of adequate accuracy. The demand for predictions is increasing, however, and the computer program for an automated prediction system is nearing completion.

At present no routine monthly predictions are being made for any circuit and the work is concentrated on systems planning requirements. Thus new circuits are always being considered and the predicted information needs to be sufficient to demonstrate the availability of the circuit at any time.

2. THE TIMES FOR WHICH PREDICTIONS ARE MADE

Predictions are made for the two solstice months and for one of the equinoxes. The remaining nine months of the year are assumed to have ionospheric characteristics similar to or intermediate between the 3 months selected. In temperate latitudes the performance of paths shorter than, say, 4000 km can be assessed by predictions for the solstice months only.

Two extreme solar cycle conditions are included in the predictions. Sunspot minimum predictions do not vary significantly from cycle to cycle since changes in the minimum values of the solar or ionospheric indices used are quite small. It is desirable, however, to use prediction data which are based on the 1964 minimum rather than on earlier cycles when fewer ionospheric observations were made.

Forecasts of the index values at sunspot maximum are less certain (1). In the last years of cycle 19, up to about 1965, an index corresponding approximately to a sunspot number, R_{12}, of 160 was adopted. Since then a lower index, $R_{12} = 100$, has been used and this has proved to be satisfactory for the present cycle.

3. FREQUENCY PREDICTIONS

Frequency predictions are made by conventional 'control-point' methods (2). The F2 region charts in C.C.I.R. Report 340(3) are used, circuit frequencies are predicted from the values read from the charts for the mid-point of paths shorter than 4000 km, and for control points 2000 km from each end of longer paths. The estimated junction frequencies (EJF) for paths up to 4000 km are obtained by the interpolation procedure given in Report 340. The $R_{12} = 0$ and $R_{12} = 100$ charts are used and, for planning purposes, it is not necessary to use the interpolation procedure for other index values. The F2 region EJFs are multiplied by 0.85 to obtain optimum working frequencies (OWF).

Prior to the publication of Report 340 the British D.S.I.R. prediction charts were used. The procedures given in the accompanying Instructions (4) were followed when interpolating for distance and for other index values.

A magneto-ionic correction (5) was added to the frequencies predicted for short

ranges since the zero-distance charts provided by D.S.I.R. were for the ordinary mode critical frequency foF2. This correction, which is already included in the EJF(zero)F2 charts of Report 340, can be economically important as it increases the predicted value for the lowest required frequency. However it is not always appropriate to assume that the extraordinary mode will be propagated efficiently (5) and the prediction process could be improved by taking the antenna polarisation and path orientation into account.

E region predictions are obtained from Piggott's nomograms (7) which have been converted for slide-rule calculation (8). This method is convenient as the k-factors are also required for the absorption loss calculations. Regrettably, predictions for sporadic-E propagation cannot be made.

The predicted frequency information is usually presented in the form shown in Fig. 1 where the diurnal variation of OWF is shown for the selected months and for both extreme solar index values. When several modes are possible only the highest frequency is usually shown but additional information is provided when, for example, the choice of antenna is likely to be affected by the presence of an E region mode with a low radiation angle.

From curves such as Fig. 1. sets of frequencies may be selected. A suitable choice for a fixed circuit might be four frequencies: a night and a day frequency for sunspot minimum conditions, together with an intermediate frequency, which may be used at night during years with high sunspot numbers, and a higher frequency for day use in those years.

It is sometimes convenient for mobile or broadcasting purposes to show how the OWF varies with distance and the presentations shown in Figs. 2 and 3 are then used. In Fig. 2, which could be called a maximum skip distance chart, the reduction in skip distance due to the E mode is also shown. Sets of equidistant azimuthal maps, Fig. 3, are produced when required. In this case the E region frequencies are shown and are extended to 4000 km, forming a composite E - F1 mode, by using a distance factor similar to that used in Report 340, p.404. In this way, it is possible to avoid discontinuities in the presentation at distances near to 2000 km.

4. PREDICTIONS OF SIGNAL-TO-NOISE RATIO

Curves showing the diurnal variation of signal-to-noise ratio are prepared for a set of selected frequencies. The curves are obtained from predictions of signal field strength and of atmospheric noise.

Field strengths are predicted by Piggott's method (7) and, again, the computations are greatly facilitated by use of the slide rule designed for the task. The active propagation modes are considered and the curves are only shown for periods when the mode is available i.e. when the working frequency is below the OWF and the mode is not screened by a lower ionospheric layer. When 2 modes with comparable strength are present at the same time, for example when both E and F2 propagation is possible, the signal levels are combined by r.m.s. addition. Often, however, it is sufficient to demonstrate continuity of communication by making predictions for one or two modes only. Fig. 4a shows the signal field strengths on a 2200 km path for the one-hop F2 (1F2) mode. The gaps in the lower frequency curves near midday are due to E region screening of this mode but these could have been filled by considering other modes. This work is unnecessary as higher frequencies, giving a better service, are available at these times. When paths of about 3000 km are considered, E region screening is sometimes enough to prohibit a 1F2 mode. In such cases more complex modes are calculated to fill the gaps, if this can be done with signals of useful strength. It is rarely necessary to consider modes more complicated than the 2E or 2F2.

Field strength predictions for path lengths greater than 4000 km are obtained by dividing the path into the minimum number of equal parts so that the length of each part is less than 4000 km. Piggott's method is used to compute the loss in each part.

The power reference level used by Piggott involves a complicated description of the reference aerial and has proved to be difficult to define clearly to prospective customers. Consequently the reference level has been changed to 1 kW e.i.r.p. (9); this is simply obtained by subtracting 4.8 dB from the unabsorbed field strengths given by Piggott.

Atmospheric noise field strengths are obtained from C.C.I.R. Report 322 (10). Median levels are usually sufficient but other percentiles are predicted when required. The field strengths are given for a reference 6 kHz receiver bandwidth. An example is given in Fig. 4b.; the horizontal parts of the curves are due to the galactic noise level or to the assumed level of man-made noise. Report 322 gives man-made noise levels at a 'quiet' site but the higher levels quoted by Lucas and Haydon (11) are

used when appropriate.

Median signal to noise ratios, for the specified reference power and bandwidth, are given by the ratio of the signal field strength to the atmospheric noise field strength and may be obtained graphically when both are plotted in decibels on the same axes. Fig. 4c shows an example of the final presentation.

C.C.I.R. Recommendations 339 and 340 (12) give the required signal to noise ratios, in the same specified bandwidth, for various classes of emission and these figures may be extended for other modulation systems and for multi-channel operation (13).

The radiated power may be determined by comparing the required signal-to-noise ratio with the predictions made for 1 kW e.i.r.p. and this comparison will indicate when economies in the installation could be made by reducing the traffic loading at the worst times.

5. LOWEST USABLE FREQUENCY

Some prediction systems give the daily variation of the lowest usable frequency (LUF). While this is probably adequate for existing circuits with specified equipments and requirements, it is insufficient for high-speed circuits when the signal dispersion becomes important (14), and it is not possible to scale an LUF curve for other powers or service requirements.

The time dispersion on selected frequencies could be estimated from predictions of median signal level and of the fading variation of the active modes; this technique is not yet in use. Nevertheless the planning advantage of showing the performance on selected frequencies is valuable, particularly in cases where the circuit loading, quality or availability may be adjusted to meet the users' resources.

6. ANTENNA SELECTION

Information is supplied, with the predictions, of typical radiation angles required for the main propagation modes on each circuit. This is an important factor when selecting the best antenna for the circuit. When estimating the circuit reliability full account is taken of the gain of the transmitting antenna at the required azimuth and radiation angle. Appropriate receiving antennas are also selected but no allowance is made for the receiving antenna gain. In some cases the antenna directivity will improve the signal to atmospheric noise ratio, but it would be too optimistic if full allowance for the gain were made (15). Receiving antenna gain and directivity is important, of course, in reducing interference levels.

7. CONCLUSIONS

The prediction system has been in use for several years and has proved satisfactory. The manual prediction methods are conventional, although there may be few other organisations which use Piggott's absorption calculation methods regularly, and attempts are made to use the latest available data.

Signal-to-noise ratios are predicted on a number of selected frequencies and the presentation of the information in this way is more useful for systems planning purposes than alternative presentations of the lowest usable frequency.

The demand for planning predictions is increasing and an automated system is now being programmed.

ACKNOWLEDGMENT

This contribution is presented by permission of the Assistant Director of Research of The Marconi Company.

REFERENCES

1. Barclay, L.W. — "The 1964 Sunspot Minimum and the next solar cycle." Point to Point Telecom. Vol. 9, No. 3, p.12, June 1965.

2. Tremellen, K.W., Cox, J.W. — "The Influence of Wave Propagation on the planning of short-wave communication." J.I.E.E. Vol. 94, Part IIIA, p.200, 1947.

3. C.C.I.R. Atlas of Ionospheric charactersitics. C.C.I.R. Report 340, Oslo 1966.

4. D.S.I.R. — "Instructions for the use of predictions of radio wave propagation conditions using the index IF2 and Bulletin A." Radio Research Station, Slough, England, January 1963.

5. Tremellen, K.W., Cox, J.W. — "The Influence of Wave Propagation on the planning of short-wave communication." J.I.E.E. Vol. 94, Part IIIA, p.204, Fig. 4. 1947.

6. Moorat, A.J.G., Bradley, P.A. — "Wave Polarisation and its influence on the power available from a radio signal propagated through the ionosphere." Proc.I.E.E. Vol. 115, No. 6, p.771 & 777. June 1968.

7. Piggott, W.R. — "The Calculation of the Median sky wave field strength in tropical regions". D.S.I.R. Radio Research Special Report No. 27, H.M.S.O. London, 1959.

8. Barclay, L.W. — "Slide Rule for the calculation of ionospheric absorption loss and of maximum usable frequency in the lower ionosphere". Proc. I.E.E. Vol. 110, No. 9, p.1523. Sept. 1963.

9. C.C.I.R. Recommendation 445 "Definitions concerning radiated power", Oslo, 1966.

10. C.C.I.R. Report 322. "World distribution and characteristics of atmospheric radio noise". Geneva, 1963.

11. Lucas, D.L., Haydon, G.W. — "Predicting statistical performance indexes for high frequency ionospheric telecommunications systems". ESSA Tech. Rep. I.E.R.1 - I.T.S.A.1, August, 1966.

12. C.C.I.R. Recommendations 339 and 340. "Bandwidths and signal-to-noise ratios in complete systems" and "Fading allowances for the various classes of emission". Oslo, 1966.

13. East, F.R. — "Planning an H.F. Transmission Circuit". Point to Point Telecom. Vol. 10, No. 2, p.26, Feb. 1966.

14. Vincent, W.R., Daly, R.F., Sifford, B.M. — "Modelling communication systems". in 'Ionospheric Radio Communications' ed. K. Foldestad. Plenum Press 1968.

15. Bradley, P.A., Clarke, C. — "Atmospheric radio noise and signals received on directional aerials at high frequencies". Proc. I.E.E. Vol. 111, No. 9, p.1534, September 1964.

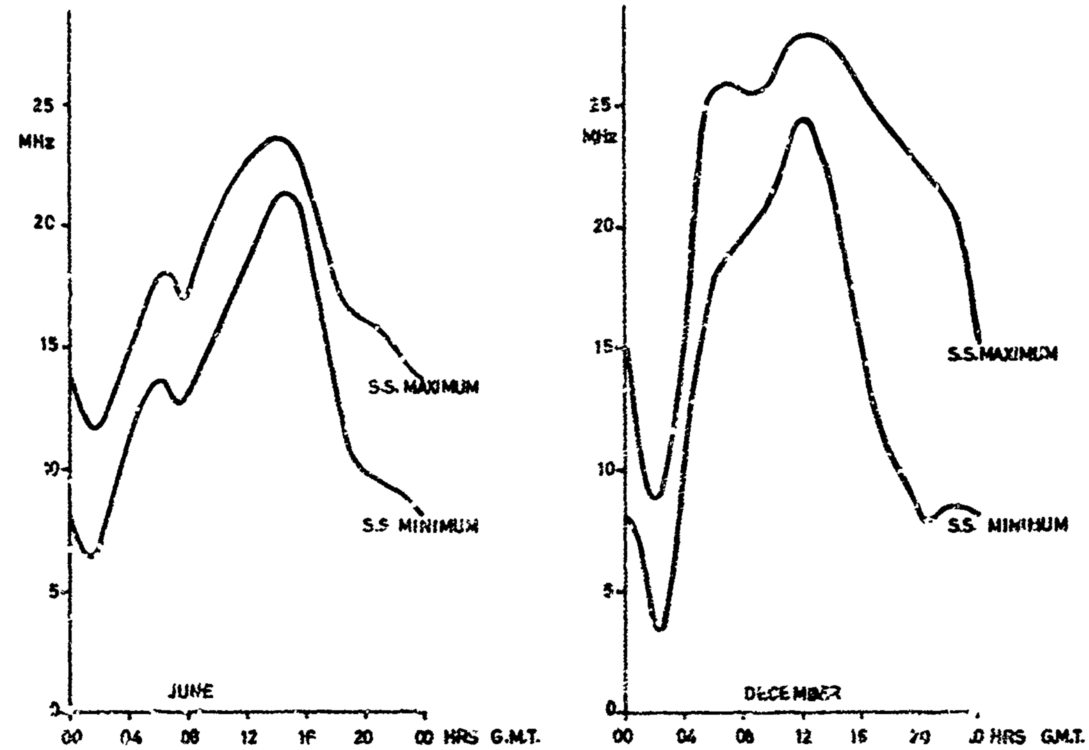

Fig.1 Diurnal variation of optimum working frequency in the two solstices and at both extremes of the sunspot cycle. Kuwait - Khartoum

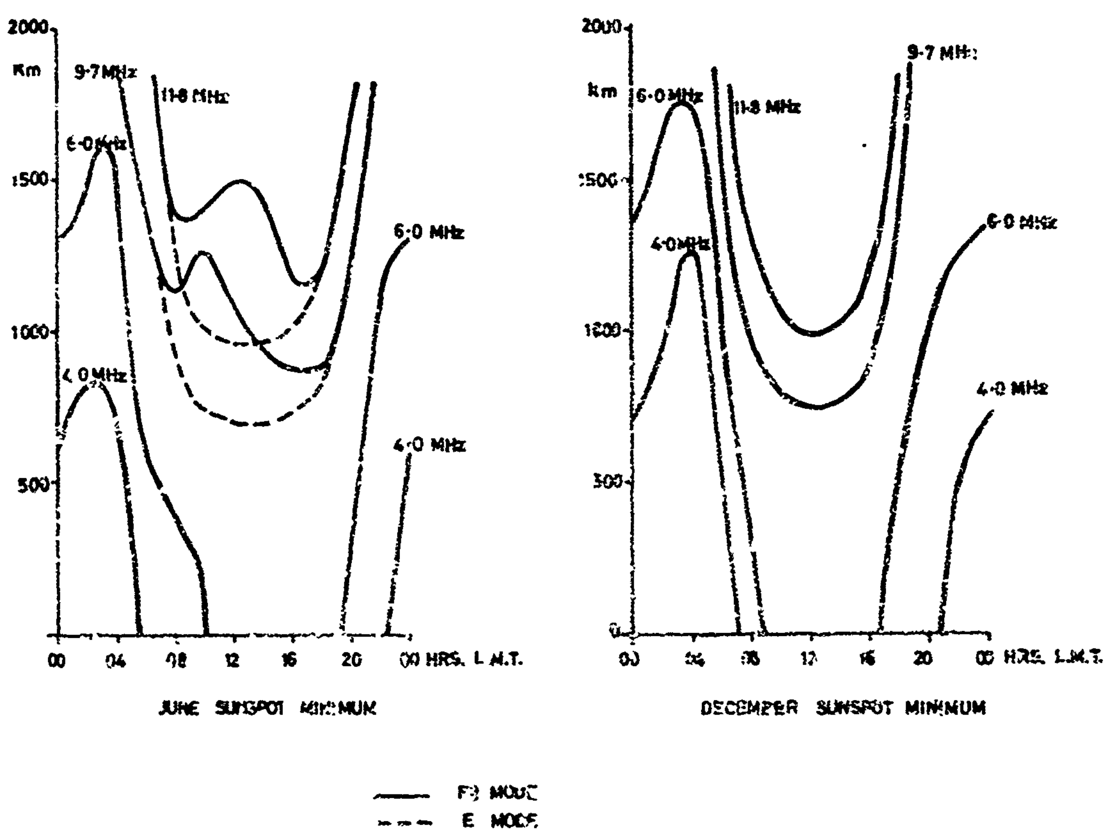

Fig.2 Diurnal variation of maximum skip distance in both solstices at sunspot minimum. Qatar

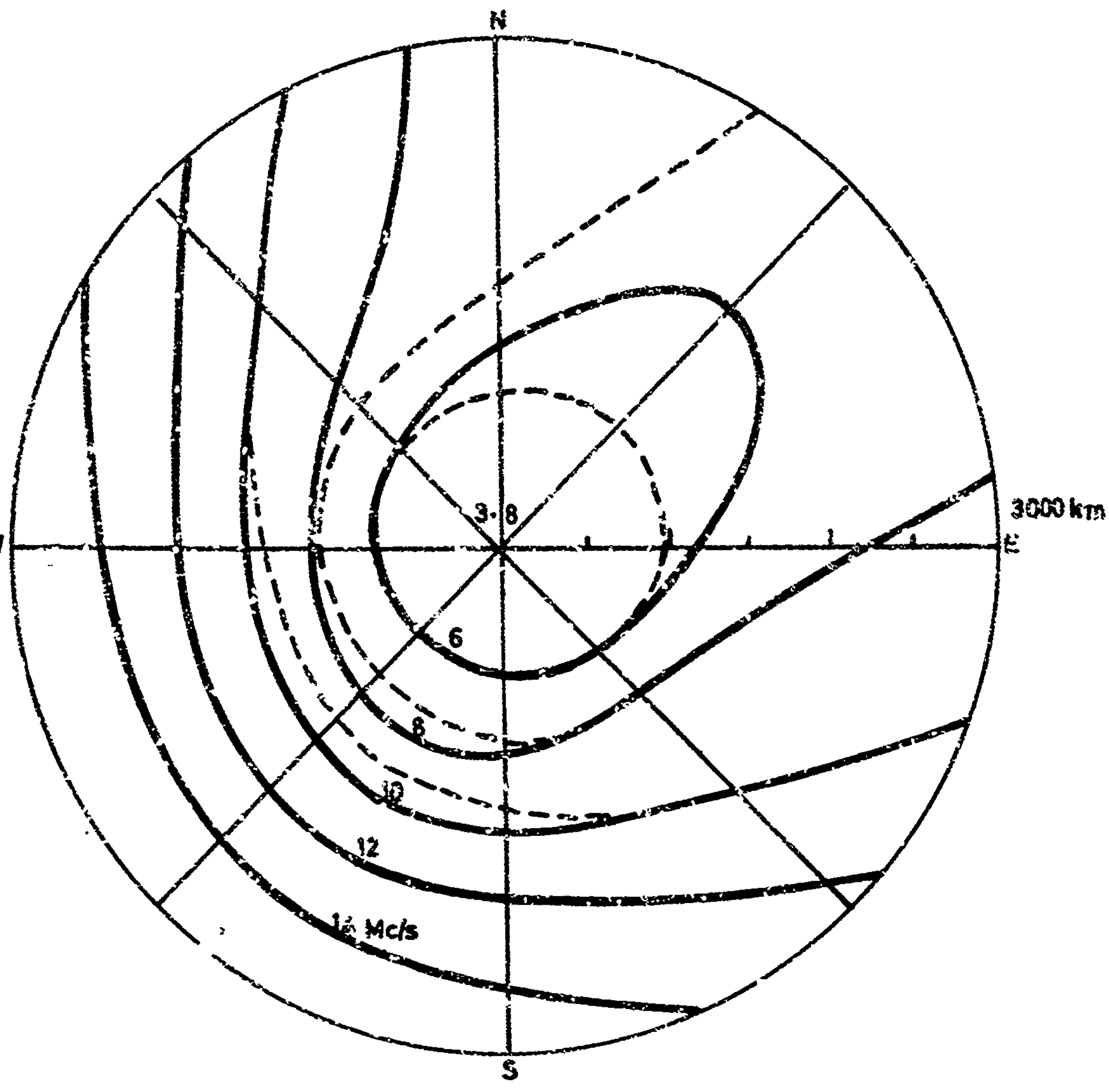

Fig.3 Equidistant-azimuthal map of maximum skip distance at 1600 GMT in December, sunspot minimum. Southern England

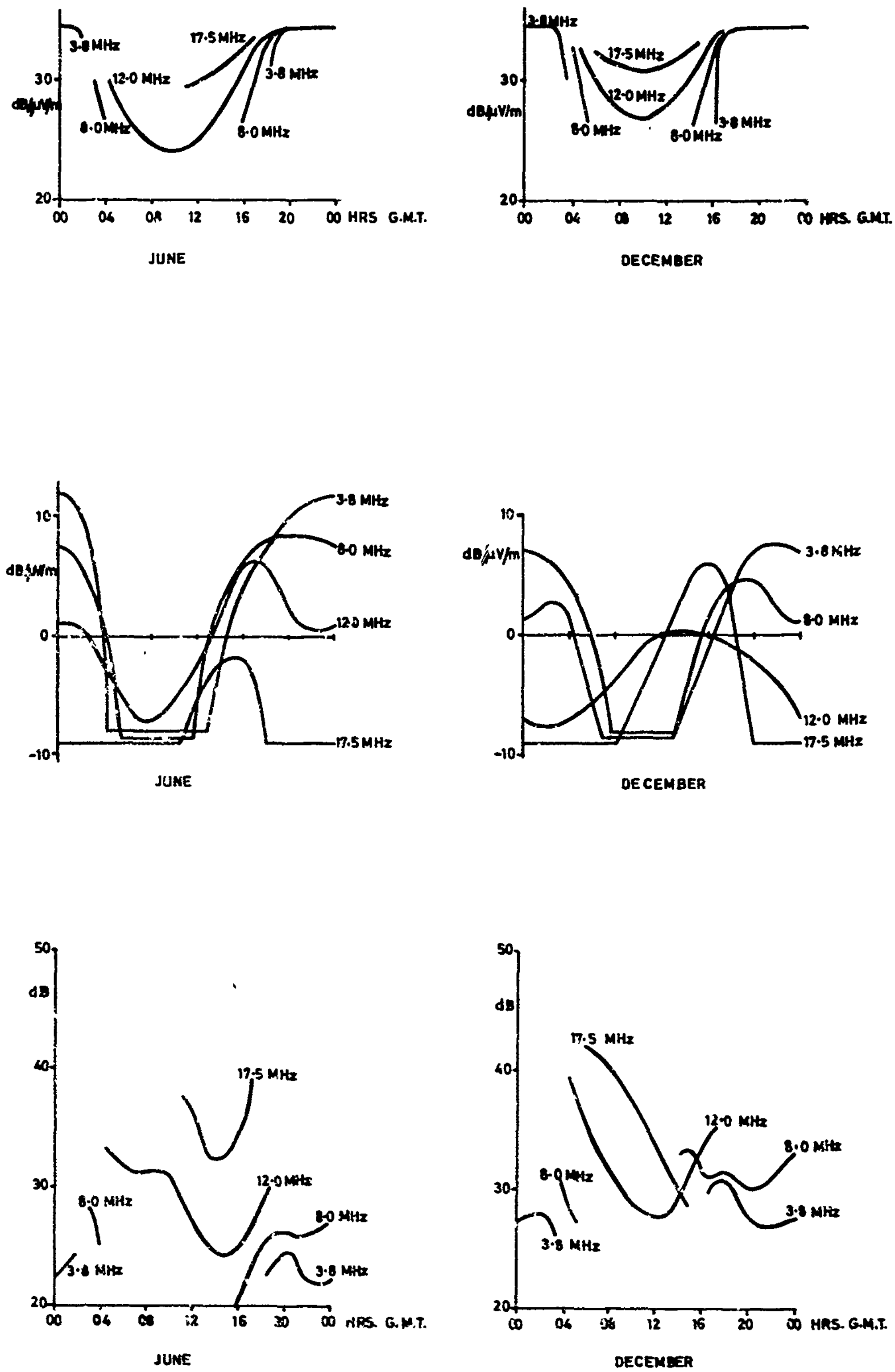

Fig.4 Prediction of signal to noise ratio in the two solstices at sunspot minimum. Kuwait - Khartoum

(a) Variation of signal field strength on selected frequencies for 1 kW e.i.r.p.

(b) Variation of median atmospheric noise field strength in a 6 kHz bandwidth at Khartoum.

(c) Median signal-to-noise ratios obtained from the above curves.

THE FORECASTING SYSTEM
OF THE FERNMELDETECHNISCHES ZENTRALAMT (FTZ)

by

A. Ochs

SUMMARY

Research Group D 33 (Ionosphere) forms part of the Wave Propagation Department of the Research Institute of the Fernmeldetechnisches Zentralamt (FTZ). It is concerned with a number of research projects in the field of ionospheric wave propagation and solar-terrestrial influences on wave propagation. In the International Ursigram and World-Days Service (IUWDS) the Group acts as a Regional Warning Center (RWC) and in the Spacewarn Network as a Satellite Regional Warning Center (SRWC).

In addition, the Research Group regularly issues monthly, weekly and daily radio predictions and forecasts for the radio stations operated by the Deutsche Bundespost and other radio services. These forecasts are based on a great number of solar, interplanetary and geophysical data, which are furnished by different institutions. The Group has some field stations carrying out measurements of ionospheric wave propagation, geomagnetic activity, solar radio emission and cosmic-ray intensity. The measured values are evaluated daily. Some of this work is done by electronic computers. A short description is given of the data evaluation and of the contents and form of the forecasts.

The Forecasting System of the Fernmeldetechnisches Zentralamt (FTZ)

by

Alfred Ochs*)

Research Institute of the Fernmeldetechnisches Zentralamt

1. Responsibilities of Research Group D 33 of the FTZ Research Institute

Research Group D 33 "Ionospheric Studies" forms part of the Research Branch "Wave Propagation" of the FTZ Research Institute. Its responsibilities (Fig. 1) comprise research work in the field of ionospheric wave propagation and of solar-terrestrial influences on wave propagation as well as the preparation of ionospheric predictions and forecasts for the assistance of the Deutsche Bundespost radio stations and other organisations. The national and international interchange of solar, interplanetary and geophysical measuring data is closely connected with the above activities. Thus the Research Group takes part in the International Ursigram and World Days Service (IUWDS) as Regional Warning Center (RWC) and in the Spacewarn Network as Satellite Regional Warning Center (SRWC).

The overall responsibilities of the Research Group are summarized below. In the following sections the preparation and distribution of short-term forecasts is dealt with in more detail.

1.1. Research

1.1.1. Ionospheric Wave Propagation

- World-wide variation of ionospheric characteristics (e.g. dependence on the earth's magnetic field)
- Field strength in the HF band
- Field strength in the MF band
- Propagation above the classical MUF by irregularities in the ionosphere and at the ground (scatter, etc.)
- Winter anomaly of ionospheric absorption

1.1.2. Solar-terrestrial Relations

- Day-to-day variation of MUF, LUF and field strength on different radio circuits (observation of the transmission frequency range)
- Effect of solar phenomena
- Precursors of ionospheric disturbances
- Statistical relations between various phenomena (solar, interplanetary, cosmic-ray, geomagnetic, auroral and other phenomena) and ionospheric disturbances
- 27-day recurrence tendency

1.1.3. Measurements

- Transmission frequency range of different "directions"
- Field strength recordings of selected HF-transmitters
- Long-distance VLF propagation
- Solar radio noise at two frequencies
- Geomagnetic activity
- Variations of cosmic-ray intensity

*) Deputy Chief of Research Group D 33 "Ionospheric Studies"

1.2. Ionospheric Predictions and Forecasts

1.2.1. Monthly Predictions

- Median receiving field strength as a function of frequency and time of day (cf. Fig. 2) for 65 long-distance radio circuits (more than 4000 km), for 21 intermediate-distance and short-distance radio circuits (less than 4000 km) and for regional radio circuits within Europe
- Median level of atmospheric noise as a function of frequency and time of day for a receiving station in Central Europe

1.2.2. Weekly and Daily Forecasts

- Weekly forecasts of radio propagation quality during day and night periods for different "directions" (i.e. groups of radio circuits)
- Daily forecasts for the same "directions"

1.2.3. Predictions and Forecasts for Special Purposes

at request

1.3. Interchange of Data

1.3.1. Regional Warning Center in the International Ursigram and World-Days Service (IUWDS)

- Collecting and coding of the data furnished by German and Austrian Institutes
- Interchange of coded data with the other RWC's and the ARWC's (Associate RWC's) at Stockholm and Prague
- Preparation of regional Ursigrams and passing on of the latter to the interested institutes
- Issue of the advice for the Geoalert and transmission of the latter to the World Warning Agency at Boulder, Colorado
- Passing on of Advance Alerts and Geoalerts to institutes, RWC's and ARWC's

1.3.2. Satellite Regional Warning Center (SRWC) in the Spacewarn Network

- Distribution of announcements on satellites, launched in the Eurafrican region, to the other SRWC's and the observation stations
- Passing on of the announcements received from other regions to the observation stations of the own region

2. Data Received Daily

A great number of the latest data concerning various solar, interplanetary and geophysical phenomena are required as a basis for the preparation of short-term forecasts. The list in Table 1 conveys an idea of the variety of different data available each day.

Table 1

Input Data for the Daily Forecasts

A.	**Solar Data**	
	Optical	Centers of activity Plages Spots Magnetic classification Corona Flares
	Radio	Single frequency - m-waves Single frequency - dm-waves Spectral observations Interferometric observations
	Other	X-rays
B.	**Interplanetary Data**	
	Particle events	Measurements made in the earth's atmosphere or in space
	Solar wind	Velocity Density Temperature
C.	**Geophysical Data**	
	Geomagnetism	Indices Disturbances
	Ionosphere	Critical frequencies SID's Polar cap absorption (PCA) Auroral absorption
	Aurora	Forms Activity Brightness Colour
	Cosmic Rays	Daily variation Special events
	Wave propagation	Transmission frequency range Received field strength Quality figures
D.	**Alerts and Forecasts**	
	Alerts	Geoalerts Advance alerts Advices
	Forecasts	Solar activity Proton events (forecasts of other Centers) Wave propagation

As shown in Fig. 1 the data originate from different sources. Part of the data are supplied by scientific institutes in Germany and abroad. The majority of the data from foreign sources are made available via the IUWDS. Moreover, the radio stations report on the handling and quality of the radio traffic. In those cases where no appropriate measurements are made by other stations or their results cannot reach us in good time, measurements are carried out by various stations of the Deutsche Bundespost.

2.1. Data Furnished by the Ursigram Service

The data interchanged within the IUWDS are the most essential basis for the preparation of the daily and weekly forecasts of radio propagation conditions. The following data are regularly obtained from the institutes in the Federal Republic of Germany and Austria listed below:

a) Optical observations of the sun:
Wendelstein, Schauinsland, Kanzelhöhe

b) Radio observations of the sun:
Kiel, Weissenau

c) Critical frequencies, ionospheric absorption:
Lindau (Harz), Breisach

d) Geomagnetic activity:
Wingst, Fürstenfeldbruck

e) Cosmic-ray intensity:
Kiel, Lindau (Harz)

Moreover, the other RWC's and the ARWC's at Stockholm and Prague furnish us regularly with their Ursigrams. They comprise data measured by a great many institutes all over the world. It is not possible to name here all the stations participating in the IUWDS [1] .

2.2. Measurements Performed by the Deutsche Bundespost

The Deutsche Bundespost established three measuring stations in order to obtain the data which other scientific institutes cannot supply in the appropriate form or in good time:

2.2.1. Lüchow (Northern Germany, 53.0°N, 11.2°E)

This overseas radio receiving station is mainly concerned with observations of the transmission frequency range. These observations allow the quality of ionospheric propagation and its development tendency to be continuously monitored, deviations from normal conditions (corresponding to the monthly median or mean value) to be recognized and the outcome of the forecasts to be checked.

For this purpose, the field strength values of a greater number of transmitters situated in a certain geographic region (e.g. East Asia) are measured at regular intervals of 90 minutes. The transmitters to be observed are so chosen that their frequencies are distributed as equally as possible throughout the entire HF range (about 2-30 MHz). If possible, only such transmitters are observed which have a regular transmission schedule and a known transmitting power. These conditions could, however, not be satisfied in all cases.

Because of the great number of transmitters to be observed, there is not much time for each identification and field strength measurement. Consequently, the individual field strength value may depart very much from the half-hourly or hourly median value. For this reason, statistical methods are always employed for the evaluation, e.g. determination of the band character figure or the propagation quality figure [2, 3] .

At present, the transmission frequency band is observed for the following geographic regions:

Canada	North America (west coast)
U.S.A. (east coast)	Australia
South America	East Asia
South Africa	Europe
India	

In addition to these observations of the transmission frequency range, Lüchow records the solar noise on 250 and 610 MHz by means of a small radio telescope so that solar bursts are indicated as early as possible.

2.2.2. Leeheim (near Darmstadt, 49.9°N, 8.4°E)

This station is also concerned with wave propagation studies. Measurements are made of the receiving field strength of a number of suitable HF transmitters at various distances and on several frequencies. A cable line is used to transmit the measured values to Darmstadt, where they are continuously recorded. They are available for the preparation of the daily and weekly forecasts. In addition, statistical evaluations are made to check and improve the monthly predictions.

Moreover, the measuring station at Leeheim records the amplitude and phase of the received field strength of remote VLF transmitters. These recordings are made to obtain information about special events in the lower ionosphere, e.g. SID's and PCA events.

These measurements are supplemented by recording the geomagnetic activity, i.e. the horizontal component of the geomagnetic field.

Efforts are made to further expand the number of propagation measurements carried out by the Leeheim station and to automize as far as possible the work of the station and the evaluation of the measuring results. We hope that at a later date these steps will allow the observation of the transmission frequency range to be discontinued which is at present carried out by a large number of operators at the overseas radio receiving station at Lüchow.

2.2.3. Predigtstuhl (Southern Germany, 47.6°N, 12.9°E)

As Dr. Beckmann has already stated in his review [4], since about 1940 the Deutsche Post Radio Propagation Prediction Service has been interested in the correlation between the variations of cosmic-ray intensity and the changes of the ionospheric conditions. Since both phenomena are consequences of solar events, attempts were made to use the variations of cosmic-ray intensity as an indicator of the events on the sun and in interplanetary space, and thus also of forthcoming disturbances of the ionosphere and the radio propagation conditions.

The measuring station on the Predigtstuhl, about 1700 m above sea level, records the cosmic-ray intensity by means of various measuring instruments. At present, the following equipment is used:

1 neutron monitor,
2 NaJ(Tl) scintillators (5 inches Ø),
2 ionization chambers with different shielding.

The results of the measurements are daily telephoned to Darmstadt.

2.3. Reports from Radio Stations

Part of the radio stations which are furnished with our ionospheric forecasts and predictions report daily on the disposal of the radio traffic on the most important overseas links. Such reports are, of course, very valuable in order to recognize and follow-up the commencement, the development and the intensity of disturbances of the propagation conditions. In evaluating these reports it must, however, be borne in mind that the quality of radio traffic does not only depend on the propagation conditions but also on several other factors. The most essential factors are listed below:

- the changing natural and man-made noise levels at the receiving station,
- the intensity of interference caused by other transmitters,
- the correct functioning and setting of the technical equipment at either terminal of the radio path,
- the choice of frequency which must be in agreement with existing frequency assignments,
- the mutual agreement by the two communicating radio stations on steps to be taken.

Frequently it is not possible to ascertain reliably the different causes to which the observed changes in the quality of traffic are to be attributed. This is particularly true in the case of the modern modes of operation such as ARQ systems, etc.

2.4. Other Measuring and Observation Data

In order to obtain a survey of the solar-terrestrial events and the ionospheric phenomena, which is as comprehensive and complete as possible, we do our best to include further reports in our evaluation. At the time being, the following reports are to be mentioned in this connection:

a) The SFC (Solar Forecast Center) Reports of the U.S. Air Force Weather Service, in which the development of the solar activity is indicated in detail every six hours.

b) The reports of the ESOC (European Space Operations Centre of the ESRO) on the increase of the particle radiation outside the magnetosphere. These reports are based on the provisional evaluation of the measurements made by the satellite HEOS (1968-109A).

2.5. Alerts and Combined Messages Issued by the IUWDS

Just as we furnish the other RWC's with our advice for the Geoalert and with our ionospheric forecasts and predictions, we use also the advices of the other RWC's and the Geoalert for the preparation of our daily forecasts.

The same applies to the concise surveys of the solar activity and the solar-terrestrial relations. These surveys which are encoded according to the GEOSOL code are included in the Ursigrams. We are very grateful because for some time the solar physicists have furnished us not only with their most essential observation data, but estimate also the probable development of the activity centres and the possible geophysical effects.

3. Synoptic Representation of Data and Evaluation for Forecasts

In spite of many endeavours and numerous investigations in the field of solar-terrestrial physics one has not yet succeeded in finding a precursor which reliably indicates the occurrence of ionospheric disturbances. The objective of our Radio Propagation Prediction Service is, therefore, to collect as many different data concerning the solar-terrestrial events as possible and to combine them in a synopsis. Thus we are able to compare the different phenomena and to weigh their importance.

3.1 Synoptic Representation

In order to daily obtain a fairly clear survey of the great many phenomena and their interrelation in space and time, the most essential data are plotted in graphs.

The most important representations are:

a) Daily solar maps which indicate the development of the centres of solar activity on the basis of optical and R.F. observations (cf. Table 1, Section A). Several maps showing the different phenomena are plotted on tracing paper. By superimposing these maps it is possible to see the correlations.

b) The sequence of the solar events, of the phenomena resulting therefrom in interplanetary space, in the magnetosphere and ionosphere, and their effects on the wave propagation conditions are plotted on general surveys.

Here these representations need not be dealt with in detail, because some examples are shown and explained in Dr. Beckmann's paper (Figs. 2a-c) [3]. All sheets are so divided that several consecutive 27-day solar rotations can be placed side by side or can be superimposed. Thus, the comparison of the actual situation with that existing 27 days earlier as well as the recognition of recurrence tendencies and the following-up of the development from one solar rotation to the next are considerably facilitated.

Further details which are extracted from the reports received daily but cannot be included in graphic representations are compiled in supplementary tables.

3.2. Evaluation of Data and Preparation of Forecasts and Predictions

As mentioned above, no clear correlation has as yet been found to exist between solar events and wave propagation disturbances, which would allow a reliable forecast to be made. All investigations showed only statistical relations so that the forecasts can only be made with a certain degree of probability. The preparation of forecasts and predictions requires, therefore, very much experience. In our Research Group this work is closely connected with the further investigation into solar-terrestrial correlations. Thus, the latest results of research can immediately be used for the preparation of forecasts. On the other hand, new problems to be studied by research arise in the light of experience gained in preparing the daily forecasts.

When preparing forecasts the forecaster generally proceeds as follows:

At first he uses the synoptic representations described above to form an opinion of the solar activity existing at that moment, of the conditions in the interplanetary space and the ionosphere and of the development tendencies as far as these can be recognized. He compares this situation with the situations which occurred one or two solar rotations earlier and tries to find similarities and dissimilarities. Needless to say, he pays special attention to the occurrence of outstanding events, such as larger flares, which he can assume to be non-recurring. In such cases he cannot assume that the radio wave propagation condition will develop similar to that during the preceding solar rotations, but he must try to estimate the effects of this event on the ionosphere. However, if such non-recurring events have not been reported, he will pay special attention to the 27-day recurrence tendency of the propagation conditions and, for instance, he will study the question whether disturbances experienced during the preceding rotations will have the tendency to increase, to decrease or to shift in time.

Frequently, the forecaster faces the problem that of the indicators available to him for estimating the further development some point into different directions. Then he must try to find further clues which will facilitate his decision in one direction or the other. For this decision he must have the experience which tells him which of the indicators are to be attached more importance in the given circumstances.

The correlations to be allowed for and the rules to be applied to the preparation of forecasts have been dealt with at some length by Dr. Beckmann [3, 5]. For this reason, this contribution will not discuss these items in detail.

4. Short-term Forecasts Issued by the FTZ

4.1. Philosophy of Forecasts

At the FTZ the forecasts and predictions are combined to form one system.

The example in Fig. 2 shows that the predictions for each radio circuit indicate the expected monthly median value of the receiving field strength as a function of frequency and time of day for a transmitter with an effective radiated power of 1 kW. The user of these predictions must know the following:

- actual transmitting power and gain of the transmitting antenna,
- gain of the receiving antenna,
- noise level at the receiving station,
- signal-to-noise ratio required according to the mode of operation applied and the requirements to be met with regard to reliability.

Then he can take the predictions to determine the limits of the frequency band (operational MUF and LUF) usable for his special requirements.

The forecasts are based on these predictions. They forecast the probable deviations of the transmission conditions from the normal value. These deviations are expressed in the form of quality figures and information on the relative position of the MUF and LUF.

4.1.1. Geographic Region to which the Forecasts Apply

The conditions are forecast separately for the following directions of traffic or areas:

North America	-	Germany	(code: NORAM)
East Asia	-	Germany	(code: EASAS)
South America	-	Germany	(code: SOUAM)
Europe			(code: EUROP)
Short circuits			(code: SHORT)

4.1.2. Forecasting Periods

For each traffic region we differentiate between a "DAY" and a "NIGHT" period. Here "day" means the period during which the day frequencies can normally be used in the direction concerned, and "night" the period during which the night frequencies can be used. In the case of short-distance circuits these two periods are determined by sunset and sunrise. Hence, the "day" and "night" periods vary according to the direction of traffic and the season. The mean trend is plotted in Fig. 3.

4.1.3. Quality Scale for Radio Propagation Conditions

The quality figure is a general description of the daily propagation conditions with respect to conditions indicated in the monthly predictions. The radio propagation quality is the better the wider the transmission frequency range and the higher the field strength within the transmission frequency range. This range is limited by the MUF and LUF which, in turn, depend on the relevant operating conditions (mode of operation, transmitting power, antennas, noise level, etc.). The quality figures are expressed in a scale from 1-9, viz.:

1 = useless
2 = very poor
3 = poor
4 = poor to fair
5 = fair
6 = good (normal, approximately corresponding to the monthly prediction)
7 = very good
8 = superior
9 = excellent

The quality figures derived from the observation of the transmission frequency range (cf. item 2.2.1) are calculated according to the above scale and included in the Ursigrams.

4.2. Weekly Forecasts

Every Friday the weekly forecasts are distributed by telegraph. They cover always ten days so that there is a three-day overlapping for two consecutive forecasts.

At first, a brief review of the conditions during the preceding week is given in plain language. This review is followed by the quality figures for the next ten days. For each traffic region one quality figure is indicated for the day period and another one for the night period.

4.3. Daily Forecasts

The daily forecasts are issued Monday to Friday at about 1300 hours U.T. by way of telegraph. They cover the forthcoming night period and the following day period. The daily forecasts for Saturday and Sunday are already issued on Friday. A similar arrangement applies to public holidays.

For the daily forecasts the day and night periode are once again sub-divided into the first half of the night (1) and the second half of the night (2), the first half of the day (3) and the second half of the day (4). The boundaries between the two halves are not clearly defined. Their purpose is only to indicate the development tendencies to be expected during the interval concerned.

The daily forecasts supplement or correct the weekly forecasts by more detailed information.

4.3.1. Quality figures

One quality figure is given for each of the five traffic regions and each of the four forecasting periods (see above).

4.3.2. Relative Position of the Limits of the Transmission Frequency Range

The general information about the radio propagation quality is supplemented by additional statements concerning the relative position of the MUF and LUF, where:

0 normal.
The MUF and LUF values obtained from the monthly prediction by allowing for the respective operation conditions are considered to be normal.

+ above normal.
In general, a higher MUF is connected with an earlier in-time or later out-time in the upper frequency range, i.e. with a prolongation of the operating time. A higher LUF means a shorter operating time on the lower frequencies

- below normal.
As a rule, a lower MUF results in a shorter operating time on higher frequencies. In the case of a lower LUF there will be a longer operating time on lower frequencies.

Moreover, a higher (lower) MUF generally means a higher (lower) field strength in the upper frequency range, whereas a higher (lower) LUF means a lower (higher) field strength in the lower frequency range.

The meaning of these statements is once again listed in Table 2.

Table 2

Meaning of the Forecasts of MUF and LUF Variations

Forecast	In-time	Out-time	Operating time	Field strength	Frequency range to which forecast applies
MUF +	early	late	prolonged	increased	on higher frequencies
MUF 0	normal	normal	normal	normal	
MUF -	late	early	shortened	decreased	
LUF +	late	early	shortened	decreased	on lower frequencies
LUF 0	normal	normal	normal	normal	
LUF -	early	late	prolonged	increased	

In the case of short-distance circuits (code: SHORT) the relative position of MUF and LUF is not indicated, since these forecasts cover only low frequencies (up to about 6 MHz) which are mainly influenced by the varying day-time absorption and are especially suitable for shorter distances (up to about 1000 km).

4.3.3. S.I.D.'s

The probability of the occurrence of SID's is indicated in four steps. It applies always to the respective day period (see item 4.1.2. and Fig. 1) because SID's can affect only the illuminated half of the earth. Moreover, the intensity of the ionospheric effects depends upon the position of the sun. Hence, when applying these SID forecasts allowance has to be made for the illumination of the relevant radio path and the season. The stronger the sun on the relevant radio path the more is the radio traffic affected by a SID. As a rule, during the summer months a SID is more pronounced on the northern circuits and during the winter on the southern circuits.

The variation of probability is indicated as follows:

0 = unlikely
1 = possible
2 = likely
3 = almost certain
(with strong ionospheric effects)

4.3.4. Explanations

A final brief explanation in plain English language comprises a review and information about the solar activity together with the expected effects on ionospheric wave propagation. If possible, some special characteristics of the radio propagation conditions and their further development are dealt with.

References

[1] I.U.W.D.S. — Synoptic Codes for Solar and Geophysical Data, Part D: Lists of Station Indicators. Second Revised Edition 1969.

[2] Ochs, A., Beckmann, B. — On the 27 days' recurrence tendency of radio propagation disturbances in the period of high solar activity. "The Effect of Disturbances of Solar Origin on Communications", G.J. Gassmann (Ed.), AGARDograph 59 (1963), pp. 235-244.

[3] Beckmann, B. — Positive phases and disturbances of ionospheric wave propagation as compared to solar-terrestrial events. Paper presented to the XVth EPC Symposium on Ionospheric Forecasting, 2-5 Sept., 1969.

[4] Beckmann, B. — Short-term forecasting in Germany. Paper presented to the XVth EPC Symposium on Ionospheric Forecasting, 2-5 Sept., 1969.

[5] Beckmann, B. — Scientific information needed for radio propagation forecasting. "Synoptic Codes for Solar and Geophysical Data", published by I.U.W.D.S., Second Revised Edition 1969, pp. 17-19.

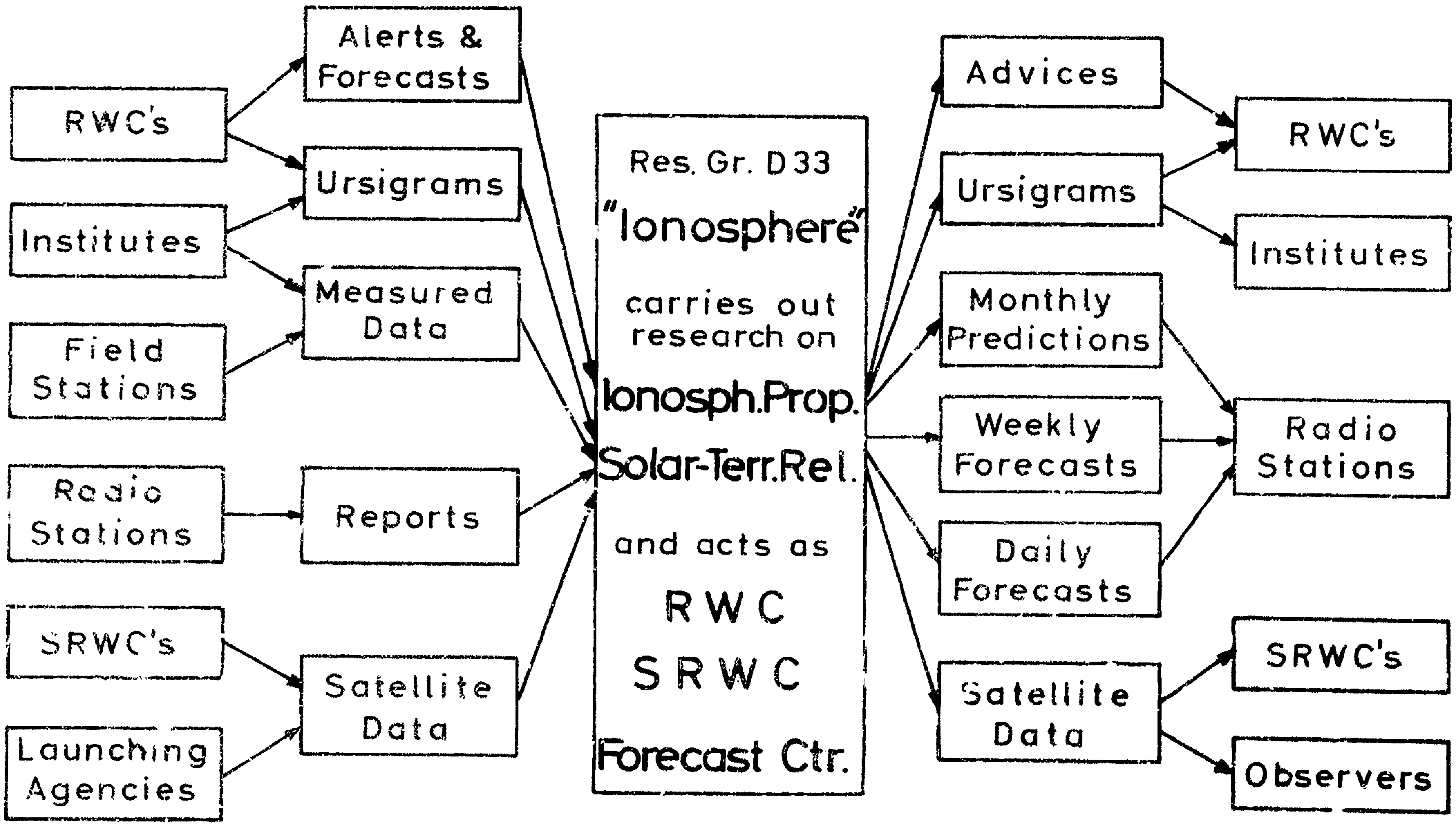

Fig. 1 Regular input and output of data

Deutsche Bundespost
Fernmeldetechnisches Zentralamt
Forschungsgruppe V C

Page 43
CIRAF 28-47

Radio Propagation Prediction

E in µV/m

ERP =	100 W	1 kW	10 kW	100 kW	1 MW
+ 40 dB	30	100	300	1000	3000
+ 30 dB	10	30	100	300	1000
+ 20 dB	3	10	30	100	300
+ 10 dB	1	3	10	30	100
0 dB	0,3	1	3	10	30
- 10 dB	0,1	0,3	1	3	10
- 20 dB	0,03	0,1	0,3	1	3
- 30 dB	0,01	0,03	0,1	0,3	1
- 40 dB	0,003	0,01	0,03	0,1	0,3

Circuit: *Frankfurt/M — Karachi*

Month: *April 1968* Azimuth *97°*

R = *104* *5680 km*

Median Oper. MUF } depending on the
" LUF } required fieldstrength
" FOF

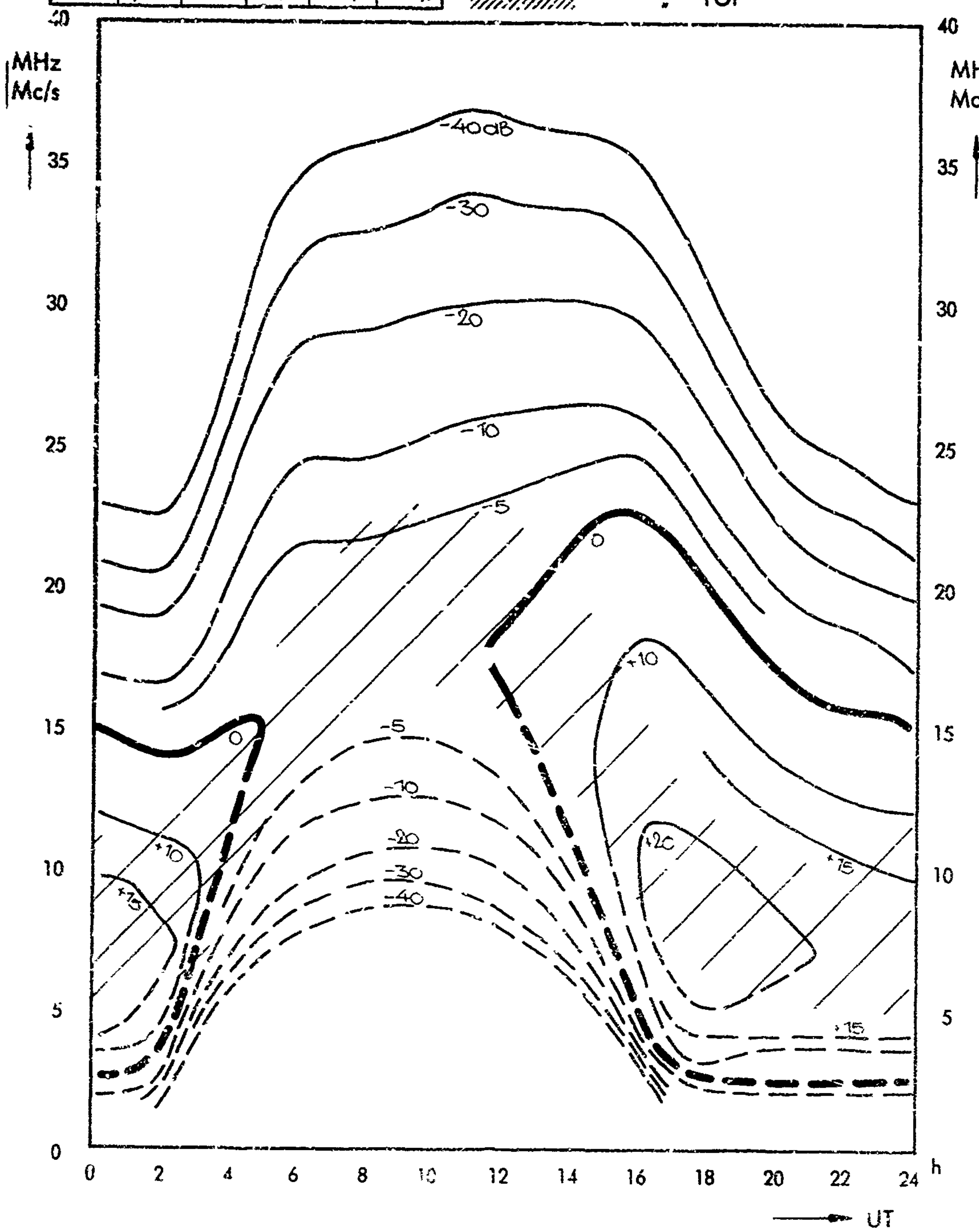

Fig. 2 Sample of the monthly predictions

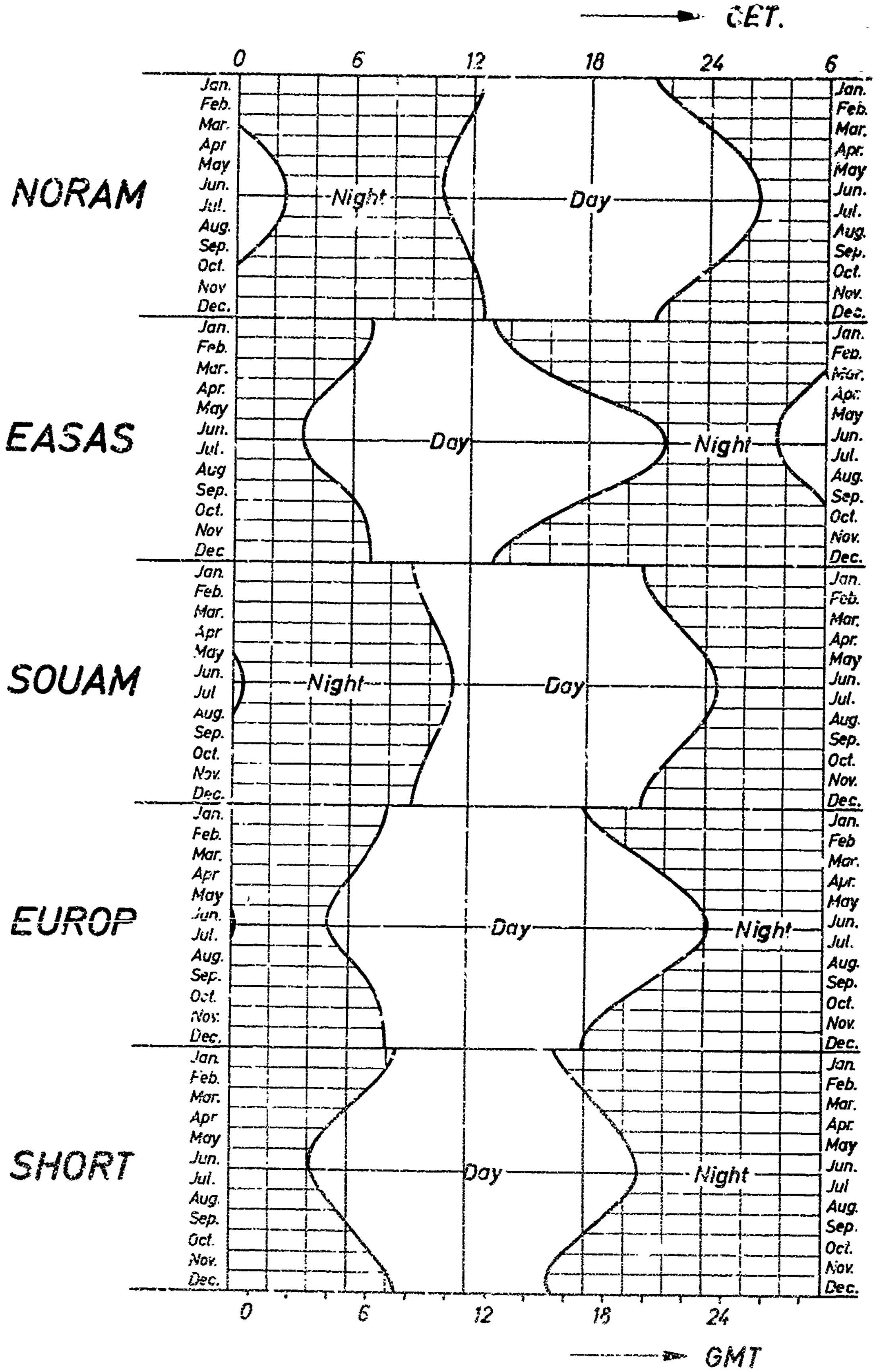

Fig. 3 Day and night periods to which the forecasts apply

CET = GMT + 1 h = Central European Time

D

DISCUSSION

D

Questions and comments concerning specific papers (referenced by number) are given first followed by more general discussion. The general discussion as given here came in part from the 'comment forms' filled out by those contributing to the discussion and by transcription from the recording tapes made during the meeting In the latter case, the remarks have been edited and paraphrased.

QUESTIONS AND COMMENTS ON SPECIFIC PAPERS

PAPER NO. 6

K. Davies (U.S.): Are forecasts of quiet solar and ionospheric conditions also useful?

P. Halley (France): A mon avis la prévision des periodes de calme assuré, permettant une propagation ionosphérique tout a fait suite est sans doute aussi importante pour l' exploitant que la prévision des periodes de perturbation.

P. A. Simon (France): In reference to Paper No. 6, the use of just one technique, the X-ray flux of the sun, seems to be insufficient to forecast the solar activity. The classical forecast uses several data together, the material coming from each technique reinforces or reduces the weight or the physical meaning of that coming from the other sources.

PAPER NO. 7

P. A. Simon (France): With regard to paper No. 7, the evaluation of a method for long term forecasting is a ticklish problem: the successful periods tend to persist in such a way that the method may appear better than it is. The problem of the sudden increase of the solar activity during a week or more with the birth of several active centers at about the same time is unsolved. Nobody has been able to forecast the starting date of this evolution.

P. Hypher (Canada): Has Dr. Blizard considered simulating the planetary conjunctions using a digital computer?

J. Blizzard (U.S.): The orbital and conjunction periods have been compared on a computer to sunspot number by several authors including Jose, Wood and Wood, Brier and Biggs. It has not seemed necessary to duplicate the work of other investigators. In addition, fifteen planetary functions have been correlated with sunspot number in a recent Lockheed report by Pimm and Bjorn, utilizing machine programming. However sunspot number may not be a sensitive indicator of major solar activity.

G. A. Kuck (U.S.): Miss Blizard, can you order the tidal forces as caused by the various planets according to the intensity of the force?

J. Blizard (U.S.): First of all, it is not clear whether the tidal force is the correct function to use. If the planets are considered singly, then Jupiter has the greatest tidal force, followed by Venus, with Earth and Mercury in third and fourth place. Mercury is highly eccentric, so the order depends on whether it is near perihelion or not.

J. P. Sudworth (U.K.): Has the relationship between conjunctions and solar activity been examined for past records, in particular for solar minimum periods?

J. Blizard (U. S.): Solar minimum is the ideal time to study this because one can detect the 10 cm flux increases with conjunction times much better when there are no active centers on the sun. I have been trying to do this for 1964; unfortunately, 1964 was not so quiet as some other minimum periods but we had no radio data earlier than that. I have checked back with large sunspot groups in the past as in January 1926, and there one gets the same correlation with conjunction as in the recent data, but there one must use sunspot areas or sunspot numbers since we have no other data.

J. Bochau (U.S.): I am one of a group of about 50 people who are on standby at Churchill waiting for a PCA event. If we had a prediction of a conjunction which will produce a flare within the next six or seven weeks, it would help us and save the government some $200,000.

H. Rishbeth (U.K.): (1) A rough calculation suggests that a conjunction between the four planets Mercury, Venus, Earth, Jupiter occurs about once every 30 days. If a 10 day "response" time, following any conjunction, is permitted in the calculation, there is a one-third probability of obtaining "positive results" by chance. If the pre-existence of an active region is also assumed, the chances would seem to be further improved. (2) Is it worth performing calculations with conjunctions of "fictitious" planets to investigate further the statistical reliability of the method?

J. Blizard (U.S.): Your calculation on conjunction frequency is correct. However, the conjunction must be in alignment with an active center on the sun, so that the "chance" probability is considerably reduced. (2) This would be a useful approach.

PAPER NO. 9

W. R. Piggott (U.K.): Do we need data we do not at present get? For example, would it be worthwhile to store X-ray data and get average and extreme data for longer periods than possible with real time observations?

R. M. Straka (U.S.): Kuck uses the Castelli criteria to predict proton events (1 proton/cm²/sec/steradian where E≥ 10Mev) where riometer absorptions would be less than 1dB. However, the Castelli criterion was designed and is used most effectively for proton prediction where the absorption is 2 dB or greater. Used properly, this criterion then gives 80% or higher success in prediction. The forecaster's guide for prediction of proton events shows 75% prediction with the Castelli criteria and type II or IV meter bursts occur. When the integrated X-ray flux 0.032 erg-min- $(cm^2 sec)^{-1}$ is added to the radio criteria the prediction still is 75%. Since no gain is apparent, why then is the integrated X-ray flux added to the radio criteria?

G. A. Kuck (U.S.): I tend to think in terms of the physical mechanism which produces the protons. If the Castelli criteria has a physical basis, then the "thousand flux units" criterion should be related to the the actual intensity of the particles produced. If the spectral shape is related to the actual production of the particles, then so is the thousand flux units criterion; and by lowering your standards a bit, one can go from 2 dB down to 1 dB. At the present, there is no easy distinction to be made between a PCA event and a proton event.

S. M. Bennett (U.S.): Based on a study of solar proton data during the previous solar cycle, it appears that a power law decay is as acceptable a fit as is an exponential decay. Furthermore, the filamentary structure observed in the interplanetary magnetic field suggests that diffusion theory is not necessarily applicable to the low energy protons responsible for PCA, especially within a flux tube connected to the flare-active center.

G. A. Kuck (U.S.): Parker stated in his book that the structure was probably filamentary but the main ideas were probably valid. This is borne out by the correlation of the interplanetery magnetic field sector structure with the active regions on the sun during solar minimum. One must consider diffusion coefficients both inside and outside the flux tube. Take a simple model of heat conduction in a copper rod surrounded by an insulator. If one measures the heat flux in the rod, one must use one diffusion coefficient. If one measures in the insulator, he will get a different answer. If he exmines figure 6 in paper 9, he finds that he must use a diffusion equation in one dimension for $\theta < 0.5$ radians (instead of the assumed 3-dimensional diffusion used in deriving figure 6. For $\theta > 0.5$ radians, diffusion in three dimensions seems adequate for forecasting. I must admit all the present theories have problems.

W. R. Piggott (U.K.): From the point of view of HF propagation we do not need to forecast events which are not observable on riometers and have little interest in the weaker events. Thus the prediction system could be simplified to give only what we want to use. For VLF and LF we need to test whether the weaker events are effective. If so, they need to be forecast but, at the same time, give a more sensitive model of proton effects.

PAPER NO. 10

G. A. Kuck (U.S.): The power of using integrated X-ray vs. particle intensities should not be neglected. Correlation coefficients for integrated cm radio data vs. integrated or peak particle fluxes are not as high as integrated X-ray vs. peak particle fluxes. Furthermore, modulation of cm radio data adds uncertainty to the integration. These modulations do not usually show up in the X-ray results. On the X-ray data, several fluxes close together in time can be resolved when they cannot be resolved in the cm radio data.

R. M. Straka (U.S.): Until the question of modulation of radio bursts is more clearly resolved, one cannot rule out that additional particle accelerations may occur during these modulalations and add to the size of the proton event. Regarding the flares, numerous radio bursts recorded at the AFCRL Sagamore Hill Radio Observatory do show that close flares can at times be resolved within the burst.

PAPER NO. 12

J. H. Duffus (Canada): I would like to draw the attention of the meeting to the prediction requirements of two potential groups of users whose needs have not yet been considered. The recent development of the superconducting magnetometer has potentially increased the available sensitivity by 10^4. This implies that the magnetic detection of submarines and geophysical prospecting will soon be more concerned with the natural electromagnetic background in the range from a few Hz down to periods of a few hundred seconds. This background is not directly related to the geomagnetic disturbances discussed in this paper, except during major disturbances. Forecasts of 12-24 hours, or less, which would permit a decision as to whether or not to work, as well as a running forecast for geophysical baseline control would be welcome.

J. H. Meek (Canada): Should not one consider that the tongue of ionization from the sun may be actually in the form of more restricted clouds. This woud account for the lack of correlation between the satellite observations and the earth observations.

K. Moe (U.S.): I hadn't thought about that aspect of the problem. But if you are interested in looking at small scale features, the Vela data would probably be more useful.

W. R. Piggott (U.K.): I wish to point out that small storms are much more common than large and often show better regularity from storm to storm. Small storm forecasting is therefore important and will become more so as the large flare-associated storms die out in the latter stages of the solar cycle.

PAPER NO. 13

L. Petrie (Canada): Is the data shown in figures 2 and 3 selected for particular periods of magnetic activity?

A. R. W. Hughes (U.K.): Yes. For periods for which Kp was less than or equal to 2+.

G. A. Kuck (U.S.): Were there particle detectors on the satellite so one could correlate the wave events with the McDiarmid and Burrows smooth or background boundaries?

A. R. W. Hughes (U.K.): No, there were no particle detectors on Ariel 3. However Ariel 4 to be launched in 1971 will carry a similar VLF experiment and on this satellite, the University of Iowa will have particle detectors.

F. A. Simon (France): The Kp is a crude index of the geomagnetic activity for the study of auroral zone events. During the last two or three years Dr. P. N. Mayaud has developed new indices of the geomagnetic activity related respectively, to high latitudes, to medium latitudes and to the Northern and Southern hemispheres. It would be interesting to use these new indices in order to improve your results.

A. R. W. Hughes (U.K.): I quite agree with this criticism, but one tends to look for relations with Kp first and our plans include looking for correlations such as you suggest, particularly in view of the failure of the intensity to show any sensible relation with Kp. We are proposing to look into the possible association between substorm activity, for, example, and the intensity of the emissions. It is rather surprising that you get a fairly good effect of the changing positions of the zone with Kp.

G. L. Nelms (Canada): I would refer you to a paper which may be of interest in view of the previous question about the relation between the zones of precipitation and energetic particles.*

W. R. Piggott (U.K.): I would draw attention to the fact that the variations of particle precipitation on the quiet days appear to be determined by different factors to those effective on disturbed days. This has not, to my knowledge been properly studied but is important to practical forecasting at high latitudes.

A. R. W. Hughes (U.K.): This is certainly in common with the VLF observations in that one can often receive one's most intense noise zones in quiet periods, periods that have been quiet for a number of days.

* The High Latitude Ionosphere: Results from the Alouette/Isis Topside Sounders by G. L. Nelms and J. H. Chapman, Proceedings of NATO Advanced Study Institute on Production and Maintenance of the Polar Ionosphere, Skeikampen, Norway, 9-18 April 1969.

PAPERS NO. 14, 15, 16, 17

J. H. Meek (Canada): I have four points to bring up: (1) It would be better to use a sequence of maps over a period of 24 hours in order to test the validity of backscatter, rather than to make comparison with single ionosonde measurements. (2) Have you done any Es mapping? This is important to the radio communicator. (3) The E and F1 cut-off are important, especially at northern latitudes in summer when F2 ionization density is low. (4) Is there a problem in dealing with E and F1 region mapping?

R. R. Bartholomew (U.S.): ESSA's technique is probably more capable of doing most of these things than ours is. We do not plan to do any Es mapping. We can detect Es but we have not yet done anything with it.

J. Blair (U.S.): I believe our technique to be suitable for Es mapping and capable, too, of separating modes, since we have rather precise elevation information.

R. R. Bartholomew (U.S.): Our system is designed more for the communicator--to give the effective gradients in the ionosphere, that is, the overall gradients that will change the raypath, rather than any determination of the structure of the ionosphere at a given point. We have started a study based on a sequence of maps. We should have results in the next 6 months or so.
To this point the E- and F1-layer cutoff has not been a problem. The sounder sensitivity, however, is such that nighttime ground backscatter via the F layer is not received. In the daytime, even in the presence of Es, F-layer propagated ground backscatter is always present. We are concerned with the effective total gradients effecting the path and both F1 and F2 may be included. We do not try to separate the layers, as perhaps can be done with the high resolution array used by Mr. Blair.

R. G. Maliphant (U.K.): The speakers from both ESSA and SRI have referred to the lack of vertical-incidence stations for checking the derived data. Have you considered constructing model backscatter records from 3-D ray-tracing, and using the known input as a check on your results?

J. Blair (U.S.): No, although this is a possibility. But, what we did was to compare our measurements in time at the equivalent distance with our backscatter high resolution array with observations made with one vertical-incidence sounder. This does give a fair check.

L. W. Barclay (U.K.): In 1967 and 1968 we undertook several series of backscatter experiments to determine the possibility of measuring ionospheric parameters at a distance. We used a high power pulse backscatter transmitter with a broad band narrow beam transmitting antenna. Reception was with a vertical stack of receiving antennas, electronically scanned to allow us to measure arrival angles. Such measurements were made with the aid of a digital integrator. On selected frequencies a narrow range gate was employed and the arrival angles of signals in this gate were measured. The results were processed graphically and the reflection heights and equivalent vertical-incidence frequencies were determined. Synthetic "equivalent vertical-incidence ionograms" for the path mid-point were constructed from a number of these observations.
Our path mid-points were over W. Germany and we compared our results with the actual ionograms obtained at Lindau and Breisach. We chose to compare our deduced reflection heights with the ionogram heights at the same vertical-incidence frequency. We made several thousand measurements and between 30% and 60% of various sets of these results were within 5% of the layer height. Our experimental limitations were equivalent to about a 5% height accuracy. We believe that our errors are due mainly to wrong identification of the propagation mode, particularly where sporadic E is involved. Other errors may well be due to ionospheric tilts, receiving antenna side-lobes and interference.

H. Moeller (Germany): It is well to point out that with the high resolution array described by Mr. Blair it may now be possible to identify specific points on the ground from which the backscatter returns. If, in fact, this can now be done, it will be possible to measure the angle of departure and with the delay time and this new information as to the location of the ground-scatter point it is possible to check to see if the propagation path is symmetric or not.

K. Davies (U.S.): One short question: in the early days of attempting to apply backscatter to communication problems, the backscatter failed just when it was needed most -- during disturbed periods. Are either of the methods described here any good during disturbance?

J. Blair (U.S.): There are still problems to overcome during disturbed periods, but, since we now have higher resolution in both azimuth and elevation as well as higher powers, we can separate modes, for example. Certainly, the new techniques are a great improvement over the old.

H. Moeller (Germany): To continue with Meek's question about F1 and E backscatter, are you not able to detect two leading edges?

R. R. Bartholomew (U.S.): First with regard to F1, the technique allows us to detect only one leading edge; future improvements may allow us to do better. With regard to E, ground scatter via the E layer is, according to my observations a very rare thing.

PAPER NO. 18

H. Albrecht (Germany): In using RTW modes, the real problem, of course, is in the mode you actually assume. Did you merely assume this mode, or did you consider others as well? Did you make very precise time-delay measurements?

C. A. Moo (U.S.): The propagation mode is that described by Fenwick after an elaborate series of experiments which demonstrated that this is essentially the only way in which signals could propagate around the world. The introduction of the tilt was due to Isted in England for the purpose of launching these ion-ion modes. We did no precise time measurements. This topic was exhaustively covered by Hess in a series of experiments in Germany during the war.

S. M. Bennett (U.S.): The measurements were range-gated, of course, so that no backscatter or other signals could affect the measurements of amplitude. The gate was set for a delay time (I think) within about 10 milliseconds of 138 milliseconds after the transmitted pulse.

Albrecht (Germany): If you had made very accurate time-of-travel measurements, you would then have been able to determine the actual mode more exactly -- the ionosphere reflection points, could have been found. These do vary, of course.

C. A. Moo (U.S.): One conclusion reached by early investigators -- one of the astounding things about RTW signals -- was that there was not very much variability.

J. H. Meek (Canada): Have you any reason to believe that your propagation follows the great circle even if you point the receiving antennas at 180° to the transmitting antenna?

C. A. Moo (U.S.): Fenwick, Hayden and Villard published a paper in 1965 in which they stated that very small bearing deviations could be detected -- less than about 5°.

J. H. Meek (Canada): I do not agree that deviations are negligible. The actual state of the ionosphere at a moment is very different from models or from estimates based on monthly averaged and smoothed observations.

S. M. Bennett (U.S.): During the course of the experiment we did attempt to measure bearing deviations, but within the azimuthal resolution of the receiving antenna (12°) none were observed.

PAPER NO. 19

J. W. Ames (U.S.): The 80 day recurrence of small scale irregularities suggests a remarkably long lived, small-geographical-extent phenomenon. Have you considered a causal mechanism?

W. R. Piggott (U.K.): You are seeing the tip of a regular perturbation which is generated by the world circulation of the neutral atmosphere pushing the F2 layer up or down. Some more details are given in the written paper. There are, however, also semi-fixed perturbations which can be seen on the maps at certain LMT's.

PAPER NO. 21

W. R. Piggott (U.K.): We need new cheap methods of getting data for forecast and prediction problems. Can you indicate the additional cost needed to exploit this possibility?
Has the data so far shown any parameters which would be useful to the forecaster, e.g., in some zones at high latitudes Es can act as a warning of future local disturbance.

H. J. Albrecht (Germany): The necessary equipment is relatively inexpensive: appropriate time-signal receivers are now available from industry: production tolerances are more than adequate for the overall accuracy aimed at. In addition, a four-channel oscillograph should be available for simple displays: automatic equipment alignment to optimum transmission frequencies would be more expensive.
As shown in 3.5 of the paper, the occurrence of Es was found in terms of appropriate changes in mode, such that short-term predictions may be based on this method

E. L. Hagg (Canada): Do you experience any difficulties due to ground sidescatter modes?

H. J. Albrecht (Germany): In the system described, ground sidescatter, similarly to any other type of scatter, would appear as time dispersion on signal pulses used for analysis. A definite interpretation of such records would require a certain minimum amount of statistical data of direct-path category, and can be attempted when this condition is fulfilled.

PAPER NO. 22

D. A. Reynolds (Canada): (1) What is the practical application of this system to a communications circuit? (2) What would it cost for an individual system?

J. W. Ames (U.S.): The practical application in a continuously operating radio station would be to greatly reduce the work load or required skill level of technical control operators while at the same time improving performance. Additional programming could provide frequency management for moving stations. It would provide immediate good performance if used to direct an intermittent or standby HF link.
The cost is about $10,000 to $20,000 for the processor. A sounder receiver and channel monitor receiver are also necessary. Sounder receivers for this single purpose can be sold for under $10,000 in quantity. A new channel monitor receiver should probably be designed using recent techniques. The cost would depend on whether or not the quick-change capability of a synthesizer is needed.

PAPER NO. 24

G. W. Haydon (U.S.): What is meant by "daily" absorption values? Is it a daily average, a comparison of power received vs. power transmitted or a comparison between day and night field strengths?

T. B. Jones (U.K.) (In absentia): The absorption was measured by the conventional A3 technique. The absorption is determined by assuming the reflection co-efficient of the Es layer at night to be unity. It is necessary to use the Es layer for calibration in order to preserve the path geometry since all these results are for 1 hop-E modes during day time.

W. R. Piggott (U.K.): The low correlation at zero distance shows the importance of the height of reflection on the observed absorption. This suggests that the paper is showing how this varies with position. Before the IGY (IGY Annals III Pt. II) we made a study of vertical-incidence absorption and found that storm-associated absorption varied rapidly with latitude. Does the difference between months depend on magnetic activity?

T. B. Jones (U.K.): It was realized that differences in reflection levels could influence the correlation obtained between the various circuits. When the correlation coefficients were examined as a function of the reflection level (i.e. in terms of the equivalent vertical-incidence frequency for the paths), no systematic trend could be detected. It was concluded, therefore, that the path mid-point separation rather than the reflection level had the greatest influence on the correlation coefficients for the circuits considered. Little change with magnetic activity was detected.

E. L. Hagg (Canada): I noticed the low correlation particularly for the May-August period. Now this is the time when sporadic E occurs most frequently -- therefore the signals at one reflection point may be reflected from Es and at another from the normal E layer. Thus the deviative absorption may differ at various reflection points.

T. B. Jones (U.K.): I agree. However, the occurrence of the Es is probably sufficiently wide-spread to influence most of the paths considered.

PAPER NO. 26

D. A. Reynolds (Canada: (1) What sort of staff complement is used in the forecast center? (2) How is the forecast information passed to the user? By mail?

T. D. Damon (U.S.): (1) By the end of this year we will have an officer forecaster, a non-commissioned-officer forecaster, an an observer (for data handling) on each shift around the clock. (2) Forecasts are disseminated to users by use of the entire military communications facilities of NORAD. telephone, teletype, etc., depending on the requirements of the customers.

J. H. Meek (U.S.): Do you have a way of getting feedback from the user to indicate the usefulness of the forecast?

T. D. Damon (U.S.): For our highest priority customers, we have a man assigned to the operation to assist them in interpreting and using our forecasts, to advise us of the usefulness of our product, to suggest changes in types of forecasts, formats, etc., and to evaluate our service in general.

J. W. Ames (U.S.): What training do your forecasters receive?

T. D. Damon (U. S.): All officer forecasters have B. S. degrees in meteorology, physics, math, or other science and M. S. degrees in astrophysics, geophysics, solar physics or related subjects. They have experience in weather forecasting and are given on-the-job training in solar and ionospheric forecasting at the forecast center. The NCO forecasters have weather forecasting experience and attend a special training course. Most of them have had experience at a solar/geophysical observatory.

R. P. Hypher (Canada): Do you have an extensive service predicting fade-outs over a large geographical area?

T. D. Damon (U. S.): The Forecast Center is responsible for predicting ionospheric conditions primarily over the northern hemisphere. Effects of solar flares and geomagnetic storms are, of course, observed in both hemispheres simultaneously, but we do not now make quantitative predictions for the southern hemisphere.

PAPER NO. 27

A. Katz (U. S.): How was Matsushita's work concerning foF2 changes during storms related to the predicted MUF changes obtained in your prediction program?

G. H. Stonehocker (U. S.): The MUF factors in the latitude bands used by Matsushita for this foF2 changes were examined. The changes in the factors were then combined with the critical frequency changes to give the storm-associated changes in MUF.

J. H. Meek (Canada): I am concerned about the use of computers for turning out forecasts in a field like this one where so many variables are involved: (a) the forecast can be no better than the hypotheses originally put into the computer program. (b) the scientist often having put his best efforts into devising the program then feels that his job is done and turns his attention to more interesting and more impractical ventures. (c) the program almost always involves smoothing of data which eliminates the detection of minor events which may be of real importance to the communicator who operates in real time and not in statistics.
Since it is not convenient to alter the program even if it is devised with that in mind, the value of the forecast quickly reaches a plateau.

J. W. Ames (U. S.): These are certainly all good points to take into consideration in building a system. However, the augmentation of a forecasters memory and giving him a way to take into consideration many extensive calculations quickly are a help which overshadows your points at this time. Improvements must be incorporated, of course. Hopefully, this will be done often and in a learned manner.

PAPER NO. 28

I. Paghis (Canada): The biggest problem in flare-to-storm correlation is that there is not a one-to-one correspondence. The problem has two parts: first, there are more flares than there are things that we identify as storms, and second, not all storms are flare-associated.

J. V. Lincoln (U. S.): To emphasize this point, if you look in any issue of "Solar-Geophysical Data", you will see that there are far too many flares for any individual flare to be associated with a later geomagnetic storm without using other criteria as well. Solar radio waves are found to be an important factor, for example. It is not easy to make the flare-storm association, but, at least Mr. Cook has had the courage to publish his associations in detail.

C. G. McCue (Australia): The problem is recognized. In Cook's work, if such confusion arises, he gives alternative analyses.

PAPER NO. 30

H. G. Moeller (Germany): For the VLF transmission measurements to investigate PCA events you used a frequency of 18.6 KHz. Would a similar effect have been found on 10 KHz?

K. K. Rinnert (Germany): The frequency range around 20 KHz seems to be the most sensitive. We have only a few measurements on a transpolar path at 10.2 KHz from the OMEGA station in Hawaii. They show only extremely small effects during solar disturbances.

D. Davidson (U. S.): You will note that amplitudes over Greenland ice-cap paths are far more sensitive to PCA effects. It would have been interesting in your pre-print paper to have parallel display of NSS-Sodankyla with NSS-Lindau. This has been discussed in a recent paper in Planetary and Space Science by Westerlund et al, who show some of your results, I believe.

K. K. Rinnert (Germany): Unfortunately, we have a lot of instrument troubles at the station in northern Finland. There is not enough data for statistical comparison, but there are special events showing PCA effects on the NSS-Sodankyla path and AZA effects on the NSS-Linday path about 2 days later. This seems to occur only for very strong geomagnetic storms, e.g., September 3-4, 1966.

T. Larsen (Norway): We see great changes in phase of the 10.2 KHz Hawaii transmitter (up to 80 or 90 μs) at Tromso during PCA's. This path seems to be very sensitive to such events.

K. K. Rinnert (Germany): At Lindau, however, for about 5 PCA events during one year, there were no very great phase effects.

K. Davies (U.S.): Is the absence of VLF phase effects during PCA's caused by mode interference?

K. K. Rinnert (Germany): We received OMEGA Hawaii on 10.2 and 13.6 KHz. In this frequency range, the 2nd mode is too much attenuated over 10,000 km. The received signal from NPG crosses the Greenland ice with very high attenuation even for the second mode. There is no interference pattern during sunset and sunrise.

P. Simon (France): I suspect that the protons responsible for the absorption at VLF are not precisely the same energy as the ones producing PCA. When you have absorption on VLF do you always have absorption indicated on riometer?

K. K. Rinnert (Germany): We correlated our VLF measurements with riometer observations made at Godhaven in Greenland. In the summertime, the sensitivity of the riometer is much greater and during the equinox it is about the same as the VLF so that then the VLF event accompanies the PCA observed by riometer. They must not be the same protons, but their effects occur during the same time.

PAPER NO. 31

J. B. Lomax (U.S.): We have found that a better predictor than the 3-day running average you used is one based on giving weight one-half to the preceding day, one-fourth to the day before that, etc.

S. M. Bennett (U.S.): It certainly should be. Something else to try is the sum of Kp over longer periods of time and this would tend to give substantial weight to the most recent previous disturbed day. This is another example of persistence.

K. Davies (U.S.): Why is it necessary to determine foF2 changes via magnetic and solar radio noise flux? Wouldn't it be just as logical to forecast foF2 and hence, to determine Kp and flux?

S. M. Bennett (U.S.): Solar flux and magnetic disturbance measures are conveniently available for analysis. They represent overall indices of the major perturbation mechanisms for the F-region plasma frequency. The response of the F region is known to vary substantially with season, time of day and location and to infer the strength of the perturbation sourse from the response seems circuitous.

P. A. Simon (France): I suggest the use of new criteria for the forecast: solar activity is more complex than it appears through the 10 cm flux.

W. R. Piggott (U.K.): I would point out that magnetic disturbance can give positive or negative perturbations of foF2 depending, for SC storms, on the UT at which the storm started. This tends to underestimate the importance of magnetic-associated terms. For a low latitude station at hours when storm effects are predominantly positive you can find large Kp factors which tend to hide the 10 cm perturbation.

S. M. Bennett (U.S.): I agree. The period chosen for study (1961) exhibited substantial 27 day periodicities in solar 10 cm flux and was particularly useful for elucidating any daily correlation between solar flux and daily-hourly foF2. The results for Washington should be taken as suggesting that the contribution to the variance by certain solar and geophysical variables may be treated quantitatively, but the relative importance of the independent variables considered changes with local time, season, and geographic location. What we really wish to know is whether their relative importance varies in a systematic way.

J. V. Lincoln (U.S.): Just a reminder that to actually use your method for the day ahead you will have to predict Kp from some local K. Thus adding to the variability.

S. M. Bennett (U.S.): The objective of the study was to establish reasonable relationships between solar-geophysical parameters and foF2 variability. To the extent that any parameter is conveniently available and well-correlated, it can be utilized for prediction purposes.

PAPER NO. 33

J. H. Meek (Canada): You have discussed the characteristics and changes in Es and absorption but I did not hear mention of the precursor events which are valid as a result of this work.

E Harnischmacher (Germany): (1) The Es anywhere is the precursor. With the drift movement, we can forecast the azimuth in which the Es will move in the next few hours, and from the periodicity we can estimate that some 12 or 24 hours later, there will be Es at the same place. (2) The precursor is the magnetic storm. Two to 4 days later you have a maximum in absorption.

H. G. Moeller (Germany): According to Mr. Harnischmacher, an increase of Kp should be used as a precursor to indicate an increase of absorption. For practical purposes this is not meaningful. One should investigate whether the same correlation exists if instead of Kp, the magnetic activity measured at the same station could be used.

E. Harnischmacher (Germany): We plan to make such an investigation.

PAPER NO. 34

P. Halley (France): Si j'ai bien compris, l'auteur indique dans la premiere partie de l'exposé que le parcours 2F est moins affaiblé que le parcours 1F et d'autre part que l'affaiblessement a l'évanouissement de l'onde et a l'absorption déviative peut être plus important que l'affaiblessement du a l'absorption non déviative. Ces resultats peuvent être obtenus par le calcul et sont conformes a l'application de la théorie magnétoionique au modele ionosphérique plan ou sphérique, en présence des chocs, pour des valeurs convenables des caracteristiques.

C. G. McCue (Australia): I agree. However, although these results are well known, they have not been applied adequately in the past. It should be done now.

PAPER NO. 36

A. F. Barghausen (U. S.): Since Mr. Gerson arrived at Gray Rocks after the symposium had been in session for two days, he could not be aware of the fact that many of his points have already been discussed. His detailed comments on the computer program used by ITS actually had to do with an older version (the '68 version) and some of his objections have been recognized and corrected in the '69 version, described in an ESSA/ERL report ITS 78. Comparisons have been made (as he suggests), sporadic E has been mapped and is now taken into account, and the absorption equation has been improved. The atmospheric noise maps are being redone to give noise sources, from WMO information of thunderstorm centers, and this should give better prediction of the effects of atmospheric noise as received by use of (usually) directive antennas. In fact however, interference is more often the limiting factor rather than atmospheric noise.
Dr. Meek has raised objection to the use of computers. Because of the large number of variables involved, a computer is essential if an adequate job is to be done, either for long-term or short-term prediction. The central facility suggested by Mr. Gerson is in operation at ITS. A time-share computer can be accessed to give the desired information rather quickly.

N. Gerson (U. S.): My remarks apply to the ITS 1968 version which I have examined in detail, and not to the 1969 version which I have not seen.

G. W. Haydon (U. S.): As a co-author of ITSA-1 (the 1968 version referred to) I wish to thank Mr. Gerson for the publicity he has given the computer methods of ionospheric predictions outlined in that publication, and for his recognition of the fact that they have been so extensively used nationwide.

N. Gerson (U. S.): You raise a good point. It would be impossible to do by hand in any reasonable time what can now be quickly done by computer. Whether it is worthwhile to do it by computer or by hand, however, is a legitimate concern of this type of conference.

R. W. Madden (U. S.): With regard to your remarks regarding the whimsy of the ionosphere, I would suggest that we should be very cautious in substituting nature's whim for that of a hostile power. I would point out that cables can be cut, and have in the past, and that satellites can be jammed and may be in the future. and I think that what we shoud be concerned with in military communications is a proper mix to make sure that neither the whimsy of nature nor the hostility of a foreign power can foul us up.

PAPER NO. 38

J. A. Reynolds (Canada): Someone should devise a system to let us know when the elaborate masses of equipment are actually working together properly.

F. Green (Canada): You have mentioned monitoring the base station as a requirement. What does this mean? What is the base station transmitting, traffic, tone, or beacon signal, etc. ?

R. P. Hypher (Canada): It means passive listening; transmissions are traffic and weather.

J. P. Sudworth (U.K.): Experience with RAF Coastal Command confirms general pattern of operation. However, in a few years there will be a need for completely automatic data transmission from aircraft, and there will then be a need for accurate automatic selection of the best frequency.

R. P. Hypher (Canada): I agree. The U.S.A.F. is now doing this, to some extent, on the C5A where impending or present maintenance problems are described to the base station so that preparations can be made before actual landing.

PAPER NO. 39

J. H. Meek (Canada): In Paper 1 I defined what I mean be "prediction" and by "forecast", and I would like to ask Mr. Probst what he means by the two terms.

S. E. Probst (U.S.): I use the word "prediction" to refer to the prediction of monthly values, medians or deciles, on a long term basis, say, three months in advance, for planning selection of frequencies to be assigned to a circuit. Or, perhaps, the frequencies may be given for entire seasons and for high and low sunspot numbers. I reserve the term "forecast" for information with regard to what is going to happen in a day or two or in an hour or two by way of deviations from the "predicted" situation.

GENERAL DISCUSSION

K. Davies (U.S.) : Why are there no forecasts issued by Britain and Canada?

L. E. Petrie (Canada) : At least in Canada, many of the users of HF communications circuits find that in many instances, the monthly predictions are quite adequate and that most of their outages are probably not due to the ionosphere but are probably due to inadequacies in equipment and installation. However, some Canadian users make extensive use of the American system discussed here by Miss Lincoln and by Mr. Salaman. One of the difficulties is that possibly some of the parameters supplied to the users are not what they require. I am not a user so I would like to hear from the users as to their requirements. Have they any use, say for a forecast 24 hours in advance and could they take advantage of such a forecast if it were reliable?

W. R. Piggott (U.K.): There are possibly three main reasons: a. It is not obvious that a forecast system is economically justified; b. a good forecast system demands a first class man for its creation and largely because of (a) such people are not attracted to the problem, c. the users who could gain most from forecasts are unorganized and do not know the possibilities. Some education is required.

D. A. Reynolds (Canada) : I represent a user--the Canadian Forces Communication System. Len Petrie mentioned that they (CRC) provide communications predictions for average conditions. Through headquarters DCN Australia broadcasts their IPSD warnings to everybody in the U.K.. We, in turn, publish the IPSD warnings to all the Canadian military radio stations and ships at sea. We also find WWV a great help. So we use these all the time: The IPSD warnings and WWV.

L. W. Barclay (U.K.): I asked an associated company who provide ship radio operators; they said they could not use short term forecasts as the circuits were controlled from the shore end and, in some cases, frequencies inappropriate from long term predictions were used. British military long term predictions have been provided by the JRPB for a number of years and we have now been asked to expand this service and to provide short term forecasts. To start with we will have to lean heavily on those organizations which are currently issuing predictions.

L. E. Petrie (Canada): I'm very happy to hear from the users, and now may I ask them: How do you use these forecasts? In what way do you make use of them on the HF communication circuits? One of the speakers mentioned using them to indicate the time when they may have outages, but this is something usually found after the event. Do you use them in real time? Do you use the actual prediction into the future in operating HF communication circuits?

P. Hypher (Canada): The users I am concerned with are those on air-ground-air circuits, and, in particular, radio officers on aircraft. We need more than the knowledge of a condition. What we need is an instantaneous system which says what frequency is or is not usable right now so that the radio officer's time is not wasted.

J. H. Meek (Canada): In answer to Ken Davies' question: We had a forecast system which we stopped in 1944 and we stopped not because we thought that these forecasts were not of use anymore but by that time after our meeting (Britain, Australia, the United States and Canada) it was obvious that the U. S. was going to set up a well staffed center for storm warnings and forecasting and there was no point in our attempting to carry on with $1\frac{1}{2}$ men and a dog which was about all we had available. So we contributed quite a bit, as did the British, to the common pool of knowledge of how to do this and the U. S. set up the service which has been going ever since. As to why we don't have a service now: The value of the system just hasn't improved very much. It has value, but in all these years it hasn't improved very much. It's still about the same sort of system, giving about the same accuracy, and a great deal more effort is put into it. Until we have a breakthrough in method, there is no point starting up another service. Such a breakthrough can be made right now, if somebody gets down to work and looks at the data to work out new patterns on a quantitative basis. We must relate the forecasts more closely to the communications circuits than has been done before. We have talked about "North Atlantic circuits" and South Atlantic circuits", but there is a great deal of evidence that circuits having a common transmitter and with receivers only 1 or 2 degrees apart (in the right direction, of course and on the southern edge of the northern auroral zone) may be outstandingly different. We have to be a little more precise, but I think we can be. And we must give the communicator an estimate of the frequency bands he can use and of the powers he needs.
One more point: There seems to be a general feeling that when there is a "blackout" nothing can be done. In fact there are always alternatives. The naval officer will tell you that the alternative is to go down to low frequencies. Since he has a worldwide network at low frequencies, this alternative is an obvious one. For those of us who are not so fortunate, however, there are still alternatives, such as using a relay station 1000 to 1500 miles to the south. Air Canada has used such a relay station to communicate with aircraft going across the Atlantic. Of course, it is not as convenient, but it is an alternative. The point is that you don't just give up and wait until the storm is over. Other possible alternatives include using different propagation modes or different types of service.

C. G. McCue (Australia): IPSD's forecasting system attempts simply to predict roughly the time of magnetic disturbances and the probability of radio fade-outs. It is left to the communicator to decide from his experience on his own circuits what he will do. IPSD uses most of the correlations described by the earlier speakers plus some of the type to be described in paper No. 28 by Coo K. IPSD has undertaken a research programme which included: (a) examining the morphology of sunspots in fine detail to identify the spots which will develop activity; (b) providing communicators with advice as to how they can minimuse the effects of ionosphere storms and fade outs; (c) forecasting the type, severity and timing of ionosphere disturbances.

P. Halley (France): Depuis quelques années certaines administrations francaises ont manifesté un interet grandissant pour les prévisions a court terme. Ce genre de prévision présente un interet militaire certain, pour les liaisons en HF avec les mobiles tels que les navires ou les avions jusqu'aux plus grandes distances (20 000 km). Citons a titre d' exemple des sousmarins dans l' océan glacial arctique ou bien encore une force aérienne stratégique qu' il faut suivre a travers les océans et les continents. La Division des Prévisions Ionospheriques du CNET, dont j' ai la charge, prepare occasionnellement des prévisions a court terme de 24 heures qui ont pour premiere base de départ des prévisions a long terme. Le réseau des stations de la DPI est progressivement équipé en materiel divers destiné a la prévision a court terme.

T. Damon (U.S.): Paper No. 26 describes the services of the Air Weather Service Solar Forecast Center.

G. A. Kuck (U.S): Is anyone familiar with the Russian forecast system? One difference I am familiar with is the use of magnetic field changes in active regions to predict when a region will flare.

J. V. Lincoln (U.S.): A Russian pamphlet by Zevakina defines their system Basically, hourly reports are received from their 12-30 odd ionosonde stations and forecasts are prepared for a few hours ahead, several times a day, of Δ foF2 both positive and negative for specific areas of USSR. Severny has a paper on solar flare forecasting to be published in proceedings of COSPAR, Prague, May 1969. Flare forecasts were actually made only at times of their manned space flights.

W. R. Piggott (U.K.): I would like to comment here to raise an important point. The Russian sector tends to be appreciably less stormy than ours and this means in practice that they have more communications difficulties due to big differences on quiet days than between quiet days and stormy days. This is, I think, the main reason for their concentration on Δ foF2 and I would mention this as forecast groups who are concerned with the world as a whole do have to bear in mind that there are sectors where the quiet day variations are greater than the quiet to stormy day variation.

B. Beckmann (Germany): The USSR forecasting method described by Zevakina distinguishes between positive and negative disturbances. Instead of positive disturbances, we would say positive phases. The forecast gives both kinds of change.

S. M. Bennett (U.S.): In connection with Dr. Meek's suggestion that more synoptic mapping be done, I would like to mention that we (AVCO) have, for many years, conducted synoptic mapping studies of both the Arctic and Antarctic and also of the Eurasian area. In our studies we find that the best parameter to use for mapping is the percentage change in foF2 rather than Δ foF2 in MHz. This organizes the data very well during storms except during the first hour or so. Recently we have reduced the plotting of maps to a computer program based on a weather mapping program developed by the U. S. Air Weather Service. While this considerably reduces the t diousness of drawing the map, I think it gives us a little less insight into what is going on during the storm. The practice of drawing the map by hand forces you to consider very carefully whether a large scale patterns exist. In fact, they do exist, both in Δ foF2 (percentage change) and also in sporadic E especially over Canada where very large patterns of sporadic E occur during magnetic storms. Finally, regarding the comment that large percentage changes in foF2 occur over Eurasia during quiet times -- I think this is true. However, I think it occurs all over the world during quiet times and, in fact, that is the basis of the paper I will be presenting later on. It appears that during portions of the solar cycle, especially where there are pronounced 27 day fluctuations in the solar activity as measured by the 10 cm solar radio wave flux, there is a corresponding daily variation in foF2 and this could account for some of the pronounced prestorm variability that we seem to have observed in some of our synoptic mapping studies.

B. Beckmann (Germany): The Δ foF2 values in the USSR forecasting method are calculated in percent. They are based not on the monthly median values but on a running mean for 10 days before. We use a running mean of 27 days for our calculated quality figure describing the daily variation of propagation conditions (as published in the Ursigram code) because some positive phases and some of the depressions due to disturbances may last longer than 10 days.

W. R. Piggott (U.K.): I wish to talk about forecasting systems as seen from the humaniti[illegible] parallels can be drawn from Mr. Dolittle in B. Shaw's Pygmalion. The majority of HF [illegible] needing forecasts are similar to "the undeserving poor." They do not know what is possible, [illegible]ding and above all cannot afford any expensive system -- an extra bottle of beer would be more [illegible]. We must consider the needs of this group and economically justified ways of meeting their needs.

T. E. Devey (Canada): Association over the past several years with the service, with the ITU, and with CCIR Study Group XIII on mobile services, suggests to me that the maritime mobile service is a substantial potential user of forecasts. The ship owners, of course, are reluctant to pay more than is necessary for equipment and they want the cheapest possible communications over the great distances from the home port to their ships. Many of the ships registered in various countries seldom see their home ports. Scandinavian tankers, for example, may be built on the other side of the world -- many are now built in Japan -- and their routes may never bring them "home"; even their overhaul may be carried out in ship yards in other parts of the world. There is a need for exchange of information, and, to an increasing extent, of data for which provision was made at the recent maritime conference in 1967. But they would like to be able to go on one of the HF bands and, of course, there are only certain frequencies they can use so that they cannot always use an optimum frequency for their communications. Because of propagation failure or interference, available frequencies may be out for days at a time. Eventually, however, as the world networks become even further developed it may be possible to tie into a coast station in almost any part of the world and through microwave systems, cable systems, or satellite systems communicate with any other part of the world. The need, then, will not be for such long direct paths via the ionosphere but for much shorter paths, relatively speaking, to a coast station -- two or three thousand miles, perhaps, rather than 10,000 miles. So, the operator on the ship needs some sort of graphical aid, perhaps, by which he could, at a particular time of year in a particular part of the world establish the optimum frequency for communication with a particular coast station, or by which he might be able to choose the coast station to feed his data into. From a synoptic point of view, if he had something that he could use as a short term deviation from the long term predictions, so that if there is a storm in progress or anticipated, or if there are variations expected in the present ionosphere conditions, he can make a more accurate estimate of the frequency to use. Similarly, the ship owner, in Oslo, say, could determine the best coast station through which to contact his ship in the Indian ocean.

H. J. Albrecht (Germany): It is well to keep in mind that future requirements may differ from the requirements we have had in communications work during the past 10 or 20 years. The ionosphere may play a different role in future communications, for instance, the transparency of the ionosphere is a rather important factor if you consider satellite communications. I would like to suggest that we may now be in a period which might be described as the eve of the new field of long distance communications: that is, satellite communications. We know that frequency ranges available for such contact are limited on the lower end by the ionosphere. We know that up to about 500 MHz, especially in auroral regions, you may find rather strong influence from scintillations and we also know that satellite communication on these frequencies will most likely become very important in military and civilian work because, at least, by the present standards of technology, the lower frequency ranges within the satellite radio window, let's call it, will be optimal for mobile operations -- for the operation of mobile ground terminals, naval applications and so on. So, we should not forget to modernize our aspects and perhaps to include predictions of the effects of scintillations and transparency of the ionosphere

J. H. Meek (Canada): We have heard a number of people mention the MUF and the LUF as if the band in between these frequencies is always available for communications. This isn't true, as the oblique-incidence soundings show. A second point has to do with the information provided the communicator. He is not interested, and, in fact, unless his training and interests are exceptionally broad, cannot use data about the sun. He needs, and can use, information on how his communication circuits are going to be affected, and this is what should be supplied him. Finally, I'd like to support the comments made on satellite communications, especially with mobile units. This follows what I said earlier about our future concern with less efficient means of communications on frequencies outside the HF band. As impractical as it may sound now, eventually we will be able to use a yagi or a dipole at the ground station, and we will then be concerned with noise coming in from the environment and with the fine structure of the ionosphere which leads to what we now call scintillations. This is in the future, of course, but the forecaster should be preparing now so that he can give the communicator of the future what he is certain to need.

P. Halley (France): Je pense que les fréquences dites MUF et LUF délimitent une bande de fréquence en general assez continue. Lorsque le sondage oblique indique discontinuités dans la bande, l'enregistrement d'amplitude d'continues, sur les fréquences en cause, montre en general la réception d'une champ utilisable.

J. H. Meek (Canada): Perhaps we see much more of these effects in the polar regions. Multiple reflections from the ionosphere (more than one mode present) can give you interference which will be unimportant if you are using Morse code, but extremely important for modern communications, i.e., for high data rates. Another effect is that of the intense sporadic E clouds just south of the auroral zone maximum. These can prevent radio waves for some frequencies and take-off angles from reaching the F region so that there will be areas on the ground at certain distances from the transmitter which can not be reached by way of reflections from the ionosphere. But I do agree with you that these effects may not be so important for communications because the antennas are relatively broad beam and you do get propagation from off the great circle path. This, too, must be taken into account if we are ever to produce a really advanced forecast system.

R. W. Madden (U.S.): We have heard discussion as to whether forecasting at HF is a thing of the future. It seems to me that that discussion has somehow degenerated into talk about whether HF will, in fact, be used as much as it is now. I think that we did predict, with the advent of the cable, that high frequencies would go out, but they didn't. It should be pointed out to those people who are trying to design mechanisms whereby we may make forecasts that whenever one has an allocation-of-resources problem which requires planning for the future, it is essential to have some method of prediction. And anything which is reasonably correct will help us manage these resources better. I think that is the situation we are in with respect to HF. In spite of the cheapness of transmitters and receivers, we require their better use and we must be able to predict reliable modes, especially for the use of cryptographic equipment, so that we can plan, say, a month ahead as to what frequencies will be used, what stations will be used, what antennas will be used. This is very valuable, and from my point of view, the better we can predict (long-term and short-term) the better off we will be. Finally, the predictions can be useful in the management of a system in another way: if contact can not be maintained by certain stations as we predict it should, they may usefully be informed of equipment problems they might not otherwise have discovered.

C. G. McCue (Australia): Hans Albrecht has suggested that I make a few suggestions to you. They will not be in logical order, but they may be worth the time. (1) We must educate the operational people. We must set up training courses for the services and for other organizations and prepare appropriate manuals for them. (2) We must realize that different customers have different needs -- they differ operationally, and their needs will differ in so far as the mode of presentation of the prediction-forecast information is concerned. For example, the overseas telecommunications people operate straight point-to-point circuits; the aviation people have a certain number of fixed terminals and mobiles going over fixed routes, the naval forces have a few bases but must cover large areas. Predictions are required for all these problems and they can readily be made by use of a computer. (3) On the matter of forecasts, some of the needs of the future relate to the work being done by Dr. Simon and by ESSA on solar forecasts to give us as much lead time for propagation events as possible. We want to be able to estimate the time between observation and event, and then the duration. (4) We must determine how the operational people can minimize the effects of fadeouts or storms. We must tell them what to do with their traffic during these conditions -- because, there is often something they can do. (5) We need feedback on the success of our predictions and our forecasts. In our case we get better response in this regard on our forecasts than we do on our predictions. This seems to be because our forecasts are used by people engaged in research as well as by communicators. The research people plan their experiments to take place during certain events, so they are actually waiting on our information -- and they do give us feedback. (6) Mr. Albrecht has spoken earlier of the need to look to the future in designing our forecasts -- we will have to forecast information on the transparency of the ionosphere and on scintillations for satellite communications. But we should also extend the forecasts to lower frequencies -- VLF, for example. (7) Research is necessary on ionosphere-stratosphere coupling and on its implications in forecasting. (8) Finally, the recognized need for forecasting services has led to the establishment of organizations for this purpose; but there are many people now being supported in their research only because such organizations exist. These people should give some attention now to the practical problems in return for this support.

(Editor's comment: During the entire conference, the user's viewpoint was continually sought. In addition to the formal papers presenting this viewpoint, informal comment from the floor was repeatedly asked for with the intention of establishing -- at long last -- fully two-way communications between forecaster and user. Comments by Hypher, Reynolds, Damon, Green, Meek, Piggott and Devey were given in response to this request. These are briefly summarized in what follows.)

F. Hypher (Canada): (1) If the aircraft pilot, for example, is the ultimate user of the forecast, it will not be enough to provide him with a set of frequency charts. He needs something -- perhaps a device -- which provides him (with essentially no effort on his part) with a frequency -- if there is one, and if it is one assigned for his use -- or, if there is none, an indication of this fact. The ground station can then be fully aware -- usually -- of any problem which makes it impossible for the pilot to make his half-hourly report to the ground station. (2) Finding the right frequency is not the only problem facing the men in the cockpit -- nor is it the most important one -- so that, if communications are to be maintained through the static of rain and thunderstorms, for example, and in spite of fatigue, the frequency predictions must be accepted with a high level of confidence. Otherwise, they may well be ignored. At the present time the user does not have much confidence in them.

D. A. Reynolds (Canada): Our ground station operators and technicians are, in general, high school graduates with many years of experience. They are, however, overworked and underpaid; their working conditions can be unpleasant -- for example, how many of you have visited a transmitter site during a lightning storm? So these men, too, have other things to think about besides the optimum frequency for communications with the aircraft that are out. We use the CRPL predictions which work well for us but we have gone to the USAF technique for providing the aircraft with usable frequencies, i.e., the ground operator has the route of the aircraft and each time the aircraft calls in he provides it with a primary and a secondary frequency, based on the predictions and on his experience. For disturbed periods we rely on the IPSL predictions from Mr. McCue's organization in Australia, which we learned about quite by accident. This is an example of failure of communications: please let us know what you have available for us to use. It is extremely difficult to find anyone who can (or is willing to) write simply expressed articles on propagation and communications that our people can understand and make use of.

T. Damon (U. S.): For about three months early this year we attempted to make MUF predictions for the aircraft flying weather reconnaissance across the North pole. They are required to report their weather observations every hour and we insisted that at the same time they report their operating frequency and communication conditions. I went along on one flight during which, after passing Thule, communications with that station went out as we continued toward Norway. The predictions indicated that contact with Anchorage was possible, however, and the major problem was to convince the co-pilot (who has the responsibility for communications) that he ought to try it. So, the operator must be educated. Two other things coming out of this experience may be mentioned. During one flight, communications were very poor on the predicted frequency until the ground station log-periodic antenna was pointed in the proper direction. The second point is that the predicted MUF was generally much higher than any of the frequencies assigned. For weather forecasting, there is a staff meteorologist who is assigned to the customer. When the customer has a weather problem, he consults the staff met. This same approach is being attempted for the solar and ionospheric predictions user.

F. Green (Canada): Experience is the best teacher. The operators must be trained in these matters, but I suggest that the forecaster will benefit and be able to do his job better, if he takes part in some of these missions, sitting at the elbow of the operator, so to speak.

J. H. Meek (Canada): In my early days, I was required to teach young service pilots elementary meteorology. I was not there to tell them about the composition of the atmosphere or the fine structure of the wind distribution with height, but about icing of their aircraft and what to do about it, and about vapor trails which could make them more easily seen and, therefore, vulnerable to enemy action. I was there to tell them about the physical basis of some of the problems they would run into and how they might be solved. Similarly, if a person from an ionospheric laboratory could spend a few hours a week for several months as one of the instructors charged with training potential operators, he would be serving a very useful purpose. In addition he would learn something about the operator's point of view. If this kind of cross-fertilization can't solve the problem, nothing will.

W. R. Piggott (U.K.): If your forecasts are to be used, it is essential that you have the confidence of the skilled man. Don't try to bluff him. You cannot afford to make a mistake. If your forecast is only a guess, tell him so.

T. E. Devey (Canada): Consider the spectrum manager (more precisely, the spectrum engineer) whose job it is to plan for efficient use of the spectrum. Even now we are not very deeply involved in MF and HF problems, but these are, in fact, more complicated than those associated with microwaves or VHF, for example, and they are getting worse. We need the information that you forecasters have in order to develop techniques for assigning frequencies so that interference can be minimized. And this is a point for your consideration. Although there has been frequent mention of "outage," an equally important possibility which renders a frequency useless may be that that frequency is already being used successfully by someone else, i. e., that interference is excessive. Your forecast must take this into account.

E. W. Peterkin (U. S.): Although the remark may be obvious, it is well to keep in mind that <u>any</u> system that uses the ionosphere will be disturbed when the ionosphere is disturbed. Although we have talked almost entirely about communications, there are other applications: navigations, surveillance systems, and possibly intelligence systems. All of these will need forecast information.

N. Gerson (U. S.): It must be kept in mind that the ionosphere, with which the predictions and the forecasts are primarily concerned, is only one aspect of the problem. If the antennas are inefficient, if there is, say, a 5 dB drop between the antenna and the receiver, required signal-to-noise ratios may not be maintained for a particular circuit and it will seem to "go out" much more readily than others where design of the antennas and coupling circuits are better. This is entirely apart from the quality of station maintenance.

I. Paghis (Canada): Like most people, I find that my initial point of view has been strengthened rather than changed during the meeting. The users have done a good job of helping us understand what their problems are; the forecasters have told us a great deal about their systems and the progress they have made in handling the large inputs of data; but the scientists have not levelled with the audience. The fact is that we do not yet have enough detailed knowledge and understanding of the physical processes to provide a really solid basis for short term forecasting. This is certainly true for the ionosphere and it may also be true for solar physics problems as well. Here is what I mean: what are the present forecast systems doing about the effects of neutral winds in the F region? What are they doing about the large scale motion of plasma in the magnetosphere (which will certainly have a large effect on the ionization we need for HF communication)? Not very much. Our understanding has not progressed to the point where these things can be built into the forecast systems. We have more work to do.

D. Jelly (Canada): I'd like to make a few comments about auroral absorption to indicate that we do know a bit about it than has been mentioned here. Absorption has been defined from the riometer records as being of three types: one is the sudden cosmic noise absorption associated with flares, the second is polar cap absorption produced by solar protons, and third is auroral absorption, originally designated as everything else. It occurs mainly in the auroral zone and at first we knew only its average characteristics. Now however, we know that it tends to occur in individual events -- the auroral sub-storms -- and that nighttime effects are associated with absorption on the day side as well. Sub-storms are known to occur most frequently during the early part of major storms. They last from one to two hours and they tend to repeat every two or three hours. As far as I know, the effects of the sub-storms on circuits have not been examined in detail and it would seem to be a worthwhile study. Sub-storm effects on the F layer should also be examined; these should be useful for short-term forecasts also.

W. R. Piggott (U.K.): This my third sunspot maximum in this field. At every sunspot maximum we've been told that we don't need predictions, we don't need forecasts. Four or five years later, sunspot minimum is upon us and a terrible cry arises, "No frequencies are available and everybody is interfering with everybody else. Can we have a system set up?" It takes two or three years to set up a system and by that time we are at sunspot maximum again. If you are to break out of this vicious circle, the time to begin is now.
Now the physicist has been told, I think quite rightly, that he is not contributing. But you must keep in mind that the physicist is perfectly happy if he knows how and why a phenomenon occurs, while to do a forecast or a prediction you must also know when and where, and the physicist isn't interested in this. There is an easy way to get the job done, and that is to cut off the funds until it is done. (I just want to make one constructive suggestion in this period.)
A lot of work was done during the war on the very problems we face today. Your best way of getting a quick answer may be to find someone who was active during the war when we had a very large number of tricks, very often very cheap, which are now completely forgotten.

T. Damon (U.S.): The Air Weather Service (and the IUCSTP, as well) is looking into the possibility of setting up an international network of existing vertical-incidence ionosphere stations so that data can be very rapidly relayed into a central location for the purpose of deriving (almost) real time synoptic maps of the ionosphere. We have found (and Mr. Piggott has shown us well) that there are features not related to solar or geomagnetic activity. These must also be forecast -- especially near solar minimum when solar activity and geomagnetic activity are low, but when ionospheric variability still plagues us. This should be a suitable research problem for someone.

S. E. Probst (U.S.): A few years ago DCA supported ESSA in some research aimed at improving our services to communications in southeast Asia; we did exactly what Major Damon is proposing. We made arrangements to get the vertical-incidence ionograms read and reported on as close as possible to real time from the stations at Manila, Taiwan, Bangkok, and Okinawa. Our principal problem was in getting the data back to the Boulder computer fast enough and the predictions back out to southeast Asia fast enough for the operator in the field to make use of it. As far as he was concerned, the major factor influencing his selection of a frequency was who else was already using the spectrum at that time and in that area. He was limited predominantly by interference and so he could rarely work near the MUF because that's where everybody else was. As we had earlier observed in our operation of the CURTS (Common User Radio Transmission System) system in the Pacific, frequently the best frequency was very close to the LUF since not so many people were using the spectrum down there.

N. Gerson (U.S.): If you look at life from the viewpoint of the man who is using the predictions, namely, the communicator, what accuracies does he need, and for these accuracies (probably to within 1 or 1.5 MHz) what is the least sophisticated system we can get away with to supply his needs?

E. Warren (Canada): That's a difficult question. For most short circuits, a very simple system could be devised. But for long circuits, say, from here to Central Africa or to Australia and for some shorter ones with special problems, a fair degree of sophistication is required. For some situations no existing system will work and a great deal of sophistication is needed. For example, Kift found that the predictions for the Ascension Island - Slough path were hardly related to what he observed; for the path between Tripoli and Accra, Ken Davies found that frequencies around 60 MHz could sometimes be used -- these were centainly not predicted. It seems to me, therefore, that the whole problem of long-term predictions is still unsolved and it is not going to have a simple solution.

R. W. Madden (U.S.): Our studies of the HF spectrum indicate that it is, in fact, very thinly used -- to no more than 10% of its capacity. Since that is so, why is QRM such a problem? I suggest that the answer lies in the fact that all of us using the HF spectrum tend to set up our circuits in the same way. For example, we would not dream of planning a link so that the transmissions travel the long way around, but such signals are frequently observed.

K. Davies (U.S.): As already indicated by a number of speakers, education and training of the operators is perhaps the area needing the most attention. It may be that we should invest some of the money now being spent for research in developing the necessary training program. I believe this should be done nationally rather than internationally, but this committee has made a contribution by the publication of a book by the Norwegian Defense Research Establishment entitled, High Frequency Radio Communications. It is a small book, quite elementary and non-mathematical. It should be useful for the purpose.

J. B. Lomax (U.S.): As an example of a forecasting failure as it bears on the question of keeping the operator's confidence I'd like to tell of an experience of several years ago in southeast Asia. We set up an oblique sounder to help in frequency selection for a very well equipped circuit which had been having trouble in the early morning hours. The operators were interested and co-operative. On one particular evening, however, the MOT determined by the sounder was varying in such a way that we were certain that it would drop through the operating frequency in the next 15 or 20 minutes. So we predicted this and recommended that they go to a lower frequency. The controller overruled us on the basis of a listening test of his own and predicted that the frequency would be good for another three or four hours. In fact, he maintained the circuit for the next four hours and it took several weeks to regain their confidence.

H. Rishbeth (U.K.): As an ionospheric physicist, I should like to ask for suggestions from the users as to the kind of problem we could undertake to help out. We know considerably more than we did a few years ago about the high latitude ionosphere (as a result of Canadian work, in particular, by Hartz and Brice), about the distribution of large irregularities (which should be important for propagation), and about the shape of the equatorial F region. I accept all that has been said about being remote from the user, but with suggestions from some of you perhaps we can help.

C. C. McCue (Australia): Perhaps we should define our terms more carefully. It should not be necessary for the pure scientist to bridge the entire gap between him and the operator any more than for the operator to take up the study of the chemistry of the upper atmosphere, for example. The "user" for the kind of help offered by Dr. Rishbeth should be the applied scientist who develops and puts out the predictions and the forecasts. We should serve as the interface between the two extremes.

F. Green (Canada): In spite of Mr. McCue's comments, I'd like to repeat that a mix of all the elements is still desirable. Experience is still the best teacher. The scientist (pure or not) should not be backward about asking to attend an operation, and the operator should certainly invite them. Visiting back and forth will provide mutual training, and it can lead to the automatic system which appears to be needed.

J. W. Ames (U.S.): At Granger, we made a few haulting attempts to assist in training military radio operators in connection with the installation of sounder systems. The training program was primarily for maintenance purposes so that out of a two-week program there would be one day with a short lecture on how the ionosphere works and what the operator can learn about the communications by watching the sounder. Some of the material for these training courses along with some appropriate more general material has been gathered in a little booklet. Copies will be made available for those who want them.

R. M. Straka (U.S.): In line with the training aspects, would it be possible for NATO or other organization could get together a series of films prepared by a responsible scientist or group of scientists, or prepared after close consultation with these scientists, which would then be given wide distribution?

R. K. Salaman (U.S.): I was involved in the program described by Ed Probst in southeast Asia and we learned quite a bit, particularly in working with the operators in the communication centers and the receiver sites and so on. It is difficult for the forecaster to provide all the answers to the communicator, and, in fact, with his current state of knowledge, I'm not sure that it can be done. Part of the necessary information can come from the forecaster, but part of it may also come from the communicator himself from what is going on over his particular circuit. Would it be possible to devise a simple system -- simple at least from his standpoint -- which gives him a box, say, with six or seven lights on it. Through a world-wide system, it might be possible to distribute a warning of a flare -- giving probable attenuation of daylight circuits -- so one of the lights would indicate this. Another light could respond to signals from a world-wide VLF network when a magnetic storm was forecast -- MUF-LUF perturbations would be expected under these conditions, especially at high latitudes. If a storm is actually detected, a third light could come on. If he is operating quite a bit below the MUF, the fading of the signal will be represented by a Rayleigh distribution (assuming, now, a one-hop path), for frequencies approaching the MUF fading between high and low ray and between ordinary and extraordinary components is very selective, for frequencies between to O- and X-MUFs the fading is very flat and above the X-MUF it becomes Rayleigh again. So if the signal could be analyzed, each of these conditions could, in effect, turn on a light to indicate to the operator the state of his circuit, and as the lights come on in turn, how much operating time remains to him.

J. H. Meek (Canada): First, I'd like to ask Mr. Salaman to stay over so he could go out to CRC on Monday to see the equipment he has just described. Ken Davies, who is now chairman of EPC has an opportunity, and I suggest that he and his cohorts take the responsibility for preparing recommendations, as a result of this meeting to promote cooperative action through AGARD and EPC for this training. Finally, it should be emphasized that Canada (and the USSR) among the more affluent nations share with those countries, called by Mr. Piggott the undeserving poor, a need for HF that not all of you may appreciate. We do not have cables criss-crossing the more remote areas (in our case, the Canadian Arctic, for example) and we cannot depend on satellites or on the less efficient means of communications like tropospheric and ionospheric scatter. This is also true in the Antarctic, of course. Part of our problem has to do with the needs of individuals who may be far from civilization, briefly as in the case of the bush pilots, or for more extended periods like the Eskimo who leaves his settlement for many weeks to hunt. It is a requirement now that these people keep in touch and high frequencies provide the only practical way to do it.